Pseudomonas adaptation to stress factors : role of membrane lipids and Pseudomonas fluorescens response to NO2

Tatiana Kondakova

Normandie Université

THESE

Pour obtenir le grade de Docteur

opéré par l'Université de Rouen

Spécialité : Microbiologie

Pseudomonas adaptation to stress factors: role of membrane lipids and *Pseudomonas fluorescens* response to NO_2

Présentée et soutenue publiquement par
Tatiana Kondakova

Thèse soutenue publiquement le 20 novembre 2015 devant le jury composé de		
Madame Angela CORCELLI	Professeur / Coordonnateur du Centre Interdépartemental de la Recherche de la Paix / Département des Sciences Médicales Fondamentales, Université de Bari, Bari, Italie	Rapporteur
Madame Janine FRÖHLICH	Docteur / Chef du groupe de recherche / Département de chimie Polyphasique / Institut Max Planck Chimie, Mayence, Allemagne	Rapporteur
Monsieur Hermann HEIPIEPER	Docteur / Chef du Groupe des Processus Microbiens / Département Biotechnologie de l'Environnement / Centre Helmholtz pour la recherche environnementale – UFZ, Leipzig, Allemagne	Examinateur
Madame Nicole ORANGE	Professeur / Enseignant-chercheur / Laboratoire de Microbiologie Signaux et Microenvironnement / Université de Rouen, Evreux, France	Examinateur
Monsieur Frédéric DIONNET	Docteur / Directeur du Centre d'Étude et de Recherche Technologique en Aérothermique et Moteurs, St Etienne du Rouvray, France	Examinateur
Madame Cécile DUCLAIROIR POC	Docteur / Enseignant-chercheur / Maître de conférences/ Laboratoire de Microbiologie Signaux et Microenvironnement / Université de Rouen, Evreux, France	Examinateur

Thèse dirigée par le Pr Nicole ORANGE et le Dr Frédéric Dionnet, co-endadrée par les Dr Cécile Duclairoir Poc et David Préterre aux Laboratoire de Microbiologie Signaux-Microenvironnement, EA 4312 de l'Université de Rouen, et Centre d'Étude et de Recherche Technologique en Aérothermique et Moteurs

UNIVERSITÉ DE ROUEN

EdNBISE
Ecole doctorale Normande Biologie Intégrative, Santé, Environnement

LMSM

CERTAM

Normandie Université

THESE

Pseudomonas adaptation to stress factors: role of membrane lipids and *Pseudomonas fluorescens* response to NO_2

The high distribution of *Pseudomonas fluorescens* group is linked to its ability to adapt to stress factors. This work goaled the response of an airborne *P. fluorescens* MFAF76a, and its clinical standard *P. fluorescens* MFN1032 to environmental changes in order to refine the specific adaptation of airborne bacteria. First the HPTLC-MALDI TOF MSI tool defined glycerophospholipid (GP) composition of both strains. In stationary growth phase, an unknown GP, in short UGP, was found and seemed to be involved in temperature adaptation for the clinical strain. After exposure to 0.1, 5 and 45 ppm concentrations, the bacterial response to NO_2 was defined through motility, biofilm formation, antibiotic resistance and expression of several chosen target genes. While no change in parameters was seen in bacteria exposed to 0.1 and 5 ppm of NO_2, several alterations were occurred with a bacterial exposure to 45 ppm. NO_2 seemed to bias the UGP production, reduced *P. fluorescens* swim and decreased swarm only for MFN1032 strain. Biofilm formed by NO_2-treated MFAF76a showed increased maximum thickness, with no change in c-di-GMP intracellular level. Expression of the *hmp*-homologue gene involved in NO detoxification was upregulated in response to NO_2, suggesting a possible common pathway between NO and NO_2 detoxification. Finally, NO_2 was found to increase bacterial resistance to ciprofloxacin and chloramphenicol. Thus the resistance nodulation cell division (RND) MexEF-OprN efflux pump encoding genes were highly upregulated in both strains. Together these findings implement the first model of bacterial response to NO_2 toxicity and the role(s) of GP in bacterial adaptation to environmental changes.

Keywords: *Pseudomonas fluorescens*, adaptation, glycerophospholipid, fatty acids, pollution, nitrogen oxides

---

Adaptation de *Pseudomonas* aux facteurs de stress : rôle des lipides membranaires et réponse de *Pseudomonas fluorescens* au NO_2

La large distribution des *Pseudomonas fluorescens* est liée à leur grande adaptabilité aux facteurs de stress tels que les variations environnementales. Ce travail avait pour objet la réponse spécifique au milieu aéroporté de *P. fluorescens*, comme l'aéroportée MFAF76a et la clinique MFN1032, comme standard. La technique récente HPTLC-MALDI-TOF MSI a permis de caractériser les divers glycérophospholipides (GP) des deux souches. En phase stationnaire de croissance, un GP inconnu (UGP - unknown GP) a été isolé et semble intervenir dans l'adaptation à la température de la souche clinique MFN1032. Quant au stress NO_2 gaz, les deux souches ont été exposées aux concentrations: 0.1, 5 et 45 ppm. Leurs phénotypes ont été confrontés à l'expression de quelques gènes ciblés. Pour les valeurs standard 0,5 and 5 ppm en NO_2, aucun paramètre n'est modifié. Par contre, une réponse bactérienne est constatée suite à l'exposition à 45 ppm de NO_2. Cette exposition semble impacter la production d'UGP. De plus *hmp* et *mexEF-oprN*, codant respectivement pour la flavohémoglobine et pour la pompe à efflux RND, se trouvent surexprimés, corroborant l'évolution de la résistance bactérienne aux antibiotiques. Contrairement au NO, aucune altération de la biomasse de biofilm n'est observée pour le NO_2, qui favorise, cependant, l'augmentation de son épaisseur chez MFAF76a, mais aussi l'inhibition du swarming et la diminution du swimming, avec un taux de c-di-GMP stable. Ce faisceau de résultats offre, pour la première fois, la réponse bactérienne et le rôle des GP lors de stress comme NO_2 ou à la température, autre modification environnementale.

Mots clefs: *Pseudomonas fluorescens*, adaptation, glycérophospholipide, acides gras, pollution, oxydes d'azote, détoxification

La science ouvre à l'esprit humain une voie infinie, et le lance, par une série d'étapes sans nombre, sur l'Asymptote de la Vérité.

Paul Bert (1933-1986)

Remerciements

This work was realized in Laboratory of Microbiology Signals and Microenvironment EA4312, of University of Rouen. I am grateful to the Haute Normandie region for the financial support for this research work.

I would like to thank Pr. **Angela CORCELLI** from University of Bari Aldo Moro, and Dr. **Janine FRÖHLICH** from Max Planck Institute for Chemistry of Mainz for agreeing to participate in my PhD defense and examine my work. It is my honor to be examined by you and I would like hereby to express my sincere gratitude. Special thanks to Dr. **Hermann HEIPIEPER** from Helmholtz Centre for Environmental Research of Leipzig for agreeing to participate in my PhD defense but also for your help in this work, your advices and support. Thank you to accepting me working in your lab, and for your help in FAME analysis and results interpretation. This allow me not only to acquire invaluable professional and personal experience, but also to obtain the European PhD grade. I am very grateful for your help in the review writing. I am glad you are present for my PhD defense today.

Je remercie également mes directeurs de thèse, le Pr. **Nicole ORANGE** et le Dr. **Frédéric DIONNET**, pour m'avoir fait confiance et acceptée dans leur équipe. Je vous suis profondément reconnaissante de m'avoir accordé du temps et des conseils tout au long de ma thèse. Merci pour toutes vos corrections pertinentes des oraux, posters et articles. Je tiens à vous exprimer ma plus profonde reconnaissance.

Je tiens également à remercier mes encadrants, le Dr. **Cécile DUCLAIROIR POC** et **David PRETERRE** pour avoir aiguillé mes travaux pendant ces trois années. Merci **Cécile** pour ta convivialité et ton soutien même dans les moments difficiles ! Merci de m'avoir fait confiance. J'ai particulièrement apprécié tes conseils, nos discussions, ton écoute ainsi que ta disponibilité à chaque moment dans ton bureau. J'ai beaucoup appris à tes cotés !

Un grand merci à toi **Nadine MERLET-MACHOUR** ! L'interprétation des spectres MALDI sans toi aurait été moins drôle ! Merci pour tes conseils et le partage de tes connaissances. Ce fut une expérience très enrichissante.

Je remercie également le Pr. **Marc FEUILLOLEY**, directeur du LMSM, pour m'avoir accueillie dans son laboratoire, pour ses conseils lors de ces trois années, son aide rédactionnelle et ses encouragements. Je n'oublierai jamais les petites pauses café et les moments de rire.

Un grand merci à tous les membres du laboratoire LMSM, **Audrey**, **Chloé**, **Alex**, **Jérémy**, **Lucille**, **Gwen**, **Irina**, **Lilly**, **Manuela**, **Noémie**, **Camille**, **Victorien**, **Andréa**, **Baoloc**, **Kelly**, **Awa**, **Florence**, **Thomas**… Je ne cite sûrement pas tout le monde, la liste est longue. Merci pour votre soutien, votre gentillesse et votre bonne humeur ! Je vous adresse mes chaleureuses pensées et je vous souhaite à tous beaucoup de chance pour la suite.

Merci beaucoup **Olivier** et **Magalie**, vous étiez toujours à l'écoute, disponible et arrangeante ! Merci à toi Magalie pour les expositions au NO_2, pour tes conseils et ton sourire. Merci à toi Olivier pour ta bonne humeur, ton rire va beaucoup me manquer !

Merci à vous mes amis, **Dorian** et **Célia**, pour votre bonne humeur, votre soutien, amitié et tout et tout ! Merci **Corinne**, pour tes conseils, le partage de tes connaissances, nos soirées. Merci à toi **Mathias**, pour les bons moments à Maastricht et ta gentillesse. Merci à vous **Charlène** et **Nicolas**, pour votre bonne humeur et amitié. Merci à toi **Thibaut** pour ta gentillesse, ton aide et soutien, nos soirées ensemble, et tout et tout ! Merci particulièrement à toi **Rachel**. Merci pour ta présence, ton amitié, ta gentillesse. Tu m'a beaucoup apporté lors de ces trois années ensemble. Tu es et resteras une personne exceptionnelle pour moi. En tous cas, il me faudrait plusieurs pages pour exprimer le bonheur d'être à vos côtés mes amis ! Vous restez pour toujours dans mon cœur.

J'adresse une chaleureuse pensée à tous mes amis. Je te remercie, **François** pour ton soutien tout au long de la thèse, ta présence, ta compréhension et ton aide précieux. Pendant ces trois années, tu étais mon amour, mon collègue et mon ami. Sans toi tout cela n'aurait pas la même valeur.

Я от всего сердца благодарю Вас, **мои родители**. Без Вас всего этого никогда бы не случилось. Благодарю Вас за ваше терпение, безграничную любовь, поддержку и заботу! Целой диссертации не хватит, чтобы выразить мою признательность и любовь к Вам! Спасибо тебе **Наташа** за любовь, понимание и поддержку, тебе **Леша** за дружеское отношение, за ревю, и пивные посиделки, Вам **Алла Федоровна** и **Леонид Устинович** за хорошее настроение и помощь во всем. Спасибо вам, мои маленькие солнышки, **Ярослава** и **Даша**. Один взгляд на вас вызывает у меня улыбку.

Наконец, спасибо огромное Вам, **Владимир Константинович**, **Катя** и **Марина**. Вы научили меня самому главное в нашей профессии: любить микробиологию.

Table of content

List of abbreviations

[Fe-S]: Iron-Sulfur cluster
µM: Micromole
2-acyl-GPE: 2-acyl-GlyceroPhosphoEthanolamine
8-oxoG: 8-oxoguanine
AA: Amino Acids
Aas: Acyl-ACP synthase
Abs: Absorbance
ACP: Acyl Carrier Protein
ADEM: French environment and energy management agency
AHL: N-Acyl Homoserine Lactone
AK: Adenylate Kinase
Ala-PG: Alanyl-PhosphatidylGlycerol
ANR: ANaerobic Regulator of arginine deiminase and nitrate reductase
ATP: Adenosine TriPhosphate
BER: Base Excision Repair
BF_3: Boron trifluoride
bNOS: bacterial Nitric Oxide Synthase
bp: base pair
BPG: BisPhosphatidylGlycerol
C20:4ω6: Arachidonic acid
C20:5ω3: Eicosapentaenoic acid
C22:5ω3: Docosapentaenoic acid
CAM: Contact Angle Measurements
cAMP: cyclic Adenosine MonoPhosphate
C-di-GMP: *bis*-(3'-5')-Cyclic dimeric guanosine MonoPhosphate
cDNA: complementary DNA
CDP: Cytidine DiPhosphate
Cfa: Cyclopropane fatty acid synthase
CFP: Cyan Fluorescent Protein
CFU: Colony-Forming Unit
CiLy: Citrate Lyase
cis*-UFA*: *cis*-Unsaturated Fatty Acid
CITEPA: Interprofessional technical center for studies on air pollution
CL: CardioLipin
CLP: Cyclic LipoPeptides
CLSM: Confocal Laser Scanning Microscopy
CO_2: Carbon dioxide
CO_3^-: Carbonate radical anion
Ct: Cycle threshold
Cti: *cis–trans*-isomerase
cXMP: Xanthosine-(3',5')-cyclic MonoPhosphate
cyclo-FA: Cyclopropane Fatty Acid
DEPC: DiEthylPyroCarbonate
DGC: DiGuanylate Cyclase
DHB: 2,5-DiHydroxyBenzoic acid (MALDI matrix)
DMB: Davis Medium Broth
DNA: DeoxyriboNucleic Acid
DNR: Dissimilatory Nitrate respiration Regulator
DSB: Double-Strand Break in DNA
E: PCR Efficiency
eDNA: extracellular DNA
EDTA: EthyleneDiamineTetraacetic Acid
EGP: Exponential Growth Phase
eNOS: endothelial Nitric Oxide Synthase
EPS: ExoPolySaccharides
ESI: ElectroSpray Ionization
ETC: Electron Transport Chain
FA: Fatty Acid
FAD: Flavin Adenine Dinucleotide
FAME: Fatty Acid Methyl Esters
Fap: Familial Amyloidotic Polyneuropathy
FAS: Fatty Acid Synthesis
FAST: Fragment Analysis and Structural TOF
Fe^{2+}: Ferrous iron
Fe^{3+}: Ferric iron
Fe_B: non-heme iron
FlavoHb: FlavoHemoglobin
Fur: Ferric uptake protein
GC: Gas Chromatography
GCyc: Guanylate Cyclase
GlyC: GlycoCardiolipin
GP (or PL): GlyceroPhospholipid
GSH: Reduced Glutathione
GSNO: S-nitrosoGlutathione
GSNOR: S-nitrosoGlutathione Reductase
GTR: Generalised Time-Reversible
HG: Head Group
HNO: Nitroxyl
H-NOX: Heme-Nitric OXide/oxygen binding domain
HONNOH: Hyponitrous acid
HONO: Nitrous acid
HOONO: Peroxynitrous acid
HPLC: High-Performance Liquid Chromatography
HPTLC-MALDI TOF MSI: High Performance Thin-Layer Chromatography - Matrix-Assisted Laser Desorption Ionization - Time Of Flight Mass Spectrometry Imaging
HR: Homologous Recombination
IM: Inner Membrane
INERIS: French National Institute for Industrial Environment and Risks
iNOS: inducible, macrophage Nitric Oxide Synthase
ISC: Iron-Sulfur Cluster system
K^+: Potassium ion
KDO: 3-deoxy-D-manno-Octulosonic acid
L(O)NO_2: Lipid epoxide
LB: Luria-Bertani medium
LO: Lipid alkoxyl radical
LOO^-: Lipid peroxyl radical
$LOONO^-$: Lipid peroxynitrite
LPA: LysoPhosphatidic Acid
LPE: LysoPhosphatidylEthanolamine
LPS: LipoPolySaccharide
MALDI: Matrix-Assisted Laser Desorption Ionization

MATS: Microbial Adhesion To Solvent
MCP: Methyl-accepting Chemotaxis Protein
MDO: Membrane-Derived Oligosaccharides
MIC: Minimum Inhibitory Concentration
ML: Maximum Likelihood
MLSA: Multi-Locus Sequence Analysis
MMR: MisMatch Repair
MRM: Multiple Reaction Monitoring
MS/MS: Tandem Mass spectrometry
MS: Mass Spectrometry
MSI: Mass Spectrometry Imaging
N_2O: Nitrous oxide
N_2O_3: Dinitrogen trioxide
N_2O_4: Dinitrogen tetroxide (dimer of NO_2)
N_2OR: Nitrous Oxide Reductase
NAD(P)H: Nicotinamide Adenine Dinucleotide
NAD^+: Oxidized form of Nicotinamide Adenine Dinucleotide (NAD)
NADH: Reduced form of Nicotinamide Adenine Dinucleotide (NAD)
$NADP^+$: Nicotinamide Adenine Dinucleotide Phosphate
NAP: Periplasmic Nitrate Reductase
NAR: Respiratory membrane-bound NitrAte Reductase
Nas: Nitrate Assimilation Enzymes
NCBI: National Center for Biotechnology Information
NDPK: Nucleoside DiPhosphate Kinase
NER: Nucleotide Excision Repair
NH_3: Ammonia
NH_4^+: Ammonium
NHEJ: Non-Homologous End-Joining
Ni:NOR: Nitrite: Nitric Oxide Reductase
NIR: NitrIte Reductase
nM: Nanomolar
NMR: Nuclear Magnetic Resonance Spectroscopy
nNOS: Neuronal Nitric Oxide Synthase
NO: Nitrogen monoxide
NO_2^-: Nitrite
NO_2: Nitrogen dioxide
NO_3^-: Nitrate
NOR: Nitric Oxide Reductase
NOS: Nitric Oxide Synthase
NO_x: Nitrogen Oxides
NR: Nitrate Reductase
$O_2NOCO_2^-$: Nitrocarbonate ion
OD: Optical Density
OM: Outer Membrane
$ONOO^-$: Peroxynitrite
$ONOOCO_2^-$: Nitrosoperoxycarbonate anion
OP: Oxidative Phosphorylation
PA: Phosphatidic Acid
PBAP: Primary Biological Aerosol Particles
PC: PhosphatidylCholine
Pcs: PhosphatidylCholine Synthase
PDE: PhosphoDiEsterase
PE: PhosphatidylEthanolamine
PEPC: PhosphoEnolPyruvate Carboxylase
PG: PhosphatidylGlycerol
PGP: PhosphatidylGlycerol Phosphate
pGpG: 5′-PhosphoGuanylyl-(3'-5')-Guanosine
$PI(3,4,5)P_3$: PhosphatidylInositol 3,4,5-trisPhosphate
$PI(4,5)P_2$: PhosphatidylInositol 4,5-biPhosphate
PI: PhosphatidylInositol
PIP: PhosphatidylInositol Phosphate
pK_a: Acidity constant
PLD: PhosphoLipase D
PM: Particulate Matter
Pmt: Phospholipid N-MeThylation
poly-UFA: polyUnsaturated Fatty Acid
PPDK: Pyruvate Phosphate DiKinase
ppGpp: Guanosine 3',5'-bisPyroPhosphate
ppm: Part Per Million
PS: PhosphatidylSerine
PSD: Post Source Decay
qRT-PCR: Quantitative RetroTranscription Polymerase Chain Reaction
R_f : Retention Factor
RNA: RiboNucleic Acid
RND: Resistance-Nodulation-cell Division
RNS: Reactive Nitrogen Species
ROS: Reactive Oxygen Species
rpm: Rotation Per Minute
RR: Response Regulator
rRNA: Ribosomal RNA
RS-NO: S-Nitrosothiols
$RS-NO_2$: S-Nitrothiol
RT: Reverse Transcription
S-DGD-5-PA: Sulfated Diglycosyl DiphytanylGlycerol Diether
SDS: Sodium Dodecyl Sulfate
SFA: Saturated Fatty Acid
SGP: Stationary Growth Phase
SM: SphingoMyelin
SSB: Single-Strand Break in DNA
S-TGD-1: Sulfo-TriGlycosyl-Diether
T3SS: Type 3 Secretion System
T6SS: Type 6 Secretion System
TAE: TetraAcetic Acid
TCA: TriCarboxylic Acid
TLC: Thin-Layer Chromatography
T_m: Transition temperature
TOF: Time Of Flight
***trans*-UFA:** *trans*-Unsaturated Fatty Acid
UFA: Unsaturated Fatty Acid
UGP: Unknown GlyceroPhospholipid
V: Viscosinamide
vol: Volume
WHO: World Health Organization
wt: WeighT

List of figures and tables

Figures

Tables

I. Introduction

Chapter 1 *Pseudomonas* genus

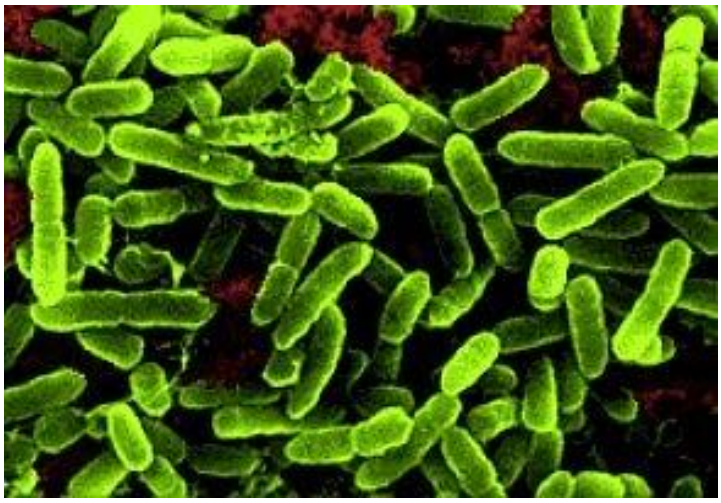

http://pseudomonasaeruginosa.blogspot.fr/

1. Properties of *Pseudomonas* genus

Bacteria of genus *Pseudomonas* belong to the phylum Proteobacteria, class *γ*-Proteobacteria, order *Pseudomonadales. Pseudomonas* are unicellular Gram-negative straight or lightly curved rods, with rounded extremity and average size of 2x0.5 µm (Palleroni, 1984). These bacteria are motile with one or several polar flagella, able to growth in minimum medium and metabolize several hydrocarbon substrata as energy and carbon source. These aerobic bacteria have a strictly respiratory type of metabolism with oxygen as the terminal electron acceptor. However, nitrate can be used by several *Pseudomonas* strains as an alternate electron acceptor, allowing an anaerobic growth. *Pseudomonas* possess oxidase and catalase activity (Brenner *et al.*, 2005). The features of these organisms are the degradation of a large number of organic compounds (Barathi & Vasudevan, 2001; Foght & Westlake, 1988; Leahy & Colwell, 1990), the interactions with plants (Mercado-Blanco & Bakker, 2007; Nomura *et al.*, 2005; Tao *et al.*, 2003) and the associations in the rhizosphere, which are advantageous for agriculture (Lugtenberg *et al.*, 2001; Rainey, 1999). In addition, *Pseudomonas* include one of the most dangerous opportunistic pathogens among all bacteria *P. aeruginosa* (Driscoll *et al.*, 2007; Srour *et al.*, 2014). *Pseudomonas* comprise taxa of metabolically versatile organisms capable of living under diverse environmental conditions. Consequently, the members of this group are able to growth in diverse environments (Ringen & Drake, 1952) as illustrated in **Figure 1**, including water (Mena & Gerba, 2009), soil (Couillerot *et al.*, 2009; Kiely *et al.*, 2006), air (Duclairoir Poc *et al.*, 2014; Morris *et al.*, 2007), food, and hospital environment (Shooter *et al.*, 1969, 1971). This worldwide distribution seems to be due to a high physiological and genetic adaptability (Spiers *et al.*, 2000), being the presence of numerous genomic islands in the genus, a key adaptability traits of individual strains to such ubiquitous environments (Peix *et al.*, 2009). Thus, the genomes of several species like *P. aeruginosa*, *P. fluorescens*, *P. syringae*, *P. putida* or *P. stutzeri* include between 3.7 and 7.1x10^6 base pairs (bps) (Spiers *et al.*, 2000).

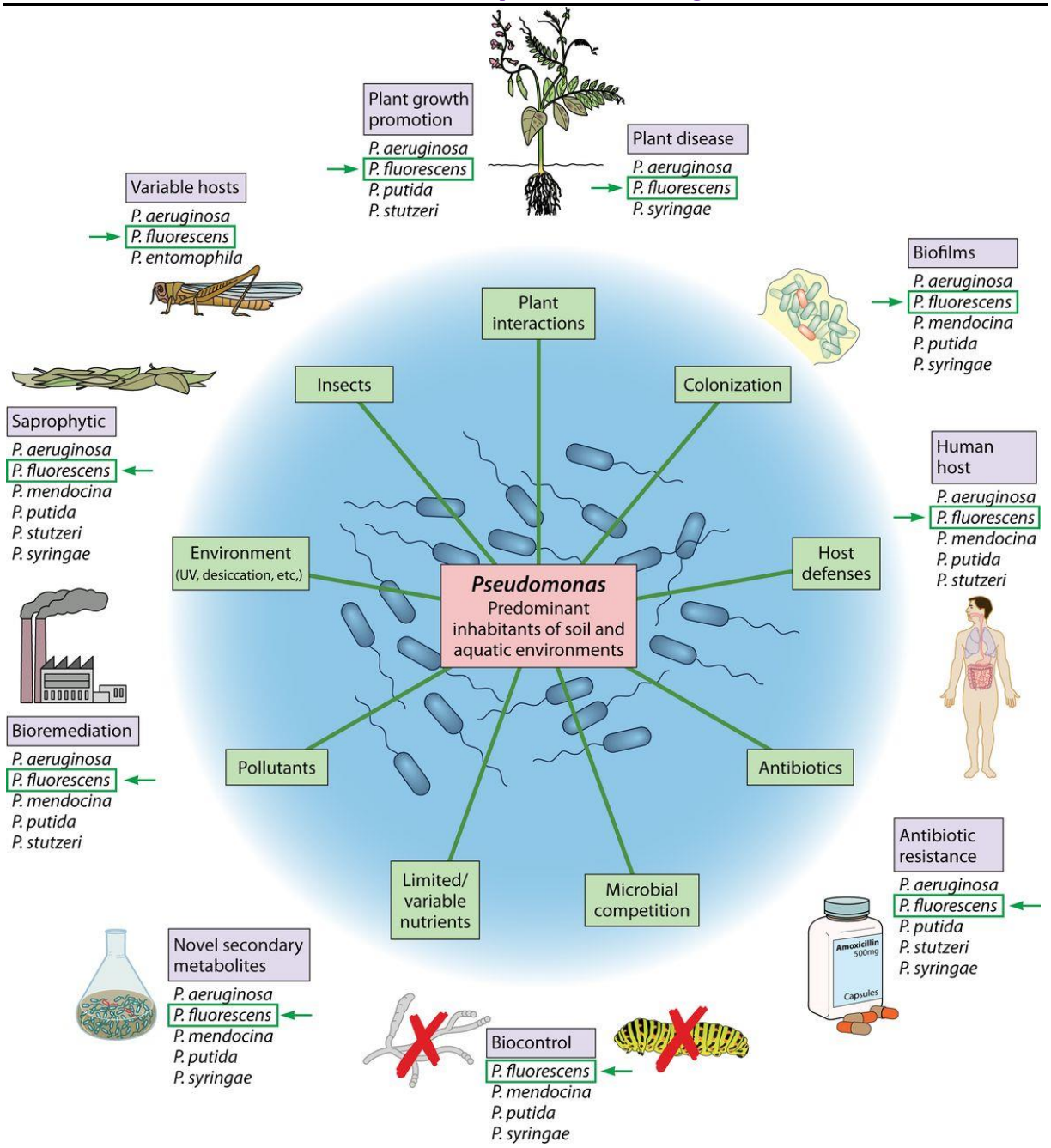

Figure 1. Functional range and environmental niches of the *Pseudomonas* genus, highlighting the broad distribution of the *P. fluorescens* species
Adapted from Scales et al., 2014.

2. Taxonomic diversity

The name *Pseudomonas* originates from the work of Migula, 1894 describing this genus as "Cells with polar organs of motility strictly". Defined in this way, the genus *Pseudomonas* was very heterogeneous and suffers several taxonomic reclassifications. In 1966 Stainer established the *Pseudomonas* classification based on the capacity of strains to metabolize the different energy sources. This fundamental work described 267 *Pseudomonas* strains with their biochemical, physiological and phenotypic properties (Stanier *et al.*, 1966). With the emergence of molecular biology, the *Pseudomonas* genus was reorganized. The study of genomic sequence

homology by DNA-DNA (Palleroni *et al.*, 1972; Palleroni & Doudoroff, 1971) or DNA-RNA (Palleroni *et al.*, 1973) hybridizations, as well as the phylogenetic analysis based on 16S ribosomal RNA (rRNA) sequence (Anzai *et al.*, 2000) have led to the division of *Pseudomonas* genus on five distinct 'rRNA homology' groups. This division explains an important heterogeneity of the *Pseudomonas* genus (Vos *et al.*, 1985, 1989; Vos & Ley, 1983). The species belonging to the 'group I' conserved the genus name and termed the *Pseudomonas sensu stricto*; the other species (‘group II-V’) *Pseudomonas sensu lato* have been reclassified and generically renamed according to their phylogenetic relationships, include nowadays the related genus, including *Ralstonia*, *Comamonas*, *Agrobacterium*, *Brevundimonas*, or *Burkholderia* (Anzai *et al.*, 2000). The genus *Pseudomonas sensu stricto* was divided on two major lineages (**Figure 2**) represented by typical species, namely *Pseudomonas aeruginosa* and *Pseudomonas fluorescens* (Bodilis *et al.*, 2012; Mulet *et al.*, 2010). The *P. aeruginosa* lineage is the more homogenous and consists of the *P. aeruginosa* species, but also of more distant species, like *P. oleovorans* or *P. stutzeri*. Basing on study of the 16S rRNA gene and targeting one or two hypervariable regions, Bodilis and coworkers divided *P. fluorescens* lineage on two r-clusters (“r”-clusters, the clusters based on “r”RNA gene data): the “*putida*” and the “*fluorescens*” (Bodilis *et al.*, 2012). The *putida* r-cluster corresponds to the *P. putida* group; the *fluorescens* r-cluster contains the *P. fluorescens*, *P. syringae* and *P. lutea* groups, as shown in **Figure 2**. The *fluorescens* r-cluster is the largest in terms of species number (about 60% of the *Pseudomonas* species described), and the most heterogeneous *Pseudomonas* group in terms of phenotypes and genotypes (Bodilis *et al.*, 2012).

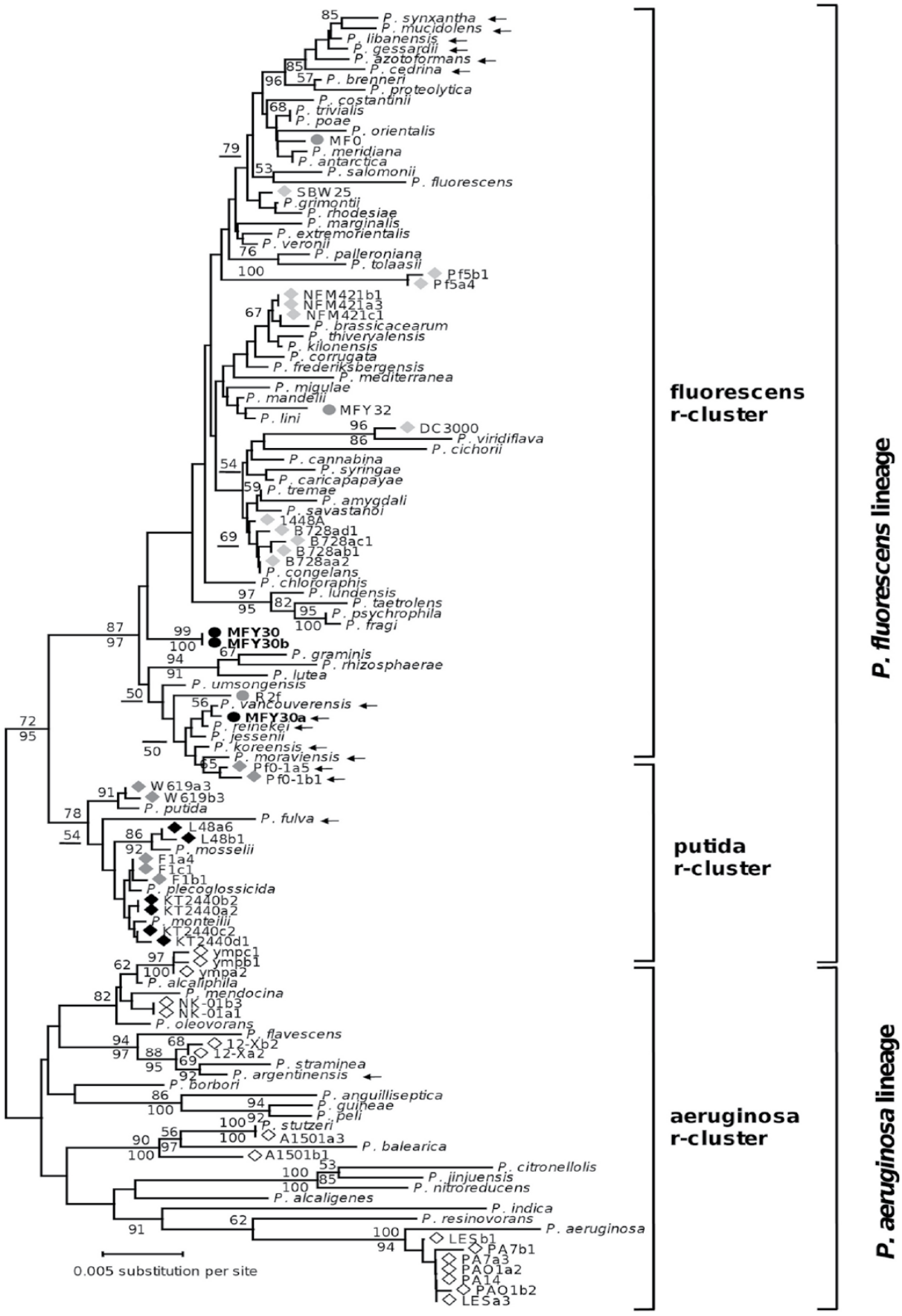

Figure 2. Phylogenetic relationships of *Pseudomonas* genus bacteria among 16S ribosomal RNA genes

Adapted form Bodilis et al., 2012.

3. *Pseudomonas fluorescens* strains

3.1. General information

The name *Pseudomonas fluorescens* was chosen because of the production of complex fluorescent peptidic siderophores called pyoverdines (**Figure 3**), which are very efficient iron scavengers in bacteria (Cornelis & Matthijs, 2002). This species is described as psychrotrophic germ with optimum growth temperature between 25°C and 30°C, able to growth at 4°C, but unable to growth at 41°C, as thermophilic bacteria. Several strains of *P. fluorescens* are sequenced (58 sequenced genomes, 5 genomes annotated without gap, in April 2015, according to NCBI, http://www.ncbi.nlm.nih.gov/). A whole variety of phenotypes and genotypes allows the classification of *P. fluorescens* as heterogeneous bacteria, with several biovars and sub-biovars. The percentage of DNA/DNA hybridization between strains of the same biovar is frequently less than 50%. Thus, the genotype of this species is difficult to define. The taxonomy of *Pseudomonas* is currently being renewed (Palleroni, 2010), as evidenced by the reclassification of CHAO or Pf-5 strains to a novel species named *P. protegens* (Ramette *et al.*, 2011). Here, we defined *P. fluorescens* as bacteria, belonging to the *fluorescens* r-cluster and previously published at the name *P. fluorescens*.

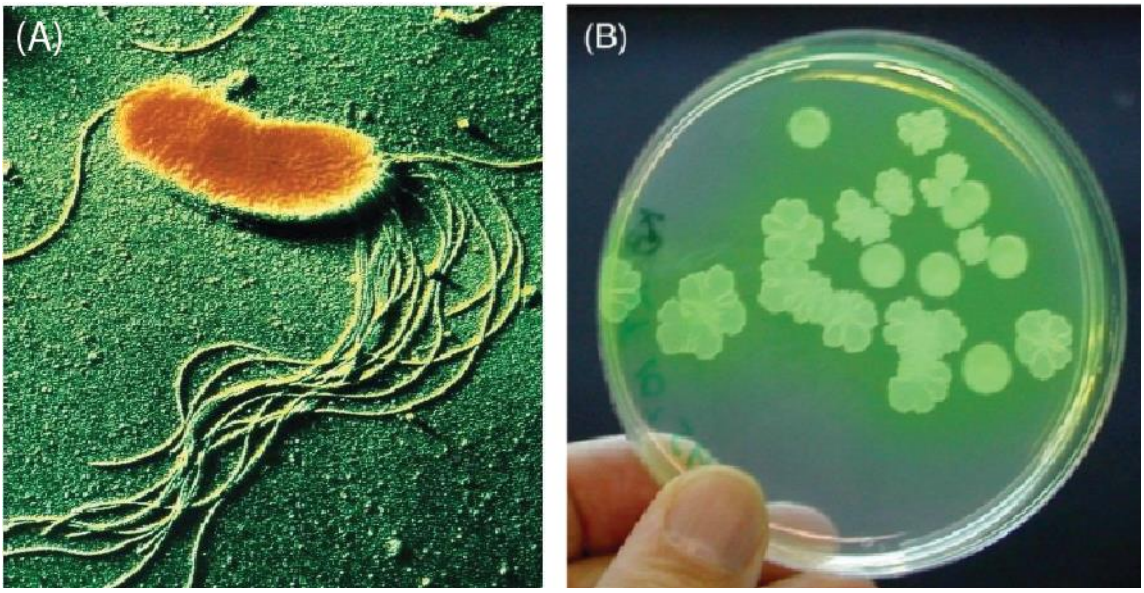

Figure 3. Microscopic and macroscopic aspect of *P. fluorescens*
A. Scanning electron micrograph of *P. fluorescens* (www.scienceclarified.com). **B.** Macroscopic aspect of *P. fluorescens* SBW25, pyoverdine production (Spiers et al., 2013).

3.2. Distribution and adaptive capacity of *Pseudomonas fluorescens*

The members of *P. fluorescens* group are highly distributed in all major environments, including water, soil and air as illustrated in **Figure 1** (Bodilis *et al.*, 2004; Duclairoir Poc *et al.*, 2014). These species contribute greatly to the turnover of organic matter and, while present

in soil, are abundant on the surfaces of plant roots and leave. This applies also the role of *P. fluorescens* as rhizosphere biocontrol agents (Walsh *et al.*, 2001). Biocontrol strains have noticeably been observed at the root surface (*i.e.* the rhizoplane), often forming microcolonies or discontinued biofilms in the grooves between epidermal cells (Couillerot *et al.*, 2009). Some of the plant-colonizing strains, such as SBW25, positively affect plant health and nutrition (Silby *et al.*, 2009).

The ability to growth at refrigerated temperatures opens to *P. fluorescens* the possibility to colonize the 'cold environments'. Thus, *P. fluorescens* was isolated from Antarctic glacier ice melt (Attard *et al.*, 2012) or from clouds and rain water (Ahern *et al.*, 2007), where these bacteria can catalyze freezing of supercooled water at a temperature as warm as -2°C (Attard *et al.*, 2012; Joly *et al.*, 2013). The low temperature adaptation makes *P. fluorescens* contamination a particular problem for the food-processing (Dogan & Boor, 2003; Jonghe *et al.*, 2011). Indeed, at low temperature *P. fluorescens* is able to product degradation enzymes, including proteases, lipases and gelatinases, modifying organoleptic food quality (Russell, 2002). In addition, *P. fluorescens* can cause blood infusion-related infections and outbreaks, contaminating the blood products or the equipment associated with intravenous infusions during storage (Gibaud *et al.*, 1984; Khabbaz *et al.*, 1984; Scales *et al.*, 2014).

Being psychrotrophic bacteria, several *P. fluorescens* strains still grow at increasing temperature (at least 37°C) (Picot *et al.*, 2004). Bodilis and coworkers proposed to split *P. fluorescens* into two groups: (1) "true psychrotrophs" able to multiply at temperatures from 4°C to at least 30°C (but no grow at 37°C); and (2) "thermo-tolerant psychrotrophs" able to grow at temperatures from 4°C to at least 37°C (but no grow at 42°C). Group (1) contains only strains from soil and water. Group (2) is composed of clinical isolates and also certain strains with soil origins (Bodilis *et al.*, 2004). This thermotolerance associated with virulence factors expression and biofilm formation (**Figure 1**) allows *P. fluorescens* to tame eukaryotic hosts. While far less virulent than *P. aeruginosa*, *P. fluorescens* can cause acute infections (opportunistic) in humans and was reported in clinical samples from the mouth, stomach and lungs of patients with compromised immune status (Chapalain *et al.*, 2008; Scales *et al.*, 2014), as shown in **Figure 1**. Species of *P. fluorescens* are associated to agents of pulmonary diseases (Bahrani-Mougeot *et al.*, 2007; Choi *et al.*, 2011; Dickson *et al.*, 2014), urinary infections (Osawa *et al.*, 2002), eye infections (Durbán *et al.*, 1996), and bloodstream infections (Benito *et al.*, 2012). Several strains are able to link to eukaryotic cells, such as intestinal cells Caco2/TC7, to modify their permeability, inducting cytotoxic and pro-inflammatory responses (Madi *et al.*, 2010a, b). Indeed, *P. fluorescens* possesses a number of functional traits, which provide to this bacterium the capacity to grow in mammalian hosts. These traits include production of bioactive

secondary metabolites (Gross & Loper, 2009; Mavrodi *et al.*, 2006; Ramette *et al.*, 2003; Rossignol *et al.*, 2008; Weller *et al.*, 2007), synthesis of siderophores (Cornelis & Matthijs, 2002), type III secretion system (Marchi *et al.*, 2013; Mavrodi *et al.*, 2011; Rezzonico *et al.*, 2005; Sperandio *et al.*, 2012), ability to form biofilms (Barahona *et al.*, 2010; Baum *et al.*, 2009), and plasticity of some strains to adapt to grow at higher temperature.

3.3. Biofilm formation as *P. fluorescens* adaptation mode

Bacteria respond to fluctuating environmental signals to coordinate adaptive changes in metabolic pathways and physiological outputs. Integration of environmental factors affords bacteria the ability to make important decisions regarding how to respond to the constantly changing environments. One of the possibilities is the change of the lifestyle. Bacteria can live in a free movement (planktonic) existence or commit to a surface attached lifestyle (biofilm). There are three major types of bacterial motility (**Figure 4**), depending on medium viscosity, namely, swimming in aqueous environments, twitching on solid surfaces, and swarming on semisolid, viscous media, such as those containing 0.4 to 0.7% (wt/vol) agar (Overhage *et al.*, 2008).

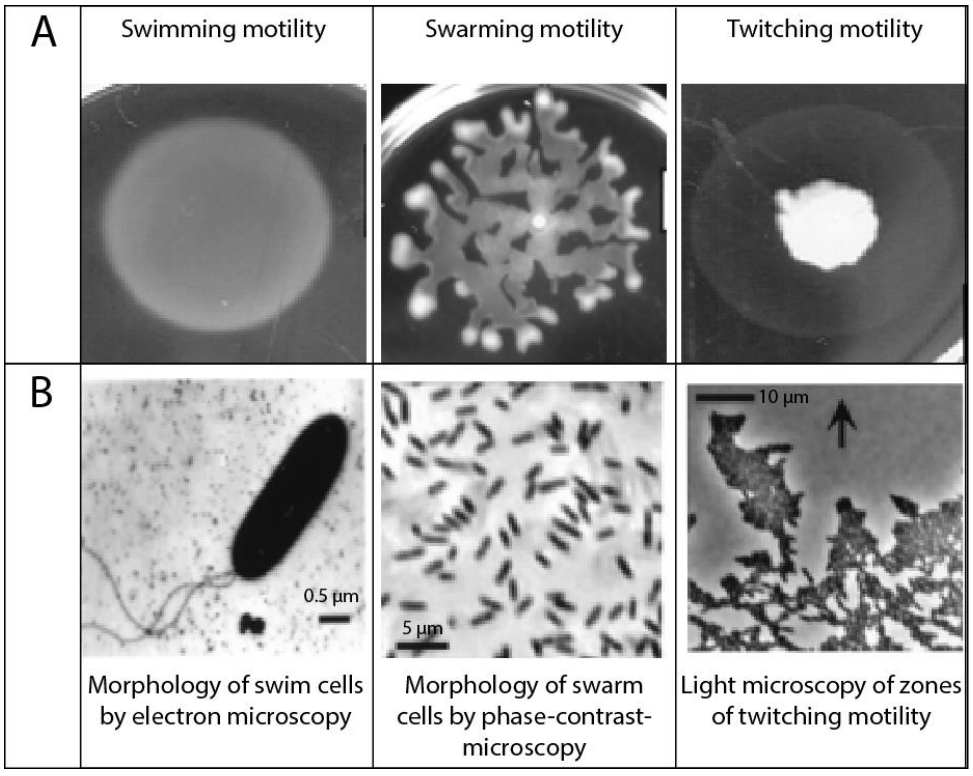

Figure 4. Swimming, swarming, and twitching motilities of *P. aeruginosa* PAO1
A. Macroscopic motility assays. Swimming motility on a semi-liquid agar plate (*Left*); Swarming motility on a semi-solid agar plate (*Middle*); Macroscopic assay of twitching motility (*Right*). **B. Microscopic aspect of *Pseudomonas* motility**. Modified according M. Harunur and A. Kornberg, 2000.

Swimming and swarming motility needs the synthesis of flagella. The swimming is brought about by individual cells independently perceiving chemical signals that trigger adaptive chemotactic responses. The swarming motility is characterized by a multicellular movement of bacteria that migrate above solid substrates in groups of tightly bound cells (Calvio *et al.*, 2005). Swarming motility requires both the functional flagella and the production of surface-wetting agent biosurfactant (Caiazza *et al.*, 2007; Kearns, 2010). Production of the biosurfactants serves

as an essential aid to swarming motility by acting as a wetting agent to overcome the surface tension of water and facilitates movement across the most surface (Caiazza et al., 2005). The nature of *Pseudomonas* biosurfactants was described as strain-dependent (Duclairoir-Poc, 2011). Unlike *P. aeruginosa*, which products biosurfactant rhamnolipid, *P. fluorescens* secretes cyclic lipopeptides (CLP), including viscosine and viscosinamide (Duclairoir-Poc, 2011; Nielsen *et al.*, 1999). Twitching motility is a flagella-independent form of bacterial translocation over moist surfaces. It occurs by the extension, tethering, and then retraction of polar type IV pili (Mattick, 2002).

When coming in contact with a surface, whether in natural, industrial, or clinical settings, bacteria must evaluate whether the surface and the environment are favorable for attachment and biofilm formation (Wei & Ma, 2013).

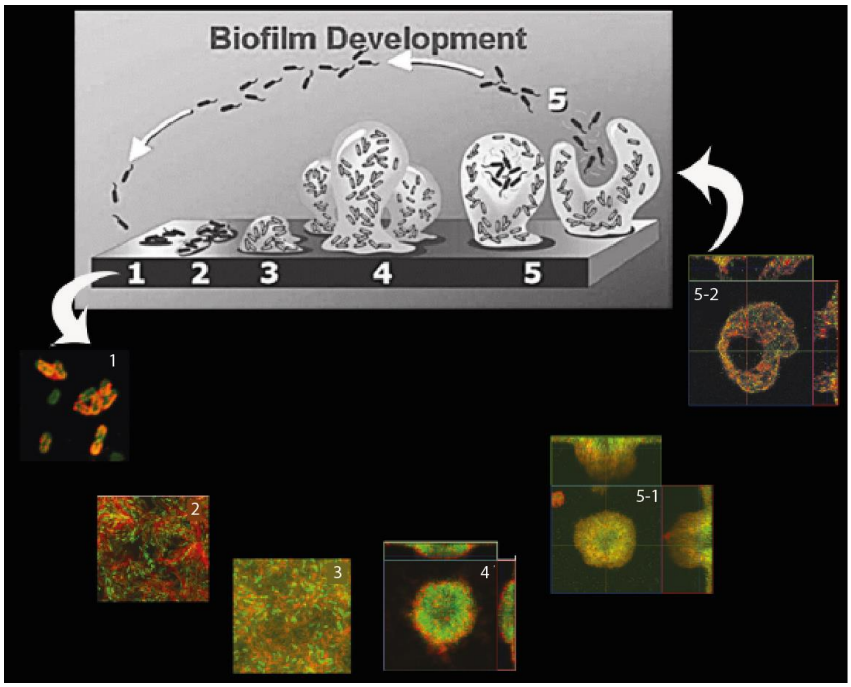

Figure 5. Pathway of biofilm development in *P. aeruginosa*
A. Scheme of biofilm development. 1. Initial attachment; 2. Irreversible attachment; 3. Microcolony formation; 4. Biofilm maturation; 5. Biofilm dispersion. **B.** Confocal microscopy of biofilm development in *P. aeruginosa*. Extra-cellular polysaccharide matrix (red fluorescence) enmeshes bacterial cells (green fluorescence) during biofilm development.
Adapted from following sources: Ma et al., 2009; Wei and Ma, 2013.

The biofilm is defined as a structured community of bacterial cells enclosed in a self-produced polymeric matrix and adherent to inert or living surfaces (Costerton *et al.*, 1999; O'Toole & Ha, 2015). The formation of biofilms occurs as a series of regulated steps displayed in **Figure 5** (Ma *et al.*, 2009; O'Toole *et al.*, 2000). Bacteria swim using flagellar-mediated motility toward a surface and initiate a reversible attachment (**Figure 5.1)** (O'Toole & Kolter, 1998). A subpopulation of transiently attached bacteria becomes irreversibly attached to the surface to form a monolayer, followed by the formation of small microcolonies (**Figure 5.2**) (Hinsa *et al.*, 2003). The microcolonies grow into a mature biofilm with a developed architecture (**Figure 5.3** and **4)**. The mature biofilm is typically characterized by macrocolonies, located in extracellular matrix and separated by fluid-filled channels as shown in **Figure 6**. These channels transport nutrients and oxygen to the bacteria and aid in waste removal (Davey & O'Toole, 2000; Hinsa

et al., 2003). The biofilm cycle is completed by the biofilm dispersion, when bacterial cells are shed from the biofilm into the medium (**Figure 5.5)**, to found best environmental conditions (Chua *et al.*, 2014; O'Toole & Kolter, 1998).

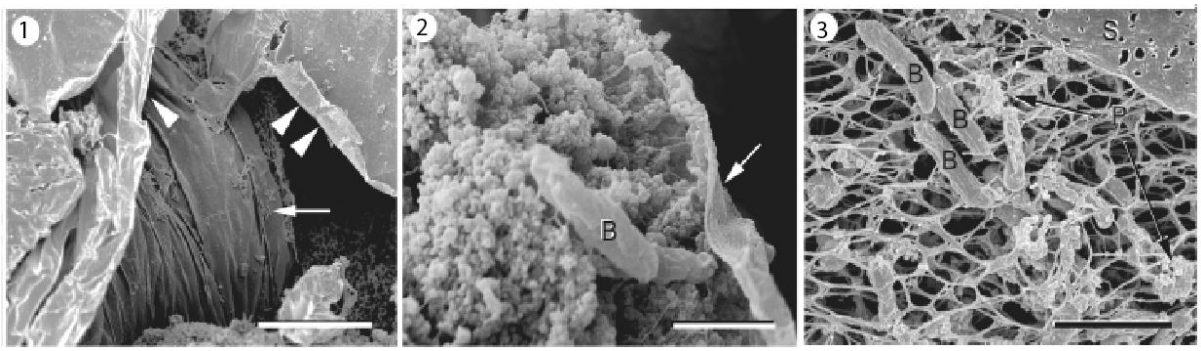

Figure 6. Scanning electron micrographs of *P. fluorescens* biofilms
The monocultures of 14-day biofilms form *P. fluorescens* EvS4-B1 were shown. **1.** Flat sheets of material (arrowheads), with some of the sheets wrapped around other structures (arrow). Bar = 1 µM. **2.** The inside core of the "wrapped" structures, consisting of bacteria (B) embedded in an extracellular matrix and thin sheet of material (arrow). Bar = 1 µM. **3.** A sheet of material (S), consisting of extracellular matrix, covering and attaching to the fiber network (potentially fluid-filled channels) and including associated bacteria (B) and particulate matter (P). Bar = 2µM.
Adapted from Baum et al., 2009; Scales et al., 2014.

The biofilm formation involves an array of cellular factors and highly regulated mechanisms, specific for each bacterial species (Monds *et al.*, 2007). Several extracellular components such as exopolysaccharides (EPS), proteins (*e.g.* adhesins, amyloid familial amyloidotic polyneuropathy (Fap) fibrils), and extracellular DNA (eDNA) are involved in adhesion and biofilm formation by the pseudomonads (Dueholm *et al.*, 2013). However, a unifying theme across bacterial species is the synthesis of the cellular signaling molecule *bis*-(3'-5')-cyclic dimeric guanosine monophosphate (c-di-GMP), which regulates both biofilm formation and motility (D'Argenio & Miller, 2004; Boyd *et al.*, 2012; Schirmer & Jenal, 2009). The c-di-GMP is a soluble molecule, which functions as a second messenger in bacteria. In general, c-di-GMP stimulates the biosynthesis of adhesins and EPS matrix in biofilms and inhibits various forms of motility. It controls switching between the motile planktonic and sessile biofilm-associated 'lifestyles' in bacteria (Hengge, 2009). This molecule is synthesized by diguanylate cyclases (DGCs) (Paul *et al.*, 2004), and is broken down into 5′-phosphoguanylyl-(3'-5')-guanosine (pGpG) by specific phosphodiesterases (PDEs) as presented in **Figure 7**. The active DGC is a dimer of two subunits with GGDEF domains. The PDE harbors EAL or HD-GYR domains (Kulesekara *et al.*, 2006; Stelitano *et al.*, 2013). While the accumulation of c-di-GMP in bacterial cells promotes the biofilm formation, favoring EPS production and suppressing motility, reduction of c-di-GMP level favors planktonic growth and/or dispersion of established biofilm (Christen *et al.*, 2005; Newell *et al.*, 2011a).

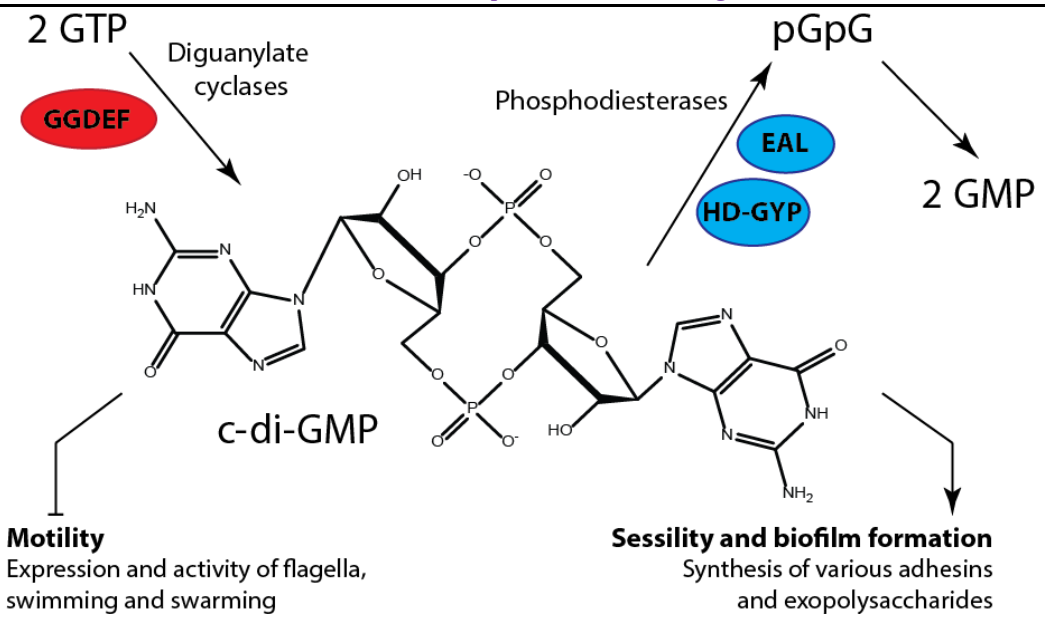

Figure 7. Structure and physiological functions of c-di-GMP
In bacteria, *bis*-(3'-5')-cyclic dimeric guanosine monophosphate (c-di-GMP) is controlled by diguanylate cyclases (DGC) with GGDEF domains (red) and specific phosphodiesterases that carry EAL or HD-GYP domains (blue). The high c-di-GMP level reduces motility and stimulates various biofilm-associated functions, such as the formation of fimbriae and other adhesins and various matrix exopolysaccharides. pGpG, 5'-phosphoguanylyl-(3'-5')- guanosine. pGpG is subsequently split into two GMP molecules.
Adapted from Hengge, 2009.

Biofilm research has utilized *P. fluorescens* as a model, because of its high adaptation capacity and typical growth on surface in nature (Newell *et al.*, 2011b). O'Toole and coworkers identified a mechanism of regulation of biofilm formation by phosphate in *P. fluorescens* **Figure 8**. This mechanism is based, in majority, on two proteins: a large adhesive protein, LapA, required for the attachment, and a periplasmic cysteine protease LapG that cleaves LapA from the cell surface, as shown in litterature (Boyd *et al.*, 2014; O'Toole & Ha, 2015). Under high phosphate level, the c-di-GMP accumulates in the cell. LapG activity is regulated by the inner membrane c-di-GMP effector protein LapD (O'Toole & Ha, 2015). LapD binds c-di-GMP and sequesters LapG at the inner membrane, promoting the maintenance of LapA on the cell surface. Under these conditions, LapA remains at the cell surface, forms irreversible attachments to the substratum, promoting biofilm formation (Newell *et al.*, 2011a).

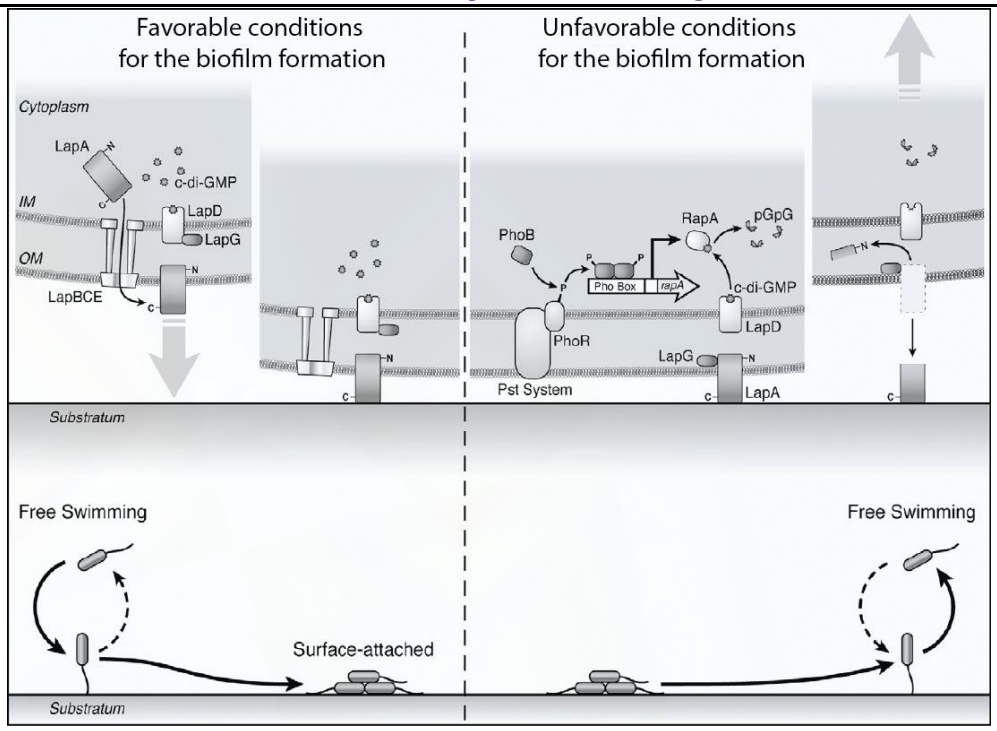

Figure 8. A proposed model for regulation of *P. fluorescens* biofilm formation
At high concentrations of phosphate, c-di-GMP accumulates in the cell. LapD binds c-di-GMP, sequesters LapG at the inner membrane, promoting the maintenance of LapA on the cell surface. In these conditions, cells attach to the surface and form the biofilm. Conversely, low phosphate concentrations are sensed by PhoR/Pst system complex, the PhoR kinase phosphorylates PhoB, which activates the transcription of *rapA*. The RapA degrades c-di-GMP to pGpG. This leads to dissociation of c-di-GMP from LapD, and the cleavage of the LapA in the periplasm, promoting the detachment of attached to substratum bacteria, and/or inhibition of future surface attachment of planktonic cells.
According Newell et al., 2011a.

Systematic analysis of *P. fluorescens* genomes revealed, that these species harbors over 20 genes, coding for putative DGCs, with 4 confirmed to be involved in the regulation of surface attachment and/or biofilm formation (Newell *et al.*, 2011b). These genes include *wspR* gene. WspR is the response regulator (RR) of the Wsp chemosensory system, which is involved in production of c-di-GMP, as its effector. The Wsp system includes the DGC WspR, a predicted membrane-bound methyl-accepting chemotaxis protein (MCP)-like receptor (WspA), two CheW-like scaffolding proteins (WspB and WspD), histidine sensor kinase (WspE), and two methyltransferases WspC and WspF (Hickman *et al.*, 2005). In addition to WspR, three other DGCs were found to promote biofilm formation in *P. fluorescens*. GcbA mainly controls swimming motility, GcbB preferentially affects localization of the LapA adhesin, and GcbC affects both LapA and motility (Newell *et al.*, 2011b).

Although the clear establishing of positive correlation between biofilm formation and c-di-GMP level, the regulation of c-di-GMP, and as result, the switch between planktonic and biofilm growth, is increasingly complex (Petrova *et al.*, 2014). Several genes (*flgZ, sadB, fgtA, flhH* or *fap*) and regulation pathways (AdnA, GacA/GacS, AlgU or FuBA) were described as required for *P. fluorescens* adhesion and motility (Casaz *et al.*, 2001; Dueholm *et al.*, 2013;

Martínez-Granero *et al.*, 2012; Mastropaolo *et al.*, 2012; Nian *et al.*, 2007; Robleto *et al.*, 2003). These systems do not precise here, and themselves can be a subject of another work.

Biofilm is not only a simple bacterial lifestyle, but also a good adaptation mode to changing environmental conditions. The highly permeable water channels interspersed throughout the biofilm allow bacterial nutrient availability and metabolic cooperativity (Davey & O'Toole, 2000); the extracellular matrix protects bacteria against environmental stressors (O'Toole & Ha, 2015), including pollution (Baumgarten *et al.*, 2012; Baum *et al.*, 2009) or temperature changes (White-Ziegler *et al.*, 2008), allowing bacterial survival in inconvenient environments. Biofilm formation is one of the strategies to colonize eukaryotic host. As a result, infections caused by bacterial biofilms are persistent and very difficult to eradicate (Drenkard, 2003; Mah *et al.*, 2003).

3.4. Envelope role in adaptation of *Pseudomonas fluorescens*

3.4.1. Introduction

To be faced with an unpredictable, dilute and often hostile environment, bacteria have evolved a sophisticated and complex cell envelope that protects them playing a role of a first selective barrier between the cell and its environment (Russell *et al.*, 1995; Silhavy *et al.*, 2010). The barrier functions of bacterial envelope are known to be depend critically on the physical state of lipid bilayer, including its structure and fluidity (Mansilla *et al.*, 2004). Microbial envelopes are responsible for a plethora of physiological processes, such as regulating the substances traffic in and out of the cells (Uratani & Aiyama, 1986). It stabilizes protein structures for a correct functioning of membrane embedded enzymes and provides a matrix for many biological reactions (Bernal *et al.*, 2007; Pogozheva *et al.*, 2014). The cell wall plays also a role of the first sensor in activating a stress response (Los & Murata, 2004) and participates in bacteria/host interactions (van der Meer-Janssen *et al.*, 2010; Vromman & Subtil, 2014; Wenk, 2006). Therefore, the precise regulation of membrane structure and fluidity, known as homeoviscous adaptation, in the face of a constantly changing environment is an important challenge for all bacteria (Baysse & O'Gara, 2007).

3.4.2. Properties of *P. fluorescens* membrane

Pseudomonas envelope, as well as envelope of all Gram-negative bacteria, is composed of two membranous structures (**Figure 9**) (Bos *et al.*, 2007; Glauert & Thornley, 1969). The inner one (IM) is composed of a glycerophospholipids (GPs) bilayer (Chatterjee & Chaudhuri, 2012). The outer membrane (OM) is an asymmetrical bilayer, consisting of GPs and lipopolysaccharides (LPS) in the inner and outer leaflet respectively (Freulet-Marrière *et al.*,

2000). The GPs bilayer of OM immerges proteins, including porins, and receptors (Bos *et al.*, 2007). The outer leaflet is composed primarily of LPS projecting outside and the inner leaflet containing GPs.

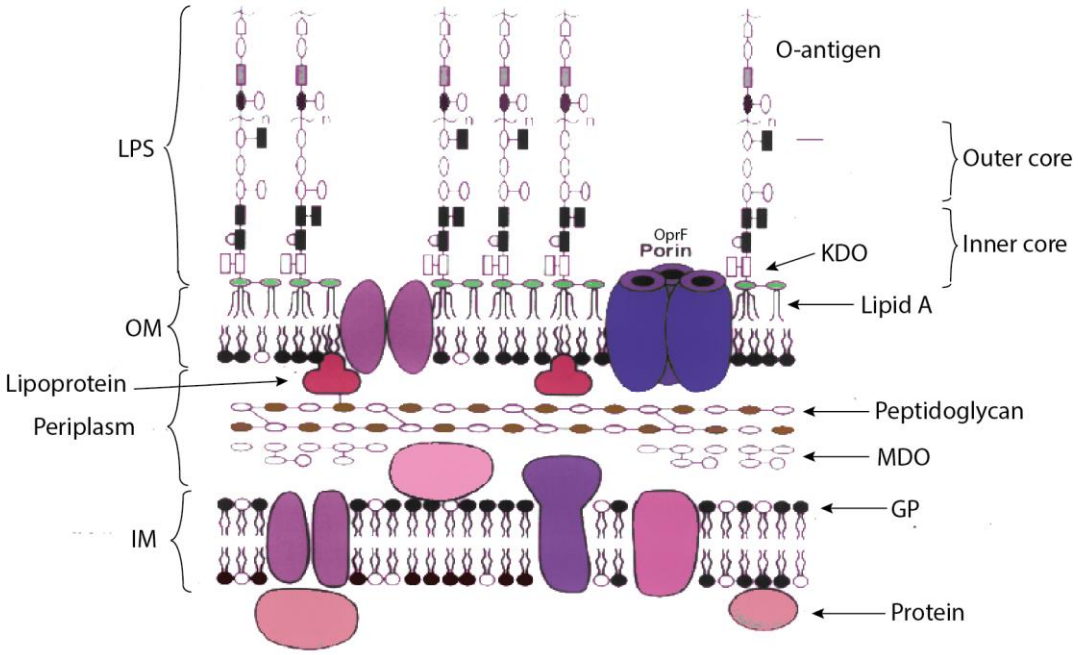

Figure 9. *Pseudomonas* cell envelope
Inner membrane (IM) is a typical glycerophospholipid (GP) bilayer, playing a role of permeability barrier of the cell. The outer membrane (OM) is composed of an inner monolayer of GP and an outer monolayer of the Lipid A component of lipopolysaccharide (LPS). Lipid A is a fatty acid substituted phosphorylated disaccharide, connected via the unusual sugar 3-deoxy-D-manno-octulosonic acid (KDO) to a polysaccharide to build up the inner core, outer core and the O-antigen repeat. The prismatic space contains the amino acid-sugar cross-linked peptidoglycan layer, which gives a structural rigidity to the cell envelope. Many proteins and membrane-derived oligosaccharides (MDO) can also be found in periplasm.
Adapted from W. Dowhan and M. Bogdanov, 2002.

The LPS consists of three different sectors: (i) lipid-A (a fatty acid substituted phosphorylated disaccharide), (ii) the core polysaccharide comprising the inner and the outer cores, and (iii) the O-specific polysaccharide chains, a heterogeneous polymer of branched oligosaccharide units, as shown in **Figure 9** (Chatterjee & Chaudhuri, 2012; Freulet-Marrière *et al.*, 2000). The lipid portion of LPS serves as the lipid anchor and is commonly composed of fatty acids (FAs), sugars, and phosphate groups. The *P. fluorescens* LPS have been described as able to associate to the major outer membrane porin OprF (Freulet-Marrière *et al.*, 2000) and essential for the outer membrane functions, particularly during host – pathogen interactions (Picot *et al.*, 2003). The *P. fluorescens* LPS is an infamous molecule because they are responsible for the endotoxin shock associated with the septicemia (Raetz & Whitfield, 2002), apoptosis and a concomitant and limited necrosis (Picot *et al.*, 2003).

Peptidoglycan layer is made up of repeating units of the disaccharide N-acetyl glucosamine and N-acetyl muramic acid, which are cross-linked by pentapeptide side chains (Heilmann, 1972;

Mirelman & Nuchamowitz, 1979; Vollmer *et al.*, 2008). Because of its rigidity, it determines the cell shape. Agents, such as enzymes or antibiotics, that damage the peptidoglycan cause cell lysis owing to the turgor pressure of the cytoplasm (Silhavy *et al.*, 2010).

P. fluorescens possesses a relatively simple GP composition with phosphatidylethanolamine (PE, 60-80%), phosphatidylglycerol (PG; 10-25%), phosphatidylcholine (PC; not defined) and cardiolipin (CL; 8-25%) being the four major GPs found in the cell envelope (Cullen *et al.*, 1971; Gill, 1975). Their relative ratio varies according experimental conditions and bacterial strains. However, these data are based on the experiments, performed in the 1970s using the thin-layer chromatography (TLC) (Cullen *et al.*, 1971; Gill, 1975). The FAs composition of *P. fluorescens* has been well described (Fouchard *et al.*, 2005). Like all members of *Pseudomonas* genus, *P. fluorescens* contains 16-18 carbons in FA chains with or without unsaturation (only one unsaturation is found). In the absence of well systematized review about *Pseudomonas* GP synthesis and homeostasis we decided to summarize all known today information about this topic in the review format.

3.4.3. Glycerophospholipid synthesis and functions in *Pseudomonas*

Tatiana Kondakova; François D'Heygère; Marc J. Feuilloley; Nicole Orange; Hermann J. Heipieper; Cécile Duclairoir Poc

Chemistry and Physics of Lipids, 190 (2015), 27–42; doi:10.1016/j.chemphyslip.2015.06.006

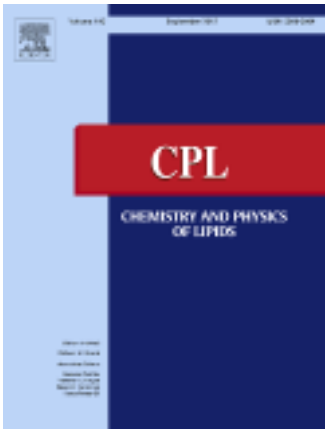

Chemistry and Physics of Lipids 190 (2015) 27–42

Contents lists available at ScienceDirect

Chemistry and Physics of Lipids

journal homepage: www.elsevier.com/locate/chemphyslip

Glycerophospholipid synthesis and functions in *Pseudomonas*

Tatiana Kondakova[a], François D'Heygère[b], Marc J. Feuilloley[a], Nicole Orange[a], Hermann J. Heipieper[c], Cécile Duclairoir Poc[a,*]

[a] Normandie University of Rouen, Laboratory of Microbiology Signals and Microenvironment (LMSM), EA 4312, 55 rue St. Germain, 27000 Evreux, France
[b] Centre de Biophysique Moléculaire, CNRS, UPR4301, rue Charles Sadron, 45071 Orléans, France
[c] Department of Environmental Biotechnology, UFZ Helmholtz Centre for Environmental Research, Permoserstr. 15, 04318 Leipzig, Germany

ARTICLE INFO

Article history:
Received 27 March 2015
Received in revised form 29 June 2015
Accepted 30 June 2015
Available online 3 July 2015

Keywords:
Biosynthesis
Lipidomics
Membranes
Phospholipids
Phosphatidylcholine
Lineage
Host
Interactions

ABSTRACT

The genus *Pseudomonas* is one of the most heterogeneous groups of eubacteria, presents in all major natural environments and in wide range of associations with plants and animals. The wide distribution of these bacteria is due to the use of specific mechanisms to adapt to environmental modifications. Generally, bacterial adaptation is only considered under the aspect of genes and protein expression, but lipids also play a pivotal role in bacterial functioning and homeostasis. This review resumes the mechanisms and regulations of pseudomonal glycerophospholipid synthesis, and the roles of glycerophospholipids in bacterial metabolism and homeostasis. Recently discovered specific pathways of *P. aeruginosa* lipid synthesis indicate the lineage dependent mechanisms of fatty acids homeostasis. *Pseudomonas* glycerophospholipids ensure structure functions and play important roles in bacterial adaptation to environmental modifications. The lipidome of *Pseudomonas* contains a typical eukaryotic glycerophospholipid – phosphatidylcholine –, which is involved in bacteria–host interactions. The ability of *Pseudomonas* to exploit eukaryotic lipids shows specific and original strategies developed by these microorganisms to succeed in their infectious process. All compiled data provide the demonstration of the importance of studying the *Pseudomonas* lipidome to inhibit the infectious potential of these highly versatile germs.

Contents

Abbreviations: ACP, acyl carrier protein; AHL, *N*-acyl homoserine lactone; CDP, cytidine diphosphate; CL, cardiolipin; FAS, fatty acid synthesis; GP, glycerophospholipid; HG, head group; HPTLC, high performance thin-layer chromatography; IM, inner membrane; LPA, lysophosphatidic acid; LPS, lipopolysaccharide; MSI, mass spectrometry imaging; OM, outer membrane; PA, phosphatidic acid; PC, phosphatidylcholine; PE, phosphatidylethanolamine; PG, phosphatidylglycerol; PGP, phosphatidylglycerol phosphate; PI, phosphoinositide; PIP, phosphatidylinositol phosphate; PI(4,5)P2, phosphatidylinositol 4,5-biphosphate; PI(3,4,5)P3, phosphatidylinositol 3,4,5-trisphosphate; PLD, phospholipase D; PS, phosphatidylserine; T3SS, type 3 secretion system; T6SS, type 6 secretion system.

* Corresponding author at: Laboratory of Microbiology Signals and Microenvironment (LMSM) EA 4312, Normandie Université, University of Rouen, 55 rue Saint Germain, 27000 Evreux, France. Fax: +33 232291550.
E-mail address: cecile.poc@univ-rouen.fr (C. Duclairoir Poc).

http://dx.doi.org/10.1016/j.chemphyslip.2015.06.006
0009-3084/

1. Introduction

The genus *Pseudomonas* is one of the most heterogeneous groups of eubacteria. These bacteria are found in all natural environments (Ringen and Drake, 1952), like water (Mena and Gerba, 2009), soil (Couillerot et al., 2009; Kiely et al., 2006) and air (Duclairoir Poc et al., 2014; Morris et al., 2007) and also in association with plants and animals. Some *Pseudomonas* species are of medical importance and count among the principal human opportunistic pathogens (Driscoll et al., 2007). The concept of *Pseudomonas* diversity originates from the biochemical studies of Stanier et al. 1966, who performed a comparative study on the growth characteristics of 267 strains on 146 different organic compounds and a wide range of physiological tests. Since their initial designation at the end of the nineteenth century and their taxonomic redefinition by Palleroni, many species have been classified in other genus (Palleroni, 2010) and, nowadays, the genus *Pseudomonas* is divided in two major lineages represented by typical species, namely *Pseudomonas aeruginosa* and *Pseudomonas fluorescens* (Mulet et al., 2010; Palleroni, 2010). The *P. aeruginosa* lineage is the most homogeneous and consists predominantly of the *P. aeruginosa* species. The *P. fluorescens* lineage is much more diverse and is by itself separated in 3 major groups: *P. fluorescens*, *Pseudomonas* putida and *Pseudomonas* syringae (Mulet et al., 2010).

The members of *P. aeruginosa* lineage are generally found in riparian soil associated with decaying plants (Jones et al., 2013; Ringen and Drake, 1952; Vasil and Ochsner, 1999). However, *P. aeruginosa* group includes important opportunistic pathogens, particularly involved in nosocomial infections in immunocompromised hosts and in cystic fibrosis (Driscoll et al., 2007). *P. aeruginosa* infections are always difficult to treat due to the natural resistance of this bacterium (Obritsch et al., 2005). Consequently, a therapy with two or three antimicrobial agents is typically used (Lodise et al., 2007; Szaff et al., 1983; Valerius et al., 1991). Thus, the utilization of antibiotics uncommonly used in clinical practice, such as polymyxins like colistin, is recommended (Gunderson et al., 2003; Sabuda et al., 2008). Bacteria of the *P. fluorescens* lineage are found preferentially in soil and in association with plants (Bodilis et al., 2006; Loper et al., 2012). Members of the *P. putida* group show an adaptation to various ecological niches and are characterized by their adaptation to grow in soils and sediments contaminated with high concentrations of heavy metals and organic contaminants (Hachicho et al., 2014; Heipieper et al., 1996; Ramos et al., 1997; Wu et al., 2011). Members of the *P. syringae* group are plant pathogens. *P. syringae* is well known for its capacity to grow epiphytically on diverse plants and for its ice-nucleation activity (Joardar et al., 2005; Kozloff et al., 1984; McCann et al., 2013). Recently, strains of *P. syringae*, virulent on diverse species of crop plants, were isolated from epilithic biofilms of rivers (Morris et al., 2007) and clouds at several kilometers altitude (Amato et al., 2007) outside the zones of agricultural production (Morris et al., 2008). Bacteria of the *P. fluorescens* group commonly found in soil (Bodilis et al., 2006) and water (Janek et al., 2010) are also able to develop in air (Duclairoir Poc et al., 2014; Kondakova et al., 2014). Some of *P. fluorescens* group members, adapted to the human temperature are members of the skin microbiota or behave as opportunistic pathogens (Chapalain et al., 2008).

The wide distribution of *Pseudomonas* suggests a remarkable degree of physiological and genetic adaptability. Physiologically, bacterial adaptability to ecological niches and environmental modifications depends essentially on the structure and organization of their envelope. Most protective membrane functions, as osmotic or heat shock response, are traditionally attributed to proteins that are immersed in the lipid bilayer (Allan et al., 1988; Gotoh et al., 1989), but the lipids are not only a matrix to accommodate proteins but play a major role in bacterial functioning (Boughton and Pollock, 1953; Lindgren et al., 1977). As in the case of proteins, bacteria have the capacity to adjust their membrane lipid composition in response to environmental modifications (Cullen et al., 1971; Fang et al., 2000; Parsons and Rock, 2013; Pepi et al., 2008; Ramos et al., 1997). This is especially true in Gram-negative bacteria, like *Pseudomonas*, because of their double envelope with outer and inner membranes. Although a considerable diversity of lipid structures exists in the bacterial world, most predominant lipids in *Pseudomonas* membranes are glycerophospholipids (GPs). GPs are defined as acylated derivatives of *sn*-glycerol-3-phosphate composed of two fatty acid chains, a glycerol unit and a phosphate group linked to a polar head group (Zhang and Rock, 2008). The variety of chemical structures and functions of GPs is due to the polar head group (HG) and fatty acid (FA) composition. GP polar HGs determine the membrane properties and associated functions, such as the barrier function to prevent the entry of noxious compounds and the passive and active influx of nutrient molecules (Sutterlin et al., 2014; Heath et al., 2002a,b). They influence membrane-related processes such as protein export and DNA replication (Nikaido, 2003). Adjustments in FA composition are related to the formation of *trans*-unsaturated or cyclopropylated FAs. Formation of unsaturated or cyclopropylated FAs by *Pseudomonas* occurs in response to osmotic stress, solvent exposition and temperature adaptation, and are interpreted as a mechanism that modifies the permeability of the GP bilayer to minimize energy expenditure and optimize growth (Heipieper et al., 1996; Pepi et al., 2008). The recent identification of lipid signaling molecules and the involvement of GPs in bacteria/eukaryotes interactions (Sato and Frank, 2014; Vromman and Subtil, 2014) demonstrate the key role of lipids apart from cell wall. GP synthesis, composition and functions in bacterial cells were determined early in bacterial lipid metabolism and homeostasis studies realized particularly on the *Escherichia coli* lipidome (Guchhait et al., 1974; Heath and Rock, 1995; Larson et al., 1984; Parsons and Rock, 2013; Wang and Cronan, 2004). However, the high ability of *Pseudomonas* to adapt to various ecological conditions could suppose the involvement of other specific mechanisms of GP homeostasis. This review is aimed at organizing the wealth of information on GP metabolism and homeostasis in *Pseudomonas*. These data provide important insights into the mechanism and the regulation of bacterial GP synthesis, role of GPs in bacterial metabolism and homeostasis as well as in host–bacteria interactions.

2. Pseudomonas lipid synthesis and functions

2.1. Fatty acid biosynthesis

Fatty acid synthesis (FAS) in *Pseudomonas* spp. is conducted by the type II FA synthetic pathway. FAS II is found in bacteria, plants and eukaryotic parasites. This mechanism is divided in individual steps wherein each component is encoded by a separate gene that produces a unique protein, catalyzing a single step in the pathway (Heath et al., 2002a,b). Proteins in this pathway are located in the cytosol, and each has been purified and biochemically characterized (White et al., 2005). In FAS II enzymes, the active sites are usually not located on the protein surface but within a deep cavity. These active sites are connected to the protein surface through narrow tunnel. The enzymatic activity and substrate specificity are dependent on the size and the shape of the tunnels and active site chemistry (Biedermannova et al., 2012; White et al., 2005).

2.1.1. Acyl carrier protein

The major player of FA biosynthesis in bacterial cells is the acyl carrier protein (ACP). It is a small protein (about 9 kDa) containing the prosthetic group 4′-phosphopantetheine (White et al., 2005; Zhang and Rock, 2008). The ACP is produced by *acpP* gene as the apoprotein. ACP is one of the most abundant proteins in the cell and is converted to its active form by ACP-synthase (AcpS). AcpS transfers the 4′-phosphopantetheine prosthetic group from CoA to apo-ACP (White et al., 2005). The 4′-phosphopantetheine prosthetic group of ACP injects the substrate into tunnels for catalysis. ACP interacts specifically and transiently with all of the enzymes of FAS. The negative residues of ACP (its prosthetic group sulfhydryl) interact with a patch of positive surficial residues of the FAS enzymes (Heath et al., 2002a,b). The ACP of *P. aeruginosa* was successively purified and characterized by Kutchma and coworkers (Kutchma et al., 1999). In addition to GP synthesis, ACP plays an essential role in synthesis of rhamnolipids, and in a broad range of other biosynthetic reactions of acyl transfer (nonribosomal peptide and depsipeptide biosynthesis). ACP is a precursor of oligosaccharides and proteins transacylation (Kutchma et al., 1999; White

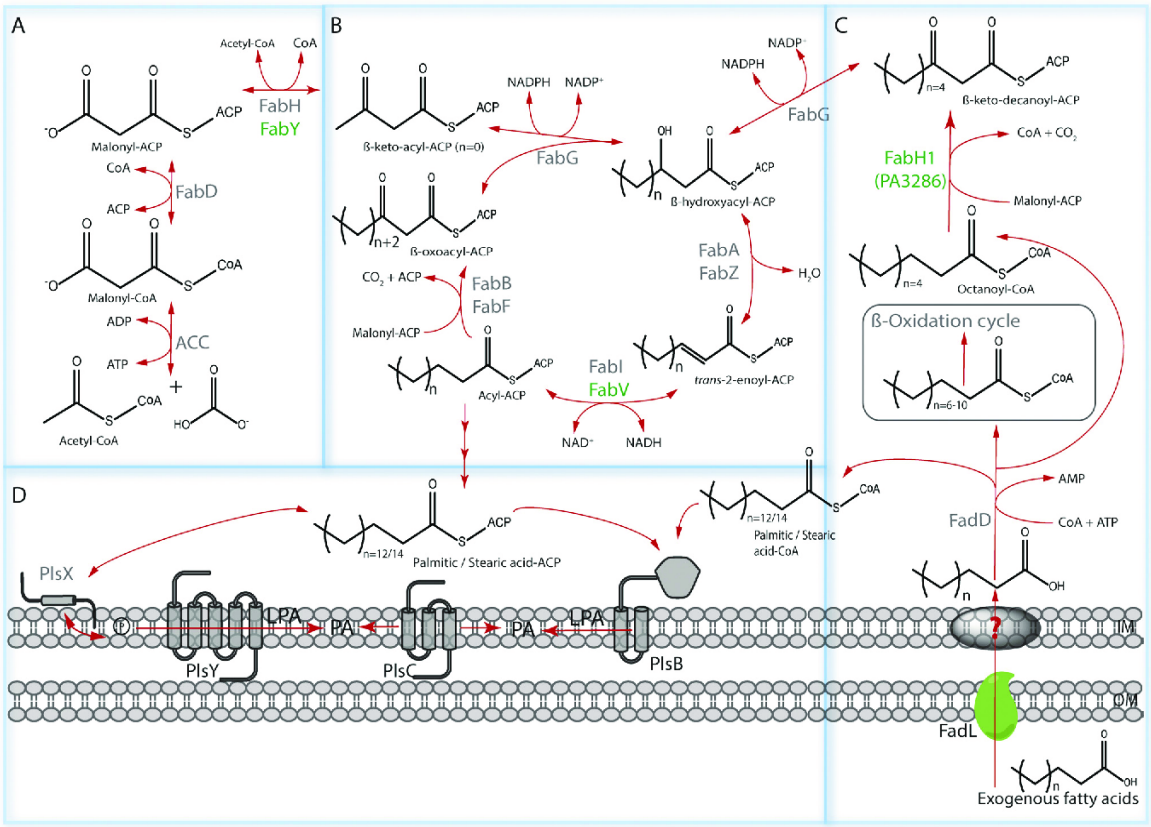

Fig. 1. Proposed pathway of fatty acid synthesis in *Pseudomonas* spp.
(A) Initiation module: the acetyl-CoA carboxylase (ACC) generates malonyl-CoA via the carboxylation of acetyl-CoA. The malonyl group is transferred to the acyl carrier protein (ACP) by malonyl-CoA:ACP acyltransferase (FabD). The initiation of the new acyl chain formation is performed by condensation of malonyl-ACP with acetyl-CoA by β-ketoacyl-ACP synthase III (FabY, PA 5174 for *P. aeruginosa* – green color – and potential FabH enzymes for *Pseudomonas* strains).
(B) Elongation module: the NADPH-dependent β-ketoacyl-ACP reductase (FabG) reduces obtained previously ketoester, and a water molecule is removed by β-hydroxyacyl-ACP dehydrases (FabA and FabZ). Then, enoyl-ACP reductases (FabI for all *Pseudomonas* spp. and FabV for *P. aeruginosa*) complete the cycle. The new cycle of elongation is initiated by β-ketoacyl-ACP synthase I and II (FabB and FabF).
(C) Incorporation of exogenous fatty acids: after diffusion across the outer membrane through FadL protein, FA is retained by FadD enzymes catalyzed esterification of FA with CoA. Further metabolism depends on acyl-CoA ester chain length. Long chains C_{16}/C_{18}-CoA esters can be incorporated directly into *de novo* GPs by the glycerol-phosphate and acylglycerol-phosphate acyltransferases PlsB/PlsC. Medium C_{10} to C_{14} acyl-CoA esters are degraded in the β-oxidation cycle. C_8-CoA esters are intercepted by FabH1 (PA3286) enzyme and condensed with malonyl-ACP to form the β-keto-decanoyl-ACP.
(D) Transfer to the membrane: C_{16}/C_{18} fatty acids chains are transferred to the membrane by acyltransferases. The PlsB enzyme catalyzes the acylation of the *sn*-1-position of glycerol-3-phosphate to form lysophosphatidic acid (LPA). Alternatively, PlsX transfers the acyl group to inorganic phosphate to form reactive acylphosphate intermediate, which is acylated in *sn*-1-position by the integral plasma-membrane protein PlsY to form LPA. Next, PlsC transfers a FA to the *sn*-2-position of LPA to form phosphatidic acid (PA). OM: outer membrane; IM: inner membrane.

et al., 2005). Acyl-ACP is an acyl donor for synthesis of *N*-acyl homoserine lactones (AHLs) of the quorum sensing mechanism (Gould et al., 2004).

2.1.2. Initiation of fatty acid biosynthesis

2.1.2.1. Acetyl-CoA carboxylase and FabD acyltransferase. The acetyl-CoA-carboxylase (ACC) performs the first step of FAS in Pseudomonas. The malonyl-coenzyme A (malonyl-CoA) is generated through the carboxylation of acetyl-CoA (Fig. 1A) (Parsons and Rock, 2013). The ACC is a four-subunit complex consisting in a biotin carboxylase (AccC), a biotin carboxyl carrier protein (AccB), and two carboxyltransferases (AccAD) (Table 1) (Guchhait et al., 1974). This enzyme complex governs the quantity of produced FA to maintain a normal lipid/protein ratio. The organization of genes encoding the component enzyme activities of ACC varies in different organisms. In *E. coli*, the *accAD* and the *accBC* genes are cotranscribed (Kondo et al., 1991; Li and Cronan, 1992). In *P. aeruginosa, accBC* genes are organized in one operon, and *accA and accD* are found in different regions of chromosome (Best and Knauf, 1993). Upon synthesis, the malonyl-CoA is transferred to ACP by a malonyl-CoA:ACP transacylase (FabD) (Fig. 1A, Table 1). The gene coordinating the production of FabD protein belongs to the *fab* gene cluster of *P. aeruginosa* (Kutchma et al., 1999).

2.1.2.2. Role of FabH and FabY in determining fatty acids structure in Pseudomonas. The following step of FAS is the initiation of new acyl chain formation by condensation of malonyl-ACP with a short-chain acyl-CoA (Fig. 1A). Usually, in γ-proteobacteria, this reaction is catalyzed by FabH enzyme. The known sequences of FabH vary according to the bacterial species, but are characterized by a conserved Cys-His-Asn catalytic triad and utilization of a ping-pong mechanism (Davies et al., 2000; Qiu et al., 1999; White et al.,

Table 1
Genes, enzymes and functions in fatty acid and glycerophospholipid synthesis.

Gene	Enzyme activity	Functions	References
acpP	Acyl carrier protein (ACP)	Production of ACP	(White et al., 2005; Kutchma et al., 1999; Best and Knauf, 1993)
accC	Acetyl-CoA carboxylase biotin carboxylase subunit (AccC)	ATP-dependent transfer of CO_2 from bicarbonate to biotin attached to AccB	
accB	Acetyl-CoA carboxylase biotin carboxyl carrier protein subunit (AccB)	Transfer of the carboxy-biotin intermediate to the transcarboxylase enzyme composed of AccA and AccD subunits	
accA	Acetyl-CoA carboxylase carboxyl transferase (α-subunit) (AccA)	Transfer of the CO_2 from carboxybiotin to acetyl-CoA	
accD	Acetyl-CoA carboxylase, carboxyl transferase (β-subunit) (AccD)	Transfer of the CO_2 from carboxybiotin to acetyl-CoA	
fabD	Malonyl-CoA:ACP transacylase (FabD)	Transfer of malonyl-CoA to the ACP	(White et al., 2005; Kutchma et al., 1999)
PA3333 (*fabH2*)	β-Ketoacyl ACP synthase III (FabH2)	Unknown functions	(Davies et al., 2000; Yuan et al., 2012a; Yuan et al., 2012b; Six et al., 2014; Zhang and Rock, 2012)
PA3286	β-Ketoacyl ACP synthase III (FabH1)	Channeling of 8-carbon acyl-CoA intermediates	
PA5174	β-Ketoacyl ACP synthase (FabY)	Condensation of malonyl-ACP with a short-chain acyl-CoA	
fabB	β-Ketoacyl-ACP synthase I (FabB)	Complementation of acyl-ACP by two-carbon unit from malonyl-ACP Essential enzyme for unsaturated FAS, elongating *cis*-3-decenoyl-ACP	(Garwin et al., 1980; Hoang and Schweizer, 1997)
fabF	β-Ketoacyl-ACP synthase II (FabF)	Complementation of acyl-ACP by two-carbon unit from malonyl-ACP Temperature-dependent production of *cis*-unsaturated FA	
fabG	3-Ketoacyl-ACP- reductase (FabG)	Reduction of ketoester to obtain the hydroxyacyl-ACP	(Fisher et al., 2000; Price et al., 2001; Ren et al., 2000)
fabA	β-Hydroxydecanoyl-ACP dehydrase (FabA)	Dehydration of hydroxyacyl-ACP to *trans*-2-ACP Isomerization of *trans*-2 to *cis*-3-decenoyl ACP	(Hoang and Schweizer, 1997; Mohan et al., 1994)
fabZ	(3R)-Hydroxymyristoyl-ACP dehydratase (FabZ)	Dehydration of hydroxyacyl-ACP to *trans*-2-ACP	
fabI	NADH-dependent enoyl-ACP reductase (FabI)	Formation of saturated fatty acid chains	(Hoang and Schweizer, 1999)
fabV	NADH-dependent enoyl-ACP reductase (FabV)	Formation of saturated fatty acid chains	(Zhu et al., 2010; Massengo-Tiassé and Cronan, 2008)
desA	Δ-9 fatty acid desaturase (DesA)	Introduction of double bond into acyl chains previously attached to phospholipids	(Zhu et al., 2006; Subramanian et al., 2010)
desB	Acyl-CoA Δ-9-desaturase (DesB)	Introduction of a double bond into saturated acyl-CoA specifically at the 9-position	
plsB	Glycerol-3-phosphate acyltransferase (PlsB)	Acylation of the 1-position of glycerol-3-phosphate, formation of LPA	(Röttig and Steinbüchel, 2013; Lu et al., 2007; Cronan and Bell, 1974; Yoshimura et al., 2007)
plsC	1-Acyl-sn-glycerol-3-phosphate acyltransferase (PlsC)	Formation of PA	
plsY	Glycerol-3-phosphate acyltransferase (PlsY)	Acylation of the 1-position of glyceril-3-phosphate, formation of LPA	
plsX	Glycerol-3-phosphate acyltransferase (PlsX)	Transfer of acyl group to inorganic phosphate to form reactive acylphosphate intermediate	
pssA	Phosphatidylserine synthase (PssA)	Condensation of CDP-diacylglycerol with serine, formation of PS	(Shi et al., 1993; Mileykovskaya and Dowhan, 1997)
psd	Phosphatidylserine decarboxylase (Psd)	Decarboxylation of PS, formation of PE	
pgsA	CDP-diacylglycerol-glycerol-3-phosphate 3-phosphatidyltransferase (PgsA)	Condensation of CDP-dyacylglycerol with glycerol phosphate, formation of PGP	(Heath et al., 2002a,b; Kikuchi et al., 2000; Suzuki et al., 2002)
pgpA	Phosphatidylglycerophosphatase A (PgpA)	Dephophorylation of PGP, formation of PG	
cls	Cardiolipin synthetase (Cls)	Condensation of two PG molecules, formation of CL	(Heath et al., 2002a,b; Bernal et al., 2007)
pcs	Phosphatidylcholine synthase (Pcs)	Condensation of choline with CDP-diacylglycerol, formation of PC	(Geiger et al., 2013; Wilderman et al., 2002)

2005). FabH selectively utilizes acetyl-CoA derived from intermediary metabolism (Parsons and Rock, 2013). Only thioesters with less than four carbons are able to pass FabH active site tunnel in *E. coli* (White et al., 2005). The FabH enzyme has many similarities with FabB and FabF condensation enzymes of elongation module, which add a two-carbon unit from malonyl-ACP to growing acyl-ACP (*see part Elongation module*) (Parsons and Rock, 2013). The most important difference between these three enzymes is the configuration of the active site: Cys-His-His triade for FabB/FabF, and Cys-His-Asn for FabH (Davies et al., 2000). *fabH* is an essential gene for bacterial FA synthesis, thus it is a target for antibacterial development (Castillo and Pérez, 2008; Davies et al., 2000; Lai and Cronan, 2003; Zhang and Cronan, 1998). Most bacteria have a single FabH enzyme. However, in *P. aeruginosa* the FAS initiation is carried out by another enzyme PA5174, named FabY. This condensing enzyme performs a task usually attributed to FabH but uses a Cys-His-His active site of FabB/FabF enzymes (Yuan et al., 2012b). The *fabY* mutant is still viable indicating a possible alternative secondary mechanism of FAS in *P. aeruginosa* (Yuan et al., 2012a). It exhibits a growth defect and a decreased production of quorum sensing signaling molecules, rhamnolipids and siderophores (Yuan et al., 2012b). The *fabY* mutant is susceptible to a number of antibiotics, including certain β-lactams (Six et al., 2014). The study of one of *E. coli* FabH ortholog in *P. aeruginosa* (FabH1-PA3286) showed that this enzyme plays a unique role in channeling of C_8 acyl-CoA intermediates arising from FA ß-oxidation (Fig. 1C green color, Table 1). Yuan and colleagues proposed that *P. aeruginosa* can incorporate exogenous FAs with C_8 via PA3286 catalysis. In this pathway exogenous FAs, intercepted by Fad enzymes, are condensed with malonyl-ACP using PA3286 to make the FAS intermediate ß-keto-decanoyl-ACP (Figure 1/C) (Yuan et al., 2012a). This case of direct utilization of long-chain acyl-CoA has been demonstrated also for *E. coli* (Black et al., 2000), *Mycobacterium tuberculosis* during the synthesis of mycolic acids (Choi et al., 2000) or *Rhodococcus opacus* (Holder et al., 2011). Structural characterization of PA3286 is needed to shed more light upon how this enzyme catalyzes the reactions with long acyl chains.

The initiation of FAS in *P. fluorescens* lineage is poorly documented. We have found the open reading frames (ORF) coding FAS enzymes in genomes of five *Pseudomonas* type strains (*P. aeruginosa* PAO1, *P. fluorescens* Pf0-1, *P. putida* KT2440, *P. fulva* 12-X, and *P. syringae* pv. *theae*). Fig. 2 shows a phylogenic distribution of protein translated from these ORFs. We observed that FabB and FabF have two FAS domain protein clusters well conserved among *P. aeruginosa* and *P. fluorescens* lineages. These enzymes are representatives from all five analyzed *Pseudomonas* strains, consistent with their role in FAS elongation. The FabY enzyme is not conserved suggesting strain specific role(s) outside primary FAS metabolism. The distribution of FabY in *Pseudomonas* is confined to *P. aeruginosa* PAO1 and *Pseudomonas fulva* 12-X (member of the *P. putida* group). Conversely, no *fabY* ortholog was detected in *P. putida, P. fluorescens*, and *P. syringae*. This indicates that this alternative metabolism observed for *P. aeruginosa* should be also active in specific members of the *P. putida* group such as *P. fulva*. However, supplementary studies are necessary to support this thesis. It is likely that FAS domain proteins should be also involved (Yuan et al., 2012b). Indeed, we found annotated sequences to *fabH* in all studied *Pseudomonas* strains. FabH proteins present two major and divergent clusters. The FabH1 enzyme was studied in *P. aerugnosa* (FabH1-PA3286) and was discussed above (Fig. 1). *fabH1* orthologous gene sequences were found in all studied *Pseudomonas* strains. This could indicate the ability of these *Pseudomonas* strains to intercept long C_8 acyl-CoA chains. Surprisingly, three strains (*P. putida* KT2440, *P. fluorescens* Pf0-1, *P. aeruginosa* PAO1) have more than one *fabH* annotated sequence (FabH2, Fig. 2). The role of FabH2 is unknown in the absence of biochemical studies of this enzyme (Zhang and Rock, 2012). Therefore, we can suppose this enzyme is involved in alternative metabolic pathway(s).

2.1.3. Elongation module

The iterative cycle of acyl chain elongation is divided in four steps catalyzed by six enzymes. In the first step, ß-ketoacyl-ACP synthase I and II (FabB and FabF) complement the growing of acyl-ACP by two-carbon unit to form malonyl-ACP (Fig. 1B). The resulting ketoester is reduced by a NADPH-dependent ß-ketoacyl-ACP reductase (FabG), and a water molecule is then removed by a ß-hydroxyacyl-ACP dehydrases (FabA and FabZ) (Fig. 1B). The last step is catalyzed by enoyl-ACP reductases (FabI/FabV) to form a saturated acyl-ACP, which in turn serves as a substrate for another

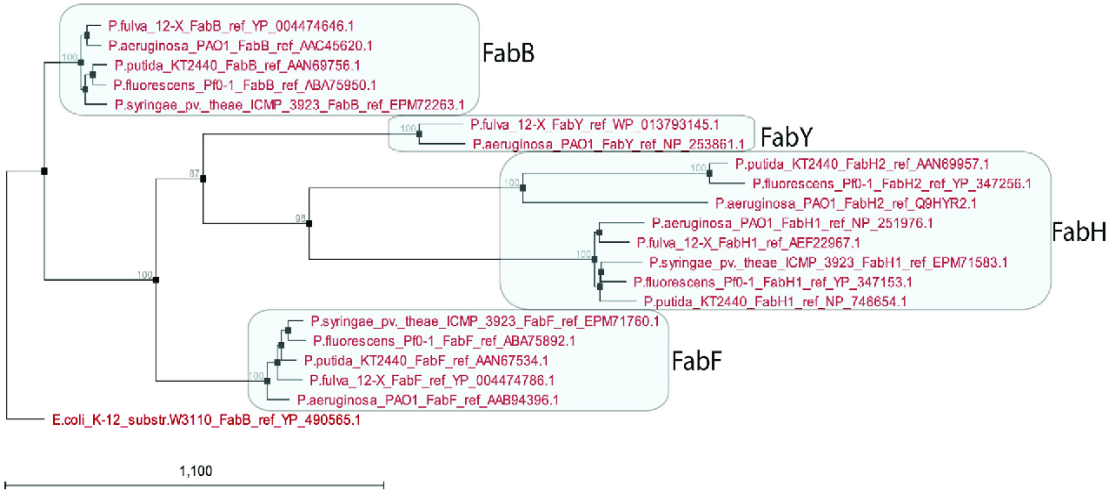

Fig. 2. Phylogenic analysis of FabB/FabF, FabH and FabY proteins among *Pseudomonas* type strains.
A phylogenic tree, based on protein sequences translated from open reading frames found in selected *Pseudomonas* genomes was established. Sequences coding FAS proteins domain clusters were found in databases and analyzed using the neighbor-joining method. Analyses were conducted by using CLC Sequence Viewer 7 (CLC bio, a QIAGEN Company, Denmark). The branches of the tree are labeled by the strain name and reference in NCBI database. The percent value of the bootstrap support is present in all nodes of tree. To scale the tree, branch lengths are calculated corresponding to the number of amino acid substitutions per site. The four main clusters (FabB, FabF, FabH and FabY) are indicated in bleu squares. The FabB of *E. coli* K-12 substr. W3110 is used for rooting the tree.

condensation reaction continuing the cycle of FA chain elongation (Fig. 1B) (Heath et al., 2002a,b).

Chemical structures of FabB and FabF enzymes are very similar (Huang et al., 1998; Olsen et al., 1999). However, FabF is responsible for temperature-dependent production of *cis*-unsaturated FA (Table 1) (Garwin et al., 1980). At low temperatures, FabF promotes the production of Δ11-18:1, whereas at higher temperatures, FabF is inactivated and the formation of Δ11-18:1 is reduced (Garwin et al., 1980; Zhang and Rock, 2008). FabB is an essential enzyme for unsaturated FAS (Hoang and Schweizer, 1997; Wang and Cronan, 2004) (see part Introduction of the double bond), which has the catalytic property of elongating *cis*-3-decenoyl-ACP, whereas FabF does not (Table 1) (Hoang and Schweizer, 1997).

The next reduction of ketoester is catalyzed by a short-chain dehydrogenase/reductase family member FabG (Fig. 1B, Table 1). It is an essential protein for bacteria and plants (Fisher et al., 2000; Price et al., 2001; Ren et al., 2000).

The third step of dehydration is catalyzed by the FabA or FabZ ß-hydroxyacyl-ACP dehydratases (Fig. 1B). Although FabA and FabZ are two isoforms, FabZ catalyzes the dehydration of hydroxyacyl-ACP to *trans*-2-ACP (Table 1). In addition to dehydration, FabA also carries out the isomerization of *trans*-2 to *cis*-3-decenoyl-ACP

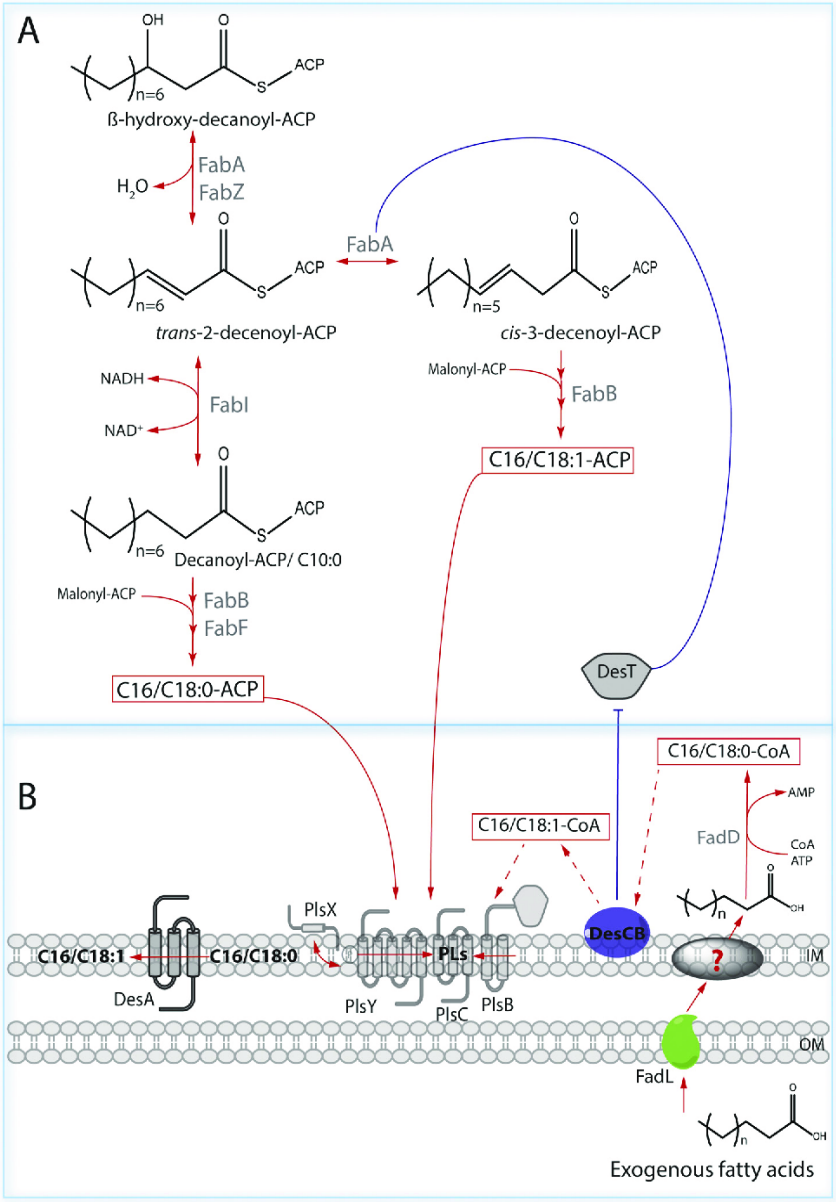

Fig. 3. Proposed mechanism of formation of unsaturated fatty acids in *Pseudomonas* strains.
(A) FabAB pathway of double bond introduction in *Pseudomonas*: At the 10-carbon stage of elongation module, the bifunctional FabA enzyme performs both the dehydration of ß-hydroxyacyl-ACP to *trans*-2-enoyl-ACP and the isomerization of *trans*-2-enoyl-ACP to *cis*-3-enoyl-ACP. Then the enoyl-ACP reductase (FabI) reduces the *trans*-isomer to form a saturated FA chain (C16/C18:0-ACP). The *cis*-3-enoyl-ACP is elongated by the FabB enzyme to form an unsaturated FA chain (C16/C18:1-ACP), which is incorporated into GPs thought the action of acyltransferases (PlsX, PlsY, PlsB and PlsC). Production of the FabA protein is under the control of the DesT transcriptional repressor.
(B) *DesCB/DesA* pathways of double bond introduction: Exogenous FAs enter the cell and are converted to their acyl-CoA derivatives by the long-chain-fatty-acid-CoA ligase (FadD). DesA is a GP acyl-desaturase that introduces a double bond in the Δ9-position into formed GPs. The GP substrates for DesA are produced from both *de novo* FA synthesis and exogenous saturated FAs. DesB is an acyl-CoA desaturase that introduces a double bond in the Δ9-position. DesC is a predicted oxidoreductase which is probably involved in electron transport supporting FA desaturation reactions. Regulation of the DesBC system is insured by DesT. OM: outer membrane; IM: inner membrane, regulation patways.

(Fig. 3A, Table 1) (Kimber et al., 2004). *P. aeruginosa* FabA and FabZ have very similar sequence characteristics, but they differ in active site residues, an Asp in FabA and a Glu in FabZ (Kimber et al., 2004; Mohan et al., 1994). The coupled transcription of the two genes coordinates the production of the two proteins (FabA and FabB) that are essential for unsaturated fatty acid biosynthesis (Hoang and Schweizer, 1997).

Usually, the fourth and final step in FAS is catalyzed by a NADH-dependent enoyl-ACP reductase FabI (Fig. 1B, Table 1). The active site of this enzyme has a Tyr-Lys catalytic diad (Roujeinikova et al., 1999; White et al., 2005). The FabI mechanism involves the transfer of a hydride to the C_3 of the $C_2{=}C_3$ bond and the development of an enolate anion on the C_1 carbonyl oxygen, which accepts a proton from a Tyr hydroxyl moiety. The obtained enol then undergoes tautomerization to yield the thioester (Rafferty et al., 1995). FabI is exclusively bacterial enzyme. The reduction of enoyl-ACP derivatives is thought to coordinate FA and GP biosynthesis and to regulate the degree of FA unsaturation (Hoang and Schweizer, 1999). The regulation of the ratio of unsaturated/saturated FAs is an essential mechanism of *Pseudomonas* adaptation to environmental modifications (Heath and Rock, 1995; Heipieper and Fischer, 2010; Ramos et al., 1997). FabI is the target of a group of antibacterial compounds, and is a typical triclosan-sensitive enoyl-ACP reductase (Chuanchuen et al., 2003; Heath and Rock, 1995). Triclosan is a very widely used biocide, which specifically inhibits enoyl-ACP-reductase activity. FabI is present in all *Pseudomonas* species (Zhu et al., 2010). Remarkably, *P. aeruginosa* possesses an another enoyl-ACP reductase isozyme FabV (Figure 1/B, *green color*, Table 1) (Zhu et al., 2010). It is considerably larger than typical short-chain dehydrogenase/reductase family members. The Tyr and the Lys active site residues of FabV are separated by eight amino acids instead of six in FabI (Massengo-Tiassé and Cronan, 2008).

In *P. aeruginosa* the genes encoding several enzymes of elongation cycle (*fabF-acpP-fabG-fabD)* are clustered (called the *fab* cluster) (Hoang and Schweizer, 1999; Kutchma et al., 1999). The genes coordinating the production of the FabH, FabY and FabZ proteins, are absent in this cluster.

2.1.4. Introduction of the double bond

Bacterial membranes should conserve the appropriate fluidity to maintain normal membrane structure and functions under various environmental changes (Heipieper and Fischer, 2010; Keweloh and Heipieper, 1996; Rühl et al., 2012). To increase membrane rigidity, *Pseudomonas* produce more saturated FAs whereas when higher fluidity is needed, unsaturated FAs are synthetized (Mansilla et al., 2004; Pepi et al., 2008; Zhu et al., 2006). A considerable diversity of mechanisms is used by *Pseudomonas* to generate unsaturated FAs. Bacteria of this genus use the bifunctional FabA enzyme which performs both the dehydration of ß-hydroxyacyl-ACP to *trans*-2-enoyl-ACP and the isomerization of *trans*-2-enoyl-ACP to *cis*-3-enoyl-ACP at 10-carbon stage of elongation module (Fig. 3A, Table 1) (Parsons and Rock, 2013). Resulting *cis*-3-enoyl-ACP is then elongated by FabB enzyme. In *E. coli* the expression of *fabA* and *fabB* genes are transcriptionally regulated by the FadR activator and the FabR repressor (Feng and Cronan, 2012). In *Pseudomonas* the FabAB pathway is positively and negatively regulated by the DesT protein (PA4890) (Subramanian et al., 2010). DesT binds to a DNA palindromic site in the gene promoter. This binding is positively and negatively regulated by acyl-CoA. The DesT binds to saturated- and unsaturated-CoA with the same affinity, but the binding to DNA is enhanced when DesT is bound to an unsaturated acyl-CoA and released when DesT is bound to a saturated acyl-CoA (Miller et al., 2010; Zhang et al., 2007).

In addition to the FabAB dependent mechanism, *P. aeruginosa* generates unsaturated FAs by two other pathways (Fig. 3B). The DesA enzyme, a membrane-associated Δ9-desaturase, introduces a double bond in Δ9-position of fatty acyl chains attached to the *sn*-2 position of existing GPs (Fig. 3B, Table 1) (Parsons and Rock, 2013). We have found *P. aeruginosa desA* orthologs in a majority of *Pseudomonas* spp. (www.pseudomonas.com, data not shown). This suggests the presence of DesA dependent mechanism in most of *Pseudomonas* strains. However, the mechanism of DesA regulation is unknown and necessitates biochemical studies. Zhu et al. suppose that *desA* expression is regulated by membrane biophysical properties (Zhu et al., 2006). DesCB proteins, encoded by the *desCB* 2-genes′ operon, are responsible for the introduction of a double bond specifically at the Δ9-position of acyl-CoA produced from exogenous saturated FAs (Fig. 3B, Table 1) (Subramanian et al., 2010). DesB is an acyl-CoA Δ9-desaturase, and the DesC is a predicted oxydoreductase which is probably involved in the electron transport that supports FA desaturation reactions catalyzed by DesB (Zhu et al., 2006). The *desB* mutants are known to be deficient in the synthesis of proteolytic enzymes, pyocyanin and rhamnolipids. They show impaired swarming and twitching motilities and reduced virulence in the *Caenorhabditis elegans* infection model. These data demonstrate that DesB is not only a FA desaturase but also a factor required for full virulence in *P. aeruginosa* (Schweizer and Choi, 2011). The DesBC pathway is like FabAB, regulated by a DesT dependent mechanism. However, the role of DesT in controlling *fabAB* expression likely accounts for the fact that DesT is conserved in both protein sequence and chromosomal location in all *Pseudomonas* species examined, yet only *P. aeruginosa* has a *desCB* operon (Subramanian et al., 2010). The reasons why *Pseudomonas* strains have three independent mechanisms of unsaturated FA formation need to be determined.

2.2. Transfer to the membrane

The FAS in *Pseudomonas* generally ends when the acyl chain has 16 or 18 carbons in length. The FA chain is then transferred into membrane to form GPs thanks to acyltransferases. Thus, the FA is transferred from acyl-ACP or acyl-CoA to the *sn*-1-position of glycerol-3-phosphate to form the 1-acyl-glycerol-3-phosphate, also known as lysophosphatidic acid (LPA). Next, the LPA is acylated in the *sn*-2-position to form phosphatidic acid (PA) (Fig. 1D) (Cullinane et al., 2005; Rock et al., 1981; Zhang and Rock, 2008).

The PlsB, an inner-membrane protein, catalyzes the acylation of the *sn*-1-position of glycerol-3-phosphate (Fig. 1D, Table 1). This enzyme can use both acyl donors: acyl-ACP and acyl-CoA (Lu et al., 2006) and has an eukaryotic ortholog. The second step of PA formation is always catalyzed by PlsC enzyme (Fig. 1D, Table 1), ubiquitously distributed in all bacteria (Röttig and Steinbüchel, 2013).

Alternatively, *Pseudomonas* spp. has a second acylation system PlsX/PlsY. The PlsX, a peripheral membrane protein, transfers the acyl group to inorganic phosphate to form a reactive acylphosphate intermediate (Fig. 1D, Table 1) (Zhang and Rock, 2008). Next, the PlsY an integral plasma-membrane protein acylates the *sn*-1-position of glycerol-3-phosphate and allows the PlsC enzyme to form the PA (Fig. 1D, Table 1) (Cullinane et al., 2005). Why *Pseudomonas* possesses two acylation systems is still an enigma.

PlsY is characterized as a remarkably small (23 kDa) membrane-bound enzyme in comparison to PlsB (93 kDa). It possesses five membrane-spanning segments and three cytoplasmic domains. This enzyme has no eukaryotic homologs (Röttig and Steinbüchel, 2013). Unlike PlsB, the PlsY unables to directly use acyl-ACP or acyl-CoA (Lu et al., 2007, 2006). An *E. coli, plsB* mutant was produced by Robert Bell's research group (Cronan and Bell,

1974). Those mutants are *sn*-glycerol 3-phosphate auxotrophs which owe their requirement to a K_m defect in *sn*-glycerol 3-phosphate acyltransferase (Cronan and Bell, 1974; Larson et al., 1984). Therefore, the *plsB* mutation was overcomed by addition of exogenous glycerol-3-phosphate in the medium (Larson et al., 1984). Yoshimura et al. generated targeted *plsX*, *plsY* and *plsB* gene deletions (Yoshimura et al., 2007). *plsB* is an essential gene in *E. coli*, whereas single deletion mutants of *plsX* or *plsY* have no effect on bacterial growth. The double *plsX*/*plsY* mutant cannot be produced, indicating the essential role of the PlsX/PlsY complex in GP biosynthesis. Despite great therapeutic value, the transfer of FA modules to the membrane GPs remains a puzzle that will require more research to unravel.

3. Glycerophospholipid biosynthesis and functions in *Pseudomonas*

3.1. Glycerophospholipid head group diversity

An assortment of different polar HGs can be attached to the PA basic structure in bacteria, creating the optimum surface charge for membrane (Boeris et al., 2007; Parsons and Rock, 2013). The membrane charge depends on the ratio between zwitterionic GPs, e.g. phosphatidylethanolamine (PE), and GPs with acidic HGs, e.g. phosphatidylglycerol (PG). The balance in electrostatic charge is required for many integral membrane proteins to adopt the correct steric conformation in the cell membrane (Parsons and Rock, 2013). Bacteria can modify membrane charge to adapt to stress factors, like high temperature or solvent stresses (De Carvalho et al., 2008; De Carvalho, 2012).

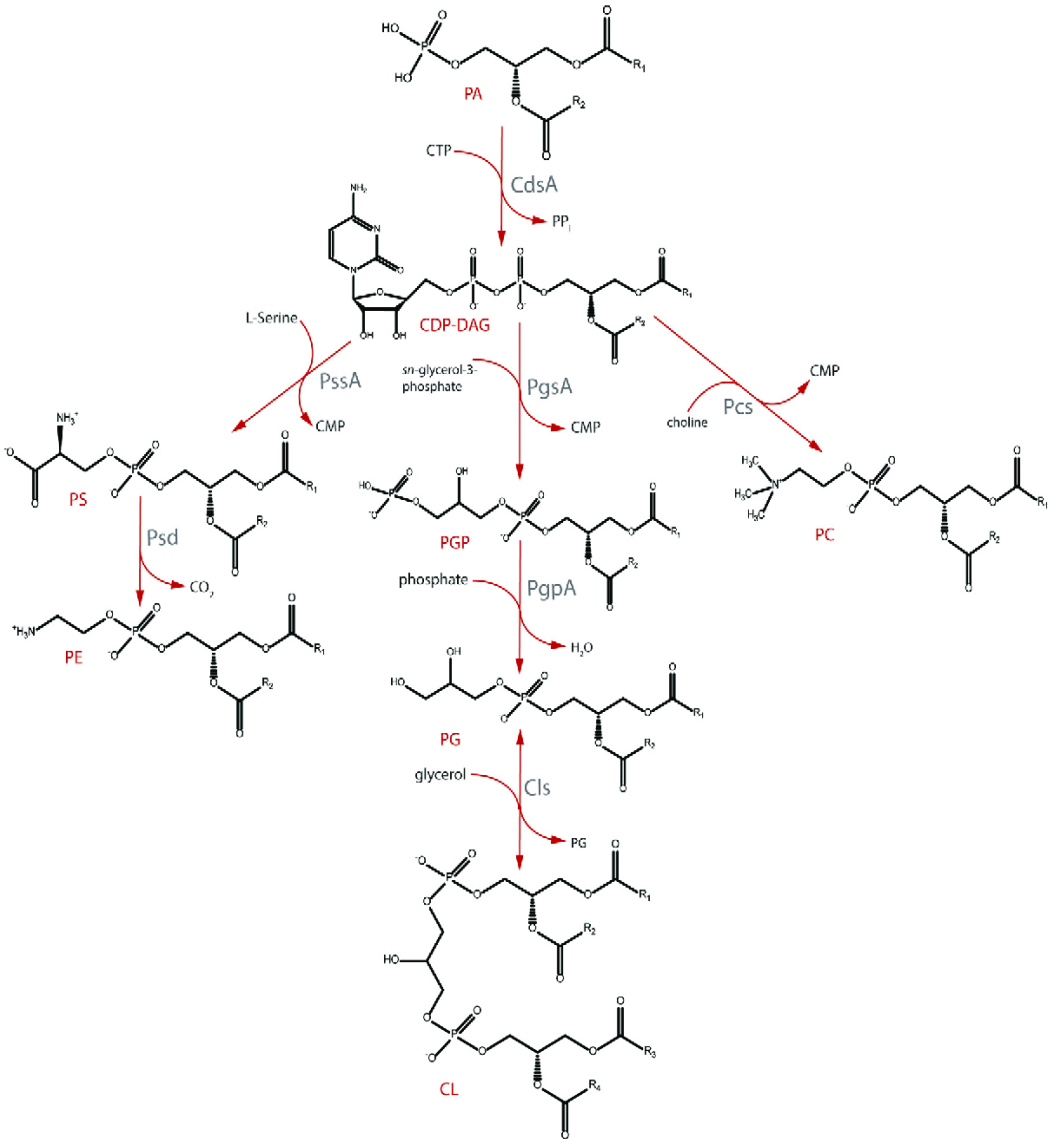

Fig. 4. Glycerophospholipid head group diversity.
Phosphatidic acid (PA) is the precursor for GPs synthesis in *Pseudomonas*. The cytidine diphosphate-diacylglycerol (CDP-DAG) is a key intermediate in the synthesis of all GPs in *Pseudomonas*. It is formed from PA and cytosine triphosphate (CTP) via CdsA catalysis. Phosphatidylethanolamine (PE), a major GP of *Pseudomonas*, is synthesized by phosphatidylserine (PS) decarboxylation. CDP-DAG is condensed with serine via the PS synthase PssA catalyze to form PS. Then, PS is decarboxylated thanks to the PS decarboxylase Psd to yield PE. For phosphatidylglycerol (PG) formation, CDP-DAG is condensed with glycerol phosphate by PgsA, to form phosphatidylglycerol phosphate (PGP). Then, PGP is dephosphorylated by a PGP phosphatase (PgpA). Cardiolipin (CL) is synthesized through condensation of two PG molecules by a CL synthase (Cls). Phosphatidylcholine (PC) is formed through the PC synthase (Pcs) pathway when choline is condensed with CDP-DAG to form the PC.

Table 2
Glycerophospholipids and their functions.

Glycerophospholipid	Chemical formula	Functions in bacterial cells	References
Phosphatidic acid (PA)	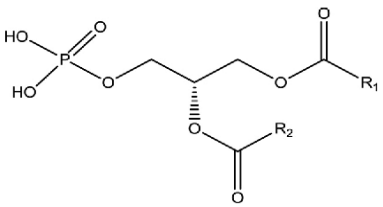	1. Basis in the synthesis of all membrane phospholipids 2. Negative membrane charge	(Parsons and Rock, 2013; Zhang and Rock, 2008) (Sutterlin et al., 2014)
Phosphatidylethanolamine (PE)	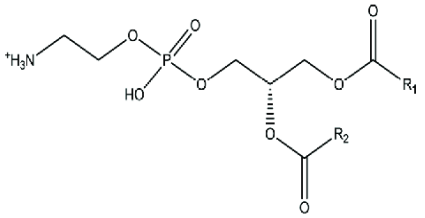	1. Most predominant phospholipid of *Pseudomonas* 2. Membrane architecture (lateral pressure and curvature stress in membranes) 3. Adaptation to organic solvents contamination and temperature stress 4. Motility and chemotaxis 5. Precursor for lipopolysaccharides synthesis	(Boeris et al., 2007; Gill, 1975; Bhakoo and Herbert, 1980) (Heath et al., 2002a,b) (Nikaido, 2003; Rühl et al., 2012; Gill, 1975; Bhakoo and Herbert, 1980) (Shi et al., 1993) (Raetz et al., 2007)
Phosphatidylserine (PS)	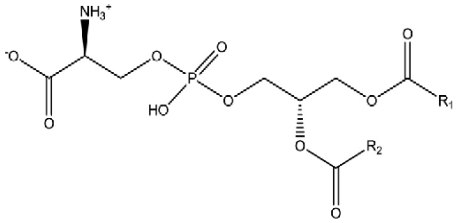	1. Precursor for PE synthesis	(Parsons and Rock, 2013)
Phosphatidylglycerol (PG)	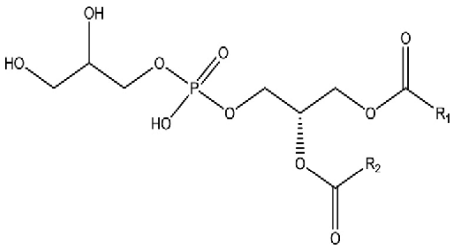	1. Major anionic phospholipid of *Pseudomonas* 2. Membrane architecture 3. Adaptation to organic solvents and temperature stress	(Rühl et al., 2012; Suzuki et al., 2002) (Zhao et al., 2008) (Nikaido, 2003; Rühl et al., 2012; Gill, 1975; Bhakoo and Herbert, 1980)
Cardiolipin (CL)	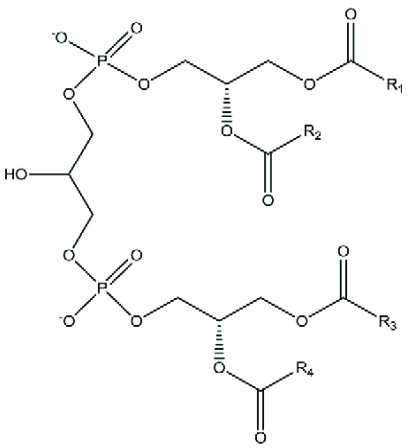	1. Formation of dynamic protein–lipid membrane domains 2. Cell division 3. Resistance to organic compounds and antibiotics	(Camberg et al., 2007; Mileykovskaya and Dowhan, 2009; Romantsov et al., 2007) (Mileykovskaya and Dowhan, 2005; Dowhan et al., 2004; Mileykovskaya and Dowhan, 2009) (Ramos et al., 1997) (Bernal et al., 2007)
Phosphatidylcholine (PC)	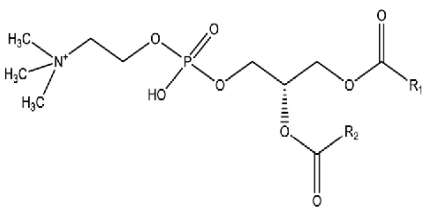	1. Interactions symbiotic/pathogenic bacteria-eukaryotic hosts 2. Membrane structure formation 3. Resistance to heavy metals 4. Metabolic cycle, biomolecules formation	(Minder et al., 2001; Sohlenkamp et al., 2003; Martínez-Morales et al., 2003) (Geiger et al., 2013) (Boeris and Lucchesi, 2012) (Geiger et al., 2013)

Lipids composition of *Pseudomonas* spp. does not vary significantly depending on the bacterial strains (Bhakoo and Herbert, 1980; Bobo and Eagon, 1968; Boeris et al., 2007; Boeris and Lucchesi, 2012; Cullen et al., 1971; Tashiro et al., 2011). *Pseudomonas* spp. possesses four major GP species. PE and PG present the two major *Pseudomonas* spp. GPs, which together account for about 95%. Integral cellular analysis gives the composition of about 75% PE and 20% PG. Remainders are represented by cardiolipin (CL) (Diedrich and Cota-Robles, 1974) and phosphatidylcholine (PC), recently found in *Pseudomonas* strains (Boeris and Lucchesi, 2012; Geiger et al., 2013; Kondakova et al., 2014). CL is accumulated in *Pseudomonas* spp. when the cells enter the stationary growth phase. This lipid can be up to 10% of total GPs, and is required for prolonged survival of bacteria (Gill, 1975; Heath et al., 2002a,b). PC is the major component of eukaryotic cells, but it was also detected in the lipidome of *P. aeruginosa*, *P. fluorescens* and *P. putida* in small quantity (less than 4%) (Wilderman et al., 2002). The schema of *Pseudomonas* GPs synthesis is shown in Fig. 4.

3.2. Phosphatidylethanolamine production and functions

PE is a major component of the *Pseudomonas* lipidome (Table 2) (Boeris et al., 2007; Fuchs and Schiller, 2008). The bacterial PE is synthesized exclusively via phosphatidylserine (PS) decarboxylation (Dowhan, 1997; Gibellini and Smith, 2010). The first step catalyzed by PS synthase (PssA) is the condensation of cytidine diphosphate-diacylglycerol (CDP-DAG) with serine to form PS. Then PS yields PE by PS decarboxylase (Psd) (Fig. 4). PS is a minor GP of *Pseudomonas* (Bhakoo and Herbert, 1980), since it is quickly converted to PE (Table 2). It has been demonstrated that the lack of PE is lethal for bacteria, but this lethality is suppressed by media supplementation with high concentration of divalent metal cations. A *pss* null mutant contains no PS and PE in its lipidome and has a defect in motility (Shi et al., 1993), in Cpx dependent signal transduction pathway (Mileykovskaya and Dowhan, 1997) and in division site selection. This last was attributed to a concomitant increase in CL content (Mileykovskaya and Dowhan, 2005; Ramos et al., 1997) (see part Cardiolipin synthesis and functions). A defect in the native folding of lactose permease LacY, which causes the loss of active membrane transport, is also observed (Dowhan et al., 2004). Complete inactivation of *psd* indicates that this gene is required for motility and chemotaxis (Ramos and Filloux, 2007; Shi et al., 1993). PE is mostly located in the inner membrane, and may be transferred from the inner to the outer membrane by lipid flippases (Sanyal and Menon, 2009). The PE plays a major role in membrane structure, because it is able to form reversed non lamellar structures like the hexagonal phase. In membrane, PE increases lateral pressure and introduces curvature stress (Birner et al., 2001). Moreover PE is the precursor of many essential biological molecules including DAG, FAs, PA (Gibellini and Smith, 2010) and lipopolysaccharides (LPS), major *Pseudomonas* virulence factor (Ham et al., 2011; Raetz et al., 2007).

3.3. Phosphatidylglycerol synthesis and functions

The second predominant *Pseudomonas* GP is phosphatidylglycerol (PG) (Table 2) (Diedrich and Cota-Robles, 1974). Unlike PE, PG is an anionic lipid at pH 7. The hydroxyl group of PG has the potential to form intermolecular hydrogen bonds (Zhao et al., 2008). The PG synthesis is organized in two steps and starts with CDP-DAG (Fig. 4). First, the CDP-DAG is condensed with glycerol phosphate by PgsA protein, to form phosphatidylglycerol phosphate (PGP). The second step is the PGP dephosphorylation by PGP phosphatase (PgpA) (Table 1) (Rühl et al., 2012; Heath et al., 2002a, b). It has long been thought that PG is an essential bacterial GP, but Kikuchi et al. (2000) showed that in *E. coli*, a null pgsA mutant is viable if the major outer membrane lipoprotein (Lpp) is deficient. In the null *pgsA* mutant, the PG production is not detected (less than 0.01% of total GPs, below the detection limit), although the PA, an acidic biosynthetic precursor, was accumulated (4%). Nonetheless, the null *pgsA* mutant does not grow at high temperature, in low-osmolality or minimal media, but it grows almost normally in rich media (Suzuki et al., 2002). PG is therefore nonessential for *Pseudomonas* viability or basic life GP functions, but it plays an important role in bacterial machinery. Studies of the toxic effects of organic solvents on bacteria revealed that an adaptive bacterial mechanism to solvent stress modifies the amount of PG relative to PE in the cell membrane (Fang et al., 2000; Murzyn et al., 2005). This alteration in the HG composition is the way of preserving stability and low membrane permeability (Murzyn et al., 2005).

3.4. Cardiolipin biosynthesis and functions

CL is also called diphosphatidylglycerol because of its unique dimeric molecular structure in which two phosphatidyl moieties are linked by a glycerol. This GP is one of the major participants in the formation of membrane domains in *Pseudomonas* spp. (Table 2) (Gill, 1975; Heath et al., 2002a,b). Although CL has two phosphate groups, it is not fully ionized at pH 7 due to intramolecular hydrogen bonding between the free hydroxyl residue of the central glycerol and a protonated phosphate (Kates et al., 1993). CL is produced in *Pseudomonas* species by condensation of two PG molecules (Figure 4) thanks to the CL synthase (Cls) (Table 1) (Heath et al., 2002a,b). Due to its propensity to form non-bilayer structures dependent on pH or divalent counter cations, CL is able to participate in the formation of dynamic protein–lipid membrane domains of higher curvature, for example in bacterial division sites (Table 1) (Mileykovskaya and Dowhan, 2005). This explains the co-localization of CL with some proteins, like osmosensory transporter ProP, or Eps system, found in the polar regions in bacterial cells (Camberg et al., 2007; Mileykovskaya and Dowhan, 2009; Romantsov et al., 2007). The long-term solvent response involves the increasing of CL production in *P. putida* (Bernal et al., 2007; Ramos et al., 1997). The *cls* null mutant has a more rigid membrane, is more sensitive to toluene stress and to several antibiotics than the parental strain, suggesting that RND efflux pumps involved in the extrusion of these drugs are not working efficiently without CL production (Bernal et al., 2007).

3.5. Phosphatidylcholine synthesis in Pseudomonas

PC is the major membrane-forming GP in eukaryotic cells (Cole et al., 2012). However, at least 15% of bacteria have the ability to synthesize PC (Geiger et al., 2013). For example, PC synthesis is described in *Agrobacterium tumefaciens* (Kaneshiro and Law, 1964), *Rhodobacter sphaeroides* (Arondel et al., 1993), *Sinorhizoum meliloti* (De Rudder et al., 2000), *Zymomonas mobilis* (Tahara et al., 1994), *Bradyrhizobium japonicum* (Minder et al., 2001) and many other eubacteria. PC is detected in small quantity (less than 4%) in the lipidome of *Pseudomonas* spp. (Geiger, 2010). PC and PE have a very similar chemical structure. Both have a zwitterionic state at pH 7 and possess a dipole moment across their respective head groups (Sohlenkamp et al., 2003). However, there are significant and important differences in chemistry and properties between the two GP. PC has a head group and hydrophobic domains of similar diameter and forms lipid bilayers. PE has a small head group relative to a large hydrophobic domain and favors the hexagonal II phase formation (Dowhan and Bogdanov, 2002). Two pathways for PC biosynthesis exist in bacteria: the glycerophospholipid *N*-methylation (Pmt) pathway and the phosphatidylcholine synthase (Pcs) pathway. In the Pmt pathway, PE is three times methylated to

yield PC involving one or more glycerophospholipid *N*-methyltransferases (Wilderman et al., 2002) whereas in the Pcs pathway, choline condenses directly with CDP-DAG to form PC (Geiger et al., 2013; Gibellini and Smith, 2010). In *P. aeruginosa* PAO1, orthologs of rhodobacterial *pmtA* (PA0798) and *pcs* (PA3857) are found (Table 1) (Wilderman et al., 2002). The *pmtA*-deficient mutant still synthesizes PC at wild type level whereas a *pcs* null mutant forms no detectable amounts of PC (Wilderman et al., 2002). These data suggest that the Pcs pathway is predominant in *P. aeruginosa* PC synthesis (Fig. 4) (Geiger et al., 2013). The both (*pcs* and *pmt* null mutants) affects the viability of PAO1, demonstrating the important role of both genes in *P. aeruginosa* (Wilderman et al., 2002). It has been shown, that *P. putida* is able to synthesize PC via the Pcs pathway (Boeris and Lucchesi, 2012). Recently, we identified the PC production in *P. fluorescens* strains (Kondakova et al., 2014). We found orthologs to *P. aeruginosa* PAO1 *pmt* and *pcs* in *P. fluorescens* Pf0-1. Tblastx analyses show *pmt*: Pfl01_0427 and *pcs*: Pfl01_2093 with 28 and 66% of amino acid identity respectively (www.pseudomonas.com, BLAST analysis, data not shown). PC plays a role in membrane formation in *P. aeruginosa* and is involved in *P. putida* resistance to heavy metals (Boeris and Lucchesi, 2012) (Table 2). In addition, pseudomonal PC can function as an intermediate during the biosynthesis of other biomolecules or form part of metabolic cycle (Geiger et al., 2013, p. 201).

4. Exploitation of host glycerophospholipids by *Pseudomonas*

Lipids have been loosely defined as biological substances that are generally hydrophobic in nature and in many cases soluble in organic solvents presenting important structural materials in living organisms (Fahy et al., 2005). The role of lipid is wider than structural material formation (Ganapathy et al., 2013), and several studies help us to understand the mysterious reason why nature synthesizes thousands of different lipids (Kanfer and Kennedy, 1964, 1963). In 1989, for the first time Irvine and Berridge showed that the phosphoinositides are involved in bacterial signaling system quorum sensing (Berridge and Irvine, 1989). Then, Haucke and Di Paolo showed the lipid implication in membrane traffic (Haucke and Di Paolo, 2007).

One example of host lipid exploitation by *Pseudomonas* is illustrated in the type 3 secretion system (T3SS). This mechanism, identified in human and plant pathogens *P. aeruginosa* and *P. fluorescens* and delivering virulence effector proteins into eukaryotic cells, appears functionally dependent on lipids (Cornelis, 2002; Mavrodi et al., 2011). At the tip of the T3SS needle, bacterial proteins are inserted into the host cell membrane to form a translocon that perturbs the membrane bilayer. *P. aeruginosa* has two translocon components, PopB and PopD, capable to bind directly to two eukaryotic lipids: cholesterol and phosphatidylserine, causing a cholesterol-dependent lyse of membrane (Schoehn et al., 2003). Approximately, 28% of strains of *P. aeruginosa* encode a potent cytotoxin, ExoU (Feltman et al., 2001), which is a marker of highly virulent *P. aeruginosa* strains isolated from patients with ventilator-associated pneumonia (Diaz and Hauser, 2010; Schulert et al., 2003). The ExoU is a cytotoxic phospholipase A2 effector protein secreted by the T3SS directly into host cells (Tyson and Hauser, 2013). Among membrane GPs, ExoU possesses high affinity for phosphatidylinositol 4,5-bisphosphate or PI(4,5)P_2, and it is capable to use this phospholipid as a substrate (Kierbel et al., 2005; Sato and Frank, 2014). Lysing cell membranes, ExoU contributes to the ability of *P. aeruginosa* to disseminate rapidly from lung tissue into the bloodstream (Van der Meer-Janssen et al., 2010). Then, *Pseudomonas* strains have a large capacity to exploit eukaryotic lipids in order to improve their host interactions. Within the last few years, bacteria–host lipid interactions became a very promising research area. For earlier studies, we highly recommend very comprehensive reviews (Ham et al., 2011; Van der Meer-Janssen et al., 2010; Vromman and Subtil, 2014).

4.1. Phosphoinositide signaling and Pseudomonas

Many internal organs such as epithelial sheets are composed by separate apical and basolateral surfaces that are defined by distinct lipid and protein compositions and are separated by tight junctions (Gibson and Perrimon, 2003). The apical surface plays a role of barrier to the environment. The basolateral surface is adapted for interaction with other cells and for exchange with the bloodstream.

Phosphoinositides (PIs) are small lipids derived from phosphatidylinositol. As key components of eukaryotic cell membranes, PIs have essential roles in a wide range of cellular processes, such as membrane dynamics, actin cytoskeleton arrangements and vesicle trafficking (Michell, 2007). This differential distribution of PIs in cell is regulated by PI kinases and phosphatases, which interconvert diverse PI species (Ham et al., 2011). Phosphatidylinositol 3,4,5-trisphosphate (PI(3,4,5)P_3) is described as stably localized at the basolateral membrane and is excluded from the apical plasma membrane (Vanhaesebroeck and Alessi, 2000). This GP is a key determinant of *P. aeruginosa* interaction with host cells (Botelho et al., 2000; Kierbel et al., 2005). Insertion of exogenous PI(3,4,5)P_3 into the apical surface results in the rapid transformation of regions of the apical membrane to one with basolateral constituents. *P. aeruginosa* could create a local microenvironment that facilitates colonization and entry into the cell (Kierbel et al., 2007). For this, polarized monolayers *P. aeruginosa* binds near cell–cell junctions and coopts PI_3 kinase generating PI(3,4,5)P_3 at the surface. Membrane protrusions enriched by PI(3,4,5)P_3 and actin accumulate at the apical surface in the site of bacterial binding. This causes the decreasing susceptibility of the intact epithelium to *P. aeruginosa*–mediated invasion or damage (Kierbel et al., 2007). The PI(3,4,5)P_3 pathway of cell invasion by *P. aeruginosa* depends on the phospholipase D (PLD) enzymes activity (Jiang et al., 2014). The PLD enzymes catalyze the hydrolysis of GP phosphodiester bonds to product PA, and have been identified as type 6 secretion system (T6SS) effectors (Russell et al., 2013). Two such effectors in *P. aeruginosa* are PldA (PA3487) (Russell et al., 2013) and PldB (PA5089) (Jiang et al., 2014) targeting bacterial and eukaryotic cells (Spencer and Brown, 2015). Both proteins have significant homology to eukaryotic PLDs, but not to any prokaryotic PLDs, suggesting they were acquired horizontally, perhaps from a eukaryotic organism (Wilderman et al., 2001). PLD proteins of *P. aeruginosa* imposed cell death occurs through PA accumulation, via degradation of the major membrane components: PC for eukaryotes (Jiang et al., 2014) or bacterial PE (Russell et al., 2013).

4.2. Eukaryotic phosphatidylcholine exploitation

As the major eukaryotic phospholipid, PC is supposed to play an important role in the interactions between symbiotic and pathogenic bacteria and their eukaryotic hosts (Martínez-Morales et al., 2003). But recent findings showing the PC presence in about 15 % of all bacteria put into question this hypothesis. However, plant-colonizing *P. syringae* species detects and exploits choline in hosts for osmoprotection and nutrition (Chen et al., 2013). *P. aeruginosa* in turn produces a number of virulence factors that facilitate the establishment of lung infections. Mammalian lungs are naturally coated by indispensable lung surfactant, which is composed of approximately 80% of PC (Bernhard et al., 2001). This lipid serves as an important nutrient for *P. aeruginosa* during cystic fibrosis lung infection (Sun et al., 2014). *P. aeruginosa* hemolytic phospholipase C (PlcH) is a secreted hydrolase that degrades host-

associated PC (Jackson et al., 2013; Sage and Vasil, 1997; Wargo et al., 2011). In the PC-rich environment of the lungs, the PlcH degradation products of PC, DAG, and phosphorylcholine play different roles in the disease process. DAG may induce the abnormal release of inflammatory mediators and increase the host inflammatory response, thereby promoting tissue damage (Johansen et al., 1994; Sage and Vasil, 1997). Phosphorylcholine can be converted to choline or glycine betaine. These compounds serve as osmoprotectant agents which shield bacteria against the effects of hyperosmolar environments (such as the lungs tissues) (Jackson et al., 2013; Sage and Vasil, 1997). Since *P. aeruginosa* is able to utilize choline and glycine betaine as sole sources of carbon; nitrogen and energy (Lisa et al., 1983). Sun et al., 2014). A null *P. aeruginosa plcH* mutant was less able to colonize epithelial cell monolayers and defective in biofilm formation when grown in lung (Jackson et al., 2013). In a mouse thermal injury model, *plcH* mutant had a 10-fold increase in its LD50, compared to that of its wild type parent (Ostroff et al., 1989), Using the transparent zebrafish model, it has been demonstrated, that the PlcH is selective for endothelial cells, and also could contribute to apoptosis in lung endothelial cells and further exacerbates chronic inflammation seen in cystic fibrosis patients (Vasil et al., 2009). However, the role of PC in *Pseudomonas* spp.—host/symbiont interactions is still a promised area of future lipidomic researches.

4.3. Pseudomonas *lipids as a target for a new antibiotic development*

The bacterial FAS II differs significantly from the mammalian and fungal system (FAS I), which uses a large complex multifunctional enzymes (White et al., 2005; Zhu et al., 2010). The differences between the FAS I and FAS II systems make the FAS II one of the most attractive biochemical pathways to be used as targets for new antibacterial agents (Heath et al., 2002a,b, 2001; Payne et al., 2001; Zhang et al., 2006). Triclosan 1 (5-chloro-2-(2, 4-dichlorophenoxy)phenol), a broad spectrum antimicrobial agent, can specifically inhibit enoyl-acyl carrier protein reductase, FabI, to block lipid biosynthesis (Castillo and Pérez, 2008; McMurry et al., 1998). Through subsequent kinetic and structural studies, triclosan was shown to be a potent inhibitor of FabIs from many organisms, such as *Staphylococcus aureus* (Suller and Russell, 2000), and *Haemophilus influenza* (Marcinkeviciene et al., 2001). However, *P. aeruginosa* is resistant to triclosan, because this species encodes triclosan-resistant enoyl-ACP reductase isozymes. As discussed above, *P. aeruginosa* contains two enoyl-ACP reductases, FabI and the triclosan resistant FabV. Upon deletion of the fabV gene, the mutant strain became extremely sensitive to triclosan (>2,000-fold more sensitive than the wild-type strain), whereas the mutant strain lacking FabI remained completely resistant to the biocide (Zhu et al., 2010).

Over the last few years, *P. aeruginosa* lipidome became a target for new antibiotic development. The family of peptidomimetic antibiotics, based on membranolytic host-defense peptide protegrin I perturbs the LPS assembly in the outer membrane (Srinivas et al., 2010). A new aminoglycoside derivative 3′,4′,6-tri-2-naphylmethylene (3′,4′6-tri-2NM neamine) also targets *P. aeruginosa* LPS (Ouberai et al., 2011). It bound to LPS inducing membrane permeabilization. The accumulation of this drug within *P. aeruginosa* phospholipids causes the membrane destabilization. Electrostatic phospholipids/antibiotic interactions are probably critical in the 3′,4′6-tri-2NM neamine efficiency. Thus the positive charge of this compound targets negatively charged phospholipids, like CL and PG (Ouberai et al., 2011). In any cases, these studies support the concept of lipid as attractive targets for drug development.

5. Conclusions and perspectives

The *Pseudomonas* genus includes ubiquitous bacteria, taming all ecological niches, which are able to adapt to highly diverse environmental modifications. In this review, we explored specific *Pseudomonas* mechanisms for FA and GP synthesis, composition and homeostasis. *Pseudomonas* spp. possesses three independent pathways to add double bonds in FA chains. These mechanisms, non-existent in many other bacteria, are known to protect *Pseudomonas* strains from stress factors. The FabV enzyme allows *P. aeruginosa* to resist to the antimicrobial agent triclosan. *P. aeruginosa* FabH enzyme was recently described as a component of the system of incorporation of long chain FAs. The *Pseudomonas* GP composition is more complex, than that one of *E. coli*. *Pseudomonas* spp. is able to synthetize the PC. This cell compound could be used by bacteria in the network of host–pathogen interactions. Improving our knowledge of GP biosynthesis in *Pseudomonas* should be helpful in understanding the physiology of these highly versatile microorganisms.

The ability of *Pseudomonas* spp. to exploit eukaryotic lipid is an emerging area of studies that will take advantage with the rapid development of high-throughput mass spectrometric, microscopic and genomic techniques. The establishment of bacterial lipid profiles should lead to the identification of the specific role of individual lipid species. Moreover the functions of minor bacterial lipids and the mechanism of lipid production in molecular level could be enlightened by the coupling of mass spectrometry with omics tools. The interactions between pseudomonal human or plant pathogens and their host, the role of individual GPs in these interactions should be investigated more finely. Hence, novel intracellular signaling or trafficking mechanisms could be revealed. This will certainly support the development of more specific drugs against *Pseudomonas* pathogens.

Acknowledgements

We wish to thank Awa N'Diaye-Renoult for linguistic insight for this manuscript. Tatiana Kondakova is recipient of a PhD grant from the GRR SeSa (Sanitary Safety Research Network) financed by the Regional Council of Haute-Normandie (France). This study was supported the Regional Council of Haute-Normandie (France) and Europe Council through the FEDER “SéSa” sponsoring.

References

Allan, B., Linseman, M., MacDonald, L.A., Lam, J.S., Kropinski, A.M., 1988. Heat shock response of *Pseudomonas aeruginosa*. J. Bacteriol. 170, 3668–3674.

Amato, P., Parazols, M., Sancelme, M., Laj, P., Mailhot, G., Delort, A.-M., 2007. Microorganisms isolated from the water phase of tropospheric clouds at the Puy de Dôme: major groups and growth abilities at low temperatures. FEMS Microbiol. Ecol. 59, 242–254. doi:http://dx.doi.org/10.1111/j.1574-6941.2006.00199.x.

Arondel, V., Benning, C., Somerville, C.R., 1993. Isolation and functional expression in *E. coli* of a gene encoding phosphatidylethanolamine methyltransferase (EC 2.1.1.17) from *Rhodobacter sphaeroides*. J. Biol. Chem. 268, 16002–16008.

Bernal, P., Muñoz-Rojas, J., Hurtado, A., Ramos, J.L., Segura, A., 2007. A *Pseudomonas putida* cardiolipin synthesis mutant exhibits increased sensitivity to drugs related to transport functionality. Environ. Microbiol. 9, 1135–1145. doi:http://dx.doi.org/10.1111/j.1462-2920.2006.01236.x.

Bernhard, W., Hoffmann, S., Dombrowsky, H., Rau, G.A., Kamlage, A., Kappler, M., Haitsma, J.J., Freihorst, J., von der Hardt, H., Poets, C.F., 2001. Phosphatidylcholine molecular species in lung surfactant. Am. J. Respir. Cell Mol. Biol. 25, 725–731. doi:http://dx.doi.org/10.1165/ajrcmb.25.6.4616.

Berridge, M.J., Irvine, R.F., 1989. Inositol phosphates and cell signaling. Nature 341, 197–205. doi:http://dx.doi.org/10.1038/341197a0.

Best, E.A., Knauf, V.C., 1993. Organization and nucleotide sequences of the genes encoding the biotin carboxyl carrier protein and biotin carboxylase protein of *Pseudomonas aeruginosa* acetyl coenzyme A carboxylase. J. Bacteriol. 175, 6881–6889.

Bhakoo, M., Herbert, R.A., 1980. Fatty acid and phospholipid composition of five psychrotrophic *Pseudomonas* spp. grown at different temperatures. Arch. Microbiol. 126, 51–55. doi:http://dx.doi.org/10.1007/BF00421890.

Biedermannova, L., Prokop, Z., Gora, A., Chovancova, E., Kovacs, M., Damborsky, J., Wade, R.C., 2012. A single mutation in a tunnel to the active site changes the mechanism and kinetics of product release in haloalkane dehalogenase LinB. J. Biol. Chem. doi:http://dx.doi.org/10.1074/jbc.M112.377853 jbc.M112.377853.

Birner, R., Bürgermeister, M., Schneiter, R., Daum, G., 2001. Roles of phosphatidylethanolamine and of its several biosynthetic pathways in Saccharomyces cerevisiae. Mol. Biol. Cell 12, 997–1007.

Black, P.N., Færgeman, N.J., DiRusso, C.C., 2000. Long-chain acyl-CoA-dependent regulation of gene expression in bacteria, yeast and mammals. J. Nutr. 130, 305.

Bobo, R.A., Eagon, R.G., 1968. Lipids of cell walls of *Pseudomonas aeruginosa* and *Brucella abortus*. Can. J. Microbiol. 14, 503–513. doi:http://dx.doi.org/10.1139/m68-086.

Bodilis, J., Hedde, M., Orange, N., Barray, S., 2006. OprF polymorphism as a marker of ecological niche in *Pseudomonas*. Environ. Microbiol. 8, 1544–1551. doi:http://dx.doi.org/10.1111/j.1462-2920.2006.01045.x.

Boeris, P.S., Domenech, C.E., Lucchesi, G.I., 2007. Modification of phospholipid composition in Pseudomonas putida A ATCC 12633 induced by contact with tetradecyltrimethylammonium. J. Appl. Microbiol. 103, 1048–1054. doi:http://dx.doi.org/10.1111/j.1365-2672.2007.03346.x.

Boeris, P.S., Lucchesi, G.I., 2012. The phosphatidylcholine synthase of Pseudomonas putida A ATCC 12633 is responsible for the synthesis of phosphatidylcholine, which acts as a temporary reservoir for Al3. Microbiology 158, 1249–1257. doi:http://dx.doi.org/10.1099/mic.0.054072-0.

Botelho, R.J., Teruel, M., Dierckman, R., Anderson, R., Wells, A., York, J.D., Meyer, T., Grinstein, S., 2000. Localized biphasic changes in phosphatidylinositol-4,5-bisphosphate at sites of phagocytosis. J. Cell Biol. 151, 1353–1368.

Boughton, B.W., Pollock, M.R., 1953. Long-chain unsaturated fatty acids as essential bacterial growth factors: further studies with *Corynebacterium* 'Q'. Biochem. J. 53, 261–265.

Camberg, J.L., Johnson, T.L., Patrick, M., Abendroth, J., Hol, W.G.J., Sandkvist, M., 2007. Synergistic stimulation of EpsE ATP hydrolysis by EpsL and acidic phospholipids. EMBO J. 26, 19–27. doi:http://dx.doi.org/10.1038/sj.emboj.7601481.

De Carvalho, C.C., Wick, L.Y., Heipieper, H.J., 2008. Cell wall adaptations of planktonic and biofilm *Rhodococcus erythropolis* cells to growth on C5 to C16 *n*-alkane hydrocarbons. Appl. Microbiol. Biotechnol. 82, 311–320. doi:http://dx.doi.org/10.1007/s00253-008-1809-3.

Castillo, Y.P., Pérez, M.A., 2008. Bacterial beta-ketoacyl-acyl carrier protein synthase III (FabH): an attractive target for the design of new broad-spectrum antimicrobial agents. Mini Rev. Med. Chem. 8, 36–45.

Chapalain, A., Rossignol, G., Lesouhaitier, O., Merieau, A., Gruffaz, C., Guerillon, J., Meyer, J.-M., Orange, N., Feuilloley, M.G.J., 2008. Comparative study of 7 fluorescent pseudomonad clinical isolates. Can. J. Microbiol. 54, 19–27. doi:http://dx.doi.org/10.1139/w07-110.

Chen, C., Li, S., McKeever, D.R., Beattie, G.A., 2013. The widespread plant-colonizing bacterial species Pseudomonas syringae detects and exploits an extracellular pool of choline in hosts. Plant J. 75, 891–902. doi:http://dx.doi.org/10.1111/tpj.12262.

Choi, K.-H., Kremer, L., Besra, G.S., Rock, C.O., 2000. Identification and substrate specificity of β-ketoacyl (acyl carrier protein) synthase III (mtFabH) from *Mycobacterium tuberculosis*. J. Biol. Chem. 275, 28201–28207.

Chuanchuen, R., Karkhoff-Schweizer, R.R., Schweizer, H.P., 2003. High-level triclosan resistance in *Pseudomonas aeruginosa* is solely a result of efflux. Am. J. Infect. Control 31, 124–127. doi:http://dx.doi.org/10.1067/mic.2003.11.

Cole, L.K., Vance, J.E., Vance, D.E., 2012. Phosphatidylcholine biosynthesis and lipoprotein metabolism. Biochim. Biophys. Acta 1821, 754–761. doi:http://dx.doi.org/10.1016/j.bbalip.2011.09.009.

Cornelis, G.R., 2002. The Yersinia Ysc–Yop Type III weaponry. Nat. Rev. Mol. Cell Biol. 3, 742–754. doi:http://dx.doi.org/10.1038/nrm932.

Couillerot, O., Prigent-Combaret, C., Caballero-Mellado, J., Moënne-Loccoz, Y., 2009. *Pseudomonas fluorescens* and closely-related fluorescent pseudomonads as biocontrol agents of soil-borne phytopathogens. Lett. Appl. Microbiol. 02566. doi:http://dx.doi.org/10.1111/j.1472-765X.

Cronan, J.E., Bell, R.M., 1974. Mutants of *Escherichia coli* defective in membrane phospholipid synthesis: mapping of *sn*-glycerol 3-phosphate acyltransferase K_m mutants. J. Bacteriol. 120, 227–233.

Cullen, J., Phillips, M.C., Shipley, G.G., 1971. The effects of temperature on the composition and physical properties of the lipids of Pseudomonas fluorescens. Biochem. J. 125, 733–742.

Cullinane, M., Baysse, C., Morrissey, J.P., O'Gara, F., 2005. Identification of two lysophosphatidic acid acyltransferase genes with overlapping function in *Pseudomonas fluorescens*. Microbiology 151, 3071–3080. doi:http://dx.doi.org/10.1099/mic.0.27958-0.

Davies, C., Heath, R.J., White, S.W., Rock, C.O., 2000. The 1. 8 Å crystal structure and active-site architecture of β-ketoacyl-acyl carrier protein synthase III (FabH) from *Escherichia coli*. Structure 8, 185–195. doi:http://dx.doi.org/10.1016/S0969-2126(00) 94-0.

De Carvalho, C.C., 2012. Adaptation of *Rhodococcus erythropolis* cells for growth and bioremediation under extreme conditions. Res. Microbiol. 163, 125–136. doi:http://dx.doi.org/10.1016/j.resmic.2011.11.003.

De Rudder, K.E., López-Lara, I.M., Geiger, O., 2000. Inactivation of the gene for phospholipid *N*-methyltransferase in *Sinorhizobium meliloti*: phosphatidylcholine is required for normal growth. Mol. Microbiol. 37, 763–772. doi:http://dx.doi.org/10.1046/j.1365-2958.2000.02032.x.

Diaz, M.H., Hauser, A.R., 2010. Pseudomonas aeruginosa cytotoxin ExoU is injected into phagocytic cells during acute pneumonia. Infect. Immun. 78, 1447–1456. doi:http://dx.doi.org/10.1128/IAI.01134-09.

Diedrich, D.L., Cota-Robles, E.H., 1974. Heterogeneity in lipid composition of the outer membrane and cytoplasmic membrane of *Pseudomonas* BAL-31. J. Bacteriol. 119, 1006–1018.

Dowhan, W., 1997. Molecular basis for membrane phospholipid diversity: why are there so many lipids? Annu. Rev. Biochem. 66, 199–232. doi:http://dx.doi.org/10.1146/annurev.biochem.66.1.199.

Dowhan, W., Bogdanov, M., 2002. Functional roles of lipids in membranes, In: Vance, D.E., Vance, J.E. (Eds.), Biochemistry of Lipids, Lipoproteins and Membranes. fourth ed. Elsevier Science, B.V.

Dowhan, W., Mileykovskaya, E., Bogdanov, M., 2004. Diversity and versatility of lipid–protein interactions revealed by molecular genetic approaches. Biochim Biophys Acta 1666, 19–39. doi:http://dx.doi.org/10.1016/j.bbamem.2004.04.010.

Driscoll, J.A., Brody, S.L., Kollef, M.H., 2007. The epidemiology, pathogenesis and treatment of *Pseudomonas aeruginosa* infections. Drugs 67, 351–368.

Duclairoir Poc, C., Verdon, J., Groboillot, A., Barreau, M., Toucourou, H., Mijouin, L., Leclerc, C., Hulen, C., Kondakova, T., Morin, J., Feuilloley, M., Merieau, A., Orange, N., 2014. Airborne fluorescent pseudomonads: what potential for virulence? Int. J. Curr. Microbiol. Appl. Sci. 3, 708–722.

Fahy, E., Subramaniam, S., Brown, H.A., Glass, C.K., Merrill, A.H., Murphy, R.C., Raetz, C.R., Russell, D.W., Seyama, Y., Shaw, W., Shimizu, T., Spener, F., van Meer, G., VanNieuwenhze, M.S., White, S.H., Witztum, J.L., Dennis, E.A., 2005. A comprehensive classification system for lipids. J. Lipid Res. 46, 839–862. doi:http://dx.doi.org/10.1194/jlr.E400004-JLR200.

Fang, J., Barcelona, M.J., Alvarez, P.J., 2000. Phospholipid compositional changes of five pseudomonad archetypes grown with and without toluene. Appl. Microbiol. Biotechnol. 54, 382–389.

Feltman, H., Schulert, G., Khan, S., Jain, M., Peterson, L., Hauser, A.R., 2001. Prevalence of type III secretion genes in clinical and environmental isolates of Pseudomonas aeruginosa. Microbiology 147, 2659–2669.

Feng, Y., Cronan, J.E., 2012. Crosstalk of *Escherichia coli* FadR with global regulators in expression of fatty acid transport genes. PLoS ONE 7, e46275. doi:http://dx.doi.org/10.1371/journal.pone.0046275.

Fisher, M., Kroon, J.T., Martindale, W., Stuitje, A.R., Slabas, A.R., Rafferty, J.B., 2000. The X-ray structure of *Brassica napus* beta-keto acyl carrier protein reductase and its implications for substrate binding and catalysis. Structure 8, 339–347 (Lond. Engl. 1993).

Fuchs, B., Schiller, J., 2008. MALDI-TOF MS analysis of lipids from cells, tissues and body fluids. Subcell. Biochem. 49, 541–565. doi:http://dx.doi.org/10.1007/978-1-4020-8831-5_21.

Ganapathy, V., Thangaraju, M., Prasad, P.D., Martin, P.M., Singh, N., 2013. Transporters and receptors for short-chain fatty acids as the molecular link between colonic bacteria and the host. Curr. Opin. Pharmacol. 13, 869–874. doi:http://dx.doi.org/10.1016/j.coph.2013.08.006.

Garwin, J.L., Klages, A.L., Cronan, J.E., 1980. Beta-ketoacyl-acyl carrier protein synthase II of *Escherichia coli*. Evidence for function in the thermal regulation of fatty acid synthesis. J. Biol. Chem. 255, 3263–3265.

Geiger, O., 2010. Lipids and *Legionella* virulence. In: Timmis, K.N. (Ed.), Handbook of Hydrocarbon and Lipid Microbiology. Springer, Berlin, Heidelberg, pp. 3195–3202.

Geiger, O., López-Lara, I.M., Sohlenkamp, C., 2013. Phosphatidylcholine biosynthesis and function in bacteria. Biochim. Biophys. Acta 1831, 503–513. doi:http://dx.doi.org/10.1016/j.bbalip.2012.08.009.

Gibellini, F., Smith, T.K., 2010. The Kennedy pathway—de novo synthesis of phosphatidylethanolamine and phosphatidylcholine. IUBMB Life 62, 414–428. doi:http://dx.doi.org/10.1002/iub.337.

Gibson, M.C., Perrimon, N., 2003. Apicobasal polarization: epithelial form and function. Curr. Opin. Cell Biol. 15, 747–752.

Gill, C.O., 1975. Effect of growth temperature on the lipids of *Pseudomonas fluorescens*. J. Gen. Microbiol. 89, 293–298. doi:http://dx.doi.org/10.1099/00221287-89-2-293.

Gotoh, N., Wakebe, H., Nishino, T., 1989. Ultrastructural aspects of fragility of Pseudomonas aeruginosa outer membrane devoid of protein F. FEMS Microbiol. Lett. 50, 51–53.

Gould, T.A., Schweizer, H.P., Churchill, M.E.A., 2004. Structure of the *Pseudomonas aeruginosa* acyl-homoserinelactone synthase LasI. Mol. Microbiol. 53, 1135–1146. doi:http://dx.doi.org/10.1111/j.1365-2958.2004.04211.x.

Guchhait, R.B., Polakis, S.E., Dimroth, P., Stoll, E., Moss, J., Lane, M.D., 1974. Acetyl Coenzyme A carboxylase system of *Escherichia coli*. Purification and properties of the biotin carboxylase, carboxyltransferase, and carboxyl carrier protein components. J. Biol. Chem. 249, 6633–6645.

Gunderson, B.W., Ibrahim, K.H., Hovde, L.B., Fromm, T.L., Reed, M.D., Rotschafer, J.C., 2003. Synergistic activity of colistin and ceftazidime against multiantibiotic-resistant *Pseudomonas aeruginosa* in an in vitro pharmacodynamic model. Antimicrob. Agents Chemother. 47, 905–909. doi:http://dx.doi.org/10.1128/AAC.47.3 905-909.2003.

Hachicho, N., Hoffmann, P., Ahlert, K., Heipieper, H.J., 2014. Effect of silver nanoparticles and silver ions on growth and adaptive response mechanisms of *Pseudomonas putida* mt-2. FEMS Microbiol. Lett. 355, 71–77. doi:http://dx.doi.org/10.1111/1574-6968.12460.

Ham, H., Sreelatha, A., Orth, K., 2011. Manipulation of host membranes by bacterial effectors. Nat. Rev. Microbiol. 9 doi:http://dx.doi.org/10.1038/nrmicro2602.

Haucke, V., Di Paolo, G., 2007. Lipids and lipid modifications in the regulation of membrane traffic. Curr. Opin. Cell Biol. 19, 426–435. doi:http://dx.doi.org/10.1016/j.ceb.2007.06.003.

Heath, R.J., Rock, C.O., 1995. Enoyl-acyl carrier protein reductase (*fabI*) plays a determinant role in completing cycles of fatty acid elongation in *Escherichia coli*. J. Biol. Chem. 270, 26538–26542. doi:http://dx.doi.org/10.1074/jbc.270.44.26538.

Heath, R.J., White, S.W., Rock, C.O., 2001. Lipid biosynthesis as a target for antibacterial agents. Prog. Lipid Res. 40, 467–497.

Heath, R.J., Jackowski, S., Rock, C.O., 2002a. Fatty acid and phospholipid metabolism in prokaryotes, In: Vance, D.E., Vance, J.E. (Eds.), Biochemistry of Lipids, Lipoproteins and Membranes. fourth ed. Elsevier Science, B.V.

Heath, R.J., White, S.W., Rock, C.O., 2002b. Inhibitors of fatty acid synthesis as antimicrobial chemotherapeutics. Appl. Microbiol. Biotechnol. 58, 695–703. doi:http://dx.doi.org/10.1007/s00253-001-0918-z.

Heipieper, H.J., Fischer, J., 2010. Bacterial solvent responses and tolerance: *cis–trans* isomerization. In: Timmis, K.N. (Ed.), Handbook of Hydrocarbon and Lipid Microbiology. Springer, Berlin, Heidelberg, pp. 4203–4211.

Heipieper, H.J., Meulenbeld, G., van Oirschot, Q., de Bont, J., 1996. Effect of environmental factors on the *trans/cis* ratio of unsaturated fatty acids in *Pseudomonas putida* S12. Appl. Environ. Microbiol. 62, 2773–2777.

Hoang, T.T., Schweizer, H.P., 1999. Characterization of *Pseudomonas aeruginosa* enoyl-acyl carrier protein reductase (FabI): a target for the antimicrobial triclosan and its role in acylated homoserine lactone synthesis. J. Bacteriol. 181, 5489–5497.

Hoang, T.T., Schweizer, H.P., 1997. Fatty acid biosynthesis in *Pseudomonas aeruginosa*: cloning and characterization of the *fabAB* operon encoding beta-hydroxyacyl-acyl carrier protein dehydratase (FabA) and beta-ketoacyl-acyl carrier protein synthase I (FabB). J. Bacteriol. 179, 5326–5332.

Holder, J.W., Ulrich, J.C., DeBono, A.C., Godfrey, P.A., Desjardins, C.A., Zucker, J., Zeng, Q., Leach, A.L.B., Ghiviriga, I., Dancel, C., Abeel, T., Gevers, D., Kodira, C.D., Desany, B., Affourtit, J.P., Birren, B.W., Sinskey, A.J., 2011. Comparative and functional genomics of *Rhodococcus opacus* PD630 for biofuels development. PLoS Genet. 7, e1002219. doi:http://dx.doi.org/10.1371/journal.pgen.1002219.

Huang, W., Jia, J., Edwards, P., Dehesh, K., Schneider, G., Lindqvist, Y., 1998. Crystal structure of beta-ketoacyl-acyl carrier protein synthase II from *E. coli* reveals the molecular architecture of condensing enzymes. EMBO J. 17, 1183–1191. doi:http://dx.doi.org/10.1093/emboj/17.5.1183.

Jackson, A.A., Gross, M.J., Daniels, E.F., Hampton, T.H., Hammond, J.H., Vallet-Gely, I., Dove, S.L., Stanton, B.A., Hogan, D.A., 2013. Anr and its activation by PlcH activity in *Pseudomonas aeruginosa* host colonization and virulence. J. Bacteriol. 195, 3093–3104. doi:http://dx.doi.org/10.1128/JB.2169-12.

Janek, T., Łukaszewicz, M., Rezanka, T., Krasowska, A., 2010. Isolation and characterization of two new lipopeptide biosurfactants produced by *Pseudomonas fluorescens* BD5 isolated from water from the Arctic Archipelago of Svalbard. Bioresour. Technol. 101, 6118–6123. doi:http://dx.doi.org/10.1016/j.biortech.2010.02.109.

Jiang, F., Waterfield, N.R., Yang, J., Yang, G., Jin, Q., 2014. A *Pseudomonas aeruginosa* type VI secretion phospholipase D effector targets both prokaryotic and eukaryotic cells. Cell Host Microbe 15, 600–610. doi:http://dx.doi.org/10.1016/j.chom.2014.04.010.

Joardar, V., Lindeberg, M., Jackson, R.W., Selengut, J., Dodson, R., Brinkac, L.M., Daugherty, S.C., DeBoy, R., Durkin, A.S., Giglio, M.G., Madupu, R., Nelson, W.C., Rosovitz, M.J., Sullivan, S., Crabtree, J., Creasy, T., Davidsen, T., Haft, D.H., Zafar, N., Zhou, L., Halpin, R., Holley, T., Khouri, H., Feldblyum, T., White, O., Fraser, C.M., Chatterjee, A.K., Cartinhour, S., Schneider, D.J., Mansfield, J., Collmer, A., Buell, C. R., 2005. Whole-genome sequence analysis of *Pseudomonas syringae* pv. phaseolicola 1448A reveals divergence among pathovars in genes involved in virulence and transposition. J. Bacteriol. 187, 6488–6498. doi:http://dx.doi.org/10.1128/JB.187.18.

Johansen, T., Bjørkøy, G., Overvatn, A., Diaz-Meco, M.T., Traavik, T., Moscat, J., 1994. NIH 3T3 cells stably transfected with the gene encoding phosphatidylcholine-hydrolyzing phospholipase C from *Bacillus cereus* acquire a transformed phenotype. Mol. Cell. Biol. 14, 646–654.

Jones, C., Allsopp, L., Horlick, J., Kulasekara, H., Filloux, A., 2013. Subinhibitory concentration of kanamycin induces the *Pseudomonas aeruginosa* type VI secretion system. PLoS ONE 8 doi:http://dx.doi.org/10.1371/journal.pone.0081132.

Kaneshiro, T., Law, J.H., 1964. Phosphatidylcholine synthesis in *Agrobacterium tumefaciens*. Purification and properties of a phosphatidylethanolamine *N*-methyltransferase. J. Biol. Chem. 239, 1705–1713.

Kanfer, J., Kennedy, E.P., 1964. Metabolism and function of bacterial lipids. II. Biosynthesis of phospholipids in *Escherichia colli*. J. Biol. Chem. 239, 1720–1726.

Kanfer, J., Kennedy, E.P., 1963. Metabolism and function of bacterial lipids. I. Biosynthesis of phospholipids in *Escherichia colli*. J. Biol. Chem. 238, 2919–2922.

Kates, M., Syz, J.Y., Gosser, D., Haines, T.H., 1993. pH-Dissociation characteristics of cardiolipin and its 2′-deoxy analogue. Lipids 28, 877–882.

Keweloh, H., Heipieper, H.J., 1996. Trans unsaturated fatty acids in bacteria. Lipids 31, 129–137.

Kiely, P.D., Haynes, J.M., Higgins, C.H., Franks, A., Mark, G.L., Morrissey, J.P., O'Gara, F., 2006. Exploiting new systems-based strategies to elucidate plant-bacterial interactions in the rhizosphere. Microb. Ecol. 51, 257–266. doi:http://dx.doi.org/10.1007/s00248-006-9019-y.

Kierbel, A., Gassama-Diagne, A., Mostov, K., Engel, J.N., 2005. The phosphoinositol-3-kinase-protein kinase B/Akt pathway is critical for Pseudomonas aeruginosa strain PAK internalization. Mol. Biol. Cell 16, 2577–2585. doi:http://dx.doi.org/10.1091/mbc.E04-08-0717.

Kierbel, A., Gassama-Diagne, A., Rocha, C., Radoshevich, L., Olson, J., Mostov, K., Engel, J., 2007. *Pseudomonas aeruginosa* exploits a PIP3-dependent pathway to transform apical into basolateral membrane. J. Cell Biol. 177, 21–27. doi:http://dx.doi.org/10.1083/jcb.200605142.

Kikuchi, S., Shibuya, I., Matsumoto, K., 2000. Viability of an *Escherichia coli pgsA* null mutant lacking detectable phosphatidylglycerol and cardiolipin. J. Bacteriol. 182, 371–376.

Kimber, M.S., Martin, F., Lu, Y., Houston, S., Vedadi, M., Dharamsi, A., Fiebig, K.M., Schmid, M., Rock, C.O., 2004. The structure of (3R)-hydroxyacyl-acyl carrier protein dehydratase (FabZ) from *Pseudomonas aeruginosa*. J. Biol. Chem. 279, 52593–52602. doi:http://dx.doi.org/10.1074/jbc.M408105200.

Kondakova, T., Merlet-Machour, N., Chapelle, M., Preterre, D., Dionnet, F., Feuilloley, M., Orange, N., Duclairoir Poc, C., 2014. A new study of the bacterial lipidome: HPTLC-MALDI-TOF imaging enlightening the presence of phosphatidylcholine in airborne *Pseudomonas fluorescens* MFAF76a. Res. Microbiol. doi:http://dx.doi.org/10.1016/j.resmic.2014.11.003.

Kondo, H., Shiratsuchi, K., Yoshimoto, T., Masuda, T., Kitazono, A., Tsuru, D., Anai, M., Sekiguchi, M., Tanabe, T., 1991. Acetyl-CoA carboxylase from *Escherichia coli*: gene organization and nucleotide sequence of the biotin carboxylase subunit. Proc. Natl. Acad. Sci. U. S. A. 88, 9730–9733.

Kozloff, L.M., Lute, M., Westaway, D., 1984. Phosphatidylinositol as a component of the ice nucleating site of *Pseudomonas syringae* and *Erwinia herbiola*. Science 226, 845–846. doi:http://dx.doi.org/10.1126/science.226.4676.845.

Kutchma, A.J., Hoang, T.T., Schweizer, H.P., 1999. Characterization of a *Pseudomonas aeruginosa* fatty acid biosynthetic gene cluster: purification of acyl carrier protein (ACP) and malonyl-coenzyme A:ACP transacylase (FabD). J. Bacteriol. 181, 5498–5504.

Lai, C.-Y., Cronan, J.E., 2003. β-Ketoacyl-acyl carrier protein synthase III (FabH) is essential for bacterial fatty acid synthesis. J. Biol. Chem. 278, 51494–51503. doi:http://dx.doi.org/10.1074/jbc.M308638200.

Larson, T.J., Ludtke, D.N., Bell, R.M., 1984. *sn*-Glycerol-3-phosphate auxotrophy of *plsB* strains of *Escherichia coli*: evidence that a second mutation, *plsX*, is required. J. Bacteriol. 160, 711–717.

Lindgren, V., Holmgren, E., Rutberg, L., 1977. *Bacillus subtilis* mutant with temperature-sensitive net synthesis of phosphatidylethanolamine. J. Bacteriol. 132, 473–484.

Lisa, T.A., Garrido, M.N., Domenech, C.E., 1983. Induction of acid phosphatase and cholinesterase activities in *Ps. aeruginosa* and their *in-vitro* control by choline, acetylcholine and betaine. Mol. Cell. Biochem. 50, 149–155.

Li, S.J., Cronan, J.E., 1992. The gene encoding the biotin carboxylase subunit of *Escherichia coli* acetyl-CoA carboxylase. J. Biol. Chem. 267, 855–863.

Lodise, T.P., Lomaestro, B., Drusano, G.L., 2007. Piperacillin-tazobactam for *Pseudomonas aeruginosa* infection: clinical implications of an extended-infusion dosing strategy. Clin. Infect. Dis. 44, 357–363. doi:http://dx.doi.org/10.1086/510590.

Loper, J.E., Hassan, K.A., Mavrodi, D.V., Davis II, E.W., Lim, C.K., Shaffer, B.T., Elbourne, L.D.H., Stockwell, V.O., Hartney, S.L., Breakwell, K., Henkels, M.D., Tetu, S.G., Rangel, L.I., Kidarsa, T.A., Wilson, N.L., van de Mortel, J.E., Song, C., Blumhagen, R., Radune, D., Hostetler, J.B., Brinkac, L.M., Durkin, A.S., Kluepfel, D.A., Wechter, W. P., Anderson, A.J., Kim, Y.C., III, Lindow, S.E., Kobayashi, D.Y., Raaijmakers, J.M., Weller, D.M., Thomashow, L.S., Allen, A.E., Paulsen, I.T., 2012. Comparative genomics of plant-associated *Pseudomonas* spp.: insights into diversity and inheritance of traits involved in multitrophic interactions. PLoS Genet. 8, e1002784. doi:http://dx.doi.org/10.1371/journal.pgen.1002784.

Lu, Y.-J., Zhang, F., Grimes, K.D., Lee, R.E., Rock, C.O., 2007. Topology and active site of PlsY: the bacterial acylphosphate: glycerol-3-phosphate acyltransferase. J. Biol. Chem. 282, 11339–11346. doi:http://dx.doi.org/10.1074/jbc.M700374200.

Lu, Y.-J., Zhang, Y.-M., Grimes, K.D., Qi, J., Lee, R.E., Rock, C.O., 2006. Acyl-phosphates initiate membrane phospholipid synthesis in Gram-positive pathogens. Mol. Cell 23, 765–772. doi:http://dx.doi.org/10.1016/j.molcel.2006.06.030.

Mansilla, M.C., Cybulski, L.E., Albanesi, D., de Mendoza, D., 2004. Control of membrane lipid fluidity by molecular thermosensors. J. Bacteriol. 186, 6681–6688. doi:http://dx.doi.org/10.1128/JB.186.20.6681-6688.

Marcinkeviciene, J., Jiang, W., Kopcho, L.M., Locke, G., Luo, Y., Copeland, R.A., 2001. Enoyl-ACP reductase (FabI) of Haemophilus influenzae: steady-state kinetic mechanism and inhibition by triclosan and hexachlorophene. Arch. Biochem. Biophys. 390, 101–108. doi:http://dx.doi.org/10.1006/abbi.2001.2349.

Martínez-Morales, F., Schobert, M., López-Lara, I.M., Geiger, O., 2003. Pathways for phosphatidylcholine biosynthesis in bacteria. Microbiology 149, 3461–3471. doi:http://dx.doi.org/10.1099/mic.026522-0.

Massengo-Tiassé, R.P., Cronan, J.E., 2008. *Vibrio cholerae* FabV defines a new class of enoyl-acyl carrier protein reductase. J. Biol. Chem. 283, 1308–1316. doi:http://dx.doi.org/10.1074/jbc.M708171200.

Mavrodi, D.V., Joe, A., Mavrodi, O.V., Hassan, K.A., Weller, D.M., Paulsen, I.T., Loper, J. E., Alfano, J.R., Thomashow, L.S., 2011. Structural and functional analysis of the type III secretion system from *Pseudomonas fluorescens* Q8r1-96. J. Bacteriol. 193, 177–189. doi:http://dx.doi.org/10.1128/JB.895-10.

McCann, H.C., Rikkerink, E.H.A., Bertels, F., Fiers, M., Lu, A., Rees-George, J., Andersen, M.T., Gleave, A.P., Haubold, B., Wohlers, M.W., Guttman, D.S., Wang, P.W., Straub, C., Vanneste, J., Rainey, P.B., Templeton, M.D., 2013. Genomic analysis of the kiwifruit pathogen *Pseudomonas syringae* pv. actinidiae provides insight into the origins of an emergent plant disease. PLoS Pathog. 9, e1003503. doi:http://dx.doi.org/10.1371/journal.ppat.1003503.

McMurry, L.M., Oethinger, M., Levy, S.B., 1998. Triclosan targets lipid synthesis. Nature 394, 531–532. doi:http://dx.doi.org/10.1038/28970.
Mena, K.D., Gerba, C.P., 2009. Risk assessment of *Pseudomonas aeruginosa* in water. Rev. Environ. Contam. Toxicol. 201, 71–115. doi:http://dx.doi.org/10.1007/978-1-4419-0032-6_3.
Michell, R.H., 2007. Evolution of the diverse biological roles of inositols. Biochem. Soc. Symp. 223–246. doi:http://dx.doi.org/10.1042/BSS0740223.
Mileykovskaya, E., Dowhan, W., 2009. Cardiolipin membrane domains in prokaryotes and eukaryotes. Biochim. Biophys. Acta 1788, 2084–2091. doi:http://dx.doi.org/10.1016/j.bbamem.2009.04.003 Biomembr., Includes Special Section: Cardiolipin.
Mileykovskaya, E., Dowhan, W., 2005. Role of membrane lipids in bacterial division-site selection. Curr. Opin. Microbiol. 8, 135–142. doi:http://dx.doi.org/10.1016/j.mib.2005.02.012.
Mileykovskaya, E., Dowhan, W., 1997. The Cpx two-component signal transduction pathway is activated in *Escherichia coli* mutant strains lacking phosphatidylethanolamine. J. Bacteriol. 179, 1029–1034.
Miller, D.J., Zhang, Y.-M., Subramanian, C., Rock, C.O., White, S.W., 2010. Structural basis for the transcriptional regulation of membrane lipid homeostasis. Nat. Struct. Mol. Biol. 17, 971–975. doi:http://dx.doi.org/10.1038/nsmb.1847.
Minder, A.C., De Rudder, K.E.E., Narberhaus, F., Fischer, H.-M., Hennecke, H., Geiger, O., 2001. Phosphatidylcholine levels in Bradyrhizobium japonicum membranes are critical for an efficient symbiosis with the soybean host plant. Mol. Microbiol. 39, 1186–1198. doi:http://dx.doi.org/10.1111/j1365-2958.2001.02325.x.
Mohan, S., Kelly, T.M., Eveland, S.S., Raetz, C.R., Anderson, M.S., 1994. An *Escherichia coli* gene (FabZ) encoding (3R)-hydroxymyristoyl acyl carrier protein dehydrase. Relation to *fabA* and suppression of mutations in lipid A biosynthesis. J. Biol. Chem. 269 (32), 896–32903.
Morris, C.E., Kinkel, L.L., Xiao, K., Prior, P., Sands, D.C., 2007. Surprising niche for the plant pathogen *Pseudomonas syringae*. Infect. Genet. Evol. 7, 84–92. doi:http://dx.doi.org/10.1016/j.meegid.2006.05.002.
Morris, C.E., Sands, D.C., Vinatzer, B.A., Glaux, C., Guilbaud, C., Buffière, A., Yan, S., Dominguez, H., Thompson, B.M., 2008. The life history of the plant pathogen *Pseudomonas syringae* is linked to the water cycle. ISME J. 2, 321–334. doi:http://dx.doi.org/10.1038/ismej.2007.113.
Mulet, M., Lalucat, J., García-Valdés, E., 2010. DNA sequence-based analysis of the *Pseudomonas* species. Environ. Microbiol. 12, 1513–1530. doi:http://dx.doi.org/10.1111/j.1462-2920.2010.02181.x.
Murzyn, K., Rog, T., Pasenkiewicz-Gierula, M., 2005. Phosphatidylethanolamine-phosphatidylglycerol bilayer as a model of the inner bacterial membrane. Biophys. J. 88, 1091–1103. doi:http://dx.doi.org/10.1529/biophysj.104.048835.
Nikaido, H., 2003. Molecular basis of bacterial outer membrane permeability revisited. Microbiol. Mol. Biol. Rev. 67, 593–656. doi:http://dx.doi.org/10.1128/MMBR.67.4.593-656.2003.
Obritsch, M.D., Fish, D.N., MacLaren, R., Jung, R., 2005. Nosocomial infections due to multidrug-resistant *Pseudomonas aeruginosa*: epidemiology and treatment options. Pharmacotherapy 25, 1353–1364. doi:http://dx.doi.org/10.1592/phco.2005.25.10.1353.
Olsen, J.G., Kadziola, A., von Wettstein-Knowles, P., Siggaard-Andersen, M., Lindquist, Y., Larsen, S., 1999. The X-ray crystal structure of beta-ketoacyl [acyl carrier protein] synthase I. FEBS Lett. 460, 46–52.
Ostroff, R.M., Wretlind, B., Vasil, M.L., 1989. Mutations in the hemolytic-phospholipase C operon result in decreased virulence of *Pseudomonas aeruginosa* PAO1 grown under phosphate-limiting conditions. Infect. Immun. 57, 1369–1373.
Ouberai, M., El Garch, F., Bussiere, A., Riou, M., Alsteens, D., Lins, L., Baussanne, I., Dufrêne, Y.F., Brasseur, R., Decout, J.-L., Mingeot-Leclercq, M.-P., 2011. The *Pseudomonas aeruginosa* membranes: a target for a new amphiphilic aminoglycoside derivative. Biochim. Biophys. Acta 1808, 1716–1727. doi:http://dx.doi.org/10.1016/j.bbamem.2011.01.014.
Palleroni, N.J., 2010. The *Pseudomonas* story. Environ. Microbiol. 12, 1377–1383. doi:http://dx.doi.org/10.1111/j.1462-2920.2009.02041.x.
Parsons, J.B., Rock, C.O., 2013. Bacterial lipids: metabolism and membrane homeostasis. Prog. Lipid Res. 52, 249–276. doi:http://dx.doi.org/10.1016/j.plipres.2013.02.002.
Payne, D.J., Warren, P.V., Holmes, D.J., Ji, Y., Lonsdale, J.T., 2001. Bacterial fatty-acid biosynthesis: a genomics-driven target for antibacterial drug discovery. Drug Discov. Today 6, 537–544.
Pepi, M, Heipieper, H.J., Fischer, J., Ruta, M., Volterrani, M., Focardi, S.E., 2008. Membrane fatty acids adaptive profile in the simultaneous presence of arsenic and toluene in *Bacillus* sp. ORAs2 and *Pseudomonas* sp. ORAs5 strains. Extremophiles 12, 343–349. doi:http://dx.doi.org/10.1007/s00792-008-0147-9.
Price, A.C., Zhang, Y.M., Rock, C.O., White, S.W., 2001. Structure of beta-ketoacyl-[acyl carrier protein] reductase from *Escherichia coli*: negative cooperativity and its structural basis. Biochemistry 40, 12772–12781 (Mosc.).
Qiu, X., Janson, C.A., Konstantinidis, A.K., Nwagwu, S., Silverman, C., Smith, W.W., Khandekar, S., Lonsdale, J., Abdel-Meguid, S.S., 1999. Crystal structure of β-ketoacyl-acyl carrier protein synthase III: a key condensing enzyme in bacterial fatty acid biosynthesis. J. Biol. Chem. 274, 36465–36471. doi:http://dx.doi.org/10.1074/jbc.274.51.36465.
Raetz, C.R., Reynolds, C.M., Trent, M.S., Bishop, R.E., 2007. Lipid A modification systems in gram-negative bacteria. Annu. Rev. Biochem. 76, 295–329. doi:http://dx.doi.org/10.1146/annurev.biochem.76.010307.145803.
Rafferty, J.B., Simon, J.W., Baldock, C., Artymiuk, P.J., Baker, P.J., Stuitje, A.R., Slabas, A.R., Rice, D.W., 1995. Common themes in redox chemistry emerge from the X-ray of oilseed rape (*Brassica napus*) enoyl acyl carrier protein reductase. Structure 3, 927–938 (Lond. Engl.).
Ramos, J.L., Duque, E., Rodríguez-Herva, J.-J., Godoy, P., Haïdour, A., Reyes, F., Fernández-Barrero, A., 1997. Mechanisms for solvent tolerance in bacteria. J. Biol. Chem. 272, 3887–3890. doi:http://dx.doi.org/10.1074/jbc.272.7.3887.
Ramos, J.-L., Filloux, A., 2007. Pseudomonas: A Model System in Biology, vol. 5. Springer.
Ren, Q., Sierro, N., Witholt, B., Kessler, B., 2000. FabG, an NADPH-dependent 3-ketoacyl reductase of Pseudomonas aeruginosa, provides precursors for medium-chain-length poly-3-hydroxyalkanoate biosynthesis in Escherichia coli. J. Bacteriol. 2000, 2978–2981. doi:http://dx.doi.org/10.1128/JB.182.102978-2981.2000.
Ringen, L.M., Drake, C.H., 1952. A study of the incidence of *Pseudomonas aeruginosa* from various natural sources. J. Bacteriol. 64, 841–845.
Rock, C.O., Goelz, S.E., Cronan, J.E., 1981. Phospholipid synthesis in *Escherichia coli*. Characteristics of fatty acid transfer from acyl-acyl carrier protein to *sn*-glycerol 3-phosphate. J. Biol. Chem. 256, 736–742.
Romantsov, T., Helbig, S., Culham, D.E., Gill, C., Stalker, L., Wood, J.M., 2007. Cardiolipin promotes polar localization of osmosensory transporter ProP in *Escherichia coli*. Mol. Microbiol. 64, 1455–1465. doi:http://dx.doi.org/10.1111/j.1365-2958.2007.05727.x.
Röttig, A., Steinbüchel, A., 2013. Acyltransferases in bacteria. Microbiol. Mol. Biol. Rev. 77, 277–321. doi:http://dx.doi.org/10.1128/MMBR.10-13.
Roujeinikova, A., Sedelnikova, S., de Boer, G.-J., Stuitje, A.R., Slabas, A.R., Rafferty, J.B., Rice, D.W., 1999. Inhibitor binding studies on enoyl reductase reveal conformational changes related to substrate recognition. J. Biol. Chem. 274, 30811–30817. doi:http://dx.doi.org/10.1074/jbc.274.43.30811.
Rühl, J., Hein, E.-M., Hayen, H., Schmid, A., Blank, L.M., 2012. The glycerophospholipid inventory of *Pseudomonas putida* is conserved between strains and enables growth condition-related alterations. Microb. Biotechnol. 5, 45–58. doi:http://dx.doi.org/10.1111/j.1751-7915.2011.00286.x.
Russell, A.B., LeRoux, M., Hathazi, K., Agnello, D.M., Ishikawa, T., Wiggins, P.A., Wai, S.N., Mougous, J.D., 2013. Diverse type VI secretion phospholipases are functionally plastic antibacterial effectors. Nature 496, 508–512. doi:http://dx.doi.org/10.1038/nature12074.
Sabuda, D.M., Laupland, K., Pitout, J., Dalton, B., Rabin, H., Louie, T., Conly, J., 2008. Utilization of colistin for treatment of multidrug-resistant Pseudomonas aeruginosa. Can. J. Infect. Dis. Med. Microbiol. 19, 413–418.
Sage, A.E., Vasil, M.L., 1997. Osmoprotectant-dependent expression of plcH, encoding the hemolytic phospholipase C, is subject to novel catabolite repression control in *Pseudomonas aeruginosa* PAO1. J. Bacteriol. 179, 4874–4881.
Sanyal, S., Menon, A.K., 2009. Flipping lipids: why an' what's the reason for? ACS Chem. Biol. 4, 895–909. doi:http://dx.doi.org/10.1021/cb900163d.
Sato, H., Frank, D.W., 2014. Intoxication of host cells by the T3SS phospholipase ExoU: $PI(4,5)P_2$-associated, cytoskeletal collapse and late phase membrane blebbing. PLoS One 9 doi:http://dx.doi.org/10.1371/journal.pone.0103127.
Schoehn, G., Di Guilmi, A.M., Lemaire, D., Attree, I., Weissenhorn, W., Dessen, A., 2003. Oligomerization of type III secretion proteins PopB and PopD precedes pore formation in *Pseudomonas*. EMBO J. 22, 4957–4967. doi:http://dx.doi.org/10.1093/emboj/cdg499.
Schulert, G.S., Feltman, H., Rabin, S.D.P., Martin, C.G., Battle, S.E., Rello, J., Hauser, A.R., 2003. Secretion of the toxin ExoU is a marker for highly virulent *Pseudomonas aeruginosa* isolates obtained from patients with hospital-acquired pneumonia. J. Infect. Dis. 188, 1695–1706. doi:http://dx.doi.org/10.1086/379372.
Schweizer, H.P., Choi, K.-H., 2011. Pseudomonas aeruginosa aerobic fatty acid desaturase DesB is important for virulence factor production. Arch. Microbiol. 193, 227–234. doi:http://dx.doi.org/10.1007/s00203-010-0665-6.
Shi, W., Bogdanov, M., Dowhan, W., Zusman, D.R., 1993. The pss and psd genes are required for motility and chemotaxis in *Escherichia coli*. J. Bacteriol. 175, 7711–7714.
Six, D.A., Yuan, Y., Leeds, J.A., Meredith, T.C., 2014. Deletion of the β-acetoacetyl synthase FabY in Pseudomonas aeruginosa induces hypoacylation of lipopolysaccharide and increases antimicrobial susceptibility. Antimicrob. Agents Chemother. 58, 153–161. doi:http://dx.doi.org/10.1128/AAC.1804-13.
Sohlenkamp, C., López-Lara, I.M., Geiger, O., 2003. Biosynthesis of phosphatidylcholine in bacteria. Prog. Lipid Res. 42, 115–162. doi:http://dx.doi.org/10.1016/S0163-7827(02) 50-4.
Spencer, C.T., Brown, H.A., 2015. Biochemical characterization of a Pseudomonas aeruginosa phospholipase D. Biochemistry doi:http://dx.doi.org/10.1021/bi501291t (Mosc.).
Srinivas, N., Jetter, P., Ueberbacher, B.J., Werneburg, M., Zerbe, K., Steinmann, J., Van der Meijden, B., Bernardini, F., Lederer, A., Dias, R.L.A., Misson, P.E., Henze, H., Zumbrunn, J., Gombert, F.O., Obrecht, D., Hunziker, P., Schauer, S., Ziegler, U., Käch, A., Eberl, L., Riedel, K., DeMarco, S.J., Robinson, J.A., 2010. Peptidomimetic antibiotics target outer-membrane biogenesis in *Pseudomonas aeruginosa*. Science 327, 1010–1013. doi:http://dx.doi.org/10.1126/science.1182749.
Stanier, R.Y., Palleroni, N.J., Doudoroff, M., 1966. The aerobic pseudomonads a aaxonomic study. J. Gen. Microbiol. 43, 159–271. doi:http://dx.doi.org/10.1099/00221287-43-2-159.
Subramanian, C., Rock, C.O., Zhang, Y.-M., 2010. DesT coordinates the expression of anaerobic and aerobic pathways for unsaturated fatty acid biosynthesis in *Pseudomonas aeruginosa*. J. Bacteriol. 192, 280–285. doi:http://dx.doi.org/10.1128/JB.404-09.

Suller, M.T.E., Russell, A.D., 2000. Triclosan and antibiotic resistance in *Staphylococcus aureus*. J. Antimicrob. Chemother. 46, 11–18. doi:http://dx.doi.org/10.1093/jac/46.1.11.

Sun, Z., Kang, Y., Norris, M.H., Troyer, R.M., Son, M.S., Schweizer, H.P., Dow, S.W., Hoang, T.T., 2014. Blocking phosphatidylcholine utilization in *Pseudomonas aeruginosa*, via mutagenesis of fatty acid, glycerol and choline degradation pathways, confirms the importance of this nutrient source *in vivo*. PLoS One 9 doi:http://dx.doi.org/10.1371/journal.pone.0103778.

Sutterlin, H.A., Zhang, S., Silhavy, T.J., 2014. Accumulation of phosphatidic acid increases vancomycin resistance in *Escherichia coli*. J. Bacteriol. 196, 3214–3220. doi:http://dx.doi.org/10.1128/JB.1876-14.

Suzuki, M., Hara, H., Matsumoto, K., 2002. Envelope disorder of *Escherichia coli* cells lacking phosphatidylglycerol. J. Bacteriol. 184, 5418–5425. doi:http://dx.doi.org/10.1128/JB.184.19 2002.

Szaff, M., Høiby, N., Flensborg, E.W., 1983. Frequent antibiotic therapy improves survival of cystic fibrosis patients with chronic *Pseudomonas aeruginosa* infection. Acta Paediatr. Scand. 72, 651–657. doi:http://dx.doi.org/10.1111/j.1651-2227.1983.tb09789.x.

Tahara, Y., Yamashita, T., Sogabe, A., Ogawa, Y., 1994. Isolation and characterization of *Zymomonas mobilis* mutant defective in phosphatidylethanolamine *N*-methyltransferase. J. Gen. Appl. Microbiol. 40, 389–396.

Tashiro, Y., Inagaki, A., Shimizu, M., Ichikawa, S., Takaya, N., Nakajima-Kambe, T., Uchiyama, H., Nomura, N., 2011. Characterization of phospholipids in membrane vesicles derived from *Pseudomonas aeruginosa*. Biosci. Biotechnol. Biochem. 75, 605–607.

Tyson, G.H., Hauser, A.R., 2013. Phosphatidylinositol 4,5-bisphosphate is a novel coactivator of the Pseudomonas aeruginosa cytotoxin ExoU. Infect. Immun. 81, 2873–2881. doi:http://dx.doi.org/10.1128/IAI.414-13.

Valerius, N.H., Koch, C., Høiby, N., 1991. Prevention of chronic Pseudomonas aeruginosa colonisation in cystic fibrosis by early treatment. The Lancet 338 (8769), 725–726. doi:http://dx.doi.org/10.1016/0140-6736(91)91446-2.

Van der Meer-Janssen, Y.P.M., van Galen, J., Batenburg, J.J., Helms, J.B., 2010. Lipids in host–pathogen interactions: pathogens exploit the complexity of the host cell lipidome. Prog. Lipid Res. 49, 1–26. doi:http://dx.doi.org/10.1016/j.plipres.2009.07.003.

Vanhaesebroeck, B., Alessi, D.R., 2000. The PI3K-PDK1 connection: more than just a road to PKB. Biochem. J. 346 (Pt 3), 561–576.

Vasil, M.L., Ochsner, U.A., 1999. The response of *Pseudomonas aeruginosa* to iron: genetics, biochemistry and virulence. Mol. Microbiol. 34, 399–413. doi:http://dx.doi.org/10.1046/j.1365-2958.1999.01586.x.

Vasil, M.L., Stonehouse, M.J., Vasil, A.I., Wadsworth, S.J., Goldfine, H., Bolcome, R.E., Chan, J., 2009. A complex extracellular sphingomyelinase of *Pseudomonas aeruginosa* inhibits angiogenesis by selective cytotoxicity to endothelial cells. PLoS Pathog. 5 doi:http://dx.doi.org/10.1371/journal.ppat.1000420.

Vromman, F., Subtil, A., 2014. Exploitation of host lipids by bacteria. Curr. Opin. Microbiol. 17, 38–45. doi:http://dx.doi.org/10.1016/j.mib.2013.11.003 Host–microbe interactions: bacteria.

Wang, H., Cronan, J.E., 2004. Functional replacement of the FabA and FabB proteins of *Escherichia coli* fatty acid synthesis by Enterococcus faecalis FabZ and FabF homologues. J. Biol. Chem. 279, 34489–34495. doi:http://dx.doi.org/10.1074/jbc.M403874200.

Wargo, M.J., Gross, M.J., Rajamani, S., Allard, J.L., Lundblad, L.K.A., Allen, G.B., Vasil, M.L., Leclair, L.W., Hogan, D.A., 2011. Hemolytic phospholipase C inhibition protects lung function during *Pseudomonas aeruginosa* infection. Am. J. Respir. Crit. Care Med. 184, 345–354. doi:http://dx.doi.org/10.1164/rccm.201103-0374OC.

White, S.W., Zheng, J., Zhang, Y.-M., Rock, C.O., 2005. The structural biology of type II fatty acid biosynthesis. Annu. Rev. Biochem. 74, 791–831. doi:http://dx.doi.org/10.1146/annurev.biochem.74.082803.133524.

Wilderman, P.J., Vasil, A.I., Johnson, Z., Vasil, M.L., 2001. Genetic and biochemical analyses of a eukaryotic-like phospholipase D of Pseudomonas aeruginosa suggest horizontal acquisition and a role for persistence in a chronic pulmonary infection model. Mol. Microbiol. 39, 291–304. doi:http://dx.doi.org/10.1046/j.1365-2958.2001.02282.x.

Wilderman, P.J., Vasil, A.I., Martin, W.E., Murphy, R.C., Vasil, M.L., 2002. Pseudomonas aeruginosa synthesizes phosphatidylcholine by use of the phosphatidylcholine synthase pathway. J. Bacteriol. 184, 4792–4799. doi:http://dx.doi.org/10.1128/JB.184.17.4792-4799.2002.

Wu, X., Monchy, S., Taghavi, S., Zhu, W., Ramos, J., van der Lelie, D., 2011. Comparative genomics and functional analysis of niche-specific adaptation in Pseudomonas putida. FEMS Microbiol. Rev. 35, 299–323. doi:http://dx.doi.org/10.1111/j.1574-6976.2010.00249.x.

Yoshimura, M., Oshima, T., Ogasawara, N., 2007. Involvement of the YneS/YgiH and PlsX proteins in phospholipid biosynthesis in both Bacillus subtilis and *Escherichia coli*. BMC Microbiol. 7, 69. doi:http://dx.doi.org/10.1186/1471-2180-7-69.

Yuan, Y., Leeds, J.A., Meredith, T.C., 2012a. Pseudomonas aeruginosa directly shunts β-oxidation degradation intermediates into de novo fatty acid biosynthesis. J. Bacteriol. 194, 5185–5196. doi:http://dx.doi.org/10.1128/JB.860-12.

Yuan, Y., Sachdeva, M., Leeds, J.A., Meredith, T.C., 2012b. Fatty acid biosynthesis in *Pseudomonas aeruginosa* is initiated by the FabY class of β-ketoacyl acyl carrier protein synthases. J. Bacteriol. 194, 5171–5184. doi:http://dx.doi.org/10.1128/JB.792-12.

Zhang, Y., Cronan, J.E., 1998. Transcriptional analysis of essential genes of the Escherichia coli fatty acid biosynthesis gene cluster by functional replacement with the analogous *Salmonella typhimurium* gene cluster. J. Bacteriol. 180, 3295–3303.

Zhang, Y.-M., Rock, C.O., 2012. Will the initiator of fatty acid synthesis in Pseudomonas aeruginosa please stand up? J. Bacteriol. 194, 5159–5161. doi:http://dx.doi.org/10.1128/JB.01198-12.

Zhang, Y.-M., Rock, C.O., 2008. Membrane lipid homeostasis in bacteria. Nat. Rev. Microbiol. 6, 222–233. doi:http://dx.doi.org/10.1038/nrmicro1839.

Zhang, Y.-M., White, S.W., Rock, C.O., 2006. Inhibiting bacterial fatty acid synthesis. J. Biol. Chem. 281, 17541–17544. doi:http://dx.doi.org/10.1074/jbc.R600004200.

Zhang, Y.-M., Zhu, K., Frank, M.W., Rock, C.O., 2007. A Pseudomonas aeruginosa transcription factor that senses fatty acid structure. Mol. Microbiol. 66, 622–632. doi:http://dx.doi.org/10.1111/j.1365-2958.2007.05934.x.

Zhao, W., Róg, T., Gurtovenko, A.A., Vattulainen, I., Karttunen, M., 2008. Role of phosphatidylglycerols in the stability of bacterial membranes. Biochimie 90, 930–938. doi:http://dx.doi.org/10.1016/j.biochi.2008.02.025.

Zhu, K., Choi, K.-H., Schweizer, H.P., Rock, C.O., Zhang, Y.-M., 2006. Two aerobic pathways for the formation of unsaturated fatty acids in Pseudomonas aeruginosa. Mol. Microbiol. 60, 260–273. doi:http://dx.doi.org/10.1111/j 1365-2958.2006.05088.x.

Zhu, L., Lin, J., Ma, J., Cronan, J.E., Wang, H., 2010. Triclosan resistance of Pseudomonas aeruginosa PAO1 is due to FabV, a triclosan-resistant enoyl-acyl carrier protein reductase. Antimicrob. Agents Chemother. 54, 689–698. doi:http://dx.doi.org/10.1128/AAC.01152-09.

3.4.4. *P. fluorescens* lipidome adaptation

Environmental changes directly affect structural membrane characteristics (Baysse & O'Gara, 2007). As demonstrated in **Figure 10**, GPs' bilayer forms different phases (*i.e.* a gel phase or a liquid-crystalline phase) (Hazel & Williams, 1990). The normal cell function requires membrane GPs bilayers that are largely fluid, in crystalline lamellar phase (planar bilayer) (Mansilla *et al.*, 2004; Russell *et al.*, 1995).

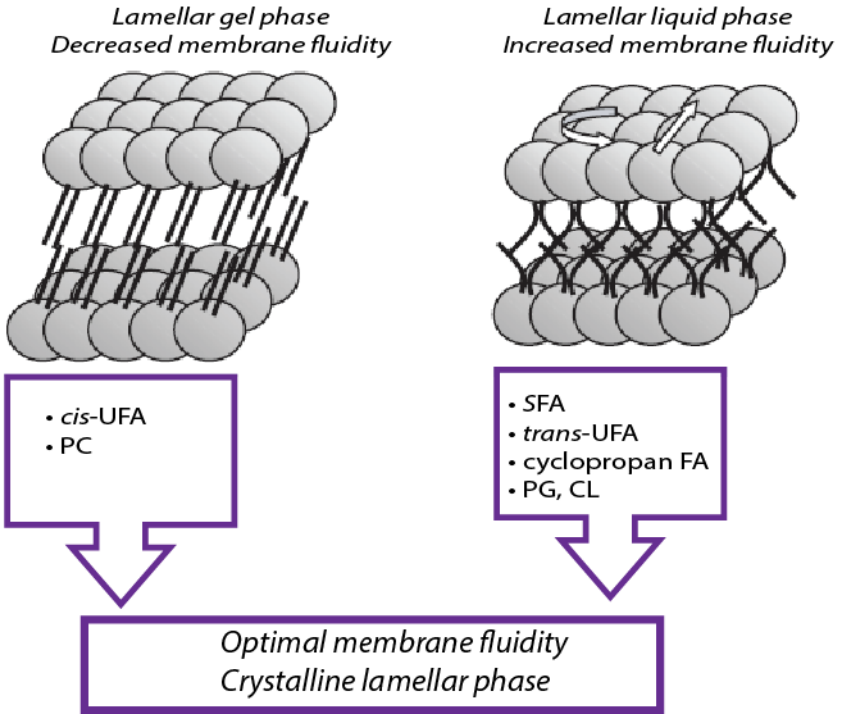

Figure 10. Adaptation of glycerophospholipid structure and composition in *Pseudomonas*
In the lamellar liquid-crystalline state, the lipid molecules are melted and disordered. Upon transition to the gel state, the glycerophospholipids (GPs) become ordered and the frequency of rotation and lateral movement is reduced. Bacteria can regulate their membrane fluidity adjusting the GPs head groups and fatty acids (FAs). In order to increase membrane fluidity, the increasing level of *cis*-unsaturated fatty acids (*cis*-UFAs) and phosphatidylcholine (PC) is required. In contrast, to decrease membrane fluidity, the levels of saturated (SFAs), *trans*-unsaturated (*trans*-UFAs), or cyclopropane FA are increased. Concerning the GP head groups, the increasing of phosphatidylglycerol (PG) and/or cardiolipin (CL) levels negatively regulates membrane fluidity.
Adapted from Baysse and O'Gara, 2007.

Environmental changes can cause the suboptimal membrane fluidity resulting in the subnormal membrane functions. The temperature at the midpoint of this transition is called the transition temperature (T_m), and the change of phase accompanying an increase in temperature is called the lipid phase transition, or most properly, the order-disorder transition. The T_m is a function of the membrane GP composition and mainly depends on the FA composition (Mansilla *et al.*, 2004). The (overly simplified) rule of thumb is that GPs that contain unsaturated fatty acids (UFAs) have much lower T_m than those lipids made of saturated fatty acids (SFAs). The effect is due to different packing of the two types of GP acyl chains as demonstrated in **Table 1**. SFA acyl chains can pack tightly, but the steric hindrance imparted by the rigid kink of the *cis* double bond results in much poorer chain packing of UFAs, even below the phase transition

temperature. The T_m depends also on the glycerophospholipid head group: T_m (CL) > T_m (PE) > T_m (PG) (Rühl *et al.*, 2012).

Table 1. Chemical structures of membrane fatty acids

Fatty acid	Structure	Effect on membrane fluidity
C16:0	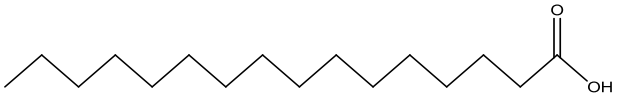	Decreases membrane fluidity
***cis*-C16:1**	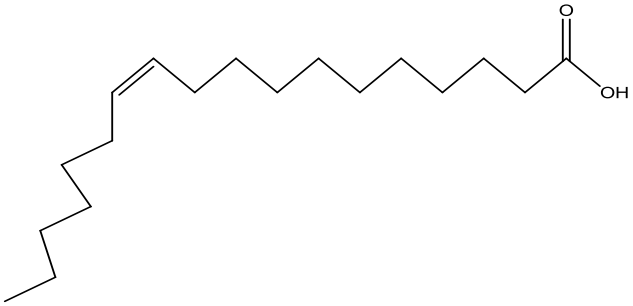	Increases membrane fluidity
***trans*-C16:1**	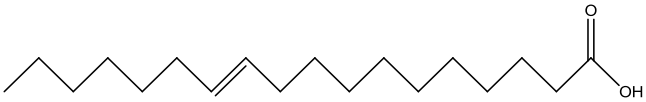	Increases resistance to solvents and temperature
cyclopropane-C17:0	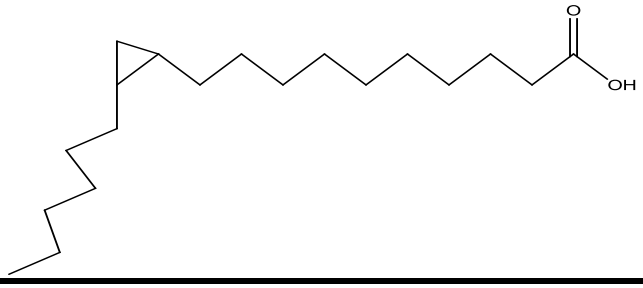	Increases resistance to osmotic stress and solvents

The ratio of GP head groups plays a pivotal role in maintain of optimal membrane properties and results in the balance between zwitterionic or neutral GPs (such as PE) and anionic GP (*i.e.* PG or CL) (Parsons & Rock, 2013). These changes affect the physico-chemical properties of membranes due to the differences in melting temperature between the GP head groups. The increase of the PG level comparing to PE in the membrane, allows the decrease of membrane permeability for lipophilic and polar molecules, and, at the same time, makes membrane more stable. This is because the PG and the CL have a higher transition temperature than PE and are more ordered and less densely packed GPs (Fang *et al.*, 2000; Murzyn *et al.*, 2005). The PC level plays also an important role in membrane properties. The increase of the PC level, comparing to PE, coincides positively with membrane fluidity. Basing on the size of the GP head group relative to the FA chains, the PC increases the membrane fluidity. Giving that the chemical structure of the choline HG is larger, than that of the PE, the PC has a relatively similar area of head group compared to FA chains. In contrast, the PE decreases the membrane fluidity, because the HG of PE is smaller, than the FA chains, resulting in a larger area of FA chains relative to the HG (Fajardo *et al.*, 2011).

From these considerations, it seems to be clear, that bacteria and the most (if not all) poikilothermic organisms must regulate their membrane fluidity in response to environmental modifications. For this, the members of genus *Pseudomonas* have various pathways, several examples of which will be discussed below.

Control of fatty acid *de novo* synthesis

The control at the level of FAS is crucial for membrane homeostasis, because the biophysical properties of bacterial membrane are determined in large part by the composition of the FAs that are produced by *de novo* synthesis (Zhang & Rock, 2008). In this way, the long-chain acyl-ACP (see part **3.4.3. Glycerophospholipid synthesis and functions in *Pseudomonas***) plays a role of a key regulator of the FAS. In *Pseudomonas* spp., the three most significant enzymes are regulated by acyl-ACP: ACC, FabH and FabI. The ACC activity is inhibited by the long-chain acyl-ACP (Davis & Cronan, 2001) and lower ACC activity decreases the quantity of malonate groups essential for the initiation and the elongation steps of FAS. The acyl-ACP-mediated inhibition of catalytic activity of FabH prevents the initiation of new acyl-chains and, as consequence, limits the production of FAs (Heath & Rock, 1996a). The FabI catalytic activity, involved in the FA elongation, is also inhibited by acyl-ACP that could also reduce the total rate of bacterial FAs (Heath & Rock, 1996b). However, it should be noted, that *P. aeruginosa* possesses the FabY and FabV enzymes (see part **3.4.3. Glycerophospholipid synthesis and functions in *Pseudomonas***), and the regulation of *de novo* FA synthesis in this bacterium could be more complex than in other *Pseudomonas* spp. species. The intracellular acyl-ACP level is controlled by PslB enzyme, which, in turn, is regulated by guanosine 3',5'-bispyrophosphate (ppGpp) (Wahl *et al.*, 2011). The ppGpp is a global regulator of gene expression and RNA synthesis in bacteria (Poole, 2012; Zhang & Rock, 2008), responsible also to peptidoglycan production and antibiotic resistance (Nguyen *et al.*, 2011). It should be nevertheless noted, that only growing *Pseudomonas* cells can modify their GP and FA composition by *de novo* synthesis (Diefenbach & Keweloh, 1994).

Regulation of membrane biophysical properties

As previously demonstrated, the mainly studied membrane regulation pathway in *Pseudomonas* spp. strains is based on the FAs modifications (Heipieper & Fischer, 2010; Pepi *et al.*, 2008; Zhang & Rock, 2008). Several physico-chemical factors (*i.e.* contamination by organic solvents or increasing temperature) can increase the membrane fluidity. To maintain the optimal membrane functions, this increase is regulated by the production of SFAs. The GPs containing 16:0 SFAs display a transition temperature that is higher than those of the 16:1 *cis*-UFAs (Heipieper *et al.*, 2003; Zhang & Rock, 2008). The double bond of a *cis*-UFA causes an unmovable 30° bend in the acyl chain as presented in **Table 1** and **Figure 11** (Roach *et al.*,

2004), leading to the increase of the membrane fluidity. The SFA/UFA ratio is commonly quantified by the degree of FA saturation (Heipieper *et al.*, 1996). The pathways, including FabAB and Des enzymes for synthesis of UFA, are discussed in the part **3.4.3. Glycerophospholipid synthesis and functions in *Pseudomonas*** and will not be included below.

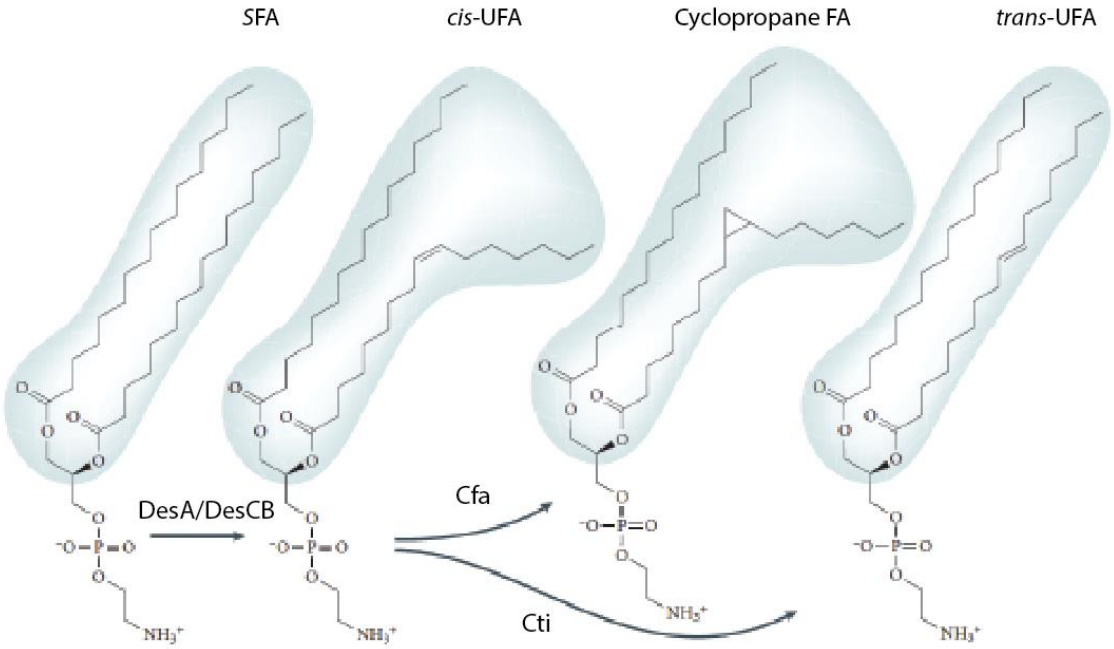

Figure 11. Modifications of fatty acids structure in *Pseudomonas* spp.
Bacteria can introduce a double bond into a saturated fatty acid (SFA) increasing membrane fluidity, via catalytic properties of Des enzymes. The rigid *cis*- double bond, introduces a pronounced kink of 30° in the acyl chain. GPs that contain *cis*-unsaturated fatty acids (*cis*-UFAs) occupy a greater molecular volume (blue shading) and do not pack as densely in the bilayer as GPs that contain SFAs. The cyclopropane FAs (a methyl group introduction across the double bond) formed by Cfa catalysis, have similar biophysical properties to the *cis*-UFAs, but render the membrane more stable to environmental insults. *Pseudomonas* cells can replace a *cis*-double bond with a *trans*-double bond via a mechanism, catalyzed by Cti isomerase. The *trans*-UFAs have properties that resemble SFAs, but give rise to the membranes that have higher transition temperatures. Phosphatidylethanolamine modifications are shown as an example.
Adapted from Zhang and Rock, 2008.

The conversion of *cis*- to *trans*-UFAs is an another adaptive mechanism documented for several *Pseudomonas* spp. species, enabling bacteria to decrease their membrane fluidity, (Heipieper *et al.*, 2003; Heipieper & Fischer, 2010). The advantage of the conversion is due to steric differences between *cis*- and *trans*-UFAs (**Figure 11**, **Table 1**). Contrary to the *cis*-UFA, the steric structure of the *trans*-configuration lacks the kink in the FA chain and is able to insert into the membrane as for the SFAs (Roach *et al.*, 2004). The conversion from the *cis*- to the *trans*-unsaturated double bond does not have the same quantitative effect on membrane fluidity as the conversion to SFAs, but still substantially influences the rigidity of the membrane, as illustrated in **Figure 12** (Heipieper *et al.*, 2003).

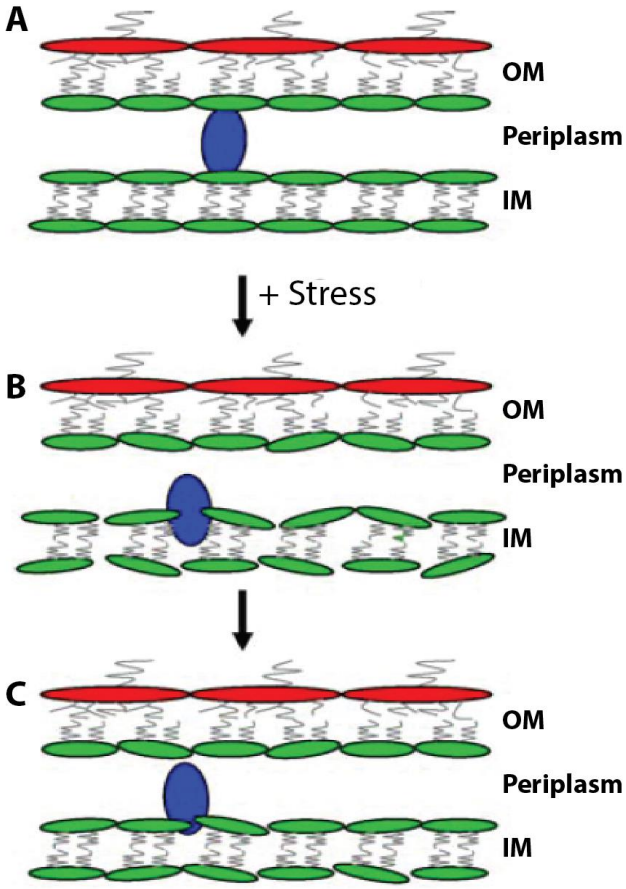

Figure 12. Schematic model of regulation of the Cti enzymatic mechanism by membrane fluidity

A. Without stress condition, the UFAs are in *cis*-configuration and the hydrophilic Cti cannot enter the rigid membrane. **B.** Several stress factors can increase the membrane fluidity. In this way, Cti enters bacterial membrane and interacts with its targets, *cis*-UFAs. **C.** Cti catalyzes the isomerization of *cis*- to *trans*-UFAs, reducing the membrane fluidity. The optimized fluidity leads to the release of Cti from the membrane. OM Outer membrane, IM Inner membrane, Green Glycerophospholipids, Red Lipid A, *Blue* Cti.
According Heipieper et al., 2003.

Besides FabA and FabZ enzymes discussed previously (see part **3.4.3. Glycerophospholipid synthesis and functions in *Pseudomonas***), the *cis–trans*-isomerase (Cti) was described in several *Pseudomonas* species (Holtwick *et al.*, 1999; Pedrotta & Witholt, 1999), including *P. fluorescens* (Heipieper *et al.*, 2003). It is a constitutively expressed periplasmic enzyme that, to exert its action, necessitates neither adenosine triphosphate (ATP) nor other cofactors, and consistently, is independent of the *de novo* FAS.

In several conditions, *Pseudomonas* spp. are able to form the cyclopropane FA (a methyl group across the double bond to form a cyclopropane ring, as presented in **Table 1** and **Figure 11**). The required methylation reaction is carried out by cyclopropane FA synthase (Cfa), which uses S-adenosylmethionine as the methyl donor to create the cyclopropane group. Studies of acyl chain dynamics by nuclear magnetic resonance spectroscopy (NMR) indicate that the cyclopropane rings restrict the overall mobility and the disorder of the acyl chain between the *cis* segment and the polar HG, compared to the *cis*- double bonds (Chang & Cronan, 1999; Dufourc *et al.*, 1983). The cyclopropane FAs have similar biophysical properties to the UFAs, but render the membrane more stable to environmental insults, such as acid stress (Zhang & Rock, 2008). Recent investigations, used molecular dynamics simulation showed, that the cyclopropane FAs may fulfill a dual function: stabilizing membranes against adverse conditions while simultaneously promoting their fluidity. Marked differences in the effect of *cis*- and

trans-cyclopropanated FAs were also observed, suggesting that they may play alternative roles in membranes (Poger & Mark, 2015).

Control of membrane glycerophospholipid composition

The GP homeostasis is controlled by the biochemical regulation of enzymes, which are previously discussed in the part **3.4.3. Glycerophospholipid synthesis and functions in *Pseudomonas***. The importance of maintaining the GP balance is illustrated by strains defective in genes, coding for GP synthesis and results in defects in solute and electron transport, the initiation of DNA replication or cell division (Zhang & Rock, 2008). For example, the PS synthase, PssA, is an extrinsic membrane protein that associated with, and activated by, membrane PG and CL (Linde *et al.*, 2004; Salamon *et al.*, 2000). Thus, the proportion of PE increases, the membrane association and activity of PssA decreases, slowing the rate of PE formation (Zhang & Rock, 2008). The CL production is regulated by induction of *cls* gene expression in stationary growth phase or in high salt environment, but may also be inhibited by high PA or CL levels, contrary to PE, that inducts the CL synthesis (Ragolia & Tropp, 1994). In addition, *Pseudomonas* spp. strains synthesize the unique lipid, alanyl-phosphatidylglycerol (Ala-PG) (Arendt *et al.*, 2013; Klein *et al.*, 2009). This positively charged GP is synthetized by the aminoacylation of PG by the transmembrane MprF enzyme (PA0919 in *P. aeruginosa* PAO1). The alanine amino acid residue change the net charge of PG from -1 to 0 (Parsons & Rock, 2013). This change is induced by acidic growth and involved in a wide range of resistance, including to several antimicrobial compounds (Arendt *et al.*, 2013).

Membrane glycerophospholipid turnover

Giving the fact, that the FA synthesis needs a high energy expenditure, the GPs could be recycled to maintain the membrane homeostasis or used, in case of need, as precursors in the synthesis of other structural compounds in the cell. This GP recycling is named GP turnover. The head group of PG undergoes a rapid turnover by transferring to MDOs, which use the PG head group as a substrate for their synthesis. The residual from PG turnover, DAG, is quickly converted to PA and can be used by DgkA enzyme for re-synthesis of PG (Zhang & Rock, 2008). The DgkA is an inner membrane lipid kinase (Wahl *et al.*, 2011). This protein is involved in MDO production and related to the tolerance to osmotic stress (Rumley *et al.*, 1992). In *E.coli*, the *dgkA* in *plsB* genes are inversely regulated by ppGpp intracellular level (Wahl *et al.*, 2011). The PE is also a subject of GP turnover. The FA at *sn*-1 position of PE is used for the post-transcriptional acylation of lipoproteins. The resulting 2-acylglycerophosphoethanolamine (2-acyl-GPE) is recycled thanks to the catalytic properties of bifunctional enzyme 2-acyl-GPE acyltransferase/acyl-ACP synthase (Aas) (Jackowski *et al.*, 1994).

It should also be noted, that the lipid synthesis must be coordinated with DNA, RNA and protein synthesis to maintain the correct proportion of GPs to proteins in the membrane (Bogdanov *et al.*, 2013; Parsons & Rock, 2013). In conclusion, *P. fluorescens* envelope is the first barrier between the bacterial cell and its environment. The components of bacterial envelope, including GPs, play a major role in sensoring of environment, and adaptation to environmental modifications. This brief report shows the major pathways for GP adaptation to environmental modifications involved in *Pseudomonas* spp. strains. In the next section of this study, the GP membrane adaptation to various stressors will be discussed in more detail.

Highlights

- *P. fluorescens* is a highly heterogeneous group of bacteria, colonizing the large variety of ecological niches and able to adapt to modifications of environment.
- The formation of biofilm is one of the various modes of *P. fluorescens* adaptation to environmental conditions. The biofilm formation is specific for each *P. fluorescens* species and involves an array of cellular factors and highly regulated mechanisms.
- The *P. fluorescens* envelope plays a role of the first selective barrier between environment and cell, protecting bacteria against hostile environmental modifications.
- The glycerophospholipids are the major constituents of *P. fluorescens* envelope. Their synthesis is a complex mechanism, which requires an activation of several enzymes. The glycerophospholipids play a pivotal role in envelope protective functions and in bacterial adaptation to environmental changes.

Chapter 2 Stress factors and *Pseudomonas fluorescens* lipid adaptation

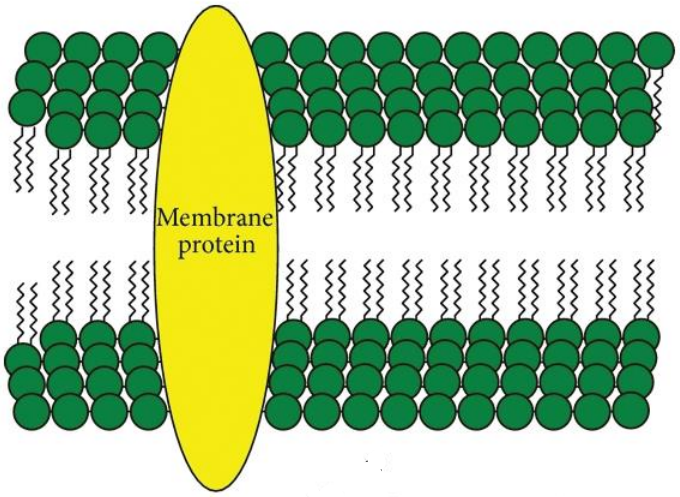

(Murínová *et al.*, 2014)

1. Stressors and bacterial survival

Bacteria, including *Pseudomonas* spp., are permanently exposed to a series of various stress factors, such as temperature alterations, availability of nutrients and water, or the presence of toxic molecules, that can make the living conditions far from optimal (Ramos *et al.*, 2001). These stressor factors have natural or anthropogenic origins and could be divided in three classes: biological, chemical and physical. The physical stressors, that bacteria cope in the environment, include temperature changes, modifications of osmotic pressure or irradiation. The chemical stressors comprise chemical pollutants found in natural environments, like organic solvents and metals. Biological factors, in turn, englobe the host defense processes, and include antimicrobials, and stresses caused by competition with other microorganisms. Bacteria have to implement adaptive mechanisms to survive under conditions of stress and cope with the challenges of changing environments. With the development of genomic and proteomic approaches, a myriad of studies based on the changes in gene expression, ensuring bacterial stress response, were realized (Boor, 2006; Kim & Park, 2014; Reva *et al.*, 2006; Ron, 2013; Rowley *et al.*, 2006). Thus, a combination of transcriptional regulatory pathways, which allow bacteria to sense and convert environmental stimuli, resulting in altered gene expression and enzyme activities (signal transduction) were well established. However, bacterial lipids play also a role of target(s) and adaptive mechanism(s) to environmental changes. Some examples of membrane lipid interactions with environmental stressors will be exposed below.

2. Impact of physical factors on membrane properties

2.1. Temperature modifications

In its natural habitats (soil, water and rhizosphere), *Pseudomonas* spp. can suffer frequent and long-term changes in temperature, which affect bacterial growth and survival. The effect of temperature on the members of *P. fluorescens* group and temperature adaptation of these bacteria were finely studied in our laboratory. Thus, it has been established, that growth temperature has an effect on *P. fluorescens* enzyme activity (Gügi *et al.*, 1991; Merieau *et al.*, 1993). *P. fluorescens*, growing at low temperatures, is much more sensitive to β-lactam mezlocillin, that the cells, growing at optimal temperature (Orange, 1994), due, in part, to the permeation of this antibiotic through bacterial membrane and the modifications in outer membrane porin OprF (Dé *et al.*, 1997; Hemery *et al.*, 2006). Temperature modifications were found to cause the variations in *P. fluorescens* cytotoxicity: low temperature increases bacterial adhesion to surface, but optimal temperature enchases the apoptotic effect (Picot *et al.*, 2004). The bacterial response on temperature fluctuations is one of the most studied topics of bacterial lipid adaptation. The temperature can change bacterial membrane fluidity (Mansilla *et al.*,

2004). The temperature higher than the optimum of growth increases membrane fluidity, allowing a membrane switch into the lamellar liquid phase (**Figure 10**). In contrast, the temperature, lower than optimum decreases membrane fluidity, switching the membrane into the gel phase. The molecular mechanism of regulation of UFA synthesis to adjust the temperature-mediated changes of membrane fluidity was elucidated more than 30 years ago (Marr & Ingraham, 1962; McGarrity & Armstrong, 1981) and was discussed in a number of studies (Mansilla *et al.*, 2004; Russell *et al.*, 1995). The lipidome adaptation to temperature modifications was also reported for members of *Pseudomonas* genus (Bhakoo & Herbert, 1980; Gill, 1975; Kropinski *et al.*, 1987). When the temperature rises, *Pseudomonas* spp. produce more SFAs, decreasing the membrane fluidity (**Figure 10**, **Table 1**). Conversely, at low membrane fluidity, caused by low temperature, bacteria produce more UFAs, increasing membrane fluidity and optimizing the growth (Mansilla *et al.*, 2004; Russell *et al.*, 1995). Concerning GP composition, modifications of the growth temperature do not elicit significant changes either in the total quantities of GP synthesized or in the concentration of individual GP components in any of the isolates (Bhakoo & Herbert, 1980). However, the tests of the temperature effect on the lipidome of *P. fluorescens* grown under carbon and nitrogen limited conditions (Gill, 1975) showed that the low temperature increases the proportion of the PE under carbon-limited conditions, but under nitrogen limitation an increase in the amount of CL is observed. The *cis*- to *trans*-UFA isomerization is an another mechanism to be described as response of *P. syringae* (Kiran *et al.*, 2004, 2005) and *Vibrio* spp. (Okuyama *et al.*, 1990, 1991) species in response to increasing temperature (**Table 1** and **Figure 10**). The role of cyclopropane-FAs in the adaptation to temperature changes is not clear so far, but there are studies demonstrated the increasing of cyclopropane-FAs with the rise of temperature (Nagamachi *et al.*, 1991).

2.2. Osmotic pressure

The osmotic strength of the environment is one of the physical parameters that determines the ability of organisms in given environment. Bacterial cells have to maintain the cell turgor, in other words, the intracellular osmotic pressure greater than in the environment in order to optimize the cell extension, growth and division (Sleator & Hill, 2002). The mechanisms involved in bacterial osmotic adaptation were well studied. The classical bacterial responses to osmotic stress were reviewed by Csonka, 1989 and Sleator & Hill, 2002. Briefly, bacteria react to osmotic stress first by taking up potassium ions (K^+) level in cytoplasm, which is followed by the increase of accumulation and/or biosynthesis of osmoprotective compounds. As shown in **Figure 13**, the latter, named compatible solutes, play a role of effective stabilisators of enzymatic functions, allowing the protection against osmotic stress. While the bacterial

cytoplasm employs the compatible solutes to protect its compounds against osmotic stress, the bacterial membrane also must undergo a number of adaptive changes. The *P. fluorescens* adaptation to osmotic stress is characterized by the alterations in porins, lipoproteins, and the flagella synthesis. In agreement with these changes, osmotic stress results in vesicle formation and modifications of bacterial motility and antibiotic susceptibility (Guyard-Nicodème *et al.*, 2008).

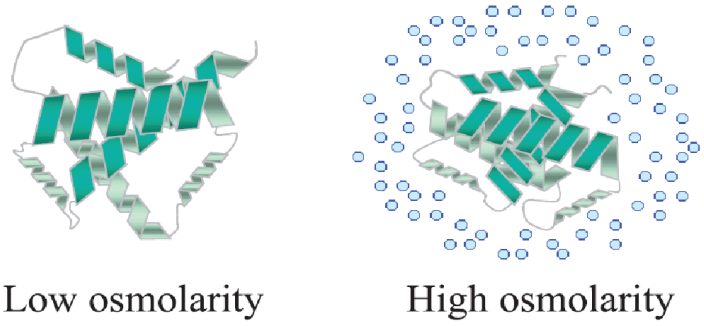

Figure 13. Enzyme stabilization at high osmolarity
The compatible solutes (blue circles) help to maintain the enzyme structure and properties at high osmolarity. Adapted from Sleator and Hill, 2002.

The membrane GPs play an important role in bacterial adaptation to osmotic stress (Sleator & Hill, 2002). The latter, caused by addition of glycerol, sodium chloride, or sucrose was evaluated in *P. putida* cells (Heipieper *et al.*, 1996). The cell responses were found to be stressor-dependent: exposure to NaCl and sucrose is correlated with an increase in the ratio of *trans/cis* UFAs, whereas glycerol does not cause any membrane response, indicating the importance of diffusive properties of these toxic compounds across the membrane. NaCl and sucrose cannot freely diffuse across the membrane and causes the accumulation of K^+ and synthesis of compatible solutes, while equilibration of a glycerol gradient across biological membranes is fast, which is not correlated with K^+ and compatible solutes synthesis. The proportion of cyclopropane FAs was also found to be increased in high salinity media (Romantsov *et al.*, 2009).

Another remarkable response to osmotic stress was observed in *Rhodococcus erythropolis* cells. The members of *Rhodococcus* genus are not only able of degrading a wide range of organic compounds (de Carvalho & da Fonseca, 2005), but also able to the growth in the presence of up to 7.5 % NaCl (de Carvalho, 2012). In hyperosmotic conditions, caused by NaCl, *R. erythropolis* completely changes its net surface charge and FA composition (Carvalho *et al.*, 2014). Interestingly, this bacterium formes the polyunsaturated long chain FAs, mainly eicosapentaenoic acid (C20:5ω3), arachidonic acid (C20:4ω6) and docosapentaenoic acid (C22:5ω3). The possible function of these very uncommon for bacteria FAs could be based on

the decrease in the number of negatively charged groups in ion channels resulting in a repellence of the NaCl.

When bacteria are grown in media of increasing salinity, the proportion of anionic GPs increases, comparing to zwitterionic GPs (Romantsov *et al.*, 2009). The role of CL seems to be very important in the context of high salinity adaptation. *Rhodobacter sphaeroides* responds to the hyperosmotic stress by increasing of the amount of CL in its membrane (Catucci *et al.*, 2004). The growth of *E. coli* and *Bacillus subtilis cls* mutants is impaired in high osmolarity medium (López *et al.*, 2006; Romantsov *et al.*, 2007).

It seems appropriate, that the lipid studies of osmotic stress adaptation are mainly performed with halophilic microorganisms that are classified, in majority, into the Archaea domain (Oren, 2002). The members of genus *Halobacterium* are halophile *par excellence*. In osmotic stress conditions, these bacteria increase the level of the archaeal CL bisphosphatidylglycerol (BPG), and synthesize normally absent in the purple membrane analogs of CL: a glycocardiolipin (GlyC) and a sulfated diglycosyl diphytanylglycerol diether (S-DGD-5-PA). This increase of CL level is correlated with a decrease of the level of sulfo-triglycosyl-diether (S-TGD-1) in the purple membrane (Lobasso *et al.*, 2003; Lopalco, 2003).

It should be however noted, that a wide range of adaptive responses to osmotic stress, based on solute or water efflux mechanisms, osmosensing and osmoregulation were described and reported in a very comprehensive review (Sleator & Hill, 2002).

3. Impact of chemical factors on membrane properties

3.1. Organic solvents

Nowadays, all kinds of motors are widely present in our environment and accidental oil spills are frequent, resulting in soil and water contamination with hydrocarbons. Bacteria are the ability to resist to hydrocarbon contamination and/or degrade these toxic compounds in polluted environments, offering an amazing possibility of bioremediation of contaminated surfaces (de Carvalho & da Fonseca, 2005).

The bacterial responses to hydrocarbons were extensively studied during the last decade. A large number of the organic-solvent-tolerant bacteria was reported, including *Pseudomonas* strains, especially *P. putida* (Heipieper *et al.*, 1994; Heipieper & Fischer, 2010). The primary site of action of organic solvents is the cell membrane.

Although no individual analytical technique is able to determine fully the effects of solvents on a membrane, several mechanisms of solvent toxicity were established (Heipieper & Martínez,

2010). The accumulation of solvents in bacterial membrane leads to the inhibition of membrane protein functions and synthesis, non-specific membrane permeabilization and its swelling (Heipieper *et al.*, 1991, 1994). The membrane fluidity is also known to be impacted by organic solvents (Heipieper & Martínez, 2010). **Figure 14** shows a scheme of the toxic effect of these molecules on the cell membrane that could cause the inhibition of bacterial growth and/or lysis of the cells.

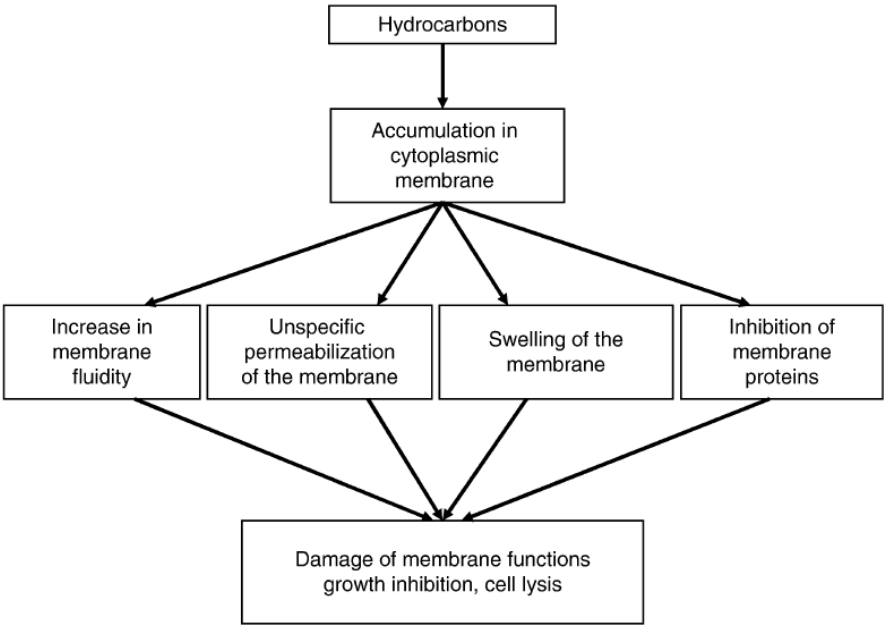

Figure 14. Scheme of the toxicity of hydrocarbons in the cell membranes
According Heipieper and Martínez, 2010.

In order to adapt to the hydrocarbon toxicity, bacteria of genus *Pseudomonas* use several membrane adaptive pathways, which could be divided to short- and long-term responses. The short-term response is based on a decrease of membrane fluidity by a rapid transformation of the *cis*-FAs to their *trans*-conformations (**Table 1**, **Figure 11** and **Figure 12**) (Heipieper & Fischer, 2010). The role of cyclopropane-FAs was also demonstrated: the *cfa* knock out mutant was found to be more sensitive to solvent shock than the wild type strain in stationary phase (Segura *et al.*, 2010). The long-term response, in turn, is based on the changes in FAs and the alterations in the ratio of zwitterionic/anionic GPs. Bacteria increase the degree of FAs saturation, that leads to the decrease of the membrane fluidity (Heipieper & de Bont, 1994). In this way, the adaptation of the FA composition to the hydrocarbons strongly resembles the well-known process of thermal adaptation (see part **2.1. Temperature modifications**). It has been established, that with addition of solvents the level of CL increases, when the level of PE decreases, leading to the increased membrane rigidity (Ramos *et al.*, 1997). Recently, the effect of n-butanol on the GP composition of four solvent-tolerant *Pseudomonas* spp. strains was evaluated (Rühl *et al.*, 2012), demonstrating strain-dependent GP response to this organic

molecule. In fact, *P. putida* DOT-T1E and KT2440 grown with 1% of n-butanol exhibit a shift from PE to PG at slightly decreasing amounts of CL. A different response was observed for *P. putida* S12 and *Pseudomonas* sp. VLB120, where the PE and CL levels are enhanced, correlated with the decrease of the relative amounts of PG.

3.2. Metal pollutants

Several metals, including Ca, Cu, or Zn, are essential for bacterial functioning, as cofactors of various enzymes, or regulators of osmotic pressure. On the other hand, many metals, such as Hg, Pb, or Au, have no biological functions and are toxic to bacterial cells. The bacterial envelope protects cell compounds against environmental pollutants, including toxic metals (Beveridge, 2005). As a consequence, the metal resistance pathways are often based on membrane functions, including metal exclusion by permeability barrier, cellular sequestration, and efflux of the metal ions from the cell (Markowicz *et al.*, 2010). In addition, the enzymatic transformation and reduction of metal to less toxic forms play also a pivotal role in bacterial metal decontamination. Bacterial cell surface carries a negative charge under optimal pH conditions, and can interact with the electropositive metal ions. The evidence of these interactions was observed by Breveridge and coworkers using electron microscopy and illustrated in **Figure 15** (Beveridge & Koval, 1981).

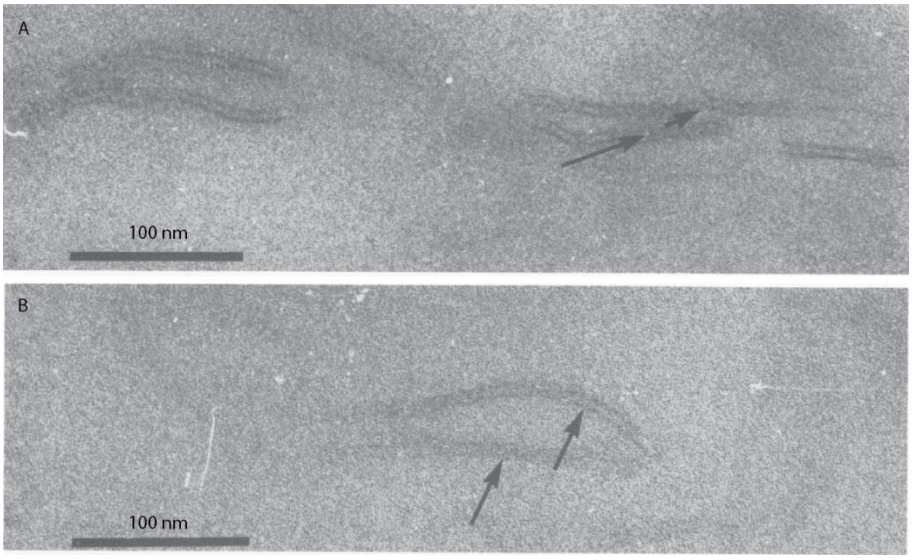

Figure 15. Interactions of cell envelope with metals
Thin section of *E. coli* K12 envelope with **A.** Cu and **B.** Mg. The arrows point to the membrane of a single vesicle. No stain other than the initial binding metal was used for contrast.
Adapted from Beveridge & Koval, 1981.

While the metals penetrate in bacterial cells through the channel for metal ion acquisition (Hohle *et al.*, 2011), bacterial GPs play a significant protective role against metal pollution. The anionic GPs, including PG and CL or phosphoryl groups, are able to react with metal cations in order to sequester these toxic compounds within the membrane. An alternate mechanism

involved in response to metal contamination is based on the FAs response to the metal binding (French *et al.*, 2013). It ws reported that an increase in the level of UFAs results in a two-fold decrease in Ca^{2+} binding to the lipid membranes (Huster *et al.*, 2000). In fact, the increased distances between adjacent HGs in *cis*-UFAs or cyclopropane-FAs comparing to the SFAs (**Figure 11**), may reduce lipid-metal binding (French *et al.*, 2013). The work of Markowicz and coworkers demonstrated the alterations in the cyclopropane-FAs level and the degree of FA saturation in bacteria, grown with several metals. Unfortunately, the observed effects are strain- and metal-dependent, making it difficult to establish the mechanism of FA adaptation to metal contamination. It was also shown, that *P. putida* adapts its membrane FAs to the heavy metals pollution by the transformation of the *cis*-UFAs to their *trans* steric conformations (Heipieper *et al.*, 1996).

Since the last years, the notion of nanoparticles (particles of size between 1 and 100 nm) became an important subject of pharmaceuticals and industrial science researches (Arvizo *et al.*, 2012; Whitesides, 2003). The membrane adaptive response of *P. putida* to silver nanoparticles was studied (Hachicho *et al.*, 2014). The silver nanoparticles were found to cause a strong increase in the *trans/cis* ratio of UFAs, as a mechanism of control of the increasing membrane fluidity.

Bacteria involved in bioremediation processes must cope the multicontaminated environment, and very often la contamination is accompanied by organic pollutants (Cébron *et al.*, 2014). The bacterial response to mixed organic and metal pollution were evaluated (Pepi *et al.*, 2008). Concerning membrane lipids, *Bacillus* sp. ORAs2 is able to increase the degree of FA saturation at high arsenic concentrations that can probably counteract the increase of arsenic uptake. *Pseudomonas* sp. ORAs5 also increases the degree of FAs saturation, but also forms the *trans*-UFAs. However, its response to heavy metals is a much lower than that to toluene.

4. Impact of biological factors on membrane properties

4.1. Antimicrobial agents

As previously reported in the part **3.4.3. Glycerophospholipid synthesis and functions in *Pseudomonas***, bacterial lipidome becomes a target for antibiotic development. The chemical nature of antimicrobial agents is quite diverse. However, many of these toxic compounds are positively charged. In addition to the net negative charge, bacterial membrane has a negatively charged GP domains (*i.e.* domains enriched by CL). There is also evidence, that bacteria are able to rearrange their membrane GPs, forming, for example, anionic GP domains to adapt to stress impact (Vanounou *et al.*, 2002). Antimicrobial agents are able to interact with the negatively charges bacteria GPs, as reported in **Figure 16**. This may protect bacteria against

positively charged antibacterial agents, sequestering antimicrobial agents outside the cell, but also lead to the lower membrane permeability and alterations in bacterial membrane functioning (Epand & Epand, 2009).

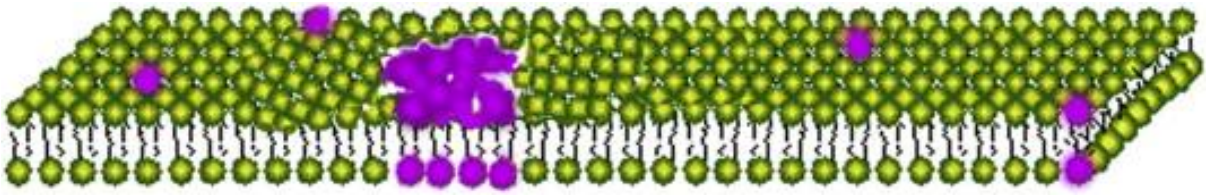

Figure 16. Glycerophospholipid rearrangement that can occur on binding cationic antimicrobial agents

Clustering of anionic GPs (purple head groups) into a domain occurs as a consequence of binding to the antimicrobial agent. This causes a rearrangement of GPs around the domain, and membrane defects.
Adapted from Epand and Epand, 2009.

The antimicrobial host defense peptides provide a good example of interactions with bacterial membrane. These molecules are small in size and have a cationic structure. The helical peptide NK-2 binds to the anionic PG, causing a rigidification of the membrane and an increase in the phase transition temperature without destroying the membrane structure. In addition, a negligible interaction was observed with pure zwitterionic PC model membranes. Whereas NK-2 has no effect on PC liposomes, it enhances the fluidity of the PE acyl chains and lowers the phase transition enthalpy of the gel to liquid crystalline transition. The most dramatic effect, however, was observed for the lamellar hexagonal transition of the PE, which is reduced by more than 10 °C. Negative charges will increase the probability of the presence of the peptide at the membrane surface (Willumeit *et al.*, 2005). In a similar way, the high concentrations of the tryptophan-rich antimicrobial peptide indolicidin lower the ratio of the gel-phase fluid domains in model membranes (Shaw *et al.*, 2006). Alternatively, it was reported that the decrease in the membrane level of PC promotes the resistance of *P. aeruginosa* to benzalkonium chloride (Loughlin *et al.*, 2002).

The antibiotic tetracycline was reported to alter the membrane fluidity in *B. cereus* and *P. putida* membranes. Whereas it has a positive effect on the cytoplasmic membrane fluidity of *B. cereus*, the opposite was observed in *P. putida*, reflecting the difference in stress induced behavior between different bacteria species (Vincent *et al.*, 2006)

The role of the recently identified Ala-PG in *P. aeruginosa* antibiotic resistance should be mentioned. Ala-PG conferrs a growth advantage when the bacteria are cultured in the presence of a diverse group of substances, including the cationic antimicrobial peptides, such as protamine, the heavy metal chromium (III), the osmolyte sodium lactate and the β-lactam cefsulodin (Klein *et al.*, 2009). The biological significance of Ala-PG is not clear, but the

addition of Ala could neutralize the negative charge of PG imparting a net positive membrane charge and decreasing the interactions of cationic antimicrobials with negatively charged PG. In addition, it was proposed that the Ala modification might be involved in changing of membrane biological properties, such as permeability and fluidity (Roy *et al.*, 2009).

In conclusion, various stress factors impact bacterial functioning. The bacterial membrane plays a role of the first barrier between the toxic compounds and the cell and is often altered with modifications of environmental conditions. As consequence, bacteria, including the members of *Pseudomona*s genus, can adapt to these modifications. The membrane GP adaptive responses to several stress factors discussed in this chapter are summarized in **Table 2**.

Table 2. Summary table of pathways, involved in bacterial lipid adaptation to various stress factors

Stress factor	Lipid adaptation mechanism					
	SFA	*cis*-UFA	*trans*-UFA	cyclo-FA	Poly-UFA	Adaptation of polar head groups
High temperature						No modification
Low temperature						No modification
Osmotic stress						Increase of the level of anionic GPs, particularly CL.
Solvents (short-term response)						
Solvents (long-term response)						Strain-dependent response. Modifications of ration zwitterionic/anionic GPs
Metals						Sequestration of metal cations into anionic GP domains
Nanoparticles						ND
Antimicrobial agents	ND	ND	ND	ND	ND	Sequestration of metal cations into anionic GP domains; increase of Ala-PG level and modification of net membrane charge

The mechanisms of bacterial adaptation to various stress factors based on the glycerophospholipid polar head groups and/or fatty acids (FAs) modifications are summarized in this table. The modifications in FAs include the formation of saturated FAs (SFA), *cis*-, *trans*-monounsaturated FAs (*cis*-UFA, *trans*-UFA), cyclopropane-FAs (cyclo-FA) and polyunsaturated FAs (poly-UFA). The green square shows the increasing level of displayed parameter, the red square shows the decreasing level of displayed parameter. ND: no determined.

Briefly, the increase of the membrane fluidity, caused by several stress factors, is controlled by the increasing levels of SFAs and *trans*-UFAs in bacterial membrane. The cyclopropane-FAs play an important role in response to osmotic stress and solvent toxicity. The GP polar head groups are also involved in response to stress. Particularly, the anionic GPs, including PG and CL, are involved in the response to osmotic stress and in the adaptation to cationic toxic compounds, such as antimicrobial agents and metal cations. This overproduction and/or rearrangements of GP bilayer cause both the sequestration of toxic compounds outside of the bacterial cells, but also the alterations in the membrane functions.

This chapter discussed only several and the most studied stress factors in terms of the membrane GP adaptation. However, the topic of bacterial adaptation is much vaster that described above. The stressors, like light (Elmnasser *et al.*, 2007; Gómez-López *et al.*, 2007), nutrient limitation (Poole, 2012) and pH (Baatout *et al.*, 2007; Padan *et al.*, 2005) should also be mentioned.

4.2. Oxidative stress

Several previously discussed stressors, like metal ions (Lemire *et al.*, 2013) and antibiotics (Marrakchi *et al.*, 2014; Poole, 2012) can cause the oxidative stress in bacterial cells. It has been reported, that free radicals can attack directly the polyunsaturated FAs in membranes and initiate the lipid peroxidation. The latter is primary reflected in a decrease of the membrane fluidity, altering the membrane properties. This effect acts as an amplifier, more radicals are formed, more polyunsaturated FAs are oxidized (Cabiscol *et al.*, 2000). However, these data should be interpreted with caution. A biochemical mechanism of lipid peroxidation was defined for membranes of eukaryotic organisms, which contain the high levels of polyunsaturated FAs. By contrast, most bacterial membranes, including *Pseudomonas* species, are composed of monounsaturated FAs, which are described as unreactive in lipid peroxide chain reactions *in vitro* (Imlay, 2003). However, others discussed the repair of *E. coli* lipid peroxidation (Bonamore *et al.*, 2003a, b). Therefore, it is still unclear whether the lipid peroxidation occurs in bacterial membranes (Lemire *et al.*, 2013). In the case of doubt, in this study, the bacterial lipid peroxidation is not taken into account. The oxidative stress is closed to the nitrosative stress, caused by nitrogen oxides (van der Heijden *et al.*, 2015). The sources of nitrogen oxides, their chemistry and bacterial adaptation to these toxic compounds will be discussed in the next chapter of this work.

Highlights

- Several environmental stressors can alter bacterial homeostasis. Giving the fact, that the membrane plays an important role of the first barrier between bacterial cell and its environment, several (if not all) environmental stress factors alter membrane functions, that often results in modifications of the membrane fluidity.
- Bacteria, including members of *Pseudomonas* genus, involve a membrane adaptive response to control the membrane fluidity and optimize growth, which is based, in part, on the modifications in membrane GPs.
- The high temperatures, solvents and metals are known to increase the membrane fluidity, which is controlled by the increasing of the level of SFAs and the rapid transformation of *cis*-UFAs to their *trans*-conformations.

- The cyclopropane-FA synthesis is required for the response to the solvent toxicity and osmotic stress. The latter is found to induce the synthesis of unusual for bacteria poly-UFAs.
- The modifications in GP polar head groups are also involved in bacterial response to stress factors. The modifications in ratio of the membrane zwitterionic/anionic GPs allows bacteria to control the membrane fluidity. The anionic GP, including PG and CL, are involved in the response to osmotic stress and in the adaptation to cationic toxic compounds, such as antimicrobial agents and metal cations. The rearrangements of GP bilayer allow the formation of the anionic GP domains, which can capture toxic molecules, but also alter the membrane properties.

Chapter 3 Nitrogen oxides, their chemistry, biological roles and atmospheric pollution

1. Nitrogen oxides (NO_x)

1.1. NO_x basic notions

Nitrogen is a basic element for life because it is a component of the two preeminent biological macromolecules: proteins and nucleic acids. Nitrogen exists in several oxidation states, from N(-III) to N(+V). Interconversions of the nitrogen species constitute the global biogeochemical nitrogen cycle, in which bacteria play a predominant role (Moreno-Vivián *et al.*, 1999). Several types of nitrogen oxides (NO_x) exist in the environment: N_2O, NO, NO_2, N_2O_3, N_2O_4, NO_3, and N_2O_5. However, the abbreviation NO_x mainly relates to nitrogen monoxide (NO) and nitrogen dioxide (NO_2) (Skalska *et al.*, 2010). The structure, reactivity and functions of these molecules were extensively studied. NO and NO_2 are more soluble in polar solvents than in water (Lide, 2004; Schwartz & White, 1981). From a Lewis structure presented in **Figure 17**, it becomes evident, that ˙NO and ˙NO_2 are the free radicals with one unpaired electron. In order to homogenize the text below, these two radicals are named as NO and NO_2.

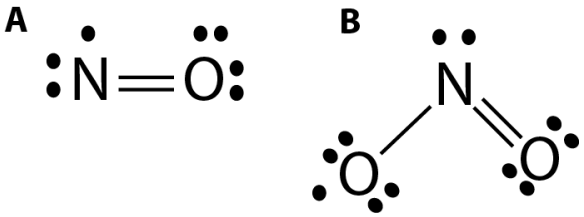

Figure 17. Lewis structure of (A) NO and (B) NO_2

1.2. Nitrogen monoxide (NO)

NO is a simple inorganic molecule, possessing unique and fascinating properties. On one hand, NO is found to be one of the major air pollutants (see part **6.1. NOx as a major air pollutant**). On the other hand, NO is known to be synthetized in several (if not all) living organisms, including mammals, plants and naturally bacteria (see part **2. NO formation in living organisms**). These NO functions have reinvigorated research into the fundamental chemistry, and led *Science* magazine to designate NO as Molecule of the Year in 1992 (Koshland, 1992). However, in presence of O_2 and light, NO is unstable and is quickly oxidized to form NO_2. The latter reacts with NO in aqueous solution to give N_2O_3, as shown in **Figure 18**. When the reaction occurs in air, NO_2 dimerizes to give N_2O_4. Given that NO is a lipophilic molecule, the reaction of NO with oxygen will be accelerated in the cell membrane (Hughes, 2008), with various and, in majority, negative consequences for the cell.

1.3.Nitrogen dioxide (NO_2)

NO_2 is described as a toxic air pollutant (see part **6.1. NOx as a major air pollutant**), which, however, can be synthesized (at low concentrations) by several organisms (*i.e.* during

denitrification process, see part **NO in bacteria**). In atmosphere, this molecule exists in form of its dimer N_2O_4 (at 27 °C, 80 % N_2O_4 for 20 % NO_2) (Fukuto *et al.*, 2000). Moreover, N_2O_4 is about 100 times more soluble in water than its monomer NO_2 that results in generation of nitrite (NO_2^-) and nitrate (NO_3^-). In cells, NO_2 and its dimer are, in majority, concentrated in the hydrophobic areas (*i.e.* cell membrane) (Hughes, 2008). As previously reported and shown in **Figure 18**, in aqueous solution, NO_2 reacts with NO to form dinitrogen trioxide (N_2O_3), which hydrolyzes to form NO_2^-. The N_2O_3 and N_2O_4 are also known for their oxidative properties and the possible reactions with proteins (see part **Proteins**) (Espey *et al.*, 2002).

Because the NO_x are able to react in the cellular environment to give a wide range of products with different biological effects, the relationship between the biological activity of NO_x and their chemistry is particularly complex (Fukuto *et al.*, 2000). Some of these reactions are represented in **Figure 18** and give rise to the generation of the reactive nitrogen species (RNS) (Wink & Mitchell, 1998). According the strict chemical definition, the RNS include a wide range of compounds, with contrasting and distinct properties, and their only unifying trait is related to the common origins from NO (Patel *et al.*, 1999). However, more and more of studies take into account the biological effect of RNS, considering as the RNS only toxic for living organism molecules. The chemistry and biological functions of RNS will be discussed below.

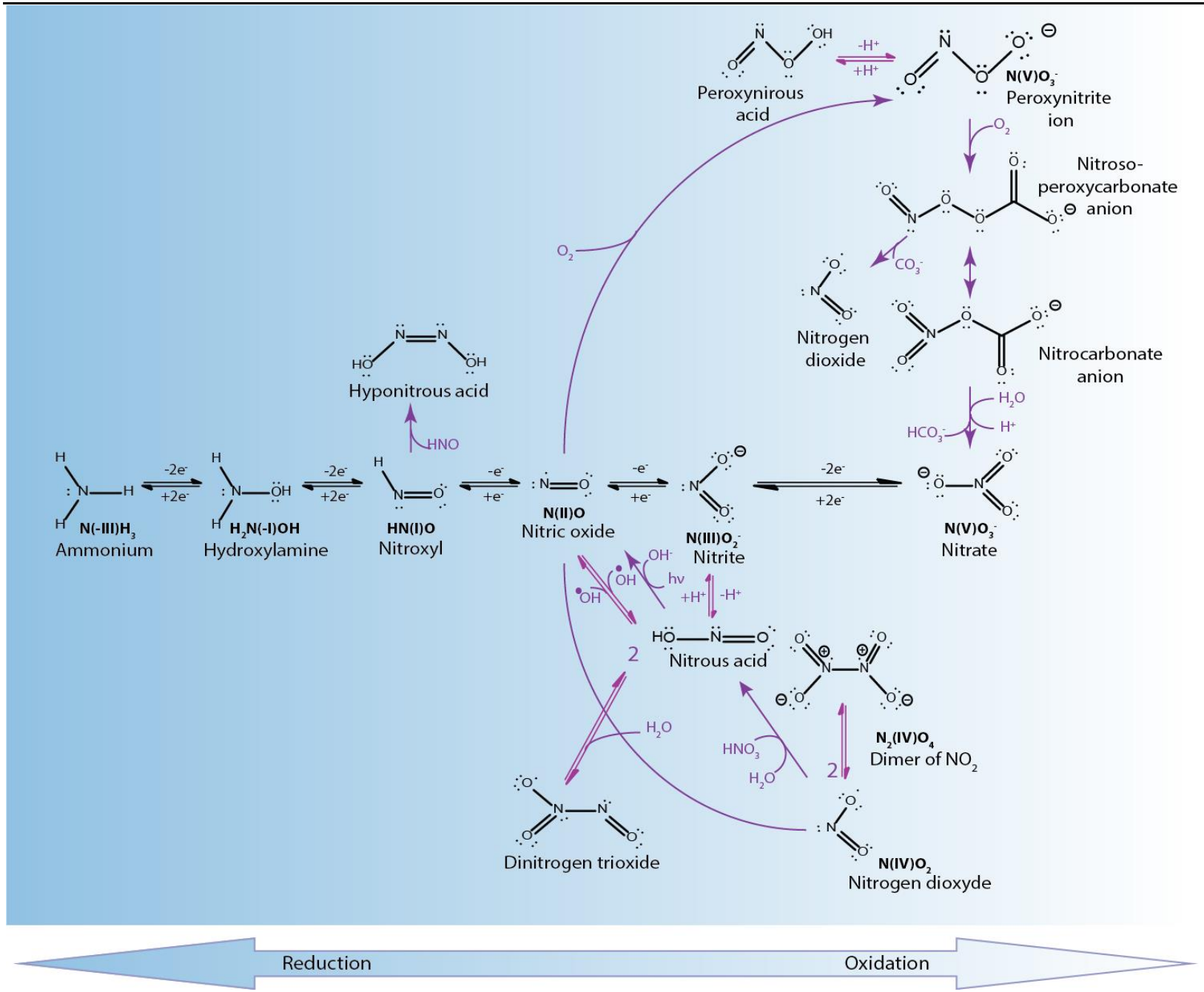

Figure 18. Redox relationships of NO_x with other RNS species

NO take a central place in the series of reactive nitrogen species (RNS). Oxidation and reduction of NO (**black arrows**) lead to the formation of several RNS, including nitrate, or ammonium. NO_2 is formed by reaction of NO with O_2 and can be dimerized to give N_2O_4. The formed reactive species can, in turn, be involved in a wide range of reactions (**purple color**). The Roman numbers in the chemical formulas refer to the oxidation state of the nitrogen atom. The color gradient shows the reduction/oxidation state from (-III) to (V).

1.4. Nitrogen oxides and reactive nitrogen species: chemistry and biological role

A wide range of RNS with various chemical structures and different (and often opposite) biological roles may be cited. First of all, the RNS play a role of a source of nitrogen. In this way, the physiological level of RNS helps to maintain the normal cell homeostasis and produce macromolecules, and/or energy for growth (Fang, 2004). However, the pathological level of RNS can cause the nitrosative stress, which negatively impacts the cell functioning. Due to the complex RNS chemistry, the excess of these compounds may induce the generation of other and probably toxic species. Nitrosative stress may lead to nitrosylation reactions that alter the structure of proteins and inhibit their normal functions. There is a difficulty with classifying the RNS according their role in the cells. However, the peroxynitrite ($ONOO^-$), among others, is recognized as a very strong oxidizing agent, causing the DNA damages and lipid oxidation (Valko *et al.*, 2007). In this part of the manuscript, we tried to summarize the currently known information about several RNS, their chemistry and function in biology and areas of application.

1.4.1. Peroxynitrite ($ONOO^-$)

Notable example of highly reactive RNS species is peroxynitrite ($ONOO^-$) that is formed through the reaction of NO with the superoxide radical O_2 as shown in **Figure 18**. The chemical properties of peroxynitrite make it a strong, and highly reactive species, which gives rise to both oxidative and nitrosative stresses (Ferrer-Sueta & Radi, 2009). Thus, this molecule plays a role of a central pathogenic mediator in a variety of diseases including cardiovascular, neurodegenerative, and inflammatory disorders. The half-life of this species is thought to be as little as 10 ms in biological systems; however, this time is sufficient for damaging bacterial cells (McLean *et al.*, 2010). Once penetrated in bacterial cytoplasm, peroxynitrite is able to react with a variety of targets (see part **NO targets in cells**) causing protein modifications, lipid oxidations, and/or DNA damages. The formation rate of peroxynitrite has been estimated at up to 100 M/min in selected cellular compartments (McLean *et al.*, 2010). However, the toxicity of this species seems to be highly dependent on ratio between the cells number and the stressor. In addition, the toxicity of peroxynitrite seems to be largely influenced by the presence of scavering compounds in culture medium. As demonstrated in **Figure 18**, $ONOO^-$ possesses nucleophilic character and is able to react with electrophiles, such as carbon dioxide (CO_2) (Fukuto *et al.*, 2000). The obtained nitrosoperoxycarbonate anion ($ONOOCO_2^-$) is unstable and gives two highly reactive radicals: NO_2 and carbonate radical anion CO_3^-. The nitrosoperoxycarbonate ion, in turn, can be isomerized in unstable nitrocarbonate ion ($O_2NOCO_2^-$), which in aqueous solution decomposes to nitrate and bicarbonate (Hughes, 2008).

1.4.2. Nitroxyl HNO

The nitroxyl (HNO) is a RNS that has emerged as a promising therapy for treating the cardiovascular diseases (Ge & Moss, 2012). Its pharmaceutical utilization is due to the chemistry of this species. HNO is a weak acid (acidity constant (pKa) 11.5), that means, that this RNS is a predominant species at physiological pH. As previously reported for peroxynitrite, HNO is able to react with proteins, which are located in key components of the cardiac electromechanical machinery, ruling myocardial function. This RNS is used to increase the cardiac force production and modulate the cardiac contractility (Tocchetti *et al.*, 2011). Nerveless, Fukudo et al. reported the metastable nature of HNO. This properties is due, in the major part, to the self-reactivity of this species: one HNO molecule can react with another to give hyponitrous acid (HONNOH) (**Figure 18**), which, in turn, is unstable and forms nitrous oxide and water (Fukuto *et al.*, 2000).

1.4.3. Nitrous oxide (N_2O)

It has been established that N_2O is one of the greenhouse gases (Skalska *et al.*, 2010). It has a ~300-fold greater warming potential than CO_2, and is involved in destruction of the atmospheric ozone layer. Unlike NO or NO_2, N_2O has a long half-life around 100 to 150 years, that makes the increasing atmospheric level of this species a serious global problem. Atmospheric N_2O concentrations have increased by 19% since pre-industrial times (Butterbach-Bahl *et al.*, 2013). The major source of N_2O is soil ecosystems, which emit approximately 65% of the total N_2O into the atmosphere. Here, the major N_2O producer are denitrifying microorganisms (see part **Nitrogen cycle and denitrifying bacteria**). In recent years, the excessive use of nitrogen-based fertilizers in agriculture has also greatly contributed to the conspicuous elevation in atmospheric N_2O concentration (Hu *et al.*, 2015).

1.4.4. Ammonia (NH_3)

Ammonia is a basic gas and one of the most abundant nitrogen-containing compounds in the atmosphere. The role of microorganisms in ammonium transformation in sols is impressive. The soil nitrification, the oxidation of ammonia to nitrate (**Figure 18**) are performed by several bacterial species, named nitrifying bacteria (see part **Nitrogen cycle and denitrifying bacteria**). This results in enormous commercial losses of ammonium-based fertilizers, with associated atmospheric and groundwater pollution by nitrous oxide/acid and nitrate (Anderson *et al.*, 2003).

1.4.5. Nitrous acid (HONO) and nitrite (NO_2^-)

Nitrous acid and nitrite are short-lived intermediates of RNS. The nitrous acid (HONO) is a RNS of high importance in urban atmosphere chemistry. In particular, HONO plays an

important role in the initiation of daytime photochemistry by its rapid photolysis to NO and OH radicals (Arens *et al.*, 2001). The photolysis of NONO can provide a significant increasing of the HO-radical rate and generate the products of photochemical smog (Czader *et al.*, 2012). As shown in **Figure 18**, the nitrite, in turn, can be oxidized to the nitrate (NO_3^-). The microorganisms, including denitrifying bacteria, can perform this reaction (see part **Nitrogen cycle and denitrifying bacteria**). The nitrate can be removed from atmosphere by plants (see part **NO in plants**) or through wet and dry deposition, leading to the acidification of ecosystems (Lammel & Cape, 1996).

In conclusion, it should be noted, that NO_x, and the derived RNS, have a complex chemistry and, as consequence, various biological, pharmaceutical, and ecological functions. All these species are in interaction with living organisms, including bacteria. However, thanks to its unique properties, the effect of NO on bacterial cells is well studied. Thus, the synthesis and roles of this molecule in living cells, including bacteria will be discussed below.

2. NO formation in living organisms

NO is known to be synthetized in mammalian (Fang & Vazquez-Torres, 2002), plant (Planchet & Kaiser, 2006) and bacterial (Plate & Marletta, 2013a) cells as a biological effector and/or mediator (Choudhari *et al.*, 2013). When engulfed by macrophages, microorganisms are exposed to the NO defense mechanisms (El-Gayar *et al.*, 2003). In the same way, the plants have a NO defense against pathogens (Delledonne *et al.*, 1998). NO functions as a messenger in defense responses and as a general key factor associated with basal resistance in various plant–pathogen systems (Arasimowicz-Jelonek & Floryszak-Wieczorek, 2014). Thus, NO assimilation and synthesis in bacterial hosts seems to be inescapable step in the understanding of the bacterial NO_x response.

2.1. Mammalian NO

NO is an important enzymatically synthesized signaling molecule responsible for a variety of physiological functions ranking from neurotransmission, relaxation of vascular endothelium, to toxicity to tumor and pathogen cells (Fang & Vazquez-Torres, 2002; Ignarro, 1990; Marletta, 1989). As illustrated in **Figure 19**, the majority of mammalian NO is synthesized enzymatically from nitric oxide synthase (NOS), through the conversion of L-arginine to L-citrulline in an O_2 and NADPH-dependent reaction (Thomas *et al.*, 2008). NO could be formed by three NOS homodimers depending on cellular localization, functions and biochemical characteristics. Two of the NOS proteins, the neuronal NOS (nNOS; NOS-1) and the endothelial NOS (eNOS; NOS-3), are dependent on elevated intracellular Ca^{2+}, besides the inducible macrophage NOS (iNOS; NOS-2) is independent on Ca^{2+} level (Bruckdorfer, 2005; Moncada *et al.*, 1997).

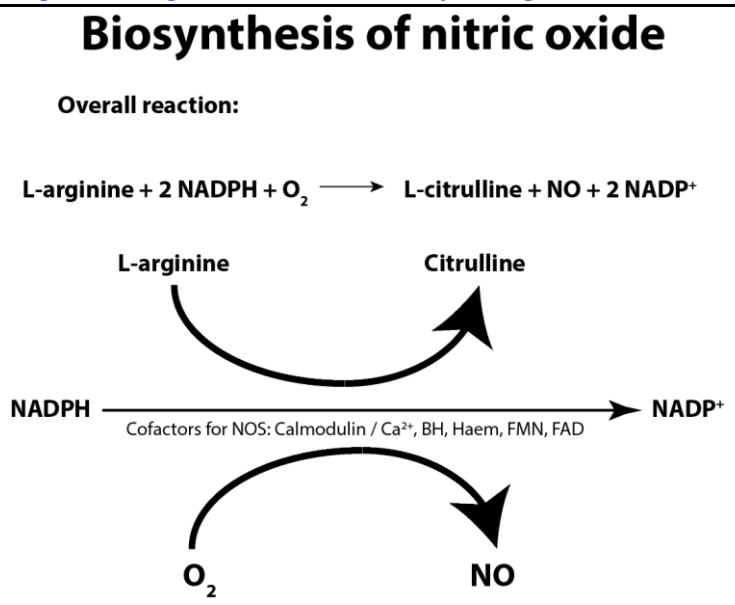

Figure 19. Scheme of biosynthesis of nitric oxide from L-arginine in mammalian cells
Adapted from Moncada et al., 1997 and Bruckdorfer, 2005.

The nNOS was isolated from mammalian brain and named neuronal NOS playing several important roles in regulation of synaptic signaling and plasticity. High levels of nNOS protein are present in skeletal muscle (Brenman *et al.*, 1995), where this molecule controls muscle contractility and local blood flow (Mungrue & Bredt, 2004). As the name implies, the eNOS is originally from vascular endothelium, and NO generated by eNOS regulates blood pressure, platelet aggregation, leukocyte adherence, and mitogenesis of vascular smooth muscle cells (Shaul, 2002). Deficient eNOS production was implicated in the pathogenesis of systemic and pulmonary hypertension (Huang *et al.*, 1995) and in other vascular disorders including atherosclerosis (Oemar *et al.*, 1998) The role of macrophage iNOS is the most interesting in terms of host-bacteria interactions. NO synthesized by iNOS is an important proinflammatory cytotoxic mediator, which defends the host toward various pathogens by inactivating and destroying infectious agents (MacMicking *et al.*, 1997). Thus, NO assures the resistance to microbial growth and antitumor immunity (Fang, 2004).

2.2. NO in plants

As previously reported, NO and the derived RNS play an important role in soil (see part **1.4. Nitrogen oxides and reactive nitrogen species: chemistry and biological role**). As consequence, the role of NO in plants appears even more multi-faceted than in animals. Briefly, NO is a signaling molecule, controlling the plant growth and development, as well as the plant responses to biotic and abiotic stresses (Planchet & Kaiser, 2006). In plants, NO is involved in mitochondrial (Zottini *et al.*, 2002) and chloroplast functionality (Jasid *et al.*, 2006), root growth and cell wall lignification (Franciele Mara Lucca Zanardo Böhm, 2010), stomatal closure (Garcia-Mata *et al.*, 2003), senescence (Hung & Kao, 2003), cell death (Pedroso *et al.*, 2000)

and plant responses toward a variety of abiotic stresses, such as wounding, salinity, drought, and hypoxia (Neill *et al.*, 2003).

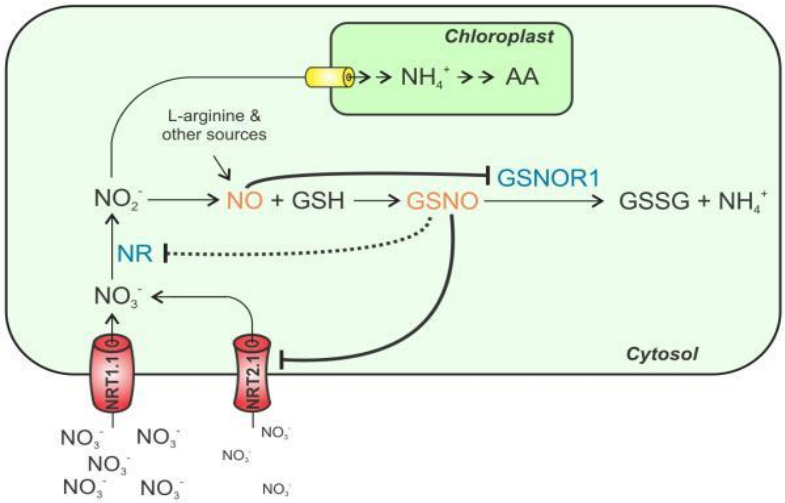

Figure 20. Schematic model of NO_x synthesis and assimilation in plants
Nitrate (NO_3^-) is taken up by nitrate transporters (NRT) in roots and reduced in leaves to nitrite (NO_2^-) by nitrate reductase (NR). In chloroplasts, nitrite is reduced to ammonium (NH_4^+) and incorporated into amino acids (AA). In cytosol, nitrite can also be reduced to nitric oxide (NO). NO, in turn, can be generated from other sources, such as L-arginine. NO reacts with reduced glutathione (GSH) producing S-nitrosoglutathione (GSNO), the major plant reservoir of NO. The levels of NO and GSNO are controlled by the enzyme GSNO reductase (GSNOR).
Adapted from Frungillo et al., 2014.

As demonstrated in **Figure 20**, the NO production in plants is based on both the synthesis of NO by NOS (*e.g.* arginine based NO synthesis, like in mammalian cells) and reductive pathways (Gupta *et al.*, 2011). Although the mechanism of arginine-dependent NO production in plants is similar to that of mammalian cells, up to now, no mammalian NOS homologs were identified in higher plants. It was described, that the polyamines and the hydroxylamines could be a potential source for the NO synthesis in higher plants (Fröhlich & Durner, 2011). In addition, S-nitrosoglutathione (GSNO), which is formed by spontaneous reaction of NO with glutathione, is a major NO reservoir and NO donor in plant cells. GSNO level is controlled by the GSNO reductase, which is known to be the main enzyme responsible for the modulation of S-nitrosothiol pools (**Figure 20**) (Frungillo *et al.*, 2014).

Assimilation of nitrate involves the sophisticated transport systems, which relies mainly on membrane-bound nitrate transporters (NRTs) (Tsay *et al.*, 2007; Wang *et al.*, 2012). Once taken up by roots, nitrite is transported to shoots for assimilation and reduced to nitrite (NO_2^-) thanks to activity of the nicotinamide adenine dinucleotide (NAD(P)H)-dependent cytosolic nitrate reductase (NR). NO_2^-, in turn, is promptly reduced by nitrite reductase into ammonium (NH_4^+) for further assimilation into organic compounds (Crawford, 1995; Zheng *et al.*, 2013). In addition to NH_4^+ production, the nitrite anion can be reduced to NO via non-enzymatic and various enzymatic pathways (Salgado *et al.*, 2013). Non-enzymatic nitrite reduction occurs in

the apoplasts (Bethke *et al.*, 2004). The NO_2^- reduction by enzymatic mechanism includes the reaction catalyzed by NO_2^-:NO reductase (Ni:NOR) in the plasma membrane (Stöhr *et al.*, 2001) and in the plant mitochondria (Frungillo *et al.*, 2014; Salgado *et al.*, 2013) and the reaction catalyzed by NR in the cytosol (Rockel *et al.*, 2002).

2.3. NO in bacteria

Bacteria, like animals and plant, tame NO in order to use this free radical as second messenger in their functioning and signaling. Here, once more, the high bacterial evolutionary potential and the ability to adapt to environmental changes are reflected. Thus, two major pathways of NO metabolism were described in bacteria. The first one includes the primary NOS-mediated NO synthesis (Sudhamsu & Crane, 2009); and the second one is based on the NO reductase activity, similar to that previously described in plants (Arai *et al.*, 2003).

2.3.1. NO synthesis by NO synthase

Several strains of mostly Gram-positive bacteria express homologs of the mammalian NOS (bNOS from bacterial NOS). Recent genome sequencing has revealed that NOS-like protein exists in many bacteria, including *Streptomyces*, *Deinococcus*, *Staphylococcus*, and *Bacillus* species (Crane, 2008). However, to the best of our knowledge, bacteria of genus *Pseudomonas* do not possess the NOS coding genes.

2.3.2. Nitrogen cycle and denitrifying bacteria

As previously reported in **Figure 18**, the interconversion of the nitrogen species (oxidation states from –III to +V) constitutes the global biogeochemical nitrogen cycle (Watmough *et al.*, 1999). As represented in **Figure 21**, the inorganic nitrogen is converted to a biologically useful form (N+V) by N_2 fixation or nitrate assimilation. Nitrogen is removed from the environment by both nitrification - the oxidative conversion of ammonia (NH_4^+) to nitrate (NO_3^-) (**Figure 21**, **green color**) - and denitrification - a respiratory process whereby nitrate is reduced by several enzymatic steps to nitrogen gas (**Figure 21**, **blue color**).

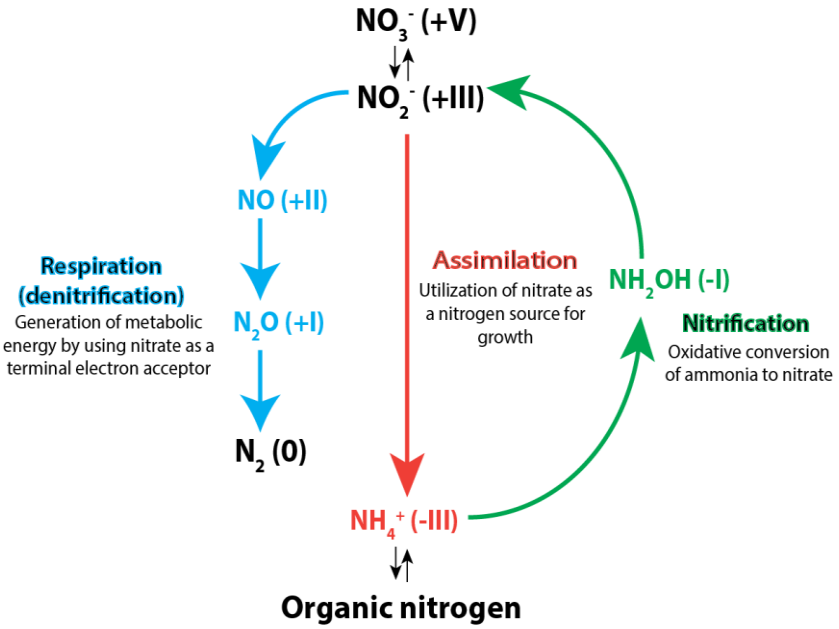

Figure 21. Bacterial nitrogen cycle
Nitrate assimilation (**red color**) leads to the conversion of inorganic nitrogen N(+V) to a biologically useful form N(-III). The nitrification (**green color**) is the oxidative conversion of ammonia N(-III) to nitrate N(+V). Denitrification (**blue color**) is a respiratory process when nitrate N(+V) is successively reduced to nitrite N(+III), nitric oxide N(+II), nitrous oxide N(+I), and dinitrogen N(0). The oxidation state of nitrogen is shown in bracket.
Adapted from Watmough et al., 1999.

Ammonia is not an intermediate of the denitrification pathway. The overall respiratory reduction of nitrate to nitrogen gas is coupled to ATP generation, allowing the organism to grow in the absence of oxygen (Sias *et al.*, 1980; Takaya *et al.*, 2003). Many bacterial species, especially the members of *Pseudomonas* genus (in majority *P. aeruginosa*), can perform the denitrification under anaerobic conditions (Almeida *et al.*, 1995; Kumita *et al.*, 2004).

Since NO could be formed during the denitrification pathway in *Pseudomonas* species, this mechanism will be discussed below. As demonstrated in **Figure 22**, the denitrification consists of four sequential steps catalyzed by the denitrification enzymes, such as nitrate reductase (NAR/NAP), nitrite reductase (NIR), nitric oxide reductase (NOR), and nitrous oxide reductase (N_2OR).

Figure 22. Denitrification pathway in *Pseudomonas* spp. species and enzymes, catalyzed the NO_x reduction

Nitrate reductases

In the first step of the denitrification pathway, bacteria have to reduce the nitrate -N(+V)- to the nitrite -N(+III)- thanks to the catalytic properties of nitrate reductases (**Figure 22**) (Bedzyk *et al.*, 1999; Carlson *et al.*, 1982). Two different nitrate reductases were found in denitrifying *P. aeruginosa* (Bedzyk *et al.*, 1999). One is known as a respiratory membrane-bound nitrate reductase (NAR) (Carlson *et al.*, 1982), which is directly associated with denitrification and

anaerobic nitrate respiration. The second is a periplasmic nitrate reductase (NAP) (Van Alst *et al.*, 2009). Why have two enzymes, catalyzing the same reaction remains to be understood.

The membrane-bound nitrate reductase complex consists of three polypeptides α, β, and γ, which are encoded by the *narK1K2GHJI* operon (**Figure 23A**). The α- and β-subunits NarGH extend into the cytoplasm and are associated with a molybdopterin cofactor. The enzyme is attached to the cytoplasmic membrane by the γ subunit NarI, which accepts electrons from the quinol pool and transfers them via β-heme to NarG. The NarJ is a chaperone involved in NarGHI assembly, and $NarK_1K_2$ are possibly involved in nitrate and nitrite transport (Van Alst *et al.*, 2009).

The periplasmic nitrate reductase, encoded by the *napEFDABC* operon (**Figure 23B**), consists of two subunits, NapA and NapB. The cytochrome c-type protein NapC is involved in the electron transfer to NapAB. NapA is the large subunit with the molybdenum cofactor and a [4Fe-4S] cluster. NapB is a *c*-type cytochrome (Carlson *et al.*, 1982).

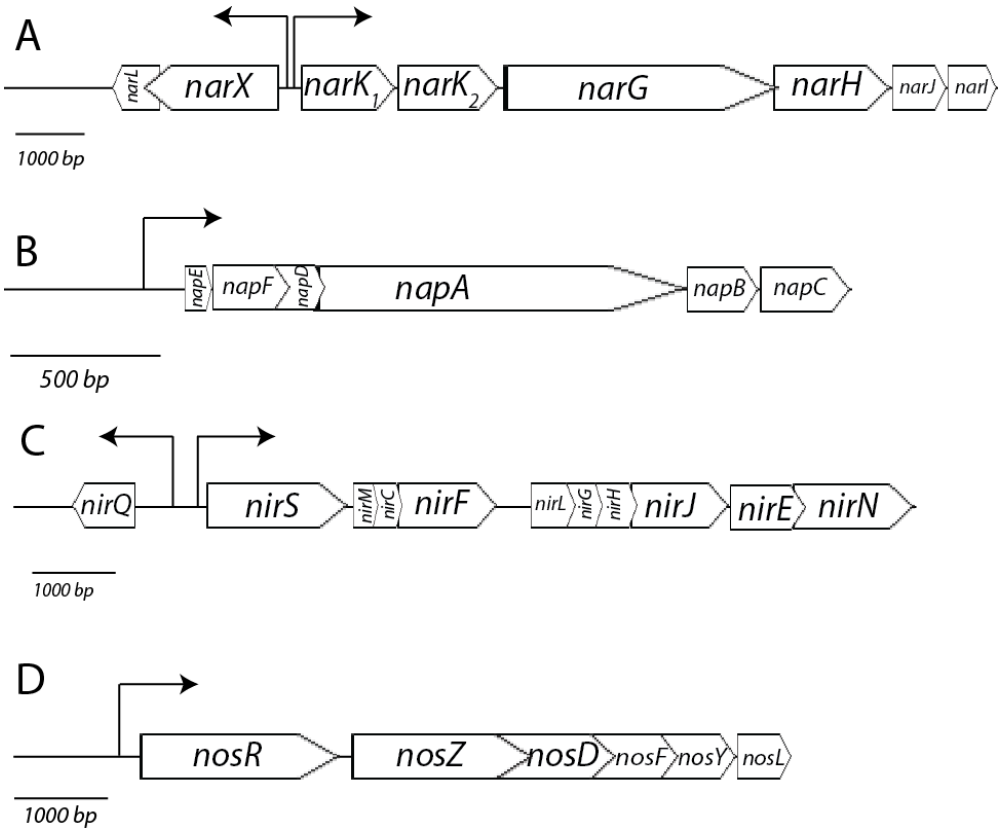

Figure 23. Schematic representation of the denitrification genes locus in *Pseudomonas aeruginosa* PAO1

A. The *nar* locus. The *narXL* and *narK1K2GHJI* share a divergently oriented promoter region. B. The *nap* locus. C. The *nir* locus. D. The *nos* locus. The scale is made for each locus. bp: base pair.
According: www.pseudomonas.com.

The *narK1K2GHJI* operon was described as involving in the nitrate respiration, whereas the physiological role of the NAP periplasmic nitrate reduction may vary in different organisms or

even in the same bacterium under different metabolic conditions (Moreno-Vivián *et al.*, 1999). The physiological role of NAP in *P. aeruginosa* is not certain in present. Bedzyk and colleges supposed, that the latter is used for the denitrification during aerobic to anaerobic transition, as well as to maintain the redox balance during the reduction of NO_3^- to NO_2^- (Bedzyk *et al.*, 1999). Thus, the 'aerobic' denitrification was found to be performed by the coupling of the NAP to the NIR and NOR enzymes (Bell *et al.*, 1990; Berks *et al.*, 1995). Aerobic denitrification can be an advantage for bacteria growing under microaerobic conditions (*i.e.* biofilm) or in environments, rapidly changing between aerobic and anaerobic conditions (Moreno-Vivián *et al.*, 1999).

Nitrite reductases

As previously reported (see part **1.4. Nitrogen oxides and reactive nitrogen species: chemistry and biological role**), the nitrite is a toxic molecule, which must be quickly reduced in nitric oxide using the nitrite reductases (**Figure 22**). Three different types of NIR were found in bacteria. The cytochrome *c* NIR reduces nitrite to ammonia while the other two classes of NIR (a cytochrome *cd1* NIR and a trimeric copper containing NIR) located in the periplasm and catalyze the one electron reduction of NO_2^- to NO (Watmough *et al.*, 1999). The cytochrome *cd1* was isolated from a number of denitrifying bacteria (van Wonderen *et al.*, 2007; Zajicek *et al.*, 2004), including members of *Pseudomonas* genus (Cutruzzolà *et al.*, 2003; Rinaldo *et al.*, 2011). This enzyme functions as a homodimer (Nurizzo *et al.*, 1998), when each subunit contains a covalently attached heme *c* and a non-covalently bound heme d_1 (Nurizzo *et al.*, 1997). In *P. aeruginosa*, the NIR is encoded by the *nirSMCFDLGHJEN* gene cluster (**Figure 23C**), where *nirS* is the structural gene for the enzyme (Silvestrini *et al.*, 1989). The *nirM* and *nirC* encode two cytochromes *c*, and both these cytochromes mediate electron transfer from the cytochrome bc_1 complex to the nitrite reductase (Arai *et al.*, 1990; Hasegawa *et al.*, 2001). The *nirFDLGHJE* genes are necessary for the biosynthesis of the heme d_1 (Arai, 2011). The *nirN* encodes a c-type cytochrome, which is similar to *nirS*, but its function is not certain (Hasegawa *et al.*, 2001).

Nitric oxide reductases

Three types of bacterial NORs have been identified: cNOR, qNOR and qCu_ANOR (Shiro *et al.*, 2012). Cytochrome *c*-dependent NOR (cNOR) was characterized in *P. aeruginosa* and *P. stutzeri* (Field *et al.*, 2008; Kastrau *et al.*, 1994). It is a heterodimeric enzyme consisting of a small (NorC) and a large (NorB) subunits. NorC is a membrane-bound subunit with a heme *c*, which accepts electrons from an external protein electron donor. NorB contains three iron centers (two *b*-type hemes and one non-heme iron, Fe_B). The *b*-type heme mediates electron

transfer from the heme *c* in the NorC subunit to the binuclear catalytic center, which consists of another *b*-type heme and Fe_B (Hino *et al.*, 2010; Shiro, 2012). In *P. aeruginosa*, the NOR is encoded by the *norCBD* operon. The *norC* and *norB* encode cytochrome *c* and *b* subunits, respectively, and *norD* encodes a soluble protein involved in the enzyme activation (Arai, 2011; Arai *et al.*, 1995a; Zumft, 2005).

Nitrous oxide reductase

As shown in **Figure 22**, the last step of the denitrification, including the reduction of N_2O to N_2, is catalyzed by the multicopper enzyme N_2O reductase (N_2OR) (Zumft, 1997; Zumft & Kroneck, 2007). In *P. aeruginosa*, the N_2OR is encoded in the *nosRZDFYL* operon (**Figure 23D**), where *nosZ* is a structural gene (Arai *et al.*, 2003). The *nosDFY* genes products are involved in the copper insertion into the enzyme, the *nosL* gene product is an outer membrane disulfide isomerase, and the *nosR* gene codes for a membrane protein with unknown functions.

Transcriptional regulation of denitrification genes in *P. aeruginosa*

Two transcriptional regulators, ANR (ANaerobic Regulator of arginine deiminase and nitrate reductase) and DNR (Dissimilatory Nitrate respiration Regulator), which both belong to the FNR (Fumarate and Nitrate reductase Regulator)/cAMP (cyclic adenosine monophosphate) receptor protein family, hierarchically control the expression of the denitrification genes in *P. aeruginosa* (**Figure 24**) (Kuroki *et al.*, 2014). ANR senses intracellular oxygen levels by the $[4Fe\text{-}4S]^{2+}$cluster and is activated upon the oxygen depletion (Sawers, 1991). DNR is a NO-sensing regulator, which senses NO molecules through heme (Castiglione *et al.*, 2009; Giardina *et al.*, 2008). Expression of the *dnr* gene is under control of ANR and is induced under low oxygen or anaerobic conditions (Arai *et al.*, 1997). The transcription of NAR complex is regulated by NarXL two-component nitrate sensor-Response Regulator (RR) proteins (**Figure 24**) (Van Alst *et al.*, 2009; Arat *et al.*, 2015). NarXL is a classic two-component bacterial regulatory system, in which a histidyl-aspartyl phosphorelay controls the gene expression in response to specific environmental stimuli (Härtig *et al.*, 1999). The periplasmic domain of the sensor protein NarX, contains a highly conserved nitrate recognition region. The nitrate recognition results in the autophosphorylation of a conserved histidyl residue in the NarX cytoplasmic transmitter domain. Transfer of phosphate to the conserved aspartyl residue in the receiver domain of the RR, NarL results in the transcriptional regulation of the target operons. NarL, in conjunction with Anr and Dnr, induces the *narK1K2GHJI* operon expression, and potentially represses the expression of *napEFDABC* operon in *P. aeruginosa* (Van Alst *et al.*, 2009; Schreiber *et al.*, 2007). NirQ is an ATP-binding protein, which is required for the activation of nitrite reduction (**Figure 24**). The *nirQ* expression is dependent on *dnr* and *narL*

expression and strongly induced under anaerobic conditions (Arai *et al.*, 1994; Schreiber *et al.*, 2007). The transcription of *norC* is also dependent on Anr and Dnr and the presence of nitrite (Arai *et al.*, 1995b).

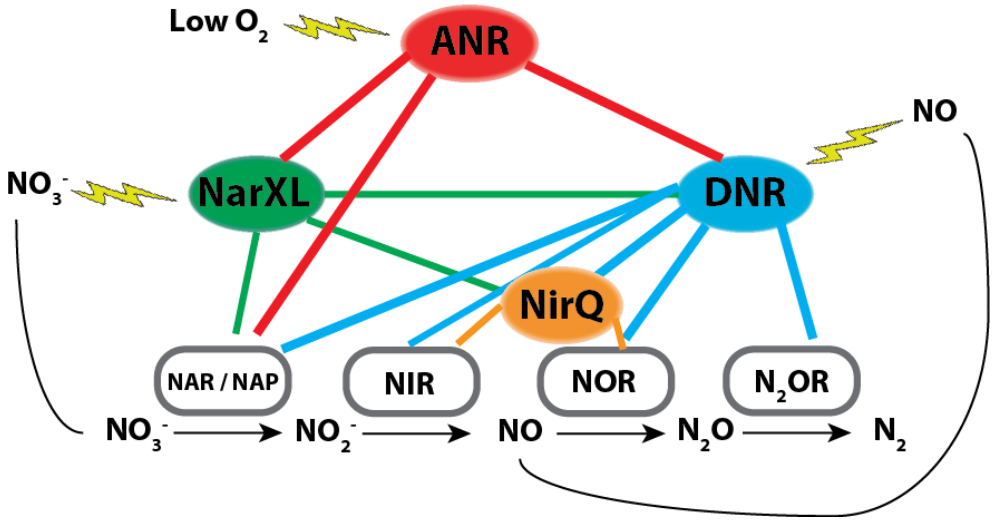

Figure 24. Schematic model of the regulatory network controlling the denitrification genes in *P. aeruginosa*
Under anaerobic or low O_2 conditions, ANR (red color) activates the expression of DNR (blue color). The latter activates the expression of all denitrification genes in response to NO_x. A two-component nitrate sensor regulator, NarXL (green color) positively regulates expression of the *nar* genes, and represses the expression of *nap* genes. The NirQ (orange color) is involved in the fine tuning of the activities of *nir* and *nor* genes.
Adapted from Arai, 2011.

However, it should be noted, that not all *Pseudomonas* spp. strains possess nitrate respiration coding genes. Among currently sequenced strains, the genomes of most *P. aeruginosa*, several *P. stutzeri*, *P. brassicacearum* subsp. brassicacearum NFM421 and just *P. fluorescens* F113 are found to contain such genes coding for Nar, Nap, and Nir enzymes (www. pseudomonas.com).

3. NO targets in cells

NO and RNS were found to damage bacterial cells. The complexity of RNS chemistry and their high reactivity (especially in presence of O_2 and reactive oxygen species (ROS)) make difficult to assign the specific antimicrobial actions to individual molecular species (see part **1.4. Nitrogen oxides and reactive nitrogen species: chemistry and biological role**). The dependence of antimicrobial action of RNS on the redox environment in and outside the bacterial cell is an additional complication. However, the RNS were found to interact with numerous targets in a microbial cell, including thiols, metal centers, tyrosines, nucleotide bases and lipids (Fang, 2004; Nathan & Shiloh, 2000). Many of these interactions are reversible, which reflects once again, the high bacterial adaptability to counteract the nitrosative stress.

Some of the most important antibacterial actions of RNS are shown in **Figure 25** and discussed below.

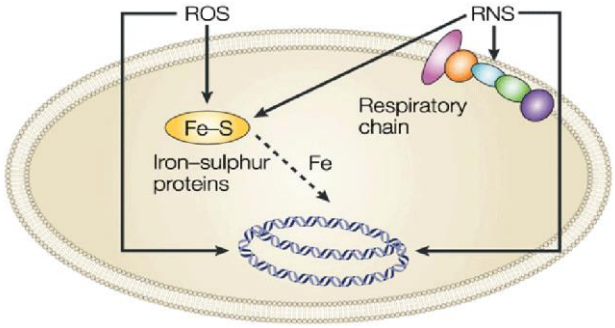

Figure 25. Bacterial targets of RNS
A scheme of simplified bacterial cell is shown. Reactive nitrogen species (RNS) mainly interact with thiols, metal centers and DNA. RNS inhibit bacterial respiration and alter DNA replication through the inactivation of zinc metalloproteins. RNS can mobilize iron from iron–sulphur [Fe-S] proteins. The reactive oxygen species (ROS) provoke mainly a direct DNA damage and, like RNS, interact with bacterial proteins.
Adapted from (Fang, 2004).

3.1. Membrane glycerophospholipids

As previously reported in **Chapter 2 Stress factors and *Pseudomonas fluorescens* lipid adaptation**, bacterial membrane plays a role of the first barrier between the environment and the cell. However, the GP membrane itself is not inert towards several toxic compounds and could be chemically modified. The prototypical effect of RNS on membrane is reflected in lipid oxidation and/or nitrosation (Möller *et al.*, 2008; Pryor *et al.*, 1982). It was shown, that several RNS affect mainly polyunsaturated FAs, leading to form lipid hydroperoxides, lipid alcohols, and aldehydes. The NO_2 effect on GPs is well studied (Augusto *et al.*, 2002; Pryor *et al.*, 1982; Pryor & Lightsey, 1981). It was proposed that the reaction is dependent on the O_2 level. At high O_2 concentrations, NO_2 will predominantly mediate lipid oxidation (see part **1.1. Oxidative stress**). Conversely, at low O_2 level, nitration reactions may preferentially occur (**Figure 26**) (O'Donnell *et al.*, 1999). The GP nitration reaction proceeds via addition of NO_2 to the double bond of FA chain, forming an instable nitro alkyl radical, which will be efficiently transformed in the presence of O_2 or additional NO_2 to peroxynitroalkyl and dinitroalkyl respectively (**Figure 26.1 and 2**) (Pryor *et al.*, 1982; Pryor & Lightsey, 1981). In the absence of adequate concentrations of O_2 and NO_2, nitrous acid is dissociated from alkyl radical, leading to the double bond formation (**Figure 26.3**) (Augusto *et al.*, 2002). This reaction drives to *cis/trans* isomerization (Jiang *et al.*, 1999). Conversely, the hydrogen abstraction reaction can support the formation of alkyl radical, which, in turn, can be nitrated or oxidized as described previously (**Figure 26.4 and 5**).

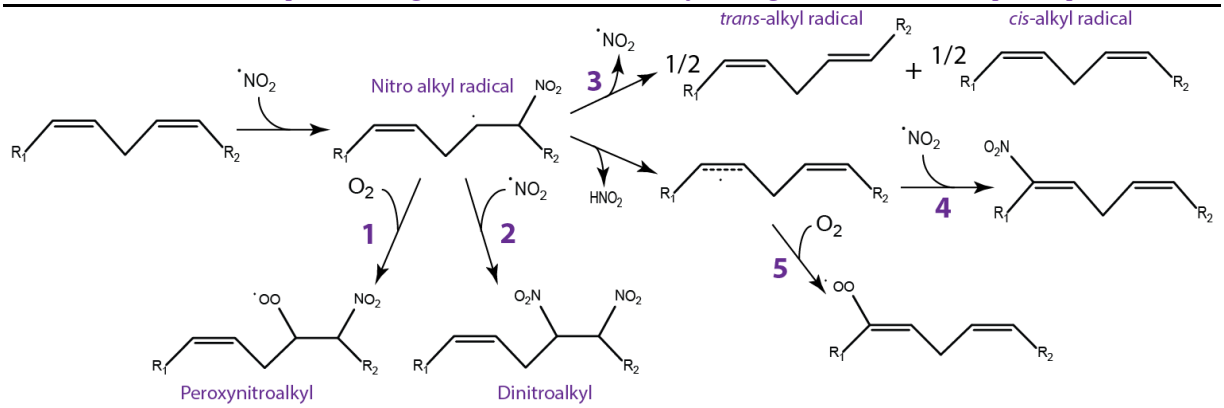

Figure 26. Schematic representation of NO_2 reaction with polyunsaturated lipids
Adapted from Augusto et al., 2002.

As the NO oxidation by O_2 is accelerated in hydrophobic conditions of lipid membrane (Liu *et al.*, 1998), the damage of GPs is not the major role of NO radical. As consequence, NO alone (without O_2 or $ONOO^-$) does not modify bacterial FAs (Rubbo *et al.*, 1994).

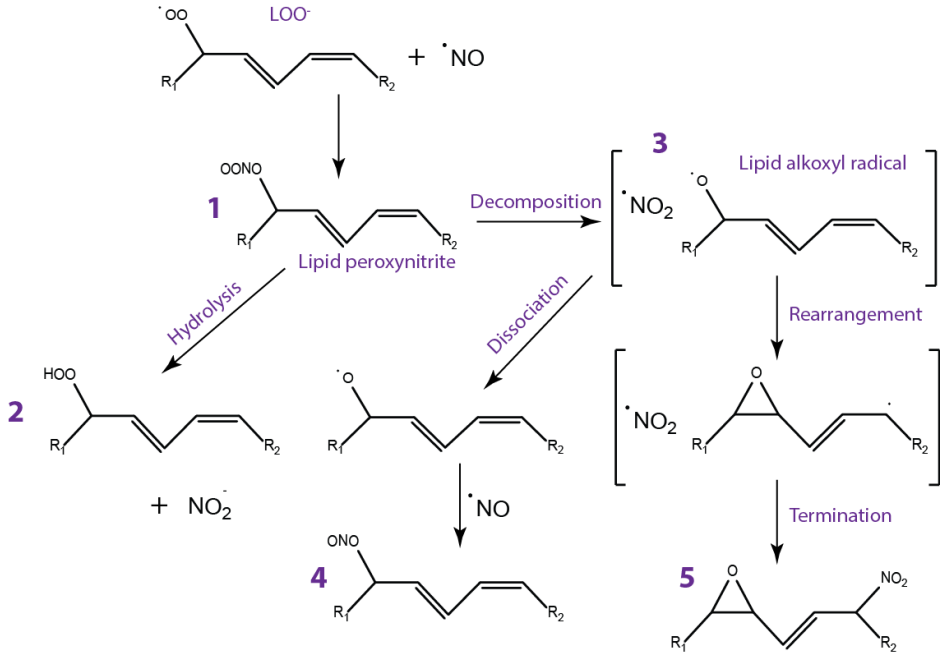

Figure 27. Reaction of NO and lipid peroxyl radicals
Adapted from O'Donnell et al., 1999.

Therefore, NO potentially interacts with oxidized lipid at several levels. Rubbo proposed that, depending of the rate of ROS production, NO both stimulates and inhibits lipid peroxidation and yields to the nitrogen-containing derivatives of oxidized lipids. Its protective role includes (i) redirection of O_2^-- and $ONOO^-$-mediated cytotoxic reactions to other oxidative pathways, and (ii) termination of lipid peroxidation propagation reaction (**Figure 27.1**) (Rubbo *et al.*, 1994). Thus, NO reacts with a lipid peroxyl radical (LOO^-) to give the lipid peroxynitrite ($LOONO^-$) intermediate, which is rapidly hydrolyzed to secondary radical species (**Figure 27.2**). Two free radicals, NO_2 and lipid alkoxyl radical (LO) may be formed (**Figure 27.3**) and could react with additional NO (**Figure 26.4**), or undergo a termination of lipid peroxidation

(**Figure 27.5**) (O'Donnell *et al.*, 1999). Concerning another RNS species, peroxynitrite can both oxidize and nitrate polyunsaturated FAs via NO_2 formation (**Figure 26**) (O'Donnell *et al.*, 1999).

It should be noted, that all previously discussed mechanisms of NO_x – lipids interactions were established in eukaryotic cells, containing polyunsaturated FAs. The question "Can NO_x modify bacterial monounsaturated FAs or GPs composition?" is still an enigma.

3.2. Proteins

Among the RNS targets in bacterial cell, the proteins play one of the most important roles. Nitrosative stress can cause several types of protein damage. Binding to the protein metal centers, the RNS impact several vital functions in bacteria, such as biofilm formation, or DNA repair. The reaction of RNS with phenols provokes a tyrosine nitration, and the ones with thiol groups of cysteines cause the S-nitrosylation of several proteins (Hill *et al.*, 2010; McLean *et al.*, 2010). All these mechanisms are of high importance in bacterial functioning, reflecting once more the complex RNS chemistry and the high reactivity of these species, but also a high bacterial adaptability to the RNS toxicity. The brief description of RNS reactions with proteins are sum up below.

3.2.1. Reaction of RNS with thiols

Thiols is organosulfur compounds that contain a carbon-bonded sulfhydryl group (–C–SH or R–SH, where R represents alkane, alkene, or other carbon-containing chemical group). The chemistry of thiols is intimately associated with the chemistry of RNS, which lead to the reversible nitrosation and/or oxidation of thiols (Fukuto *et al.*, 2000). The involvement of NO_2, N_2O_4 or N_2O_3 in these reactions was particularly studied. The thiol nitrosation results in the formation of S-nitrosothiols (RS-NO) (Hughes, 2008) or S-nitrothiol species (RS-NO_2) (Antelmann & Helmann, 2011). The different modifications appear to be dependent on the nature of RNS, the protein itself, and its subcellular localization. The protein S-nitrosylation was found to be an obligate concomitant of anaerobic respiration on nitrate in *E. coli*, controlled by OxyR transcription factor (see part **4.6. Secondary NO sensors**) (Seth *et al.*, 2012). Overall, the thiol group belongs to cysteine, an indispensable α-amino acid for all forms of life. It serves as a precursor for protein synthesis. The unique chemistry of its free thiol group forms the active moiety of several essential metabolites, such as CoA, glutathione and its derivatives (Dominy *et al.*, 2006). Nitrosation may cause toxic effects on bacterial cells, altering protein 'normal' functions (Sigfrid *et al.*, 2003). However, the impact of RNS on bacterial proteins is not always negative. For instance, the S-nitrosylation could play a role of a conserved mechanism for control of protein function. This non common control pathway appears to activate several

proteins, essential in response to nitrosative stress (see part **5.1. [Fe - S] cluster repair**). The mechanism of this activation is based on the reaction of RNS with protein metal centers, which will be described below.

3.2.2. RNS complexes with metal centers

NO is able to reversibly bind to ferrous (Fe^{2+}) and ferric (Fe^{3+}) irons of several prokaryotic and eukaryotic proteins. This binding could both inhibit enzyme activity (*i.e.* catalase inhibition, (Brown, 1995)) and activates several enzymes, such as guanylate cyclase (GCyc) (Ding & Demple, 2000). The notable example of the NO signaling in bacterial cells is the NO binding to iron-sulfur protein clusters [Fe-S] (Cooper, 1999). The [Fe-S] clusters are common, almost ubiquitous, prosthetic groups that are essential for the function of proteins, involved in a wide range of biological processes, including electron transfer chains, redox and non-redox catalysis of reactions involved in metabolic pathways, and gene regulation (Justino *et al.*, 2007). These prosthetic groups are inorganic moieties, whose iron atoms are coordinated to inorganic sulfides and usually linked to protein by cysteine thiolates (Drapier, 1997).

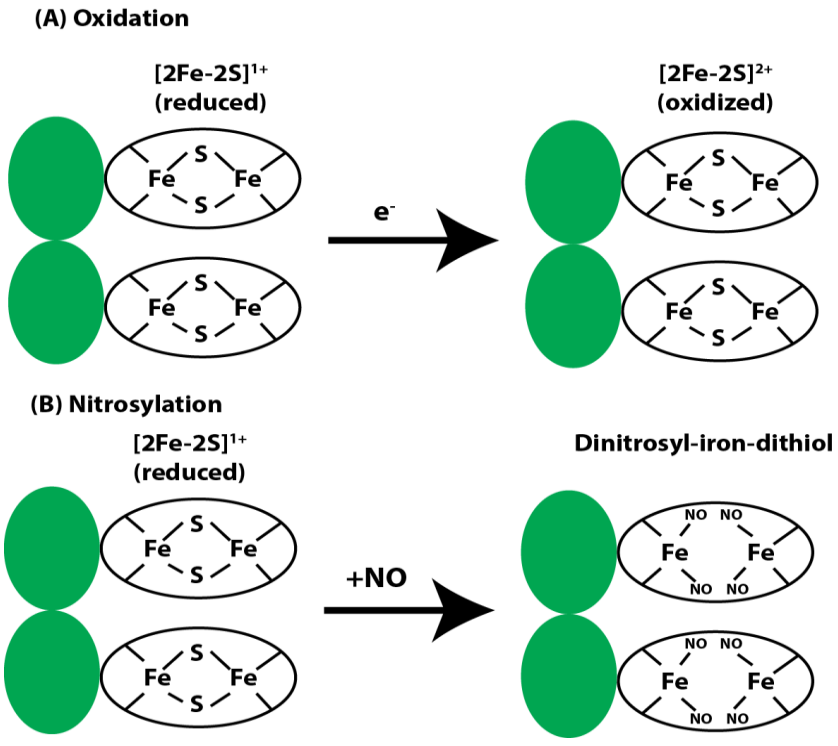

Figure 28. Reaction of RNS with [Fe-S] cluster
The RNS reaction with [Fe-S] cluster is demonstrated in example of SoxR activation. **Green ovals:** DNA binding domains; colorless ovals: iron-binding domains. SoxR is shown as a homodimer. **(A) Redox-regulation**. When the [2Fe-2S] centers of SoxR are in the reduced state, the protein transcriptionally inactive. One-electron oxidation converts the protein to a potent transcription activator. **(B) Model for activation of SoxR by nitrosylation**. The intact [2Fe-2S] cluster of SoxR is directly modified by NO to generate dinitrosyl-iron-dithiol clusters. Adapted from Ding and Demple, 2000.

One of attractive examples of this reaction is presented in **Figure 28** by SoxR transcriptional regulator that controls an oxidative stress response in *E. coli* (Ding & Demple, 2000). When the [2Fe-2S] centers of SoxR are in the reduced state $[2Fe\text{-}2S]^{1+}$, the protein is transcriptionally inactive. As shown in **Figure 28A**, the ROS cause one-electron oxidation to yield $[2Fe\text{-}2S]^{2+}$ clusters that activates the protein (Ding *et al.*, 1996; Gaudu & Weiss, 1996). The RNS, as well, activate SoxR in *E. coli* (Nunoshiba *et al.*, 1993) generating, in turn, dinitrosyl-iron-dithiol clusters (**Figure 28B**) (Ding & Demple, 2000).

3.2.3. Tyrosine nitration

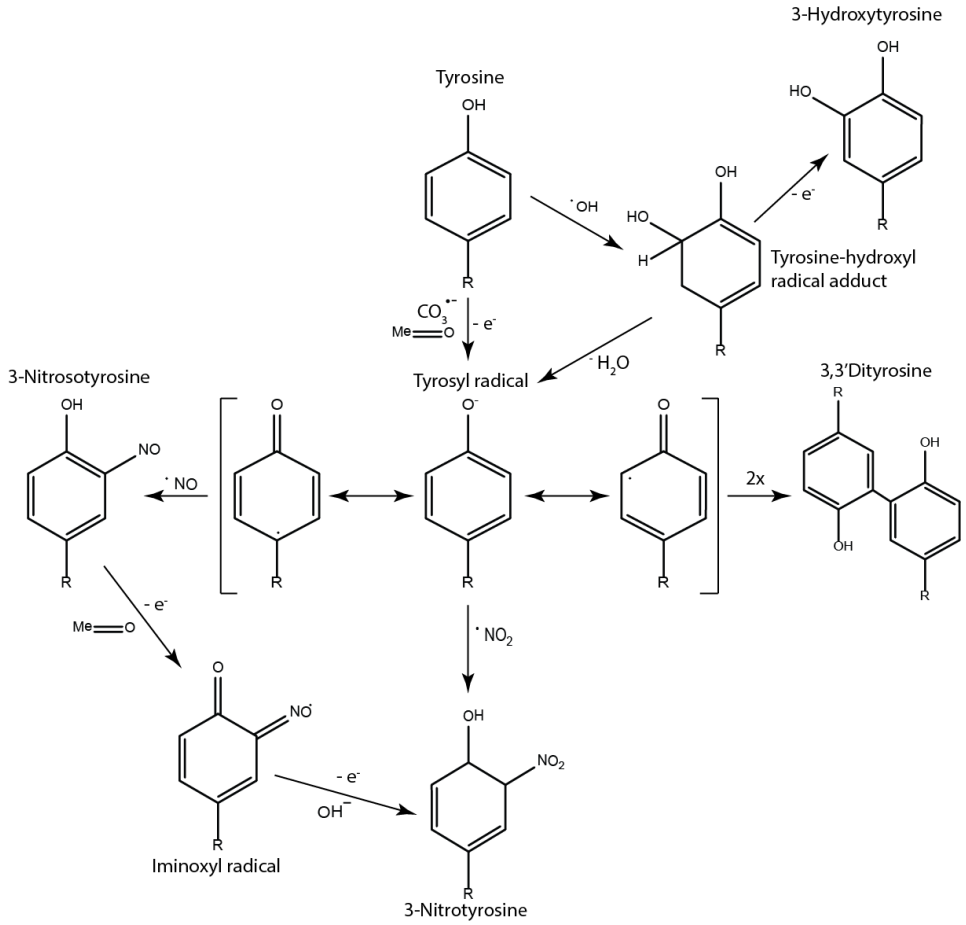

Figure 29. Free radical pathways to tyrosine nitration
Adapted form Radi, 2004.

The RNS react with phenols, occurring in the protein tyrosine residues nitration to form the 3-nitrotyrosine (**Figure 29**). This post-translational protein modification draws attention of biochemical researches, because it may alter the protein functions. RNS do not able to directly perform the nitration, because they have to react with previously formed tyrosine radical. These latter are formed via tyrosine oxidation by $CO_3^{\bullet-}$ and OH radicals, or oxo-metal complexes. An alternative radical mechanism for tyrosine nitration involves the reaction of tyrosyl radicals with NO, giving 3-nitrosotyrosine, which, after sequential two-electron oxidation, forms tyrosine iminoxyl radical and 3-nitrotyrosine (Radi, 2004). Although stabilization of tyrosyl radicals, they could form a dimer, 3,3'-dityrosine. Several studies found that RNS, particularly peroxynitrite, cause the massive tyrosine nitration (Alvarez & Radi, 2003; Lindemann *et al.*, 2013; McLean *et al.*, 2010). Unlike in the case of cysteines, the tyrosine nitration is fairly unspecific, affecting a large number of *E. coli* proteins. These modifications are thought to be irreversible and probably damages proteins irreparably (Lindemann *et al.*, 2013).

In conclusion, the reactivity of RNS with proteins results in various noxious consequences for bacterial cells. The reactions with heme iron centers are known to be involved in respiratory arrest, limiting the ability of cells to maintain the redox balance and generate the energy for

growth (Richardson *et al.*, 2008; Stevanin *et al.*, 2000). Thus, nitrosative stress helds to severely impair oxidative phosphorylation (OP), a major process generating ATP in an O_2-dependent manner in bacteria. This ATP-generating system relies on the tricarboxylic acid (TCA) cycle and the electron transport chain (ETC) (Appanna *et al.*, 2014). NO directly reacts with metal prosthetic groups of cytochromes in the ETC and [Fe-S] clusters of dehydratases (*i.e.* aconitase) (Husain *et al.*, 2008). This underscores the tendency of RNS to inhibit aerobic respiration, necessitating the expression of anaerobic metabolic genes. The sensitivity of aconitase [Fe-S] cluster to NO affects the TCA cycle (Gardner *et al.*, 1997; Richardson *et al.*, 2008). Bacterial survival under conditions of nitrosative stress indicates that diverse bacterial species respond to nitrosative stress by altering the expression of metabolic pathways (see part **4.5. Metabolic reprogramming**).

3.3. DNA damage

As previously reported, RNS react with [Fe-S] clusters to inactivate proteins that contribute to the DNA stability, such as ribonucleotide reductase (necessary for normal DNA replication) and several enzymes involved in DNA repair (*e.g.* Fpg DNA glycosylase, DNA repair methyltransferase and DNA ligase) (Spek *et al.*, 2001). In addition to the potentially deleterious effects of loss of function of these important DNA-metabolizing proteins, RNS may induce DNA modifications such as cross-links and base damage (reviewed in Burney *et al.*, 1999).

NO does not directly react with DNA, but can become a potent DNA damaging agent once it has been transformed to N_2O_3, or peroxynitrite. These RNS react with DNA via multiple pathways (Burney *et al.*, 1999; Tamir *et al.*, 1996), which are briefly mentioned here and reported in **Figure 30**. The N_2O_3 leads particularly to either direct or indirect nitrosative DNA damage. Direct damage results in the nitrosation of primary amines on DNA bases leading to the deamination. Any DNA base containing an exocyclic amino group can undergo deamination, whose the end result is the net replacement of an amino group by a hydroxyl group. Therefore, adenine, cytosine, 5-methylcytosine, and guanine can all be deaminated to form hypoxanthine, uracil, thymine and xanthine respectively, all of which are potentially mutagenic if unrepaired. The DNA repair pathways present a very interesting area of current researches and resumed in this work (see part **4.2. Repair of DNA damage**). As reported in **Figure 30**, in addition to deamination, the N_2O_3 can also cause the formation of single- and double-strand breaks in DNA (SSB and DSB respectively) (Burney *et al.*, 1999).

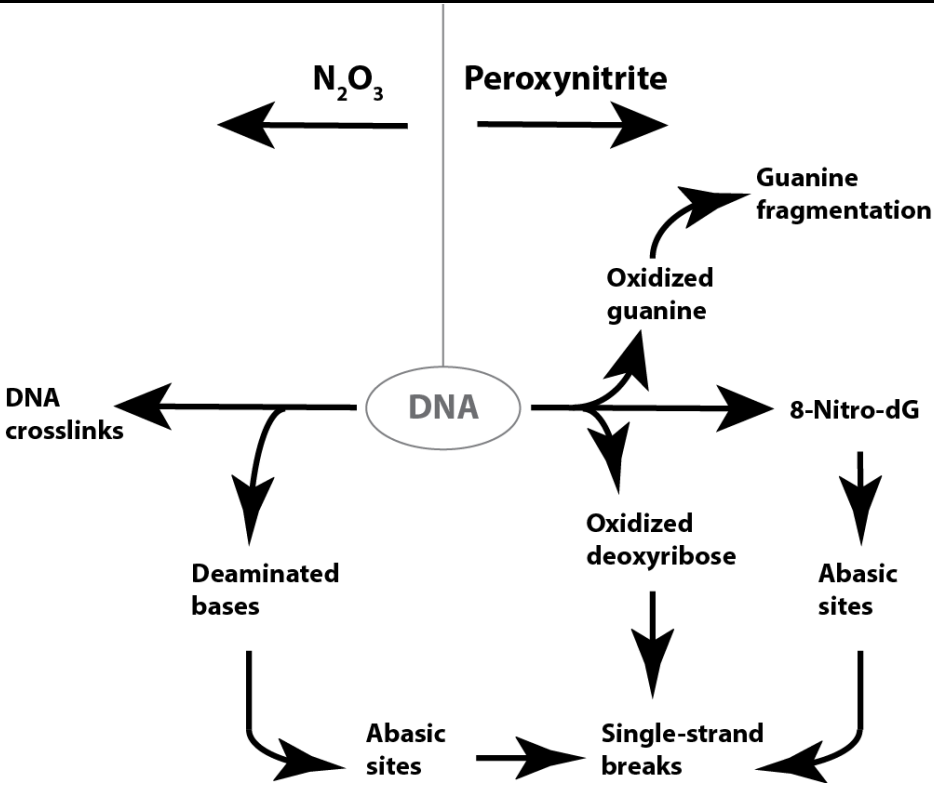

Figure 30. DNA damage pathways resulting from RNS exposure
Adapted from (Burney *et al.*, 1999).

In contrast to N_2O_3, which is primarily involved in the deamination of DNA, most of the DNA damages caused by peroxynitrite is oxidative (**Figure 30**). DNA treatment with peroxynitrite generally leads to the deoxyribose oxidation and oxidation of bases, most notably guanine (Hughes *et al.*, 2009). This reaction results in predominantly 8-oxoguanine (8-oxoG) and 8-nitroguanine (8-nitro-dG) formation. Its biological consequences include both cytotoxicity and mutagenicity. In fact, 8-nitro-dG is unstable and readily depurinates to form abasic sites. The formed 8-oxoG can actually react again with peroxynitrite to form secondary oxidation products, whose biological consequences are currently under investigation. In addition to base lesions, peroxynitrite, like N_2O_3, can also lead to SSBs (Spek *et al.*, 2001).

4. Bacterial strategies of response to RNS

It becomes increasingly evident, that NO and derived RNS damage several (if not all) compounds of bacterial cells, but bacteria have developed a wide range of adaptive responses to counteract the RNS toxicity. These responses, including NO sensing, metabolism modifications, NO detoxification pathway(s) and GP barrier, will be discussed in this part of the work.

4.1. Membrane glycerophospholipid barrier

As described before, bacterial membrane offers a significant resistance to the passage of most toxic species. It is therefore relevant to know whether GP membranes are permeable to RNS, to define if these molecules could penetrate into the cell and react with another targets within bacteria. As shown in **Figure 31**, the lipid membranes do not present a barrier against the diffusion of NO and O_2 (Signorelli *et al.*, 2011), but significantly decrease the diffusion of HNO_3 and H_2O_2, and prevent the diffusion of $ONOO^-$, O_2 and carbonate radical (CO_3^-) (Möller *et al.*, 2008). The NO_2 membrane permeability was investigated in several studies (Khairutdinov *et al.*, 2000; Möller *et al.*, 2008; Signorelli *et al.*, 2011). Khairutdinov et al. estimated the NO_2 permeability coefficient is between 4×10^{-4} and 10 cm s^{-1} (Khairutdinov *et al.*, 2000), a range too wide to make appropriate predictions, ranging from minimal to significant membrane resistance to NO_2 permeation. Signorelli and colleagues estimated the NO_2 permeability coefficient at 5 cm s^{-1}, suggesting that the GP membrane is permeable to this free radical, but 10 times slower than to NO (Signorelli *et al.*, 2011). So, the order of permeability across lipid membrane is: NO, O_2 then ONOOH, NO_2, $HOO^{\cdot}$, H_2O, which are quicker than $O_2^{\bullet-}$, $ONOO^-$, $CO_3^{\bullet-}$ as illustrated in **Figure 31**.

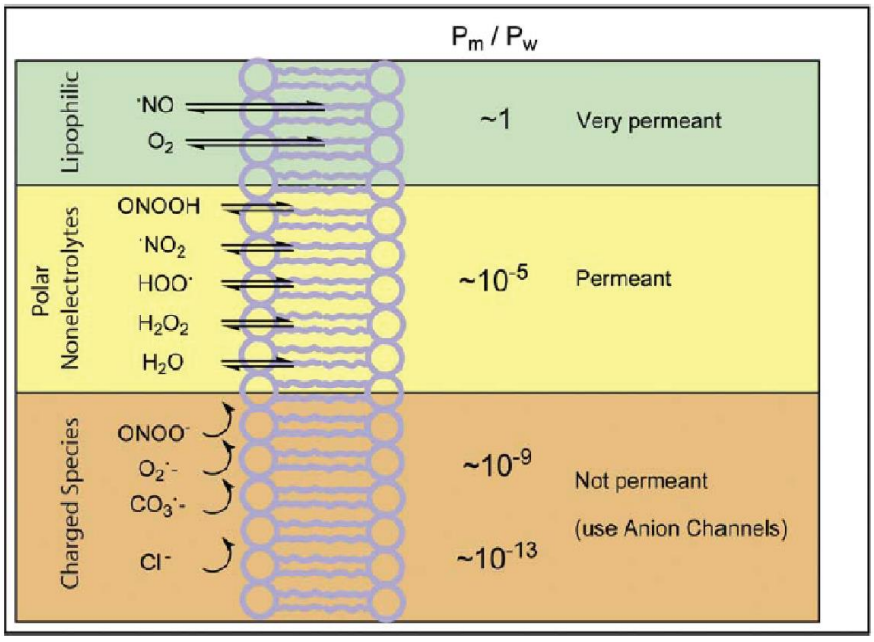

Figure 31. Permeability of reactive species across lipid membrane
P_m/P_w is the ratio between membrane permeability and the permeability through an equivalent layer of water. Lipid membranes are not barrier to NO, but a moderate barrier to the permeation of ONOOH or NO_2. The permeability of charged molecules, like $ONOO^-$ is not significant.
Adapted from Möller et al., 2008.

While the charged molecules do not able to freely cross GP bilayer, they are able to penetrate bacterial membrane. The peroxynitrite, for example, can enter the cell either by passive diffusion (as peroxynitrous acid, ONOOH) or by anion channels (as peroxynitrite anion, $ONOO^-$) (Ferrer-Sueta & Radi, 2009). However, it should be noted, that these studies were

performed in PC membrane models to establish the response of eukaryotic membrane to free radical toxicity. Bacterial membrane composition is quite different of that of eukaryotic cell. We assume, that the permeability of NO_x through bacterial membrane could (or could not) be different of previously studied.

4.2. Repair of DNA damage

All living organisms have evolved several mechanisms to repair the DNA damages, preventing the genome instability and limiting the accumulation of deleterious mutations. As previously demonstrated, The RNS can damage bacterial genomes that result in aberrant base pairing, DNA crosslinks, abasic sites, SSBs or DSBs (see part **DNA damage**). These modifications lead to the reduction in viability by impairing the transcription of essential genes and the stalling of DNA replication; furthermore, the incorporation of incorrect bases can itself be harmful and affects the viability of progeny. The DNA repair was extensively studied in both prokaryotes and eukaryotes (Boiteux & Guillet, 2004; Eisen & Hanawalt, 1999; van der Veen & Tang, 2015). Given the diverse nature of DNA damages caused by RNS, several repair pathways have evolved to rectify them and to restore lost genetic information, including the base excision repair (BER), nucleotide excision repair (NER) or mismatch repair (MMR) pathways. The BER pathway assures the cells protection from the deamination, alkylation and hydrolysis of bases (Huffman *et al.*, 2005). Briefly, in this pathway, damaged bases are recognized and removed by DNA glycosylases. The DNA backbone is then cut and the single-strand gap is replaced with nucleotide(s) (van der Veen & Tang, 2015). The NER pathway recognizes bulky adducts that distort the DNA helix (Kisker *et al.*, 2013). There is another NER pathway, which is coupled to the transcription machinery, when the NER system recognizes RNA polymerases that are stopped at an abnormal base during transcription (Deaconescu *et al.*, 2006). The MMR pathway is involved in repair of mismatched nucleotides and insertions/deletions, which occur during DNA replication or direct DNA damage (Jiricny, 2013). Repair of DSBs is mediated by the homologous recombination (HR) or non-homologous end-joining (NHEJ) systems (Ayora *et al.*, 2011). All these systems are well described in *E. coli* cells. For more information about the DNA repair we encourage readers to refer to a recent and a very comprehensive review of van der Veen and Tang, 2015.

4.3. Detoxification

In order to copy the toxic NO_x effects, bacteria have evolved a number of detoxification mechanisms based on NO_x transformation, such as reduction, or oxygenation. In *Pseudomonas* spp., two major NO detoxification pathways were demonstrated. The first is the reduction of NO by nitric oxide reductase (Arai & Iiyama, 2013; Shiro, 2012). NO_2 reduction can be

performed with two purposes: nitrite/nitrate respiration (see part **Nitrogen cycle and denitrifying bacteria**), and the utilization of nitrite as a nitrogen source for growth (assimilation) (**Figure 21**). Since the NO_2 and NO reductases involved in respiration were discussed above, here, we focus on nitrite reductase involved in the nitrite assimilation. In this assimilatory pathway, conducted by Nas enzymes (for nitrate assimilation), nitrate is reduced to nitrite, which is then reduced by assimilatory nitrite reductase (NirBD in *Pseudomonas* spp. species) to ammonia, which serves as a source of nitrogen for biosynthesis (**Figure 21**).

In nitrate-assimilating *Pseudomonas* strains, ammonium is generated in the cytoplasm by a NADH-dependent assimilatory nitrite reductase (NirBD) to detoxify the nitrite that accumulates in anaerobic nitrate-respiring cells and to regenerate NAD^+ (Romeo *et al.*, 2012). NirBD contains a single siroheme, a [4Fe-4S] center, NADH- and flavin adenine dinucleotide (FAD)-binding domain (Campbell & Kinghorn, 1990; Guerrero *et al.*, 1981).

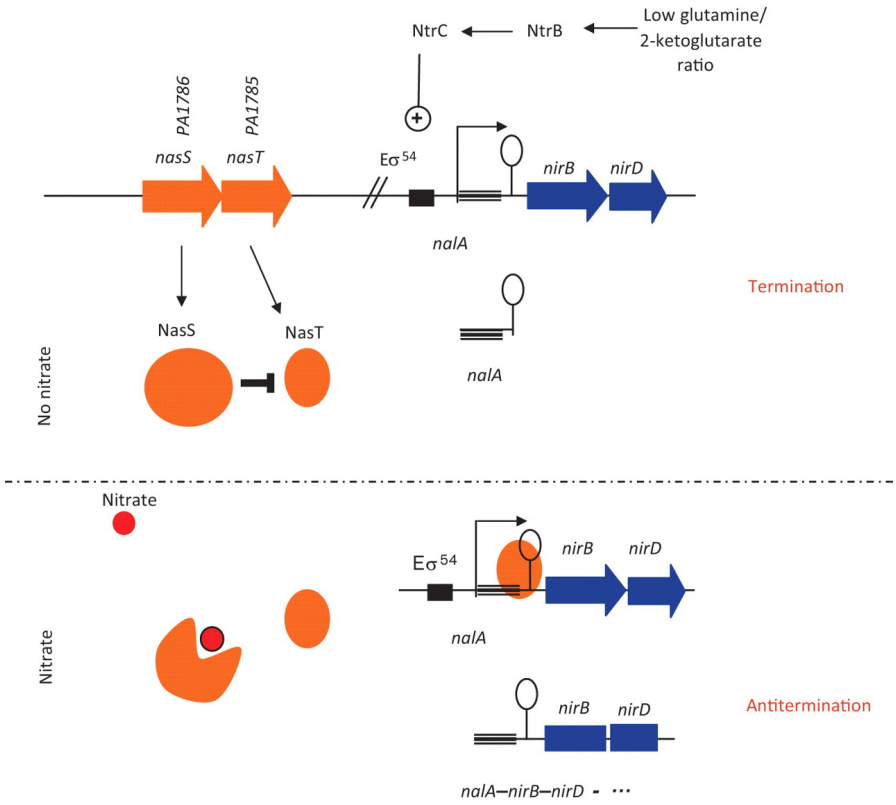

Figure 32. Model of NalA- and NasT/S-dependent expression of nitrate assimilation operon in *P. aeruginosa* PAO1
In absence of nitrate, the ratio of glutamate/2-ketoglutarate decreases, which leads to the activation of NtrBC system and σ^{54} dependent *nalA* promoter. Thus, NalA is synthesized and NasT is sequestrated by NasS. In the presence of nitrate, the NasS-mediated NasT sequestration is decreased, resulting in antitermination within the *nalA* leader and transcription of operon. Adapted from Romeo et al., 2012.

The *nirBD* genes were found to encode the two subunits of nitrite reductase, large and small respectively and, as shown in **Figure 32**, are located in operon with nitrate reductase coding gene (Romeo *et al.*, 2012). The expression of these genes is subject to dual regulation, mediated by the antiterminator protein NasT, activity of which is negatively controlled by nitrate sensitive regulator NasS (**Figure 32**) (Lin & Stewart, 1998; Romeo *et al.*, 2012). In the absence of nitrate, transcription terminates in the operon leader *nalA* as NasS inactivates NasT. In contrast, binding of nitrate to NasS leads to antitermination within *nalA*, and consequently to *nirBD* expression. Transcription of this operon is carried out by a σ^{54}-dependent promoter and mediated by

activation of the two-component system NtrBC (**Figure 32**). The Nas pathway is not regulated by oxygen level, and could be expressed under anaerobic and aerobic conditions. In addition, it seems to be largely distributed among *Pseudomonas* spp. species, and was found in majority of sequenced strains, including several *P. aeruginosa, P. fluorescens, P. putida, P. stutzeri* and *P. syringae* strains (www. pseudomonas.com).

However, the most fully studied and understood NO detoxification pathway is based on the flavohemoglobin (FlavoHb) (Cruz-Ramos *et al.*, 2002). FlavoHb is a NO detoxifying protein distributed among a wide variety of bacteria (Poole *et al.*, 1996; Poole & Hughes, 2000), including *P. aeruginosa* Fhp (Arai *et al.*, 2005). Functional properties of this enzyme is dependent on the O_2 level. Aerobically, FlavoHb detoxifies NO by acting as an NO dioxygenase (Gardner *et al.*, 1998a) and affords inducible protection of aconitase activity (Gardner *et al.*, 1998b) and respiration (Stevanin *et al.*, 2000). Anaerobically, FlavoHb serves as a NO reductase, generating nitrous oxide (Hausladen *et al.*, 1998). The *E. coli* flavohaemoglobin (Hmp) was the first described microbial globin (Wu *et al.*, 2003). This is a monomer with C-terminal domain that closely resembles to ferredoxin- nicotinamide adenine dinucleotide phosphate ($NADP^+$) reductase with FAD and NAD(P)H binding sites. In addition to its role in NO detoxification, FlavoHb is involved in bacterial protection against reactive oxygen species (Koskenkorva-Frank & Kallio, 2009). Furthermore, FlavoHb is involved in the repair of the polyunsaturated FAs in the cell membranes, which are damaged during oxidative/nitrosative stress (see part **Membrane glycerophospholipids**) (Bonamore *et al.*, 2003b). In *P. aeruginosa,* transcription of the *fhp* gene is activated by FhpR, a NorR-type σ54-dependent transcriptional activator, located upstream of *fhp*. The studies of *fhp* promoter region demonstrated that the expression of *fhp* is independent on DNR or ANR. Thus, DNR activates the genes for denitrification, which utilizes NO as an electron acceptor under anaerobic conditions. FhpR activates the *fhp* transcription, which detoxifies NO under aerobic conditions (Arai *et al.*, 2005). It addition, two another genes, *asrA*, and PA3697 coding for aminoglycoside-induced stress response ATP-dependent protease and hypothetical protein, were described as regulators of *fhp* transcription in *P. aeruginosa*. Interestingly, AsrA protein is involved in short-term protection of *P. aeruginosa* against high concentrations of tobramycin (Kindrachuk *et al.*, 2011), suggesting that NO detoxification could modify *P. aeruginosa* antibiotic sensitivity.

4.4. NO release

Bacteria are able not only to transform NO through detoxification pathways, but also to release this toxic molecules from the cells. This release seems to be entrust to RND (Resistance-nodulation-cell division) family efflux pumps, and particularly MexEF-OprN (Poole, 2014). Like other tripartite RND family pumps, the MexEF-OprN efflux system consists of an inner

membrane drug-proton antiporter (MexF), an outer membrane channel-forming component (OprN), and a prismatic membrane fusion protein (MexE) (**Figure 33**) (Alvarez-Ortega *et al.*, 2013). In *P. aeruginosa* the *mexEF-oprN* is positively controlled by MexT, which, in turn, is probably negatively regulated by MexS (Uwate *et al.*, 2013). Moreover, that the *mexEF-oprN* multidrug efflux locus is induced by nitrosative stress (Fetar *et al.*, 2011). This induction is dependent on both the MexT transcriptional activator and the MexS repressor (Poole, 2005a), which together with *mexEF-oprN* are involved in response to NO detoxification.

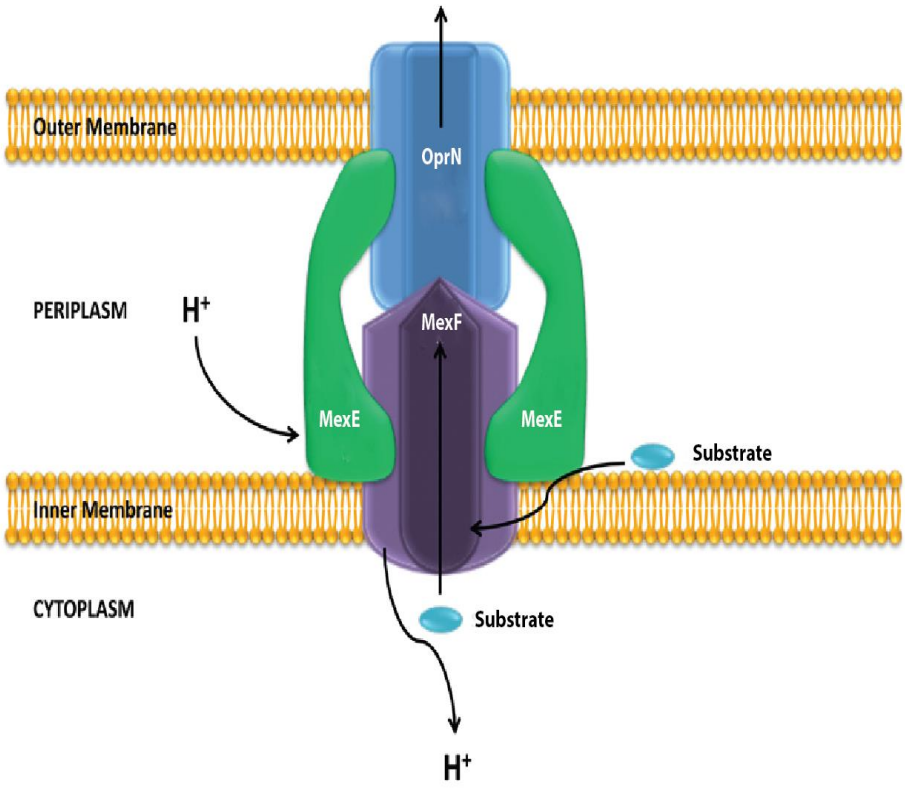

Figure 33. Schematic illustration of the MexEF-OprN RND efflux pump
The MexEF-OprN system is formed by the inner membrane MexF protein, the outer membrane protein OprN and the membrane fusion protein MexE. The activity of the MexE RND protein is coupled to the proton gradient. This efflux pump can extrude different compounds, including antibiotics and NO_x from the bacterial cytoplasm and the periplasm.
Adapted from Alvarez-Ortega et al., 2013.

The primarily role of RDN pumps is an antibiotic resistance. Activation of MexEF-OprN gives rise to the bacterial resistance to, among others, chloramphenicol, fluoroquinolones, trimethoprim and triclosan (Köhler *et al.*, 1997). The activity of MexEF-OprN pump also influences the *quorum sensing*, and reduces virulence factors (biofilm formation, pyocyanin production) and swarming motility (Lamarche & Déziel, 2011). As the overproduction of MexEF-OprN pump is involved in response to NO, it seems likely that NO could modify bacterial sensitivity to antimicrobial agents, targeted by these pump.

4.5. Metabolic reprogramming

As reported in the part **Proteins**, nitrosative stress causes the alterations in the cell respiration, altering the ATP production via oxidative phosphorylation (OP) (Husain *et al.*, 2008). Recent investigations found, that to adapt to these aspects of RNS toxicity, bacteria of *P. fluorescens* group reprogram their metabolism (Auger *et al.*, 2011; Auger & Appanna, 2015). To counteract the ineffectivity of aconitase and TCA cycle caused by NO donor, *P. fluorescens* was found to

use the citrate lyase (CiLy), phosphoenolpyruvate carboxylase (PEPC) and pyruvate phosphate dikinase (PPDK) to convert citrate into pyruvate and ATP (**Figure 34**).

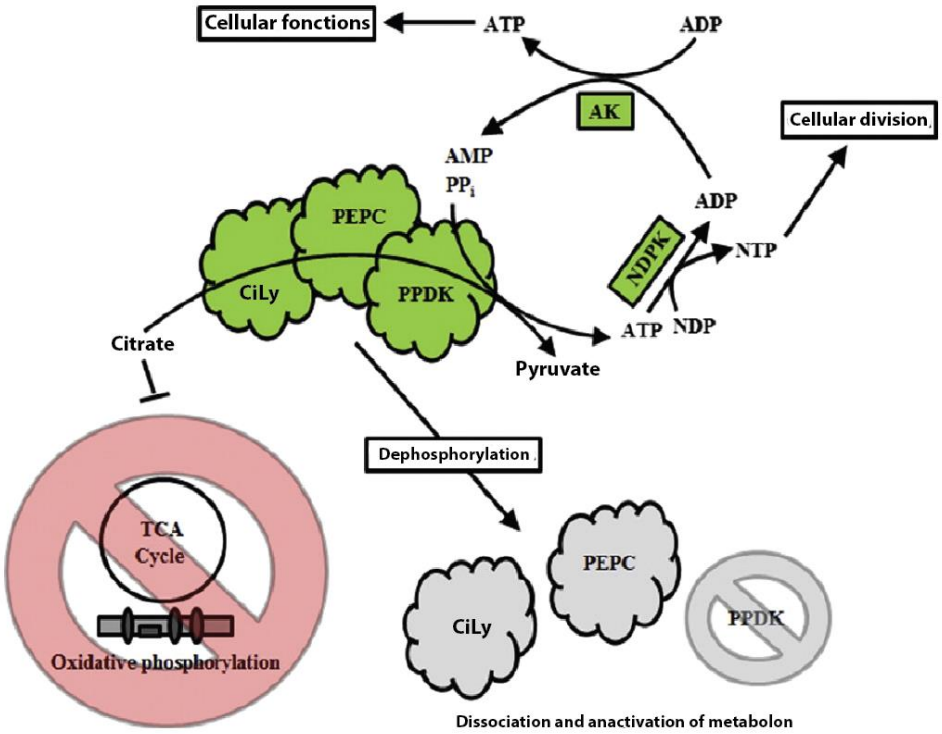

Figure 34. Reprogramming of *P. fluorescens* metabolism in order to adapt to nitrosative stress

The RNS reactions with [Fe-S] clusters and metal centers of tricarboxylic acid (TCA) cycle and ETC alter the ATP production via oxidative phosphorylation pathway (red). A supercomplex involving citrate lyase (CiLy), phosphoenolpyruvate carboxylase (PEPC) and pyruvate phosphate dikinase (PPDK) (green) is assembled by the organism to effectively produce ATP, the phosphotransfer networks, including adenylate kinase (AK) and nucleoside diphophate kinase (NDPK), permit the storage of this crucial moiety. This supercomplex can be disassociated by dephosphorylation (gray).
Adapted from Auger et al., 2015.

Interestingly, these enzymes appear to be transiently assembled as a supercomplex to form a metabolon, which completly reprogramms the metabolic networks assuring a bacterial surviving in presence of RNS. In this way, the CiLy degrades citrate into oxaloacetate and acetate. The dicarboxylic acid delivers the two compounds, pyruvate and ATP, allowing the survival of *P. fluorescens* under nitrosative stress conditions. This machinestry is coupled to the increased activities of phosphotransfer enzymes like adenylate kinase (AK) and nucleoside diphophate kinase (NDPK) (**Figure 34**), which ensure the efficacy of this ATP-making machine (Appanna *et al.*, 2014; Auger & Appanna, 2015). This elegant strategy allows bacteria to form ATP. Thus, metabolic modifications present the underlying force at the center of bacterial adaptation in order to generate and store ATP anaerobically when the electron transport chain is defective (Auger & Appanna, 2015).

4.6. Secondary NO sensors

The NO sensing in bacterial cell is a complex mechanism, involving a wide range of 'secondary' sensors. The discussed below systems, as the name of chapter indicates, have as principal function to sense another signal, but NO can modulate their activity and so, potentially influences processes mediated by these sensors. One of these mechanisms is based on the cellular redox signaling/regulation and mediated through proteins that have redox-sensitive cysteines (Antelmann & Helmann, 2011). In fact, redox-regulated proteins typically contain one or several redox-sensing cysteines, which are in the free thiol state in the reducing environment of the cytosol. When the cell encounters RNS, the redox-sensitive cysteine(s) become(s) nytrosated (see part **Reaction of RNS with thiols**), which leads to a change in protein structure, often activating protein. Once the cell has overcome the redox stress, cellular systems, such as glutaredoxin or thioredoxin, reduce the redox-sensing cysteines and return the proteins activity back to 'normal' (Brandes *et al.*, 2007; Lindemann *et al.*, 2013).

The SoxRS provides one of the prototypical examples of this mechanism. In *E. coli* the SoxRS regulon protects bacteria against NO (Ding & Demple, 2000). As previously described in part **RNS complexes with metal centers**, the sensor of this regulon is SoxR protein, activated by NO (**Figure 28**). Its target *soxS*, in turn, increases the transcription of several genes, including superoxide dismutase, *sodA*, glucose-6-phosphate dehydrogenase, *zwf*, two flavodoxins *fdlA* and *fdlB* and *fur* regulator, involved in iron metabolism. The *sodA* gene allows the removing $O_2^{\bullet-}$ that may react with NO to form NO_2 and $ONOO^-$ (Feld *et al.*, 2012). The *zwf* is involved in the repair of [Fe-S] clusters (Giró *et al.*, 2006). SoxRS activation protects *E. coli* from macrophage killing (Nunoshiba *et al.*, 1993). However, SoxRS is still a minor player in the physiological response to the RNS toxicity. SoxR orthologues are present in many bacteria, including *P. aeruginosa*. However, its target, SoxS, was not found in *P. aeruginosa* (Kobayashi & Tagawa, 2004). Thus, in this bacterium, SoxR is a functional redox-responsive activator, which is probably directly linked to $O_2^{\bullet-}$ or NO. Its activity is required for *P. aeruginosa* virulence and antibiotic resistance (Palma *et al.*, 2005).

The transcription factor OxyR is a major H_2O_2 transcriptional activator. H_2O_2 is a toxic for bacteria oxidative species, produced by plants (Ohwada *et al.*, 1999) and macrophages (Loegering & Schwacha, 1991), during host – pathogen interactions. Like SoxR, OxyR is activated by oxidation under aerobic conditions, and also by S-nitrosylation under anaerobic conditions. Activated by H_2O_2, OxyR induces the gene expression in a distinct regulon through alternative post-translational modifications. However, the S-nitrosylated OxyR induces the gene expression in other regulon, whose the components protect bacteria against nitrosative stress at least by limiting the S-nitrosylation (Seth *et al.*, 2012).

Catalase is an enzyme involved in bacterial response to oxidative stress, and able to catalyze the decomposition of H_2O_2 to O_2 and H_2O (Chelikani *et al.*, 2004). *P. aeruginosa* defense against this oxidizing biocide is mediated by three catalases: KatA, KatB and KatC (Elkins *et al.*, 1999). The transcription of *katA* is regulated, in part, by the intercellular signaling system called *quorum sensing* (Hassett *et al.*, 1999), OxyR (Heo *et al.*, 2010), IscR (an [Fe-S] cluster assembly regulator) (Kim *et al.*, 2009) and ANR (Trunk *et al.*, 2010). The high level of *katA* expression was detected in anaerobic *P. aeruginosa* cultures, indicating that KatA possesses functions beyond the removal of H_2O_2. KatA may directly interact with NO to protect bacterial cells against NO toxicity by buffering of free NO when potentially toxic concentrations of NO are approached (Su *et al.*, 2014) (**Figure 35**).

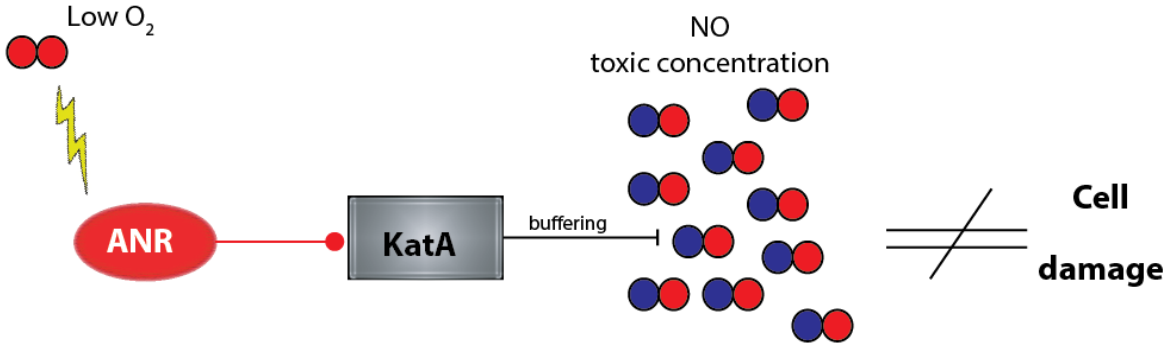

Figure 35. The proposal model of the KatA-mediated NO sensing
Under anaerobic or low O_2 conditions, ANR activates *katA* expression, resulting in KatA production. Using an unidentified mechanism, KatA may sense a toxic concentration of NO and buffers NO to protect bacteria against nitrosative stress.

Ferric uptake protein (Fur) is a global regulator, conserved in Gram-negative bacteria. It acts as a transcriptional repressor when it binds ferrous ion (Cornelis *et al.*, 2009). This dimeric protein is activated by the Fe^{2+} ion. The active form is able to bind to specific DNA sequences, located in the promoter region of genes involved in iron acquisition (Ochsner *et al.*, 1995). This binding leads to the repression of the downstream genes. In contrast, when iron concentration is not sufficient, the active Fur releases the Fe^{2+} irons. In this case, Fur is not able to bind specific DNA sequences and iron acquisition is then stimulated (D'Autréaux *et al.*, 2004). The iron centers of Fur can react with NO molecules to form iron-nitrosyl complex, unable to bind DNA, causing a derepression of Fur-regulated promoters (D'Autréaux *et al.*, 2002). It is particularly interesting, because the functions of Fur are not only limited to iron homeostasis. A wide variety of genes involved in various mechanisms, such as manganese superoxide dismutase or catalase, are under Fur control (Hassett *et al.*, 1996). The Fur-mediated bacterial response to NO seems to be dependent on experimental conditions (*i.e.* growing medium) (Flatley *et al.*, 2005). Fur was found to be insensitive to NO *in vivo* in minimal medium, and, in contrast, was inactivated in rich medium. The suggested explanation for this paradox is therefore that the rich medium is

sufficiently poor in iron to reveal Fur-mediated, NO-sensitive repression of genes involved in iron acquisition (Flatley *et al.*, 2005; Spiro, 2007).

In response to NO, bacteria product the enzymes, which reduce or oxidize this molecule to decrease its toxic effect, and the regulatory proteins that respond to NO (Spiro, 2007). As NO is formed in bacterial hosts, the pathogens require mechanisms to detect and detoxify this molecule (Stevanin *et al.*, 2005). Metabolism of NO is important for virulence of *P. aeruginosa* (Arai & Iiyama, 2013). Anaerobic biofilms of *P. aeruginosa* actively denitrify, and NO reduction is required for biofilm viability (Yoon *et al.*, 2002). Thus, it is not surprising that bacteria possess numerous and diverse NO-mediated regulatory networks. So, in bacteria, NO is a signal molecule, which regulates several important processes. This NO-mediated regulation is discussed in the next part of this work.

5. NO-mediated regulation in bacteria

5.1. [Fe - S] cluster repair

As previously discussed in this study, NO is involved in the redox regulation within bacterial cells (see part **4.6. Secondary NO sensors**). Since the protein dinitrosyl iron complexes are stable *in vivo*, they are not degraded, but efficiently repaired in bacterial cells (Ding & Demple, 2000; Rogers & Ding, 2001). Ferredoxin dinitrosyl iron complex may be converted to the ferredoxin [2Fe-2S] cluster thanks to ISC (iron-sulfur cluster) system (Yang *et al.*, 2002). The latter consists of cysteine desulfurase IscS, which provides the atomic sulfur during cluster assembly. The IscU protein provides scaffold for IscS-mediated assembly. IscA is an assembly protein, involved in the delivery of irons to the sites of assembly. IscR plays a role of their regulator, that senses the demand for [Fe-S] cluster formation/repair (Rogers & Ding, 2001; Schwartz *et al.*, 2001). These proteins, in conjunction with chaperons *hscAB* and ferredoxin *fdx*, are involved in both repair of [Fe - S] cluster and its *de novo* assembly (Djaman *et al.*, 2004). In fact, IscS is able to directly convert the ferredoxin dinitrosyl iron complex to the [2Fe-2S] cluster in the presence of L-cysteine. All these proteins are encoded by *iscSUA-hscBA-fdx* operon in *E. coli* (Rogers & Ding, 2001). Furthermore, only IscS protein was described as mediated the repair process (Djaman *et al.*, 2004). ISC system is well distributed among bacteria (Jones-Carson *et al.*, 2008), including *Pseudomonas* spp. strains (Choi *et al.*, 2007). In *P. aeruginosa* ISC system is encoded by *yfhJ-fdx2-hscAB-iscAUSR* operon (www.pseudomonas.com). In addition, the ISC system is involved in many physiological pathways, such as iron homeostasis or resistance to oxidative stress (Romsang *et al.*, 2014).

Other proteins are implicated in [Fe-S] cluster repair. The YtfE of *E. coli*, ScdA of *S. aureus* and NorA of *Ralstonia eutropha* are homologous to Dnr of *P. aeruginosa*. These proteins are important for the repair process of [Fe-S] clusters of aconitase and furmatase, damaged by nitrosative stress (Justino *et al.*, 2007; Overton *et al.*, 2008; Strube *et al.*, 2007). A *ytfE* deletion mutant grows poorly under anaerobic conditions, has increased sensibility to iron starvation, and decreased activity of [Fe-S] cluster containing enzymes (Justino *et al.*, 2007).

5.2. Biofilm and motility

Bacteria employ NO in non-lethal concentrations as signaling agent to control biofilm formation/dispersion and motility. NO-mediated biofilm dispersion was observed in a wide range of mono- or multispecies bacterial biofilms. Addition of NO donors was shown to induce the biofilm dispersion in *E. coli*, *Vibrio cholera*, *Bacillus licheniformis*, and *Serratia marcescens* (Barraud *et al.*, 2009a), *Neisseria gonorrhoeae* (Potter *et al.*, 2009), *Staphylococcus aureus* (Davidson *et al.*, 2004). In *B. subtilis*, inhibition of endogenous NO production leads to the decrease of biofilm biomass (Schreiber *et al.*, 2011). Addition of NO donors induces biofilm dispersion in drinking water and recycled-water systems (Barraud *et al.*, 2009a). In *Pseudomonas* spp. species, NO also causes biofilm dispersion. In fact, addition of low NO doses (25 to 500 nM) promotes dispersion of *P. aeruginosa* biofilm. *P. aeruginosa* mutant, lacking NO reductase exhibits greatly enhanced biofilm dispersion (Barraud *et al.*, 2006). In *P. putida*, heterologous expression of NOS genes is involved in increase of motility and biofilm dispersion (Liu *et al.*, 2012b). In *Pseudomonas* spp., NO stimulates PDE activity, which decreases the c-di-GMP level interlocking the biofilm dispersion (Barraud *et al.*, 2009b). Several *P. aeruginosa* PDE are involved in NO-dependent biofilm dispersion, including DipA, RbdA and NdbA (Li *et al.*, 2013; Roy *et al.*, 2012).

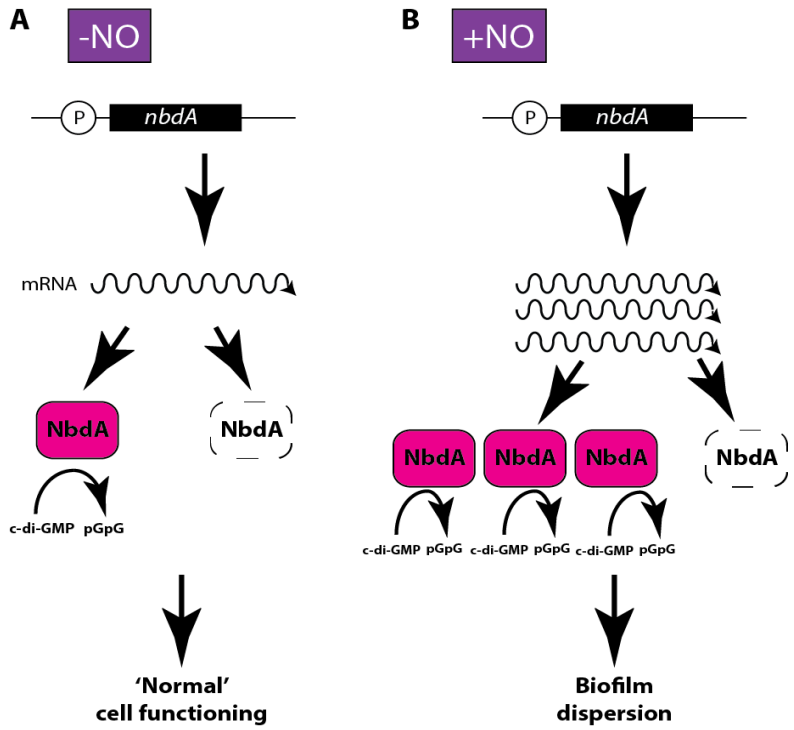

Figure 36. Model for the transcriptional regulation of *nbdA* through NO

(A) Without NO addition *nbdA* expression is low, resulting in only a few NbdA proteins that do not significantly contribute to the cellular c-di-GMP concentration. **(B)** NO induces expression of *nbdA*, resulting in elevated level of NbdA proteins, reduced cellular c-di-GMP levels and increased biofilm dispersion.
Adapted from Li et al., 2013.

In addition, the chemotaxis transducer BdlA is essential for NO-mediated biofilm dispersion (Morgan *et al.*, 2006). However, none of these proteins are specific to NO. In fact, without NO addition, *nbdA* is only weakly expressed and does not affect the c-di-GMP level (**Figure 36**). Upon NO exposure, transcription of *nbdA* is significantly induced, leading to enhanced PDE activity and biofilm dispersion. The MHYT domain of NbdA serves as a copper-binding gas sensor is responsible to the NO-mediated biofilm regulation (Hay *et al.*, 2009; Li *et al.*, 2013).

The RbdA and DipA are required to biofilm dispersion in response to NO. These PDEs directly interact with BdlA, regulating the c-di-GMP level in order to enable the process of dispersion (Petrova & Sauer, 2012a). Recent evidence also suggests a feedback regulation between c-di-GMP and BdlA. While BdlA indirectly regulates c-di-GMP level via PDE activity, activation of BdlA is, in turn, dependent on c-di-GMP abundance (Petrova & Sauer, 2012b). In addition, the c-di-GMP-synthesizing DGC GcbA is required for biofilm dispersion by regulating the posttranscriptional processing of BdlA (Petrova *et al.*, 2014). In fact, GcbA contributes to the cleavage of BdlA in *P. aeruginosa*, allowing an initial cell attachment to the surface. So, GcbA indirectly plays a surprising for DGC role in biofilm dispersion (**Figure 37**). The both GcbA and BdlA are dependent on the c-di-GMP level and are inversely regulated during the sessile-motile and motile-sessile transitions.

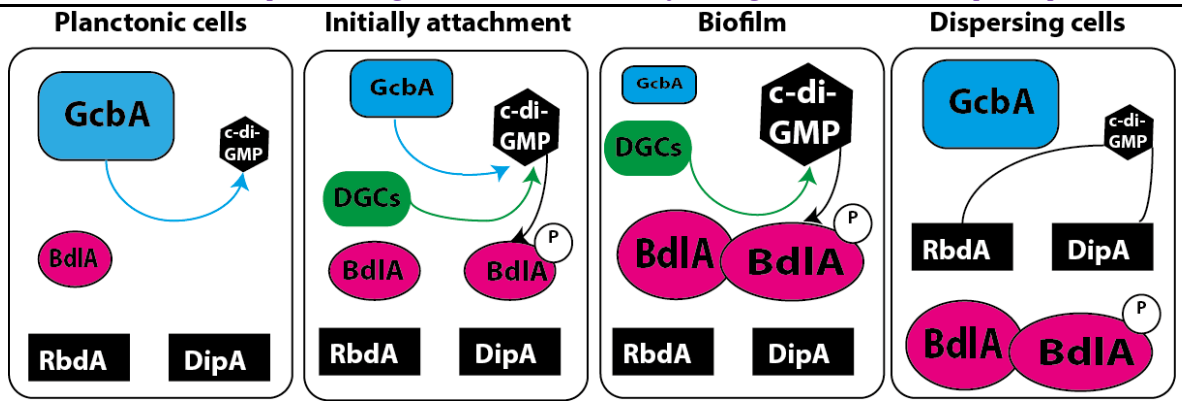

Figure 37. GcbA-mediated modulation of the BdlA-dependent biofilm dispersion
In planktonic and initially attached cells, GcbA is produced and synthesizes the c-di-GMP (blue line). This promotes the transition from reversible to irreversible surface attachment. *Via* c-di-GMP level, GcbA contributes to the cleavage of BdlA in initially attached cells (**black line**). Other DGC(s) (green line) potentially act in concert with GcbA to regulate the c-di-GMP level and, as consequence, BdlA. Conditions of reduced cellular motility and NO production lead to a reduction in GcbA. BdlA directly interacts with the PDEs RbdA and DipA, modulating their activity to reduce c-di-GMP levels. During the dispersion process, DipA and RbdA reduce c-di-GMP level to facilitate the sessile-motile transition and to induce GcbA production, activating a mechanism, which will allow the detached cells to attach to a new surface. The relative sizes of symbols indicating proteins and c-di-GMP correlate with their relative abundances in the cell during the indicated growth mode.
Adapted from Petrova et al., 2015.

In eukaryotes, the major receptor for NO is the GCyc, which has both haem and nonhaem binding site for NO (Cary *et al.*, 2006). Similar domains are encoded in bacteria and revealed a NO receptor family, named Heme-Nitric Oxide/Oxygen binding (H-NOX) proteins (Iyer *et al.*, 2003). The H-NOX genes are found in operons with diverse bacterial signaling genes (Plate & Marletta, 2013a), the majority of which can be divided in two classes: (i) containing histidine kinase (HK) and (ii) DGCs and PDE.

As shown in **Figure 38B**, H-NOX proteins control the HK activity in *Shewanella oneidensis* and *Vibrio cholerae* (Arora & Boon, 2012; Henares *et al.*, 2012; Price *et al.*, 2007). The NO-bound HnoX state inhibits associated HK (HnoK) autophosphorylation. HnoK, in turn, targets three different RR: HnoB, HnoC and HnoD. HnoB contains a PDE effector domain and its phosphorylation by HnoK stimulates hydrolysis of c-di-GMP (Plate & Marletta, 2012). HnoD functions as an inhibitor of HnoB. HnoC mediates transcriptional control for all of the signaling compounds of this network to regulate the dynamics of the NO response (Plate & Marletta, 2013b). All together, these proteins increase c-di-GMP levels in response to NO that leads to increased biofilm formation (**Figure 38B**).

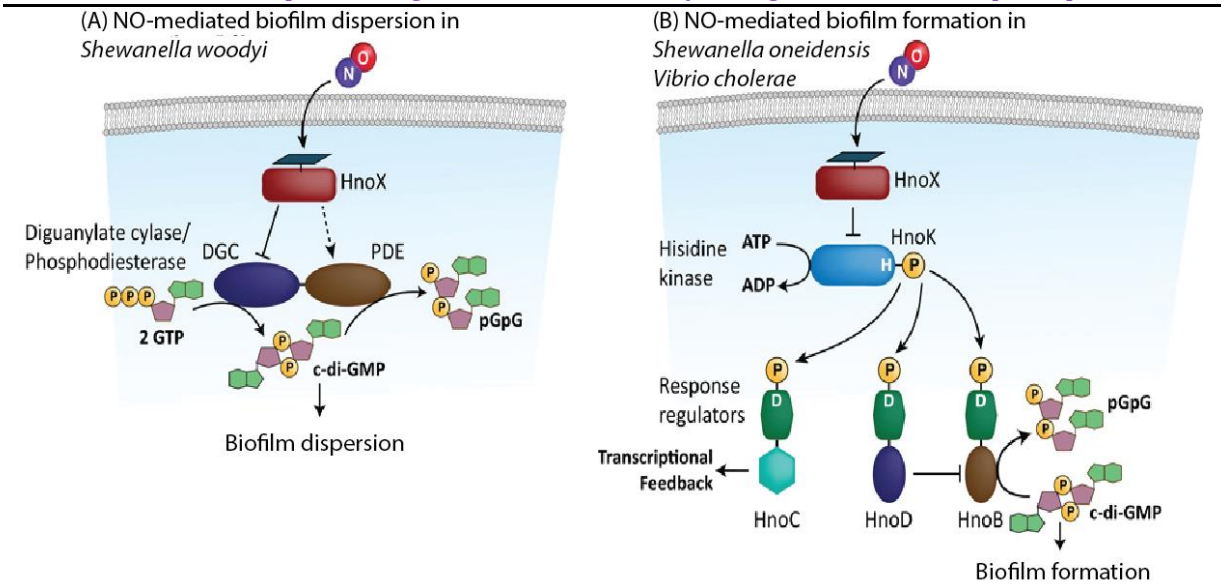

Figure 38. H-NOX-dependent control of biofilm formation through the regulation of c-di-GMP level

(A) H-NOX signaling in *S. woodyi*. The H-NOX protein HnoX interacts with a dual diguanylate cyclase/phosphodiesterase (DGC/PDE) enzyme. The NO-bound H-NOX state inhibits DGC, and increases PDE activity, leading to increased c-di-GMP hydrolysis and lower biofilm formation in response to NO. **(B)** H-NOX signaling promotes biofilm formation in response to NO in *S. oneidensis* and *V. cholerae*. The NO-bound H-NOX state inhibits autophosphorylation of the associated histidine kinase HnoK. HnoK possesses three phosphotransfer targets: HnoB, HnoC, and HnoD.
Adapted from Plate & Marletta, 2013a.

As shown in **Figure 38A**, in *Shewanella woodyi* H-NOX protein plays an opposite role. This protein contains both PDE and DGC domains, capable of the synthesis and degradation of c-di-GMP (Liu *et al.*, 2010). Without NO, H-NOX activates DGC, leading to 'normal' biofilm formation. NO-bound H-NOX increases PDE activity, allowing the decrease of intracellular c-di-GMP level and decrease of biofilm formation (Liu *et al.*, 2012a). Sequences with 15-40% identity to the GCyc H-NOX were identified in many bacteria, nonetheless, certain bacterial genus, such as *Bacillus* or *Pseudomonas*, lack H-NOX containing genes (Iyer *et al.*, 2003; Karow *et al.*, 2004, 2005).

Overall, NO-mediated regulation of biofilm formation and motility has emerged as a common theme, regulated by c-di-GMP level (D'Argenio & Miller, 2004). This process can be carried out through either direct control of DGC and PDE activity or through more sophisticated multi-component systems, based on H-NOX NO-mediated activation. The simpler direct system seems to cause dispersion of biofilm in response to NO, while the more sophisticated systems seem to react in opposite way, increasing the biofilm formation.

It should be noted, that NO-mediated effect on bacterial biofilm is described as to be concentration-dependent. At low NO concentrations, in the micromolar and nanomolar ranges, a decrease in biofilm biomass is observed. In contrast, at high (millimolar) concentrations, NO causes an increase in biofilm biomass and a decrease in planktonic biomass, related to a rapid

conversion of NO to NO_3^- and enhances anaerobic metabolism (Barnes *et al.*, 2013; Barraud *et al.*, 2006).

Unfortunately, to the best of our knowledge, the studies of effect of RNS on bacterial biofilm and/or motility are practically non-existent, only nitrate sensing and metabolism were a subject of study (Van Alst *et al.*, 2007). Analyze of *narXL* and NAR genes mutants shows altered swimming and swarming motility. No modification is noted in biofilm biomass, but in biofilm architecture compared to the wild-type *P. aeruginosa*. As authors proposed, these biofilm alterations are due to the inefficient motility and biosurfactant production. However, a NAR mutant, as well as a NAR/NAP double mutant had no defect in swimming, but in swarming motility and in biofilm formation. The deletion of *P. aeruginosa nirS* gene demonstrates the decrease of swarming, but not swimming motility. The *norC* mutant does not show any motility modification (Van Alst *et al.*, 2007). This study suggests a possible link between nitrate sensing, metabolism and biofilm formation/motility in *P. aeruginosa*. However, future investigation is necessary to rule out the mechanism of these interactions.

5.3. Antibiotic resistance

Several studies of NO-mediated resistance to antibiotics were performed (Gusarov *et al.*, 2009; McCollister *et al.*, 2011; van Sorge *et al.*, 2013). Gusarov and coworkers (Gusarov *et al.*, 2009) investigated the role of NOS genes (bNOS) of *B. subtilis* and *S. aureus* in resistance to antimicrobial agents. Thus, the effect of a wide range of antibiotics on wild type and *nos* mutated strains was compared. The bNOS protects Gram-positive bacteria against antimicrobial agents, through a direct reaction of NO with antimicrobials, making the latter less toxic, and against oxidative stress, caused by these antimicrobials. It is remarkable, that the pretreatment of *Δnos* strains with exogenous NO also temporarily protects cell against antibiotic toxicity (Gusarov *et al.*, 2009). McCollister et al. investigated the mechanism, by which NO induces resistance of Gram-positive and Gram-negative bacteria to aminoglycosides (McCollister *et al.*, 2011). Aminoglycosides are often used in the treatment of infections caused by Gram-positive (Bayer & Murray, 2009) or Gram-negative (Poole, 2005b) bacteria. These antibiotics are a vital component of antipseudomonal chemotherapy (Cheer *et al.*, 2003). Aminoglycosides cause bacterial cell death targeting the 30S subunit of ribosomes, and the protein synthesis (Morita *et al.*, 2014). Given the intracellular localization of ribosomal targets, aminoglycosides must penetrate bacterial membrane thanks to electrochemical gradient and electron flow of the respiratory chain (Taber *et al.*, 1987). As NO represses bacterial respiration (see part **Proteins**), the authors proposed, that this repression of respiration prevents drug uptake, protecting bacteria from the aminoglycoside activity (McCollister *et al.*, 2011). Surprisingly, van Sorge and colleagues (van Sorge *et al.*, 2013) demonstrated, that, bNOS-deficient *S. aureus* gains

resistance to aminoglycosides. These results are in opposition to previous studies, suggesting that the role of NO in bacterial aminoglycoside resistance still a mysterious and complex question. All together these data indicate, that both endogenous and exogenous NO seem to affect bacterial antibiotic sensitivity, but the mechanism of NO-dependent modifications of antibiotic resistance remains to be defined.

6. Abiotic RNS and air pollution

6.1. NO_x as a major air pollutant

The air pollution is one of the major problems especially in urban areas, because of the urban population growth, combined with development of industrial areas, where the airborne pollutant are concentrated (Chaloulakou *et al.*, 2008; Mayer, 1999). The notion of 'air pollutant' includes all substances, which can damage human health, animals, vegetation and also materials (Skalska *et al.*, 2010). Air pollution exists as a complex mixture, whose the effects in majority are attributed to NO_x, sulfur dioxide and particulate matter (PM). As reported by World Health Organization (Harrison, 2006) and shown in **Figure 39**, the major atmospheric source of NO_x is anthropogenic, including principally the combustion processes in stationary or mobile sources, such as emissions from diesel vehicles and fossil fuels (Brunekreef & Holgate, 2002; Mayer, 1999).

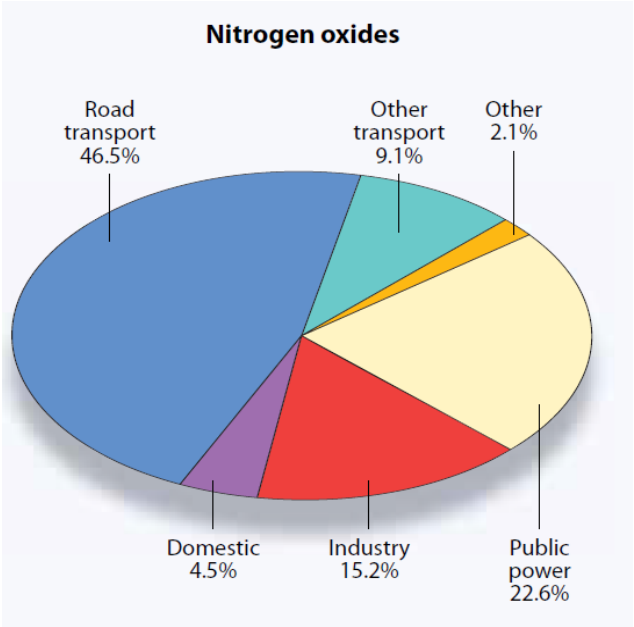

Figure 39. NO_x sources in atmosphere

According Harrison, 2006.

However, the atmospheric NO_x can be naturally produced by lightning (Schumann & Huntrieser, 2007), and volcano eruption (B. Huebert, 1999), considered as a natural sources for NO_x production (Boichu *et al.*, 2011).

The chemical, biological (Ghenu *et al.*, 2008; Ramaroson *et al.*, 2006) and toxicological (Fall *et al.*, 2008) studies of these air pollutants were made in order to estimate their effect on human

health and environment and develop the new technologies of air decontamination. As described in part **1. Nitrogen oxides (NOx)**, these nitrogen derivatives cause several environmental problems, including photochemical smog, acid rain, ozone layer depletion, and, as consequence, global warming. According WHO (Sivertsen, 2006), this pollution effect could be explained by: (i) the capacity of NO_x to absorb visible solar radiation and their contribution to impaired atmospheric visibility; (ii) the NO_x ability to absorb visible radiation and a direct role in global climate change; (iii) their regulation of the oxidizing capacity of the atmosphere by controlling the radical species level, including hydroxyl radicals; and (iv) the role of NO_x in determining of ozone concentrations. However, NO_x, especially NO_2, are known for their toxicity to human health, as reported below.

6.2. NO_x effect on human health

As humans, we are always in contact with air all around us. Due to the low NO_x solubility in aqueous solutions, the major pathway of NO_x action in humans is pulmonary (inhalation). The effects of exposure to urban air pollution on health are now well established. Several studies performed during the 1990s, demonstrated, that the traffic related NO_x emission enhances the risk of respiratory symptoms and allergic diseases especially in children (Ciccone *et al.*, 1998; Duhme *et al.*, 1996, 1998; van Vliet *et al.*, 1997). For example, traffic-related air pollution is correlated with symptoms of cough during the first 2 years of life (Gehring *et al.*, 2002). Exposure to combustion products, containing NO_x, is related to the development of wheezing bronchitis in children (Pershagen *et al.*, 1995). In animal experiment, NO_2 alters lung barrier function, suggesting the possible NO_2 damage of alveolar epithelium (McElroy *et al.*, 1997). Unfortunately, these data were confirmed by recent researches, which highlight the effect of air pollutants on cardiovascular disease (Brook *et al.*, 2010; Declercq *et al.*, 2012). Others identified a possible link between the air pollution and life expectancy (Pope *et al.*, 2009). The low air pollution increases the life expectancy in European cities, and save about €7.8 billion per year (Declercq *et al.*, 2012). According a similar calculation mode, the French citizens could gain about 6 month of life expectancy thanks to the 'good' air quality. However, this simple comparison is not very convincing, because of a myriad of factors, except air quality, that must impact the life expectancy. Nonetheless, these data aim to highlight the impact of air pollution on the human health and the importance of studying this topic.

The effects of air pollutants on human health are dependent on pollutant concentration and on time of exposure, demonstrating short- and long-term effects. Thus, individuals exposed for 2 hours to 1 ppm of NO show a significant decrease of specific airway conductance, without any clinical sign (Kagawa, 1982). The short-term exposure at low NO_2 concentrations was found to slightly affects human bronchial responsiveness in subjects with mild asthma (Bylin *et al.*,

1988). With rise of concentration, NO_2 induces a neutrophilic inflammation in the airways that was detectable in bronchial washing at 6 h after NO_2 exposure. The increase in neutrophils could be related to the enhanced IL-8 secretion observed at 1.5 h after exposure (Blomberg *et al.*, 1997). The French Environment and Energy Management Agency (ADEME) reports, that the long-term exposure to air pollutants may increase the risk of respiratory allergy, inflammatory response of blood vessels, affect the cardiac function and cause the cardiovascular diseases especially in children and elderly persons. The short-term exposures cause the discomfort, eye stinging effects, irritation to eyes, nose and throat. However, the more important effects, like nausea, cough, respiratory disorders or worsening of asthma symptom, are also observed (ADEME, 2015).

6.3. NO_x level in atmosphere

According the Interprofessional Technical Centre for Studies on Air Pollution (CITEPA), the NO_x emission trends observed during the period from 1990 to 2013 are on the decrease (CITERA, 2014). These observations are globally encouraging and especially reflect the reduction actions implemented by European Union and French government (see par **6.4. NOx standards**).The **Figure 40** below summarizes total emissions over the period 1990 – 2013 for NO_x in France.

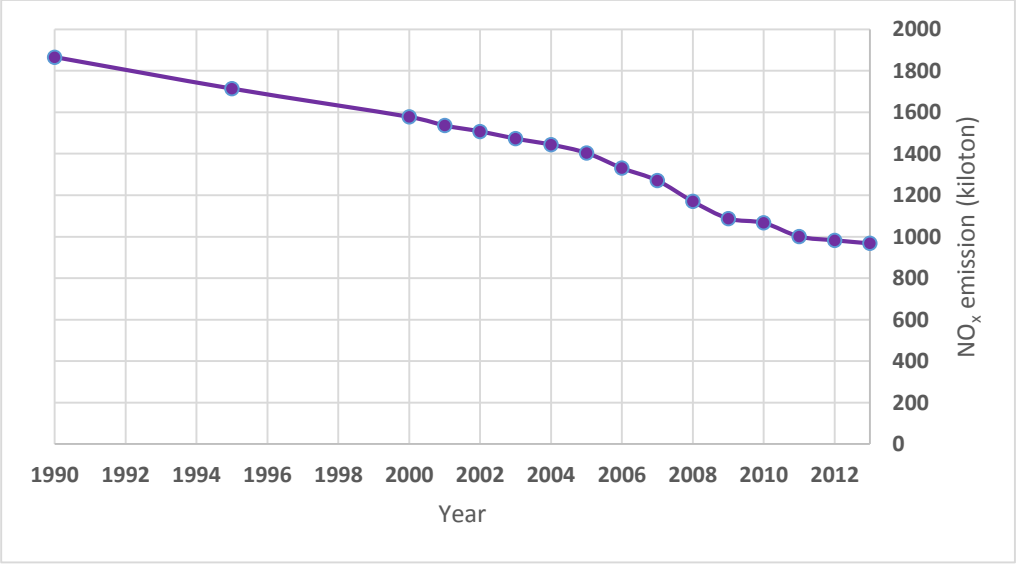

Figure 40. Evolution of NO_x emission in metropolitan France from 1990 to 2013
The data are presented as total NO_x emission according Interprofessional Technical Centre for Studies on Air Pollution.
According CITEPA, 2014.

These data are all the more encouraging, because the NO_x emission value in 2013 (990 kiloton) is close to the objective for 2010, fixed in Gothenburg Protocol as 860 kiloton of NO_x per year (*Review of the Gothenburg Protocol. Report of the Task Force on Integrated Assessment Modelling and the Centre for Integrated Assessment Modelling*, 2007). However, there is a

critic point of this decreasing. As previously reported (see part **1. Nitrogen oxides (NOx)**), in atmosphere, NO is quickly transformed to NO_2. Consequently, this reaction is regarded as the most important route for atmospheric NO_2 production. Given that NO_2 is much more toxic than NO, the ratio of NO_2/NO_x in air must to be taken into consideration. However, the main feature of recently obtained results is the elevation of the NO_2/NO_x ratio, indicating the drastic increase of NO_2 concentration. The increase of NO_2 concentration in road tunnel was found to be based on the post-processing techniques of the exhaust gas from road vehicles (Bernagaud *et al.*, 2014). The study of diesel emission toxicological impacts shows that increased NO_2 levels correlates with the production of a systemic oxidant stress in rats lung tissue (Morin *et al.*, 2013a).

According WHO, the rural annual concentrations of NO_2 in industrialized countries were measured at around 15–30 $\mu g/m^3$. In urban areas, the annual NO_2 concentrations exceed 40 $\mu g/m^3$ (Sivertsen, 2006). However, the NO_2 concentrations may vary considerably within cities and from time to time during the day and night. In 2002, the annual average NO_2 concentrations in France was reported to 44 $\mu g/m^3$, although the annual NO_2 level in Paris was found to be higher, and reported to 57 $\mu g/m^3$. Hourly average values of NO_2 near very busy roads can exceed 940 $\mu g/m^3$ (0.5 ppm). The personal exposure in vehicles in tunnels can be very high, a range of 179–688 $\mu g/m^3$ of NO_2 inside a car in a road tunnel during rush hours was established (Svartengren *et al.*, 2000).

During last decades, the rising restrictions regarding NO_x emission were imposed. The ratification of the Geneva Convention, Kyoto and Gothenburg Protocols require the 'Parties' to control the emission of NO_x, recognizing the harmful effect of these pollutants (Reilly *et al.*, 1999; UNECE, 2015). According the National competence center for Industrial Safety and Environmental Protection (INERIS), NO_x are classed as dangerous chemicals and their exposure thresholds were established (INERIS, 2011a, b) and reported in **Table 3**.

Table 3. Threshold values for NO_x

NO_x threshold	Time (min)							
	10		20		30		60	
	NO	NO_2	NO	NO_2	NO	NO_2	NO	NO_2
Significant lethal effect (ppm)	NF	118	NF	98	NF	88	NF	73
Irreversible effects (ppm)	150	60	120	55	100	50	80	40
Reversible effects (ppm)	NF	5	NF	5	NF	5	NF	5

According INERIS, 2011a, b. NF: not found

The 'lethal effect threshold' corresponds to the NO/NO_2 concentrations, above which mortality can be observed in the exposed population. The 'irreversible and reversible effect thresholds' correspond to the NO/NO_2 concentrations, above which the irreversible and reversible effects

can be observed in the exposed population. On this basis, European Environmental commission and French government developed the NO_x standards ranking from hourly NO_x limits to industrial NO_x standards ('WHO | Ambient (outdoor) air quality and health', 2015).

6.4. NO_x standards

The annual and 1-hour means of NO_2 were set to 40 µg/m^3 and 200 µg/m^3 respectively (**Table 4**). Annual NO_2 threshold is calculated as average value of daily NO_2 concentrations.

Table 4. NO_2 air quality standards

NO_2 standard	Concentration	
	µg/m^3	ppb
Hourly NO_2 standard	200	106
Annual NO_2 standard	40	21.2

According 'WHO | Ambient (outdoor) air quality and health', 2015

In order to limit pollution caused by road vehicles, European Union introduced the stricter limits on NO_2 for emissions from motor vehicles and their specific replacement parts (Euro 5 and Euro 6 standards) ('Reduction of pollutant emissions from light vehicles', 2015). The standards for pollutant emissions from road vehicles are set separately for light-duty (cars and light vans) and for heavy-duty (trucks and buses) vehicles. For light-duty vehicles, the maximal NO_x emissions from diesel is set to 180 mg/km; the NO_x emissions from petrol vehicles or those running on natural gas is 60 mg/km.

In conclusion, it should be mentioned, that NO_x, especially NO_2, present a toxic atmospheric pollutant, which has a negative effect on human health, but also on environment. The latter, in turn, includes, among others, the microorganisms.

6.5. Microorganisms in atmosphere

The air is a biotic environment, which contains the myriads of primary biological aerosol particles (PBAP). The latter are defined as solid airborne particles derived from biological organisms, including microorganisms and fragments of biological materials, such as plant debris and animal dander (Després *et al.*, 2012). To gain a better understanding of their composition, concentration, seasonal fluctuation and regional diversity, several methods were developed and/or adapted (Georgakopoulos *et al.*, 2009) ranking from cell culture, immunological detection, microscopy, flow cytometry, to methods of molecular biology. In this way, bacteria, archaea and fungi are known as the major compounds of PBAP. With regard to airborne fungi, Fröhlich-Nowoisky team detected *Basidiomycota* (club fungi, 64%) as major phylum in a semi-urban environment in central Europe (Fröhlich-Nowoisky *et al.*, 2009). However, the preponderance of *Ascomycota* (sac fungi, 80-92%) was noted at a mountain site

in North America (Bowers *et al.*, 2009), indicating the regional differences and possible seasonal variations in airborne fungal distribution (Fröhlich-Nowoisky *et al.*, 2012). The sequencing of 16S rRNA and *amoA* genes in samples of air particulate matter allows to identify the airborne archaea as members of phylums *Thaumarchaeota* and *Euryarchaeota* (Fröhlich-Nowoisky *et al.*, 2014). Bacteria are one of the major compounds of PBAP (Burrows *et al.*, 2009a; Després *et al.*, 2012). Mean bacterial concentrations in ambient air can be greater than 1×10^4 cells m^{-3} (Bauer *et al.*, 2002; Burrows *et al.*, 2009b; Morin *et al.*, 2013b). Due to their size, bacteria have a long atmospheric residence time and can be transported by wind over long distances (Womack *et al.*, 2010). Although a wide range of research on bacteria in the atmosphere, it remains difficult to establish a clear picture of the actual composition of bacteria in the air. The bacterial composition in the atmosphere is strongly dependent on many factors, such as seasonality, climate and meteorological factors, or anthropogenic influence (Després *et al.*, 2012). Thus, bacterial diversity in rural areas is generally higher than at urban sites (Després *et al.*, 2007). The concentrations of bacteria in urban seem to be higher than in rural environments (Bovallius *et al.*, 1978; Fang *et al.*, 2007; di Giorgio *et al.*, 1996). There is evidence that the bacterial communities in urban environment are influenced by human activities (Bovallius *et al.*, 1978; Fang *et al.*, 2007). Although instability of bacterial composition in air, the literature often reports members of *Pseudomonas* genus to be found among airborne species (Després *et al.*, 2012; Dybwad *et al.*, 2012; Fang *et al.*, 2007; Pearce *et al.*, 2010; Šantl-Temkiv *et al.*, 2015). However, to the best of our knowledge, the effect of air pollution on bacterial functioning and/or mechanisms of adaptation of airborne bacteria to air pollution were poorly studied.

Highlights

- NO_x are free radicals, which include NO and NO_2. Thanks to an unpaired electron, NO_x can react with other species, containing unpaired electron, forming reactive nitrogen species (RNS). The chemistry of NO_x and derived RNS is complex and dependent on a myriad of factors. However, the oxygen level plays a major role in RNS reactions.
- NO occupies a central position in RNS chemistry and may be reduced and/or oxidized to form a large number of reactive and frequently toxic species.
- Bacterial membrane is permeable to NO and NO_2, but prevents the diffusion of charged RNS, like $ONOO^-$. The membrane glycerophospholipids are not inert towards NO_x. The polyunsaturated fatty acid chains may be oxidized and/or nitrated by NO_x depending on the oxygen level.
- NO and its derivatives can react with proteins, causing the protein nitration, which may alter their functions and sometimes activate proteins. The related protein nitration and/or

nitrosylation are efficiently repaired thanks to several very elegant mechanisms, including ISC (iron-sulfur cluster) system.

- The RNS are able to damage the DNA directly (DNA deamination), or indirectly (alteration of DNA replication). These damages are also quickly repaired.
- The major NO_x sources are usually into two classes: abiotic and biotic. Abiotic NO_x principally come from combustion processes. Biotic NO_x production is based primarily on the NO synthesis by mammalian cells, plants and bacteria.
- In bacterial cells, NO is synthesized by NO synthases and nitrate/nitrite reductases. Several members of *Pseudomonas* genus are denitrifying bacteria, able to transform nitrate to nitrogen by reduction pathway. NO synthase coding genes are not found in sequenced genomes of *Pseudomonas* spp. species.
- Bacteria can detoxify NO using nitrate/nitrite reductase and flavohemoglobin catalytic properties.
- NO is involved in a wide range of processes in bacterial cells, including regulation of bacterial biofilm formation and antibiotic resistance.
- NO_x are one of major air pollutant, which appear to have a harmful effect on human health, but also on environment.
- European Union with World Health Organization and French government established the NO_x emission standards in order to control the air quality.
- The air contains a wide variety of primary biological aerosol particles (PBAPs), including bacteria, fungi or archaea. Bacterial composition of atmosphere is diverse and depends on various factors. However, the members of *Pseudomonas* genus are often detected among airborne microbiota.

II. Goals

With growth of the urban population, air pollution, caused in majority by urban activities, including motor traffic and industry, attracts global attention. Airborne bacteria undergo the air pollution effect and have to adapt to both fast natural and anthropogenic modifications in the environment. The high diversity and ubiquitous distribution of *P. fluorescens* suggest a remarkable degree of physiological and genetic adaptability. Physiologically, bacterial adaptability to various ecological niches and environmental modifications depends on the structure and organization of the envelope, composed of glycerophospholipids, which plays a major role in bacterial functioning.

In this context the aims of this work are:

- Characterization of the lipidome of airborne *P. fluorescens* strain using a new mass spectrometric method HPTLC-MALDI TOF MSI.
- Establishment of the membrane response of airborne *P. fluorescens* to environmental modifications, like increasing temperature in the context of climate change, and NO_2 as a marker of air pollution. For this, the membrane response of airborne *P. fluorescens* was compared to that of clinical *P. fluorescens* strain. This analogy of *P. fluorescens* strains from different ecological niches could give supplementary information about the specific for airborne bacteria mechanism(s) of adaptation to environmental modifications.
- Evaluation of the response of airborne *P. fluorescens* to air pollution. This investigation includes the first screen of potential mechanism(s) of adaptation of airborne bacteria to NO_2 air contamination, including NO_2 detoxification pathways, modification of phenotypes and genes expression caused by NO_2.

III. Materials and methods

Materials

1. Chemicals

GPs standards, MALDI matrix (2,5-dihydroxybenzoic acid; DHB), solvents (chloroform, methanol, ethanol, trimethylamine, acetonitrile, hexane, ethyl acetate, hexadecane and decane) and GP dyes (ninhydrin, azure A and primuline) were obtained from Sigma-Aldrich (Saint-Quentin-Fallavier, France). The 1,2-di-(9Z-octadecenoyl)-*sn*-glycero-3-phosphoethanolamine-N-nonadecanoyl [19:0-PE (18:1/18:1)+Na]$^{+}$ was provided by Avanti Polar Lipids, Inc. (Alabaster, Alabama, USA). HPTLC silica gel 60 plates F_{254} (75 x 50 mm in size, on aluminum backs) were obtained from Merck (Darmstadt, Germany).

Sodium acetate, sodium dodecyl sulfate (SDS), ethylenediaminetetraacetic acid (EDTA), acid phenol, chloroform/isoamyl alcohol, diethylpyrocarbonate, tris–acetate–ethylenediamine tetraacetic acid (TAE), used in RNA manipulations, as well as xanthosine-(3',5')-cyclic monophosphate (cXMP) used in c-di-GMP quantification, were provided by Sigma-Aldrich (Saint-Quentin-Fallavier, France). All chemicals were of the highest commercially available purity and used without any further purification.

The enzymes and kits for qRT-PCR assays (RNase, TurboDnase I, cDNA RT Kit, SYBR Green DNA Poymerase, dNTPs and dUTPs), as well as the PCR primers were obtained from Life Technology (Life Technology, Brumath, France).

2. Bacterial strains

Two *P. fluorescens* strains MFN1032 and MFAF76a were used in this study. *P. fluorescens* MFN1032 is a clinical strain isolated from the sputum of a pneumonia patient (Rossignol *et al.*, 2008; Sperandio *et al.*, 2010). The airborne strain *P. fluorescens* MFAF76a was collected in the dust cloud of cereal docks in harbor installations of Rouen (France) (Morin *et al.*, 2013b). The both strains are psychrotrophic bacteria with optimum of growth at 28°C. However, they are able to growth at 37°C (Chapalain *et al.*, 2008; Duclairoir Poc *et al.*, 2014).

Methods

1. Methods of microbiology

1.1. Bacterial culture

The strains are kept on glass beads at -80°C in 15% glycerol solution, from a bacterial culture at the end of exponential growth phase in Luria-Bertani (LB) medium. Precultures were realized

from one bead added in 10 mL of LB. After overnight incubation at 28°C, precultures were used to prepare bacterial culture. The added volume of preculture was calculated to ensure the optical density (OD) of culture A_{580}=0.08 (Spectrometer Termo Spectronic, Cambridge, UK). Bacterial cultures were grown at 28°C or at 37°C under limited agitation (180 rpm) in LB or DMB (Davis Medium Broth) minimal medium with glucose as carbon source (2.16 g per liter). The compositions of growth media are presented in **Table 5**.

Table 5. Composition of growth media

Medium	Composition (per liter)	
Luria Bertani (LB) (pH 7)	Tryptone	10 g
	Yeast extract	5 g
	NaCl	5 g
	Agar (solid medium)	15 g
	H_2O qsp	
Davis Medium Broth (DMB)	K_2HPO_4	10.450 g
	KH_2PO_4	3.810 g
	$(NH_4)SO_4$	2.010 g
	$MgSO_4$	0.049 g
	Glucose	4.320 g
	Agar	15.000 g
	H_20 qsp	

1.2. Growth monitoring

The bacterial growth was monitored by turbidimetry at A_{580} using Bioscreen C MBR (Oy Growth Curves Ab Ltd., Helsinki, Finland). Bacteria were resuspended in DMB minimal medium and added to Bioscreen Honeycomb plates (Oy Growth Curves Ab Ltd., Helsinki, Finland) in a total volume of 200 µL of DMB (A_{580}=0.08). Growth was measured every 15 min for 24 h. The generation time was calculated following formula: $T_{EGP} / ((\log_{10} N_t - \log_{10} N_0) / \log_{10}2)$. Where T_{EGP}: time of exponential growth phase; N_t: CFU at the end of exponential growth phase; N_0: CFU at the beginning of exponential growth phase. The bacterial growth was assayed in at least three independent experiments with two replicates for each experimental condition.

1.3. Minimum inhibitory concentration (MIC) assays

Bacterial sensitivity to ciprofloxacin, chloramphenicol and two aminoglycosides (tobramycin and kanamycin) was tested. The MICs of antibiotics were determined by broth microdilution method in DMB minimal medium. Bacterial solution were diluted in the appropriate broth to A_{580}=0.08 and added to a 96-well test plate (Nunc™, Roskilde, Denmark) containing different concentrations of antibiotics in triplicate. The test plate containing antibiotic dilutions and

targeted bacteria was incubated at 28°C for 24 h. MIC was defined to be the lowest concentration of antibiotic that inhibited bacteria growth as determined by turbidimetry at A_{580}.

1.4. Motility assays

Swimming and swarming motility assays were performed on agar plates using DMB medium containing 0.2% (wt/vol) and 0.5 % (wt/vol) agar, respectively as previously described (Déziel *et al.*, 2001). The resultant diameters of swim and swarm zones were measured after 24 h of incubation at 28 °C. All motility types were assayed in at least three independent experiments with three replicates for each experimental condition.

1.5. Study of biofilm monitoring by confocal laser scanning microscopy (CLSM)

Samples for CLSM were prepared in 175 µm glass-bottom dishes (SensoPlate™, VWR, Fontenay-sous-Bois, France) by inoculation of 300 µL of bacterial suspension in sterile saline solution (A_{580} =1). After 2 h of incubation at 28°C, planktonic bacteria were removed and the adhesion of *P. fluorescens* was observed using confocal laser scanning microscope (LSM 710, ZEISS) with an immersion objective 63x. After addition of DMB medium, bacterial biofilms were incubated at 28°C for 24 h. DMB medium was removed, biofilms were rinsed with 1 mL of saline solution and observed using CLSM. All biofilm assays were analyzed using the fluorescence of Cyan Fluorescent Protein (CFP, excitation by the 405 nm laser line and detection at 485 nm) through at least three independent experiments with two replicates for each experimental condition. The biofilm thickness and related biovolumes (bacterial volume (μm^3) by μm^2) were estimated from 6 fields on 3 independent experiments using COMSTAT software (Heydorn *et al.*, 2000).

2. Physico-chemical methods

2.1. Bacterial contact angle measurements by sessile drop

The contact angle formed by water droplet, θ_w, on microbial lawns was measured by sessile drop method using a goniometer DSA 100 (Krüss GmbH, Germany). Bacterial lawns were prepared in suspension of physiological saline in order to obtain at least 2 mL with A_{580} of at least 5. To obtain homogeneous, continuous bacterial lawns, the suspension was slowly deposited on the filter by applying negative pressure, rinsed with 10 mL of physiological saline and dried at room temperature for 2 h under standardized conditions. To capture the contact angle of water θ_w on the bacterial lawn, four water droplets were observed on each biological triplicate. To determine this contact angle, the drop contour was mathematically described by the Young –Laplace equation using DSA 100, and the contact angle was evaluated as the slope

of the contour line at the three -phase contact point. The θ_w acquisition was made in the first 10 s once the drop stabilized.

2.2. Evaluation of bacterial surface hydrophobicity

The hydrophobicity of bacterial surface was evaluated by the microbial adhesion to solvent (MATS) test (Bellon-Fontaine *et al.*, 1996). It consisted in assessing the affinity of the cells to two solvents duos consisting of a monopolar solvent and an apolar solvent. In each set, both solvents have similar surface tension, but the monopolar one is acidic (electron accepting, e.g. chloroform) or basic (electron donating, *e.g.* ethyl acetate). The apolar solvents are respectively hexadecane and decane. For the experiments, bacterial cells were resuspended in saline solution to A_{400}=0.8 (Abs1). This bacterial suspension was mixed with each solvent at 1/6 (v/v) by vigorous agitation for 1 min in order to form an emulsion. This mixture was then left for at least 15 min until the separation of the two phases. The aqueous phase absorbance (Abs2) was measured and the percentage of adhesion was expressed as: $\%_{affinity}$ = (1-Abs2/Abs1) x100.

2.3. Exposition to NO_2

Bacterial culture at the end of exponential growth phase (about $3x10^7$ bacteria per filter) was transferred on cellulose nitrate membrane filter (pore size 0.2 µm, diameter 47 mm, Sartorius Biolab Products, Gottingen, Germany) and grown in DMB agar plates at 28°C for 4 h to obtain the single layer's bacterial population. After 4 h of incubation, the cellulose membranes were placed on agar 1 well dishes (size 127.8 x 85.5 mm, Thermo Scientific Nunc, Roshester, USA) that were directly transferred in gas delivery device.

In order to restore the environmental conditions, bacterial NO_2 exposure was done in gas phase for 2 h, according to Ghaffari *et al.*, 2005. The delivery device consisted of two sterile cylindrical Plexiglas exposure chambers (one for the NO_2 exposure, the second one for the control - exposure to the synthetic air), deposed in drying oven at 28°C creating a thermally isolated environment. The NO_2, N_2, and O_2 obtained to Air Liquide GMP Europe (Mitry-Mory, France) were mixed together using digital mass flowregulators (Alicat Scientific, Inc., Tucson, USA) to obtain pre-calculated concentration of NO_2 and maintain the O_2/N_2 ratio at 2/8, (v/v). The obtained gas mixture and synthetic air (Air Liquide GMP Europe, Mitry-Mory, France) were routed independently to each of the exposure chambers at a constant flow rate of 2 L/min. The parallel NO_2/synthetic air circuits allow utilization of the same bacterial culture for exposed to NO_2 and control samples. After passing through exposure chamber, the NO_2 concentrations were monitored by AC32M nitrogen oxides analyzer (Environnement S.A, Poissy, France) and safely vented to a chemical hood. Chamber temperature and relative humidity data were

monitored and collected to control reliable steady-state environmental conditions inside the exposure chambers. Three concentrations of NO_2 were used in this study: 0.1 ppm; 5 ppm and 45 ppm. After exposure bacteria were resuspended to A_{580}=2 in 20 mL of sterile saline solution.

3. Methods of biochemistry

3.1. Lipid extraction

3.1.1. Extraction of glycerophospholipids (GP)

Lipids were extracted according to the method of Bligh and Dyer (Bligh & Dyer, 1959). About 1 g of lyophilized bacteria was resuspended in 3 mL of $CHCl_3$/CH_3OH (1/2, v/v). The obtained mixture was completed by 1 mL of $CHCl_3$, and 1.8 mL of H_2O successively. Samples were centrifuged 15 min at 3,000 *g*. The chloroform phase containing lipids was collected and stored at -20°C under N_2 atmosphere.

3.1.2. Extraction of fatty acid methyl esters (FAME)

The FAME were prepared from lipid extract samples by incubation for 15 min at 95°C in a boron trifluoride/ethanol mixture (140 g BF_3 per liter of CH_3OH) and extracted with hexane as described by Morrison & Smith, 1964. Briefly, the FAME were added to 0.3 mL of H_2O and 0.5 mL of hexane. After shaking the hexane phase was transferred in GC-autosampler flasks. The hexane was removed by N_2-gasstream. To unify volumes, 0.5 mL of hexane was added in each simple before GC analysis.

3.2. Glycerophospholipid analysis

3.2.1. Separation of GPs by high performance thin-layer chromatography (HPTLC)

The GPs were separated by high performance thin-layer chromatography (HPTLC) using method adapted from Fuchs *et al.*, 2007a. Beforehand, HPTLC plates were washed with the separation solvent system: $CHCl_3$/ CH_3-CH_2OH/ H_2O/ $N(CH_2CH_3)_3$ (35/35/7/35, v/v/v/v), and activated at 110°C under vacuum for 2 hours. Bacterial GP extracts were spotted in triplicates on HPTLC plates and separated at room temperature.

After development, GPs spots were labeled with spray of 0.05% primuline dye in acetone/water, (8/2, v/v) and visualized by UV fluorescence (365 nm). The primuline binds non-covalently to the apolar fatty acyl residues of lipids and does not affect a subsequent MS analysis (Richter *et al.*, 2008). Moreover, the staining with ninhydrin and azure A were performed in order to identify the lipid classes having a free amino groups and sulfatides and/or sulfoglycolipids respectively (Kates, 1972; Kean, 1968). The 3% solution of ninhydrin prepared in absolute

ethanol was sprayed on HPTLC plate. The plate was heated at 110°C for 15 min to visualize the phospholipid spots. The 2% azure A in 1 mM sulfuric acid was applied to HPTLC plate. Retention factors (R_f) are calculated using the Sweday JustTLC software (v. 4.0.3, Lund, Sweden).

3.2.2. Glycerophospholipid identification by MALDI TOF MS

GLs were identified directly on HPTLC plates by matrix-assisted laser desorption ionization mass spectrometry – time of flight (MALDI-TOF) using an Autoflex III mass spectrometer equipped with a laser Optibeam TM Nd/YAG (355 nm, 200-Hz tripled-frequency) (Bruker Daltonics, Bremen, Germany). DHB was chosen as MALDI matrix since it generates positive ion spectra of lipids and does not interfere with the silica of HPTLC plates. HPTLC plate containing GP spots was coated by DHB matrix solution (200 g/L in C_2H_3N /0.1% TFA, 90/10, v/v) (Fuchs *et al.*, 2007a) and immediately dried under dust-free atmosphere. Matrix coating was made twice to reach a mean of DHB matrix of 5 mg/cm^2. Matrix coated HPTLC plate were fixed on a TLC-MALDI target developed by Bruker Daltonics (Bremen, Germany).

The Autoflex III mass spectrometer was run in the reflector positive ion mode using the TLC-MALDI software (v. 1.1.7.0, Bruker Daltonics, Bremen, Germany). The excitation voltage was 19.5 kV, the reflector voltage was 21.0 kV. The laser strength was kept about 30% above threshold to have a good signal-to-noise ratio. A major strength is needed to desorb lipids from silica (Lobasso *et al.*, 2012). 200 single laser shoots were averaged for each point. The distance between two points was determined as 1 mm. Obtained 2D mass spectra enable the rapid MS analysis of lipid spots. Post Source Decay (PSD) spectra were acquired on a Bruker Autoflex III mass spectrometer (Bruker Daltonics), as previously described (Fuchs *et al.*, 2007b). The precursor ions were isolated using a time ion selector. The fragment ions were refocused onto the detector by stepping the voltage applied to the reflectron in appropriate increments. This was done automatically by using the "FAST" ("fragment analysis and structural TOF") subroutine of the FlexAnalysis software.

Calibration was performed in two steps. The external calibration of the apparatus is performed daily in FlexControl software. This calibration was made using the DHB matrix and the Peptide Calibration Standard II (Bruker Daltonics, Bremen, Germany) covering a mean mass range between 200 and 3500 Da. Supplementary internal calibration was made using sphingomyelin (1 µg/mL) mixed with the matrix solution before dipping. Peaks generated by these standards were used to calibrate TLC MALDI software. This double calibration improved the measurement accuracy of bellow 0.1 Da for lipid identification. Lipids were identified manually

using the LIPID MAPS database. All experiments were performed in at least three independent experiments with three replicates for each experimental condition.

3.2.3. Imaging HPTLC-MALDI TOF MS assays

Mass spectrometry imaging (MSI) of GP spots was performed using the FlexImaging software (v. 2.1., Bruker Daltonics, Bremen, Germany). A polygon measurement region was defined according the GP spots of single sample with a spatial resolution of 200 µM. The GP spots were imaged with 500 laser shots per pixel with multiple additions of single position acquisition run (every 40 shots). Each MS spectrum was baselined and smoothed in FlexAnalysis software. Following previous MS and PSD identification (see part **Glycerophospholipid identification by MALDI TOF MS**), individual GP spots were labeled by a specific color code according to their m/z.

3.3. Fatty acid analysis

3.3.1. Separation and identification of fatty acids (FAs)

The FAs were separated and analyzed by gas chromatography (GC) coupled to flame ionization detection using an Agilent Technology, 6890 Network GC System, 7683 Series Injector equipped with a split/splitless injector. The apparatus was equipped with a CP-Sil 88 capillary column (length, 50m; inner diameter, 0.25 mm; 0.25 mm film; Chrompack, Middelburg, the Netherlands). FAs were identified by coinjection as internal standards of reference compounds obtained from Supelco (Bellefonte, Pennsylvania, USA).

3.3.2. Quantification of fatty acids

The FAs were quantified on the basis of their peak areas in total ion chromatograms. All experiments were performed in triplicate. The degree of FA saturation was determined as the ratio between the saturated FAs and the unsaturated FAs (Heipieper *et al.*, 1996).

4. Methods of molecular biology

4.1. Nucleotide extraction

4.1.1. C-di-GMP extraction

Extraction and quantification of intracellular c-di-GMP was performed as previously described (Spangler *et al.*, 2010; Strehmel *et al.*, 2014). Aliquots of bacterial culture (CFU=$3.3x10^9$) were harvested by centrifugation for 2 min, 8,000 g, 4°C. Bacterial pellets were resuspended in 600 µL ice-cold extraction buffer, composing to C_2H_3N/ CH_3OH/ H_2O (2/2/1, v/v/v) with and without of 5 µL of a 10 µg/mL solution of xanthosine-(3',5')-cyclic monophosphate (cXMP)

as an internal standard. After 15 min of incubation on ice, bacterial cells were lysed at 95°C for 10 min, followed by centrifugation at 20,000 g, 4°C for 5 min. Supernatants were collected and stored on ice. Remaining pellets were resuspended in 400 µL of extraction buffer, incubated on ice for 15 min, and centrifuged at 15,000 g, 4°C for 5 min. The extraction was repeated thrice, the supernatants were pooled and evaporated using a DNA SpeedVac® DNA 120 (Thermo Savant, Holbrook, USA) at 43°C. The remaining residues were resuspended in 500 µL of H_2O.

4.1.2. Extraction of total RNA

The total RNA were extracted as previously described by Gicquel *et al.*, 2013. One volume of absolute ethanol was added to collected bacterial cells (about 10^8 of bacteria). The pellet bacteria were harvested by centrifugation at 13,000 g, 10 min and lysed in 300 µL of buffer I (0.02 M sodium acetate; 0.5% sodium dodecyl sulfate (SDS); 1 mM ethylenediaminetetraacetic acid (EDTA)). After homogenization, the total RNA were extracted twice in 600 µL of hot acid phenol (pH 4.3; 60°C). After 3 min incubation at 60°C, the aqueous phase containing the RNA was separated from organic phase, containing the genomics DNA and proteins by centrifugation at 13,000 g for 4 min. 500 µL of chloroform/isoamyl alcohol (24/1, v/v) were added to aqueous phase. The centrifugation at 13,000 g for 2 min was performed to separate two phases. Aqueous phase, containing the total RNA, was collected. The total RNA was precipitated in cold 100% ethanol with 100 mM sodium acetate, harvested by centrifugation at 13,000 g 30 min at 4°C, rinsed with 1 mL of 75% ethanol and dissolved in 50 µL of H_2O treated by diethylpyrocarbonate (DEPC), inactivating RNase enzyme.

The contamination by genomic DNA was eliminated with addition of 10U TurboDnase I (Life Technology, Brumath, France) in reaction mixture containing 6.25 mM $MgCl_2$. The reaction was performed at 37°C for 2 h. The absence of genomic DNA was controlled by PCR with the pair of primers F*mexX*/R*mexX* (**Table 6**). If necessary the samples were retreated with TubroDnase for 1 h. The TurboDnase was inactivated by adding of 1 µL of 0.5M EDTA at 75°C for 10 min. The quality of total RNA was controlled by 2% agarose gel electrophoresis with Tris–Acetate–Ethylenediamine tetraacetic acid (TAE) 1X. The RNA concentration was measured by spectrophotometry at A_{260}. The absence of contamination by proteins and organic solvents was controlled by measurement of ratios A_{260}/A_{280} and A_{260}/A_{230}.

4.2. Quantitative retrotranscription polymerase chain reaction (qRT-PCR)

4.2.1. Reverse transcription reaction

Reverse transcription (RT) of total RNA into complementary DNA (cDNA) was performed using "High capacity cDNA RT Kit" (Applied Biosystems®, Life Technology, Brumath, France) according to provider recommendations. The cDNA synthesis was performed in a final volume of 50 µL from 2.5 µL of RNA during 2 h at 37°C. The reaction was stopped by samples heating at 85°C during 5 min. The control samples (negative RT) were made at the same conditions without addition of reverse transcriptase in reaction mixture. The control of cDNA synthesis was performed by 2% agarose gel electrophoresis.

4.2.2. Design and optimization of primers

The sequences of target genes were identified using Blast+ v2.2.30 software (Altschul *et al.*, 1997). The primers of target genes were designated using Primer Express® software v3.0.1 (Applied biosystem®, Life Technology, Fontenay-sous-Bois, France) and are compiled in **Table 6**. Temperature of melting of qRT-PCR primers was 60°C.

Table 6. Primer sequences used for quantitative RT-PCR assay

Gene	Forward primer (5'-3')	Reverse primer (5'-3')
***Pseudomonas fluorescens* MFAF76a**		
hmp	AAACCGCGATCTATGACCAG	GCTTCATGCCGATGTACTGA
Pfl76a_nirB	AATTGAAAGTCACCGGCATC	GAATCTGCCGGAAATACCAA
bdlA	ACATTCTTACCGCCAACCAG	ACTGTCCGTGGAAGAACTCG
ndbA	AGATGAAAGAGCCGATCGAA	TGAAGAAGTGCAGACCGTTG
mexE	ACTCAAACATTTGCGCTTCC	AATTCGTCCCACTCGTTGAC
mexF	GAGTGGACCGACCTGACCTA	GCAAGTCCCACCAGTACGAT
oprN	ACCTCAACAACCAGCAGGAG	AGGTCGACGGTCAGTTTGTC
mexX	CGCAGCGAGTTTCCCAAT	TGGATGGTTGCCTGCTCAA
mexY	GGCTGGGTCGGCTATGC	TCAGCAGGACCACGTAGATCAT
***Pseudomonas fluorescens* MFN1032**		
hmp	GATAAACCGCTGGTGCTGAT	ATCCTCGGCGTAGCAGTAGA
Pfl1032_nirB	CGCCCTATGTGCTGGTGTT	ATCTGCCGGGCCATCTC
dipA	ACGAAGACATCACCCAGACC	TTGATGCGCTTGAAGTTGTC
mucR	CCTTGTCGTGATTTCCCTGT	GCCAACATCCCGATAAAGTG
mexE	CCGACAAGGTTTACGCCTAC	GTGTATTCGCCCTTGCTGTT
mexF	CTGACCCTGACCATCACCTT	ATTGAGGATCGCGTAGTTGG
oprN	GTTGCTGGCATTGGAAGAGT	GTCGAGCAACACCAGGAAGT
mexX	CCGTTGCCGGGTAAATTG	GAACTCGCTGCGCAGGAT
mexY	CAGTGGTTTTGAGTTCCGTTTG	GCAGCGTCCAGCAATTCAGT

All pairs of primers were tested with serial dilutions of cDNA mixture obtained previously. Each dilution of cDNA quantity spectrum was analyzed in duplicate. Based on results of cDNA

quantity spectrum, the slope was obtained using a linear equation to determine the PCR efficiency (E): $E=10^{(1/slope)}$. The reaction specificity was tested using melting curves of amplification products, amplification of negative RT and H_2O replacing the cDNA.

4.2.3. Real-time quantitative amplification

Real time quantitative amplification was realized using 7500 Fast Real Time PCR system (Applied biosystem®, Life Technology, Fontenay-sous-Bois, France). The reaction was realized according to provider recommendations. The reaction was made in 13 µL with 6.5 µL of SYBR Green DNA Poymerase, dNTPs and dUTPs. The simples contained 300 nM of each primer and 7.5 of cDNA. For amplification the following program was used: one step at 95°C - 20 min, 40 cycles at 95°C - 10 s, 60°C – 30 s and 72°C – 6 s. The relative RNA quantification was realized by comparison of cycle threshold (Ct) ($2^{-\Delta\Delta Ct}$) using 16S RNA as control.

4.3. Transformation of *Pseudomonas* by electroporation

4.3.1. Plasmid preparation

The Cyan Fluorescent Protein (CFP) transformed *P. fluorescens* MFN1032 and MFAF76a were used in this study. The fluorescent gene *cfpopt* was introduced in pPSV35 vector (Rietsch *et al.*, 2005; Vallet-Gely *et al.*, 2007). The CFP cassette was obtained from pTetONCFPopt plasmid containing 729-bp *cfpopt* gene (Sastalla *et al.*, 2009) by double digesting with PstI and Xmal. This gene was inserted into the *lacZ* site of the polylinker of pPSV35 by ligation into the pPSV35 vector digested with the same enzymes.

4.3.2. Preparation of *P. fluorescens* competent cells

The competent cells of *P. fluorescens* were prepared as follows Enderle & Farwell, 1998: bacteria were collected on the agar plate and washed twice in 500 µL of distilled water at 4°C. The pellet cells were collected by two centrifugations at 10,000 g, 4°C for 1 min and resuspended in 40 µL of cold distillated water.

4.3.3. Transformation by electroporation

The transformation by electroporation helps to make the bacterial cells permeable to DNA through electric shock. About 150 ng of plasmid were added to 100 µL of competent cells. The mixture was transferred into electroporation chamber with electrical voltage 1,800 V during 5 ms (Gene transformer GTF100, Savant). The reaction volume was transferred in 1 mL of LB medium and incubated at 28°C during 1 h to obtain the first phenotypic expression. After chosen the clones by antibiotic selection (gentamycin 15µg/mL), the transformation was confirmed by confocal laser scanning microscope (LSM 710, ZEISS).

4.4. Bis-(3', 5')-cyclic dimeric guanosine monophosphate (c-di-GMP) analysis

4.4.1. Separation of c-di-GMP by high-performance liquid chromatography (HPLC)

The c-di-GMP levels were quantified by HPLC MS/MS as described previously (Strehmel *et al.*, 2014). The chromatographic separation was performed on a 1100 Series HPLC system (Agilent, Waldbronn, Germany) using a Multospher AQ RP 18.5 µm, 250 x 4.0 mm HPLC column (CS Chromatography Service GmbH, Landenwehe, Germany) in a gradient mode using 10 mM ammonium acetate with 0.1% acetic acid as eluent A and methanol a eluent B. The injection volume of each sample was set to 40 µL and the flow rate was 0.4 mL/min. The gradient program was as follows: from 0-4 min 100% A, followed by a linear gradient from 100% to 80% A in 1 min, held for 2 min at 80% A, followed by a linear gradient from 80% to 60% A in 1 min and held for additional 9 min at 60%. Finally, re-equilibration of the column was obtained by constantly running 100% A for 16 min. All experiments were performed in at least three independent experiments with three replicates for each experimental condition.

4.4.2. Quantification of c-di-GMP by Electrospray Ionization (ESI) MS

ESI MS was performed on an API 4000 triple quadrupole mass spectrometer (Applied Biosystems, Toronto, Canada) using a turbo ion spray interface in positive mode. The ionization potential was of 5,000 V and a temperature of 400°C using nitrogen a curtain, nebulizer and collision gas. The parameter settings were optimized by infusion experiments. Data were acquired in multiple reaction monitoring (MRM) mode using the Analyst software version 1.6. (Applied Biosystems, Toronto, Canada). Identification and quantification of c-di-GMP was performed by using three specific mass transitions from molecule ion m/z 691 to the product ions: m/z 152, m/z 135 and m/z 540. The external calibration was carried out at c-di-GMP concentrations ranging from 10 ng to 200 ng in 500 µL H_2O using the internal standard cXMP (50 ng). Obtained concentrations of c-di-GMP were normalized against total protein contents of respective cultures, which was determined by the bicinchoninic acid assay (Smith *et al.*, 1985). All experiments were performed in at least three replicates for each experimental condition.

5. Methods of bioinformatics

5.1. Gene sequences identification

The nucleotide sequences identified in this study were obtained using the non-annotated genome drafts of *P. fluorescens* MFN1032 and MFAF76a. First of all, a research of homologous sequences in *P. fluorescens* annotated genomes was performed using *Pseudomonas* genome database (http://pseudomonas.com/). The conserved nucleotide sequences were identified in *P. fluorescens* MFN1032 and MFAF76a using Blast+ (Stand-alone) software (v. 2.2.30, NCBI, USA) according to Altschul *et al.*, 1997 and compiled in **Table 7**. The genome alignment and the studies of genomic neighborhood were performed in multiple genome alignment software Mauve v. 2.3.1 (Darling lab, Sydney, Australia), according to Darling *et al.*, 2004.

5.2. Phylogenetic analyses

The nucleic sequences of 12 *Pseudomonas* type strains used in this study were obtained from a previous study (Bodilis *et al.*, 2011). Some nucleic sequences from 8 sequenced genomes were also included in this analysis, from the PAO1 (Stover *et al.*, 2000), PA14 (Lee *et al.*, 2006), SBW25 (Rainey & Bailey, 1996), Pf0-1 (Silby *et al.*, 2009), CHAO (Jousset *et al.*, 2014, p. 0), PF-5 (Silby *et al.*, 2009), MFN1032 (KP119846 for 16S RNA (Mazurier *et al.*, 2015); *unpublished data*: KT350505 for *gyrB*, KT350506 for *rpoB*, KT350507 for *rpoD*), and MFAF76a (*this study:* KT350501 for 16S RNA, KT350502 for *gyrB*, KT350503 for *rpoB*, KT350504 for *rpoD*).

From the 20 *Pseudomonas* strains, nucleic alignments of four partial housekeeping genes (*gyrB* gene, 798 bp; *rpoB* gene, 642 bp; *rpoD* gene, 564bp; and 16S rRNA gene, 1182 bp) were optimized individually then concatenated, leading to 3,186 nucleotide positions. Protein sequences were aligned with ClustalW2 with default parameters (Bodilis *et al.*, 2011) implemented in Seaview 4.2.4 (Gouy *et al.*, 2010). Conserved blocks of the multiple alignment were selected by using Gblocks 0.91b with default parameters (Talavera & Castresana, 2007) and then, nucleic alignment was deduced from this corrected protein alignment. For the 16S rRNA gene alignment, a preliminary step was conducted before selecting the conserved blocks by using Gblocks 0.91b: the regions in which the secondary structures differed were eliminated, as described previously by Anzai *et al.*, 2000.

Phylogenetic analysis was conducted by using BioNJ implemented in Seaview 4.2.4, with JC correction. Bootstrap analysis was conducted from 1000 replicates. The maximum likelihood (ML) tree was inferred using RAxML version 7.2.6 (Stamatakis, 2006) with partitioned analysis

for the third codon position. A third partition corresponding to the 16S rRNA gene was defined. The generalised time-reversible (GTR) model parameters, branch lengths, proportion of invariant sites and alpha parameter of the gamma distribution had been estimated independently for each partition. Support values were evaluated based on 100 bootstrap replicates.

The *pcs* nucleic sequences of 6 *P. fluorescens* strains Pf-5, CHAO, Pf0-1, SBW25, MFN1032 (GenBank accession number KT338639) and MFAF76a (GenBank accession number KT338638) and *P. aeruginosa* PAO1 were obtained as described before. The *pcs* nucleic sequence form A506 sequenced genome (Loper *et al.*, 2012) was also included in this analysis. The sequences were analyzed using the neighbor-joining method (Saitou & Nei, 1987). Analyses were conducted using CLC Sequence Viewer 7 (CLC bio, a QIAGEN Company, Denmark). Bootstrap analysis was performed from 1000 replicates.

Table 7. Genes identified with the Blast 2.2.30+ software

	Gene name	GenBank accession number		Protein name	Protein description	References	
		MFAF76a	MFN1032			Strain	Bibliographies
NO_2 detoxification	*hmp*	KR818822	KR818823	flavohemoglobin	nitric oxide dioxygenase	*E. coli* *P. aeruginosa*	Arai et al., 2005; Poole et al., 1996; Gardner et al., 1998
	Pfl76a_nirB *Pfl1032_nirB*	KT186428	KT070320	putative nitrite reductase large subunit NirB	assimilatory nitrite reductase	*P. aeruginosa*	Romeo et al., 2012
Biofilm and motility	*bdlA*	KT186436		putative protein BdlA	biofilm dispersion protein BdlA	*P. aeruginosa*	Petrova and Sauer, 2012b
	dipA		KT186437	putative phosphodiesterase DipA	protein, possessing EAL domain and involved in biofilm dispersion	*P. aeruginosa*	Roy et al., 2012
	mucR		KT186445	putative phosphodiesterase MucR	protein possessing both GGDEF and EAL domains and involved in NO-mediated biofilm dispersion	*P. aeruginosa*	Li et al., 2013
	ndbA	KT186444		putative phosphodiesterase NdbA	protein possessing both GGDEF and EAL domains and involved in NO-mediated biofilm dispersion	*P. aeruginosa*	Li et al., 2013
Antibiotic resistance	*mexE*	KT070324	KT070323	putative membrane fusion protein MexE	RND family efflux transporter	*P. aeruginosa*	Maseda et al., 2000; Fetar et al., 2011; Poole K., 2005b
	mexF	KT070321	KT070322	putative cation efflux protein MexF	multidrug efflux transporter		
	oprN	KT070325	KT186432	putative multidrug efflux RND transporter, outer membrane factor lipoprotein OprN	outer membrane component of multidrug efflux system		

	mexX	KT070313	KT186462	putative MexX	MexX family efflux pump subunit	*P. aeruginosa*	Poole, 2005a; Morita et al., 2014; Sobel et al., 2003
	mexY	KT070314	KT070315	putative MexY	multidrug efflux protein		
Phylogenetic analyses	*pcs*	KT338638	KT338639	Putative phosphatidylcholine synthase Pcs	phosphatidylcholine synthase activity	*P. aeruginosa* *P. putida*	Wilderman et al., 2002; Boeris and Lucchesi, 2012
	gyrB	KT350502	KT350505	DNA gyrase subunit B, GyrB	Type IIA topoisomerase (DNA gyrase/topo II, topoisomerase IV), B subunit	*Pseudomonas* spp. species	Bodilis et al., 2011
	rpoB	KT350503	KT350506	DNA-directed RNA polymerase beta chain, RpoB	DNA-directed RNA polymerase, beta subunit		
	rpoD	KT350504	KT350507	sigma factor RpoD	DNA-directed RNA polymerase, sigma subunit		

IV. Results

Chapter 4 Study of lipidome of airborne *P. fluorescens*

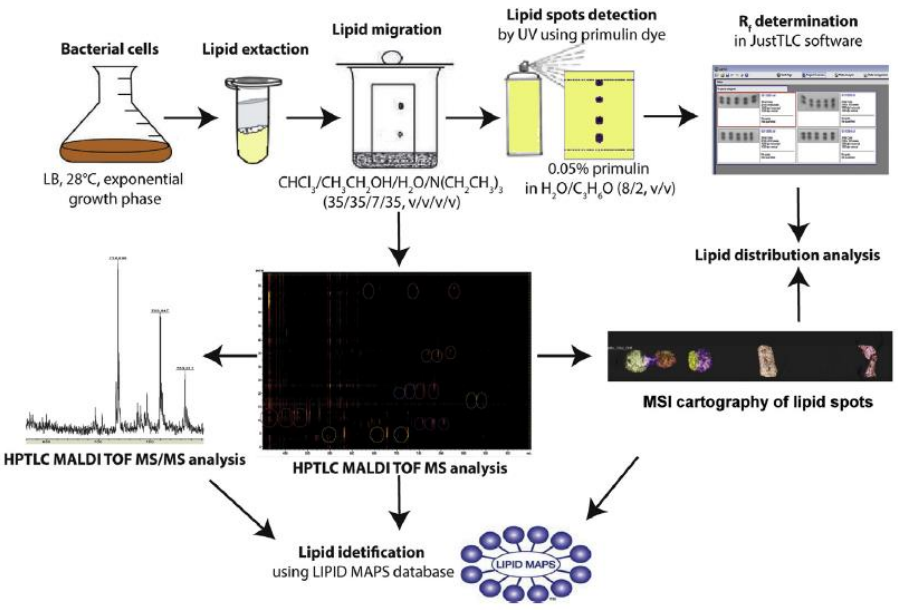

A new study of the bacterial lipidome: HPTLC-MALDI-TOF imaging enlightening the presence of phosphatidylcholine in airborne *Pseudomonas fluorescens* MFAF76a

Tatiana Kondakova, Nadine Merlet-Machour, Manuel Chapelle, David Preterre, Frédéric Dionnet, Marc Feuilloley, Nicole Orange, Cécile Duclairoir Poc

Research in Microbiology 166 (2015) 1-8; doi:10.1016/j.resmic.2014.11.003

Framework

In previous studies, several *P. fluorescens* strains have been isolated from harbor terminal in Rouen (France), including MFAF76a strain, characterized as able to growth at 37°C and express noticeable virulence, particularly against human epithelial pulmonary cells. Although a myriad of proteomics and genomics studies of *P. fluorescens* adaptability to ecological niches and environmental conditions, the lipidome of *P. fluorescens* and its role(s) in bacterial adaptation were poorly studied. The *P. fluorescens* glycerophospholipid studies undergo the excessive development of genomic and proteomic methods and were realized only using thin-layer chromatography (TLC) methods, currently used in the 1970s. In this study, we were interested to characterize the membrane glycerophospholipid composition of this airborne *P. fluorescens* MFAF76a in order to (i) establish a complete picture of *P. fluorescens* lipidome; and (ii) use obtained data in future studies of response of *P. fluorescens* lipidome to environment modifications.

Institut Pasteur
Research in Microbiology 166 (2015) 1–8
www.elsevier.com/locate/resmic

Original article

A new study of the bacterial lipidome: HPTLC-MALDI-TOF imaging enlightening the presence of phosphatidylcholine in airborne *Pseudomonas fluorescens* MFAF76a

Tatiana Kondakova [a,d], Nadine Merlet-Machour [b], Manuel Chapelle [c], David Preterre [d], Frédéric Dionnet [d], Marc Feuilloley [a], Nicole Orange [a], Cécile Duclairoir Poc [a,*]

[a] *Laboratory of Microbiology Signals and Microenvironment (LMSM) EA4312, Normandy Univ., Univ. Rouen, 55 rue St Germain, 27000 Evreux, France*
[b] *Team Modified to Surface and Interface Analysis (SIMA), UMR 6014 COBRA, Normandy Univ., Univ. Rouen, 55 rue St Germain, 27000 Evreux, France*
[c] *Bruker AXS S.A.S., 77420 Champs-sur-Marne, France*
[d] *Aerothermic and Internal Combustion Engine Technological Research Center (CERTAM), 1 Rue Joseph Fourier, 76800 Saint Etienne du Rouvray, France*

Received 6 October 2014; accepted 20 November 2014
Available online 2 December 2014

Abstract

Lipids are major functional components of bacterial cells that play fundamental roles in bacterial metabolism and the barrier function between cells and the environment. In an effort to investigate the bacterial lipidome, we adopted a protocol using MALDI-TOF MS imaging coupled to HPTLC to screen a large number of phospholipid classes in a short span of time.

With this method, phospholipids of airborne *Pseudomonas fluorescens* MFAF76a were visualized and identified in sample extracts (measurement accuracy below 0.1 Da, phospholipid identification by means of four characteristic fragment peaks). Via this technique, the *P. fluorescens* lipidome was shown to comprise three major lipid classes: phosphatidylethanolamine, phosphatidylglycerol and phosphatidylcholine.

The protocol described herein is simple, rapid and effective for screening of bacterial phospholipid classes. The remarkable presence of a eukaryotic phospholipid, phosphatidylcholine, was observed in *P. fluorescens* MFAF76a. This lipid is known to play a role in bacteria–host interactions and had not been known to be found in *P. fluorescens* cells.

Keywords: Lipidomics; Phospholipids; Phosphatidylcholine; Mass spectrometry imaging; HPTLC MALDI TOF MSI; *Pseudomonas fluorescens*

1. Introduction

The emergence of molecular biology techniques at the end of the 20th century was at the origin of complete renewal of microbiology and, as a consequence, research focused essentially on gene and protein expression. However, there is a growing interest in the analysis and identification of bacterial lipids [1]. Accordingly, in addition to terms such as "proteomics", "genomics", and "metabolomics", the term "lipidomics" was introduced in microbiology [2].

Lipids are major compounds of bacterial cells and share a large variety of biological functions. Among these molecules, phospholipids, the major constituents of the cell membrane, play a fundamental role in metabolism, maintenance of membrane integrity, nutrient transport and signal transduction [3]. Bacterial phospholipids (PLs) are constituted by different long-chain (C_{14}–C_{20}) fatty acids linked by ester bonds to the major phosphatidyl moiety. Phosphatidic acid (PA),

* Corresponding author.
E-mail addresses: tatiana.kondakova@etu.univ-rouen.fr (T. Kondakova), nadine.merlet@univ-rouen.fr (N. Merlet-Machour), manuel.chapelle@bruker.fr (M. Chapelle), david.preterre@certam-rouen.com (D. Preterre), frederic.dionnet@certam-rouen.com (F. Dionnet), marc.feuilloley@univ-rouen.fr (M. Feuilloley), nicole.orange@univ-rouen.fr (N. Orange), cecile.poc@univ-rouen.fr (C. Duclairoir Poc).

http://dx.doi.org/10.1016/j.resmic.2014.11.003
0923-2508/

phosphatidylcholine (PC), phosphatidylethanolamine (PE), phosphatidylglycerol (PG), phosphatidylinositol (PI), phosphatidylserine (PS) and cardiolipin (CL) represent the main classes of PLs [4].

Screening of PLs is usually performed using a variety of mass spectrometric techniques. For structural analysis fast-atom bombardment in combination with tandem mass spectrometry, electrospray ionization and matrix-assisted laser desorption ionization (MALDI) have been employed [5–7]. Electrospray ionization MS applied in negative ion mode and combined with liquid chromatography enables separating most of the different classes of phospholipids and identifying these molecules on the basis of the length of fatty acyl chains and unsaturated bond numbers or positions [8]. Although seldom used to provide detailed information for particular molecular species, MALDI is also potentially an excellent analytical method for rapid screening of lipids in biological matrices [9,10]. The use of MALDI MS for PLs analysis helps to overcome numerous problems related to the complexity and diversity of the extracts, as often encountered in bacterial material, and appears to be the most convenient method for complete screening in bacterial lipid extracts [2,11].

In the present report, we describe an analytical method coupling HPTLC to MALDI TOF for bacterial lipid analysis, fragmentation and identification. This method was used to identify PLs expressed in an airborne strain of *Pseudomonas fluorescens* MFAF76a, of particular interest. The adaptation potential of this environmental strain, elsewhere characterized [12], could reside at least by part in the composition of its outer and/or cytoplasmic membrane; thus, its lipidome was established by HPTLC-MALDI TOF imaging.

2. Materials and methods

2.1. Bacterial strain and growth conditions

P. fluorescens MFAF76a is an airborne strain isolated from a sample of air in dust clouds generated during crop ship loading in Rouen harbor installations (Normandy, France) [12]. This strain was grown at 28 °C under gentle agitation (180 rpm) in Luria-Bertani medium (AES, France). Aliquots of cells from 3 independent cultures were collected at the end of the exponential phase (OD 0.7). Cells were harvested by centrifugation at 4 °C (13,000 *g*) for 15 min. After removal of supernatant, cells were washed with sterile saline solution and centrifuged at 4 °C (13,000 *g*) for 10 min. Three successive washes were done. Aliquots of cells were resuspended in deionized water and lyophilized using a Freeze Dryer Heto PowerDry PL9000-50/HSC500 (Thermo Fisher Scientific, Saint-Herblain, France).

2.2. Reagents and chemicals

PL standards, 2,5-dihydroxybenzoic acid (DHB) and solvents (chloroform ($CHCl_3$), methanol (CH_3OH), ethanol ($CH_3–CH_2OH$), triethylamine ($N(CH_2–CH_3)_3$), acetone ($CH_3–CO–CH_3$) and acetonitrile ($CH_3–CN$)) were obtained from Sigma–Aldrich (Saint-Quentin-Fallavier, France). Stock solutions of PL standards were prepared in $CHCl_3$ or in mixture of $CHCl_3/CH_3OH$ (2/1, v/v). All chemicals were of the highest commercially available purity and used without any further purification.

HPTLC silica gel 60 plates F_{254} (75 × 50 mm, on aluminum backs) were obtained from Merck (Darmstadt, Germany). TLC chambers (80 × 120 mm) were purchased from Fisher Scientific SAS (Illkirch, France).

2.3. Bacterial lipid extraction

Lipids were extracted according to the method of Bligh and Dyer [13]. In summary, 5.5 mL of $CHCl_3/CH_3OH/H_2O$ (2/2/1.8, v/v/v) were added to about 1 g of lyophilized bacteria. Samples were mixed for 2 min and centrifuged for 10 min at 3000 *g*. The chloroform phase containing PLs was then collected and stored at −20 °C under N_2 atmosphere.

2.4. High performance thin-layer chromatography (HPTLC)

PLs were first separated by HPTLC using a method adapted from Fuchs et al. [10]. HPTLC plates allowing electric current conduction were washed with $CHCl_3/CH_3–CH_2OH/H_2O/N(CH_2–CH_3)_3$ (35/35/7/35, v/v/v/v) and activated at 110 °C under a vacuum for 2 h. Lipid extracts (100 µL) were deposited on HPTLC plates in triplicate and separated using $CHCl_3/CH_3–CH_2OH/H_2O/N(CH_2–CH_3)_3$ (35/35/7/35, v/v/v/v) as a running separation solution.

Individual lipid spots were visualized by UV fluorescence at 365 nm after spraying of a primulin dye solution (0.05% in $CH_3–CO–CH_3/H_2O$, 8/2, v/v). Retention factors (R_f) were calculated using the Sweday JustTLC software (v. 4.0.3, Lund, Sweden).

2.5. HPTLC-MALDI coupling

DHB was selected as the MALDI matrix, since it allows positive ion spectra of lipids and does not interfere with silica of HPTLC plates. Its peaks can be used as calibration standards.

HPTLC plates were dip-coated using a solution of DHB (200 g/L in C_2H_3N/0.1% trifluoro-acetic acid, 90/10, v/v) [7] and immediately dried under a dust-free atmosphere. This operation was repeated a second time, leading to a mean of DHB of 5 mg/cm^2. HPTLC plates were then fixed on a TLC MALDI target provided by Bruker Daltonics (Bremen, Germany).

2.6. MALDI TOF analysis

MALDI TOF mass spectra were acquired using an Autoflex III mass spectrometer equipped with a laser OptibeamTM Nd/YAG (355 nm) with 200-Hz tripled-frequency (Bruker Daltonics, Bremen, Germany). The excitation voltage was 19.5 kV and the reflector voltage was 21.0 kV. Laser strength

was kept about 30% above threshold for a good signal-to-noise ratio. Substantial strength is needed to desorb lipids from silica [14]. All MS spectra were obtained in reflector positive ion mode using TLC MALDI software (v. 1.1.7.0) provided by Bruker Daltonics (Bremen, Germany). 200 single laser shoots were averaged for each point. The distance between two points was then determined as 1 mm. When obtained via this technique, 2D mass spectra enable rapid analysis of each lipid spot. Post-source decay (PSD) spectra were acquired on a Bruker Autoflex mass spectrometer (Bruker Daltonics), as previously described [15]. Briefly, precursor ions were isolated using a time ion selector. The fragment ions were refocused onto the detector by stepping the voltage applied to the reflectron in appropriate increments. This was done automatically using the "FAST" ("fragment analysis and structural TOF") subroutine of FlexAnalysis software.

Calibration was performed in two steps. External calibration was performed using the DHB matrix and Peptide Calibration Standard II (ref 822570, Bruker Daltonics, Bremen, Germany) covering a mean mass range between 200 and 3500 Da. The external calibration of the apparatus was performed daily in FlexControl software. Supplementary internal calibration was made using sphingomyelin (1 μg/mL) mixed with the matrix solution before dipping. Peaks generated by these standards were used to calibrate TLC MALDI software. This double calibration method improved measurement accuracy to below 0.1 Da for lipid identification. Lipids were identified using the LIPID MAPS database.

2.7. HPTLC-MALDI TOF imaging

Mass spectrometry imaging (MSI) of each spot was performed using FlexImaging software (v. 2.1., Bruker Daltonics, Bremen, Germany). A polygon measurement region was defined starting from the lipid migration line. The number of laser shots per pixel was set at 200 and the distance between two adjacent pixels was 200 μm, with multiple additions of single position acquisition run (every 40 shots). Following MS and MS/MS identification, the lipid line migration was reconstructed according to lipid-identified areas. Individual lipid spots were labeled by a specific color code according to *m/z*.

3. Results

3.1. HPTLC MALDI-TOF MS analysis of lipid standards

A lipid standard mixture was analyzed in order to check identification against MS and MS/MS lipid databases (www.lipidmaps.org) and to identify specific fragmentation mechanisms. The general protocol employed for standards and subsequently bacterial lipid extracts is presented in Fig. 1.

Typical HPTLC-MALDI TOF MSI of lipid standard mixture is presented in Fig. 2. The reconstructed lipid standard line migration is presented on the left side of Fig. 2. The R_f of lipid spots were calculated in JustTLC software using primulin-dyed HPTLC plates (data not shown). MS spectra of each lipid, identified on the basis of their R_f and encoded in artificial colors, are on the right side of Fig. 2. Lipid identification was completed by MS, PDS and MSI analysis directly on the HPTLC plate using TLC MALDI and FlexImaging software.

3.2. HPTLC-MALDI-TOF MSI analysis of bacterial PLs

MSI analysis of *P. fluorescens* MFAF76a lipids is presented in Fig. 3. As visible on its left side, 3 spots were separated

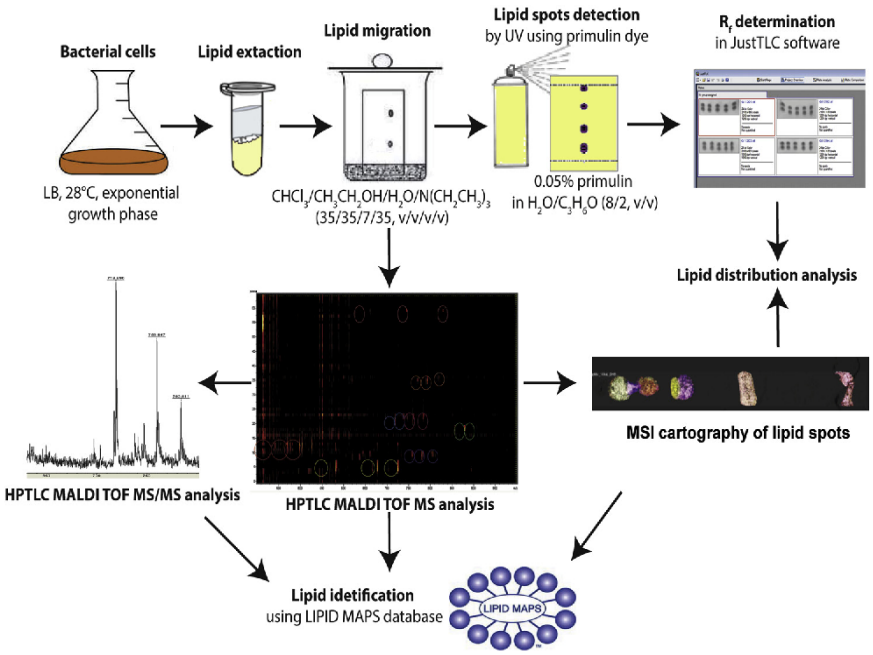

Fig. 1. Scheme illustrating the general HPTLC-MALDI TOF MSI method of PL class analysis.

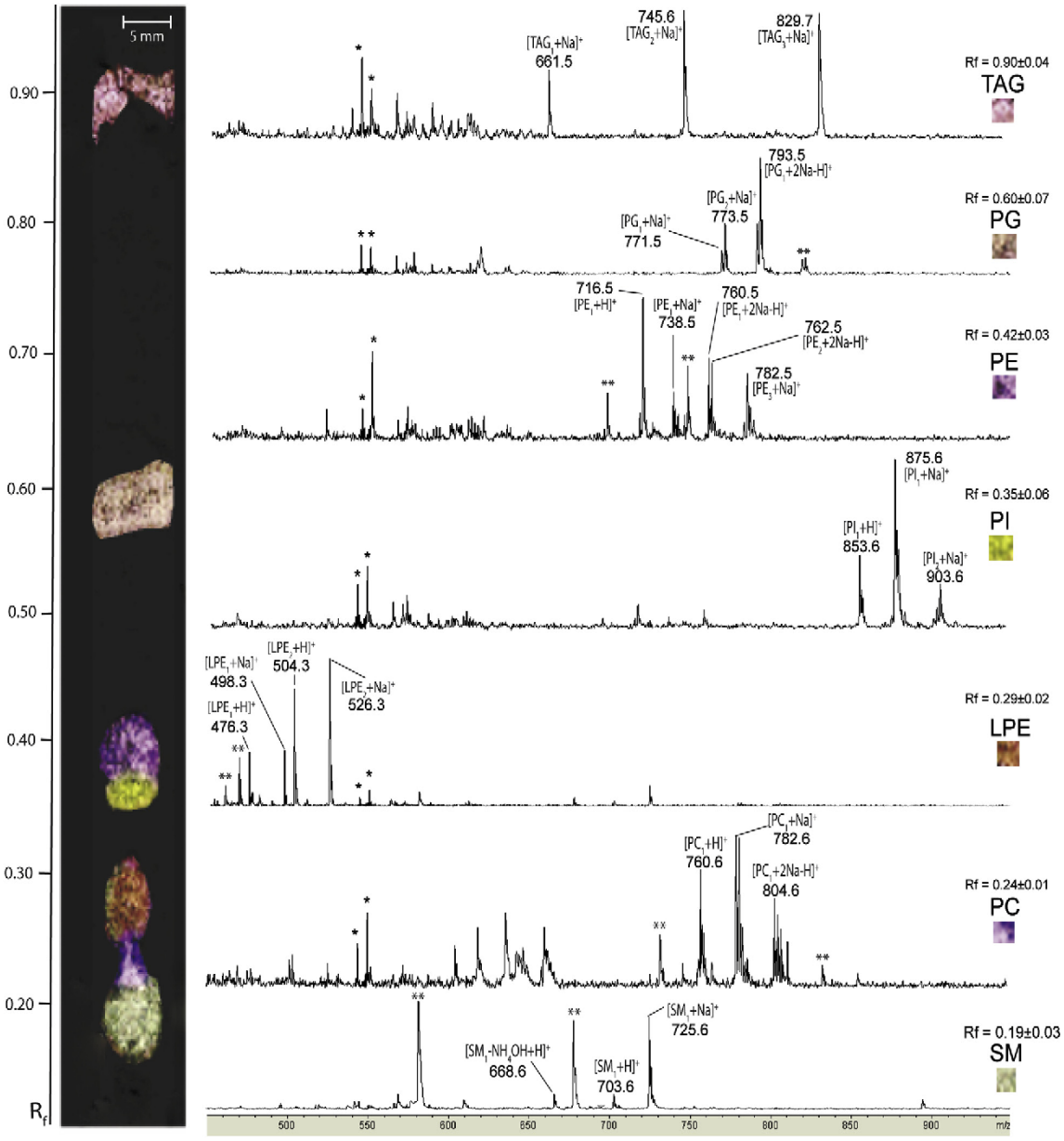

Fig. 2. HPTLC-MALDI TOF MS analysis of lipid standard mixture. Lipid mixture (100 µL) was deposited in triplicate on the HPTLC plate and developed with $CHCl_3/CH_3{-}CH_2OH/H_2O/N(CH_2{-}CH_3)_3$ (35/35/7/35, v/v/v/v) as a solvent system. Lipid standards were purchased from Sigma–Aldrich and used in $CHCl_3$ or in mixture of $CHCl_3/CH_3OH$ (2/1, v/v). The DHB matrix was used as a 200 g/L solution in $CH_3{-}CN$/0.1% trifluoro-acetic acid, 90/10, v/v. After matrix application, MALDI TOF MS, PSD and MSI analyses are performed. All spectra were acquired on an Autoflex III MS equipped with a laser OptibeamTM Nd/YAG (355 nm, 200-Hz tripled-frequency) (Bruker Daltonics, Bremen, Germany). MSI analysis of lipid spots is presented on the left side of the figure. Following MS and PSD identification, the lipid line migration was reconstructed according to lipid-identified areas. Individual lipid spots were labeled with a specific color code according to *m/z*. Sphingomyelin (SM) – (■); PC – (■); lysophosphatidylethanolamine (LPE) – (■); PI – (■); PE – (■); PG – (■) and triglycerides (TAG) – (■); *matrix peaks; **unidentified peaks. (For interpretation of the references to color in this figure legend, the reader is referred to the web version of this article.)

with R_f 0.24 ± 0.01; 0.43 ± 0.02 and 0.62 ± 0.03. On the right side of Fig. 3, the 2D representation shows the lipid line migration versus MS peak intensity (increasing *m/z*). The different lipid spots had specific regions of *m/z* localization. To eliminate most of the matrix peaks, only *m/z* from 500 to 2000 were studied.

Based on the response factors, the following PLs were identified: PC (R_f = 0.24 ± 0.01), PE (R_f = 0.43 ± 0.02) and PG (R_f = 0.62 ± 0.03) (Fig. 4). Detailed MS and PDS spectra are presented on the right side of Fig. 4. PDS spectra of selected peaks are superposed on the lipid MS spectrum.

2,5-dihydroxybenzoic acid (DHB), selected as matrix, enables cleavage of phosphate-glycerol bond and induces loss of the hydrophilic head group, i.e. $[M\text{-}HG + H]^+$, characteristic of each lipid class [1]. This loss is caused by a positive charge localized on the phosphate group [16].

The spot with R_f = 0.62 ± 0.03 was identified as PG. Two most intense peaks, at *m/z* 743.5 and 765.5, showed one PG species singly and doubly sodiated, respectively [PG(16:0/

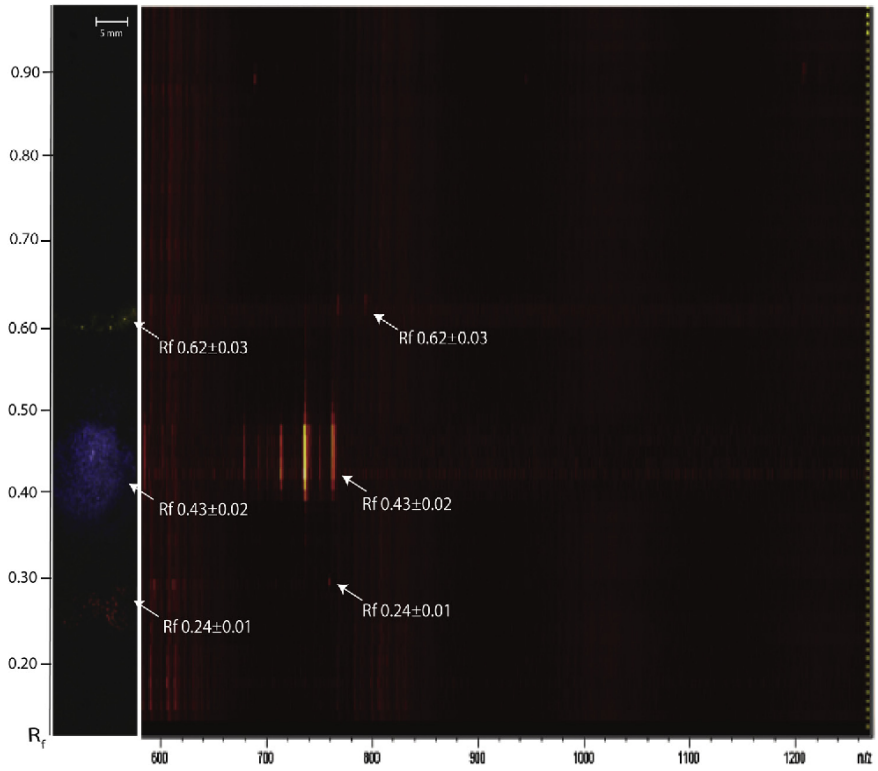

Fig. 3. HPTLC MALDI TOF MS analysis of bacterial PLs. MSI analyses were performed in triplicate using FlexImaging software (v. 2.1., Bruker Daltonics, Bremen, Germany). On the left side of the figure, MSI analysis shows *P. fluorescens* lipid distribution. On the right side, 2D MS representation obtained via TLC MALDI software is shown. The 2D MS image presents the *P. fluorescens* lipid line migration versus MS peak intensity (increasing *m/z* between *m/z* = 500–1300). PLs and retention factor (R_f): PC-0.24 ± 0.01 (■); PE-0.43 ± 0.02 (■); PG-0.62 ± 0.03 (■). The analyses were performed for three independent bacterial lipid extracts.

16:1)+Na]$^+$ and [PG(16:0/16:1)+2Na−H]$^+$ (Fig. 4/A). The peak at *m/z* 791.6 was related to another doubly sodiated PG molecule [PG(16:0/18:1)+2Na−H]$^+$. The PDS fragment at *m/z* 195.1 was characteristic of PG and corresponded to the sodiated head group [HG + Na]$^+$ (Fig. 4/A/1 & 2). The peaks at *m/z* 550.5 and 572.5, corresponding respectively to protonated and monosodiated species, illustrate loss of the head group of PG (Fig. 4/A/1). The peaks at *m/z* 576.5 and 598.5 indicate loss of protonated and sodiated polar head groups of PG species [PG(16:0/18:1)-HG + H]$^+$ and [PG(16:0/18:1)-HG + Na]$^+$ (Fig. 4/A/2, Table 1). The alkyl chain length was confirmed by GC MS analysis of PL fatty acids (see supplementary data Table S1).

The spot with an R_f value of 0.43 ± 0.02 led us to assume the presence of PE, a typical constituent of the *Pseudomonas* lipidome [17–19]. Two pairs of MS peaks (*m/z* 712.5 and 734.5; 738.5 and 760.5), separated by 22 Da, suggested the presence of two PE molecules (Fig. 4/B). This lipid class is characterized by a specific PDS fragments peak at *m/z* = 123.4 corresponding to the dehydrated PE head group [HG-H_20]$^+$ (Fig. 4/B/3 & 4); and *m/z* = 164 to the sodiated head group: [HG + Na]$^+$ (Fig. 4/B/3 & 4). The peaks at *m/z* = 669.5 and 695.5 corresponded to loss of ethanolamine [PE(16:0/16:1)-C_2H_5N + Na]$^+$ and [PE(16:0/18:1)-C_2H_5N + Na]$^+$, respectively. For PE(16:0/16:1), two fragments at *m/z* = 550.5 and 572.5, showed loss of the protonated and sodiated ethanolamine head groups, [PE(16:0/16:1)-HG + H]$^+$ and [PE(16:0/16:1)-HG + Na]$^+$ (Fig. 4/B/3). Peaks at *m/z* = 576.5 and 598.5 were characteristic of the loss of protonated and sodiated head groups of PE(16:0/18:1) (Fig. 4/B/4). Remarkably, the same fragments were found for PG, indicating the same length of alkyl chains in PE and PG molecules (Table 1).

The spot with $R_f = 0.24 \pm 0.01$ was unexpectedly identified as PC. Two MS peaks (*m/z* = 732.6 and 754.5) of one PC(16:0/16:0) species differentiated with 22 Da were found (Fig. 4/C). Fragments at *m/z* = 184.1 and *m/z* = 147.0 were characteristic of PC and corresponded to loss of the polar head group with specific rearrangements [HG + H]$^+$ and [HG-$(CH_3)_3$ + Na]$^+$ (Fig. 4/5) [20]. The peaks at *m/z* = 548.5 and 570.5, Fig. 4/5, were attributed to the loss of the sodiated and protonated polar head groups, [PC(16:0/16:0)-HG + H]$^+$ and [PC(16:0/16:0)-HG + Na]$^+$, respectively. The predominant fragment at *m/z* = 697.6 showed the loss of ammonia from the polar head group [PC(16:0/16:0)-NH_4OH + H]$^+$. The results of this study are summarized in Table 1.

4. Discussion

It is noteworthy that, up until now, the HPTLC-MALDI TOF MSI method was only used for PL analysis in eukaryotic cell lipidomes and human tissue and body fluid [21]. We

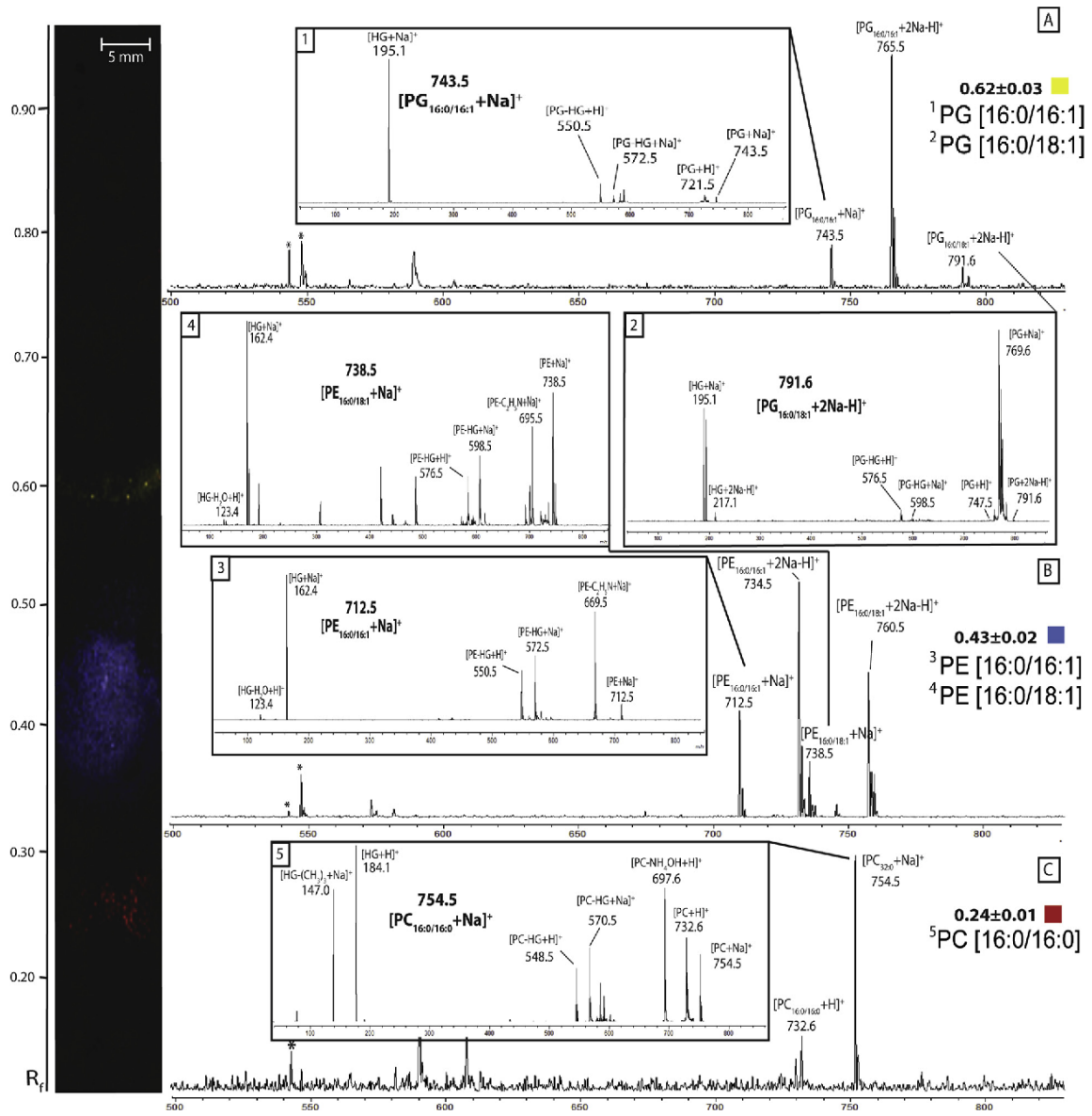

Fig. 4. HPTLC-MALDI TOF MS and PDS analysis of bacterial PLs. MS analysis of R_f 0.24 ± 0.01-PC; R_f 0.43 ± 0.02-PE and R_f 0.62 ± 0.03-PG realized in TLC MALDI software. Lipid peaks were detected in positive MALDI mode on an HPTLC plate. PSD spectra with identification of PL fragments are superimposed. Lipid identification was performed on the basis of MS, PSD and MSI analyses using the LIPID MAPS database, MS and PSD spectra of lipid standards obtained previously. The alkyl chain length was confirmed by GC MS analysis of PL fatty acids (supplementary data, Table S1). The analyses were performed for three independent bacterial lipid extracts. *DHB peaks; **unidentified peaks; HG: head group.

propose herein the first adaptation of this method to the study of the bacterial lipidome. Thus, total lipids of airborne *P. fluorescens* MFAF76a were extracted and separated on HPTLC plates to resolve individual PL spots. This HPTLC technique was coupled to MALDI TOF MS. A complete study of detected spots by MS, PDS and MSI was carried out, enabling PL identification in the lipidome of *P. fluorescens* MFAF76a. The HPTLC-MALDI TOF MSI method of PL analysis appears perfectly adapted to the analysis of bacterial lipids, as demonstrated in the present study.

This method has many key advantages: 1) due to access to a MALDI TOF spectrometer, it is inexpensive, since HPTLC plates only need to have an electric conductor metal back, but are inserted into the spectrometer using a reusable TLC MALDI adapter; 2) HPTLC-MALDI TOF MS is a rather rapid method; TLC MALDI software enable screening of one sample in 5 min; 3) coupling between MALDI MS and HPTLC for separating individual lipids increases the sensitivity of the method compared to other existing techniques; 4) MS imaging, designed for MS analysis of tissue, is a good method for mapping individual lipid species distribution in HPTLC plates.

However, the method continues to have its drawbacks. It suffers from a lack of sensitivity; the required quantity of extracted lipid remains high. A volume of 100 µL of bacterial lipid extract (containing a mean of 40 µg lipids) was necessary

Table 1
PL composition of *P. fluorescens* MFAF76a.

Retention factor	Lipid class	Peak position (*m/z*) and adducts		Species	Molar mass (Da)
0.24 ± 0.01	PC	732.6	$[PC + H]^+$	PC (16:0/16:0)	731.5
		754.5	$[PC + Na]^+$		
0.43 ± 0.02	PE	712.5	$[PE + Na]^+$	PE (16:0/16:1)	689.5
		734.5	$[PE+2Na-H]^+$		
		738.5	$[PE + Na]^+$	PE (16:0/18:1)	715.5
		760.5	$[PE+2Na-H]^+$		
0.62 ± 0.03	PG	743.5	$[PG + Na]^+$	PG (16:0/16:1)	720.5
		765.5	$[PG+2Na-H]^+$		
		791.6	$[PG+2Na-H]^+$	PG (16:0/18:1)	746.5

for one migration line; this implies starting extraction from a large volume of bacterial culture (generally 100 mL).

Moreover, difficulties in PSD fragmentation and identification of PL alkyl chains remain an issue. Since analysis was performed with DHB as the MALDI matrix, the spectrometer was run in a positive mode and non-polar alkyl chain fragments have low intensity. Other experiences with other MALDI matrices, such as 9-aminoacridine or trihydro xyacetophenone in negative MALDI mode, showed weak intensity of individual lipids (data not shown). This makes PDS fragmentation of lipid peaks too insensitive and complicates lipid identification.

The HPTLC-MALDI TOF MSI method led to original results on the lipidome of *P. fluorescens*. In bacteria, most lipids are located in the cell wall. For Gram-negative bacteria like *P. fluorescens,* this cell wall consists of an association of a multiplicity of individual proteins with a somewhat limited series of major lipid species, with the main constituents of PL essentially considered to be PE, PG, CL and minor lysoPLs, like lysoPE and lysoPG [17,18,22,22–25]. The absence of CL in our results can be explained by the extraction method employed. As shown by Lopalco et al. [14], after lipidic extraction, CL is found with denatured proteins in the aqueous phase and thus not in the chloroform phase that was presently analyzed [26]. In any case, the presence of PE and PG was confirmed by our method, and these two lipid classes are considered as major components of the *Pseudomonas* lipidome [17,27]. Conversely, the detection of PC is quite unusual in a bacterial cell [9,10]. This lipid is the major constituent of the membrane bilayer in eukaryotes [28], but it is rarely found in prokaryotes, and only 10% of bacterial species are known to synthesize PC [29]. This PL is found only in the lipidome of very specific bacteria, particularly eukaryotes, symbiotic or pathogenic. Even in an opportunistic pathogen such as *P. aeruginosa*, PC is only detected in small amounts (less 4% of total lipids), but its role appears essential in virulence expression [30,31]. Thus, PC could facilitate the assembly or localization of specific proteins to *P. fluorescens*. Further proteomics studies should help to better understand the role of PC in this bacterial lipidome.

In conclusion, the HPTLC-MALDI TOF MSI technique appears to be a rapid and inexpensive method for the study of the bacterial lipidome. Mass spectrometric analysis can be realized directly after lipid separation on HPTLC plates. This method, adapted from eukaryotic lipid analysis, should efficiently complete proteomic tools for investigating bacterial adaptation to host and stress. In the present study, HPTLC-MALDI TOF MSI enabled revealing expression of different forms of PE and PG in the lipidome of an airborne *P. fluorescens* strain. Moreover, it shows the presence of PC, suggesting potential for adaptation to interactions with eukaryotic hosts.

Conflict of interest

There is no conflict of interest.

Acknowledgments

Tatiana Kondakova is recipient of a PhD grant from the GRR SeSa (Sanitary Safety Research Network) financed by the Regional Council of Haute-Normandie (France). This study was supported by the Conseil général de l'Eure and Grand Evreux Agglomeration.

Appendix A. Supplementary data

Supplementary data related to this article can be found at http://dx.doi.org/10.1016/j.resmic.2014.11.003.

References

[1] Gidden J, Denson J, Liyanage R, Ivey DM, Lay JO. Lipid compositions in *Escherichia coli* and *Bacillus subtilis* during growth as determined by MALDI-TOF and TOF/TOF mass spectrometry. Int J Mass Spectrom 2009;283:178–84.
[2] Fuchs B, Süß R, Schiller J. An update of MALDI-TOF mass spectrometry in lipid research. Prog Lipid Res 2010;49:450–75.
[3] Zhang Y-M, Rock CO. Membrane lipid homeostasis in bacteria. Nat Rev Microbiol 2008;6:222–33.
[4] Wolf C, Quinn PJ. Lipidomics: practical aspects and applications. Prog Lipid Res 2008;47:15–36.
[5] Jensen NJ, Tomer KB, Gross ML. FAB MS/MS for phosphatidylinositol, -glycerol, -ethanolamine and other complex phospholipids. Lipids 1987;22:480–9.
[6] Pulfer M, Murphy RC. Electrospray mass spectrometry of phospholipids. Mass Spectrom Rev 2003;22:332–64.
[7] Fuchs B, Schiller J, Süss R, Zscharnack M, Bader A, Müller P, et al. Analysis of stem cell lipids by offline HPTLC-MALDI-TOF MS. Anal Bioanal Chem 2008;392:849–60.
[8] Milne S, Ivanova P, Forrester J, Alex Brown H. Lipidomics: an analysis of cellular lipids by ESI-MS. Methods 2006;39:92–103.
[9] Schiller J, Süß R, Fuchs B, Muller M, Zschornig O, Arnold K. MALDI-TOF MS in lipidomics. Front Biosci J Virtual Libr 2007;12:2568–79.
[10] Fuchs B, Schiller J, Süss R, Schürenberg M, Suckau D. A direct and simple method of coupling matrix-assisted laser desorption and ionization time-of-flight mass spectrometry (MALDI-TOF MS) to thin-layer chromatography (TLC) for the analysis of phospholipids from egg yolk. Anal Bioanal Chem 2007;389:827–34.
[11] Fuchs B, Süß R, Nimptsch A, Schiller J. MALDI-TOF-MS directly combined with TLC: a review of the current state. Chromatographia 2009;69:95–105.
[12] Duclairoir Poc C, Verdon J, Groboillot A, Barreau M, Toucourou H, Mijouin L, et al. Airborne fluorescent pseudomonads: what potential for virulence? Int J Curr Microbiol Appl Sci 2014;3(8):708–22.

[13] Bligh EG, Dyer WJ. A rapid method of total lipid extraction and purification. Biochem Cell Biol 1959;37:911–7.
[14] Lobasso S, Lopalco P, Angelini R, Vitale R, Huber H, Müller V, et al. Coupled TLC and MALDI-TOF/MS analyses of the lipid extract of the hyperthermophilic archaeon Pyrococcus furiosus. Archaea 2012;2012:1–10.
[15] Fuchs B, Schober C, Richter G, Süß R, Schiller J. MALDI-TOF MS of phosphatidylethanolamines: different adducts cause different post source decay (PSD) fragment ion spectra. J Biochem Biophys Methods 2007;70:689–92.
[16] Harvey DJ. Matrix-assisted laser desorption/ionization mass spectrometry of phospholipids. J Mass Spectrom 1995;30:1333–46.
[17] Boeris PS, Domenech CE, Lucchesi GI. Modification of phospholipid composition in *Pseudomonas putida* A ATCC 12633 induced by contact with tetradecyltrimethylammonium. J Appl Microbiol 2007;103:1048–54.
[18] Fouchard S, Abdellaoui-Maâne Z, Boulanger A, Llopiz P, Neunlist S. Influence of growth conditions on *Pseudomonas fluorescens* strains: a link between metabolite production and the PLFA profile. FEMS Microbiol Lett 2005;251:211–8.
[19] Oursel D, Loutelier-Bourhis C, Orange N, Chevalier S, Norris V, Lange CM. Lipid composition of membranes of *Escherichia coli* by liquid chromatography/tandem mass spectrometry using negative electrospray ionization. Rapid Commun Mass Spectrom 2007;21:1721–8.
[20] Al-Saad KA, Siems WF, Hill HH, Zabrouskov V, Knowles NR. Structural analysis of phosphatidylcholines by post-source decay matrix-assisted laser desorption/ionization time-of-flight mass spectrometry. J Am Soc Mass Spectrom 2003;14:373–82.
[21] Fuchs B, Schiller J. MALDI-TOF MS analysis of lipids from cells, tissues and body fluids. Subcell Biochem 2008;49:541–65.
[22] Diedrich DL, Cota-Robles EH. Heterogeneity in lipid composition of the outer membrane and cytoplasmic membrane of *Pseudomonas* BAL-31. J Bacteriol 1974;119:1006–18.
[23] Gill CO. Effect of growth temperature on the lipids of *Pseudomonas fluorescens*. J Gen Microbiol 1975;89:293–8.
[24] Rowe NJ, Tunstall J, Galbraith L, Wilkinson SG. Lipid composition and taxonomy of [*Pseudomonas*] *echinoides*: transfer to the genus *Sphingomonas*. Microbiol Read Engl 2000;146(Pt 11):3007–12.
[25] Rühl J, Hein E-M, Hayen H, Schmid A, Blank LM. The glycerophospholipid inventory of *Pseudomonas putida* is conserved between strains and enables growth condition-related alterations. Microb Biotechnol 2012;5:45–58.
[26] Lopalco P, Angelini R, Lobasso S, Köcher S, Thompson M, Müller V, et al. Adjusting membrane lipids under salt stress: the case of the moderate halophilic organism *Halobacillus halophilus*. Environ Microbiol 2013;15:1078–87.
[27] Bhakoo M, Herbert RA. Fatty acid and phospholipid composition of five psychrotrophic *Pseudomonas spp*. grown at different temperatures. Arch Microbiol 1980;126:51–5.
[28] Cole LK, Vance JE, Vance DE. Phosphatidylcholine biosynthesis and lipoprotein metabolism. Biochim Biophys Acta 2012;1821:754–61.
[29] Conde-Alvarez R, Grilló MJ, Salcedo SP, de Miguel MJ, Fugier E, Gorvel JP, et al. Synthesis of phosphatidylcholine, a typical eukaryotic phospholipid, is necessary for full virulence of the intracellular bacterial parasite *Brucella abortus*. Cell Microbiol 2006;8:1322–35.
[30] Geiger O, López-Lara IM, Sohlenkamp C. Phosphatidylcholine biosynthesis and function in bacteria. Biochim Biophys Acta 1831;2013:503–13.
[31] Geiger O. Lipids and *Legionella* virulence. In: Timmis KN, editor. Handb hydrocarb lipid microbiol. Springer Berlin Heidelberg; 2010. p. 3195–202.

Highlight

- A new HPTLC-MALDI TOF MSI tools may be successively used in study of bacterial lipidome. This method has many advantages in bacterial lipidome studies, including promptness of analysis and low detection limit. However, the quantification of glycerophospholipids with this technic appears to be difficult.
- The fatty acid composition of *P. fluorescens* reveals 16 and 18 C-atoms in alkyl chains.
- The phosphatidylcholine, phosphatidylethanolamine and phosphatidylglycerol are the major compounds of *P. fluorescens* lipidome.
- The phosphatidylcholine is identified in *P. fluorescens* lipidome for the first time and this glycerophospholipid could be involved in a wide range of bacterial functions, including interactions with eukaryotic hosts.

Chapter 5 Effect of stress factors on membrane of *P. fluorescens*

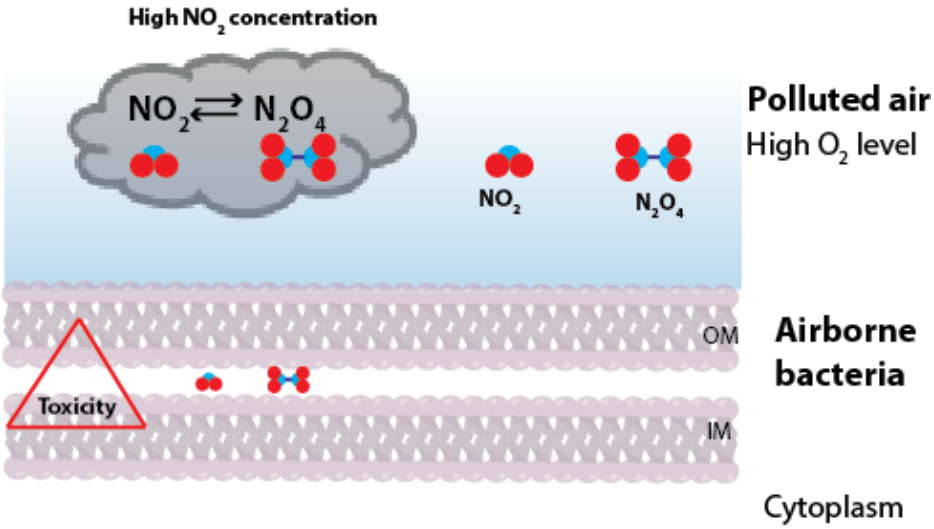

Framework

As humans, airborne bacteria undergo the effect(s) of atmospheric changes, including urban air pollution. After characterization of lipidome of airborne *P. fluorescens* MFAF76a, we decided to initiate the study of membrane response of this bacterial strain to well-known air pollutant NO_2. To the best of our knowledge, the effect of NO_2 on membrane of airborne bacteria was not established yet. In this study the lipidome of airborne *P. fluorescens* was investigated in exponential and stationary growth phase using the new HPTLC-MALDI TOF MSI tool presented in **Chapter 4 Study of lipidome of airborne *P. fluorescens***. First, the effect of increasing temperature (37°C) on *P. fluorescens* membrane was studied in order to establish the pathway(s) employed by *P. fluorescens* membrane to adapt to environmental modifications. This is all the more important in view of the fact that 37°C is an optimal temperature of human body, and several *P. fluorescens* strains were identified as the indigenous microbiota of various body sites. As previously mentioned, MFAF76a was characterized as able to grow at 37°C (Duclairoir Poc *et al.*, 2014). These adaptive properties could be used by this bacterium to adapt to climate warming and/or to tame the 'hot environments', like human body, and would involve the changes in its membrane properties. In this way, we decided to add to this study the clinical *P. fluorescens* strain MFN1032, isolated from the sputum of a pneumonia patient. This bacterium was characterized as growing at 37°C and showing increased virulence against human cells (Rossignol *et al.*, 2009; Sperandio *et al.*, 2012). It shows intense secretion-dependent hemolytic activity (Rossignol *et al.*, 2008; Sperandio *et al.*, 2010), involving the production of phospholipases C and biosurfactants, and has the common characteristics of opportunistic pathogen, similar to that seen for *P. aeruginosa*. After establishment of *P. fluorescens* response to increasing temperature, the membrane response to NO_2 was studied. For this, bacteria were exposed to three NO_2 concentrations, corresponding to the 1-hour NO_2 standard, the threshold, causing reversible effects on human health, and the high NO_2 concentration, provoking irreversible effects, according World Health Organization.

Original article

Submitted in Research in Microbiology, RESMIC-D-15-00333

Effect of air pollution on membrane of airborne bacteria: NO_2 modifies both *Pseudomonas fluorescens* glycerophospholipids and membrane electron-accepting character

Tatiana Kondakova[a,d], Nadine Merlet Machour[b], Josselin Bodilis[a], Magalie Barreau[a], Frédéric Dionnet[d], Marc Feuilloley[a], Nicole Orange[a], Hermann J. Heipieper[c], Cécile Duclairoir Poc[a1]

[a] *Laboratory of Microbiology Signals and Microenvironment (LMSM) EA4312, Normandy Univ., Univ. Rouen, 55 rue St Germain, 27000, Evreux, France.*
[b] *UMR 6014 COBRA, Normandy Univ., Univ. Rouen, 55 rue St Germain, 27000 Evreux, France.*
[c] *Department of Environmental Biotechnology, UFZ Helmholtz Centre for Environmental Research, Permoserstr. 15, 04318 Leipzig, Germany.*
[d] *Aerothermic and Internal Combustion Engine Technological Research Centre (CERTAM), 1 Rue Joseph Fourier, 76800 - Saint Etienne du Rouvray, France.*

Abstract

Nitrogen dioxide (NO_2) is an air pollutant of increasing interest in biology. The aim of the present work was to establish if the response of an airborne *Pseudomonas fluorescens* to NO_2 involves changes in the structure and composition of its membrane glycerophospholipids.

The lipidome was investigated in exponential and stationary growth phases, after exposing to different NO_2 concentrations, using an HPTLC-MALDI TOF MSI tool. Because the effects of temperature modifications on *Pseudomonas* membrane lipids have been already well studied, exposure to increasing temperature was used as control.

Phosphatidylethanolamine, phosphatidylglycerol and phosphatidylcholine were found to be the main compounds of this *P. fluorescens* lipidome. While the glycerophospholipid composition was independent of growth temperature, NO_2 was found to inhibit the synthesis of the newly identified glycerophospholipid and to change bacterial surface properties. In contrast, the degree of saturation of bacterial fatty acids increased with high temperature, but was not modified by NO_2.

This study provides evidence that the bacterial membrane response to NO_2 is specific and quite different of temperature adaptation. NO_2 can freely penetrate membrane of airborne bacteria without modification of its fluidity. In contrast, production of a newly identified membrane glycerophospholipid was modulated by NO_2.

Keywords: Glycerophospholipids; Fatty acid; Airborne; *Pseudomonas fluorescens;* Nitrogen dioxide; Temperature

[1] Corresponding author.
E-mail addresses: tatiana.kondakova@etu.univ-rouen.fr (T. Kondakova), nadine.merlet@univ-rouen.fr (N. Merlet-Machour), josselin.bodilis@univ-rouen.fr (J. Bodilis), magalie.barreau@univ-rouen.fr (M. Barreau), hermann.heipieper@ufz.de (H.J. Heipieper), frederic.dionnet@certam-rouen.com (F. Dionnet), marc.feuilloley@univ-rouen.fr (M. Feuilloley), nicole.orange@univ-rouen.fr (N. Orange), cecile.poc@univ-rouen.fr (C. Duclairoir Poc).

1. Introduction

Air quality is a world-wide problem that attracts important international research efforts. A major probable reason for air quality problems is the growth of urban population combined with changes in land uses due to increasing urban areas [1]. Emissions of air pollutants are caused, in majority, by urban activities, like motor traffic, industry, power plants or trade. Among air pollutants, nitrogen dioxide (NO_2) has been described as widely present in air and its risk for human health was confirmed by several studies. Particularly, high concentrations of NO_2 have been associated with cough, wheezing, and shortness of breath in children [2], emergence of allergic diseases [3] and increased occurrence of asthma [4] or bronchitis [5]. Thus, within the context of Kyoto and Gothenburg Protocols, restrictions of NO_2 emissions were imposed, conducting to the establishment of the toxic NO_2 thresholds, as well as the NO_2 standards.

It is essential to remember that air is a biotic environment and bacteria are one of the major compounds of primary atmosphere aerosol particles [6]. Biogeographic studies demonstrated that the mean concentration of bacteria in ambient air can exceed 10^4 cells / m^3 [7]. Because of seasonal, or meteorological variations, it remains to be difficult to establish a precise picture of bacterial composition in air [8]. However, members of the genus *Pseudomonas* have been frequently found among airborne bacterial populations [9–12].

Members of the *Pseudomonas* genus are highly versatile environmental germs, including the highly adaptable and ubiquitously distributed *Pseudomonas fluorescens* group [13]. Members of this group are found in all natural environments, like water [13], soil [14] and air [15]. Despite a psychrotrophic character of these species, with generally an optimal growth temperature between 25°C and 30°C, several *P. fluorescens* strains are able to grow at up to 37°C [16]. This 'thermotolerance' associated with virulence factors expression and biofilm formation allows *P. fluorescens* to colonize eukaryotic hosts. *P. fluorescens* promotes acute infections in humans, particularly in patients with compromised immune status [17].

The high diversity and large distribution of *P. fluorescens* is linked to its remarkable degree of physiological and genetic adaptability. A key physiological parameter of bacterial adaptability is the structure and organization of the envelope. Most protective membrane functions, as osmotic or heat shock response, are traditionally attributed to proteins that are immersed in the lipid bilayer [18]. Even if lipids themselves are a matrix to accommodate proteins, they also play a major role in bacterial adaptation [19]. This is particularly important in Gram-negative bacteria, like *P. fluorescens*, because of the presence of the distinct outer and inner membranes. Although there is a considerable diversity of lipid structures in the bacterial world, the most predominant components are glycerophospholipids (GPs) [20]. Variety of chemical structures and functions of GPs are due to the polar head group (HG) and fatty acid (FA) composition. The HGs determine the membrane properties and associated functions. They play a role of barrier to prevent the entry of noxious compounds and the influx of nutrient molecules [21]. The adjustments in FA

composition result, primarily, in the formation of unsaturated FAs. This mechanism is used by *Pseudomonas* to control the membrane fluidity to optimize membrane properties and growth in response to environmental modifications [22]. Although the effects of organic compounds [23], or temperature modifications [24] on *Pseudomonas* spp. membrane lipids were well studied, the membrane response(s) to air pollutant NO_2 remain(s) to be investigated.

In previous studies, atmosphere aerosol particles from harbor terminal in Rouen (France) were investigated in terms of size, number and mass distribution. In parallel, the content of pesticide and mycotoxins, as well as microorganism composition (bacteria, yeasts and fungi) were established [25]. Several *P. fluorescens* strains were isolated and identified. Among them, the airborne *P. fluorescens* strain MFAF76a was characterized as able to grow at 37°C and express noticeable virulence, particularly against human epithelial pulmonary cells [15]. Furthermore, the lipidome of this airborne bacterium was investigated [26]. The GP composition of MFAF76a was characterized as containing three major GP classes: phosphatidylethanolamine (PE), phosphatidylglycerol (PG) and phosphatidylcholine (PC), including, in majority, between 16 and 18 C-atoms.

In the present study, we investigated the membrane response of airborne *P. fluorescens* MFAF76a to NO_2, as a marker of air pollution. This response was tested using an HPTLC-MALDI TOF MSI tool and compared to the well-studied temperature response. Airborne MFAF76a was exposed to three NO_2 concentrations: 0.1 ppm as environmental standard; 5 ppm as the threshold, causing reversible effects on human health, and 45 ppm as a high NO_2 concentration, provoking irreversible effects, according World Health Organization. The parameters of bacterial NO_2 exposure were adapted to mimic real-life air conditions. For the first time, the membrane modifications, involved in response of airborne bacteria to NO_2 were investigated, through the analysis of bacterial lipidome coupled with physicochemical characterization of bacterial surface.

2. Materials and methods

2.1. Phylogenetic analyses of the Pseudomonas fluorescens strains

The nucleic sequences of 12 *Pseudomonas* type strains used in this study were obtained from a previous study [27]. Some nucleic sequences from 8 sequenced genomes were also included in this analysis: PAO1[28], PA14 [29], SBW25 [30], Pf0-1 [31], CHAO [32], PF-5 [31], MFN1032 (KP119846 for 16S RNA [33]; *unpublished data*: KT350505 for *gyrB,* KT350506 for *rpoB,* KT350507 for *rpoD*), and MFAF76a (*this study:* KT350501 for 16S RNA, KT350502 for *gyrB,* KT350503 for *rpoB,* KT350504 for *rpoD*).

From the 20 *Pseudomonas* strains, nucleic alignments of four partial housekeeping genes (*gyrB* gene, 798 bp; *rpoB* gene, 642 bp; *rpoD* gene, 564bp; and 16S rRNA gene, 1182 bp) were optimized individually then concatenated, leading to 3,186 nucleotide positions. Protein sequences deduced from *gyrB*, *rpoB* and *rpoD* genes were aligned with ClustalW2 with default parameters implemented in Seaview 4.2.4. Conserved blocks of the multiple alignment were selected by using

Gblocks 0.91b with default parameters and then, nucleic alignment was deduced from this corrected protein alignment. For the 16S rRNA gene alignment, a preliminary step was conducted before selecting the conserved blocks by using Gblocks 0.91b: the regions in which the secondary structures differed were eliminated, as described previously by Anzai et al.[34].

Phylogenetic analysis was conducted by using BioNJ implemented in Seaview 4.2.4, with JC correction. Bootstrap analysis was conducted from 1000 replicates. The maximum likelihood (ML) tree was inferred using RAxML version 7.2.6 with partitioned analysis for the third codon position. A third partition corresponding to the 16S rRNA gene was defined. GTR model parameters, branch lengths, proportion of invariant sites and alpha parameter of the gamma distribution had been estimated independently for each partition. Support values were evaluated based on 100 bootstrap replicates.

The *pcs* nucleic sequences of 6 *P. fluorescens* strains Pf-5, CHAO, Pf0-1, SBW25, MFN1032 (GenBank accession number KT338639) and MFAF76a (GenBank accession number KT338638) and *P. aeruginosa* PAO1 were obtained as described before. The *pcs* nucleic sequence form A506 sequenced genome [35] was also included in this analysis. The sequences were analyzed using the neighbor-joining method. Analyses were conducted using CLC Sequence Viewer 7 (CLC bio, a QIAGEN Company, Denmark). Bootstrap analysis was performed from 1000 replicates.

2.2. Bacterial strain and growth conditions

MFAF76a was grown at 28°C or at 37°C under limited agitation (180 rpm) in Luria-Bertani medium (LB, AES, France) or DMB (Davis Medium Broth) minimal medium with glucose as carbon source (2.16 g/L).

For study of increasing temperature effect on lipid composition, bacterial aliquots were collected in triplicate at the middle of the exponential growth phase ($4.5x10^8$ CFU/mL) or in the early stationary growth phase ($9x10^8$ CFU/mL). After removal of supernatant and three successive rinses with sterile saline solution, bacteria were centrifuged at 4°C (13,000xg). Aliquots were resuspended in deionized water and lyophilized using a Freeze Dryer Heto PowerDry PL9000-50/ HSC500 (Thermo Fisher Scientific, Saint-Herblain, France).

For study of NO_2 effect on bacterial membrane, overnight cultures were diluted (A_{580}=0.08) in fresh DMB and grown to the end of the exponential phase A_{580}=2 ($13x10^8$ CFU/mL). Bacterial cultures at the end of the exponential growth phase (about $3x10^7$ bacteria per filter) were transferred on cellulose nitrate membrane filter (pore size 0.2 µm, diameter 47 mm, Sartorius Biolab Products, Gottingen, Germany) and grown on DMB agar plates at 28°C for 4 h to obtain the single layer's bacterial population. After 4 h of incubation, the cellulose membranes were placed on agar 1 well dishes (size 127.8 x 85.5 mm, Thermo Scientific Nunc, Roshester, USA), which were directly transferred into the gas delivery device (Fig. S1).

2.3. Exposition to nitrogen dioxide

In order to restore the atmospheric conditions, bacterial NO_2 exposure was done in gas phase for 2 h, according [36]. The gas delivery device consisted of two sterile cylindrical Plexiglas exposure chambers (one for the NO_2 exposure, the second one for the control simple - exposure to the synthetic air). The exposure chambers were deposed in drying oven at 28°C (Fig. S1). The NO_2, N_2, and O_2 obtained from Air Liquide GMP Europe (Mitry-Mory, France) were mixed together using digital mass flow regulators (Alicat Scientific, Inc., Tucson, USA) in order to obtain pre-calculated concentration of NO_2 and maintain the O_2/N_2 ratio at 8/2, (v/v). The obtained gas mixture and synthetic air (Air Liquide GMP Europe, Mitry-Mory, France) were routed independently to each of the exposure chambers at a constant flow rate of 2 L/min. The parallel NO_2/synthetic air circuits allow utilization of the same bacterial culture for exposed to NO_2 and control samples. After passing through exposure chamber, the NO_2 concentrations were monitored by AC32M nitrogen oxides analyzer (Environnement S.A, Poissy, France). After this, the gas mixtures were safely vented to a chemical hood. Chamber temperature and relative humidity were monitored and collected to control reliable steady-state environmental conditions inside the exposure chambers. Three concentrations of NO_2 were used in this study: 0.1 ppm; 5 ppm and 45 ppm. After exposure, bacteria were resuspended to A_{580}=2 in sterile saline solution.

2.4. Chemicals

GPs standards, MALDI matrix (2,5-dihydroxybenzoic acid; DHB) and solvents (chloroform, methanol, ethanol, trimethylamine, acetonitrile, hexane, ethyl acetate, hexadecane and decane) were obtained from Sigma-Aldrich (Saint-Quentin-Fallavier, France). The 1,2-di-(9Z-octadecenoyl)-*sn*-glycero-3-phosphoethanolamine-N-nonadecanoyl [19:0-PE (18:1/18:1) + $Na]^+$ was provided by Avanti Polar Lipids, Inc. (Alabaster, Alabama, USA). All chemicals were of the highest commercially available purity and used without any further purification. The HPTLC silica gel 60 plates F_{254} (75 x 50 mm in size, on aluminum backs) were obtained from Merck (Darmstadt, Germany).

2.5. HPTLC-MALDI TOF MSI analysis of glycerophospholipids

The bacterial GP analysis was performed as previously described [26]. After exposure and resuspension at A_{580}=2 in sterile saline solution, bacteria were centrifuged at 4°C (13,000xg) and rinsed three times with sterile saline solution. Aliquots were resuspended in deionized water and lyophilized using a Freeze Dryer Heto PowerDry PL9000-50/ HSC500 (Thermo Fisher Scientific, Saint-Herblain, France). Lipid extraction was performed according to the method of Bligh and Dyer [37]. Bacterial lipid extracts (100 µL) were separated in triplicates on High Performance Thin-Layer Chromatography (HPTLC) plates using $CHCl_3/CH_3CH_2OH/H_2O/N(CH_2CH_3)_3$ (35/35/7/35, v/v/v/v) as mobile phase. The GP spots were visualized by UV fluorescence (365nm) after labeling with 0.05% primulin dye in

acetone/water, (8/2, v/v). Retention factors (R_f) are calculated using the Sweday JustTLC software (v. 4.0.3, Lund, Sweden). Moreover, the following staining was performed in order to identify the lipid classes present in the HPTLC bands: (i) 2% azure A in 1 mM sulfuric acid for sulfatides and sulfoglycolipids, and (ii) 0.25% ninhydrin prepared in acetone-lutidine (9:1, v/v) for phosphatides and lipids having a free amino group. GPs were identified directly on HPTLC plates by Matrix-Assisted Laser Desorption Ionization mass spectrometry – Time of Flight (MALDI-TOF) using an Autoflex III mass spectrometer equipped with a laser Optibeam TM Nd/YAG (355 nm) with a 200-Hz tripled-frequency (Bruker Daltonics, Bremen, Germany). The DHB (200 g/L in acetonitrile/0.1% TFA, 90/10, v/v) was chosen as MALDI matrix. Autoflex III mass spectrometer was run in the reflector positive ion mode using the TLC-MALDI software (v. 1.1.7.0, Bruker Daltonics, Bremen, Germany). The Post Source Decay (PSD) spectra were acquired using FlexControl software (Bruker Daltonics). The Mass Spectrometry Imaging (MSI) was performed using the FlexImaging software (v. 2.1., Bruker Daltonics, Bremen, Germany). The GP distribution was reconstructed according to the m/z of GPs, identified by MS and PSD spectra in combination with LIPID MAPS database and previously obtained data [26]. Individual lipid spots were labeled by a specific color code according to their m/z.

2.6. Fatty acids analysis

Fatty acid methyl esters were prepared by incubation for 15 min at 95°C in a boron trifluoride (BF_3)/methanol (140 g BF_3 per liter of methanol) and extracted with hexane as described by Morrison and Smith [38]. Fatty acid methyl esters were separated and analyzed by gas chromatography (GC) coupled to flame ionization detection using an Agilent Technology, 6890 Network GC System, 7683 Series Injector equipped with a split/splitless injector. The apparatus was equipped with a CP-Sil 88 capillary column (Chrompack, Middelburg, the Netherlands; length, 50m; inner diameter, 0.25 mm; 0.25 mm film). FAs were identified by coinjection as internal standards of reference compounds obtained from Supelco (Bellefonte, Pennsylvania, USA) and were quantified on the basis of their peak areas in total ion chromatograms. All experiments were performed in triplicate. The degree of FA saturation was determined as the ratio between the saturated FAs and the unsaturated FAs [39].

2.7. Bacterial contact angle measurements by sessile drop

After NO_2 exposure, the bacterial suspension at A_{580}=2 in sterile saline solution was filtered on cellulose nitrate membrane filter (pore size 0.2 µm, diameter 47 mm, Sartorius Biolab Products, Gottingen, Germany). The contact angle formed by water droplet, θ_w, on microbial lawns was measured by sessile drop method using a goniometer, DSA 100 (Krüss GmbH, Germany). Bacterial lawns were prepared in suspension of physiological saline in order to obtain at least 2 mL with A_{580} of at least 5. To obtain homogeneous, continuous bacterial lawns, the suspension was slowly deposited on the filter by applying negative pressure, rinsed with 10 mL of

physiological saline and dried at room temperature for 2 h under standardized conditions. To capture the contact angle of water θ_w on the bacterial lawn, four water droplets were observed on each biological triplicate. To determine this contact angle, the drop contour was mathematically described by the Young –Laplace equation using DSA100, and the contact angle was evaluated as the slope of the contour line at the three-phase contact point. The θ_w acquisition is made in the first 10 s once the drop stabilized.

2.8. Evaluation of microbial adhesion to solvent (MATS)

The hydrophobicity of MFAF76a was evaluated by the microbial adhesion to solvent (MATS) test [40]. It consisted in assessing the affinity of the cells to two solvents duos consisting of a mono- and an apolar solvent. In each set, both solvents have similar surface tension, but the monopolar one is acidic (electron accepting, e.g. chloroform) or basic (electron donor, e.g. ethyl acetate). The apolar solvents are respectively hexadecane and decane. For the experiments, bacterial cells were resuspended in saline solution to A_{400}=0.8 (Abs1). This bacterial suspension was mixed with each solvent at 1/6 (v/v) by vigorous agitation for 1 min in order to form an emulsion. This mixture was then left for at least 15 min until the separation of the two phases. The aqueous phase absorbance (Abs2) was measured and the percentage of adhesion was expressed as: affinity % = (1-Abs2/Abs1) x100

2.9. Statistical analysis

All experiments were carried out at least three times. Significances of differences between mean values were assessed using Mann-Whitney test with significance set at $p < 0.05$ (*), < 0.01 (**) and < 0.001 (***).

3. Results and discussion

3.1. Phylogenetic characterisation of Pseudomonas fluorescens *MFAF46a*

Given the current heterogeneity of *P. fluorescens* group, it was first necessary to perform the phylogenetic characterization of *P. fluorescens* MFAF76a in order to characterize its physiological potential. This was carried out by multi-locus sequence analysis (MLSA) using four housekeeping genes, 16S rRNA gene; *gyrB*; *rpoB*; and *rpoD*, as previously described by Mulet et al. [41]. Resulting groups issued from this analysis are supported by high bootstrap values as shown in Fig. 1. The two main lineages, *P. aeruginosa* and *P. fluorescens*, are clearly defined. The *P. fluorescens* lineage is complex [42], six groups being distinguished: *P. fluorescens*, *P. putida*, *P. syringae*, *P. lutea* and *P. fulva* groups. Next, the *P. fluorescens* group could be divided into several subgroups: *P. koreensis, P. chlororaphis, P. corrugata,* and *P. fluorescens* (Fig. 1), with common fluorescens emitting molecules [41]. The airborne MFAF76a strain appeared to be included in the *P. koreensis* subgroup of the *P. fluorescens* group (bootstrap values of 90-100%). This result is in agreement with previous identification studies [15].

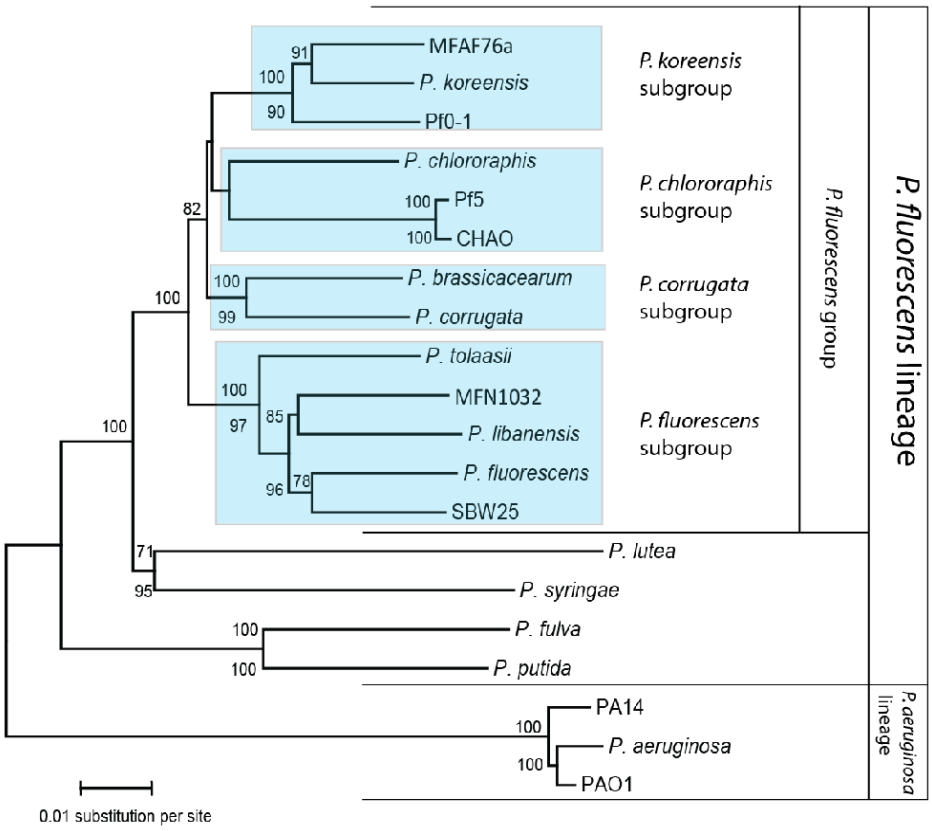

Figure 1. Phylogenetic characterization of airborne *P. fluorescens* MFAF76a
Unrooted phylogenetic tree was based on BioNJ analysis of four concatenated housekeeping genes (*gyrB*, *rpoB*, *rpoD* genes, and 16S rRNA gene) from 20 *Pseudomonas* spp. strains. Phylogenetic analysis was conducted using BioNJ implemented in Seaview 4.2.4. Bootstrap values of more than 80% (from 1000 replicates) are indicated at the nodes (above branch). The node supports below the branches corresponded to ML analysis inferred using RAxML version 7.2.6 (based on 100 bootstrap replicates). The bar indicates sequence divergence.

3.2. Effect of increasing temperature on the glycerophospholipid composition of the airborne Pseudomonas fluorescens *MFAF76a*

The study of *P. fluorescens* MFAF76a lipidome was performed using an HPTLC-MALDI TOF MSI tool [26]. Bacteria were cultivated at 28°C (optimal temperature) and 37°C (high temperature). Total GPs and FAs were extracted in the mid-exponential growth phase (EGP) and in the early stationary growth phase (SGP) in order to (i) study the *P. fluorescens* lipidome all along bacterial growth and (ii) establish the response of a psychrotrophic *P. fluorescens* to increasing temperature.

Results of MSI analyses of the total MFAF76a lipidome are presented in Fig. 2. In all experiments, three GP spots (with R_f 0.24±0.01 - *red color*; 0.43±0.02 - *blue color* and 0.62±0.03 - *yellow color*) were visualized. These GPs were identified in our previous study [26] as PC, PE and PG respectively (Fig. 2, Table 1). The PE and PG, as major bacterial GPs, have been extensively studied in recent literature [43]. The PC was identified in about 15 % of all known bacteria [44], including *P. aeruginosa* [45] and *P. putida* [46] and makes up *circa* 4% of the total membrane GP content in these *Pseudomonas* strains. Although PC, as the major eukaryotic GP, is supposed to play an important role in the

interactions between symbiotic and pathogenic bacteria and their eukaryotic hosts [47], it becomes increasingly evident, that the role of PC in bacterial functioning is much more extensive than previously reported. The identification of PC in *P. fluorescens* MFAF76a conducted us to analyze the possible pathway(s) for synthesis of this GP. Two different pathways for PC synthesis have been described in bacteria: the phospholipid N-methylation (Pmt) and the phosphatidylcholine synthase (Pcs). In the Pmt pathway, PE is methylated to yield PC by a mechanism involving phospholipid N-methyltransferase(s) [44]. In the Pcs pathway, choline condenses directly with cytidyldiphosphate-diacylglycerol to form PC [48]. In *P. aeruginosa* PAO1, *pmtA* (PA0798) and *pcs* (PA3857) genes were described, but the PC seems to be synthesized by Pcs pathway [45]. In *P. putida,* PC was also found to be produced via the Pcs pathway [46].

In order to establish the PC synthesis pathway in *P. fluorescens* strains, the analysis of *pcs* and *pmt* gene sequences among *P. fluorescens* type strains was performed. The gene coding for the Pmt protein was not found in the genomes of tested bacteria (*data not shown*). In consequence, we hypothesize that the synthesis of PC in *P. fluorescens* is conducted by the Pcs pathway. The phylogenetic characterisation of *pcs* gene distribution among *Pseudomonas* spp. strains was realised. The resulting groups were supported by high bootstrap values as shown in Fig. 3, indicating that the Pcs pathway for PC synthesis is well conserved among *Pseudomonas* genus. Three main groups of *pcs*, including *P. aeruginosa*, *P. fluorescens and P. protegens*, were clearly defined. Sequences from the *P. fluorescens* group are pooled together, and contain the airborne MFAF76a *pcs* gene.

The fourth spot, with R_f 0.26±0.02, was detected in the lipidome of MFAF76a (Fig. 2A, *green color*). This lipid was negative to both azure A and amine straining (*data not shown*). The obtained data, based on R_f, MS and PSD analyses, did not allow to a complete identification of this molecule, named in this study unknown glycerophospholipid (UGP). Three MS peaks (m/z 927.5; 941.5; 953.5) were found (Fig. 2C) and present the sodiated molecular forms $[UGP(16:0/17:0)+Na]^+$, $[UGP(16:0/18:0)+Na]^+$, $[UGP(17:1/18:0)+Na]^+$. The PSD spectra of these three m/z were similar to the GP fragmentation mechanism (Fig. 2D), described previously by Al-Saad et al. [49,50]. Fragments at m/z 356.1 and 378.1 look like the glycerophospholipid HG with specific rearrangements, probably $[HG+H]^+$ and $[HG+Na]^+$ respectively (Fig. 2D). Fragment at m/z 195 seems to be a part of HG. Considering previously obtained data [26] and described in literature fragmentation mechanism of GPs, the m/z 195 could be assigned as PG head group, indicating the presence of glycero- group in the molecular structure of UGP. The alkyl chain length and number of unsaturations were identified using PSD spectra (Fig. 2D) and confirmed by GC MS analysis of FAs (Table S1).

In spite of the incomplete MS and PSD identification of UGP, several hypotheses concerning its chemical structure were tested. First of all, the R_f, MS and PSD of several lipid standard were analyzed. The HPTLC analyses of phosphatidylserine (PS), phosphatidic acid (PA), lysophosphatidylethanolamine (LPE) and phosphatidylinositol phosphate (PIP) show the R_f

close to that of UGP (0.10±0.05; 0.29±0.07; 0.19±0.09 and 0.17±0.02 respectively). In contrast, the PSD fragmentation mechanisms of these GP standards (*data not shown*) were quite different of that observed for UGP. The R_f and PSD spectra of cardiolipin (CL), sphingomyelin (SM), phosphatidylinositol (PI) or several triglycerides (TAG) did not match with that of UGP (*data not shown*), indicating that this molecule has a specific structure quite different to that of major GP classes tested in this study. The remarkably high m/z of UGP (*i.e.* m/z 927, comparing to m/z 712 for PE) lets us suppose the addition of acyl radical to the HG (acyl-PE or acyl-PG). The GPs of quite similar structures were previously reported in *Salmonella typhimurium* [51]. The tests of [19:0-PE (18:1/18:1)+Na]$^+$ did not show any similarity in R_f, and in PSD mechanisms with UGP, allowing to reject a potential homology with this compounds. However, a similar but also non identified molecule with close R_f and MS peaks (m/z 924.3; 938.5; 952.3 in negative MALDI mode) was recently identified in *Halobacillus halophilus* [52]. In our study, the UGP appeared to be produced only in SGP, indicating its potential role in this state of bacterial development. However, we cannot exclude a low level of UGP synthesis in EGP because of detection limit of HPTLC-MALDI.

The effect of temperature on GPs and FAs in the airborne *P. fluorescens* MFAF76a confirmed previous studies [24, 54]. No modification in GP composition was found in airborne MFAF76a grown at 37°C in comparison with 28°C (Fig. 2A and Table 1). Although no modification in GP composition was observed, an adaptation to environmental modifications of the GP head groups could not be excluded. Indeed, PC and PE have been treated as interchangeable in many experimental designs [54], and could be transferred from the inner to the outer membrane by lipid flippases to adapt to environmental modifications [55]. This alteration in the HG composition is a way of preserving the stability and low membrane permeability of bacterial membrane [56].

Analysis of FAs revealed an increase of the degree of FA saturation at 37°C when compared to 28°C (Fig. 2B, Table S1). The increase of the degree of FA saturation is a well-studied mechanism used by *Pseudomonas* spp. to preserve the membrane stability [22,57]. It is well known, that the rise of temperature leads to an increase of membrane fluidity. In order to control the properties of membrane lipid bilayer, bacteria react by the synthesis of saturated FAs [57].

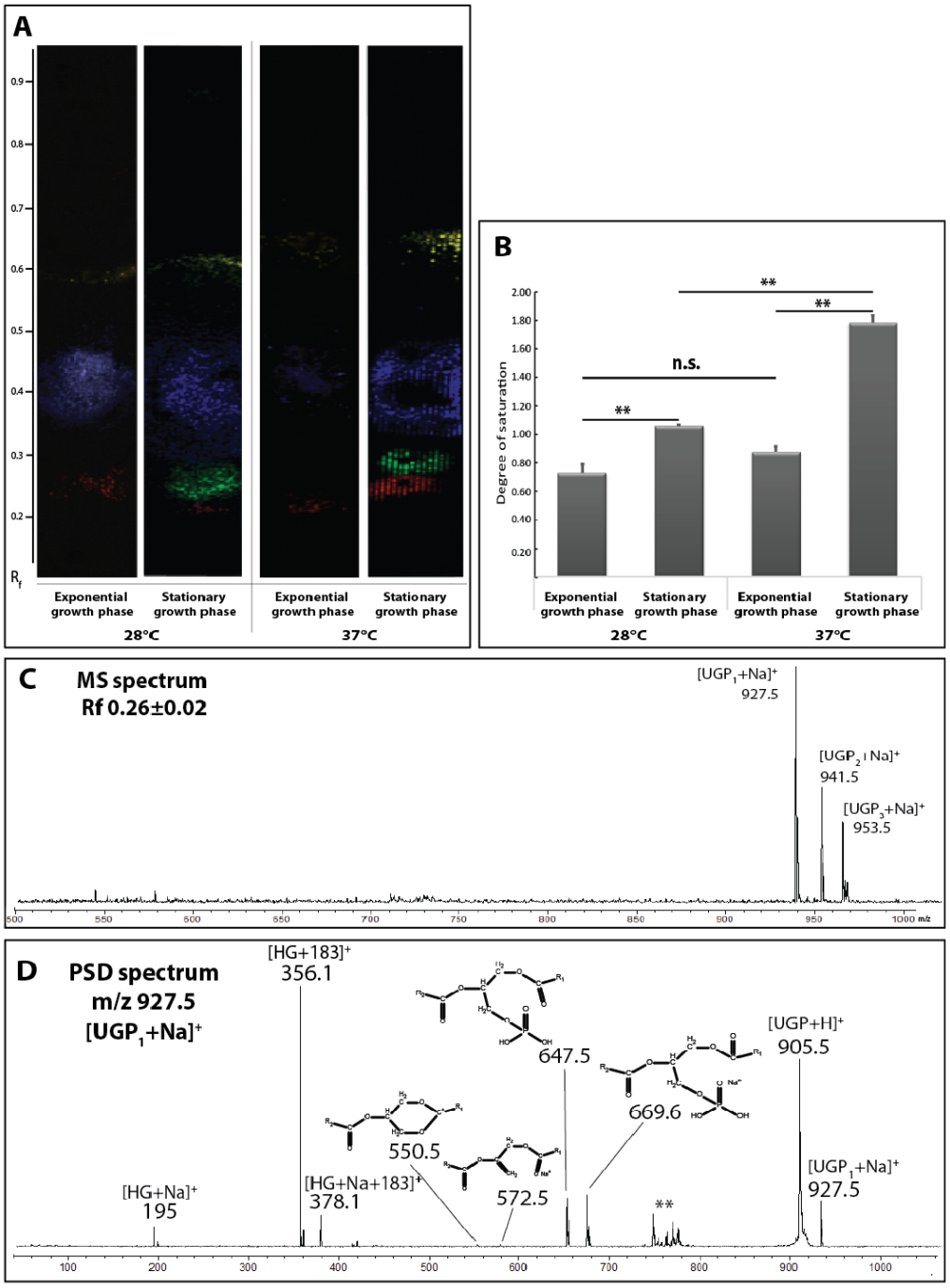

Figure 2. Effect of increasing temperature on membrane glycerophospholipids of airborne *P. fluorescens*

A. Effect of increasing temperature on glycerophospholipid composition. Glycerophospholipid composition of *P. fluorescens* MFAF76a was analyzed using HPTLC-MALDI TOF MSI tool. Bacterial lipid extract (100 µL) was developed in triplicate on HPTLC plates. MALDI TOF MS, PSD and MSI analyses of glycerophospholipid spots were performed directly on HPTLC plate in positive MALDI mode with DHB as MALDI matrix. MSI experiments were performed using FlexImaging software. Glycerophospholipids' distribution was analyzed according to their m/z, previously found using TLC-MALDI software and confirmed by PSD analysis. Individual glycerophospholipid classes were labeled by a specific color code. Glycerophospholipids and retention factor (R_f): phosphatidylcholine (PC) - 0.24±0.01 (*red*); unknown glycerophospholipid (UGP) - 0.26±0.02 (*green*); phosphatidylethanolamine (PE) - 0.43±0.02 (*blue*); phosphatidylglycerol (PG) - 0.62±0.03 (*yellow*). **B. Effect of increasing temperature on fatty acid composition.** Bacterial fatty acids were analyzed and quantified using the GC from at least three independent lipid extracts. The degree of fatty acid saturation was calculated as the ratio between saturated fatty acids and unsaturated fatty acids, and presented as average value ± SEM. Statistical significance was calculated by the non-parametric Mann-Whitney-Test. *P < 0.05; **P < 0.01; n.s. non-significant. **C and D. Identification of unknown glycerophospholipid (UGP).** HPTLC-MALDI TOF MS (**C**) and PSD (**D**) spectra of R_f 0.26±0.02 was realized in positive MALDI mode on HPTLC plates using TLC MALDI and FlexControl software respectively. Analyses of PSD spectra were performed using LIPID MAPS database, MS and PSD spectra of lipid standards. The alkyl chain length was confirmed by GC analysis. The experiments are performed for three independent bacterial lipid extracts. **: unidentified peaks; HG: head group.

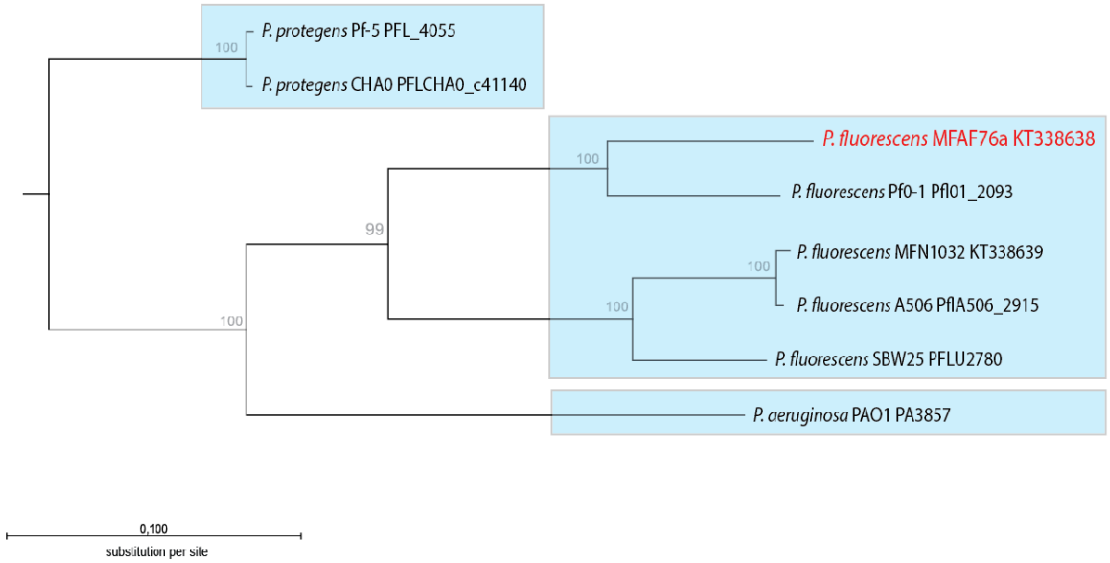

Figure 3. Phylogenic analysis of *pcs* gene distribution among *Pseudomonas fluorescens* type strains
Unrooted phylogenetic tree was based on analysis of *pcs* gene, coding for phosphatidylcholine synthesis in 7 *P. fluorescens* type strains, airborne MFAF76a and *P. aeruginosa* PAO1. The *pcs* gene sequences were analyzed using the neighbor-joining method. Analyses were conducted by using CLC Sequence Viewer 7. The branches of the tree are labeled by the strain name and gene reference in NCBI database. The percent value of the bootstrap support is present in all nodes of tree. The bar indicates sequence divergence. The three main clusters are indicated in blue squares.

Table 1. Effect of temperature change on glycerophospholipid inventory in airborne *P. fluorescens* MFAF76a

Glycerophospholipid identification[a]						Temperature, °C / growth phase			
						28°C		37°C	
Retention factor	GP[d] class	Species	Molar mass (M), g/mol	m/z	Assignement	EGP[b]	SGP[c]	EGP	SGP
0.24±0.01	PC[e]	PC [16:0 + 16:1]	731.5	732.6	$[PC_1+H]^+$	■	■	■	■
		PC [16:0 + 16:1]	731.5	754.5	$[PC_1+Na]^+$	■	■	■	■
		PC [16:0 + 18:1]	759.6	782.6	$[PC_2+Na]^+$				■
0.26±0.02	UGP[f]	UGP [16:0 + 17:0]	904.5	927.5	$[PAL_1+Na]^+$		■		■
		UGP [16:0 + 18:0]	918.5	941.5	$[PAL_2+Na]^+$		■		■
		UGP [17:1 + 18:0]	930.5	953.5	$[PAL_3+Na]^+$		■		■
0.43±0.02	PE[g]	PE [16:0 + 16:1]	689.5	712.5	$[PE_1+Na]^+$	■	■	■	■
				734.5	$[PE_1+2Na-H]^+$	■	■	■	■
		PE [16:0 + 17:1]	703.5	726.5	$[PE_2+Na]^+$		■		
				748.5	$[PE_2+2Na-H]^+$		■		
		PE [16:0 + 18:1]	715.5	738.5	$[PE_3+Na]^+$	■	■	■	■
				760.5	$[PE_3+2Na-H]^+$	■	■	■	■
0.62±0.03	PG[h]	PG [16:0 + 16:1]	720.5	743.5	$[PG_1+Na]^+$	■	■	■	■
				765.5	$[PG_1+2Na-H]^+$	■	■	■	■
		PG [16:0 + 18:1]	746.5	769.5	$[PG_2+Na]^+$		■		■
				791.6	$[PG_2+2Na-H]^+$	■	■		■

[a] The lipid identification was performed on the basis of MS and PSD spectra using LIPID MAPS database and the analysis of lipid standard. The presence of assigned m/z in lipid extract in triplicate is shown by grey squares. The colorless squares show the absence of assigned m/z in lipid extract. The lipid extractions, MS and PSD analysis in all studied conditions were performed in three replicates. [b]**EGP**: exponential growth phase; [c]**SGP**: stationary growth phase; [d]**GP**: glycerophospholipid; [e]**PC**: phosphatidylcholine; [f]**UGP**: unknown glycerophospholipid; [g]**PE**: phosphatidylethanolamine; [h]**PG**: phosphatidylglycerol.

Table 2. Effect of NO_2 on glycerophospholipid inventory in airborne *P. fluorescens* MFAF76a

Glycerophospholipid identification[a]						NO_2 level, ppm			
Retention factor	GP[b] class	Species	Molar mass (M), g/mol	m/z	Assignement	0	0.1	5	45
0.24±0.01	**PC**[c]	PC [16:0 + 16:1]	731.5	732.6	$[PC_1+H]^+$	■	■	■	■
		PC [16:0 + 16:1]	731.5	754.5	$[PC_1+Na]^+$	■	■	■	■
		PC [16:0 + 18:1]	759.6	782.6	$[PC_2+Na]^+$	■	□	□	□
0.26±0.02	**UGP**[d]	UGP [16:0 + 17:0]	904.5	927.5	$[PAL_1+Na]^+$	■	■	■	□
		UGP [16:0 + 18:0]	918.5	941.5	$[PAL_2+Na]^+$	■	■	■	□
		UGP [17:1 + 18:0]	930.5	953.5	$[PAL_3+Na]^+$	■	■	■	□
0.43±0.02	**PE**[e]	PE [16:0 + 16:1]	689.5	712.5	$[PE_1+Na]^+$	■	■	■	■
				734.5	$[PE_1+2Na-H]^+$	■	■	■	■
		PE [16:0 + 17:1]	703.5	726.5	$[PE_2+Na]^+$	■	■	■	■
				748.5	$[PE_2+2Na-H]^+$	■	■	■	■
		PE [16:0 + 18:1]	715.5	738.5	$[PE_3+Na]^+$	□	■	■	■
				760.5	$[PE_3+2Na-H]^+$	■	■	■	■
0.62±0.03	**PG**[f]	PG [16:0 + 16:1]	720.5	743.5	$[PG_1+Na]^+$	■	■	■	■
				765.5	$[PG_1+2Na-H]^+$	■	■	■	■
		PG [16:0 + 18:1]	746.5	769.5	$[PG_2+Na]^+$	□	□	□	□
				791.6	$[PG_2+2Na-H]^+$	■	■	■	■

[a] The lipid identification was performed on the basis of MS and PSD spectra using LIPID MAPS database and the analysis of lipid standard. The presence of assigned m/z in lipid extract in triplicate is shown by grey squares. The colorless squares show the absence of assigned m/z in lipid extract. The lipid extractions, MS and PSD analysis in all studied conditions were performed in three replicates. [b]**GP**: glycerophospholipid; [c]**PC**: phosphatidylcholine; [d]**UGP**: unknown glycerophospholipid; [e]**PE**: phosphatidylethanolamine; [f]**PG**: phosphatidylglycerol.

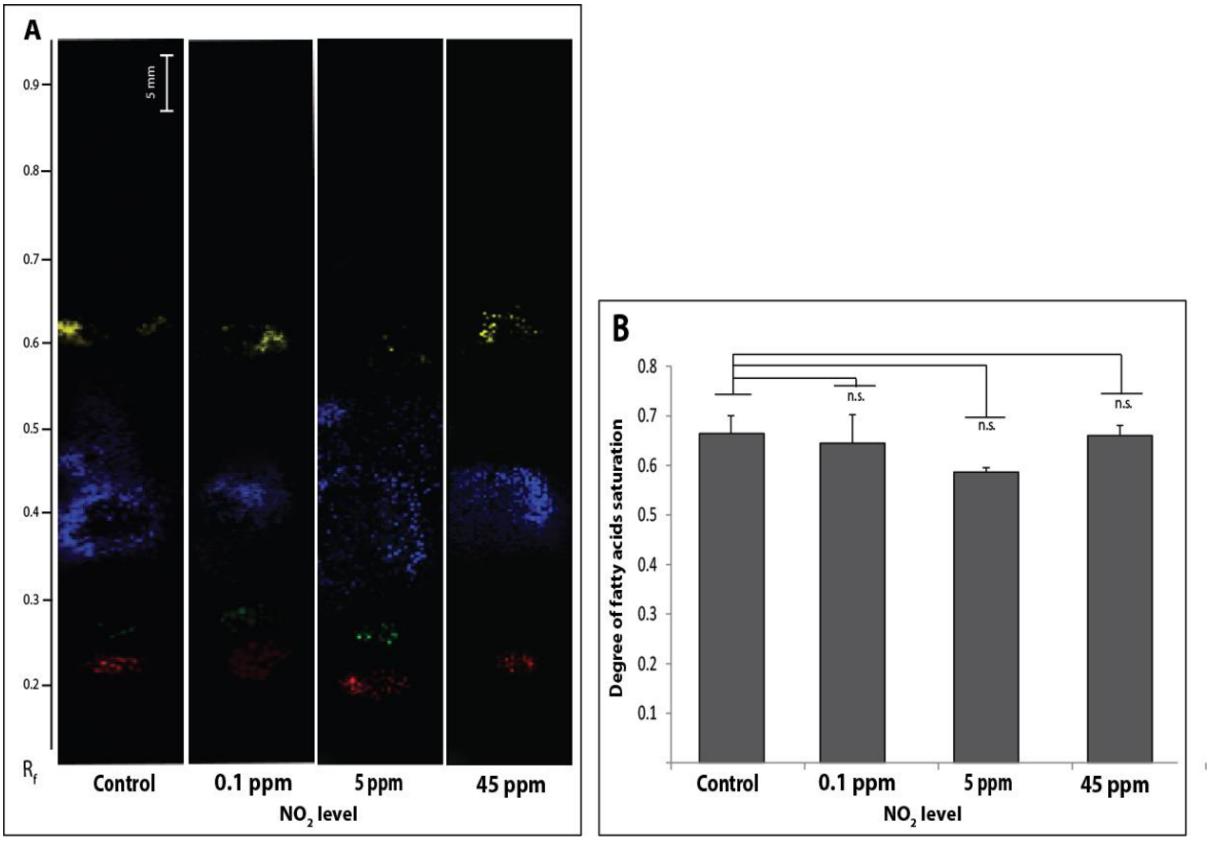

Figure 4. Effect of NO_2 on membrane glycerophospholipids of airborne *P. fluorescens*
Bacteria were exposed to NO_2 in three concentrations: 0.1 ppm; 5 ppm and 45 ppm. After exposure, effect of NO_2 on glycerophospholipid (**A**) and on fatty acid (**B**) composition was examined. Glycerophospholipid composition of exposed to NO_2 *P. fluorescens* MFAF76a was tested using HPTLC-MALDI TOF MS Imaging tool and compared to control sample. Bacterial lipid extract (100 µL) was developed in triplicate on HPTLC plates. MALDI TOF MS, PSD and MSI analyses of glycerophospholipid spots were performed directly on HPTLC plate in positive MALDI mode with DHB as MALDI matrix. MSI experiments were performed using FlexImaging software. Glycerophospholipid distribution was analyzed according to their m/z, previously found using TLC-MALDI software and confirmed by PSD analysis. Individual glycerophospholipid classes were labeled by the specific color code. Glycerophospholipids and retention factor (R_f): phosphatidylcholine (PC) - 0.24±0.01 (*red*); unknown glycerophospholipid (UGP) - 0.26±0.02 (*green*); phosphatidylethanolamine (PE) - 0.43±0.02 (*blue*); phosphatidylglycerol (PG) - 0.62±0.03 (*yellow*). **B.** Bacterial fatty acids were identified and quantified using the GC in triplicate. The degree of fatty acid saturation was calculated as the ratio between saturated and unsaturated fatty acids, and is presented as the average value from three assays ± SEM. Statistical significance was calculated by the non-parametric Mann-Whitney-Test. n.s. non-significant.

Table 3. Effect of exposure to 45 ppm of NO_2 on surface properties of airborne *P. fluorescens* MFAF76a

NO_2 concentration (ppm)	Sessile Drop[b]	MATS: solvent affinity (%)[b]			
	Contact angle (°)	Chloroform	Hexadecane	Decane	Ethyl acetate
0[a]	19.5±6.3	62±10	10±8	4±3	24±10
45	14.6±3.6	41±10	0±6	4±4	1±1

[a] Control sample: bacteria exposed to synthetic air. [b] The results are presented as the average value from at least three assays ± SEM. Statistical significance was calculated by the non-parametric Mann-Whitney-Test.

3.3. *Effect of NO_2 on glycerophospholipids in the airborne* Pseudomonas fluorescens *MFAF76a*

In order to test the effect of NO_2, as a marker of air pollution, on GPs of airborne bacteria, MFAF76a was exposed to three NO_2 concentrations: 0.1 ppm, 5 ppm and 45 ppm. Extracted GPs and FAs were analysed as described above. The GP composition of MFAF76a, exposed to three concentrations of NO_2 was comparable to that of control sample, exposed to synthetic air (Fig. 4, Table 2). PC, PE and PG were found in all experimental conditions. In contrast, the UGP was not detected in bacteria exposed to 45 ppm of NO_2, indicating that this GP is affected by this free radical. The degree of FA saturation after NO_2 exposure was also tested (Fig. 4B). Interestingly, no significant modification was detected, indicating, that NO_2-mediated stress has not the same effect on bacterial FAs than the temperature increase. This lets us suppose, that NO_2 does not change bacterial membrane fluidity and could freely penetrate through the bacterial membrane. These data are supported by computational model developed by Signorelli et al., demonstrated that lipid membranes are not significant barriers to NO_2 transport [58].

The literature reports, that the nitrogen reactive species could mediate the oxidation and/or nitration of membrane GPs, leading to the formation of lipid hydroperoxides, alcohols, and aldehydes [59]. In this way, an addition of -OOH (33 Da) or -NO_2 (44 Da) to GP masses should be observed. However, in this study, no modification of GP m/z was found, indicating that NO_2 does not react with the GPs of MFAF76a in tested conditions. A biochemical mechanism of lipid oxidation and nitration by NO_2 has been described in eukaryotic cells, which contain the high levels of polyunsaturated FAs in their membranes [60]. Given that the lipidome of *P. fluorescens* was described as including only monounsaturated FAs [26], the absence of GP reaction with NO_2 appears to be logical. In coherence, the bacterial GPs are described as unreactive oxygen reactive species *in vitro* [61], confirming our results.

3.4. *Effect of NO_2 on the physicochemical properties of the airborne* Pseudomonas fluorescens *MFAF76a membrane*

Given its lipophilic character, NO_2 can be accumulated in the bacterial membrane [62]. Although NO_2 is not reacting with membrane GPs, it can react with other membrane compounds (*i.e.* proteins or lipopolysaccharides) [63]. Bacteria are known to adapt to NO_2 toxicity by both overproduction of several membrane proteins (*i.e.* efflux pumps) [64] and as previously mentioned GP flipping [55]. Then, the synthesis of membrane GPs and proteins must, in turn, be coordinated to maintain the correct proportion of GPs to proteins in the membrane [65,66]. In this way, the membrane physiological properties, like tension or interfacial curvature, could be impacted by NO_2 consecutively to changes in hydrophobic interactions, hydrogen bonding or electrostatic interactions. Such physicochemical properties of bacterial cell wall are related to the hydrophobicity and electron donor–acceptor (acid–base) properties and are usually measured by Contact Angle Measurements (CAM). Thus, the cell lawns after exposure to 45 ppm of NO_2 were evaluated by CAM. The hydrophilic character of the surface of the airborne *P. fluorescens* MFAF76a remained stable after exposure to 45 ppm of NO_2 (Table 3),

indicating that the high NO_2 concentration causes no surface modification. In this way, the effect of NO_2 on bacterial membrane seems to be quite different of that of organic solvents, which impact the lipopolysaccharides (LPS) and modify the global charge of the bacterial surface [67]. This absence of membrane charge modification is not surprising in the context of the coordination of membrane lipid/protein ratio. To sharpen our knowledge, microbial adhesions to solvent (MATS) were realized using bacteria exposed to 45 ppm of NO_2. Despite the secondary electrostatic contribution [68], the hydrophilic character of the airborne strain was confirmed by its very poor affinity for apolar solvents (*i.e.* decane and hexadecane) (Table 3). The absence of significant modification in the affinity to chloroform, decane and hexadecane between exposed to NO_2 and control samples showed an absence of modification in surface charge and confirmed the CAM results. However, the significant decreasing of the affinity of NO_2-treated bacteria for acetyl acetate (Table 3) indicates a decrease of electron-accepting property of the membrane. These results could be explained by modifications in both membrane proteins and GPs. From the lipidic standpoint, this decrease could be related to the changes in HGs of zwitterionic GPs. Indeed, both found in *P. fluorescens* membrane, PE and PC do not exhibit similar acido-basic strength: PE is more electron accepting than PC. Then, their relative proportion could be modified in favour of PC, without considering the drastic decrease of UGP (or even its loss).

In conclusion, the membrane GP composition of the airborne *P. fluorescens* MFAF76a was found to include PE, PG and PC, which seems to be synthesized via the Pcs pathway. A new UGP with PSD spectra quite different to all tested GPs or TAGs was found. This UGP was found only in stationary growth phase and was not affected by increasing temperature. In bacteria, exposed to high NO_2 concentration, no UGP was detected, indicating that this GP is sensitive to NO_2. Complementary studies using analytic tools not presently accessible should be necessary to identify this UGP, its metabolic pathway(s) and its potential role in *P. fluorescens*. Unlike the effect of increasing temperature, NO_2 does not modify the membrane fluidity and appears to freely penetrate through the bacterial membrane. However, membrane itself is not inert towards this toxic pollutant, which causes a decrease of the electron-acceptor character of the bacterial surface. These results denote real impact of NO_2 exposure on the bacterial envelope being the first element involved in adhesion to the target cells and virulence expression.

Conflict of interest

All authors declare that they have no competing interests.

Acknowledgements

We are grateful to Anne Groboillot for the help with development of gas delivery system. We thank Olivier Maillot for the technical assistance. This study was supported by a PhD grant from the GRR SESA (Research Network of Sanitary Safety) and was financially supported by Regional Council of Haute-Normandie, the Conseil Général de l'Eure and the Grand Evreux Agglomeration

(France). Fatty acids analysis was financially supported by grants from the German Academic Exchange Service (DAAD), the Doctoral Normandy's Graduate School of Integrative Biology, Health and Environment's, University of Rouen and the Regional Council of Haute-Normandie, France.

Supplementary data

Supplementary data related to this article can be found in Annexes.

References

[1] Mayer H. Air pollution in cities. Atmos Environ 1999;33:4029–37. doi:10.1016/S1352-2310(99)00144-2.

[2] Takizawa H. Impact of air pollution on allergic diseases. Korean J Intern Med 2011;26:262–73. doi:10.3904/kjim.2011.26.3.262.

[3] Ring J, Eberlein-Koenig B, Behrendt H. Environmental pollution and allergy. Ann Allergy Asthma Immunol 2001;87:2–6. doi:10.1016/S1081-1206(10)62332-0.

[4] Rehwagen M, Schlink U, Herbarth O, Fritz GJ. Pollution profiles at different kindergarten sites in Leipzig, Germany. Environ Toxicol 1999;14:321–7. doi:10.1002/(SICI)1522-7278(199907)14:3<321::AID-TOX5>3.0.CO;2-L.

[5] Pershagen G, Rylander E, Norberg S, Eriksson M, Nordvall SL. Air pollution involving nitrogen dioxide exposure and wheezing bronchitis in children. Int J Epidemiol 1995;24:1147–53. doi:10.1093/ije/24.6.1147.

[6] Burrows SM, Elbert W, Lawrence MG, Pöschl U. Bacteria in the global atmosphere – Part 1: Review and synthesis of literature data for different ecosystems. Atmos Chem Phys 2009;9:9263–80. doi:10.5194/acp-9-9263-2009.

[7] Burrows SM, Butler T, Jöckel P, Tost H, Kerkweg A, Pöschl U, et al. Bacteria in the global atmosphere – Part 2: Modeling of emissions and transport between different ecosystems. Atmos Chem Phys 2009;9:9281–97. doi:10.5194/acp-9-9281-2009.

[8] Després VR, Alex Huffman J, Burrows SM, Hoose C, Safatov AS, Buryak G, et al. Primary biological aerosol particles in the atmosphere: a review. Tellus B 2012;64. doi:10.3402/tellusb.v64i0.15598.

[9] Dybwad M, Granum PE, Bruheim P, Blatny JM. Characterization of airborne bacteria at an underground subway station. Appl Environ Microbiol 2012;78:1917–29. doi:10.1128/AEM.07212-11.

[10] Fang Z, Ouyang Z, Zheng H, Wang X, Hu L. Culturable airborne bacteria in outdoor environments in Beijing,China. Microb Ecol 2007;54:487–96. doi:10.1007/s00248-007-9216-3.

[11] Pearce DA, Hughes KA, Lachlan-Cope T, Harangozo SA, Jones AE. Biodiversity of air-borne microorganisms at Halley Station, Antarctica. Extrem Life Extreme Cond 2010;14:145–59. doi:10.1007/s00792-009-0293-8.

[12] Šantl-Temkiv T, Sahyoun M, Finster K, Hartmann S, Augustin-Bauditz S, Stratmann F, et al. Characterization of airborne ice-nucleation-active bacteria and bacterial fragments. Atmos Environ 2015;109:105–17. doi:10.1016/j.atmosenv.2015.02.060.

[13] Bodilis J, Calbrix R, Guérillon J, Mérieau A, Pawlak B, Orange N, et al. Phylogenetic relationships between environmental and clinical isolates of *Pseudomonas fluorescens* and related species deduced from 16S rRNA gene and OprF protein sequences. Syst Appl Microbiol 2004;27:93–108. doi:10.1078/0723-2020-00253.

[14] Varivarn K, Champa LA, Silby MW, Robleto EA. Colonization strategies of *Pseudomonas fluorescens* Pf0-1: activation of soil-specific genes important for diverse and specific environments. BMC Microbiol 2013;13:92. doi:10.1186/1471-2180-13-92.

[15] Duclairoir Poc C, Verdon J, Groboillot A, Barreau M, Toucourou H, Mijouin L, et al. Airborne fluorescent pseudomonads : What potential for virulence? Int J Curr Microbiol Appl Sci 2014:708–22.

[16] Picot L, Mezghani-Abdelmoula S, Chevalier S, Merieau A, Lesouhaitier O, Guerillon J, et al. Regulation of the cytotoxic effects of *Pseudomonas fluorescens* by growth temperature. Res Microbiol 2004;155:39–46. doi:10.1016/j.resmic.2003.09.014.

[17] Chapalain A, Rossignol G, Lesouhaitier O, Merieau A, Gruffaz C, Guerillon J, et al. Comparative study of 7 fluorescent pseudomonad clinical isolates. Can J Microbiol 2008;54:19–27. doi:10.1139/w07-110.

[18] Poole K. Bacterial stress responses as determinants of antimicrobial resistance. J Antimicrob Chemother 2012:dks196. doi:10.1093/jac/dks196.

[19] Kondakova T, D'Heygère F, Feuilloley MJ, Orange N, Heipieper HJ, Duclairoir Poc C. Glycerophospholipid synthesis and functions in *Pseudomonas*. Chem Phys Lipids 2015;190:27–42. doi:10.1016/j.chemphyslip.2015.06.006.

[20] Zhang Y-M, Rock CO. Membrane lipid homeostasis in bacteria. Nat Rev Microbiol 2008;6:222–33. doi:10.1038/nrmicro1839.

[21] Nikaido H. Molecular basis of bacterial outer membrane permeability revisited. Microbiol Mol Biol Rev 2003;67:593–656. doi:10.1128/MMBR.67.4.593-656.2003.

[22] Pepi M, Heipieper HJ, Fischer J, Ruta M, Volterrani M, Focardi SE. Membrane fatty acids adaptive profile in the simultaneous presence of arsenic and toluene in *Bacillus* sp. ORAs2 and *Pseudomonas* sp. ORAs5 strains. Extrem Life Extreme Cond 2008;12:343–9. doi:10.1007/s00792-008-0147-9.

[23] Heipieper HJ, Weber FJ, Sikkema J, Keweloh H, de Bont JAM. Mechanisms of resistance of whole cells to toxic organic solvents. Trends Biotechnol 1994;12:409–15. doi:10.1016/0167-7799(94)90029-9.

[24] Fouchard S, Abdellaoui-Maâne Z, Boulanger A, Llopiz P, Neunlist S. Influence of growth conditions on *Pseudomonas fluorescens* strains: A link between metabolite production and the PLFA profile. FEMS Microbiol Lett 2005;251:211–8. doi:10.1016/j.femsle.2005.08.003.

[25] Morin J-P, Preterre D, Gouriou F, Delmas V, François A, Orange N, et al. Particules urbaines et céréalières, micro-organismes, mycotoxines et pesticides. Pollut Atmos 2013.

[26] Kondakova T, Merlet-Machour N, Chapelle M, Preterre D, Dionnet F, Feuilloley M, et al. A new study of the bacterial lipidome: HPTLC-MALDI-TOF imaging enlightening the presence of phosphatidylcholine in airborne *Pseudomonas fluorescens* MFAF76a. Res Microbiol 2014. doi:10.1016/j.resmic.2014.11.003.

[27] Bodilis J, Nsigue Meilo S, Cornelis P, De Vos P, Barray S. A long-branch attraction artifact reveals an adaptive radiation in *Pseudomonas*. Mol Biol Evol 2011;28:2723–6. doi:10.1093/molbev/msr099.

[28] Stover CK, Pham XQ, Erwin AL, Mizoguchi SD, Warrener P, Hickey MJ, et al. Complete genome sequence of *Pseudomonas aeruginosa* PAO1, an opportunistic pathogen. Nature 2000;406:959–64. doi:10.1038/35023079.

[29] Lee DG, Urbach JM, Wu G, Liberati NT, Feinbaum RL, Miyata S, et al. Genomic analysis reveals that *Pseudomonas aeruginosa* virulence is combinatorial. Genome Biol 2006;7:R90. doi:10.1186/gb-2006-7-10-r90.

[30] Rainey PB, Bailey MJ. Physical and genetic map of the *Pseudomonas fluorescens* SBW25 chromosome. Mol Microbiol 1996;19:521–33.

[31] Silby MW, Cerdeño-Tárraga AM, Vernikos GS, Giddens SR, Jackson RW, Preston GM, et al. Genomic and genetic analyses of diversity and plant interactions of *Pseudomonas fluorescens*. Genome Biol 2009;10:R51. doi:10.1186/gb-2009-10-5-r51.

[32] Jousset A, Schuldes J, Keel C, Maurhofer M, Daniel R, Scheu S, et al. Full-genome sequence of the plant growth-promoting bacterium *Pseudomonas protegens* CHA0. Genome Announc 2014;2. doi:10.1128/genomeA.00322-14.

[33] Mazurier S, Merieau A, Bergeau D, Decoin V, Sperandio D, Crépin A, et al. Type III secretion system and virulence markers highlight similarities and differences between human- and plant-associated pseudomonads related to *Pseudomonas fluorescens* and *P. putida*. Appl Environ Microbiol 2015;81:2579–90. doi:10.1128/AEM.04160-14.

[34] Anzai Y, Kim H, Park JY, Wakabayashi H, Oyaizu H. Phylogenetic affiliation of the pseudomonads based on 16S rRNA sequence. Int J Syst Evol Microbiol 2000;50 Pt 4:1563–89.

[35] Loper JE, Hassan KA, Mavrodi DV, Davis EW II, Lim CK, Shaffer BT, et al. Comparative genomics of plant-associated *Pseudomonas* spp.: Insights into diversity and inheritance of traits involved in multitrophic interactions. PLoS Genet 2012;8:e1002784. doi:10.1371/journal.pgen.1002784.

[36] Ghaffari A, Neil DH, Ardakani A, Road J, Ghahary A, Miller CC. A direct nitric oxide gas delivery system for bacterial and mammalian cell cultures. Nitric Oxide 2005;12:129–40. doi:10.1016/j.niox.2005.01.006.

[37] Bligh EG, Dyer WJ. A rapid method of total lipid extraction and purification. Biochem Cell Biol 1959;37:911–7. doi:10.1139/o59-099.

[38] Morrison WR, Smith LM. Preparation of fatty acid methyl esters and dimethylacetals from lipids with boron fluoride–methanol. J Lipid Res 1964;5:600–8.

[39] Heipieper HJ, Meulenbeld G, van Oirschot Q, de Bont J. Effect of environmental factors on the *trans/cis* ratio of unsaturated fatty acids in

Pseudomonas putida S12. Appl Environ Microbiol 1996;62:2773–7.

[40] Bellon-Fontaine M-N, Rault J, van Oss CJ. Microbial adhesion to solvents: a novel method to determine the electron-donor/electron-acceptor or Lewis acid-base properties of microbial cells. Colloids Surf B Biointerfaces 1996;7:47–53. doi:10.1016/0927-7765(96)01272-6.

[41] Mulet M, Lalucat J, García-Valdés E. DNA sequence-based analysis of the *Pseudomonas* species. Environ Microbiol 2010;12:1513–30. doi:10.1111/j.1462-2920.2010.02181.x.

[42] Yamamoto S, Kasai H, Arnold DL, Jackson RW, Vivian A, Harayama S. Phylogeny of the genus *Pseudomonas*: intrageneric structure reconstructed from the nucleotide sequences of *gyrB* and *rpoD* genes. Microbiology 2000;146:2385–94.

[43] Gidden J, Denson J, Liyanage R, Ivey DM, Lay JO. Lipid compositions in *Escherichia coli* and *Bacillus subtilis* during growth as determined by MALDI-TOF and TOF/TOF mass spectrometry. Int J Mass Spectrom 2009;283:178–84. doi:10.1016/j.ijms.2009.03.005.

[44] Geiger O, López-Lara IM, Sohlenkamp C. Phosphatidylcholine biosynthesis and function in bacteria. Biochim Biophys Acta 2013;1831:503–13. doi:10.1016/j.bbalip.2012.08.009.

[45] Wilderman PJ, Vasil AI, Martin WE, Murphy RC, Vasil ML. *Pseudomonas aeruginosa* synthesizes phosphatidylcholine by use of the phosphatidylcholine synthase pathway. J Bacteriol 2002;184:4792–9. doi:10.1128/JB.184.17.4792-4799.2002.

[46] Boeris PS, Lucchesi GI. The phosphatidylcholine synthase of *Pseudomonas putida* AATCC 12633 is responsible for the synthesis of phosphatidylcholine, which acts as a temporary reservoir for Al^{3+}. Microbiology 2012;158:1249–57. doi:10.1099/mic.0.054072-0.

[47] Martínez-Morales F, Schobert M, López-Lara IM, Geiger O. Pathways for phosphatidylcholine biosynthesis in bacteria. Microbiology 2003;149:3461–71. doi:10.1099/mic.0.26522-0.

[48] Gibellini F, Smith TK. The Kennedy pathway — *de novo* synthesis of phosphatidylethanolamine and phosphatidylcholine. IUBMB Life 2010;62:414–28. doi:10.1002/iub.337.

[49] Al-Saad KA, Siems WF, Hill HH, Zabrouskov V, Knowles NR. Structural analysis of phosphatidylcholines by post-source decay matrix-assisted laser desorption/ionization time-of-flight mass spectrometry. J Am Soc Mass Spectrom 2003;14:373–82. doi:10.1016/S1044-0305(03)00068-0.

[50] Al-Saad KA, Zabrouskov V, Siems WF, Knowles NR, Hannan RM, Hill HH. Matrix-assisted laser desorption/ionization time-of-flight mass spectrometry of lipids: ionization and prompt fragmentation patterns. Rapid Commun Mass Spectrom 2003;17:87–96. doi:10.1002/rcm.858.

[51] Hsu F-F, Turk J, Shi Y, Groisman EA. Characterization of acylphosphatidylglycerols from *Salmonella typhimurium* by tandem mass spectrometry with electrospray ionization. J Am Soc Mass Spectrom 2004;15:1–11. doi:10.1016/j.jasms.2003.08.006.

[52] Lopalco P, Angelini R, Lobasso S, Köcher S, Thompson M, Müller V, et al. Adjusting membrane lipids under salt stress: the case of the moderate halophilic organism *Halobacillus halophilus*. Environ Microbiol 2013;15:1078–87. doi:10.1111/j.1462-2920.2012.02870.x.

[53] Gill CO. Effect of growth temperature on the lipids of *Pseudomonas fluorescens*. J Gen Microbiol 1975;89:293–8. doi:10.1099/00221287-89-2-293.

[54] Rinella ME, Elias MS, Smolak RR, Fu T, Borensztajn J, Green RM. Mechanisms of hepatic steatosis in mice fed a lipogenic methionine choline-deficient diet. J Lipid Res 2008;49:1068–76. doi:10.1194/jlr.M800042-JLR200.

[55] Sanyal S, Menon AK. Flipping lipids: Why an' what's the reason for? ACS Chem Biol 2009;4:895–909. doi:10.1021/cb900163d.

[56] Murzyn K, Rog T, Pasenkiewicz-Gierula M. Phosphatidylethanolamine-phosphatidylglycerol bilayer as a model of the inner bacterial membrane. Biophys J 2005;88:1091–103. doi:10.1529/biophysj.104.048835.

[57] Mansilla MC, Cybulski LE, Albanesi D, Mendoza D de. Control of membrane lipid fluidity by molecular thermosensors. J Bacteriol 2004;186:6681–8. doi:10.1128/JB.186.20.6681-6688.2004.

[58] Signorelli S, Möller MN, Coitiño EL, Denicola A. Nitrogen dioxide solubility and permeation in lipid membranes. Arch Biochem Biophys 2011;512:190–6. doi:10.1016/j.abb.2011.06.003.

[59] Möller MN, Lancaster Jr. JR, Denicola A. Chapter 2 The interaction of reactive oxygen and nitrogen species with membranes. In: Matalon S, editor. Curr. Top. Membr., vol. 61, Academic Press; 2008, p. 23–42.

[60] Augusto O, Bonini MG, Amanso AM, Linares E, Santos CCX, De Menezes SL. Nitrogen dioxide and carbonate radical anion: two emerging radicals in biology. Free Radic Biol Med 2002;32:841–59. doi:10.1016/S0891-5849(02)00786-4.

of a phospholipase C in the hemolytic activity of a clinical strain of *Pseudomonas fluorescens*. BMC Microbiol 2008;8:189. doi:10.1186/1471-2180-8-189.

[21] Rokni-Zadeh H, Li W, Sanchez-Rodriguez A, Sinnaeve D, Rozenski J, Martins JC, et al. Genetic and functional characterization of cyclic lipopeptide white-line-inducing principle (WLIP) production by rice rhizosphere isolate *Pseudomonas putida* RW10S2. Appl Environ Microbiol 2012;78:4826–34. doi:10.1128/AEM.00335-12.

[22] Mandal SM, Sharma S, Pinnaka AK, Kumari A, Korpole S. Isolation and characterization of diverse antimicrobial lipopeptides produced by *Citrobacter* and *Enterobacter*. BMC Microbiol 2013;13:152. doi:10.1186/1471-2180-13-152.

[23] Heipieper HJ, Keweloh H, Rehm HJ. Influence of phenols on growth and membrane permeability of free and immobilized *Escherichia coli*. Appl Environ Microbiol 1991;57:1213–7.

[24] Signorelli S, Möller MN, Coitiño EL, Denicola A. Nitrogen dioxide solubility and permeation in lipid membranes. Arch Biochem Biophys 2011;512:190–6. doi:10.1016/j.abb.2011.06.003.

[25] Möller MN, Lancaster Jr. JR, Denicola A. Chapter 2 The interaction of reactive oxygen and nitrogen species with membranes. In: Matalon S, editor. Curr. Top. Membr., vol. 61, Academic Press; 2008, p. 23–42.

[26] Augusto O, Bonini MG, Amanso AM, Linares E, Santos CCX, De Menezes SL. Nitrogen dioxide and carbonate radical anion: two emerging radicals in biology. Free Radic Biol Med 2002;32:841–59. doi:10.1016/S0891-5849(02)00786-4.

Effect of temperature and NO_2 on membrane glycerophospholipids of clinical *Pseudomonas fluorescens* strain MFN1032

Tatiana Kondakova[a,d], Nadine Merlet Machour[b], Frédéric Dionnet[d], Marc Feuilloley[a], Nicole Orange[a], Hermann J. Heipieper[c], Cécile Duclairoir Poc[a1]

[a] *Laboratory of Microbiology Signals and Microenvironment (LMSM) EA4312, Normandy Univ., Univ. Rouen, 55 rue St Germain, 27000, Evreux, France.*
[b] *UMR 6014 COBRA, Normandy Univ., Univ. Rouen, 55 rue St Germain, 27000 Evreux, France.*
[c] *Department of Environmental Biotechnology, UFZ Helmholtz Centre for Environmental Research, Permoserstr. 15, 04318 Leipzig, Germany.*
[d] *Aerothermic and Internal Combustion Engine Technological Research Centre (CERTAM), 1 Rue Joseph Fourier, 76800 - Saint Etienne du Rouvray, France.*

In preparation

Abstract

Although the most widely studied role for members of *Pseudomonas fluorescens* group in the soil and the rhizosphere, these bacteria were identified in the indigenous microbiota of various body sites. Among other factors, this high distribution depends on membrane lipid composition. The aims of this work were to establish the lipidome composition of clinical *P. fluorescens* MFN1032 and to study its membrane response to human body temperature and air pollution toxicity.

The lipidome of MFN1032 was investigated using HPTLC-MALDI TOF MSI tool in exponential and stationary growth phase. Phosphatidylethanolamine, phophatidylglycerol and phosphatidylcholine were identified as its main compounds. In exponential growth phase, a newly identified glycerophospholipid was detected at 37°C, but not at 28°C, indicating its role in *P. fluorescens* temperature adaptation. The NO_2 was found to inhibit the synthesis of this new glycerophospholipid. The degree of saturation of bacterial fatty acids was found to be increased with rise of temperature, but was not modified after NO_2 exposure. The results of this study provide evidence of a glycerophospholipid role in adaptation of clinical *P. fluorescens* to human temperature and NO_2 air pollutant.

Keywords: Glycerophospholipids; Fatty acids; Clinical *Pseudomonas fluorescens*; Nitrogen dioxide; Temperature; Growth phase; Environment; Stress; Adaptation

1. Introduction

Pseudomonas fluorescens is not generally considered as a bacterial pathogen in humans. However, multiple studies have identified it at low levels in the indigenous microbiota of various body sites [1]. Being psychrotrophic bacteria with optimum of growth at 28°C, several *P. fluorescens* strains still grow at increasing temperature (37°C) [2]. This thermotolerance associated with virulence factors expression and biofilm formation allows *P. fluorescens* to tame

[1] Corresponding author.
E-mail addresses: tatiana.kondakova@etu.univ-rouen.fr (T. Kondakova), nadine.merlet@univ-rouen.fr (N. Merlet-Machour), hermann.heipieper@ufz.de (H.J. Heipieper), frederic.dionnet@certam-rouen.com (F. Dionnet), marc.feuilloley@univ-rouen.fr (M. Feuilloley), nicole.orange@univ-rouen.fr (N. Orange), cecile.poc@univ-rouen.fr (C. Duclairoir Poc).

eukaryotic hosts. While far less virulent than *P. aeruginosa*, *P. fluorescens* can promote acute infections in humans and was reported in clinical samples from the mouth, stomach and lungs of patients with compromised immune status [1,3]. However, the members of *P. fluorescens* group are present in large number of natural environments, including water [4], soil, rhizosphere [5,6], and air [7]. Physiologically, the high distribution of *P. fluorescens*, as well as its adaptation to environmental modifications, depends essentially on the structure and the organization of the envelope. Although a well-studied role of proteins in membrane protective functions [8], the glycerophospholipids (GPs) also play a major role in bacterial adaptation [9]. The structure and functions of GPs are dependent on their polar head groups (HGs) and fatty acid (FA) composition. The HGs play a role of barrier to prevent the entry of noxious compounds and the influx of nutrient molecules [11]. The FAs modifications control the membrane fluidity altered by several environmental modifications [12].

In this study, the effect of the human body temperature (37°C) and of the NO_2, as a marker of air pollution, on the membrane GPs of *P. fluorescens* MFN1032 were investigated. The GP composition of this strain was tested in exponential and stationary growth phases using HPTLC-MALDI TOF MSI tool. The understanding of lipid adaptation of psychrotrophic bacteria to human body temperature could offer the supplementary knowledge about infections caused by *P. fluorescens* and about potential antipseudomonal drug development. In order to study the effect of air pollution on the MFN1032 membrane, bacteria were exposed to NO_2 in gas phase to mimic the environmental conditions. Three NO_2 concentrations was tested in this study: 0.1 ppm as environmental standard; 5 ppm as the threshold, causing reversible effects on human health, and 45 ppm as a high NO_2 concentration, provoking irreversible effects, according World Health Organization. The comparison of the MFN1032 responses to increasing temperature and to NO_2 could provide a supplemental information about the membrane response of *P. fluorescens* to environmental modifications.

2. Materials and methods

2.1. Bacterial strain and growth conditions

MFN1032 was grown at 28°C or at 37°C under limited agitation (180 rpm) in Luria-Bertani medium (LB, AES, France) or DMB (Davis Medium Broth) minimal medium with glucose as carbon source (2.16 g/L).

For study of increasing temperature effect on lipid composition, bacterial aliquots were collected in triplicate at the middle of the exponential growth phase ($4.5x10^8$ CFU/mL) or in the early stationary phase ($9x10^8$ CFU/mL). After removal of supernatant and three successive rinses with sterile saline solution, bacteria were centrifuged at 4°C (13,000xg). Aliquots were resuspended in deionized water and lyophilized using a Freeze Dryer Heto PowerDry PL9000-50/ HSC500 (Thermo Fisher Scientific, Saint-Herblain, France).

For study of the NO_2 effect on bacterial membrane, overnight cultures were diluted (A_{580}=0.08) in fresh DMB and grown to the end of exponential growth phase A_{580}=2 ($13x10^8$

CFU/mL). Then, bacterial culture (about $3x10^7$ bacteria per filter) was transferred on cellulose nitrate membrane filters (pore size 0.2 µm, diameter 47 mm, Sartorius Biolab Products, Gottingen, Germany) and grown on DMB agar plates at 28°C for 4 h to obtain the single layer's bacterial population. After 4 h of incubation, the cellulose membranes, containing bacteria, were placed on agar 1 well dishes (size 127.8 x 85.5 mm, Thermo Scientific Nunc, Roshester, USA) and directly transferred into the gas delivery device (Figure S1).

2.2. Exposition to nitrogen dioxide

In order to restore the atmospheric conditions, bacterial NO_2 exposure was done in gas phase for 2 h, according [13]. The delivery device consisted of two sterile cylindrical Plexiglas exposure chambers (one for the NO_2 exposure, the second one for the control simple - exposure to the synthetic air), deposed in drying oven at 28°C (Figure S1). The NO_2, N_2, and O_2 obtained from Air Liquide GMP Europe (Mitry-Mory, France) were mixed together using digital mass flow regulators (Alicat Scientific, Inc., Tucson, USA) in order to obtain pre-calculated concentrations of NO_2 and to maintain the O_2/N_2 ratio at 8/2, (v/v). The obtained gas mixture and synthetic air (Air Liquide GMP Europe, Mitry-Mory, France) were routed independently to each of the exposure chambers at a constant flow rate of 2 L/min. The parallel NO_2/synthetic air circuits allow utilization of the same bacterial culture for exposed to NO_2 and control samples. After passing through exposure chamber, the NO_2 concentrations were monitored by AC32M nitrogen oxides analyzer (Environnement S.A, Poissy, France). After this, the gas mixture was safely vented to a chemical hood. Chamber temperature and relative humidity data were monitored to control reliable steady-state environmental conditions inside the exposure chambers. Three concentrations of NO_2 were used in this study: 0.1 ppm; 5 ppm and 45 ppm. After exposure, bacteria were resuspended to A_{580}=2 in sterile saline solution. After removal of supernatant and three successive rinses with sterile saline solution, bacteria were centrifuged at 4°C (13,000xg). Aliquots were resuspended in deionized water and lyophilized using a Freeze Dryer Heto PowerDry PL9000-50/ HSC500 (Thermo Fisher Scientific, Saint-Herblain, France).

2.3. Chemicals

GPs standards, MALDI matrix (2,5-dihydroxybenzoic acid; DHB) and solvents (chloroform, methanol, ethanol, trimethylamine, acetonitrile and hexane) were obtained from Sigma-Aldrich (Saint-Quentin-Fallavier, France). All chemicals were of the highest commercially available purity and used without any further purification. HPTLC silica gel 60 plates F_{254} (75 x 50 mm in size, on aluminum backs) were obtained from Merck (Darmstadt, Germany).

2.4. HPTLC-MALDI TOF MSI analysis of glycerophospholipids

The analysis of bacterial GPs was performed as previously described by [14]. All experiments were performed in at least three replicates corresponding to three independent bacterial cultures.

2.5. *Fatty acids analysis*

Fatty acid methyl esters were prepared by incubation for 15 min at 95°C in a boron trifluoride (BF_3)/methanol (140 g BF_3 per liter of methanol) and extracted with hexane as described by Morrison and Smith [15]. Fatty acid methyl esters were separated and analyzed by gas chromatography (GC) coupled to flame ionization detection using an Agilent Technology, 6890 Network GC System, 7683 Series Injector equipped with a split/splitless injector. The apparatus was equipped with a CP-Sil 88 capillary column (Chrompack, Middelburg, the Netherlands; length, 50m; inner diameter, 0.25 mm; 0.25 mm film). Fatty acids were identified by coinjection as internal standards of reference compounds obtained from Supelco (Bellefonte, Pennsylvania, USA) and were quantified on the basis of their peak areas in total ion chromatograms. All experiments were performed in triplicate. The degree of fatty acid saturation was determined as the ratio between the saturated fatty acids and the unsaturated fatty acids [16].

2.6. *Statistical analysis*

All experiments were carried out at least three times. Significances of differences between mean values were assessed using Mann-Whitney test with significance set at $p < 0.05$ (*), < 0.01 (**) and < 0.001 (***).

3. Results

3.1. Effect of increasing temperature on glycerophospholipid of clinical Pseudomonas fluorescens MFN1032

The study of bacterial lipidome was realised using an HPTLC-MALDI TOF MSI tool according [14]. Bacteria were cultivated at 28°C (optimal temperature) and at 37°C (human body temperature). Total GPs and FAs were extracted in the mid-exponential growth phase (EGP) and in the early stationary growth phase (SGP) in order to (i) study the MFN1032 lipidome all along bacterial growth and (ii) establish the GP adaptation of phychrotrophic *P. fluorescens* to human temperature.

Results of MSI analyses of the total MFN1032 lipidome are presented in Fig. 1A. In all experiments, three GP spots (with R_f 0.24±0.01-*red color*; 0.43±0.02-*blue color* and 0.62±0.03-*yellow color*) were detected. These GPs were identified in our previous study of *P. fluorescens* lipidome [14] as phosphatidylcholine (PC), phosphatidylethanolamine (PE) and phosphatidylglycerol (PG) respectively (Fig. 1A, Table 1). A fourth spot with R_f 0.26±0.02 was detected (Fig. 1A, *green color*). This GP was not completely identified yet (named UGP from unknown glycerophospholipid), but have been detected and characterized in our previous studies of airborne *P. fluorescens* lipidome (*unpublished data*), indicating the conservation of UGP among *P. fluorescens* strains. Surprisingly, another compound (Figure 1A, R_f = 0.46±0.03, *maroon color*), with high for a GP m/z 1147.5, was found in all experimental conditions. Its PSD analyses *(data not shown)* did not correspond to the mechanism of GP fragmentation and were similar to the sodiated form of a lipoprotein. The MS and PSD spectra, confirmed by LC MS analysis, allow its identification as a cyclic lipoprotein viscosinamide (V).

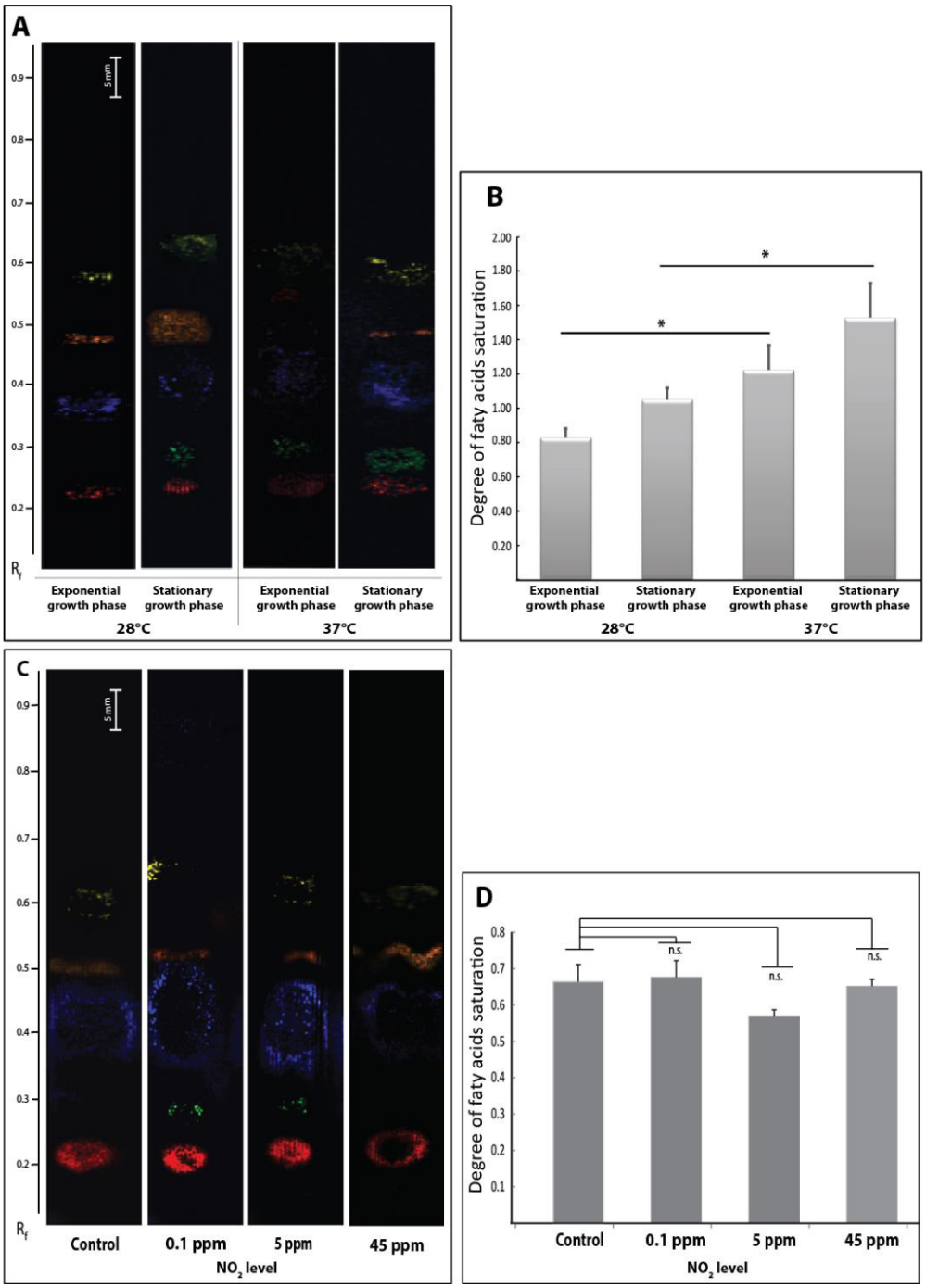

Figure 1. Effect of increasing temperature and NO_2 on membrane glycerophospholipids of clinical *P. fluorescens*

A. Effect of increasing temperature on glycerophospholipid composition. Glycerophospholipid composition of *P. fluorescens* MFN1032 was analyzed using HPTLC-MALDI TOF MSI tool. Bacterial lipid extract (100 µL) was developed in triplicate on HPTLC plates. MALDI TOF MS, PSD and MSI analyses of glycerophospholipid spots were performed directly on HPTLC plate in positive MALDI mode with DHB as MALDI matrix. MSI experiments were performed using FlexImaging software. Glycerophospholipid distribution was analyzed according to their m/z, previously found using TLC-MALDI software and confirmed by PSD analysis. Individual glycerophospholipid classes were labeled by a specific color code. Glycerophospholipids and retention factors (R_f): phosphatidylcholine (PC) - 0.24±0.01 (*red*); unknown glycerophospholipid (UGP) - 0.26±0.02 (*green*); phosphatidylethanolamine (PE) - 0.43±0.02 (*blue*); phosphatidylglycerol (PG) - 0.62±0.03 (*yellow*). Viscosinamide (V) has the R_f = 0.46±0.03, and was labeled by *maroon color*. **B. Effect of increasing temperature on fatty acid composition.** Bacterial fatty acids were analyzed and quantified using GC from at least three independent lipid extracts. The degree of fatty acid saturation was determined as the ratio between saturated and unsaturated fatty acids, and presented as average value ± SEM. Statistical significance was calculated by the non-parametric Mann-Whitney-Test. *P < 0.05; n.s. non-significant. **C. and D. Effect of NO_2 on membrane glycerophospholipids of clinical *P. fluorescens*.** Bacteria were exposed to NO_2 in three concentrations: 0.1 ppm; 5 ppm and 45 ppm. After exposure, effect of NO_2 on glycerophospholipids (**C**) and on fatty acids (**D**) was examined. Glycerophospholipid composition of exposed to NO_2 *P. fluorescens* MFN1032 was tested using HPTLC-MALDI TOF MSI tool and compared to control, exposed to synthetic air.

Table 1. Effect of increasing temperature and NO_2 on glycerophospholipid inventory in clinical *P. fluorescens* MFN1032

Glycerophospholipid identification[a]						Temperature, °C / growth phase				NO_2 level, ppm			
						28°C		37°C					
Retention factor	GP[b] class	Species	Molar mass (M), g/mol	m/z	Assignement	EGP[c]	SGP[d]	EGP	SGP	0	0.1	5	45
0.24±0.01	**PC[e]**	PC [16:0 + 16:1]	731.5	732.6	$[PC_1+H]^+$	■	■	■	■	■	■	■	■
		PC [16:0 + 16:1]	731.5	754.5	$[PC_1+Na]^+$	■	■		■	■	■	■	■
		PC [16:0 + 18:1]	759.6	782.6	$[PC_2+Na]^+$		■	■	■	■			
0.26±0.02	**UGP[f]**	UGP [16:0 + 17:0]	904.5	927.5	$[UGP_1+Na]^+$		■	■	■	■	■	■	
		UGP [16:0 + 18:0]	918.5	941.5	$[UGP_2+Na]^+$		■	■	■	■		■	
		UGP [17:1 + 18:0]	930.5	953.5	$[UGP_3+Na]^+$		■	■	■			■	
0.43±0.02	**PE[g]**	PE [16:0 + 16:1]	689.5	712.5	$[PE_1+Na]^+$	■	■	■	■	■	■	■	■
				734.5	$[PE_1+2Na-H]^+$	■	■	■	■	■	■	■	■
		PE [16:0 + 17:1]	703.5	726.5	$[PE_2+Na]^+$	■	■		■	■	■	■	■
				748.5	$[PE_2+2Na-H]^+$		■	■	■			■	■
		PE [16:0 + 18:1]	715.5	738.5	$[PE_3+Na]^+$		■		■		■	■	■
				760.5	$[PE_3+2Na-H]^+$		■	■	■	■	■	■	■
0.62±0.03	**PG[h]**	PG [16:0 + 16:1]	720.5	743.5	$[PG_1+Na]^+$	■	■	■	■	■	■	■	
				765.5	$[PG_1+2Na-H]^+$	■	■	■	■	■	■	■	
		PG [16:0 + 18:1]	746.5	769.5	$[PG_2+Na]^+$		■		■	■	■		■
				791.6	$[PG_2+2Na-H]^+$		■		■	■	■		■

[a]The lipid identification was performed on the basis of MS and PSD analyses using LIPID MAPS database and the analysis of lipid standard. The presence of assigned m/z in lipid extrac triplicate is shown by grey squares. The colorless squares show the absence of assigned m/z in lipid extract. The lipid extractions, MS and PSD analysis in all studied conditions were perfor in three replicates. [b]**GP**: glycerophospholipid; [c]**EGP**: exponential growth phase; [d]**SGP**: stationary growth phase; [e]**PC**: phosphatidylcholine; [f]**UGP**: unknown glycerophospholipid; [g] phosphatidylethanolamine; [h]**PG**: phosphatidylglycerol.

In SGP, any modification in the GP composition of clinical MFN1032 grown at 37°C was not found when compared to 28°C: all previously discussed GP classes were observed (Fig. 1A and Table 1). However, in EGP, the UGP was detected at 37°C, but was not detected at 28°C, indicating that this GP could be used by MFN1032 to adapt to human temperature. Analyses of the FAs reveal a slight increase of the degree of FA saturation at 37°C comparing to 28°C (Fig. 1B).

3.2. Effect of NO_2 on the glycerophospholipids of the clinical Pseudomonas fluorescens *MFN1032*

P. fluorescens MFN1032 was exposed to NO_2 in three concentrations: 0.1 ppm, 5 ppm and 45 ppm, and the extracted GPs and FAs were analysed as described above. The results of this study are presented in Fig. 1C/D and Table 1. The GP composition of NO_2-treated MFN1032 was comparable to that of control, exposed to synthetic air (Fig. 1C, Table 1). The PC, PE and PG were found in all experimental conditions. In contrast, the UGP was not detected in bacteria, exposed to 45 ppm of NO_2, indicating that this GP is affected by NO_2. Interestingly, any significant modification in the degree of FA saturation was not detected in the exposed to NO_2 MFN1032 comparing to control (Fig. 1D), indicating the difference between the effect of increasing temperature and effect of NO_2 on the MFN1032 membrane.

3. Discussion

In this study, the membrane response of the clinical *P. fluorescens* MFN1032 to the human body temperature and the toxicity of NO_2, as marker of air pollution was studied. The MFN1032 was cultivated at 28°C and 37°C and/or exposed to NO_2 in gas phase in order to mimic the atmospheric conditions.

In order to establish the GP composition of this clinical *P. fluorescens* strain, the analyses of GPs and FAs were performed in EGP and SGP. Thus, PE, PG and PC were identified as major GPs of MFN1032 (Fig. 1A). This results are in accord with our previous studies of *P. fluorescens* lipidome [14] and with literature [17,18]. Together with the GPs, a cyclic lipopeptide viscosinamide was detected (Fig. 1A). Cyclic lipopeptides are composed of a fatty acid chain linked to a short oligopeptide, which is cyclized to form a lactone ring between two amino acids in the peptide chain [19]. Although the production of viscosinamide by MFN1032 is already observed [20], for the first time a peptide molecule was detected in study of bacterial lipids. Since the cyclic lipopeptides are composed of peptide and the lipid moieties, they are soluble and extractable in methanol [21,22], which is a major compound of extraction solution used in our study. However, this work is focused on GPs analysis, so the production of viscosinamide and its role(s) in *P. fluorescens* MFN1032 membrane adaptation will not be discussed below.

Another, and, unfortunately, non-identified GP was found (UGP) was found in lipidome of MFN1032. At 28°C, the UGP seems to be synthetized only in SGP. In contrast, at 37°C, the UGP was detected in both EGP and SGP. These data let us speculate, that the UGP is more quickly synthetized at 37°C that at 28°C and could be involved in *P. fluorescens* temperature adaptation. However, the complete identification of the UGP

and the establishment of metabolic pathway(s) for its production are necessary to understand its role in *P. fluorescens* metabolism and homeostasis. In response to human body temperature, the membrane of MFN1032 becomes more fluid, than at 28°C, which alters the membrane functions. To decrease the membrane fluidity, MFN1032, like other members of *Pseudomonas* genus [12,23], increases the degree of FA saturation, producing more of saturated FAs.

The effect of NO_2 on the membrane of MFN1032 was quite different than this one of temperature. After NO_2 exposure, any modification in the degree of FA saturation was not detected, indicating that the NO_2 does not change bacterial membrane fluidity and could freely penetrate bacterial membrane. These data are supported by our previous studies of the lipidome of airborne *P. fluorescens* (*unpublished data*) and a computational model developed by Signorelli et al. [24], demonstrating that the lipid membrane is not significant barrier to the NO_2 transport. In contrast, in MFN1032 treated with NO_2 in high concentration, the UGP was not detected. Although incomplete identification of this molecule, we propose that this GP could be 'sensitive' to NO_2. Despite the NO_2 can freely pass across the bacterial membrane, the latter could be chemically modified in the transport process. The nitrogen reactive species were found to cause oxidation and/or nitration of GPs [25], leading to the formation of lipid hydroperoxides, lipid alcohols, and aldehydes [26]. However, the addition of -OOH (33 Da) or -NO_2 (44 Da) to GP masses was not found in our study, indicating that NO_2 does not react with the membrane GPs of MFN1032 in tested conditions. These data are in accord with our previous study of NO_2 effect on *P. fluorescens* lipidome (*unpublished data*), supporting the fact that the NO_2 can react only with the polyunsaturated FA chains, which were not found to be produced by *P. fluorescens* [14].

In conclusion, this study reveals a potential role of the UGP in adaptation of clinical *P. fluorescens* MFN1032 to human temperature and the sensitivity of this GP to the NO_2. These data, completed by identification of chemical structure of UGP and its metabolic pathway(s) should help to understand the membrane aspects of high adaptation capacity of *P. fluorescens* and could be potentially explored to develop antipseudomonal treatment.

Conflict of interest

All authors declare that they have no competing interests.

Acknowledgements

We are grateful to Anne Groboillot for help with development of gas delivery system. We thank Magalie Barreau and Olivier Maillot for technical assistance. This study was supported by a PhD grant from the GRR SESA (Reserch Network of Sanitary Safety) and was financially supported by Regional Council of Haute-Normandie, the Conseil Général de l'Eure and the Grand Evreux Agglomeration (France). Fatty acids analysis was financially supported by grants from the German Academic Exchange Service (DAAD), the Doctoral Normandy's Graduate School of Integrative Biology, Health and Environment's, University of Rouen and the Regional Council of Haute-Normandie, France.

Supplementary data

Supplementary data related to this article can be found in Annexes.

References

[1] Scales BS, Dickson RP, LiPuma JJ, Huffnagle GB. Microbiology, genomics, and clinical significance of the *Pseudomonas fluorescens* species complex, an unappreciated colonizer of humans. Clin Microbiol Rev 2014;27:927–48. doi:10.1128/CMR.00044-14.

[2] Picot L, Mezghani-Abdelmoula S, Chevalier S, Merieau A, Lesouhaitier O, Guerillon J, et al. Regulation of the cytotoxic effects of *Pseudomonas fluorescens* by growth temperature. Res Microbiol 2004;155:39–46. doi:10.1016/j.resmic.2003.09.014.

[3] Chapalain A, Rossignol G, Lesouhaitier O, Merieau A, Gruffaz C, Guerillon J, et al. Comparative study of 7 fluorescent pseudomonad clinical isolates. Can J Microbiol 2008;54:19–27. doi:10.1139/w07-110.

[4] Rajmohan S, Dodd CER, Waites WM. Enzymes from isolates of *Pseudomonas fluorescens* involved in food spoilage. J Appl Microbiol 2002;93:205–13. doi:10.1046/j.1365-2672.2002.01674.x.

[5] Couillerot O, Prigent-Combaret C, Caballero-Mellado J, Moënne-Loccoz Y. *Pseudomonas fluorescens* and closely-related fluorescent pseudomonads as biocontrol agents of soil-borne phytopathogens. Lett Appl Microbiol 2009;48:505–12. doi:10.1111/j.1472-765X.2009.02566.x.

[6] Kiely PD, Haynes JM, Higgins CH, Franks A, Mark GL, Morrissey JP, et al. Exploiting new systems-based strategies to elucidate plant-bacterial interactions in the rhizosphere. Microb Ecol 2006;51:257–66. doi:10.1007/s00248-006-9019-y.

[7] Morin J-P, Preterre D, Gouriou F, Delmas V, François A, Orange N, et al. Particules urbaines et céréalières, micro-organismes, mycotoxines et pesticides. Pollution Atmospherique 2013.

[8] Poole K. Bacterial stress responses as determinants of antimicrobial resistance. J Antimicrob Chemother 2012:dks196. doi:10.1093/jac/dks196.

[9] Kondakova T, D'Heygère F, Feuilloley MJ, Orange N, Heipieper HJ, Duclairoir Poc C. Glycerophospholipid synthesis and functions in *Pseudomonas*. Chem Phys Lipids 2015;190:27–42. doi:10.1016/j.chemphyslip.2015.06.006.

[10] Zhang Y-M, Rock CO. Membrane lipid homeostasis in bacteria. Nat Rev Microbiol 2008;6:222–33. doi:10.1038/nrmicro1839.

[11] Nikaido H. Molecular basis of bacterial outer membrane permeability revisited. Microbiol Mol Biol Rev 2003;67:593–656. doi:10.1128/MMBR.67.4.593-656.2003.

[12] Pepi M, Heipieper HJ, Fischer J, Ruta M, Volterrani M, Focardi SE. Membrane fatty acids adaptive profile in the simultaneous presence of arsenic and toluene in *Bacillus* sp. ORAs2 and *Pseudomonas* sp. ORAs5 strains. Extrem Life Extreme Cond 2008;12:343–9. doi:10.1007/s00792-008-0147-9.

[13] Ghaffari A, Neil DH, Ardakani A, Road J, Ghahary A, Miller CC. A direct nitric oxide gas delivery system for bacterial and mammalian cell cultures. Nitric Oxide 2005;12:129–40. doi:10.1016/j.niox.2005.01.006.

[14] Kondakova T, Merlet-Machour N, Chapelle M, Preterre D, Dionnet F, Feuilloley M, et al. A new study of the bacterial lipidome: HPTLC-MALDI-TOF imaging enlightening the presence of phosphatidylcholine in airborne *Pseudomonas fluorescens* MFAF76a. Res Microbiol 2014. doi:10.1016/j.resmic.2014.11.003.

[15] Morrison WR, Smith LM. Preparation of fatty acid methyl esters and dimethylacetals from lipids with boron fluoride–methanol. J Lipid Res 1964;5:600–8.

[16] Heipieper HJ, Meulenbeld G, van Oirschot Q, de Bont J. Effect of environmental factors on the *trans/cis* ratio of unsaturated fatty acids in *Pseudomonas putida* S12. Appl Environ Microbiol 1996;62:2773–7.

[17] Gill CO. Effect of growth temperature on the lipids of *Pseudomonas fluorescens*. J Gen Microbiol 1975;89:293–8. doi:10.1099/00221287-89-2-293.

[18] Fouchard S, Abdellaoui-Maâne Z, Boulanger A, Llopiz P, Neunlist S. Influence of growth conditions on *Pseudomonas fluorescens* strains: A link between metabolite production and the PLFA profile. FEMS Microbiol Lett 2005;251:211–8. doi:10.1016/j.femsle.2005.08.003.

[19] Raaijmakers JM, de Bruijn I, de Kock MJD. Cyclic lipopeptide production by plant-associated *Pseudomonas* spp.: diversity, activity, biosynthesis, and regulation. Mol Plant-Microbe Interact MPMI 2006;19:699–710. doi:10.1094/MPMI-19-0699.

[20] Rossignol G, Merieau A, Guerillon J, Veron W, Lesouhaitier O, Feuilloley MG, et al. Involvement

of a phospholipase C in the hemolytic activity of a clinical strain of *Pseudomonas fluorescens*. BMC Microbiol 2008;8:189. doi:10.1186/1471-2180-8-189.

[21] Rokni-Zadeh H, Li W, Sanchez-Rodriguez A, Sinnaeve D, Rozenski J, Martins JC, et al. Genetic and functional characterization of cyclic lipopeptide white-line-inducing principle (WLIP) production by rice rhizosphere isolate *Pseudomonas putida* RW10S2. Appl Environ Microbiol 2012;78:4826–34. doi:10.1128/AEM.00335-12.

[22] Mandal SM, Sharma S, Pinnaka AK, Kumari A, Korpole S. Isolation and characterization of diverse antimicrobial lipopeptides produced by *Citrobacter* and *Enterobacter*. BMC Microbiol 2013;13:152. doi:10.1186/1471-2180-13-152.

[23] Heipieper HJ, Keweloh H, Rehm HJ. Influence of phenols on growth and membrane permeability of free and immobilized *Escherichia coli*. Appl Environ Microbiol 1991;57:1213–7.

[24] Signorelli S, Möller MN, Coitiño EL, Denicola A. Nitrogen dioxide solubility and permeation in lipid membranes. Arch Biochem Biophys 2011;512:190–6. doi:10.1016/j.abb.2011.06.003.

[25] Möller MN, Lancaster Jr. JR, Denicola A. Chapter 2 The interaction of reactive oxygen and nitrogen species with membranes. In: Matalon S, editor. Curr. Top. Membr., vol. 61, Academic Press; 2008, p. 23–42.

[26] Augusto O, Bonini MG, Amanso AM, Linares E, Santos CCX, De Menezes SL. Nitrogen dioxide and carbonate radical anion: two emerging radicals in biology. Free Radic Biol Med 2002;32:841–59. doi:10.1016/S0891-5849(02)00786-4.

Highlight

- The members of *P. fluorescens* group are highly adaptable and ubiquitously distributed bacteria. Physiologically, these properties could be related with membrane lipid changes, as the first barrier between bacterial cell and its environment.
- The lipidome of clinical *P. fluorescens* strain MFN1032 includes the phosphatidylcholine, phosphatidylethanolamine and phosphatidylglycerol, as major glycerophospholipid compounds produced in exponential and stationary growth phases.
- In stationary growth phase, a new glycerophospholipid (UGP) is found in both *P. fluorescens* strains. Its identification is not completed yet, but it is clear, that this molecule has a PSD fragmentation mechanism characteristic for a glycerophospholipid. Interestingly, in airborne MFAF76a, this molecule is found only in stationary growth phase, contrary to clinical strain MFN1032, which seems to product the UGP in exponential growth phase at 37°C, but not at 28°C, indicating the potential role of this membrane compound in increasing temperature adaptation of clinical strain.
- The supra-optimal temperature modifies the membrane fluidity that is compensated by increasing of degree of fatty acid saturation in both tested *P. fluorescens* strains.
- Both *P. fluorescens* strains do not increase the degree of fatty acid saturation after exposure to NO_2. Thus, NO_2 does not alter membrane fluidity, can freely cross bacterial membrane and penetrates in bacterial cytoplasm.
- No modification in membrane properties of *P. fluorescens* exposed to hourly NO_2 standard, or industrial limit is found.
- In both studied bacteria exposed to high NO_2 concentration, the new UGP is not found, indicating the sensitivity of this glycerophospholipid to NO_2.
- The exposure to high NO_2 concentration does not change the surface charge of airborne MFAF76a, but decreases its electron-accepting character. The latter modifications could be caused by the decreasing (if not complete loss) of UGP, but also by the increasing level of phosphatidylcholine comparing to the phosphatidylethanolamine.

Chapter 6 *Pseudomonas fluorescens* response to NO_2 toxicity

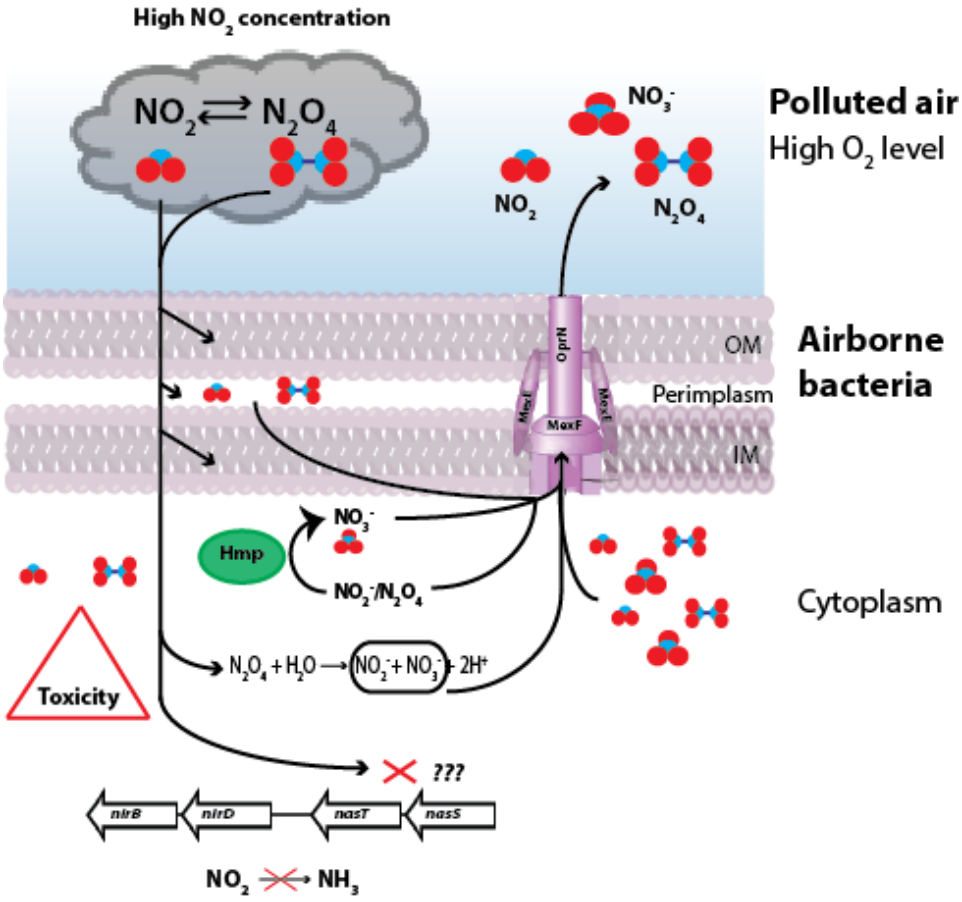

P. fluorescens airborne strain MFAF76a and clinical strain MFN1032 response to NO_2 stress

Tatiana Kondakova, Chloé Catovic, Magalie Barreau, Michael Nusser, Gerald Brenner-Weiss, Sylvie Chevalier, Frédéric Dionnet, Nicole Orange, Cécile Duclairoir Poc

Submitted in Frontiers in Microbiology

Research Topic Atmospheric Microbiology

Framework

After the establishment of *P. fluorescens* membrane response to NO_2 contamination, we were interested by the question "what happens when NO_2 penetrate in bacterial cytoplasm?" Given the high adaptability of *P. fluorescens* to various environmental conditions, these bacteria have to develop the pathway(s) for NO_2 detoxification. In addition, NO_2 may change genetic and/or phenotypic expression, including surface adhesion or motility. Given the lack of information about bacteria – NO_2 interactions, this study was based on the hypothesis of the similarity of bacterial response to NO_2 and, its homolog, NO. Thus, as previously described, two *P. fluorescens* strains, airborne MFAF76a and clinical MFN1032 were exposed to three NO_2 concentrations, in order to (i) establish concentration-dependent response of both *P. fluorescens* to NO_2 and (ii) to test the bacterial adaptation mode to NO_2 thresholds. As results, this study establishes the pathways, employed by both *P. fluorescens* to detoxify and release NO_2 from cytoplasm, as well as the modifications in bacterial biofilm formation and antibiotic resistance, caused by NO_2 exposure.

frontiers in MICROBIOLOGY

ORIGINAL RESEARCH ARTICLE
In preparation for submission

P. fluorescens airborne strain MFAF76a and clinical strain MFN1032 response to NO_2 stress

Tatiana Kondakova[1,3], Chloé Catovic[1], Magalie Barreau[1], Michael Nusser[2], Gerald Brenner-Weiss[2], Sylvie Chevalier[1], Frédéric Dionnet[3], Nicole Orange[1], Cécile Duclairoir Poc[1*]

[1] Laboratory of Microbiology Signals and Microenvironment (LMSM) EA4312, Normandy Univ., Univ. Rouen, 55 rue St Germain, 27000, Evreux, France.
[2] Karlsruhe Institute of Technology, Institute of Functional Interfaces, 76021 Karlsruhe, Germany.
[3] Aerothermic and Internal Combustion Engine Technological Research Centre (CERTAM), 1 Rue Joseph Fourier, 76800 - Saint Etienne du Rouvray, France.

*** *Correspondence*:**

Dr Cécile Duclairoir Poc
Laboratory of Microbiology Signals and Microenvironment (LMSM) EA 4312
Normandy University, University of Rouen
55 rue Saint Germain
27000 Evreux, France
Phone +33(0)232291549;
Fax: +33(0)232291550;
E-mail: cecile.poc@univ-rouen.fr

Human exposure to nitrogen dioxide (NO_2), an air pollutant of increasing interest in biology, results in several toxic effects to human health and also to the air microbiota. The aim of this study was to investigate the bacterial response to gaseous NO_2. Two *P. fluorescens* strains, namely the airborne strain MFAF76a and the clinical strain MFN1032, were exposed to 0.1, 5 or 45 ppm concentrations of NO_2, and their effects on bacteria were evaluated in terms of motility, biofilm formation, antibiotic resistance, as well as expression of several chosen target genes. While 0.1 and 5 ppm of NO_2 did not lead to any detectable modification in studied phenotypes of both two bacteria, several alterations were observed when the bacteria were exposed to 45 ppm of gaseous NO_2. We thus choose to focus on this high concentration. NO_2-exposed *P. fluorescens* strains showed reduced swimming motility, and decreased swarming in case of the strain MFN1032. Biofilm formed by NO_2-treated airborne strain MFAF76a showed increased maximum thickness compared to non-treated cells, while NO_2 had no apparent effect on the clinical MFN1032 biofilm structure. It is well known that biofilm and motility are inversely regulated by intracellular c-di-GMP level. The c-di-GMP level was however not affected in response to NO_2 treatment. Finally, NO_2-exposed *P. fluorescens* strains were found to be more resistant to ciprofloxacin and chloramphenicol. Accordingly, the resistance nodulation cell division (RND) MexEF-OprN efflux pump encoding genes were highly upregulated in the two *P. fluorescens* strains. Noticeably, similar phenotypes had been previously observed following a NO treatment. Interestingly, expression of the *hmp*-homologue gene in *P. fluorescens* strains MFAF76a and MFN1032, which encodes a NO dioxygenase that is involved in NO detoxification into nitrites, was upregulated in response to NO_2, suggesting a possible common pathway between NO and NO_2 detoxification. Taken together, our study provides evidences for the bacterial response to NO_2 toxicity.

Keywords: airborne, *Pseudomonas fluorescens*, nitrogen dioxide, biofilm, antibiotic sensitivity, motility, air pollution

Introduction

Most cities world-wide have serious air-quality problems, which have attracted attention in the past decade. One of the most common sources of air pollution is engine emission, which includes, among other toxic molecules, the nitrogen oxides (NO_x) (*reviewed in* Sher, 1998; Skalska et al., 2010). The general term nitrogen oxides (NO_x) includes nitric oxide (NO) and nitrogen dioxide (NO_2). According to the World Health Organization (WHO), NO contributes to global atmospheric pollution, but also plays a role as signaling molecule, responsible for a variety of physiological functions ranking from neurotransmission, relaxation of vascular endothelium, and toxicity to tumor and pathogen cells (Fang and Vazquez-Torres, 2002; Marletta, 1989). In consequence, the properties of NO in bacterial cells were well described (Giardina et al., 2008; Spiro, 2007). The NO can damage bacterial proteins (Laver et al., 2013; McLean et al., 2010) and DNA (Burney et al., 1999; Tamir et al., 1996)

either directly, or via formation of reactive nitrogen species (RNS), causing alterations in bacterial metabolism and homeostasis. As a result, bacteria have developed specific NO detoxification pathways and defense mechanisms (Cruz-Ramos et al., 2002; Flatley et al., 2005; Spiro, 2007). In order to counteract the NO-mediated respiratory arrest (Husain et al., 2008), the detoxification processes are completed in several bacteria by reprogramming of metabolism (Auger et al., 2011; Auger and Appanna, 2015). NO was described as a signaling molecule, which promotes the biofilm dispersion in a range of bacterial strains, including *P. aeruginosa* (Barraud et al., 2009; Cutruzzola and Frankenberg-Dinkel, 2015) and *P. putida* (Liu et al., 2012). This molecule is also known to modulate bacterial antibiotic sensitivity, protecting bacteria from a wide range of antibacterial agents (Gusarov et al., 2009; McCollister et al., 2011; van Sorge et al., 2013).

In natural environment, at high atmospheric O_2 level and light, NO is unstable and quickly oxidized to form NO_2 (Skalska et al., 2010). The latter is also a free radical, recognized as an air pollutant and finely studied by environmental chemists (Augusto et al., 2002; Gao et al., 1991; Skalska et al., 2010). However, NO_2 has a low solubility in water (Augusto et al., 2002), a property that has limited its studies in aqueous solutions. The NO_2 toxicity to human health is confirmed by several studies. This molecule was found to increase cardiovascular diseases (Chaloulakou et al., 2008), and to aggravate respiratory symptoms in the presence of coexistent infection (Chauhan et al., 1998). Thus, European environmental commission together with WHO established the NO_2 toxic thresholds and, as a consequence, recommended standards for NO_2 emission (INERIS, 2011; Reduction of pollutant emissions from light vehicles, 2015, WHO | Ambient (outdoor) air quality and health, 2015).

It is increasingly evident, that the air is a biotic environment, containing bacteria as one of the major compounds of primary atmosphere aerosol particles (Burrows et al., 2009b; Després et al., 2012). Mean bacterial concentrations in ambient air can indeed be greater than 1×10^4 cells m^{-3} (Bauer et al., 2002; Burrows et al., 2009a). Although unstable composition of air microbiota (Després et al., 2012), the members of *Pseudomonas* genus were frequently found among airborne bacterial population (Dybwad et al., 2012; Fang et al., 2007; Pearce et al., 2010; Šantl-Temkiv et al., 2015). The *Pseudomonas* genus includes highly versatile environmental bacteria, among which the *P. fluorescens* strains are described as highly distributed and adaptable (Bodilis et al., 2004). The latter are found in all major natural environments, including water (Bodilis et al., 2004), soil (Varivarn et al., 2013) and air (Ahern et al., 2007). Several *P. fluorescens* strains were found to promote acute infections in humans and were reported in clinical samples of patients with compromised immune status (Chapalain et al., 2008; Scales et al., 2014). All these properties make *P. fluorescens* a good model for further investigations of airborne bacteria.

In previous studies, the atmosphere aerosol particles that were isolated from harbor terminal in Rouen (France), were investigated in terms of size, number and mass distribution; the content of pesticides and mycotoxins, as well as the microbiological composition (bacteria, yeasts and

fungi) were established (Morin et al., 2013). Thus, several *P. fluorescens* strains were isolated. Among them, the airborne *P. fluorescens* strain MFAF76a was characterized as a virulent strain, particularly against human epithelial pulmonary cells (Duclairoir Poc et al., 2014). In this study, the response of airborne *P. fluorescens* MFAF76a to NO_2 as a marker of air pollution, was investigated. This response was compared to that of clinical strain *P. fluorescens* MFN1032, isolated from the sputum of a pneumonia patient (Chapalain et al., 2008). The parameters of bacterial NO_2 exposure were adapted to mimic real-life air conditions. Both strains were exposed to three NO_2 concentrations: 0.1 ppm as environmental standard; 5 ppm as the threshold, causing reversible effects on human health, and 45 ppm as a high NO_2 concentration, provoking irreversible effects, according WHO.

Material and Methods

Strains and growth conditions

Cyan Fluorescent Protein (CFP)-labelled *P. fluorescens* MFN1032 and MFAF76a were used in this study. The fluorescent gene *cfpopt* was introduced in pPSV35 vector (Rietsch et al., 2005; Vallet-Gely et al., 2007). The CFP cassette was obtained from pTetONCFPopt plasmid containing 729-bp *cfpopt* gene (Sastalla et al., 2009) by double digesting with *Pst*I and *Xma*I. This gene was inserted into the *lacZ* site of the polylinker of pPSV35 by ligation into the pPSV35 vector digested with the same enzymes. After chosen the clones by antibiotic selection (gentamycin 15µg/mL), the transformation was confirmed by confocal laser scanning microscope (LSM 710, ZEISS).

Bacterial strains were grown at 28°C under limited agitation (180 rpm) in DMB (Davis Medium Broth) minimal medium with glucose as carbon source (2.16 g/L) (Duclairoir-Poc, 2011). Overnight cultures were diluted (A_{580}=0.08) in fresh DMB and grown to the end of exponential phase A_{580}=2 ($13x10^8$ CFU/mL). Bacterial cultures at the end of exponential growth phase (about $3x10^7$ bacteria per filter) were transferred on cellulose nitrate membrane filter (0.45µm, pore size 0.2 µm, diameter 47 mm, Sartorius Biolab Products, Gottingen, Germany) and grown on DMB agar plates at 28°C for 4 h to obtain the single layer's bacterial population. After 4 h of incubation, the cellulose membranes containing bacteria were placed on agar one-well dishes (size 127.8 x 85.5 mm, Thermo Scientific Nunc, Roshester, USA), which were directly transferred into the gas delivery device (**Figure 1**).

Exposition to nitrogen dioxide

In order to restore the atmospheric conditions, bacterial NO_2 exposure was achieved in gas phase for 2 h, according to Ghaffari et al., 2005. The gas delivery device consisted of two sterile cylindrical Plexiglas exposure chambers (one for the NO_2 exposure, the second one for the control - exposure to the synthetic air). The exposure chambers were deposed in a drying oven at 28°C (**Figure 1**). The NO_2, N_2, and O_2 obtained from Air Liquide GMP Europe (Mitry-Mory, France) were mixed together using digital mass flow regulators (Alicat Scientific, Inc., Tucson, USA) in order to obtain pre-calculated concentrations of NO_2 and maintain the O_2/N_2 ratio at 8/2 (v/v). The obtained gas mixture and the synthetic air were routed independently to each of the exposure chamber at a constant flow rate of 2 L/min.

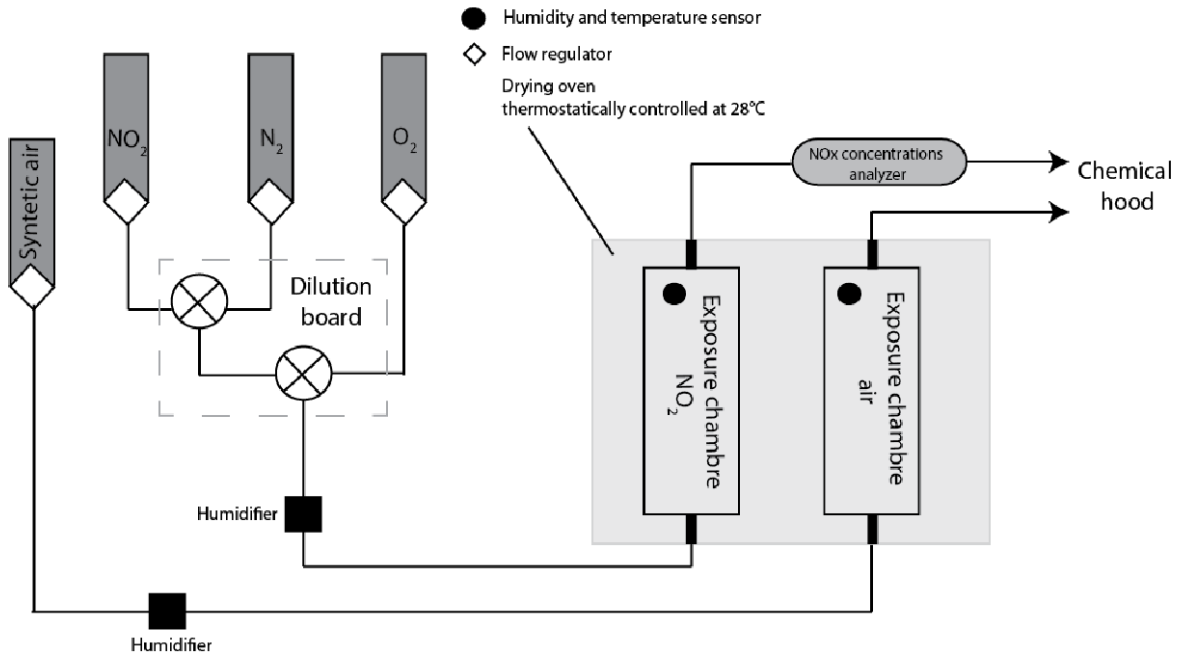

Figure 1. Schematic representation of NO_2 gas delivery system
Bacterial NO_2 exposure was done in gas phase for 2h. Two exposure chambers (one for the NO_2 exposure, the second one for the control simple - exposure to the synthetic air) were used. The gases, including NO_2, N_2 and O_2 were mixed together to obtain pre-calculated concentration of NO_2 and maintain the O_2/N_2 ratio at 2/8 (v/v). All experimental parameters (NO_2 concentration, temperature, relative humidity) were controlled.

The parallel NO_2/synthetic air circuits allow utilization of the same bacterial culture for exposed to NO_2 and control samples. After passing through the exposure chamber, the NO_2 concentrations were monitored by AC32M nitrogen oxides analyzer (Environnement S.A, Poissy, France). After this, the gas mixture was safely vented to a chemical hood. Temperature and relative humidity data were monitored to control reliable steady-state environmental conditions inside the exposure chambers. Three concentrations of NO_2 were used 0.1 ppm; 5 ppm and 45 ppm. After exposure, bacteria were resuspended to A_{580}=2 in sterile saline solution.

Antibiotic sensitivity assays

After NO_2 exposure, bacterial sensitivity to ciprofloxacin, chloramphenicol, tobramycin and kanamycin (Sigma-Aldrich, St. Quentin Fallavier, France) was tested. The minimum inhibitory concentration (MIC) was determined by broth microdilution method in DMB. Briefly, exposed to NO_2 bacterial cells were diluted to A_{580}=0.08 and added to a 96-well test plate (Nunc™, Roskilde, Denmark) containing different concentrations of antibiotics in triplicate. The test plates were incubated at 28°C for 24 h. As control sample, bacteria exposed to synthetic air were used. MIC was defined to be the lowest concentration of antibiotic that inhibited bacteria growth as determined by turbidimetry at A_{580}.

Growth inhibition assays were achieved as previously described by van Sorge and co-workers (van Sorge et al., 2013). Exposed bacteria were diluted in DMB supplemented by indicated antibiotics in subinhibitory concentrations (the last antibiotic concentrations allowing bacterial growth). Bacteria were added to Bioscreen Honeycomb plates (Oy Growth Curves Ab Ltd., Helsinki, Finland) in a total volume of 200 µL of DMB (A_{580}=0.08). Growth was measured every 15

min (A_{580}) for 24 h. The NO_2 effect on the bacterial antibiotic sensitivity was calculated as the percentage of bacterial growth with antibiotics after NO_2 exposure on the bacterial growth with antibiotics after exposure to synthetic air, using the following formula: 100 × A_{580} NO_2 exposed bacteria/A_{580} synthetic air exposed bacteria (%).

Motility assays

Swimming and swarming motility assays were performed on agar plates using DMB containing 0.2% (wt/vol) and 0.5 % (wt/vol) agar respectively, as previously described (Déziel et al., 2001). Briefly, 5 µL of suspension from NO_2 exposed bacteria were spotted on the surface of agar plates. The resultant diameters of swim and swarm zones were measured after 24 h of incubation at 28°C taking into account the generation time if necessary. As control, bacteria exposed to synthetic air were used. Motilities were assayed in at least three independent experiments with three replicates for each experimental condition.

Biofilm monitoring by confocal laser scanning microscopy

After NO_2 exposure, bacteria were diluted in sterile saline solution to A_{580}=1 and added to glass-bottom dishes (SensoPlate™, VWR, Fontenay-sous-Bois, France). After 2 h of incubation at 28°C, planktonic bacteria were removed and bacterial adhesion on glass-bottom dishes was observed using a confocal laser scanning microscope (LSM 710, ZEISS) with an immersion objective 63x. After addition of DMB, the samples were incubated at 28°C for 24h. Formed biofilms were rinsed with saline solution and observed using confocal laser scanning microscope. As control samples, bacteria exposed to synthetic air were used. All biofilm assays were performed in at least three independent experiments with two replicates for each experimental condition. The biofilm thickness and related biomass (bacterial volume, $\mu m^3/\mu m^2$) were estimated from 6 fields on 3 independent experiments using COMSTAT software (Heydorn et al., 2000).

Gene sequences identification

The identified nucleotide sequences were obtained using the non-annotated genome drafts of MFN1032 and MFAF76a (data not shown). Homologous sequences searches in *P. fluorescens* annotated genomes were performed using pseudomonas genome database (http://pseudomonas.com/). The conserved nucleotide sequences were identified in *P. fluorescens* MFN1032 and MFAF76A using Blast+ (Stand-alone) software (v. 2.2.30, NCBI) according to Altschul et al., 1997, and are listed in Table S1.

Extraction and quantification of bis-(3', 5')-cyclic dimeric guanosine monophosphate (c-di-GMP)

Extraction and quantification of intracellular c-di-GMP level were performed as previously described (Spangler et al., 2010; Strehmel et al., 2014). Identification and quantification of c-di-GMP was performed using three specific mass transitions from molecule ion m/z 691 to the product ions: m/z 152, m/z 135 and m/z 540. The external calibration was carried out at c-di-GMP concentrations ranging from 10 ng to 200 ng in 500 µL H_2O using the internal standard cXMP (50 ng). Obtained concentrations of c-di-GMP were normalized against total protein contents of respective cultures, which was determined by the bicinchoninic acid assay (Smith et al., 1985). All

experiments were performed in at least three replicates for each experimental condition.

Quantitative RT-PCR

RNA extraction, cDNA synthesis and real-time PCR were achieved as previously described (Gicquel et al., 2013) using the primers listed in Table S2.

Statistical analysis

All experiments were carried out at least three times. Significances of differences between mean values were assessed using Mann-Whitney test or pairwise strain comparisons (t-test) with significance set at $p < 0.05$ (*), < 0.01 (**) and < 0.001 (***).

Results and discussion

NO_2 is one of the most common air pollutants, but the effect of this molecule on air microbiota is poorly studied. To pursue our objective of assessing the bacterial response to NO_2, airborne *P. fluorescens* MFAF76a and clinical control MFN1032 were exposed to gaseous NO_2 at 0.1, 5 or 45 ppm concentrations, and their effects on bacteria were evaluated in terms of motility, biofilm formation, antibiotic resistance, as well as expression of several chosen target genes. While 0.1 and 5 ppm of NO_2 did not lead to any significant modification of the studied parameters in both the two bacteria (data not shown), several alterations were observed when the bacteria were exposed to 45 ppm of gaseous NO_2. We thus choose to focus on this latter condition.

NO_2-mediated modifications of bacterial biofilm and motility

In order to test the NO_2 effect on *P. fluorescens* biofilm, both airborne MFAF76a and clinical MFN1032 were exposed to NO_2 and synthetic air and grown for 4 h in static conditions. The formed biofilms were observed by confocal laser microscopy (**Figure 2A and B**). In both strains exposed to 45 ppm of NO_2, the biofilm biomass was comparable to that of the control, exposed to synthetic air (**Figure 2A and B**). However, the NO_2-treated airborne strain MFAF76a formed microcolony aggregates with increased maximum thickness (**Figure 2A**). Remarkably, this phenotype was not observed for clinical strain MFN1032 (**Figure 2B**), suggesting the strain-dependent NO_2-mediated biofilm modifications. The c-di-GMP levels after NO_2 exposure were quantified and compared with control samples, exposed to synthetic air. Both NO_2-exposed *P. fluorescens* strains did not exhibited statistically significant variations of intracellular c-di-GMP concentrations (**Figure 2C**), in correlation with biofilm biomass results. In order to better understand the NO_2 effect on *P. fluorescens* biofilm, the mRNA levels of genes, coding for several phosphodiesterases (PDE), including *dipA, mucR, ndbA* and *bdlA* genes (KT186437, KT186445, KT186444 and KT186436 respectively, Table S1) were tested. No modification of their mRNA levels comparing to control samples was observed (data not shown), confirming the observed phenotypes.

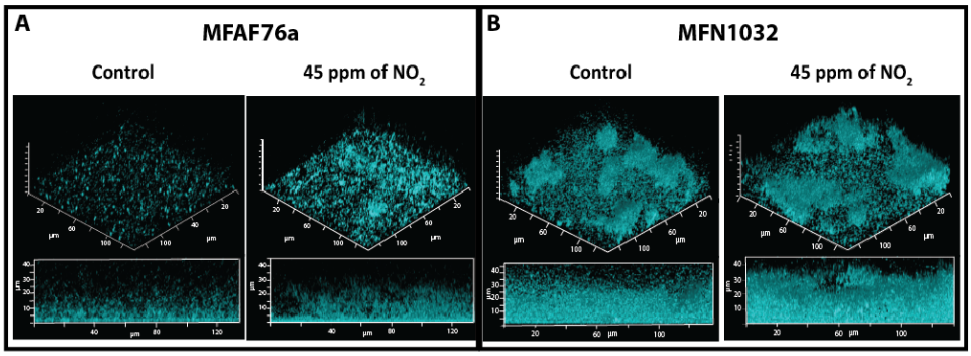

	MFAF76a		MFN1032	
	Control	45 ppm of NO_2	Control	45 ppm of NO_2
Total biomass ($\mu m^3 \mu m^{-2}$)	0.64±0.18	0.78±0.24	1.38±0.42	2.37±0.49
Max thickness (µm)	9.25±1.43	22.50±1.22	29.00±3.02	33.56±3.58

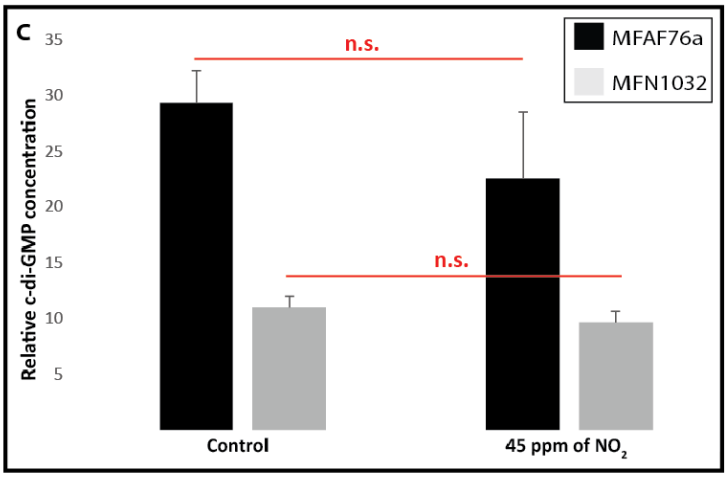

Figure 2. NO_2 effect on *P. fluorescens* biofilm
(A) Airborne MFAF76a and **(B)** clinical MFN1032 *P. fluorescens* strains were exposed in triplicate to 45 ppm of NO_2. Biofilm formation was analyzed in static conditions after 24 h development using confocal laser scanning microscope. The biofilm biomass and the maximum thickness were estimated from 6 fields on 3 independent experiments using COMSTAT software. Intracellular c-di-GMP concentrations **(C)** were measured in triplicate by LC-MS/MS for MAFA76a (■) and MFN1032 (■). Statistical significance was calculated by the non-parametric Mann-Whitney-Test. n.s. non-significant.

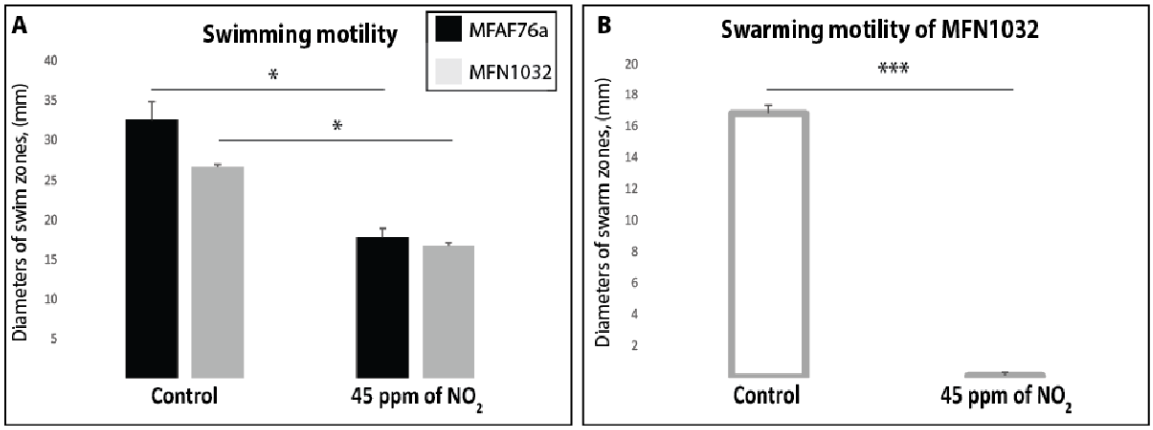

Figure 3. NO_2 decreases *P. fluorescens* motility
Airborne MFAF76a (■) and clinical MFN1032 (■) *P. fluorescens* strains were exposed in triplicate to 45 ppm of NO_2. Swimming **(A)** and swarming **(B)** motilities were assayed on DMB-swim/swarm plates after 24 h incubation. Agar plate surface coverage was determined of at least three independent experiments with three replicates. The data were compared with control samples exposed to synthetic air. Obtained results are presented as average values ± SEM. Statistical significance was calculated by the non-parametric Mann-Whitney-Test $p < 0.05$ (*) and < 0.001 (***).

In order to test the NO_2 effect on bacterial motility, swimming and swarming assays were performed for NO_2-treated clinical and airborne strains (**Figure 3A and B**). After exposure to 45 ppm of NO_2, swimming assays demonstrated slight statistically significant decreases in comparison to the control samples, suggesting that the flagellar motion was impacted (**Figure 3A**). These results were calculated considering the slight failure of bacterial growth after NO_2 exposure (generation times of 60 and 40 min for MFAF76a and MFN1032 without stress addition; 100 and 60 min for bacteria treated with 45 ppm of NO_2 respectively). In absence of tensioactive production (Duclairoir Poc et al., 2014), airborne strain MFAF76a did not swarm. In clinical strain, the swarming motility was found to be completely inhibited in response to NO_2 exposure (**Figure 3B**). The lack of modification in biofilm biomass and in intracellular c-di-GMP level compiled with data of motility assays, let us suggest that the decrease of swimming and inhibition of swarming motility was not caused by the c-di-GMP regulatory pathway, and, among others, could be dependent on alterations in flagellar motion, type IV pili and biosurfactant production.

While NO is known to be involved in biofilm dispersion (Barraud et al., 2015), we did not found any NO_2-mediated alteration in bacterial biomass and c-di-GMP level. Once more in contradiction with results obtained for NO (Barnes et al., 2013; Barraud et al., 2006), this phenotype seems to be independent on the NO_2 concentration. NO-induced dispersion of *P. aeruginosa* biofilm coincides with increased PDE activity (Petrova and Sauer, 2012; Roy et al., 2012). Several proteins, including DipA, MucR, NdbA and BdlA were identified as actors in NO-mediated biofilm dispersal (Li et al., 2013; Petrova et al., 2014; Petrova and Sauer, 2012; Roy et al., 2012). The tests of mRNA levels of *dipA, mucR, ndbA* and *bdlA* genes did not demonstrate the NO_2 effect on that gene expression. Taken together, these data suggest the difference between NO- and NO_2-mediated effects on bacterial biofilm.

Effect of NO_2 on *P. fluorescens* antibiotic resistance

In order to study the effect of NO_2 on *mexEF-oprN* efflux pump, the transcription levels of *mexE, mexF* and *oprN* genes (KT070324, KT070321 and KT070325 for MFAF76a; KT070323, KT070322 and KT186432 for MFN1032, respectively) were compared using qRT-PCR in two *P. fluorescens* strains exposed to 45 ppm of NO_2 and synthetic air. In airborne and clinical strains, the *mexE* mRNA level was increased almost 14- and 100-fold respectively; that of *mexF* almost 3.5- and 47-fold respectively and that of *oprN* almost 4.6- and 73-fold respectively (**Figure 4**). Thus, we suggest that NO_2 promoted *mexEF-oprN* expression, potentially causing the modification(s) in *P. fluorescens* antibiotic resistance.

Since the MexEF-OprN RND efflux pump is involved in fluoroquinolone resistance, we next assayed NO_2- or synthetic air-exposed bacterial sensitivity against ciprofloxacin by evaluating their MICs. As shown in **Table 1**, both the two *P. fluorescens* strains were more resistant to this antibiotic following exposure to NO_2 compared to synthetic air. Chloramphenicol is a nitroaromatic antimicrobial that is a substrate for MexEF-OprN (Köhler et al., 1997; Sobel et al., 2005).

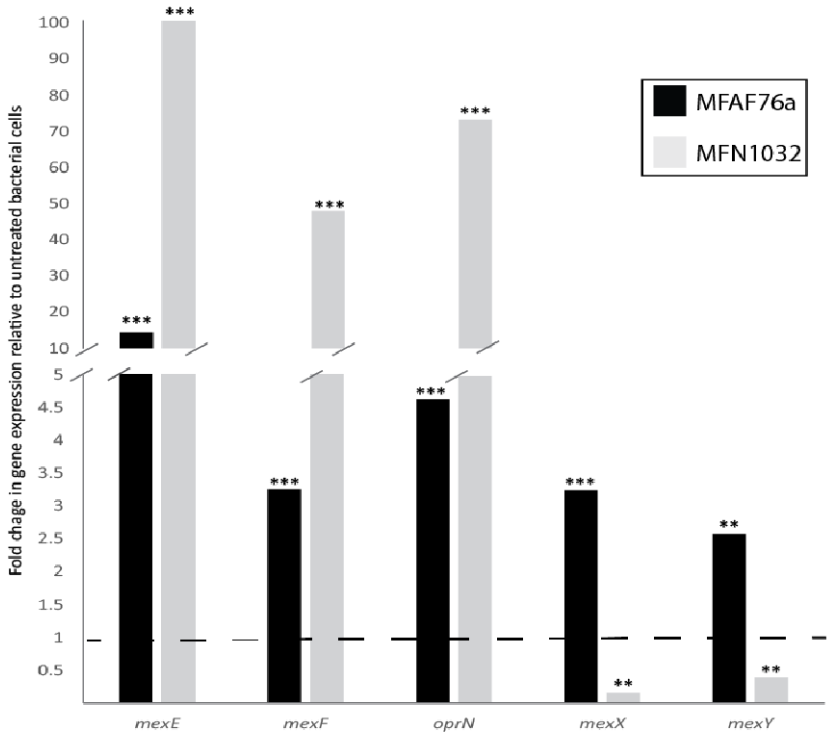

Figure 4. NO_2 effect on MexEF-OprN and MexXY efflux pump gene transcription
The nucleotide sequences of the *mexEF-oprN*- and *mexXY*-homologue genes were obtained using the non-annotated genome drafts of airborne MFAF76a (■) and clinical MFN1032 (■) *P. fluorescens.* The GenBank accession numbers of nucleotide sequences are listed in Table S1. Quantification of mRNA level was assayed using qRT-PCR on RNAs extracted from NO_2- and synthetic air-exposed *P. fluorescens*. The PCR reactions were performed in triplicate and the standard deviations were lower than 0.15 Ct. Statistical analysis used pairwise strain comparisons (t-test) $p < 0.01$ (**) and < 0.001 (***). Dotted line shows the gene expression in synthetic air-exposed control.

Table 1. NO_2 exposure increases *Pseudomonas fluorescens* antibiotic resistance

Strain	**NO_2 concentration** (ppm)	**Ciprofloxacin** MIC(µg/mL)	**Chloramphenicol** MIC(µg/mL)
MFAF76a	0	6.25	50
	45	12.5	> 100
MFN1032	0	3.125	150
	45	6.25	200

Accordingly, NO_2 exposed *P. fluorescens* strains MFAF76a and MFN1032 were about 2 fold more resistant to this antibiotic than the control synthetic air-treated bacteria (**Table 1**). Taken together, these data suggest a possible higher activity of this efflux pump in response to NO_2 exposure.

We next followed the growth of the NO_2- and synthetic air-exposed *P. fluorescens* strains in DMB medium containing ciprofloxacin or chloramphenicol at the higher antibiotic concentration leading to bacterial growth (**Figure 5**; see materials and methods). Data are given as the ratio of the NO_2-exposed bacteria versus the control (synthetic air)-treated cells (**Figure 5**). While ciprofloxacin had no effect on NO_2-exposed bacteria, chloramphenicol, at a concentration of 25 and 100 µg/mL for strain MFAF76a and MFN1032, respectively, led to increase the growth of both the two NO_2-exposed *P. fluorescens* strains (**Figure 5**). Remarkably, the statistically significant increase of bacterial

growth was maintained from 2 to 10 h, suggesting a possible NO_2 protective effect that could be conserved for 8 hours after exposure. Taken together, our data show that NO_2 induced *mexEF oprN* gene expression, and consequently increased resistance to ciprofloxacin and chloramphenicol.

MexEF-OprN-overproducing mutants with enhanced fluoroquinolone resistance often increase bacterial susceptibility to aminoglycosides apparently owing to impairment of the MexXY system (Morita et al., 2015; Sobel et al., 2005). In order to elucidate the effect of NO_2 on *P. fluorescens* aminoglycoside sensitivity, we performed the analysis of *mexX* (KT070313 for MFAF76a and KT186462 for MFN1032) and *mexY* (KT070314 and KT070315 for MFAF76a and MFN1032 respectively) genes expression. In NO_2-exposed airborne strain, the *mexX* and *mexY* mRNA levels were increased almost 3.2- and 2.6-fold respectively (**Figure 4**), indicating that, in airborne MFAF76a, NO_2 is involved in upregulation of *mexEF-oprN* as well as *mexXY*. The remarkable overexpression of two resistance nodulation cell division (RND) -type multidrug efflux operons, *mexEF-oprN* and *mexXY-(oprA)* was previously demonstrated in multiresistant *P. aeruginosa* PA7 and linked with enhanced fluoroquinolone resistance (Morita et al., 2015). In contrast, in NO_2-treated clinical MFN1032 strain, the *mexX* and *mexY* mRNA levels were decreased almost 5- and 2-fold respectively comparing to air-treated control (**Figure 4**). The MICs of tobramycin and kanamycin were tested and completed by tests of bacterial growth after NO_2 exposure in presence of these antibiotics. The 2-fold decrease of the MICs of kanamycin and tobramycin was observed for NO_2-treated bacteria, indicating that NO_2 could make bacteria more sensitive to both the antibiotics (**Table 2**). In addition, tobramycin and kanamycin at subinhibitory concentration of 1.55 and 3.1 µg/mL, respectively, were found to decrease the growth of NO_2-exposed bacteria (**Figure 6**). This effect was observed only from 6 to 10 h of growth for MFN1032 and from 6 to 18 h of growth for MFAF76a, highlighting the time-limited NO_2 effect on bacterial antibiotic sensitivity. Altogether, our data show that NO_2 increased *P. fluorescens* sensitivity to tobramycin and kanamycin. However, the difference in *mexXY* genes expression between the two *P. fluorescens* strains indicates, that NO_2 effect on bacterial aminoglycoside resistance could be complex and strain-dependent, involving, among other factors, the membrane properties. The NO_2 effect on *P. fluorescens* membrane was recently investigated (Kondakova et al., 2015; personal communication), demonstrating the NO_2-mediated modifications in both membrane glycerophospholipid composition (*i.e.* ratio zwitterionic/anionic glycerophospholipids) and in the membrane electron-accepting properties. We imagine, that these membrane modifications, could alter bacterial membrane permeability, facilitating the aminoglycoside penetration in bacterial cell.

Overall, similarly to the results observed in our study, NO was found to induce the expression of *mexEF-oprN* genes (Fetar et al., 2011) and modulate bacterial resistance to several antibiotics (Gusarov et al., 2009; McCollister et al., 2011; van Sorge et al., 2013). In this way, basing on the well-studied NO bacterial response, the NO_2 effect on several chosen target genes was tested.

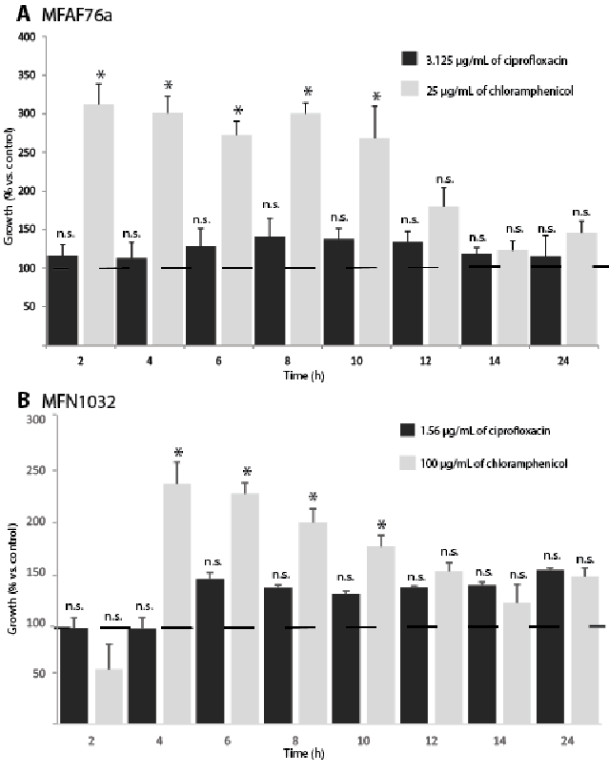

Figure 5. NO_2 protects *Pseudomonas fluorescens* from chloramphenicol toxicity

After 2h exposure to 45 ppm of NO_2, growth of airborne MFAF76a **(A)** and clinical MFN1032 **(B)** *P. fluorescens* with ciprofloxacin (■) and chloramphenicol ( ) was assayed. Growth curves were performed with ciprofloxacin (3.125 µg/mL for MFAF76a and 1.156 µg/mL for MFN1032) and chloramphenicol (25 and 100 µg/mL respectively), and A_{580} was recorded at the indicated time points. The control sample was bacteria exposed to synthetic air, and grown in presence of antibiotics in indicated concentrations. The data are shown as percentages of growth relative to synthetic air-exposed control. Pooled data from three independent experiments in duplicate ± SEM are reported. Statistical significance was calculated by the non-parametric Mann-Whitney-Test $p < 0.05$ (*); n.s. non-significant. Dotted line shows the control (100%).

Table 2. NO_2 decreases *Pseudomonas fluorescens* resistance to aminoglycosides

Strain	**NO_2 concentration** (ppm)	**Kanamycin** MIC(µg/mL)	**Tobramycin** MIC(µg/mL)
MFAF76a	0	8.3	6.2
	45	6.2	3.1
MFN1032	0	20.0	12.5
	45	16.7	8.3

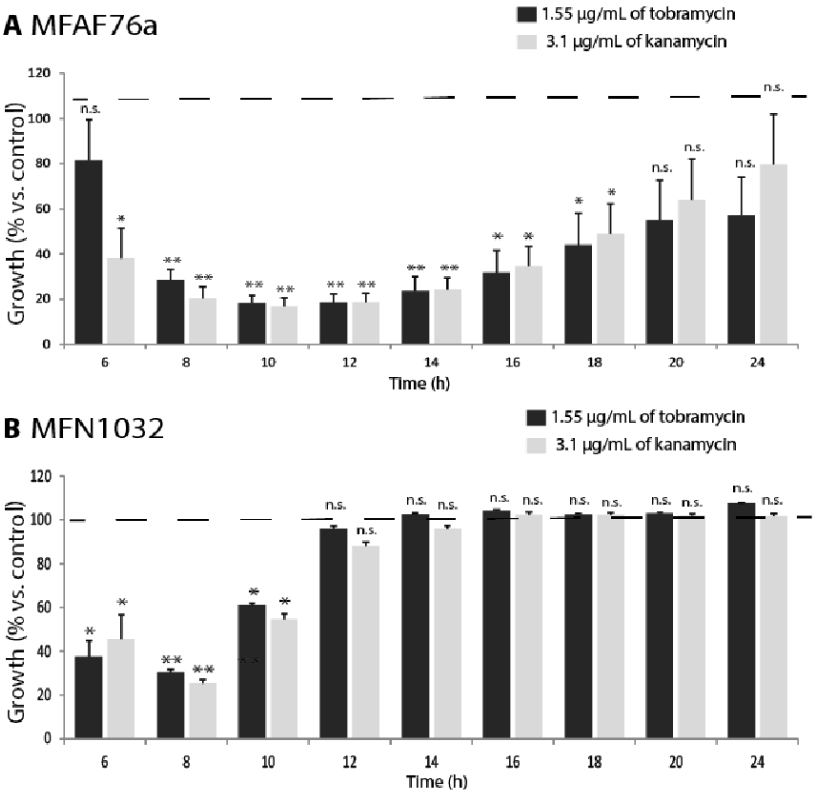

Figure 6. NO_2 exposure affects *Pseudomonas fluorescens* growth with aminoglycosides

After 2h exposure to 45 ppm of NO_2, growth of airborne MFAF76a **(A)** and clinical MFN1032 **(B)** in presence of tobramycin (1.55 µg/mL; ■) and kanamycin (3.1 µg/mL;) was tested. A_{580} was recorded at indicated time points. The control sample was bacteria exposed to synthetic air, and grown in presence of antibiotics in indicated concentrations. The data are presented as percentages of growth relative to air-exposed control. Pooled data from three independent experiments in duplicate ± SEM are reported. Statistical significance was calculated by the non-parametric Mann-Whitney-Test $p < 0.05$ (*), < 0.01 (**); n.s. non-significant. Dotted line shows the control (100%).

NO_2-mediated gene expression in *P. fluorescens*

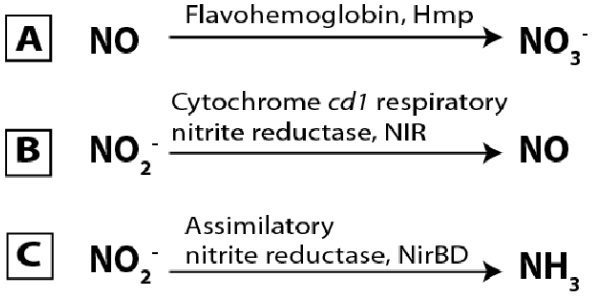

Figure 7. Scheme of Hmp-mediated NO detoxification and NO_2 reduction pathways in *Pseudomonas* spp.
(A) Flavohemoglobin (Hmp) is involved in NO detoxification acting as an NO dioxygenase to transform NO to NO_3^-. The NO_2 reduction is performed by nitrite reductase enzymes, including the respiratory cytochrome *cd1* nitrite reductase, NIR **(B)** and the assimilatory nitrite reductase NirBD **(C)**. The respiratory NIR is involved in NO_2^- reduction to NO in anaerobic conditions. NirBD takes a part of the nitrate assimilatory pathway, and reduces nitrite to ammonia.

The most well-studied pathway for NO detoxification is based on flavohemoglobin (FlavoHb) (Hmp for *E. coli* and Fhp for *P. aeruginosa*), which acts as an NO dioxygenase to transform NO to NO_3^- (**Figure 7A**) (Arai et al., 2005; Corker and Poole, 2003). In order to investigate the NO_2 effect on *hmp* expression, the mRNA levels of the *hmp*-homologue gene in both *P. fluorescens* strains (KR818822 for MFAF76a and KR818823 for MFN1032, Table S1) were tested. After exposure to 45 ppm of NO_2, the *hmp* mRNA levels were increased almost 25- and 23-fold in MFAF76a and in MFN1032 respectively (**Figure 8**), indicating that NO_2 induces *hmp* expression in both *P. fluorescens* and suggesting a possible involvement of Hmp in NO_2 detoxification. The NO_2 effect on Hmp synthesis was observed in other studies, where to activate the Hmp-dependent detoxification pathway, NO_2 was proposed to be reduced to NO (Poole et al., 1996).

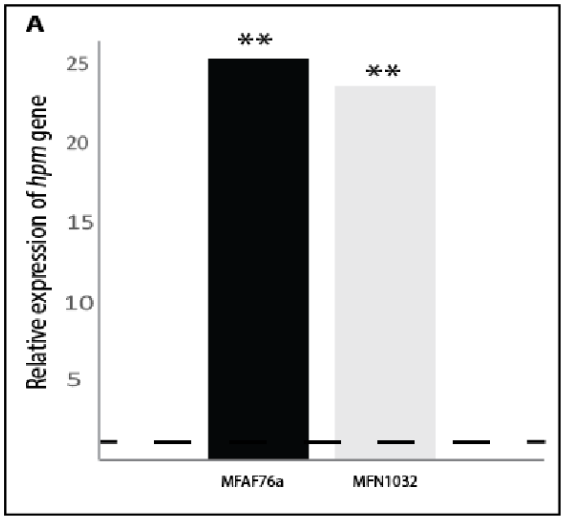

Figure 8. Transcription of *hmp* is increased in response to NO_2 exposure
The nucleotide sequences of the *hmp*-homologue gene in *P. fluorescens* strains were obtained using the non-annotated genome drafts of airborne *P. fluorescens* MFAF76a (■) and clinical MFN1032 (■). The GenBank accession numbers of *hmp* nucleotide sequences are listed in Table S1. Quantification of mRNA level was assayed using qRT-PCR on RNAs extracted from NO_2- and synthetic air-exposed *P. fluorescens*. The PCR reactions were performed in triplicate and the standard deviations were lower than 0.15 Ct. Statistical analysis used pairwise strain comparisons (t-test) $p < 0.01$ (**). Dotted line shows the gene expression in air-exposed control.

In *Pseudomonas* spp., NO_2 reduction can be performed by nitrite reductase (NIR) enzymes (**Figure 7B and C**), including the well-studied respiratory cytochrome *cd1* nitrite reductase (**Figure 7B**) of the denitrification pathway (Arai et al., 2005; Shiro, 2012). According the genome draft analysis (data not shown), both MFAF76a and MFN1032, like the majority of *P. fluorescens* strains (Redondo-Nieto et al., 2013), do not possess denitrifying genes. However, according to genome analysis (data not shown), the two studied strains harbor the genes, encoding for the assimilatory nitrite reductase NirBD (**Figure 7C**). The latter is part of the Nas assimilatory pathway (from nitrate assimilation), where nitrate is reduced to nitrite, which is then reduced to ammonia (Jeter et al., 1984; Moreno-Vivián et al., 1999). In order to test the NO_2 effect on the

expression of *nirBD* operon, the *nirB* mRNA level (*Pfl76a_nirB* (KT186428) and *Pfl1032_nirB* (KT070320), Table S1) was compared in the NO_2- and synthetic air-exposed *P. fluorescens* strains. In both strains, the mRNA level of *nirB* was not modified compared to control (data not shown), indicating the absence of NO_2 effect on the genes coding for assimilatory NIR. To the best of our knowledge, the involvement of Nas pathway in NO/NO_2 detoxification was not demonstrated. Given the presence of ammonium in DMB medium (Duclairoir-Poc, 2011), we imagine that the production of supplementary ammonium through the nitrite reduction is not appropriate. However, in order to better understand the mechanism of NO_2 detoxification, the Hmp-, Nir- and Nas-mediated mechanisms should be investigated in more details.

In this study, for the first time, the response of airborne *P. fluorescens* MFAF76a to toxicity of NO_2, as a marker of air pollution, was studied. Contrarily to a myriad of studies of NO-mediated biofilm dispersion, we did not observe the NO_2-mediated modifications of bacterial biomass. However, the alteration in the biofilm architecture of NO_2-treated airborne *P. fluorescens* MFAF76a was found. In tested experimental conditions, the NO_2 completely inhibited bacterial swarming motility and provoked a slight decreasing of swimming that could be correlated, among other factors, with alterations in flagellar motion, type IV pili and surfactant production. Anyway, the NO_2-mediated modifications in biofilm architecture and in bacterial motility seem to not be linked to c-di-GMP regulatory network. The analyses of NO_2-mediated gene expression demonstrated, that NO_2, like its homolog NO, induces the expression of *mexEF-oprN* genes, coding for the RND efflux pump. Its overexpression could, among others, be involved in the observed increase of *P. fluorescens* resistance to ciprofloxacin and chloramphenicol. Thus, the high *P. fluorescens* adaptability and a possible NO_2 propensity to increase bacterial antibiotic resistance may diminish the effectiveness of antibiotic therapies in polluted area. In addition, our study showed the NO_2-mediated upregulation of the *hmp*-homologue gene in *P. fluorescens* strains MFAF76a and MFN1032, suggesting a possible common pathway between NO and NO_2 detoxification. While the mechanism of NO_2 detoxification have been proposed to carry out through the NO_2 reduction pathway (Poole et al., 1996), the role(s) of Hmp in NO_2 detoxification should be confirmed and elucidated in future studies. In conclusion, in the context of the worrying increase of atmospheric NO_2 concentrations (Bernagaud et al., 2014), this preliminary investigation, for the first time, clarifies the response of airborne *P. fluorescens* to the air pollutant NO_2. Fortunately, no modification in tested parameters was found in bacteria, exposed to the environmental NO_2 standards. Since NO_2 air pollution is a serious urban problem with growing attention in recent years, these findings are of ecological relevance, especially because of the high NO_2 concentrations, found in the close vicinity of any vehicle.

Acknowledgements

We thank Emeline Bouffartigues for the constructive comments and the help in manuscript writing. We are grateful to Anne Groboillot for help with development of gas delivery system. We

thank Audrey Garreau and Olivier Maillot for technical assistance. This study was supported by a PhD grant from the GRR SESA (Research Network of Sanitary Safety) and was financially supported by Regional Council of Haute-Normandie, the Conseil Général de l'Eure and the Grand Evreux Agglomeration (France).

Supplementary data

Supplementary data related to this article can be found in Annexes.

References

Ahern, H. E., Walsh, K. A., Hill, T. C. J., and Moffett, B. F. (2007). Fluorescent pseudomonads isolated from Hebridean cloud and rain water produce biosurfactants but do not cause ice nucleation. *Biogeosciences* 4, 115–124. doi:10.5194/bg-4-115-2007.

Altschul, S. F., Madden, T. L., Schäffer, A. A., Zhang, J., Zhang, Z., Miller, W., et al. (1997). Gapped BLAST and PSI-BLAST: a new generation of protein database search programs. *Nucleic Acids Res.* 25, 3389–3402. doi:10.1093/nar/25.17.3389.

Arai, H., Hayashi, M., Kuroi, A., Ishii, M., and Igarashi, Y. (2005). Transcriptional regulation of the flavohemoglobin gene for aerobic nitric oxide detoxification by the second nitric oxide-responsive regulator of *Pseudomonas aeruginosa*. *J. Bacteriol.* 187, 3960–3968. doi:10.1128/JB.187.12.3960-3968.2005.

Auger, C., and Appanna, V. D. (2015). A novel ATP-generating machinery to counter nitrosative stress is mediated by substrate-level phosphorylation. *Biochim. Biophys. Acta BBA - Gen. Subj.* 1850, 43–50. doi:10.1016/j.bbagen.2014.09.028.

Auger, C., Lemire, J., Cecchini, D., Bignucolo, A., and Appanna, V. D. (2011). The metabolic reprogramming evoked by nitrosative stress triggers the anaerobic utilization of citrate in *Pseudomonas fluorescens*. *PLoS ONE* 6. doi:10.1371/journal.pone.0028469.

Augusto, O., Bonini, M. G., Amanso, A. M., Linares, E., Santos, C. C. X., and De Menezes, S. L. (2002). Nitrogen dioxide and carbonate radical anion: two emerging radicals in biology. *Free Radic. Biol. Med.* 32, 841–859. doi:10.1016/S0891-5849(02)00786-4.

Barnes, R. J., Bandi, R. R., Wong, W. S., Barraud, N., McDougald, D., Fane, A., et al. (2013). Optimal dosing regimen of nitric oxide donor compounds for the reduction of *Pseudomonas aeruginosa* biofilm and isolates from wastewater membranes. *Biofouling* 29, 203–212. doi:10.1080/08927014.2012.760069.

Barraud, N., Hassett, D. J., Hwang, S.-H., Rice, S. A., Kjelleberg, S., and Webb, J. S. (2006). Involvement of nitric oxide in biofilm dispersal of *Pseudomonas aeruginosa*. *J. Bacteriol.* 188, 7344–7353. doi:10.1128/JB.00779-06.

Barraud, N., Kelso, M. J., Rice, S. A., and Kjelleberg, S. (2015). Nitric oxide: a key mediator of biofilm dispersal with applications in infectious diseases. *Curr. Pharm. Des.* 21, 31–42.

Barraud, N., Storey, M. V., Moore, Z. P., Webb, J. S., Rice, S. A., and Kjelleberg, S. (2009). Nitric oxide-mediated dispersal in single- and multi-species biofilms of clinically and industrially relevant microorganisms. *Microb. Biotechnol.* 2, 370–378. doi:10.1111/j.1751-7915.2009.00098.x.

Bauer, H., Kasper-Giebl, A., Löflund, M., Giebl, H., Hitzenberger, R., Zibuschka, F., et al. (2002). The contribution of bacterial and fungal spores to the organic carbon content of cloud water, precipitation and aerosols. *Atmospheric Res.* 64, 109–119. doi:10.1016/S0169-8095(02)00084-4.

Bernagaud, C., Burkhart, J.-F., Vidal, B., Lepriol, T., Petit, J.-F., Brunel, T., et al. (2014). Observations du ratio [NO_2]/[NO_x] en tunnel routier. *Pollution-Atmospherique*. Available at: http://lodel.irevues.inist.fr/pollution-atmospherique/index.php?id=2659 [Accessed August 18, 2015].

Bodilis, J., Calbrix, R., Guérillon, J., Mérieau, A., Pawlak, B., Orange, N., et al. (2004). Phylogenetic relationships between environmental and clinical isolates of *Pseudomonas fluorescens* and related species deduced from 16S rRNA gene and OprF protein sequences. *Syst. Appl. Microbiol.* 27, 93–108. doi:10.1078/0723-2020-00253.

Burney, S., Caulfield, J. L., Niles, J. C., Wishnok, J. S., and Tannenbaum, S. R. (1999). The chemistry of DNA damage from nitric oxide and peroxynitrite. *Mutat. Res. Mol. Mech. Mutagen.* 424, 37–49. doi:10.1016/S0027-5107(99)00006-8.

Burrows, S. M., Butler, T., Jöckel, P., Tost, H., Kerkweg, A., Pöschl, U., et al. (2009a). Bacteria in the global atmosphere – Part 2: Modeling of emissions and transport between different ecosystems. *Atmos Chem Phys* 9, 9281–9297. doi:10.5194/acp-9-9281-2009.

Burrows, S. M., Elbert, W., Lawrence, M. G., and Pöschl, U. (2009b). Bacteria in the global atmosphere – Part 1: Review and synthesis of literature data for different ecosystems. *Atmos Chem Phys* 9, 9263–9280. doi:10.5194/acp-9-9263-2009.

Chaloulakou, A., Mavroidis, I., and Gavriil, I. (2008). Compliance with the annual NO_2 air quality standard in Athens. Required NO_x levels and expected health implications. *Atmos. Environ.* 42, 454–465. doi:10.1016/j.atmosenv.2007.09.067.

Chapalain, A., Chevalier, S., Orange, N., Murillo, L., Papadopoulos, V., and Feuilloley, M. G. J. (2009). Bacterial ortholog of mammalian translocator

protein (TSPO) with virulence regulating activity. *PLoS ONE* 4, e6096. doi:10.1371/journal.pone.0006096.

Chapalain, A., Rossignol, G., Lesouhaitier, O., Merieau, A., Gruffaz, C., Guerillon, J., et al. (2008). Comparative study of 7 fluorescent pseudomonad clinical isolates. *Can. J. Microbiol.* 54, 19–27. doi:10.1139/w07-110.

Chauhan, A. J., Krishna, M. T., Frew, A. J., and Holgate, S. T. (1998). Exposure to nitrogen dioxide (NO_2) and respiratory disease risk. *Rev. Environ. Health* 13, 73–90.

Corker, H., and Poole, R. K. (2003). Nitric oxide formation by *Escherichia coli*: Dependence on nitrite reductase, the NO-sensing regulator Fnr and flavohemoglobin Hmp. *J. Biol. Chem.* 278, 31584–31592. doi:10.1074/jbc.M303282200.

Cruz-Ramos, H., Crack, J., Wu, G., Hughes, M. N., Scott, C., Thomson, A. J., et al. (2002). NO sensing by FNR: regulation of the *Escherichia coli* NO-detoxifying flavohemoglobin, Hmp. *EMBO J.* 21, 3235–3244. doi:10.1093/emboj/cdf339.

Cutruzzola, F., and Frankenberg-Dinkel, N. (2015). Origin and impact of nitric oxide in *Pseudomonas aeruginosa* biofilms. *J. Bacteriol.*, JB.00371–15. doi:10.1128/JB.00371-15.

Després, V. R., Alex Huffman, J., Burrows, S. M., Hoose, C., Safatov, A. S., Buryak, G., et al. (2012). Primary biological aerosol particles in the atmosphere: a review. *Tellus B* 64. doi:10.3402/tellusb.v64i0.15598.

Déziel, E., Comeau, Y., and Villemur, R. (2001). Initiation of biofilm formation by *Pseudomonas aeruginosa* 57RP correlates with emergence of hyperpiliated and highly adherent phenotypic variants deficient in swimming, swarming, and twitching motilities. *J. Bacteriol.* 183, 1195–1204. doi:10.1128/JB.183.4.1195-1204.2001.

Duclairoir-Poc, C. (2011). Influence of growth temperature on cyclolipopeptides production and on adhesion behaviour in environmental strains of *Pseudomonas fluorescens*. *J. Bacteriol. Parasitol.* 04. doi:10.4172/2155-9597.S1-002.

Duclairoir Poc, C., Verdon, J., Groboillot, A., Barreau, M., Toucourou, H., Mijouin, L., et al. (2014). Airborne fluorescent pseudomonads : What potential for virulence? *Int. J. Curr. Microbiol. Appl. Sci.*, 708–722.

Dybwad, M., Granum, P. E., Bruheim, P., and Blatny, J. M. (2012). Characterization of airborne bacteria at an underground subway station. *Appl. Environ. Microbiol.* 78, 1917–1929. doi:10.1128/AEM.07212-11.

Fang, F. C., and Vazquez-Torres, A. (2002). Nitric oxide production by human macrophages: there's NO doubt about it. *Am. J. Physiol. - Lung Cell. Mol. Physiol.* 282, L941–L943. doi:10.1152/ajplung.00017.2002.

Fang, Z., Ouyang, Z., Zheng, H., Wang, X., and Hu, L. (2007). Culturable airborne bacteria in outdoor environments in Beijing, China. *Microb. Ecol.* 54, 487–496. doi:10.1007/s00248-007-9216-3.

Fetar, H., Gilmour, C., Klinoski, R., Daigle, D. M., Dean, C. R., and Poole, K. (2011). *mexEF-oprN* Multidrug efflux operon of *Pseudomonas aeruginosa*: Regulation by the MexT activator in response to nitrosative stress and chloramphenicol. *Antimicrob. Agents Chemother.* 55, 508–514. doi:10.1128/AAC.00830-10.

Flatley, J., Barrett, J., Pullan, S. T., Hughes, M. N., Green, J., and Poole, R. K. (2005). Transcriptional responses of *Escherichia coli* to S-nitrosoglutathione under defined chemostat conditions reveal major changes in methionine biosynthesis. *J. Biol. Chem.* 280, 10065–10072. doi:10.1074/jbc.M410393200.

Gao, W., Wesely, M. L., and Lee, I. Y. (1991). A numerical study of the effects of air chemistry on fluxes of NO, NO_2, and O_3 near the surface. *J. Geophys. Res. Atmospheres* 96, 18761–18769. doi:10.1029/91JD02106.

Ghaffari, A., Neil, D. H., Ardakani, A., Road, J., Ghahary, A., and Miller, C. C. (2005). A direct nitric oxide gas delivery system for bacterial and mammalian cell cultures. *Nitric Oxide* 12, 129–140. doi:10.1016/j.niox.2005.01.006.

Giardina, G., Rinaldo, S., Johnson, K. A., Di Matteo, A., Brunori, M., and Cutruzzolà, F. (2008). NO sensing in *Pseudomonas aeruginosa*: Structure of the transcriptional regulator DNR. *J. Mol. Biol.* 378, 1002–1015. doi:10.1016/j.jmb.2008.03.013.

Gicquel, G., Bouffartigues, E., Bains, M., Oxaran, V., Rosay, T., Lesouhaitier, O., et al. (2013). The extra-cytoplasmic function sigma factor SigX modulates biofilm and virulence-related properties in *Pseudomonas aeruginosa*. *PLoS ONE* 8, e80407. doi:10.1371/journal.pone.0080407.

Gusarov, I., Shatalin, K., Starodubtseva, M., and Nudler, E. (2009). Endogenous nitric oxide protects bacteria against a wide spectrum of antibiotics. *Science* 325, 1380–1384. doi:10.1126/science.1175439.

Heydorn, A., Nielsen, A. T., Hentzer, M., Sternberg, C., Givskov, M., Ersbøll, B. K., et al. (2000). Quantification of biofilm structures by the novel computer program comstat. *Microbiology* 146, 2395–2407.

Husain, M., Bourret, T. J., McCollister, B. D., Jones-Carson, J., Laughlin, J., and Vázquez-Torres, A. (2008). Nitric oxide evokes an adaptive response to oxidative stress by arresting respiration. *J. Biol. Chem.* 283, 7682–7689. doi:10.1074/jbc.M708845200.

INERIS (2011). Dioxyde d'azote: Données toxicologiques et environnementales. *Portail Subst. Chim.* Available at: http://www.ineris.fr/substances/fr/substance/cas/10102-44-0/2 [Accessed September 17, 2015].

Jeter, R. M., Sias, S. R., and Ingraham, J. L. (1984). Chromosomal location and function of genes affecting *Pseudomonas aeruginosa* nitrate assimilation. *J. Bacteriol.* 157, 673–677.

Köhler, T., Michéa-Hamzehpour, M., Henze, U., Gotoh, N., Curty, L. K., and Pechère, J. C. (1997). Characterization of MexE-MexF-OprN, a positively regulated multidrug efflux system of *Pseudomonas aeruginosa*. *Mol. Microbiol.* 23, 345–354.

Laver, J. R., McLean, S., Bowman, L. A. H., Harrison, L. J., Read, R. C., and Poole, R. K. (2013). Nitrosothiols in bacterial pathogens and pathogenesis. *Antioxid. Redox Signal.* 18, 309–322. doi:10.1089/ars.2012.4767.

Liu, P., Huang, Q., and Chen, W. (2012). Heterologous expression of bacterial nitric oxide synthase gene: a potential biological method to control biofilm development in the environment. *Can. J. Microbiol.* 58, 336–344. doi:10.1139/w11-141.

Li, Y., Heine, S., Entian, M., Sauer, K., and Frankenberg-Dinkel, N. (2013). NO-induced biofilm dispersion in *Pseudomonas aeruginosa* is mediated by an MHYT Domain-coupled phosphodiesterase. *J. Bacteriol.* 195, 3531–3542. doi:10.1128/JB.01156-12.

Marletta, M. A. (1989). Nitric oxide: biosynthesis and biological significance. *Trends Biochem. Sci.* 14, 488–492.

McCollister, B. D., Hoffman, M., Husain, M., and Vazquez-Torres, A. (2011). Nitric oxide protects bacteria from aminoglycosides by blocking the energy-dependent phases of drug uptake▽. *Antimicrob. Agents Chemother.* 55, 2189–2196. doi:10.1128/AAC.01203-10.

McLean, S., Bowman, L. A. H., Sanguinetti, G., Read, R. C., and Poole, R. K. (2010). Peroxynitrite toxicity in *Escherichia coli* K12 elicits expression of oxidative stress responses and protein nitration and nitrosylation. *J. Biol. Chem.* 285, 20724–20731. doi:10.1074/jbc.M109.085506.

Moreno-Vivián, C., Cabello, P., Martínez-Luque, M., Blasco, R., and Castillo, F. (1999). Prokaryotic nitrate reduction: molecular properties and functional distinction among bacterial nitrate reductases. *J. Bacteriol.* 181, 6573–6584.

Morin, J.-P., Preterre, D., Gouriou, F., Delmas, V., François, A., Orange, N., et al. (2013). Particules urbaines et céréalières, micro-organismes, mycotoxines et pesticides. *Pollut. Atmos.* Available at: http://lodel.irevues.inist.fr/pollution-atmospherique/index.php?id=759 [Accessed January 14, 2014].

Morita, Y., Tomida, J., and Kawamura, Y. (2015). Efflux-mediated fluoroquinolone resistance in the multidrug-resistant *Pseudomonas aeruginosa* clinical isolate PA7: identification of a novel MexS variant involved in upregulation of the *mexEF-oprN* multidrug efflux operon. *Antimicrob. Resist. Chemother.* 6, 8. doi:10.3389/fmicb.2015.00008.

Pearce, D. A., Hughes, K. A., Lachlan-Cope, T., Harangozo, S. A., and Jones, A. E. (2010). Biodiversity of airborne microorganisms at Halley Station, Antarctica. *Extrem. Life Extreme Cond.* 14, 145–159. doi:10.1007/s00792-009-0293-8.

Petrova, O. E., Cherny, K. E., and Sauer, K. (2014). The *Pseudomonas aeruginosa* diguanylate cyclase GcbA, a homolog of *P. fluorescens* GcbA, promotes initial attachment to surfaces, but not biofilm formation, via regulation of motility. *J. Bacteriol.* 196, 2827–2841. doi:10.1128/JB.01628-14.

Petrova, O. E., and Sauer, K. (2012). PAS Domain residues and prosthetic group involved in BdlA-dependent dispersion response by *Pseudomonas aeruginosa* biofilms. *J. Bacteriol.* 194, 5817–5828. doi:10.1128/JB.00780-12.

Poole, R. K., Anjum, M. F., Membrillo-Hernández, J., Kim, S. O., Hughes, M. N., and Stewart, V. (1996). Nitric oxide, nitrite, and Fnr regulation of *hmp* (flavohemoglobin) gene expression in *Escherichia coli* K-12. *J. Bacteriol.* 178, 5487–5492.

Redondo-Nieto, M., Barret, M., Morrissey, J., Germaine, K., Martínez-Granero, F., Barahona, E., et al. (2013). Genome sequence reveals that *Pseudomonas fluorescens* F113 possesses a large and diverse array of systems for rhizosphere function and host interaction. *BMC Genomics* 14, 54. doi:10.1186/1471-2164-14-54.

Reduction of pollutant emissions from light vehicles (2015). *Access Eur. Union Law*. Available at: http://eur-lex.europa.eu/legal-content/EN/TXT/?uri=uriserv:l28186 [Accessed September 17, 2015].

Rietsch, A., Vallet-Gely, I., Dove, S. L., and Mekalanos, J. J. (2005). ExsE, a secreted regulator of type III secretion genes in *Pseudomonas aeruginosa*. *Proc. Natl. Acad. Sci. U. S. A.* 102, 8006–8011. doi:10.1073/pnas.0503005102.

Roy, A. B., Petrova, O. E., and Sauer, K. (2012). The phosphodiesterase DipA (PA5017) is essential for *Pseudomonas aeruginosa* biofilm dispersion. *J. Bacteriol.* 194, 2904–2915. doi:10.1128/JB.05346-11.

Šantl-Temkiv, T., Sahyoun, M., Finster, K., Hartmann, S., Augustin-Bauditz, S., Stratmann, F., et al. (2015). Characterization of airborne ice-nucleation-active bacteria and bacterial fragments. *Atmos. Environ.* 109, 105–117. doi:10.1016/j.atmosenv.2015.02.060.

Sastalla, I., Chim, K., Cheung, G. Y. C., Pomerantsev, A. P., and Leppla, S. H. (2009). Codon-optimized fluorescent proteins designed for expression in low-GC Gram-positive bacteria. *Appl. Environ. Microbiol.* 75, 2099–2110. doi:10.1128/AEM.02066-08.

Scales, B. S., Dickson, R. P., LiPuma, J. J., and Huffnagle, G. B. (2014). Microbiology, genomics, and clinical significance of the *Pseudomonas fluorescens* species complex, an unappreciated colonizer of humans. *Clin. Microbiol. Rev.* 27, 927–948. doi:10.1128/CMR.00044-14.

Sher, E. (1998). *Handbook of Air Pollution from Internal Combustion Engines: Pollutant Formation and Control*. Academic Press.

Shiro, Y. (2012). Structure and function of bacterial nitric oxide reductases: Nitric oxide reductase, anaerobic enzymes. *Biochim. Biophys. Acta BBA -*

Bioenerg. 1817, 1907–1913. doi:10.1016/j.bbabio.2012.03.001.

Skalska, K., Miller, J. S., and Ledakowicz, S. (2010). Trends in NO_x abatement: A review. *Sci. Total Environ.* 408, 3976–3989. doi:10.1016/j.scitotenv.2010.06.001.

Smith, P. K., Krohn, R. I., Hermanson, G. T., Mallia, A. K., Gartner, F. H., Provenzano, M. D., et al. (1985). Measurement of protein using bicinchoninic acid. *Anal. Biochem.* 150, 76–85. doi:10.1016/0003-2697(85)90442-7.

Sobel, M. L., Neshat, S., and Poole, K. (2005). Mutations in PA2491 (*mexS*) promote MexT-dependent *mexEF-oprN* expression and multidrug resistance in a clinical strain of *Pseudomonas aeruginosa*. *J. Bacteriol.* 187, 1246–1253. doi:10.1128/JB.187.4.1246-1253.2005.

van Sorge, N. M., Beasley, F. C., Gusarov, I., Gonzalez, D. J., Köckritz-Blickwede, M. von, Anik, S., et al. (2013). Methicillin-resistant *Staphylococcus aureus* bacterial nitric oxide synthase affects antibiotic sensitivity and skin abscess development. *J. Biol. Chem.*, jbc.M112.448738. doi:10.1074/jbc.M112.448738.

Spangler, C., Böhm, A., Jenal, U., Seifert, R., and Kaever, V. (2010). A liquid chromatography-coupled tandem mass spectrometry method for quantitation of cyclic di-guanosine monophosphate. *J. Microbiol. Methods* 81, 226–231. doi:10.1016/j.mimet.2010.03.020.

Spiro, S. (2007). Regulators of bacterial responses to nitric oxide. *FEMS Microbiol. Rev.* 31, 193–211. doi:10.1111/j.1574-6976.2006.00061.x.

Strehmel, J., Neidig, A., Nusser, M., Geffers, R., Brenner-Weiss, G., and Overhage, J. (2014). The sensor kinase PA4398 modulates swarming motility and biofilm formation in *Pseudomonas aeruginosa* PA14. *Appl. Environ. Microbiol.* doi:10.1128/AEM.02832-14.

Tamir, S., Burney, S., and Tannenbaum, S. R. (1996). DNA damage by nitric oxide. *Chem. Res. Toxicol.* 9, 821–827. doi:10.1021/tx9600311.

Vallet-Gely, I., Sharp, J. S., and Dove, S. L. (2007). Local and global regulators linking anaerobiosis to *cupA* fimbrial gene expression in *Pseudomonas aeruginosa*. *J. Bacteriol.* 189, 8667–8676. doi:10.1128/JB.01344-07.

Varivarn, K., Champa, L. A., Silby, M. W., and Robleto, E. A. (2013). Colonization strategies of *Pseudomonas fluorescens* Pf0-1: activation of soil-specific genes important for diverse and specific environments. *BMC Microbiol.* 13, 92. doi:10.1186/1471-2180-13-92.

WHO | Ambient (outdoor) air quality and health (2015). *WHO*. Available at: http://www.who.int/mediacentre/factsheets/fs313/en/ [Accessed September 17, 2015].

Conflict of Interest

We have no conflict of interest to declare.

Author and Contributors

TK contributed to the design of project, experiments, acquisition, analysis, interpretation of data, and wrote the manuscript. CC contributed in genes identification and qRT-PCR analysis. MB contributed to the transformation of *P. fluorescens* strains. MN and GBW participated in c-di-GMP quantification. FD encouraged the study on the airborne bacteria. MF, NO and SC participated in the design and drafted the manuscript. CDP led and coordinated the global project by conceiving the study, and participated in manuscript writing. All authors have read and approved the final manuscript.

Highlight

- The human exposure to well-known air pollutant, NO_2, results in several toxic effects, but bacterial response to NO_2 is not established yet. The NO_2 effects on bacteria were evaluated in terms of motility, biofilm formation, antibiotic resistance, as well as expression of several chosen target genes.
- No modification in tested phenotypes and genes expression was found in bacteria exposed to 0.1 and 5 ppm of NO_2. However, several alterations were observed when the bacteria were exposed to 45 ppm of NO_2.
- *P. fluorescens* strains exposed to NO_2 show reduced swimming motility, and decreased swarming in case of the strain MFN1032.
- Biofilm formed by NO_2-treated airborne *P. fluorescens* MFAF76a shows increased maximum thickness, while NO_2 had no apparent effect on the clinical MFN1032 biofilm structure. However, the c-d-GMP, which is involved in *Pseudomonas* spp. biofilm regulation, seems not to be affected by NO_2 treatment.
- The both NO_2-treated *P. fluorescens* were found to be more resistant to ciprofloxacin and chloramphenicol. Accordingly, the resistance nodulation cell division (RND) MexEF-OprN efflux pump encoding genes were highly upregulated in the two *P. fluorescens* strains.
- Expression of the *hmp*-homologue gene in both tested bacteria, which encodes a NO dioxygenase that is involved in NO detoxification into nitrites, was upregulated in response to NO_2, suggesting a possible common pathway between NO and NO_2 detoxification.

V. General discussion

The members of *P. fluorescens* group are defined as ubiquitously distributed and highly adaptive bacteria, found in majority environmental niches (Scales et al., 2014). This high adaptation capacity is linked with the ability of these bacteria to respond to various stress factors. In this study, the response of *P. fluorescens* to important air pollutant, NO_2 was studied. For this purpose, the airborne *P. fluorescens* MFAF76a strain was exposed to gaseous NO_2 to mimic as far as possible the natural atmospheric conditions. Three NO_2 concentrations were chosen in correlation with NO_2 standards and toxic thresholds. Thus, bacteria were exposed to hourly NO_2 standard 0.1 ppm, recommended by WHO ('WHO | Ambient (outdoor) air quality and health', 2015). In addition, 5 ppm and 45 ppm of NO_2 were studied as concentrations, caused the reversible and irreversible effects on human health respectively. In order to establish the specific to airborne bacteria response to NO_2, the *P. fluorescens* strain MFN1032 with clinical origins was used. In our study for the first time, the bacterial response to the NO_2 contamination was evaluated in terms of membrane response, phenotypic modification, such as motility, biofilm formation, antibiotic resistance, as well as expression of several chosen target genes. After exposure to 0.1 ppm of NO_2 any detectable modification in tested parameters was not found. While the establishment of NO_2 standards on the basis of human health effects, our results could enlarge the NO_2 guideline values to the air microbiota. The similar response was found for bacteria treated with 5 ppm of NO_2. The short-term human exposure to NO_2 in concentrations, close to 5 ppm has been examined in several studies, demonstrating various responses. In healthy volunteers, a two-hour exposure to NO_2 in concentrations from 2.5 ppm to 5 ppm shows a slight, but significant increase of bronchial hyper responsiveness (Beil & Ulmer, 1976). By contrast, the same clinical symptom is not observed after an 75 min exposure to 4 ppm of NO_2 (Linn *et al.*, 1985). Although the absence of detectable modification in bacteria exposed to 0.1 and 5 ppm of NO_2, this free radical could however alter other non-tested targets (*i.e.* DNA and/or protein damages).

Several alterations were observed when the bacteria were exposed to 45 ppm of NO_2. Contrarily to NO, which is involved in biofilm dispersion (Barraud *et al.*, 2015; Cutruzzola & Frankenberg-Dinkel, 2015), we did not observe the NO_2-mediated modifications of bacterial biomass. However, biofilm formed by NO_2-treated airborne strain MFAF76a showed increased maximum thickness, while NO_2 had no apparent effect on the clinical MFN1032 biofilm structure. Given that this phenotype was observed only in airborne *P. fluorescens*, its apparent inability to produce biosurfactant may not counteract the biofilm expansion, contrary to MFN1032, producer of cyclolipopeptides CLP (Rossignol *et al.*, 2008) or to *P. aeruginosa*, rhamnolipid producer (Caiazza *et al.*, 2005; Ochsner *et al.*, 1994). In addition, NO_2 completely inhibits bacterial swarming motility and provokes a slight decreasing of swimming. It is

increasingly evident that biofilm and motility are inversely regulated. The well-known second messenger c-di-GMP plays a central role in this regulation (Hengge, 2009). The c-di-GMP level, as well as the expression of genes, coding for several PDEs was however not affected in response to NO_2 treatment, suggesting that the observed modifications in biofilm architecture and motility seem not to be linked with c-di-GMP pathway, and could be correlated, among other factors, with alterations in flagellar motion, type IV pili and surfactant production.

In addition, our study showed the NO_2-mediated upregulation of the *hmp*-homologue gene in *P. fluorescens* strains MFAF76a and MFN1032, suggesting a possible common pathway between NO and NO_2 detoxification. While the mechanism of NO_2 detoxification was proposed to carry out through the NO_2 reduction pathway (Poole *et al.*, 1996), the expression of the *nirB*-homolog gene, coding for the assimilatory nitrite reductase, which reduces nitrite to ammonium, was not found to be impacted by NO_2. We incline to think, that in presence of ammonium in DMB medium (see **III. Materials and methods**), the production of supplementary ammonium through the nitrite reduction is not appropriate.

The analyses of NO_2-mediated gene expression demonstrated, that NO_2, like its homolog NO, induces the expression of *mexEF-oprN* genes, coding for the RND efflux pump. Its overexpression could be involved in the observed increase of *P. fluorescens* resistance to ciprofloxacin and chloramphenicol. Thus, we could suppose, that NO_2 may stimulate bacterial antibiotic resistance, probably creating antibiotic resistant bacteria, diminishing the effectiveness of antibiotic therapies in polluted area. Although a potential role of MexEF-OprN efflux pump in NO_2-mediated increase of antibiotic resistance, several other mechanisms could also be highlighted. As described in part **3.2. Proteins**, NO is able to impair the oxidative phosphorylation, altering the TCA cycle and ATP production (Appanna *et al.*, 2014). The antibiotic uptake is an energy-dependent process, which requires both an electrochemical gradient across the membrane and an electron flow through the respiratory chain (Fernandes *et al.*, 2007; McCollister *et al.*, 2011; Pagès *et al.*, 2008). In this context, the recently reported NO-mediated metabolism reprogramming and utilization of CiLy-PEPC-PPDK complex for ATP production (Auger & Appanna, 2015) could also be correlated with the NO-mediated modification of bacterial antibiotic resistance. Taken together, these findings let us suspect that, in the similar to NO manner, NO_2 could alter *P. fluorescens* respiration, decreasing the drug uptake, and making bacteria more resistant to antibiotics. In addition to antibiotic resistance, the overexpression of *mexEF-oprN* genes could also impact bacterial motility, as previously described (see part **4.4. NO release**) and reported by (Lamarche & Déziel, 2011).

Therefore, the question of NO_2 impact on bacterial virulence remains to be studied in more details. An arsenal of virulence factors was reported and appears to impact on the pathogenicity of *P. fluorescens*. Included among these are cell-associated factors such as lipopolysaccharide (Picot *et al.*, 2003), the exopolysaccharide alginate (Bakkevig *et al.*, 2005), and secreted factors including toxins, proteases and lipases (Russell, 2002), phospholipases (Rossignol *et al.*, 2008; Sperandio *et al.*, 2010) and small molecules such as phenazines (Laursen & Nielsen, 2004; Weller *et al.*, 2007), cyclolipopeptides (Duclairoir-Poc, 2011), hydrogen cyanide (Ramette *et al.*, 2003), 2,4-diacetylphloroglucinol (Moynihan *et al.*, 2009), and rhizoxin (Gross & Loper, 2009). Quorum-sensing, type 3 and type 6 secretion (Decoin *et al.*, 2014; Marchi *et al.*, 2013; Mavrodi *et al.*, 2011) and many other regulatory systems are important for *P. fluorescens* virulence (Scales *et al.*, 2014). To refine the role of NO_2 in the regulation of bacterial virulence, the mechanism of bacterial response to its toxicity could be clarified with a better knowledge of the effect of such exposition on the expression of those virulence factors.

Furthermore, in study of bacterial response to stressor factors, the membrane response must to be kept in mind. First of all, the lipidome of two tested *P. fluorescens* strains was characterized using a HPTLC-MALDI-TOF MSI tool. The PE, PG and PC are found as major compounds of lipidome of these bacteria. In addition, the presence of another, new and not identified yet GP spot (UGP) was detected. This GP is found predominantly in stationary growth phase, indicating its role at this stage of bacterial development. Interestingly, in exposed to 45 ppm of NO_2 bacteria, the UGP was not detected, that means at least a decrease, if not a complete loss of this lipid with a possible modification of its production. Opposite results are demonstrated in study of *P. fluorescens* adaptation to the increasing temperature. In clinical MFN1032 grown at 37°C, the UGP is detected even in exponential growth phase indicating its potential role in temperature adaptation. All together, these results let us suppose, that the UGP may play a role in membrane adaptation to several stress factors. As reported in **Chapter 2 Stress factors and *Pseudomonas fluorescens* lipid adaptation** and **Table 1**, CL often plays an important role in bacterial adaptation to stress (Romantsov *et al.*, 2009). Like our UGP, CL has a "high" molar mass for bacterial GP and is synthesized, in majority, in stationary growth phase (Kondakova *et al.*, 2015; Mileykovskaya & Dowhan, 2009). In correlation with the similarities of PSD spectra of UGP with that ones of PG, these observations let us imagine a possible analogy between CL and UGP, especially since the various analogs of CL were found in Archaea (Corcelli, 2009). Naturally, without a complete identification of its chemical structure and metabolic pathway(s) for its synthesis, the role(s) of UGP is still unknown.

Many studies reported the involvement of FAs in membrane adaptive response to stress factors (Hachicho *et al.*, 2014; Heipieper & Fischer, 2010). Our results demonstrate that NO_2 does not

modify the degree of FA saturation, indicating that bacterial FAs are not involved in response to NO_2. In fact, in atmosphere, NO_2 and its dimer, N_2O_4 are simple, not charged and lipophilic molecules (see part **1. Nitrogen oxides (NOx)**), which freely penetrate bacterial membrane (Signorelli *et al.*, 2011) without any modification of FA composition. However, the study of bacterial surface after NO_2 exposure demonstrates a significant decrease in membrane electron-accepting properties. Thus, the membrane response to NO_2 may be based, among others, on the modifications in GP head groups (Möller *et al.*, 2008; Pryor *et al.*, 1982). The MS and PSD analyses, performed in our study, did not show any modification (nitration and/or oxidation) of GPs, suggesting the absence of NO_2 reactions with bacterial monounsaturated FA chains. However, the GP composition, in other words the ratio of anionic to zwitterionic GPs, could be modified in order to adapt to nitrosative stress. Thus, the increase of PC production, as well as a possible loss of UGP may explain this membrane modification. In addition, the membrane electron-accepting properties are directly linked with respiratory chain, which was found to be damaged by RNS (Auger *et al.*, 2011; Husain *et al.*, 2008). In accord with the NO-mediated inhibition of *P. aeruginosa* respiration (McCollister *et al.*, 2011), NO_2 could also cause the nitrosylation of [Fe-S] clusters of respiratory chain proteins (for more details see part **Proteins**), decreasing the electron-accepting membrane properties. In the context of recently demonstrated involvement of bacterial lipids in biofilm regulation (Blanka *et al.*, 2015; Davies & Marques, 2009), the modifications in GP composition could be related with NO_2-mediated biofilm modifications. The NO_2-mediated alterations of membrane GPs could also impact membrane permeability, facilitating the penetration of several antibiotics, including aminoglycosides, into bacterial cells. Altogether, these data indicate a possible link between the NO_2-mediated decrease of aminoglycoside resistance observed in our study and the observed alterations in membrane GP composition.

VI. Conclusions and perspectives

For the first time, the response of airborne *P. fluorescens* to stress factors, such as a major air pollutant NO_2, was studied. The tests of the effect of NO_2 contamination in terms of membrane response, motility, biofilm formation, antibiotic resistance, as well as expression of several chosen target genes did not show any detectable modification in bacteria, treated with 0.1 and 5 ppm of NO_2. While this absence of modification, NO_2 could cause bacterial functioning alterations, which are unrevealed through used approaches. In order to better understand the NO_2 effect on airborne bacteria, the protein modifications (*i.e.* S-nitrosylation, reactions of NO_2 with metal centers, or tyrosine nitration) and NO_2-mediated DNA damages, as well as the possible NO_2 sensors and repair mechanisms may be investigated. In this context, it will be interesting to add for this study other NO_2 concentrations, such as the mean annual NO_2 concentration in France (44 $\mu g/m^3$ - 0.02 ppm, see part **6.3. NOx level in atmosphere**) and to test various exposure times and/or cycles of exposure. In addition, NO in low concentrations between 0.001 and 0.02 ppm (52 and 500 nM respectively) has an effect on bacterial metabolism and homeostasis, altering, bacterial biofilm formation and damaging DNA (Barraud *et al.*, 2006; Woodmansee & Imlay, 2003). Thus, the assays of such NO_2 concentrations might clarify the correlation between the NO and NO_2 stress, and establish the response of airborne bacteria to atmospheric NO_2 level. Finally, to better mimic environmental conditions, bacteria could be directly exposed to the exhaust gas stream.

Several alterations were observed when the bacteria were treated with 45 ppm of NO_2. Contrarily to the well-studied NO induction of biofilm dispersion, we did not observe the NO_2-mediated modifications of bacterial biomass. However, the alteration in the biofilm architecture of NO_2-treated airborne *P. fluorescens* MFAF76a is monitores. NO_2-exposed *P. fluorescens* strains show reduced swimming motility, and decreased swarming in case of the strain MFN1032. These NO_2-mediated modifications seem to not be linked to c-di-GMP regulatory network, and could be correlated, among other factors, with alterations in flagellar motion, type IV pili and surfactant production. In this way, the supplementary studies concerning NO_2-medited surfactant production, and flagellar synthesis will complete this study, allowing an enhanced understanding of the NO_2 effect on bacterial cells.

The analyses of NO_2-mediated gene expression demonstrated, that NO_2, like its homolog NO, upregulated the *hmp*-homologue gene in *P. fluorescens* strains MFAF76a and MFN1032 expression, suggesting a possible common pathway between NO and NO_2 detoxification. While the Hmp-meidiated NO_2 detoxification was proposed to carry out through the NO_2 reduction pathway (Poole *et al.*, 1996), the expression of *nirB*-homolog genes, coding for assimilatory nitrite reductase NirBD was not found to be impacted by NO_2 treatment in the present work. However, in order to better understand the mechanism of NO_2 detoxification, the Hmp-, Nir-

and Nas-mediated mechanisms should be investigated in more details. Thus, the supplementary proteomic studies in combination with the site-directed mutagenesis could be performed. In addition, NO_2 appears to induce the expression of *mexEF-oprN* genes, coding for the RND efflux pump. Its overexpression could be involved in the observed increase of *P. fluorescens* resistance to ciprofloxacin and chloramphenicol, while the resistance to aminoglycosides, including tobramycin and kanamycin is decreased. This decrease seems to be independent on the expression of *mexXY* genes, and could be linked, among other factors, with observed in our study NO_2-mediated alterations of membrane GPs.

Concerning the lipidome studies, for the first time, in the lipidome of *P. fluorescens*, a new and currently unknown glycerophospholipid (UGP) is observed. Remarkably, this GP is undetected in bacteria exposed to high NO_2 concentration. Interestingly, in airborne *P. fluorescens* grown without stress addition, this UGP is only detected in stationary growth phase. Conversely, in clinical *P. fluorescens* strain growing at human body temperature, the UGP is supposed to be produced even in exponential phase of growth. All together, these data indicate, that UGP may be involved in *P. fluorescens* adaptation to stress conditions. In this way, the complete chemical characterization of this GP, with the establishment of pathway(s) for its synthesis is an attractive research opportunity. No NO_2 effect on fatty acid composition was observed, indicating that NO_2 does not modify the membrane fluidity. While the absence of NO_2-mediated modification of the net membrane charge, the membrane electron-accepting properties were deceased after NO_2 exposure. Given that several factors could be involved in these NO_2-mediated surface modifications, the supplementary quantitative studies of NO_2 effect on membrane GPs and proteins, as well as the bacterial respiration upon NO_2-mediated nitrosative stress conditions could be evaluated.

Finally, the bacterial response to NO_2 contamination, established here, is just the beginning of the long road ahead to achieve the goal(s) of a wide area of researches about the effect of atmospheric pollution on air microbiota. The ultimate goals of this topic would be to establish the NO_2 effect on bacterial functioning, as well as toxicity and pathogenicity against eukaryotic hosts. In this context, the virulence factors expression, in combination with genomic studies and cytotoxicity tests should be used.

VII. References

ADEME. **(2015, Mai).** La pollution de l'air extérieur.

Ahern, H. E., Walsh, K. A., Hill, T. C. J. & Moffett, B. F. (2007). Fluorescent pseudomonads isolated from Hebridean cloud and rain water produce biosurfactants but do not cause ice nucleation. *Biogeosciences* **4**, 115–124.

Almeida, J. S., Júlio, S. M., Reis, M. A. & Carrondo, M. J. (1995). Nitrite inhibition of denitrification by *Pseudomonas fluorescens*. *Biotechnol Bioeng* **46**, 194–201.

Van Alst, N. E., Picardo, K. F., Iglewski, B. H. & Haidaris, C. G. (2007). Nitrate sensing and metabolism modulate motility, biofilm formation, and virulence in *Pseudomonas aeruginosa*. *Infect Immun* **75**, 3780–3790.

Van Alst, N. E., Sherrill, L. A., Iglewski, B. H. & Haidaris, C. G. (2009). Compensatory periplasmic nitrate reductase activity supports anaerobic growth of *Pseudomonas aeruginosa* PAO1 in the absence of membrane nitrate reductase. *Can J Microbiol* **55**, 1133–1144.

Altschul, S. F., Madden, T. L., Schäffer, A. A., Zhang, J., Zhang, Z., Miller, W. & Lipman, D. J. (1997). Gapped BLAST and PSI-BLAST: a new generation of protein database search programs. *Nucleic Acids Res* **25**, 3389–3402.

Alvarez, B. & Radi, R. (2003). Peroxynitrite reactivity with amino acids and proteins. *Amino Acids* **25**, 295–311.

Alvarez-Ortega, C., Olivares, J. & Martinez, J. L. (2013). RND multidrug efflux pumps: what are they good for? *Antimicrob Resist Chemother* **4**, 7.

Anderson, N., Strader, R. & Davidson, C. (2003). Airborne reduced nitrogen: ammonia emissions from agriculture and other sources. *Environ Int*, Future Directions in air quality research : Ecological, Atmospheric, Regulatory / Policy / Economic, and Educational Issues **29**, 277–286.

Antelmann, H. & Helmann, J. D. (2011). Thiol-based redox switches and gene regulation. *Antioxid Redox Signal* **14**, 1049–1063.

Anzai, Y., Kim, H., Park, J. Y., Wakabayashi, H. & Oyaizu, H. (2000). Phylogenetic affiliation of the pseudomonads based on 16S rRNA sequence. *Int J Syst Evol Microbiol* **50 Pt 4**, 1563–1589.

Appanna, V. P., Auger, C., Thomas, S. C. & Omri, A. (2014). Fumarate metabolism and ATP production in *Pseudomonas fluorescens* exposed to nitrosative stress. *Antonie Van Leeuwenhoek* **106**, 431–438.

Arai, H., Kodama, T. & Igarashi, Y. (1997). Cascade regulation of the two CRP/FNR-related transcriptional regulators (ANR and DNR) and the denitrification enzymes in *Pseudomonas aeruginosa*. *Mol Microbiol* **25**, 1141–1148.

Arai, H. (2011). Regulation and function of versatile aerobic and anaerobic respiratory metabolism in *Pseudomonas aeruginosa*. *Front Microbiol* **2**.

Arai, H. & Iiyama, K. (2013). Role of nitric oxide-detoxifying enzymes in the virulence of *Pseudomonas aeruginosa* against the silkworm, *Bombyx mori*. *Biosci Biotechnol Biochem* **77**, 198–200.

Arai, H., Sanbongi, Y., Igarashi, Y. & Kodama, T. (1990). Cloning and sequencing of the gene encoding cytochrome *c*-551 from *Pseudomonas aeruginosa*. *FEBS Lett* **261**, 196–198.

Arai, H., Igarashi, Y. & Kodama, T. (1994). Structure and ANR-dependent transcription of the *nir* genes for denitrification from *Pseudomonas aeruginosa*. *Biosci Biotechnol Biochem* **58**, 1286–1291.

Arai, H., Igarashi, Y. & Kodama, T. (1995a). The structural genes for nitric oxide reductase from *Pseudomonas aeruginosa*. *Biochim Biophys Acta BBA - Gene Struct Expr* **1261**, 279–284.

Arai, H., Igarashi, Y. & Kodama, T. (1995b). Expression of the *nir* and *nor* genes for denitrification of *Pseudomonas aeruginosa* requires a novel CRP/FNR-related transcriptional regulator, DNR, in addition to ANR. *FEBS Lett* **371**, 73–76.

Arai, H., Mizutani, M. & Igarashi, Y. (2003). Transcriptional regulation of the *nos* genes for nitrous oxide reductase in *Pseudomonas aeruginosa*. *Microbiology* **149**, 29–36.

Arai, H., Hayashi, M., Kuroi, A., Ishii, M. & Igarashi, Y. (2005). Transcriptional regulation of the flavohemoglobin gene for aerobic nitric oxide detoxification by the second nitric oxide-responsive regulator of *Pseudomonas aeruginosa*. *J Bacteriol* **187**, 3960–3968.

Arasimowicz-Jelonek, M. & Floryszak-Wieczorek, J. (2014). Nitric oxide: an effective weapon of the plant or the pathogen? *Mol Plant Pathol* **15**, 406–416.

Arat, S., Bullerjahn, G. S. & Laubenbacher, R. (2015). A network biology approach to denitrification in *Pseudomonas aeruginosa*. *PLoS ONE* **10**, e0118235.

Arendt, W., Groenewold, M. K., Hebecker, S., Dickschat, J. S. & Moser, J. (2013). Identification and characterization of a periplasmic aminoacyl-phosphatidylglycerol hydrolase responsible for *Pseudomonas aeruginosa* lipid homeostasis. *J Biol Chem* **288**, 24717–24730.

Arens, F., Gutzwiller, L., Baltensperger, U., Gäggeler, H. W. & Ammann, M. (2001). Heterogeneous reaction of NO_2 on diesel soot particles. *Environ Sci Technol* **35**, 2191–2199.

D'Argenio, D. A. & Miller, S. I. (2004). Cyclic di-GMP as a bacterial second messenger. *Microbiology* **150**, 2497–2502.

Arora, D. P. & Boon, E. M. (2012). Nitric oxide regulated two-component signaling in *Pseudoalteromonas atlantica*. *Biochem Biophys Res Commun* **421**, 521–526.

Arvizo, R. R., Bhattacharyya, S., Kudgus, R., Giri, K., Bhattacharya, R. & Mukherjee, P. (2012). Intrinsic therapeutic applications of noble metal nanoparticles: past, present and future. *Chem Soc Rev* **41**, 2943–2970.

Attard, E., Yang, H., Delort, A.-M., Amato, P., Pöschl, U., Glaux, C., Koop, T. & Morris, C. E. (2012). Effects of atmospheric conditions on ice nucleation activity of *Pseudomonas*. *Atmospheric Chem Phys* **12**, 10667–10677.

Auger, C. & Appanna, V. D. (2015). A novel ATP-generating machinery to counter nitrosative stress is mediated by substrate-level phosphorylation. *Biochim Biophys Acta BBA - Gen Subj* **1850**, 43–50.

Auger, C., Lemire, J., Cecchini, D., Bignucolo, A. & Appanna, V. D. (2011). The metabolic reprogramming evoked by nitrosative stress triggers the anaerobic utilization of citrate in *Pseudomonas fluorescens*. *PLoS ONE* **6**.

Augusto, O., Bonini, M. G., Amanso, A. M., Linares, E., Santos, C. C. X. & De Menezes, S. L. (2002). Nitrogen dioxide and carbonate radical anion: two emerging radicals in biology. *Free Radic Biol Med* **32**, 841–859.

D'Autréaux, B., Touati, D., Bersch, B., Latour, J.-M. & Michaud-Soret, I. (2002). Direct inhibition by nitric oxide of the transcriptional ferric uptake regulation protein via nitrosylation of the iron. *Proc Natl Acad Sci U S A* **99**, 16619–16624.

D'Autréaux, B., Horner, O., Oddou, J.-L., Jeandey, C., Gambarelli, S., Berthomieu, C., Latour, J.-M. & Michaud-Soret, I. (2004). Spectroscopic description of the two nitrosyl-iron complexes responsible for *fur* inhibition by nitric oxide. *J Am Chem Soc* **126**, 6005–6016.

Ayora, S., Carrasco, B., Cárdenas, P. P., César, C. E., Cañas, C., Yadav, T., Marchisone, C. & Alonso, J. C. (2011). Double-strand break repair in bacteria: a view from *Bacillus subtilis*. *FEMS Microbiol Rev* **35**, 1055–1081.

Baatout, S., Leys, N., Hendrickx, L., Dams, A. & Mergeay, M. (2007). Physiological changes induced in bacteria following pH stress as a model for space research. *Acta Astronaut*, Benefits of human presence in space - historical, scientific, medical, cultural and political aspects. A selection of papers presented at the 15th IAA Humans in Space Symposium, Graz, Austria, 2005 **60**, 451–459.

Bahrani-Mougeot, F. K., Paster, B. J., Coleman, S., Barbuto, S., Brennan, M. T., Noll, J., Kennedy, T., Fox, P. C. & Lockhart, P. B. (2007). Molecular analysis of oral and respiratory bacterial species associated with ventilator-associated pneumonia. *J Clin Microbiol* **45**, 1588–1593.

Bakkevig, K., Sletta, H., Gimmestad, M., Aune, R., Ertesvåg, H., Degnes, K., Christensen, B. E., Ellingsen, T. E. & Valla, S. (2005). Role of the *Pseudomonas fluorescens* alginate lyase (AlgL) in clearing the periplasm of alginates not exported to the extracellular environment. *J Bacteriol* **187**, 8375–8384.

Barahona, E., Navazo, A., Yousef-Coronado, F., Aguirre de Cárcer, D., Martínez-Granero, F., Espinosa-Urgel, M., Martín, M. & Rivilla, R. (2010). Efficient rhizosphere colonization by *Pseudomonas fluorescens* f113 mutants unable to form biofilms on abiotic surfaces. *Environ Microbiol* **12**, 3185–3195.

Barathi, S. & Vasudevan, N. (2001). Utilization of petroleum hydrocarbons by *Pseudomonas fluorescens* isolated from a petroleum-contaminated soil. *Environ Int*, Environmental Geochemistry in the Tropics and Subtropics **26**, 413–416.

Barnes, R. J., Bandi, R. R., Wong, W. S., Barraud, N., McDougald, D., Fane, A., Kjelleberg, S. & Rice, S. A. (2013). Optimal dosing regimen of nitric oxide donor compounds for the reduction of *Pseudomonas aeruginosa* biofilm and isolates from wastewater membranes. *Biofouling* **29**, 203–212.

Barraud, N., Hassett, D. J., Hwang, S.-H., Rice, S. A., Kjelleberg, S. & Webb, J. S. (2006). Involvement of nitric oxide in biofilm dispersal of *Pseudomonas aeruginosa*. *J Bacteriol* **188**, 7344–7353.

Barraud, N., Storey, M. V., Moore, Z. P., Webb, J. S., Rice, S. A. & Kjelleberg, S. (2009a). Nitric oxide-mediated dispersal in single- and multi-species biofilms of clinically and industrially relevant microorganisms. *Microb Biotechnol* **2**, 370–378.

Barraud, N., Schleheck, D., Klebensberger, J., Webb, J. S., Hassett, D. J., Rice, S. A. & Kjelleberg, S. (2009b). Nitric oxide signaling in *Pseudomonas aeruginosa* biofilms mediates phosphodiesterase activity, decreased cyclic di-GMP levels, and enhanced dispersal. *J Bacteriol* **191**, 7333–7342.

Barraud, N., Kelso, M. J., Rice, S. A. & Kjelleberg, S. (2015). Nitric oxide: a key mediator of biofilm dispersal with applications in infectious diseases. *Curr Pharm Des* **21**, 31–42.

Bauer, H., Kasper-Giebl, A., Löflund, M., Giebl, H., Hitzenberger, R., Zibuschka, F. & Puxbaum, H. (2002). The contribution of bacteria and fungal spores to the organic carbon content of cloud water, precipitation and aerosols. *Atmospheric Res* **64**, 109–119.

Baumgarten, T., Sperling, S., Seifert, J., Bergen, M. von, Steiniger, F., Wick, L. Y. & Heipieper, H. J. (2012). Membrane vesicle formation as a multiple-stress response mechanism enhances *Pseudomonas putida* DOT-T1E cell surface hydrophobicity and biofilm formation. *Appl Environ Microbiol* **78**, 6217–6224.

Baum, M. M., Kainović, A., O'Keeffe, T., Pandita, R., McDonald, K., Wu, S. & Webster, P. (2009). Characterization of structures in biofilms formed by a

Pseudomonas fluorescens isolated from soil. *BMC Microbiol* **9**, 103.

Bayer, A. S. & Murray, B. E. (2009). Initial low-dose aminoglycosides in *Staphylococcus aureus* bacteremia: good science, urban legend, or just plain toxic? *Clin Infect Dis* **48**, 722–724.

Baysse, C. & O'Gara, F. (2007). Role of membrane structure during stress signaling and adaptation in *Pseudomonas*. In *Pseudomonas Vol 6 Mol Microbiol Infect Biodivers*. Juan-Luis Ramos and Alain Filloux.

Bedzyk, L., Wang, T. & Ye, R. W. (1999). The periplasmic nitrate reductase in *Pseudomonas* sp. strain G-179 catalyzes the first step of denitrification. *J Bacteriol* **181**, 2802–2806.

Beil, M. & Ulmer, W. T. (1976). Effect of NO_2 in workroom concentrations on respiratory mechanics and bronchial susceptibility to acetylcholine in normal persons. *Int Arch Occup Environ Health* **38**, 31–44.

Bell, L. C., Richardson, D. J. & Ferguson, S. J. (1990). Periplasmic and membrane-bound respiratory nitrate reductases in *Thiosphaera pantotropha*. The periplasmic enzyme catalyzes the first step in aerobic denitrification. *FEBS Lett* **265**, 85–87.

Bellon-Fontaine, M.-N., Rault, J. & van Oss, C. J. (1996). Microbial adhesion to solvents: a novel method to determine the electron-donor/electron-acceptor or Lewis acid-base properties of microbial cells. *Colloids Surf B Biointerfaces* **7**, 47–53.

Benito, N., Mirelis, B., Luz Gálvez, M., Vila, M., López-Contreras, J., Cotura, A., Pomar, V., March, F., Navarro, F. & other authors. **(2012).** Outbreak of *Pseudomonas fluorescens* bloodstream infection in a coronary care unit. *J Hosp Infect* **82**, 286–289.

Berks, B. C., Ferguson, S. J., Moir, J. W. B. & Richardson, D. J. (1995). Enzymes and associated electron transport systems that catalyse the respiratory reduction of nitrogen oxides and oxyanions. *Biochim Biophys Acta BBA - Bioenerg* **1232**, 97–173.

Bernagaud, C., Burkhart, J.-F., Vidal, B., Lepriol, T., Petit, J.-F., Brunel, T., Gouriou, F. & Préterre, D. (2014, février). Observations du ratio NO_2/NO_x en tunnel routier. *Pollution-Atmospherique*.

Bernal, P., Muñoz-Rojas, J., Hurtado, A., Ramos, J. L. & Segura, A. (2007). A *Pseudomonas putida* cardiolipin synthesis mutant exhibits increased sensitivity to drugs related to transport functionality. *Environ Microbiol* **9**, 1135–1145.

Bethke, P. C., Badger, M. R. & Jones, R. L. (2004). Apoplastic synthesis of nitric oxide by plant tissues. *Plant Cell* **16**, 332–341.

Beveridge, T. J. (2005). Bacterial cell wall structure and implications for interactions with metal ions and minerals.

Beveridge, T. J. & Koval, S. F. (1981). Binding of metals to cell envelopes of *Escherichia coli* K-12. *Appl Environ Microbiol* **42**, 325–335.

Bhakoo, M. & Herbert, R. A. (1980). Fatty acid and phospholipid composition of five psychrotrophic *Pseudomonas* spp. grown at different temperatures. *Arch Microbiol* **126**, 51–55.

B. Huebert, P. V. (1999). Volcano fixes nitrogen into plant-available forms. *Biogeochemistry* **47**, 111–118.

Blanka, A., Düvel, J., Dötsch, A., Klinkert, B., Abraham, W.-R., Kaever, V., Ritter, C., Narberhaus, F. & Häussler, S. (2015). Constitutive production of c-di-GMP is associated with mutations in a variant of *Pseudomonas aeruginosa* with altered membrane composition. *Sci Signal* **8**, ra36–ra36.

Bligh, E. G. & Dyer, W. J. (1959). A rapid method of total lipid extraction and purification. *Biochem Cell Biol* **37**, 911–917.

Blomberg, A., Krishna, M. T., Bocchino, V., Biscione, G. L., Shute, J. K., Kelly, F. J., Frew, A. J., Holgate, S. T. & Sandström, T. (1997). The inflammatory effects of 2 ppm NO_2 on the airways of healthy subjects. *Am J Respir Crit Care Med* **156**, 418–424.

Bodilis, J., Calbrix, R., Guérillon, J., Mérieau, A., Pawlak, B., Orange, N. & Barray, S. (2004). Phylogenetic relationships between environmental and clinical isolates of *Pseudomonas fluorescens* and related species deduced from 16S rRNA gene and OprF protein sequences. *Syst Appl Microbiol* **27**, 93–108.

Bodilis, J., Nsigue Meilo, S., Cornelis, P., De Vos, P. & Barray, S. (2011). A long-branch attraction artifact reveals an adaptive radiation in *Pseudomonas*. *Mol Biol Evol* **28**, 2723–2726.

Bodilis, J., Nsigue-Meilo, S., Besaury, L. & Quillet, L. (2012). Variable copy number, intra-genomic heterogeneities and lateral transfers of the 16S rRNA gene in *Pseudomonas*. *PLoS ONE* **7**, e35647.

Bogdanov, M., Dowhan, W. & Vitrac, H. (2013). Lipids and topological rules governing membrane protein assembly. *Biochim Biophys Acta*.

Boichu, M., Oppenheimer, C., Roberts, T. J., Tsanev, V. & Kyle, P. R. (2011). On bromine, nitrogen oxides and ozone depletion in the tropospheric plume of Erebus volcano (Antarctica). *Atmos Environ* **45**, 3856–3866.

Boiteux, S. & Guillet, M. (2004). Abasic sites in DNA: repair and biological consequences in *Saccharomyces cerevisiae*. *DNA Repair* **3**, 1–12.

Bonamore, A., Farina, A., Gattoni, M., Schininà, M. E., Bellelli, A. & Boffi, A. (2003a). Interaction with membrane lipids and heme ligand binding properties of *Escherichia coli* flavohemoglobin. *Biochemistry (Mosc)* **42**, 5792–5801.

Bonamore, A., Gentili, P., Ilari, A., Schininà, M. E. & Boffi, A. (2003b). *Escherichia coli* flavohemoglobin is an efficient alkylhydroperoxide reductase. *J Biol Chem* **278**, 22272–22277.

Boor, K. J. (2006). Bacterial stress responses: what doesn't kill them can make them stronger. *PLoS Biol* **4**.

Bos, M. P., Robert, V. & Tommassen, J. (2007). Biogenesis of the Gram-negative bacterial outer membrane. *Annu Rev Microbiol* **61**, 191–214.

Bovallius, A., Bucht, B., Roffey, R. & Anäs, P. (1978). Long-range air transmission of bacteria. *Appl Environ Microbiol* **35**, 1231–1232.

Bowers, R. M., Lauber, C. L., Wiedinmyer, C., Hamady, M., Hallar, A. G., Fall, R., Knight, R. & Fierer, N. (2009). Characterization of airborne microbial communities at a high-elevation site and their potential to act as atmospheric ice nuclei. *Appl Environ Microbiol* **75**, 5121–5130.

Boyd, C. D., Chatterjee, D., Sondermann, H. & O'Toole, G. A. (2012). LapG, required for modulating biofilm formation by *Pseudomonas fluorescens* Pf0-1, is a calcium-dependent protease. *J Bacteriol* **194**, 4406–4414.

Boyd, C. D., Smith, T. J., El-Kirat-Chatel, S., Newell, P. D., Dufrêne, Y. F. & O'Toole, G. A. (2014). Structural features of the *Pseudomonas fluorescens* biofilm adhesin LapA required for LapG-dependent cleavage, biofilm formation, and cell surface localization. *J Bacteriol* **196**, 2775–2788.

Brandes, N., Rinck, A., Leichert, L. I. & Jakob, U. (2007). Nitrosative stress treatment of *E. coli* targets distinct set of thiol-containing proteins. *Mol Microbiol* **66**, 901–914.

Brenman, J. E., Chao, D. S., Xia, H., Aldape, K. & Bredt, D. S. (1995). Nitric oxide synthase complexed with dystrophin and absent from skeletal muscle sarcolemma in Duchenne muscular dystrophy. *Cell* **82**, 743–752.

Brenner, D. J., Krieg, N. R., Staley, J. T., Garrity, G. M., Boone, D. R., De Vos, P., Goodfellow, M., Rainey, F. A. & Schleifer, K.-H. (Eds.). (2005). *Bergey's Manual® of Systematic Bacteriology*. Boston, MA: Springer US.

Brook, R. D., Rajagopalan, S., Pope, C. A., Brook, J. R., Bhatnagar, A., Diez-Roux, A. V., Holguin, F., Hong, Y., Luepker, R. V. & other authors. (2010). Particulate matter air pollution and cardiovascular disease: an update to the scientific statement from the American Heart Association. *Circulation* **121**, 2331–2378.

Brown, G. C. (1995). Reversible binding and inhibition of catalase by nitric oxide. *Eur J Biochem* **232**, 188–191.

Bruckdorfer, R. (2005). The basics about nitric oxide. *Mol Aspects Med*, Nitric oxide in physiology and pathology **26**, 3–31.

Brunekreef, B. & Holgate, S. (2002). Air pollution and health. *The Lancet* **360**, 1233–1242.

Burney, S., Caulfield, J. L., Niles, J. C., Wishnok, J. S. & Tannenbaum, S. R. (1999). The chemistry of DNA damage from nitric oxide and peroxynitrite. *Mutat Res Mol Mech Mutagen* **424**, 37–49.

Burrows, S. M., Elbert, W., Lawrence, M. G. & Pöschl, U. (2009a). Bacteria in the global atmosphere – Part 1: Review and synthesis of literature data for different ecosystems. *Atmos Chem Phys* **9**, 9263–9280.

Burrows, S. M., Butler, T., Jöckel, P., Tost, H., Kerkweg, A., Pöschl, U. & Lawrence, M. G. (2009b). Bacteria in the global atmosphere – Part 2: Modeling of emissions and transport between different ecosystems. *Atmos Chem Phys* **9**, 9281–9297.

Butterbach-Bahl, K., Baggs, E. M., Dannenmann, M., Kiese, R. & Zechmeister-Boltenstern, S. (2013). Nitrous oxide emissions from soils: how well do we understand the processes and their controls? *Philos Trans R Soc Lond B Biol Sci* **368**, 20130122.

Bylin, G., Hedenstierna, G., Lindvall, T. & Sundin, B. (1988). Ambient nitrogen dioxide concentrations increase bronchial responsiveness in subjects with mild asthma. *Eur Respir J* **1**, 606–612.

Cabiscol, E., Tamarit, J. & Ros, J. (2000). Oxidative stress in bacteria and protein damage by reactive oxygen species. *Int Microbiol Off J Span Soc Microbiol* **3**, 3–8.

Caiazza, N. C., Shanks, R. M. Q. & O'Toole, G. A. (2005). Rhamnolipids modulate swarming motility patterns of *Pseudomonas aeruginosa*. *J Bacteriol* **187**, 7351–7361.

Caiazza, N. C., Merritt, J. H., Brothers, K. M. & O'Toole, G. A. (2007). Inverse regulation of biofilm formation and swarming motility by *Pseudomonas aeruginosa* PA14. *J Bacteriol* **189**, 3603–3612.

Calvio, C., Celandroni, F., Ghelardi, E., Amati, G., Salvetti, S., Ceciliani, F., Galizzi, A. & Senesi, S. (2005). Swarming differentiation and swimming motility in *Bacillus subtilis* are controlled by *swrA*, a newly identified dicistronic operon. *J Bacteriol* **187**, 5356–5366.

Campbell, W. H. & Kinghorn, J. R. (1990). Functional domains of assimilatory nitrate reductases and nitrite reductases. *Trends Biochem Sci* **15**, 315–319.

Carlson, C. A., Ferguson, L. P. & Ingraham, J. L. (1982). Properties of dissimilatory nitrate reductase purified from the denitrifier *Pseudomonas aeruginosa*. *J Bacteriol* **151**, 162–171.

de Carvalho, C. C. (2012). Adaptation of *Rhodococcus erythropolis* cells for growth and bioremediation under extreme conditions. *Res Microbiol* **163**, 125–136.

de Carvalho, C. C. & da Fonseca, M. M. (2005). Degradation of hydrocarbons and alcohols at different temperatures and salinities by *Rhodococcus erythropolis* DCL14. *FEMS Microbiol Ecol* **51**, 389–399.

de Carvalho, C. C., Marques, M. P., Hachicho, N. & Heipieper, H. J. (2014). Rapid adaptation of *Rhodococcus erythropolis* cells to salt stress by synthesizing polyunsaturated fatty acids. *Appl Microbiol Biotechnol* **98**, 5599–5606.

Cary, S. P. L., Winger, J. A., Derbyshire, E. R. & Marletta, M. A. (2006). Nitric oxide signaling: no longer simply on or off. *Trends Biochem Sci* **31**, 231–239.

Casaz, P., Happel, A., Keithan, J., Read, D. L., Strain, S. R. & Levy, S. B. (2001). The *Pseudomonas fluorescens* transcription activator AdnA is required for adhesion and motility. *Microbiology* **147**, 355–361.

Castiglione, N., Rinaldo, S., Giardina, G. & Cutruzzolà, F. (2009). The transcription factor DNR from *Pseudomonas aeruginosa* specifically requires nitric oxide and haem for the activation of a target promoter in *Escherichia coli*. *Microbiol Read Engl* **155**, 2838–2844.

Catucci, L., Depalo, N., Lattanzio, V. M. T., Agostiano, A. & Corcelli, A. (2004). Neosynthesis of cardiolipin in *Rhodobacter sphaeroides* under osmotic stress. *Biochemistry (Mosc)* **43**, 15066–15072.

Cébron, A., Arsène-Ploetze, F., Bauda, P., Bertin, P. N., Billard, P., Carapito, C., Devin, S., Goulhen-Chollet, F., Poirel, J. & Leyval, C. (2014). Rapid impact of phenanthrene and arsenic on bacterial community structure and activities in sand batches. *Microb Ecol* **67**, 129–144.

Chaloulakou, A., Mavroidis, I. & Gavriil, I. (2008). Compliance with the annual NO_2 air quality standard in Athens. Required NO_x levels and expected health implications. *Atmos Environ* **42**, 454–465.

Chang, Y. Y. & Cronan, J. E. (1999). Membrane cyclopropane fatty acid content is a major factor in acid resistance of *Escherichia coli*. *Mol Microbiol* **33**, 249–259.

Chapalain, A., Rossignol, G., Lesouhaitier, O., Merieau, A., Gruffaz, C., Guerillon, J., Meyer, J.-M., Orange, N. & Feuilloley, M. G. J. (2008). Comparative study of 7 fluorescent pseudomonad clinical isolates. *Can J Microbiol* **54**, 19–27.

Chatterjee, S. N. & Chaudhuri, K. (2012). *Outer membrane vesicles of bacteria*. Springer briefs in Microbiology. Berlin, Heidelberg: Springer Berlin Heidelberg.

Cheer, S. M., Waugh, J. & Noble, S. (2003). Inhaled tobramycin (TOBI): a review of its use in the management of *Pseudomonas aeruginosa* infections in patients with cystic fibrosis. *Drugs* **63**, 2501–2520.

Chelikani, P., Fita, I. & Loewen, P. C. (2004). Diversity of structures and properties among catalases. *Cell Mol Life Sci CMLS* **61**, 192–208.

Choi, H. J., Seo, C. H., Park, S. H., Yang, H., Do, K. H., Kim, J., Kim, H.-K., Chung, D.-H., Ahn, J. H. & Moon, Y. (2011). Involvement of epidermal growth factor receptor-linked signaling responses in *Pseudomonas fluorescens*-infected alveolar epithelial cells. *Infect Immun* **79**, 1998–2005.

Choi, Y.-S., Shin, D.-H., Chung, I.-Y., Kim, S.-H., Heo, Y.-J. & Cho, Y.-H. (2007). Identification of *Pseudomonas aeruginosa* genes crucial for hydrogen peroxide resistance. *J Microbiol Biotechnol* **17**, 1344–1352.

Choudhari, S. K., Chaudhary, M., Bagde, S., Gadbail, A. R. & Joshi, V. (2013). Nitric oxide and cancer: a review. *World J Surg Oncol* **11**, 118.

Christen, M., Christen, B., Folcher, M., Schauerte, A. & Jenal, U. (2005). Identification and characterization of a cyclic di-GMP-specific phosphodiesterase and its allosteric control by GTP. *J Biol Chem* **280**, 30829–30837.

Chua, S. L., Liu, Y., Yam, J. K. H., Chen, Y., Vejborg, R. M., Tan, B. G. C., Kjelleberg, S., Tolker-Nielsen, T., Givskov, M. & Yang, L. (2014). Dispersed cells represent a distinct stage in the transition from bacterial biofilm to planktonic lifestyles. *Nat Commun* **5**.

Ciccone, G., Forastiere, F., Agabiti, N., Biggeri, A., Bisanti, L., Chellini, E., Corbo, G., Dell'Orco, V., Dalmasso, P. & other authors. **(1998).** Road traffic and adverse respiratory effects in children. SIDRIA Collaborative Group. *Occup Environ Med* **55**, 771–778.

CITERA. **(2014).** Inventaire des émissions de polluants atmosphériques et de gaz à effet de serre en France - Format SECTEN.

Cooper, C. E. (1999). Nitric oxide and iron proteins. *Biochim Biophys Acta BBA - Bioenerg* **1411**, 290–309.

Corcelli, A. (2009). The cardiolipin analogues of Archaea. *Biochim Biophys Acta BBA - Biomembr* **1788**, 2101–2106.

Cornelis, P. & Matthijs, S. (2002). Diversity of siderophore-mediated iron uptake systems in fluorescent pseudomonads: not only pyoverdines. *Environ Microbiol* **4**, 787–798.

Cornelis, P., Matthijs, S. & Van Oeffelen, L. (2009). Iron uptake regulation in *Pseudomonas aeruginosa*. *Biometals Int J Role Met Ions Biol Biochem Med* **22**, 15–22.

Costerton, J. W., Stewart, P. S. & Greenberg, E. P. (1999). Bacterial biofilms: a common cause of persistent infections. *Science* **284**, 1318–1322.

Couillerot, O., Prigent-Combaret, C., Caballero-Mellado, J. & Moënne-Loccoz, Y. (2009). *Pseudomonas fluorescens* and closely-related fluorescent pseudomonads as biocontrol agents of soil-borne phytopathogens. *Lett Appl Microbiol* **48**, 505–512.

Crane, B. R. (2008). The enzymology of nitric oxide in bacterial pathogenesis and resistance. *Biochem Soc Trans* **36**, 1149–1154.

Crawford, N. M. (1995). Nitrate: nutrient and signal for plant growth. *Plant Cell* **7**, 859–868.

Cruz-Ramos, H., Crack, J., Wu, G., Hughes, M. N., Scott, C., Thomson, A. J., Green, J. & Poole, R. K. (2002). NO sensing by FNR: regulation of the *Escherichia coli* NO-detoxifying flavohaemoglobin, Hmp. *EMBO J* **21**, 3235–3244.

Csonka, L. N. (1989). Physiological and genetic responses of bacteria to osmotic stress. *Microbiol Rev* **53**, 121–147.

Cullen, J., Phillips, M. C. & Shipley, G. G. (1971). The effects of temperature on the composition and physical properties of the lipids of P*seudomonas fluorescens*. *Biochem J* **125**, 733–742.

Cutruzzola, F. & Frankenberg-Dinkel, N. (2015). Origin and impact of nitric oxide in *Pseudomonas aeruginosa* biofilms. *J Bacteriol* JB.00371–15.

Cutruzzolà, F., Rinaldo, S., Centola, F. & Brunori, M. (2003). NO production by *Pseudomonas aeruginosa cd1* nitrite reductase. *IUBMB Life* **55**, 617–621.

Czader, B. H., Rappenglück, B., Percell, P., Byun, D. W., Ngan, F. & Kim, S. (2012). Modeling nitrous acid and its impact on ozone and hydroxyl radical during the Texas Air Quality Study 2006. *Atmos Chem Phys* **12**, 6939–6951.

Darling, A. C. E., Mau, B., Blattner, F. R. & Perna, N. T. (2004). Mauve: multiple alignment of conserved genomic sequence with rearrangements. *Genome Res* **14**, 1394–1403.

Davey, M. E. & O'toole, G. A. (2000). Microbial biofilms: from ecology to molecular genetics. *Microbiol Mol Biol Rev* **64**, 847–867.

Davidson, S. K., Koropatnick, T. A., Kossmehl, R., Sycuro, L. & McFall-Ngai, M. J. (2004). NO means 'yes' in the squid-vibrio symbiosis: nitric oxide (NO) during the initial stages of a beneficial association. *Cell Microbiol* **6**, 1139–1151.

Davies, D. G. & Marques, C. N. H. (2009). A fatty acid messenger is responsible for inducing dispersion in microbial biofilms. *J Bacteriol* **191**, 1393–1403.

Davis, M. S. & Cronan, J. E. (2001). Inhibition of *Escherichia coli* acetyl coenzyme A carboxylase by acyl-acyl carrier protein. *J Bacteriol* **183**, 1499–1503.

Deaconescu, A. M., Chambers, A. L., Smith, A. J., Nickels, B. E., Hochschild, A., Savery, N. J. & Darst, S. A. (2006). Structural basis for bacterial transcription-coupled DNA repair. *Cell* **124**, 507–520.

Declercq C, Pascal M, Chanel O, Corso M, Ung A, Pascal L, Blanchard M, Larrieu S, Medina S & DSE. (2012). *Impact sanitaire de la pollution atmosphérique dans neuf villes françaises. Résultats du projet Aphekom*.

Decoin, V., Barbey, C., Bergeau, D., Latour, X., Feuilloley, M. G. J., Orange, N. & Merieau, A. (2014). A type VI secretion system is involved in *Pseudomonas fluorescens* bacterial competition. *PLoS ONE* **9**.

Dé, E., Orange, N., Saint, N., Guérillon, J., De Mot, R. & Molle, G. (1997). Growth temperature dependence of channel size of the major outer-membrane protein (OprF) in psychrotrophic *Pseudomonas fluorescens* strains. *Microbiol Read Engl* **143 (Pt 3)**, 1029–1035.

Delledonne, M., Xia, Y., Dixon, R. A. & Lamb, C. (1998). Nitric oxide functions as a signal in plant disease resistance. *Nature* **394**, 585–588.

Després, V. R., Alex Huffman, J., Burrows, S. M., Hoose, C., Safatov, A. S., Buryak, G., Fröhlich-Nowoisky, J., Elbert, W., Andreae, M. O. & other authors. (2012). Primary biological aerosol particles in the atmosphere: a review. *Tellus B* **64**.

Després, V. R., Nowoisky, J. F., Klose, M., Conrad, R., Andreae, M. O. & Pöschl, U. (2007). Characterization of primary biogenic aerosol particles in urban, rural, and high-alpine air by DNA sequence and restriction fragment analysis of ribosomal RNA genes. *Biogeosciences* **4**, 1127–1141.

Déziel, E., Comeau, Y. & Villemur, R. (2001). Initiation of biofilm formation by *Pseudomonas aeruginosa* 57RP correlates with emergence of hyperpiliated and highly adherent phenotypic variants deficient in swimming, swarming, and twitching motilities. *J Bacteriol* **183**, 1195–1204.

Dickson, R. P., Erb-Downward, J. R., Freeman, C. M., Walker, N., Scales, B. S., Beck, J. M., Martinez, F. J., Curtis, J. L., Lama, V. N. & Huffnagle, G. B. (2014). Changes in the lung microbiome following lung transplantation include the emergence of two distinct *Pseudomonas* species with distinct clinical associations. *PLoS ONE* **9**.

Diefenbach, R. & Keweloh, H. (1994). Synthesis of *trans*-unsaturated fatty acids in *Pseudomonas putida* P8 by direct isomerization of the double bond of lipids. *Arch Microbiol* **162**, 120–125.

Ding, H., Hidalgo, E. & Demple, B. (1996). The redox state of the [2Fe-2S] clusters in SoxR protein regulates its activity as a transcription factor. *J Biol Chem* **271**, 33173–33175.

Ding, H. & Demple, B. (2000). Direct nitric oxide signal transduction via nitrosylation of iron-sulfur centers in the SoxR transcription activator. *Proc Natl Acad Sci U S A* **97**, 5146–5150.

Djaman, O., Outten, F. W. & Imlay, J. A. (2004). Repair of oxidized iron-sulfur clusters in *Escherichia coli*. *J Biol Chem* **279**, 44590–44599.

Dogan, B. & Boor, K. J. (2003). Genetic diversity and spoilage potentials among *Pseudomonas* spp. isolated from fluid milk products and dairy processing plants. *Appl Environ Microbiol* **69**, 130–138.

Dominy, J. E., Simmons, C. R., Karplus, P. A., Gehring, A. M. & Stipanuk, M. H. (2006). Identification and characterization of bacterial cysteine dioxygenases: a new route of cysteine degradation for *Eubacteria*. *J Bacteriol* **188**, 5561–5569.

Drapier, J.-C. (1997). Interplay between NO and [Fe-S] clusters: relevance to biological systems. *Methods* **11**, 319–329.

Drenkard, E. (2003). Antimicrobial resistance of *Pseudomonas aeruginos*a biofilms. *Microbes Infect Inst Pasteur* **5**, 1213–1219.

Driscoll, J. A., Brody, S. L. & Kollef, M. H. (2007). The epidemiology, pathogenesis and treatment of *Pseudomonas aeruginosa* infections. *Drugs* **67**, 351–368.

Duclairoir Poc, C., Verdon, J., Groboillot, A., Barreau, M., Toucourou, H., Mijouin, L., Leclerc, C., Hulen, C., Kondakova, T. & other authors. (2014, August). Airborne fluorescent pseudomonads : what potential for virulence? *Int J Curr Microbiol Appl Sci* 708–722.

Duclairoir-Poc, C. (2011). Influence of growth temperature on cyclolipopeptides production and on adhesion behaviour in environmental strains of *Pseudomonas fluorescens*. *J Bacteriol Parasitol* **04**.

Dueholm, M. S., Søndergaard, M. T., Nilsson, M., Christiansen, G., Stensballe, A., Overgaard, M. T., Givskov, M., Tolker-Nielsen, T., Otzen, D. E. & Nielsen, P. H. (2013). Expression of Fap amyloids in *Pseudomonas aeruginosa*, *P. fluorescens*, and *P. putida* results in aggregation and increased biofilm formation. *MicrobiologyOpen* **2**, 365–382.

Dufourc, E. J., Smith, I. C. P. & Jarrell, H. C. (1983). A 2H-NMR analysis of dihydrosterculoyl-containing lipids in model membranes: structural effects of a cyclopropane ring. *Chem Phys Lipids* **33**, 153–177.

Duhme, H., Weiland, S. K., Keil, U., Kraemer, B., Schmid, M., Stender, M. & Chambless, L. (1996). The association between self-reported symptoms of asthma and allergic rhinitis and self-reported traffic density on street of residence in adolescents. *Epidemiol Camb Mass* **7**, 578–582.

Duhme, H., Weiland, S. K., Rudolph, P., Wienke, A., Kramer, A. & Keil, U. (1998). Asthma and allergies among children in West and East Germany: a comparison between Munster and Greifswald using the ISAAC phase I protocol. International Study of Asthma and Allergies in Childhood. *Eur Respir J* **11**, 840–847.

Durbán, J. J., Villaverde, E. H., Monteoliva-Sanchez, M. & Ramos-Cormenzana, A. (1996). Bacterial contamination of hydrophilic contact lens solutions marketed in spain. *Optom Vis Sci Off Publ Am Acad Optom* **73**, 529–532.

Dybwad, M., Granum, P. E., Bruheim, P. & Blatny, J. M. (2012). Characterization of airborne bacteria at an underground subway station. *Appl Environ Microbiol* **78**, 1917–1929.

Eisen, J. A. & Hanawalt, P. C. (1999). A Phylogenomic study of DNA repair genes, proteins, and processes. *Mutat Res* **435**, 171–213.

Elkins, J. G., Hassett, D. J., Stewart, P. S., Schweizer, H. P. & McDermott, T. R. (1999). Protective role of catalase in *Pseudomonas aeruginosa* biofilm resistance to hydrogen peroxide. *Appl Environ Microbiol* **65**, 4594–4600.

Elmnasser, N., Guillou, S., Leroi, F., Orange, N., Bakhrouf, A. & Federighi, M. (2007). Pulsed-light system as a novel food decontamination technology: a review. *Can J Microbiol* **53**, 813–821.

Enderle, P. J. & Farwell, M. A. (1998). Electroporation of freshly plated *Escherichia coli* and *Pseudomonas aeruginosa* cells. *BioTechniques* **25**, 954–956, 958.

Epand, R. M. & Epand, R. F. (2009). Lipid domains in bacterial membranes and the action of antimicrobial agents. *Biochim Biophys Acta BBA - Biomembr*, Lipid interactions, domain formation, and lateral structure of membranes **1788**, 289–294.

Espey, M. G., Thomas, D. D., Miranda, K. M. & Wink, D. A. (2002). Focusing of nitric oxide mediated nitrosation and oxidative nitrosylation as a consequence of reaction with superoxide. *Proc Natl Acad Sci U S A* **99**, 11127–11132.

Fajardo, V. A., McMeekin, L. & LeBlanc, P. J. (2011). Influence of phospholipid species on membrane fluidity: a meta-analysis for a novel phospholipid fluidity index. *J Membr Biol* **244**, 97–103.

Fall, M., Bion, A., Keravec, V., Ciss, M., Diouf, A., Dionnet, F. & Morin, J.-P. (2008). Réponse toxicologique d'une culture organotypique de tissu pulmonaire exposée à des gazes d'échappement issus d'un moteur à combustion. *Environ Risques Santé* **7**, 123–129.

Fang, F. C. (2004). Antimicrobial reactive oxygen and nitrogen species: concepts and controversies. *Nat Rev Microbiol* **2**, 820–832.

Fang, F. C. & Vazquez-Torres, A. (2002). Nitric oxide production by human macrophages: there's NO doubt about it. *Am J Physiol - Lung Cell Mol Physiol* **282**, L941–L943.

Fang, J., Barcelona, M. J. & Alvarez, P. J. (2000). Phospholipid compositional changes of five pseudomonad archetypes grown with and without toluene. *Appl Microbiol Biotechnol* **54**, 382–389.

Fang, Z., Ouyang, Z., Zheng, H., Wang, X. & Hu, L. (2007). Culturable airborne bacteria in outdoor environments in Beijing, China. *Microb Ecol* **54**, 487–496.

Feld, L., Knudsen, G. M. & Gram, L. (2012). Bactericidal antibiotics do not appear to cause oxidative stress in *Listeria monocytogenes*. *Appl Environ Microbiol* **78**, 4353–4357.

Fernandes, F., Neves, P., Gameiro, P., Loura, L. M. S. & Prieto, M. (2007). Ciprofloxacin interactions with bacterial protein OmpF: Modelling of FRET from a multi-tryptophan protein trimer. *Biochim Biophys Acta BBA - Biomembr* **1768**, 2822–2830.

Ferrer-Sueta, G. & Radi, R. (2009). Chemical biology of peroxynitrite: kinetics, diffusion, and radicals. *ACS Chem Biol* **4**, 161–177.

Fetar, H., Gilmour, C., Klinoski, R., Daigle, D. M., Dean, C. R. & Poole, K. (2011). *mexEF-oprN* Multidrug efflux operon of *Pseudomonas aeruginosa*: regulation by the MexT activator in response to nitrosative stress and chloramphenicol. *Antimicrob Agents Chemother* **55**, 508–514.

Field, S. J., Thorndycroft, F. H., Matorin, A. D., Richardson, D. J. & Watmough, N. J. (2008). The respiratory nitric oxide reductase (NorBC) from *Paracoccus denitrificans*. *Methods Enzymol* **437**, 79–101.

Flatley, J., Barrett, J., Pullan, S. T., Hughes, M. N., Green, J. & Poole, R. K. (2005). Transcriptional responses of *Escherichia coli* to S-nitrosoglutathione under defined chemostat conditions reveal major changes in methionine biosynthesis. *J Biol Chem* **280**, 10065–10072.

Foght, J. M. & Westlake, D. W. S. (1988). Degradation of polycyclic aromatic hydrocarbons and aromatic heterocycles by a *Pseudomonas* species. *Can J Microbiol* **34**, 1135–1141.

Fouchard, S., Abdellaoui-Maâne, Z., Boulanger, A., Llopiz, P. & Neunlist, S. (2005). Influence of growth conditions on *Pseudomonas fluorescens* strains: a link between metabolite production and the PLFA profile. *FEMS Microbiol Lett* **251**, 211–218.

Böhm F. M. L. Z., Ferrarese M. L. L., Zanardo D. I. L., Magalhaes J. R. & Ferrarese-Filho O. (2010). Nitric oxide affecting root growth, lignification and related enzymes in soybean seedlings. *Acta Physiol Plant* **32**, 1039–1046.

French, S., Puddephatt, D., Habash, M. & Glasauer, S. (2013). The dynamic nature of bacterial surfaces: implications for metal-membrane interaction. *Crit Rev Microbiol* **39**, 196–217.

Freulet-Marrière, M.-A., Hamel, C. El, Chevalier, S., Dé, E., Molle, G. & Orange, N. (2000). Evidence for association of lipopolysaccharide with *Pseudomonas fluorescens* strain MF0 porin OprF. *Res Microbiol* **151**, 873–876.

Fröhlich, A. & Durner, J. (2011). The hunt for plant nitric oxide synthase (NOS): is one really needed? *Plant Sci* **181**, 401–404.

Fröhlich-Nowoisky, J., Burrows, S. M., Xie, Z., Engling, G., Solomon, P. A., Fraser, M. P., Mayol-Bracero, O. L., Artaxo, P., Begerow, D. & other authors. **(2012).** Biogeography in the air: fungal diversity over land and oceans. *Biogeosciences* **9**, 1125–1136.

Fröhlich-Nowoisky, J., Ruzene Nespoli, C., Pickersgill, D. A., Galand, P. E., Müller-Germann, I., Nunes, T., Gomes Cardoso, J., Almeida, S. M., Pio, C. & other authors. **(2014).** Diversity and seasonal dynamics of airborne archaea. *Biogeosciences* **11**, 6067–6079.

Fröhlich-Nowoisky, J., Pickersgill, D. A., Després, V. R. & Pöschl, U. (2009). High diversity of fungi in air particulate matter. *Proc Natl Acad Sci* **106**, 12814–12819.

Frungillo, L., Skelly, M. J., Loake, G. J., Spoel, S. H. & Salgado, I. (2014). S-nitrosothiols regulate nitric oxide production and storage in plants through the nitrogen assimilation pathway. *Nat Commun* **5**.

Fuchs, B., Schiller, J., Süss, R., Schürenberg, M. & Suckau, D. (2007a). A direct and simple method of coupling matrix-assisted laser desorption and ionization time-of-flight mass spectrometry (MALDI-TOF MS) to thin-layer chromatography (TLC) for the analysis of phospholipids from egg yolk. *Anal Bioanal Chem* **389**, 827–834.

Fuchs, B., Schober, C., Richter, G., Süß, R. & Schiller, J. (2007b). MALDI-TOF MS of phosphatidylethanolamines: different adducts cause different post source decay (PSD) fragment ion spectra. *J Biochem Biophys Methods* **70**, 689–692.

Fukuto, J. M., Cho, J. Y. & Switzer, C. H. (2000). The chemical properties of nitric oxide and related nitrogen oxides. In *Nitric Oxide Biol Pathobiol*. Academic Press.

Garcia-Mata, C., Gay, R., Sokolovski, S., Hills, A., Lamattina, L. & Blatt, M. R. (2003). Nitric oxide regulates K^+ and Cl^- channels in guard cells through a subset of abscisic acid-evoked signaling pathways. *Proc Natl Acad Sci U S A* **100**, 11116–11121.

Gardner, P. R., Gardner, A. M., Martin, L. A. & Salzman, A. L. (1998a). Nitric oxide dioxygenase: an enzymic function for flavohemoglobin. *Proc Natl Acad Sci U S A* **95**, 10378–10383.

Gardner, P. R., Costantino, G. & Salzman, A. L. (1998b). Constitutive and adaptive detoxification of nitric oxide in *Escherichia coli:* role of nitric oxide dioxygenae in the protection of aconistase. *J Biol Chem* **273**, 26528–26533.

Gardner, P. R., Costantino, G., Szabó, C. & Salzman, A. L. (1997). Nitric oxide sensitivity of the aconitases. *J Biol Chem* **272**, 25071–25076.

Gaudu, P. & Weiss, B. (1996). SoxR, a [2Fe-2S] transcription factor, is active only in its oxidized form. *Proc Natl Acad Sci U S A* **93**, 10094–10098.

El-Gayar, S., Thüring-Nahler, H., Pfeilschifter, J., Röllinghoff, M. & Bogdan, C. (2003). Translational control of inducible nitric oxide synthase by IL-13 and arginine availability in inflammatory macrophages. *J Immunol Baltim Md 1950* **171**, 4561–4568.

Gehring, U., Cyrys, J., Sedlmeir, G., Brunekreef, B., Bellander, T., Fischer, P., Bauer, C. P., Reinhardt, D., Wichmann, H. E. & Heinrich, J. (2002). Traffic-related air pollution and respiratory health during the first 2 yrs of life. *Eur Respir J* **19**, 690–698.

Georgakopoulos, D. G., Després, V., Fröhlich-Nowoisky, J., Psenner, R., Ariya, P. A., Pósfai, M., Ahern, H. E., Moffett, B. F. & Hill, T. C. J. (2009). Microbiology and atmospheric processes: biological, physical and chemical characterization of aerosol particles. *Biogeosciences* **6**, 721–737.

Ge, Y. & Moss, R. L. (2012). Nitroxyl, redox switches, cardiac myofilaments, and heart failure a prequel to novel therapeutics? *Circ Res* **111**, 954–956.

Ghaffari, A., Neil, D. H., Ardakani, A., Road, J., Ghahary, A. & Miller, C. C. (2005). A direct nitric

oxide gas delivery system for bacterial and mammalian cell cultures. *Nitric Oxide* **12**, 129–140.

Ghenu, A., Rosant, J.-M. & Sini, J.-F. (2008). Dispersion of pollutants and sstimation of emissions in a street canyon in Rouen, France. *Env Model Softw* **23**, 314–321.

Giardina, G., Rinaldo, S., Johnson, K. A., Di Matteo, A., Brunori, M. & Cutruzzolà, F. (2008). NO sensing in *Pseudomonas aeruginosa*: structure of the transcriptional regulator DNR. *J Mol Biol* **378**, 1002–1015.

Gibaud, M., Martin-Dupont, P., Dominguez, M., Laurentjoye, P., Chassaing, B. & Leng, B. (1984). *Pseudomonas fluorescens* septicemia following transfusion of contaminated blood. *Presse Médicale Paris Fr 1983* **13**, 2583–2584.

Gicquel, G., Bouffartigues, E., Bains, M., Oxaran, V., Rosay, T., Lesouhaitier, O., Connil, N., Bazire, A., Maillot, O. & other authors. **(2013).** The extra-cytoplasmic function sigma factor SigX modulates biofilm and virulence-related properties in *Pseudomonas aeruginosa*. *PLoS ONE* **8**, e80407.

Gill, C. O. (1975). Effect of growth temperature on the lipids of *Pseudomonas fluorescens*. *J Gen Microbiol* **89**, 293–298.

di Giorgio, C., Krempff, A., Guiraud, H., Binder, P., Tiret, C. & Dumenil, G. (1996). Atmospheric pollution by airborne microorganisms in the city of Marseilles. *Atmos Environ* **30**, 155–160.

Giró, M., Carrillo, N. & Krapp, A. R. (2006). Glucose-6-phosphate dehydrogenase and ferredoxin-NADP(H) reductase contribute to damage repair during the *soxRS* response of *Escherichia coli*. *Microbiol Read Engl* **152**, 1119–1128.

Glauert, A. M. & Thornley, M. J. (1969). The topography of the bacterial cell wall. *Annu Rev Microbiol* **23**, 159–198.

Gómez-López, V. M., Ragaert, P., Debevere, J. & Devlieghere, F. (2007). Pulsed light for food decontamination: a review. *Trends Food Sci Technol* **18**, 464–473.

Gouy, M., Guindon, S. & Gascuel, O. (2010). SeaView version 4: A multiplatform graphical user interface for sequence alignment and phylogenetic tree building. *Mol Biol Evol* **27**, 221–224.

Gross, H. & Loper, J. E. (2009). Genomics of secondary metabolite production by *Pseudomonas* spp. *Nat Prod Rep* **26**, 1408–1446.

Guerrero, M. G., Vega, J. M. & Losada, M. (1981). The assimilatory nitrate-reducing system and its regulation. *Annu Rev Plant Physiol* **32**, 169–204.

Gügi, B., Orange, N., Hellio, F., Burini, J. F., Guillou, C., Leriche, F. & Guespin-Michel, J. F. (1991). Effect of growth temperature on several exported enzyme activities in the psychrotrophic bacterium *Pseudomonas fluorescens*. *J Bacteriol* **173**, 3814–3820.

Gupta, K. J., Fernie, A. R., Kaiser, W. M. & van Dongen, J. T. (2011). On the origins of nitric oxide. *Trends Plant Sci* **16**, 160–168.

Gusarov, I., Shatalin, K., Starodubtseva, M. & Nudler, E. (2009). Endogenous nitric oxide protects bacteria against a wide spectrum of antibiotics. *Science* **325**, 1380–1384.

Guyard-Nicodème, M., Bazire, A., Hémery, G., Meylheuc, T., Mollé, D., Orange, N., Fito-Boncompte, L., Feuilloley, M., Haras, D. & other authors. **(2008).** Outer membrane modifications of *Pseudomonas fluorescens* MF37 in response to hyperosmolarity. *J Proteome Res* **7**, 1218–1225.

Hachicho, N., Hoffmann, P., Ahlert, K. & Heipieper, H. J. (2014). Effect of silver nanoparticles and silver ions on growth and adaptive response mechanisms of *Pseudomonas putida* mt-2. *FEMS Microbiol Lett* **355**, 71–77.

Harrison, R. M. (2006). Sources of air pollution. In *Air Qual Guidel*, World Health Organization., pp. 9–31.

Härtig, E., Schiek, U., Vollack, K.-U. & Zumft, W. G. (1999). Nitrate and nitrite control of respiratory nitrate reduction in denitrifying *Pseudomonas stutzeri* by a two-component regulatory system homologous to NarXL of *Escherichia coli*. *J Bacteriol* **181**, 3658–3665.

Hasegawa, N., Arai, H. & Igarashi, Y. (2001). Two *c*-type cytochromes, NirM and NirC, encoded in the *nir* gene cluster of *Pseudomonas aeruginosa* act as electron donors for nitrite reductase. *Biochem Biophys Res Commun* **288**, 1223–1230.

Hassett, D. J., Sokol, P. A., Howell, M. L., Ma, J. F., Schweizer, H. T., Ochsner, U. & Vasil, M. L. (1996). Ferric uptake regulator (Fur) mutants of *Pseudomonas aeruginosa* demonstrate defective siderophore-mediated iron uptake, altered aerobic growth, and decreased superoxide dismutase and catalase activities. *J Bacteriol* **178**, 3996–4003.

Hassett, D. J., Ma, J. F., Elkins, J. G., McDermott, T. R., Ochsner, U. A., West, S. E., Huang, C. T., Fredericks, J., Burnett, S. & other authors. **(1999).** Quorum sensing in *Pseudomonas aeruginosa* controls expression of catalase and superoxide dismutase genes and mediates biofilm susceptibility to hydrogen peroxide. *Mol Microbiol* **34**, 1082–1093.

Hausladen, A., Gow, A. J. & Stamler, J. S. (1998). Nitrosative stress: metabolic pathway involving the flavohemoglobin. *Proc Natl Acad Sci U S A* **95**, 14100–14105.

Hay, I. D., Remminghorst, U. & Rehm, B. H. A. (2009). MucR, a novel membrane-associated regulator of alginate biosynthesis in *Pseudomonas aeruginosa*. *Appl Environ Microbiol* **75**, 1110–1120.

Hazel, J. R. & Williams, E. E. (1990). The role of alterations in membrane lipid composition in enabling physiological adaptation of organisms to their physical environment. *Prog Lipid Res* **29**, 167–227.

Heath, R. J. & Rock, C. O. (1996a). Inhibition of -ketoacyl-acyl carrier protein synthase III (FabH) by acyl-acyl carrier protein in *Escherichia coli*. *J Biol Chem* **271**, 10996–11000.

Heath, R. J. & Rock, C. O. (1996b). Regulation of fatty acid elongation and initiation by acyl-acyl carrier protein in *Escherichia coli*. *J Biol Chem* **271**, 1833–1836.

van der Heijden, J., Bosman, E. S., Reynolds, L. A. & Finlay, B. B. (2015). Direct measurement of oxidative and nitrosative stress dynamics in *Salmonella* inside macrophages. *Proc Natl Acad Sci* **112**, 560–565.

Heilmann, H.-D. (1972). On the peptidoglycan of the cell walls of *Pseudomonas aeruginosa*. *Eur J Biochem* **31**, 456–463.

Heipieper, H. J., Weber, F. J., Sikkema, J., Keweloh, H. & de Bont, J. A. M. (1994). Mechanisms of resistance of whole cells to toxic organic solvents. *Trends Biotechnol* **12**, 409–415.

Heipieper, H. J., Meinhardt, F. & Segura, A. (2003). The *cis-trans* isomerase of unsaturated fatty acids in *Pseudomonas* and *Vibrio:* biochemistry, molecular biology and physiological function of a unique stress adaptive mechanism. *FEMS Microbiol Lett* **229**, 1–7.

Heipieper, H. J. & de Bont, J. A. (1994). Adaptation of *Pseudomonas putida* S12 to ethanol and toluene at the level of fatty acid composition of membranes. *Appl Environ Microbiol* **60**, 4440–4444.

Heipieper, H. J. & Fischer, J. (2010). Bacterial solvent responses and tolerance: *cis–trans* isomerization. In *Handb Hydrocarb Lipid Microbiol*, pp. 4203–4211. Edited by K. N. Timmis. Springer Berlin Heidelberg.

Heipieper, H. J. & Martínez, P. M. (2010). Toxicity of hydrocarbons to microorganisms. In *Handb Hydrocarb Lipid Microbiol*, pp. 1563–1573. Edited by K. N. Timmis. Springer Berlin Heidelberg.

Heipieper, H. J., Keweloh, H. & Rehm, H. J. (1991). Influence of phenols on growth and membrane permeability of free and immobilized *Escherichia coli*. *Appl Environ Microbiol* **57**, 1213–1217.

Heipieper, H. J., Meulenbeld, G., van Oirschot, Q. & de Bont, J. (1996). Effect of environmental factors on the *trans/cis* ratio of unsaturated fatty acids in *Pseudomonas putida* S12. *Appl Environ Microbiol* **62**, 2773–2777.

Hemery, G., Chevalier, S., Bellon-Fontaine, M.-N., Haras, D. & Orange, N. (2006). Growth temperature and OprF porin affect cell surface physicochemical properties and adhesive capacities of Pseudomonas fluorescens MF37. *J Ind Microbiol Biotechnol* **34**, 49–54.

Henares, B. M., Higgins, K. E. & Boon, E. M. (2012). Discovery of a nitric oxide responsive quorum sensing circuit in *Vibrio harveyi*. *ACS Chem Biol* **7**, 1331–1336.

Hengge, R. (2009). Principles of c-di-GMP signalling in bacteria. *Nat Rev Microbiol* **7**, 263–273.

Heo, Y.-J., Chung, I.-Y., Cho, W.-J., Lee, B.-Y., Kim, J.-H., Choi, K.-H., Lee, J.-W., Hassett, D. J. & Cho, Y.-H. (2010). The major catalase gene (*katA*) of *Pseudomonas aeruginosa* PA14 is under both positive and negative control of the global transactivator OxyR in response to hydrogen peroxide. *J Bacteriol* **192**, 381–390.

Heydorn, A., Nielsen, A. T., Hentzer, M., Sternberg, C., Givskov, M., Ersbøll, B. K. & Molin, S. (2000). Quantification of biofilm structures by the novel computer program comstat. *Microbiology* **146**, 2395–2407.

Hickman, J. W., Tifrea, D. F. & Harwood, C. S. (2005). A chemosensory system that regulates biofilm formation through modulation of cyclic diguanylate levels. *Proc Natl Acad Sci U S A* **102**, 14422–14427.

Hill, B. G., Dranka, B. P., Bailey, S. M., Lancaster, J. R. & Darley-Usmar, V. M. (2010). What part of NO don't you understand? Some answers to the cardinal questions in nitric oxide biology. *J Biol Chem* **285**, 19699–19704.

Hino, T., Matsumoto, Y., Nagano, S., Sugimoto, H., Fukumori, Y., Murata, T., Iwata, S. & Shiro, Y. (2010). Structural basis of biological N_2O generation by bacterial nitric oxide reductase. *Science* **330**, 1666–1670.

Hinsa, S. M., Espinosa-Urgel, M., Ramos, J. L. & O'Toole, G. A. (2003). Transition from reversible to irreversible attachment during biofilm formation by *Pseudomonas fluorescens* WCS365 requires an ABC transporter and a large secreted protein. *Mol Microbiol* **49**, 905–918.

Hohle, T. H., Franck, W. L., Stacey, G. & O'Brian, M. R. (2011). Bacterial outer membrane channel for divalent metal ion acquisition. *Proc Natl Acad Sci U S A* **108**, 15390–15395.

Holtwick, R., Keweloh, H. & Meinhardt, F. (1999). *cis/trans* Isomerase of unsaturated fatty acids of *Pseudomonas putida* P8: evidence for a heme protein of the cytochrome *c* type. *Appl Environ Microbiol* **65**, 2644–2649.

Huang, P. L., Huang, Z., Mashimo, H., Bloch, K. D., Moskowitz, M. A., Bevan, J. A. & Fishman, M. C. (1995). Hypertension in mice lacking the gene for endothelial nitric oxide synthase. *Nature* **377**, 239–242.

Huffman, J. L., Sundheim, O. & Tainer, J. A. (2005). DNA base damage recognition and removal: new twists and grooves. *Mutat Res Mol Mech Mutagen*, Mechanisms of DNA repair special issue dedicated to Phil Hanawalt **577**, 55–76.

Hughes, K. J., Meares, G. P., Chambers, K. T. & Corbett, J. A. (2009). Repair of nitric oxide-damaged DNA in β-cells requires JNK-dependent GADD45α expression. *J Biol Chem* **284**, 27402–27408.

Hughes, M. N. (2008). Chapter one - Chemistry of nitric oxide and related species. In *Methods Enzymol*, Globins and other nitric oxide-reactive proteins, Part A, pp. 3–19. Edited by R. K. Poole. Academic Press.

Hu, H.-W., Chen, D. & He, J.-Z. (2015). Microbial regulation of terrestrial nitrous oxide formation: understanding the biological pathways for prediction of emission rates. *FEMS Microbiol Rev* fuv021.

Hung, K. T. & Kao, C. H. (2003). Nitric oxide counteracts the senescence of rice leaves induced by abscisic acid. *J Plant Physiol* **160**, 871–879.

Husain, M., Bourret, T. J., McCollister, B. D., Jones-Carson, J., Laughlin, J. & Vázquez-Torres, A. (2008). Nitric oxide evokes an adaptive response to oxidative stress by arresting respiration. *J Biol Chem* **283**, 7682–7689.

Huster, D., Arnold, K. & Gawrisch, K. (2000). Strength of Ca^{2+} binding to retinal lipid membranes: consequences for lipid organization. *Biophys J* **78**, 3011–3018.

Ignarro, L. J. (1990). Biosynthesis and metabolism of endothelium-derived nitric oxide. *Annu Rev Pharmacol Toxicol* **30**, 535–560.

Imlay, J. A. (2003). Pathways of oxidative damage. *Annu Rev Microbiol* **57**, 395–418.

INERIS. **(2011a, November 10).** Dioxyde d'azote: données toxicologiques et environnementales. *Portail Subst Chim*.

INERIS. **(2011b, November 10).** Monoxyde d'azote: Données toxicologiques et environnementales. *Portail Subst Chim*.

Iyer, L. M., Anantharaman, V. & Aravind, L. (2003). Ancient conserved domains shared by animal soluble guanylyl cyclases and bacterial signaling proteins. *BMC Genomics* **4**, 5.

Jackowski, S., Jackson, P. D. & Rock, C. O. (1994). Sequence and function of the *aas* gene in *Escherichia coli*. *J Biol Chem* **269**, 2921–2928.

Jasid, S., Simontacchi, M., Bartoli, C. G. & Puntarulo, S. (2006). Chloroplasts as a nitric oxide cellular source. Effect of reactive nitrogen species on chloroplastic lipids and proteins. *Plant Physiol* **142**, 1246–1255.

Jiang, H., Kruger, N., Lahiri, D. R., Wang, D., Vatèle, J.-M. & Balazy, M. (1999). Nitrogen dioxide induces *cis-trans*-isomerization of arachidonic acid within cellular phospholipids. Detection of *trans*-arachidonic acids *in vivo*. *J Biol Chem* **274**, 16235–16241.

Jiricny, J. (2013). Postreplicative mismatch repair. *Cold Spring Harb Perspect Biol* **5**.

Joly, M., Attard, E., Sancelme, M., Deguillaume, L., Guilbaud, C., Morris, C. E., Amato, P. & Delort, A.-M. (2013). Ice nucleation activity of bacteria isolated from cloud water. *Atmos Environ* **70**, 392–400.

Jones-Carson, J., Laughlin, J., Hamad, M. A., Stewart, A. L., Voskuil, M. I. & Vázquez-Torres, A. (2008). Inactivation of [Fe-S] metalloproteins mediates nitric oxide-dependent killing of *Burkholderia mallei*. *PLoS ONE* **3**.

Jonghe, V. D., Coorevits, A., Hoorde, K. V., Messens, W., Landschoot, A. V., Vos, P. D. & Heyndrickx, M. (2011). Influence of storage conditions on the growth of *Pseudomonas* species in refrigerated raw milk. *Appl Environ Microbiol* **77**, 460–470.

Jousset, A., Schuldes, J., Keel, C., Maurhofer, M., Daniel, R., Scheu, S. & Thuermer, A. (2014). Full-genome sequence of the plant growth-promoting bacterium *Pseudomonas protegens* CHA0. *Genome Announc* **2**.

Justino, M. C., Almeida, C. C., Teixeira, M. & Saraiva, L. M. (2007). *Escherichia coli* di-iron YtfE protein is necessary for the repair of stress-damaged iron-sulfur clusters. *J Biol Chem* **282**, 10352–10359.

Kagawa, J. (1982). Respiratory effects of 2-hr exposure to 1.0 ppm nitric oxide in normal subjects. *Environ Res* **27**, 485–490.

Karow, D. S., Pan, D., Tran, R., Pellicena, P., Presley, A., Mathies, R. A. & Marletta, M. A. (2004). Spectroscopic characterization of the soluble guanylate cyclase-like heme domains from *Vibrio cholerae* and *Thermoanaerobacter tengcongensis*. *Biochemistry (Mosc)* **43**, 10203–10211.

Karow, D. S., Pan, D., Davis, J. H., Behrends, S., Mathies, R. A. & Marletta, M. A. (2005). Characterization of functional heme domains from soluble guanylate cyclase. *Biochemistry (Mosc)* **44**, 16266–16274.

Kastrau, D. H., Heiss, B., Kroneck, P. M. & Zumft, W. G. (1994). Nitric oxide reductase from *Pseudomonas stutzeri*, a novel cytochrome *bc* complex. Phospholipid requirement, electron paramagnetic resonance and redox properties. *Eur J Biochem FEBS* **222**, 293–303.

Kates, M. (1972). *Techniques of lipidology: isolation, analysis and identification of lipids*. North-Holland Pub. Co.

Kean, E. L. (1968). Rapid, sensitive spectrophotometric method for quantitative determination of sulfatides. *J Lipid Res* **9**, 319–327.

Kearns, D. B. (2010). A field guide to bacterial swarming motility. *Nat Rev Microbiol* **8**, 634–644.

Khabbaz, R. F., Arnow, P. M., Highsmith, A. K., Herwaldt, L. A., Chou, T., Jarvis, W. R., Lerche, N. W. & Allen, J. R. (1984). *Pseudomonas fluorescens* bacteremia from blood transfusion. *Am J Med* **76**, 62–68.

Khairutdinov, R. F., Coddington, J. W. & Hurst, J. K. (2000). Permeation of phospholipid membranes by peroxynitrite. *Biochemistry (Mosc)* **39**, 14238–14249.

Kiely, P. D., Haynes, J. M., Higgins, C. H., Franks, A., Mark, G. L., Morrissey, J. P. & O'Gara, F. (2006). Exploiting new systems-based strategies to elucidate plant-bacterial interactions in the rhizosphere. *Microb Ecol* **51**, 257–266.

Kim, J. & Park, W. (2014). Oxidative stress response in *Pseudomonas putida*. *Appl Microbiol Biotechnol* **98**, 6933–6946.

Kim, S.-H., Lee, B.-Y., Lau, G. W. & Cho, Y.-H. (2009). IscR modulates catalase A (KatA) activity, peroxide resistance and full virulence of *Pseudomonas aeruginosa* PA14. *J Microbiol Biotechnol* **19**, 1520–1526.

Kindrachuk, K. N., Fernández, L., Bains, M. & Hancock, R. E. W. (2011). Involvement of an ATP-dependent protease, PA0779/AsrA, in inducing heat shock in response to tobramycin in *Pseudomonas aeruginosa*. *Antimicrob Agents Chemother* **55**, 1874–1882.

Kiran, M. D., Annapoorni, S., Suzuki, I., Murata, N. & Shivaji, S. (2005). *cis-trans* Isomerase gene in psychrophilic *Pseudomonas syringae* is constitutively expressed during growth and under conditions of temperature and solvent stress. *Extrem Life Extreme Cond* **9**, 117–125.

Kiran, M. D., Prakash, J. S. S., Annapoorni, S., Dube, S., Kusano, T., Okuyama, H., Murata, N. & Shivaji, S. (2004). Psychrophilic *Pseudomonas syringae* requires *trans*-monounsaturated fatty acid for growth at higher temperature. *Extrem Life Extreme Cond* **8**, 401–410.

Kisker, C., Kuper, J. & Van Houten, B. (2013). Prokaryotic nucleotide excision repair. *Cold Spring Harb Perspect Biol* **5**, a012591.

Klein, S., Lorenzo, C., Hoffmann, S., Walther, J. M., Storbeck, S., Piekarski, T., Tindall, B. J., Wray, V., Nimtz, M. & Moser, J. (2009). Adaptation of *Pseudomonas aeruginosa* to various conditions includes tRNA-dependent formation of alanyl-phosphatidylglycerol. *Mol Microbiol* **71**, 551–565.

Kobayashi, K. & Tagawa, S. (2004). Activation of SoxR-dependent transcription in *Pseudomonas aeruginosa*. *J Biochem (Tokyo)* **136**, 607–615.

Köhler, T., Michéa-Hamzehpour, M., Henze, U., Gotoh, N., Curty, L. K. & Pechère, J. C. (1997). Characterization of MexE-MexF-OprN, a positively regulated multidrug efflux system of *Pseudomonas aeruginosa*. *Mol Microbiol* **23**, 345–354.

Kondakova, T., D'Heygère, F., Feuilloley, M. J., Orange, N., Heipieper, H. J. & Duclairoir Poc, C. (2015). Glycerophospholipid synthesis and functions in *Pseudomonas*. *Chem Phys Lipids* **190**, 27–42.

Koshland, D. E. (1992). The molecule of the year. *Science* **258**, 1861.

Koskenkorva-Frank, T. S. & Kallio, P. T. (2009). Induction of *Pseudomonas aeruginosa fhp* and *fhpR* by reactive oxygen species. *Can J Microbiol* **55**, 657–663.

Kropinski, A. M., Lewis, V. & Berry, D. (1987). Effect of growth temperature on the lipids, outer membrane proteins, and lipopolysaccharides of *Pseudomonas aeruginosa* PAO. *J Bacteriol* **169**, 1960–1966.

Kulesekara, H., Lee, V., Brencic, A., Liberati, N., Urbach, J., Miyata, S., Lee, D. G., Neely, A. N., Hyodo, M. & other authors. **(2006).** Analysis of *Pseudomonas aeruginosa* diguanylate cyclases and phosphodiesterases reveals a role for bis-(3′-5′)-cyclic-GMP in virulence. *Proc Natl Acad Sci U S A* **103**, 2839–2844.

Kumita, H., Matsuura, K., Hino, T., Takahashi, S., Hori, H., Fukumori, Y., Morishima, I. & Shiro, Y. (2004). NO reduction by nitric-oxide reductase from denitrifying bacterium *Pseudomonas aeruginosa:* characterization of reaction intermediates that appear in the single turnover cycle. *J Biol Chem* **279**, 55247–55254.

Kuroki, M., Igarashi, Y., Ishii, M. & Arai, H. (2014). Fine-tuned regulation of the dissimilatory nitrite reductase gene by oxygen and nitric oxide in *Pseudomonas aeruginosa*. *Environ Microbiol Rep* **6**, 792–801.

Lamarche, M. G. & Déziel, E. (2011). MexEF-OprN efflux pump exports the *Pseudomonas* quinolone signal (PQS) precursor HHQ (4-hydroxy-2-heptylquinoline). *PLoS ONE* **6**, e24310.

Lammel, G. & Cape, J. N. (1996). Nitrous acid and nitrite in the atmosphere. *Chem Soc Rev* **25**, 361–369.

Laursen, J. B. & Nielsen, J. (2004). Phenazine natural products: biosynthesis, synthetic analogues, and biological activity. *Chem Rev* **104**, 1663–1686.

Leahy, J. G. & Colwell, R. R. (1990). Microbial degradation of hydrocarbons in the environment. *Microbiol Rev* **54**, 305–315.

Lee, D. G., Urbach, J. M., Wu, G., Liberati, N. T., Feinbaum, R. L., Miyata, S., Diggins, L. T., He, J., Saucier, M. & other authors. **(2006).** Genomic analysis reveals that *Pseudomonas aeruginosa* virulence is combinatorial. *Genome Biol* **7**, R90.

Lemire, J. A., Harrison, J. J. & Turner, R. J. (2013). Antimicrobial activity of metals: mechanisms, molecular targets and applications. *Nat Rev Microbiol* **11**, 371–384.

Lide, D. R. (2004). *CRC Handbook of Chemistry and Physics, 85th Edition*. CRC Press.

Linde, K., Gröbner, G. & Rilfors, L. (2004). Lipid dependence and activity control of phosphatidylserine synthase from *Escherichia coli*. *FEBS Lett* **575**, 77–80.

Lindemann, C., Lupilova, N., Müller, A., Warscheid, B., Meyer, H. E., Kuhlmann, K., Eisenacher, M. & Leichert, L. I. (2013). Redox proteomics uncovers peroxynitrite-sensitive proteins that help *Escherichia coli* to overcome nitrosative stress. *J Biol Chem* **288**, 19698–19714.

Lin, J. T. & Stewart, V. (1998). Nitrate assimilation by bacteria. *Adv Microb Physiol* **39**, 1–30, 379.

Linn, W. S., Solomon, J. C., Trim, S. C., Spier, C. E., Shamoo, D. A., Venet, T. G., Avol, E. L. & Hackney, J. D. (1985). Effects of exposure to 4 ppm nitrogen

dioxide in healthy and asthmatic volunteers. *Arch Environ Health Int J* **40**, 234–239.

Liu, N., Pak, T. & Boon, E. M. (2010). Characterization of a diguanylate cyclase from *Shewanella woodyi* with cyclase and phosphodiesterase activities. *Mol Biosyst* **6**, 1561–1564.

Liu, N., Xu, Y., Hossain, S., Huang, N., Coursolle, D., Gralnick, J. A. & Boon, E. M. (2012a). Nitric oxide regulation of cyclic di-GMP synthesis and hydrolysis in *Shewanella woodyi*. *Biochemistry (Mosc)* **51**, 2087–2099.

Liu, P., Huang, Q. & Chen, W. (2012b). Heterologous expression of bacterial nitric oxide synthase gene: a potential biological method to control biofilm development in the environment. *Can J Microbiol* **58**, 336–344.

Liu, X., Miller, M. J. S., Joshi, M. S., Thomas, D. D. & Lancaster, J. R. (1998). Accelerated reaction of nitric oxide with O_2 within the hydrophobic interior of biological membranes. *Proc Natl Acad Sci U S A* **95**, 2175–2179.

Li, Y., Heine, S., Entian, M., Sauer, K. & Frankenberg-Dinkel, N. (2013). NO-induced biofilm dispersion in *Pseudomonas aeruginosa* is mediated by an MHYT domain-coupled phosphodiesterase. *J Bacteriol* **195**, 3531–3542.

Lobasso, S., Lopalco, P., Lattanzio, V. M. T. & Corcelli, A. (2003). Osmotic shock induces the presence of glycocardiolipin in the purple membrane of *Halobacterium salinarum*. *J Lipid Res* **44**, 2120–2126.

Lobasso, S., Lopalco, P., Angelini, R., Vitale, R., Huber, H., Müller, V. & Corcelli, A. (2012). Coupled TLC and MALDI-TOF/MS analyses of the lipid extract of the hyperthermophilic archaeon *Pyrococcus furiosus*. *Archaea* **2012**, 1–10.

Loegering, D. J. & Schwacha, M. G. (1991). Macrophage hydrogen peroxide production and phagocytic function are decreased following phagocytosis mediated by Fc receptors but not complement receptors. *Biochem Biophys Res Commun* **180**, 268–272.

Lopalco, P. (2003). Osmotic shock stimulates *de novo* synthesis of two cardiolipins in an extreme halophilic archaeon. *J Lipid Res* **45**, 194–201.

Loper, J. E., Hassan, K. A., Mavrodi, D. V., Davis, E. W., II, Lim, C. K., Shaffer, B. T., Elbourne, L. D. H., Stockwell, V. O., Hartney, S. L. & other authors. (2012). Comparative genomics of plant-associated *Pseudomonas* spp.: insights into diversity and inheritance of traits involved in multitrophic interactions. *PLoS Genet* **8**, e1002784.

López, C. S., Alice, A. F., Heras, H., Rivas, E. A. & Sánchez-Rivas, C. (2006). Role of anionic phospholipids in the adaptation of *Bacillus subtilis* to high salinity. *Microbiol Read Engl* **152**, 605–616.

Los, D. A. & Murata, N. (2004). Membrane fluidity and its roles in the perception of environmental signals. *Biochim Biophys Acta BBA - Biomembr*, Lipid-Protein Interactions **1666**, 142–157.

Loughlin, M. F., Jones, M. V. & Lambert, P. A. (2002). *Pseudomonas aeruginosa* cells adapted to benzalkonium chloride show resistance to other membrane-active agents but not to clinically relevant antibiotics. *J Antimicrob Chemother* **49**, 631–639.

Lugtenberg, B. J. J., Dekkers, L. & Bloemberg, G. V. (2001). Molecular determinants of rhizosphere colonization by *Pseudomonas*. *Annu Rev Phytopathol* **39**, 461–490.

MacMicking, J., Xie, Q. & Nathan, C. (1997). Nitric oxide and macrophage function. *Annu Rev Immunol* **15**, 323–350.

Madi, A., Lakhdari, O., Blottière, H. M., Guyard-Nicodème, M., Roux, K. L., Groboillot, A., Svinareff, P., Doré, J., Orange, N. & other authors. (2010a). The clinical *Pseudomonas fluorescens* MFN1032 strain exerts a cytotoxic effect on epithelial intestinal cells and induces Interleukin-8 via the AP-1 signaling pathway. *BMC Microbiol* **10**, 215.

Madi, A., Svinareff, P., Orange, N., Feuilloley, M. G. & Connil, N. (2010b). *Pseudomonas fluorescens* alters epithelial permeability and translocates across Caco-2/TC7 intestinal cells. *Gut Pathog* **2**, 16.

Mah, T.-F., Pitts, B., Pellock, B., Walker, G. C., Stewart, P. S. & O'Toole, G. A. (2003). A genetic basis for *Pseudomonas aeruginosa* biofilm antibiotic resistance. *Nature* **426**, 306–310.

Ma, L., Conover, M., Lu, H., Parsek, M. R., Bayles, K. & Wozniak, D. J. (2009). Assembly and development of the *Pseudomonas aeruginosa* biofilm matrix. *PLoS Pathog* **5**, e1000354.

Mansilla, M. C., Cybulski, L. E., Albanesi, D. & Mendoza, D. de. (2004). Control of membrane lipid fluidity by molecular thermosensors. *J Bacteriol* **186**, 6681–6688.

Marchi, M., Boutin, M., Gazengel, K., Rispe, C., Gauthier, J.-P., Guillerm-Erckelboudt, A.-Y., Lebreton, L., Barret, M., Daval, S. & Sarniguet, A. (2013). Genomic analysis of the biocontrol strain P*seudomonas fluorescens* Pf29Arp with evidence of T3SS and T6SS gene expression on plant roots. *Environ Microbiol Rep* **5**, 393–403.

Markowicz, A., Plociniczak, T. & Piotrowska-Seget, Z. (2010). Response of bacteria to heavy metals measured as changes in FAME profiles. *Pol J Environ Stud* **19**.

Marletta, M. A. (1989). Nitric oxide: biosynthesis and biological significance. *Trends Biochem Sci* **14**, 488–492.

Marrakchi, M., Liu, X. & Andreescu, S. (2014). Oxidative stress and antibiotic resistance in bacterial pathogens: state of the art, methodologies, and future trends. *Adv Exp Med Biol* **806**, 483–498.

Marr, A. G. & Ingraham, J. L. (1962). Effect of temperature on the composition of fatty acids in *Escherichia coli*. *J Bacteriol* **84**, 1260–1267.

Martínez-Granero, F., Navazo, A., Barahona, E., Redondo-Nieto, M., Rivilla, R. & Martín, M. (2012). The Gac-Rsm and SadB signal transduction pathways converge on AlgU to downregulate motility in *Pseudomonas fluorescens*. *PLoS ONE* **7**.

Mastropaolo, M. D., Silby, M. W., Nicoll, J. S. & Levy, S. B. (2012). Novel genes involved in *Pseudomonas fluorescens* Pf0-1 motility and biofilm formation. *Appl Environ Microbiol* **78**, 4318–4329.

Mattick, J. S. (2002). Type IV pili and twitching motility. *Annu Rev Microbiol* **56**, 289–314.

Mavrodi, D. V., Blankenfeldt, W. & Thomashow, L. S. (2006). Phenazine compounds in fluorescent *Pseudomonas* spp. biosynthesis and regulation. *Annu Rev Phytopathol* **44**, 417–445.

Mavrodi, D. V., Joe, A., Mavrodi, O. V., Hassan, K. A., Weller, D. M., Paulsen, I. T., Loper, J. E., Alfano, J. R. & Thomashow, L. S. (2011). Structural and functional analysis of the type III secretion system from *Pseudomonas fluorescens* Q8r1-96. *J Bacteriol* **193**, 177–189.

Mayer, H. (1999). Air pollution in cities. *Atmos Environ* **33**, 4029–4037.

Mazurier, S., Merieau, A., Bergeau, D., Decoin, V., Sperandio, D., Crépin, A., Barbey, C., Jeannot, K., Vicré-Gibouin, M. & other authors. **(2015).** Type III secretion system and virulence markers highlight similarities and differences between human- and plant-associated pseudomonads related to *Pseudomonas fluorescens* and *P. putida*. *Appl Environ Microbiol* **81**, 2579–2590.

McCollister, B. D., Hoffman, M., Husain, M. & Vazquez-Torres, A. (2011). Nitric oxide protects bacteria from aminoglycosides by blocking the energy-dependent phases of drug uptake. *Antimicrob Agents Chemother* **55**, 2189–2196.

McElroy, M. C., Pittet, J. F., Allen, L., Wiener-Kronish, J. P. & Dobbs, L. G. (1997). Biochemical detection of type I cell damage after nitrogen dioxide-induced lung injury in rats. *Am J Physiol* **273**, L1228–1234.

McGarrity, J. T. & Armstrong, J. B. (1981). The effect of temperature and other growth conditions on the fatty acid composition of *Escherichia coli*. *Can J Microbiol* **27**, 835–840.

McLean, S., Bowman, L. A. H., Sanguinetti, G., Read, R. C. & Poole, R. K. (2010). Peroxynitrite toxicity in *Escherichia coli* K12 elicits expression of oxidative stress responses and protein nitration and nitrosylation. *J Biol Chem* **285**, 20724–20731.

van der Meer-Janssen, Y. P. M., van Galen, J., Batenburg, J. J. & Helms, J. B. (2010). Lipids in host–pathogen interactions: pathogens exploit the complexity of the host cell lipidome. *Prog Lipid Res* **49**, 1–26.

Mena, K. D. & Gerba, C. P. (2009). Risk assessment of *Pseudomonas aeruginosa* in water. *Rev Environ Contam Toxicol* **201**, 71–115.

Mercado-Blanco, J. & Bakker, P. A. H. M. (2007). Interactions between plants and beneficial *Pseudomonas* spp.: exploiting bacterial traits for crop protection. *Antonie Van Leeuwenhoek* **92**, 367–389.

Merieau, A., Gugi, B., Guespin-Michel, J. F. & Orange, N. (1993). Temperature regulation of lipase secretion by *Pseudomonas fluorescens* strain MFO1. *Appl Microbiol Biotechnol* **39**, 104–109.

Mileykovskaya, E. & Dowhan, W. (2009). Cardiolipin membrane domains in prokaryotes and eukaryotes. *Biochim Biophys Acta BBA - Biomembr*, Includes Special Section: Cardiolipin **1788**, 2084–2091.

Mirelman, D. & Nuchamowitz, Y. (1979). Biosynthesis of peptidoglycan in *Pseudomonas aeruginosa*. The incorporation of peptidoglycan into the cell wall. *Eur J Biochem FEBS* **94**, 541–548.

Möller, M. N., Lancaster Jr., J. R. & Denicola, A. (2008). Chapter 2 The interaction of reactive oxygen and nitrogen species with membranes. In *Curr Top Membr*, free radical effects on membranes, pp. 23–42. Edited by S. Matalon. Academic Press.

Moncada, S., Higgs, A. & Furchgott, R. (1997). XIV. International Union of Pharmacology Nomenclature in nitric oxide research. *Pharmacol Rev* **49**, 137–142.

Monds, R. D., Newell, P. D., Gross, R. H. & O'Toole, G. A. (2007). Phosphate-dependent modulation of c-di-GMP levels regulates *Pseudomonas fluorescens* Pf0-1 biofilm formation by controlling secretion of the adhesin LapA. *Mol Microbiol* **63**, 656–679.

Moreno-Vivián, C., Cabello, P., Martínez-Luque, M., Blasco, R. & Castillo, F. (1999). Prokaryotic nitrate reduction: molecular properties and functional distinction among bacterial nitrate reductases. *J Bacteriol* **181**, 6573–6584.

Morgan, R., Kohn, S., Hwang, S.-H., Hassett, D. J. & Sauer, K. (2006). BdlA, a chemotaxis regulator essential for biofilm dispersion in *Pseudomonas aeruginosa*. *J Bacteriol* **188**, 7335–7343.

Morin, J.-P., Préterre, D., Hasson, V. & Dionnet, F. (2013a, juin). Des particules au NO_2 comme effecteur toxique principal des émissions de moteurs diesel, un problème lié à l'évolution des réglementations Euro successives. *Pollution-Atmospherique*. text, .

Morin, J.-P., Preterre, D., Gouriou, F., Delmas, V., François, A., Orange, N., Grosboillot, A., Duclairoir-Poc, C., Moretti, M. & other authors. **(2013b, avril).** Particules urbaines et céréalières, micro-organismes, mycotoxines et pesticides. *Pollution-Atmospherique*. text, .

Morita, Y., Tomida, J. & Kawamura, Y. (2014). Responses of *Pseudomonas aeruginosa* to antimicrobials. *Front Microbiol* **4**.

Morris, C. E., Kinkel, L. L., Xiao, K., Prior, P. & Sands, D. C. (2007). Surprising niche for the plant pathogen *Pseudomonas syringae*. *Infect Genet Evol* **7**, 84–92.

Morrison, W. R. & Smith, L. M. (1964). Preparation of fatty acid methyl esters and dimethylacetals from lipids with boron fluoride–methanol. *J Lipid Res* **5**, 600–608.

Moynihan, J. A., Morrissey, J. P., Coppoolse, E. R., Stiekema, W. J., O'Gara, F. & Boyd, E. F. (2009). Evolutionary history of the *phl* gene cluster in the plant-associated bacterium *Pseudomonas fluorescens*. *Appl Environ Microbiol* **75**, 2122–2131.

Mulet, M., Lalucat, J. & García-Valdés, E. (2010). DNA sequence-based analysis of the *Pseudomonas* species. *Environ Microbiol* **12**, 1513–1530.

Mungrue, I. N. & Bredt, D. S. (2004). nNOS at a glance: implications for brain and brawn. *J Cell Sci* **117**, 2627–2629.

Murínová, S., Dercová, K., Čertík, M. & Lászlová, K. (2014). The adaptation responses of bacterial cytoplasmic membrane fluidity in the presence of environmental stress factors — polychlorinated biphenyls and 3-chlorobenzoic acid. *Biologia (Bratisl)* **69**, 428–434.

Murzyn, K., Rog, T. & Pasenkiewicz-Gierula, M. (2005). Phosphatidylethanolamine - phosphatidylglycerol bilayer as a model of the inner bacterial membrane. *Biophys J* **88**, 1091–1103.

Nagamachi, E., Shibuya, S., Hirai, Y., Matsushita, O., Tomochika, K. & Kanemasa, Y. (1991). Adaptational changes of fatty acid composition and the physical state of membrane lipids following the change of growth temperature in *Yersinia enterocolitica*. *Microbiol Immunol* **35**, 1085–1093.

Nathan, C. & Shiloh, M. U. (2000). Reactive oxygen and nitrogen intermediates in the relationship between mammalian hosts and microbial pathogens. *Proc Natl Acad Sci* **97**, 8841–8848.

Neill, S. J., Desikan, R. & Hancock, J. T. (2003). Nitric oxide signalling in plants. *New Phytol* **159**, 11–35.

Newell, P. D., Boyd, C. D., Sondermann, H. & O'Toole, G. A. (2011a). A c-di-GMP effector system controls cell adhesion by inside-out signaling and surface protein cleavage. *PLoS Biol* **9**.

Newell, P. D., Yoshioka, S., Hvorecny, K. L., Monds, R. D. & O'Toole, G. A. (2011b). Systematic analysis of diguanylate cyclases that promote biofilm formation by *Pseudomonas fluorescens* Pf0-1. *J Bacteriol* **193**, 4685–4698.

Nguyen, D., Joshi-Datar, A., Lepine, F., Bauerle, E., Olakanmi, O., Beer, K., McKay, G., Siehnel, R., Schafhauser, J. & other authors. (2011). Active starvation responses mediate antibiotic tolerance in biofilms and nutrient-limited bacteria. *Science* **334**, 982–986.

Nian, H., Zhang, J., Song, F., Fan, L. & Huang, D. (2007). Isolation of transposon mutants and characterization of genes involved in biofilm formation by *Pseudomonas fluorescens* TC222. *Arch Microbiol* **188**, 205–213.

Nielsen, T. H., Christophersen, C., Anthoni, U. & Sørensen, J. (1999). Viscosinamide, a new cyclic depsipeptide with surfactant and antifungal properties produced by *Pseudomonas fluorescens* DR54. *J Appl Microbiol* **87**, 80–90.

Nomura, K., Melotto, M. & He, S.-Y. (2005). Suppression of host defense in compatible plant–*Pseudomonas syringae* interactions. *Curr Opin Plant Biol*, Biotic interactions **8**, 361–368.

Nunoshiba, T., deRojas-Walker, T., Wishnok, J. S., Tannenbaum, S. R. & Demple, B. (1993). Activation by nitric oxide of an oxidative-stress response that defends *Escherichia coli* against activated macrophages. *Proc Natl Acad Sci U S A* **90**, 9993–9997.

Nurizzo, D., Silvestrini, M. C., Mathieu, M., Cutruzzolà, F., Bourgeois, D., Fülöp, V., Hajdu, J., Brunori, M., Tegoni, M. & Cambillau, C. (1997). N-terminal *arm* exchange is observed in the 2.15 A crystal structure of oxidized nitrite reductase from *Pseudomonas aeruginosa*. *Struct Lond Engl 1993* **5**, 1157–1171.

Nurizzo, D., Cutruzzolà, F., Arese, M., Bourgeois, D., Brunori, M., Cambillau, C. & Tegoni, M. (1998). Conformational changes occurring upon reduction and NO binding in nitrite reductase from *Pseudomonas aeruginosa*. *Biochemistry (Mosc)* **37**, 13987–13996.

Ochsner, U. A., Koch, A. K., Fiechter, A. & Reiser, J. (1994). Isolation and characterization of a regulatory gene affecting rhamnolipid biosurfactant synthesis in *Pseudomonas aeruginosa*. *J Bacteriol* **176**, 2044–2054.

Ochsner, U. A., Vasil, A. I. & Vasil, M. L. (1995). Role of the ferric uptake regulator of *Pseudomonas aeruginosa* in the regulation of siderophores and exotoxin A expression: purification and activity on iron-regulated promoters. *J Bacteriol* **177**, 7194–7201.

O'Donnell, V. B., Eiserich, J. P., Chumley, P. H., Jablonsky, M. J., Krishna, N. R., Kirk, M., Barnes, S., Darley-Usmar, V. M. & Freeman, B. A. (1999). Nitration of unsaturated fatty acids by nitric oxide-derived reactive nitrogen species peroxynitrite, nitrous acid, nitrogen dioxide, and nitronium ion. *Chem Res Toxicol* **12**, 83–92.

Oemar, B. S., Tschudi, M. R., Godoy, N., Brovkovich, V., Malinski, T. & Lüscher, T. F. (1998). Reduced endothelial nitric oxide synthase expression and production in human atherosclerosis. *Circulation* **97**, 2494–2498.

Ohwada, T., Shirakawa, Y., Kusumoto, M., Masuda, H. & Sato, T. (1999). Susceptibility to hydrogen peroxide and catalase activity of root nodule bacteria. *Biosci Biotechnol Biochem* **63**, 457–462.

Okuyama, H., Sasaki, S., Higashi, S. & Murata, N. (1990). A *trans*-unsaturated fatty acid in a psychrophilic bacterium, *Vibrio* sp. strain ABE-1. *J Bacteriol* **172**, 3515–3518.

Okuyama, H., Okajima, N., Sasaki, S., Higashi, S. & Murata, N. (1991). The *cis/trans* isomerization of the double bond of a fatty acid as a strategy for adaptation to changes in ambient temperature in the psychrophilic bacterium, Vibrio sp. strain ABE-1. *Biochim Biophys Acta* **1084**, 13–20.

Orange, N. (1994). Growth temperature regulates the induction of -lactamase in *Pseudomonas fluorescens* through modulation of the outer membrane permeation of a lactam-inducing antibiotic. *Microbiology* **140**, 3125–3130.

Oren, A. (2002). Diversity of halophilic microorganisms: environments, phylogeny, physiology, and applications. *J Ind Microbiol Biotechnol* **28**, 56–63.

Osawa, K., Nakajima, M., Kataoka, N., Arakawa, S. & Kamidono, S. (2002). Evaluation of antibacterial efficacy of drugs for urinary tract infections by genotyping based on pulsed-field gel electrophoresis (PFGE). *J Infect Chemother Off J Jpn Soc Chemother* **8**, 353–357.

O'Toole, G., Kaplan, H. B. & Kolter, R. (2000). Biofilm formation as microbial development. *Annu Rev Microbiol* **54**, 49–79.

O'Toole, G. A. & Ha, D.-G. (2015). c-di-GMP and its effects on biofilm formation and dispersion: a *Pseudomonas aeruginosa* review. *Microbiol Spectr* **3**.

O'Toole, G. A. & Kolter, R. (1998). Initiation of biofilm formation in Pseudomonas fluorescens WCS365 proceeds via multiple, convergent signalling pathways: a genetic analysis. *Mol Microbiol* **28**, 449–461.

Overhage, J., Bains, M., Brazas, M. D. & Hancock, R. E. W. (2008). Swarming of *Pseudomonas aeruginosa* is a complex adaptation leading to increased production of virulence factors and antibiotic resistance. *J Bacteriol* **190**, 2671–2679.

Overton, T. W., Justino, M. C., Li, Y., Baptista, J. M., Melo, A. M. P., Cole, J. A. & Saraiva, L. M. (2008). Widespread distribution in pathogenic bacteria of di-iron proteins that repair oxidative and nitrosative damage to iron-sulfur centers. *J Bacteriol* **190**, 2004–2013.

Padan, E., Bibi, E., Ito, M. & Krulwich, T. A. (2005). Alkaline pH homeostasis in bacteria: new insights. *Biochim Biophys Acta* **1717**, 67–88.

Pagès, J.-M., James, C. E. & Winterhalter, M. (2008). The porin and the permeating antibiotic: a selective diffusion barrier in Gram-negative bacteria. *Nat Rev Microbiol* **6**, 893–903.

Palleroni, N. J. & Doudoroff, M. (1971). Phenotypic characterization and deoxyribonucleic acid homologies of *Pseudomonas solanacearum*. *J Bacteriol* **107**, 690–696.

Palleroni, N. J., Ballard, R. W., Ralston, E. & Doudoroff, M. (1972). Deoxyribonucleic acid homologies among some *Pseudomonas* species. *J Bacteriol* **110**, 1–11.

Palleroni, N. J., Kunisawa, R., Contopoulou, R. & Doudoroff, M. (1973). Nucleic acid homologies in the genus *Pseudomonas*. *Int J Syst Bacteriol* **23**, 333–339.

Palleroni, N. J. (1984). Genus I. *Pseudomonas migula* 1894. In *Bergeys Man Syst Bacteriol*, The Wiliams and Wilkins Co., pp. 141–199. Baltimore: N. R. Krieg and J. G. Hol.

Palleroni, N. J. (2010). The *Pseudomonas* story. *Environ Microbiol* **12**, 1377–1383.

Palma, M., Zurita, J., Ferreras, J. A., Worgall, S., Larone, D. H., Shi, L., Campagne, F. & Quadri, L. E. N. (2005). *Pseudomonas aeruginosa* SoxR does not conform to the archetypal paradigm for SoxR-dependent regulation of the bacterial oxidative stress adaptive response. *Infect Immun* **73**, 2958–2966.

Parsons, J. B. & Rock, C. O. (2013). Bacterial lipids: metabolism and membrane homeostasis. *Prog Lipid Res* **52**, 249–276.

Patel, R. P., McAndrew, J., Sellak, H., White, C. R., Jo, H., Freeman, B. A. & Darley-Usmar, V. M. (1999). Biological aspects of reactive nitrogen species. *Biochim Biophys Acta BBA - Bioenerg* **1411**, 385–400.

Paul, R., Weiser, S., Amiot, N. C., Chan, C., Schirmer, T., Giese, B. & Jenal, U. (2004). Cell cycle-dependent dynamic localization of a bacterial response regulator with a novel di-guanylate cyclase output domain. *Genes Dev* **18**, 715–727.

Pearce, D. A., Hughes, K. A., Lachlan-Cope, T., Harangozo, S. A. & Jones, A. E. (2010). Biodiversity of air-borne microorganisms at Halley Station, Antarctica. *Extrem Life Extreme Cond* **14**, 145–159.

Pedroso, M. C., Magalhaes, J. R. & Durzan, D. (2000). A nitric oxide burst precedes apoptosis in angiosperm and gymnosperm callus cells and foliar tissues. *J Exp Bot* **51**, 1027–1036.

Pedrotta, V. & Witholt, B. (1999). Isolation and characterization of the *cis-trans*-unsaturated fatty acid isomerase of *Pseudomonas oleovorans* GPo12. *J Bacteriol* **181**, 3256–3261.

Peix, A., Ramírez-Bahena, M.-H. & Velázquez, E. (2009). Historical evolution and current status of the taxonomy of genus *Pseudomonas*. *Infect Genet Evol*, Includes papers from the Special Issue 'Parasitology in Mexico' **9**, 1132–1147.

Pepi, M., Heipieper, H. J., Fischer, J., Ruta, M., Volterrani, M. & Focardi, S. E. (2008). Membrane fatty acids adaptive profile in the simultaneous presence of arsenic and toluene in *Bacillus* sp. ORAs2 and *Pseudomonas* sp. ORAs5 strains. *Extrem Life Extreme Cond* **12**, 343–349.

Pershagen, G., Rylander, E., Norberg, S., Eriksson, M. & Nordvall, S. L. (1995). Air pollution involving

nitrogen dioxide exposure and wheezing bronchitis in children. *Int J Epidemiol* **24**, 1147–1153.

Petrova, O. E. & Sauer, K. (2012a). PAS domain residues and prosthetic group involved in BdlA-dependent dispersion response by *Pseudomonas aeruginosa* biofilms. *J Bacteriol* **194**, 5817–5828.

Petrova, O. E. & Sauer, K. (2012b). Dispersion by *Pseudomonas aeruginosa* requires an unusual posttranslational modification of BdlA. *Proc Natl Acad Sci U S A* **109**, 16690–16695.

Petrova, O. E., Cherny, K. E. & Sauer, K. (2014). The *Pseudomonas aeruginosa* diguanylate cyclase GcbA, a homolog of *P. fluorescens* GcbA, promotes initial attachment to surfaces, but not biofilm formation, via regulation of motility. *J Bacteriol* **196**, 2827–2841.

Picot, L., Chevalier, S., Mezghani-Abdelmoula, S., Merieau, A., Lesouhaitier, O., Leroux, P., Cazin, L., Orange, N. & Feuilloley, M. G. J. (2003). Cytotoxic effects of the lipopolysaccharide from *Pseudomonas fluorescens* on neurons and glial cells. *Microb Pathog* **35**, 95–106.

Picot, L., Mezghani-Abdelmoula, S., Chevalier, S., Merieau, A., Lesouhaitier, O., Guerillon, J., Cazin, L., Orange, N. & Feuilloley, M. G. J. (2004). Regulation of the cytotoxic effects of *Pseudomonas fluorescens* by growth temperature. *Res Microbiol* **155**, 39–46.

Planchet, E. & Kaiser, W. M. (2006). Nitric oxide production in plants. *Plant Signal Behav* **1**, 46–51.

Plate, L. & Marletta, M. A. (2012). Nitric oxide modulates bacterial biofilm formation through a multicomponent cyclic-di-GMP signaling network. *Mol Cell* **46**, 449–460.

Plate, L. & Marletta, M. A. (2013a). Nitric oxide-sensing H-NOX proteins govern bacterial communal behavior. *Trends Biochem Sci* **38**, 566–575.

Plate, L. & Marletta, M. A. (2013b). Phosphorylation-dependent derepression by the response regulator HnoC in the *Shewanella oneidensis* nitric oxide signaling network. *Proc Natl Acad Sci U S A* **110**, E4648–E4657.

Poger, D. & Mark, A. E. (2015). A ring to rule them all: the effect of cyclopropane fatty acids on the fluidity of lipid bilayers. *J Phys Chem B* **119**, 5487–5495.

Pogozheva, I. D., Mosberg, H. I. & Lomize, A. L. (2014). Life at the border: adaptation of proteins to anisotropic membrane environment. *Protein Sci* **23**, 1165–1196.

Poole, K. (2005a). Efflux-mediated antimicrobial resistance. *J Antimicrob Chemother* **56**, 20–51.

Poole, K. (2005b). Aminoglycoside resistance in *Pseudomonas aeruginosa*. *Antimicrob Agents Chemother* **49**, 479–487.

Poole, K. (2012). Bacterial stress responses as determinants of antimicrobial resistance. *J Antimicrob Chemother* dks196.

Poole, K. (2014). Stress responses as determinants of antimicrobial resistance in *Pseudomonas aeruginosa*: multidrug efflux and more. *Can J Microbiol* **60**, 783–791.

Poole, R. K. & Hughes, M. N. (2000). New functions for the ancient globin family: bacterial responses to nitric oxide and nitrosative stress. *Mol Microbiol* **36**, 775–783.

Poole, R. K., Anjum, M. F., Membrillo-Hernández, J., Kim, S. O., Hughes, M. N. & Stewart, V. (1996). Nitric oxide, nitrite, and Fnr regulation of *hmp* (flavohemoglobin) gene expression in *Escherichia coli* K-12. *J Bacteriol* **178**, 5487–5492.

Pope, C. A., Ezzati, M. & Dockery, D. W. (2009). Fine-particulate air pollution and life expectancy in the United States. *N Engl J Med* **360**, 376–386.

Potter, A. J., Kidd, S. P., Edwards, J. L., Falsetta, M. L., Apicella, M. A., Jennings, M. P. & McEwan, A. G. (2009). Thioredoxin reductase is essential for protection of *Neisseria gonorrhoeae* against killing by nitric oxide and for bacterial growth during interaction with cervical epithelial cells. *J Infect Dis* **199**, 227–235.

Price, M. S., Chao, L. Y. & Marletta, M. A. (2007). *Shewanella oneidensis* MR-1 H-NOX regulation of a histidine kinase by nitric oxide. *Biochemistry (Mosc)* **46**, 13677–13683.

Pryor, W. A. & Lightsey, J. W. (1981). Mechanisms of nitrogen dioxide reactions: initiation of lipid peroxidation and the production of nitrous Acid. *Science* **214**, 435–437.

Pryor, W. A., Lightsey, J. W. & Church, D. F. (1982). Reaction of nitrogen dioxide with alkenes and polyunsaturated fatty acids: addition and hydrogen-abstraction mechanisms. *J Am Chem Soc* **104**, 6685–6692.

Radi, R. (2004). Nitric oxide, oxidants, and protein tyrosine nitration. *Proc Natl Acad Sci* **101**, 4003–4008.

Raetz, C. R. H. & Whitfield, C. (2002). Lipopolysaccharide endotoxins. *Annu Rev Biochem* **71**, 635–700.

Ragolia, L. & Tropp, B. E. (1994). The effects of phosphoglycerides on *Escherichia coli* cardiolipin synthase. *Biochim Biophys Acta* **1214**, 323–332.

Rainey, P. B. (1999). Adaptation of *Pseudomonas fluorescens* to the plant rhizosphere. *Environ Microbiol* **1**, 243–257.

Rainey, P. B. & Bailey, M. J. (1996). Physical and genetic map of the *Pseudomonas fluorescens* SBW25 chromosome. *Mol Microbiol* **19**, 521–533.

Ramaroson, R., Lelievre, C. P., Magnani, G., Talbaut, M., Gouriou, F., Frejafon, E., Schaefer, K. & Copalle, A. (2006). Field measurements of airport emissions and air pollutants including aerosols at Paris CDG airports. The AIRPUR project. Presented at the Joint CACGP/IGAC/WMO Symposium 'Atmospheric chemistry at the interfaces 2006'.

Ramette, A., Moënne-Loccoz, Y. & Défago, G. (2003). Prevalence of fluorescent pseudomonads producing antifungal phloroglucinols and/or hydrogen cyanide in soils naturally suppressive or conducive to tobacco black root rot. *FEMS Microbiol Ecol* **44**, 35–43.

Ramette, A., Frapolli, M., Saux, M. F.-L., Gruffaz, C., Meyer, J.-M., Défago, G., Sutra, L. & Moënne-Loccoz, Y. (2011). *Pseudomonas protegens* sp. nov., widespread plant-protecting bacteria producing the biocontrol compounds 2,4-diacetylphloroglucinol and pyoluteorin. *Syst Appl Microbiol* **34**, 180–188.

Ramos, J. L., Duque, E., Rodríguez-Herva, J.-J., Godoy, P., Haïdour, A., Reyes, F. & Fernández-Barrero, A. (1997). Mechanisms for solvent tolerance in bacteria. *J Biol Chem* **272**, 3887–3890.

Ramos, J. L., Gallegos, M.-T., Marqués, S., Ramos-González, M.-I., Espinosa-Urgel, M. & Segura, A. (2001). Responses of Gram-negative bacteria to certain environmental stressors. *Curr Opin Microbiol* **4**, 166–171.

Reilly, J., Prinn, R., Harnisch, J., Fitzmaurice, J., Jacoby, H., Kicklighter, D., Melillo, J., Stone, P., Sokolov, A. & Wang, C. (1999). Multi-gas assessment of the Kyoto Protocol. *Nature* **401**, 549–555.

Reva, O. N., Weinel, C., Weinel, M., Böhm, K., Stjepandic, D., Hoheisel, J. D. & Tümmler, B. (2006). Functional genomics of stress response in *Pseudomonas putida* KT2440. *J Bacteriol* **188**, 4079–4092.

Rezzonico, F., Binder, C., Défago, G. & Moënne-Loccoz, Y. (2005). The type III secretion system of biocontrol *Pseudomonas fluorescens* KD targets the phytopathogenic *Chromista Pythium* ultimum and promotes cucumber protection. *Mol Plant-Microbe Interact MPMI* **18**, 991–1001.

Richardson, A. R., Libby, S. J. & Fang, F. C. (2008). A nitric oxide-inducible lactate dehydrogenase enables *Staphylococcus aureus* to resist innate immunity. *Science* **319**, 1672–1676.

Richter, G., Schober, C., Süß, R., Fuchs, B., Müller, M. & Schiller, J. (2008). The reaction between phosphatidylethanolamines and HOCl investigated by TLC: fading of the dye primuline is induced by dichloramines. *J Chromatogr B* **867**, 233–237.

Rietsch, A., Vallet-Gely, I., Dove, S. L. & Mekalanos, J. J. (2005). ExsE, a secreted regulator of type III secretion genes in *Pseudomonas aeruginosa*. *Proc Natl Acad Sci U S A* **102**, 8006–8011.

Rinaldo, S., Giardina, G., Castiglione, N., Stelitano, V. & Cutruzzolà, F. (2011). The catalytic mechanism of *Pseudomonas aeruginosa cd1* nitrite reductase. *Biochem Soc Trans* **39**, 195–200.

Ringen, L. M. & Drake, C. H. (1952). A study of the incidence of Pseudomonas aeruginosa from various natural sources. *J Bacteriol* **64**, 841–845.

Roach, C., Feller, S. E., Ward, J. A., Shaikh, S. R., Zerouga, M. & Stillwell, W. (2004). Comparison of *cis*- and *trans*- fatty acid containing phosphatidylcholines on membrane properties. *Biochemistry (Mosc)* **43**, 6344–6351.

Robleto, E. A., López-Hernández, I., Silby, M. W. & Levy, S. B. (2003). Genetic analysis of the AdnA regulon in *Pseudomonas fluorescens*: nonessential role of flagella in adhesion to sand and biofilm formation. *J Bacteriol* **185**, 453–460.

Rockel, P., Strube, F., Rockel, A., Wildt, J. & Kaiser, W. M. (2002). Regulation of nitric oxide (NO) production by plant nitrate reductase *in vivo* and *in vitro*. *J Exp Bot* **53**, 103–110.

Rogers, P. A. & Ding, H. (2001). Cysteine-mediated destabilization of dinitrosyl iron complexes in proteins. *J Biol Chem* **276**, 30980–30986.

Romantsov, T., Helbig, S., Culham, D. E., Gill, C., Stalker, L. & Wood, J. M. (2007). Cardiolipin promotes polar localization of osmosensory transporter ProP in *Escherichia coli*. *Mol Microbiol* **64**, 1455–1465.

Romantsov, T., Guan, Z. & Wood, J. M. (2009). Cardiolipin and the osmotic stress responses of bacteria. *Biochim Biophys Acta BBA - Biomembr*, Includes Special Section: Cardiolipin **1788**, 2092–2100.

Romeo, A., Sonnleitner, E., Sorger-Domenigg, T., Nakano, M., Eisenhaber, B. & Bläsi, U. (2012). Transcriptional regulation of nitrate assimilation in *Pseudomonas aeruginosa* occurs via transcriptional antitermination within the *nirBD*-PA1779-*cobA* operon. *Microbiol Read Engl* **158**, 1543–1552.

Romsang, A., Duang-Nkern, J., Leesukon, P., Saninjuk, K., Vattanaviboon, P. & Mongkolsuk, S. (2014). The iron-sulphur cluster biosynthesis regulator IscR contributes to iron homeostasis and resistance to oxidants in *Pseudomonas aeruginosa*. *PLoS ONE* **9**, e86763.

Ron, P. E. Z. (2013). Bacterial stress response. In *The Prokaryotes*, pp. 589–603. Edited by E. Rosenberg, E. F. DeLong, S. Lory, E. Stackebrandt & F. Thompson. Springer Berlin Heidelberg.

Rossignol, G., Sperandio, D., Guerillon, J., Duclairoir Poc, C., Soum-Soutera, E., Orange, N., Feuilloley, M. G. J. & Merieau, A. (2009). Phenotypic variation in the *Pseudomonas fluorescens* clinical strain MFN1032. *Res Microbiol* **160**, 337–344.

Rossignol, G., Merieau, A., Guerillon, J., Veron, W., Lesouhaitier, O., Feuilloley, M. G. & Orange, N. (2008). Involvement of a phospholipase C in the hemolytic activity of a clinical strain of *Pseudomonas fluorescens*. *BMC Microbiol* **8**, 189.

Rowley, G., Spector, M., Kormanec, J. & Roberts, M. (2006). Pushing the envelope: extracytoplasmic stress responses in bacterial pathogens. *Nat Rev Microbiol* **4**, 383–394.

Roy, A. B., Petrova, O. E. & Sauer, K. (2012). The phosphodiesterase DipA (PA5017) is essential for

Pseudomonas aeruginosa biofilm dispersion. *J Bacteriol* **194**, 2904–2915.

Roy, H., Dare, K. & Ibba, M. (2009). Adaptation of the bacterial membrane to changing environments using aminoacylated phospholipids. *Mol Microbiol* **71**, 547–550.

Rubbo, H., Radi, R., Trujillo, M., Telleri, R., Kalyanaraman, B., Barnes, S., Kirk, M. & Freeman, B. A. (1994). Nitric oxide regulation of superoxide and peroxynitrite-dependent lipid peroxidation. Formation of novel nitrogen-containing oxidized lipid derivatives. *J Biol Chem* **269**, 26066–26075.

Rühl, J., Hein, E.-M., Hayen, H., Schmid, A. & Blank, L. M. (2012). The glycerophospholipid inventory of *Pseudomonas putida* is conserved between strains and enables growth condition-related alterations. *Microb Biotechnol* **5**, 45–58.

Rumley, M. K., Therisod, H., Weissborn, A. C. & Kennedy, E. P. (1992). Mechanisms of regulation of the biosynthesis of membrane-derived oligosaccharides in *Escherichia coli*. *J Biol Chem* **267**, 11806–11810.

Russell, N. J. (2002). Bacterial membranes: the effects of chill storage and food processing. An overview. *Int J Food Microbiol* **79**, 27–34.

Russell, N. J., Evans, R. I., ter Steeg, P. F., Hellemons, J., Verheul, A. & Abee, T. (1995). Membranes as a target for stress adaptation. *Int J Food Microbiol*, Physiology of Food Poisoning Microorganisms, AAIR Concerted Action PL920630 **28**, 255–261.

Saitou, N. & Nei, M. (1987). The neighbor-joining method: a new method for reconstructing phylogenetic trees. *Mol Biol Evol* **4**, 406–425.

Salamon, Z., Lindblom, G., Rilfors, L., Linde, K. & Tollin, G. (2000). Interaction of phosphatidylserine synthase from *E. coli* with lipid bilayers: coupled plasmon-waveguide resonance spectroscopy studies. *Biophys J* **78**, 1400–1412.

Salgado, I., Martínez, M. C., Oliveira, H. C. & Frungillo, L. (2013). Nitric oxide signaling and homeostasis in plants: a focus on nitrate reductase and S-nitrosoglutathione reductase in stress-related responses. *Braz J Bot* **36**, 89–98.

Šantl-Temkiv, T., Sahyoun, M., Finster, K., Hartmann, S., Augustin-Bauditz, S., Stratmann, F., Wex, H., Clauss, T., Nielsen, N. W. & other authors. (2015). Characterization of airborne ice-nucleation-active bacteria and bacterial fragments. *Atmos Environ* **109**, 105–117.

Sastalla, I., Chim, K., Cheung, G. Y. C., Pomerantsev, A. P. & Leppla, S. H. (2009). Codon-optimized fluorescent proteins designed for expression in low-GC Gram-positive bacteria. *Appl Environ Microbiol* **75**, 2099–2110.

Sawers, R. G. (1991). Identification and molecular characterization of a transcriptional regulator from *Pseudomonas aeruginosa* PAO1 exhibiting structural and functional similarity to the FNR protein of *Escherichia coli*. *Mol Microbiol* **5**, 1469–1481.

Scales, B. S., Dickson, R. P., LiPuma, J. J. & Huffnagle, G. B. (2014). Microbiology, genomics, and clinical significance of the *Pseudomonas fluorescens* species complex, an unappreciated colonizer of humans. *Clin Microbiol Rev* **27**, 927–948.

Schirmer, T. & Jenal, U. (2009). Structural and mechanistic determinants of c-di-GMP signalling. *Nat Rev Microbiol* **7**, 724–735.

Schreiber, F., Beutler, M., Enning, D., Lamprecht-Grandio, M., Zafra, O., González-Pastor, J. E. & de Beer, D. (2011). The role of nitric-oxide-synthase-derived nitric oxide in multicellular traits of *Bacillus subtilis* 3610: biofilm formation, swarming, and dispersal. *BMC Microbiol* **11**, 111.

Schreiber, K., Krieger, R., Benkert, B., Eschbach, M., Arai, H., Schobert, M. & Jahn, D. (2007). The anaerobic regulatory network required for *Pseudomonas aeruginosa* nitrate respiration. *J Bacteriol* **189**, 4310–4314.

Schumann, U. & Huntrieser, H. (2007). The global lightning-induced nitrogen oxides source. *Atmos Chem Phys* **7**, 3823–3907.

Schwartz, C. J., Giel, J. L., Patschkowski, T., Luther, C., Ruzicka, F. J., Beinert, H. & Kiley, P. J. (2001). IscR, an Fe-S cluster-containing transcription factor, represses expression of *Escherichia coli* genes encoding Fe-S cluster assembly proteins. *Proc Natl Acad Sci U S A* **98**, 14895–14900.

Schwartz, S. E., Brookhaven N. L. & White, W. H. (1981). Solubility equilibria of the nitrogen oxides and oxyacids in dilute aqueous solution. *Adv Env Sci Eng U S* **4**.

Segura, A., Bernal, P., Pini, C., Krell, T., Daniels, C. & Ramos, J.-L. (2010). Membrane composition and modifications in response to aromatic hydrocarbons in Gram-negative bacteria. In *Handb Hydrocarb Lipid Microbiol*, pp. 1595–1603. Edited by K. N. Timmis. Springer Berlin Heidelberg.

Seth, D., Hausladen, A., Wang, Y.-J. & Stamler, J. S. (2012). Endogenous protein S-nitrosylation in *E. coli*: regulation by OxyR. *Science* **336**, 470–473.

Shaul, P. W. (2002). Regulation of endothelial nitric oxide synthase: location, location, location. *Annu Rev Physiol* **64**, 749–774.

Shaw, J. E., Alattia, J.-R., Verity, J. E., Privé, G. G. & Yip, C. M. (2006). Mechanisms of antimicrobial peptide action: studies of indolicidin assembly at model membrane interfaces by in situ atomic force microscopy. *J Struct Biol* **154**, 42–58.

Shiro, Y. (2012). Structure and function of bacterial nitric oxide reductases: Nitric oxide reductase, anaerobic enzymes. *Biochim Biophys Acta BBA - Bioenerg*, 17th European Bioenergetics Conference **1817**, 1907–1913.

Shiro, Y., Sugimoto, H., Tosha, T., Nagano, S. & Hino, T. (2012). Structural basis for nitrous oxide generation by bacterial nitric oxide reductases. *Philos Trans R Soc B Biol Sci* **367**, 1195–1203.

Shooter, R. A., Gaya, H., Cooke, E. M., Kumar, P., Patel, N., Parker, M. T., Thom, B. T. & France, D. (1969). Food and medicaments as possible sources of hospital strains of *Pseudomonas aeruginosa*. *The Lancet*, Originally published as Volume 1, Issue 7608 **293**, 1227–1229.

Shooter, R. A., Cooke, E. M., Faiers, M., Breaden, A. & O'Farrell, S. (1971). Isolation of Escherichia coli, Pseudomonas aeruginosa, and Klebsiella from food in hospitals, canteens, and schools. *The Lancet*, Originally published as Volume 2, Issue 7721 **298**, 390–392.

Sias, S. R., Stouthamer, A. H. & Ingraham, J. L. (1980). The assimilatory and dissimilatory nitrate reductases of *Pseudomonas aeruginosa* are encoded by different genes. *J Gen Microbiol* **118**, 229–234.

Sigfrid, L. A., Cunningham, J. M., Beeharry, N., Lortz, S., Tiedge, M., Lenzen, S., Carlsson, C. & Green, I. C. (2003). Cytokines and nitric oxide inhibit the enzyme activity of catalase but not its protein or mRNA expression in insulin-producing cells. *J Mol Endocrinol* **31**, 509–518.

Signorelli, S., Möller, M. N., Coitiño, E. L. & Denicola, A. (2011). Nitrogen dioxide solubility and permeation in lipid membranes. *Arch Biochem Biophys* **512**, 190–196.

Silby, M. W., Cerdeño-Tárraga, A. M., Vernikos, G. S., Giddens, S. R., Jackson, R. W., Preston, G. M., Zhang, X.-X., Moon, C. D., Gehrig, S. M. & other authors. (2009). Genomic and genetic analyses of diversity and plant interactions of *Pseudomonas fluorescens*. *Genome Biol* **10**, R51.

Silhavy, T. J., Kahne, D. & Walker, S. (2010). The bacterial cell envelope. *Cold Spring Harb Perspect Biol* **2**.

Silvestrini, M. C., Galeotti, C. L., Gervais, M., Schininà, E., Barra, D., Bossa, F. & Brunori, M. (1989). Nitrite reductase from *Pseudomonas aeruginosa*: sequence of the gene and the protein. *FEBS Lett* **254**, 33–38.

Sivertsen, B. (2006). Global ambient air pollution concentrations and trends. In *Air Qual Guidel*, World Health Organization., pp. 31–59.

Skalska, K., Miller, J. S. & Ledakowicz, S. (2010). Trends in NO_x abatement: A review. *Sci Total Environ* **408**, 3976–3989.

Sleator, R. D. & Hill, C. (2002). Bacterial osmoadaptation: the role of osmolytes in bacterial stress and virulence. *FEMS Microbiol Rev* **26**, 49–71.

Smith, P. K., Krohn, R. I., Hermanson, G. T., Mallia, A. K., Gartner, F. H., Provenzano, M. D., Fujimoto, E. K., Goeke, N. M., Olson, B. J. & Klenk, D. C. (1985). Measurement of protein using bicinchoninic acid. *Anal Biochem* **150**, 76–85.

van Sorge, N. M., Beasley, F. C., Gusarov, I., Gonzalez, D. J., Köckritz-Blickwede, M. von, Anik, S., Borkowski, A., Dorrestein, P. C., Nudler, E. & Nizet, V. (2013). Methicillin-resistant *Staphylococcus aureus* bacterial nitric oxide synthase affects antibiotic sensitivity and skin abscess development. *J Biol Chem* jbc.M112.448738.

Spangler, C., Böhm, A., Jenal, U., Seifert, R. & Kaever, V. (2010). A liquid chromatography-coupled tandem mass spectrometry method for quantitation of cyclic di-guanosine monophosphate. *J Microbiol Methods* **81**, 226–231.

Spek, E. J., Wright, T. L., Stitt, M. S., Taghizadeh, N. R., Tannenbaum, S. R., Marinus, M. G. & Engelward, B. P. (2001). Recombinational repair is critical for survival of *Escherichia coli* exposed to nitric oxide. *J Bacteriol* **183**, 131–138.

Sperandio, D., Rossignol, G., Guerillon, J., Connil, N., Orange, N., Feuilloley, M. G. & Merieau, A. (2010). Cell-associated hemolysis activity in the clinical strain of *Pseudomonas fluorescens* MFN1032. *BMC Microbiol* **10**, 124.

Sperandio, D., Decoin, V., Latour, X., Mijouin, L., Hillion, M., Feuilloley, M. G. J., Orange, N. & Merieau, A. (2012). Virulence of the *Pseudomonas fluorescens* clinical strain MFN1032 towards *Dictyostelium discoideum* and macrophages in relation with type III secretion system. *BMC Microbiol* **12**, 223.

Spiers, A. J., Buckling, A. & Rainey, P. B. (2000). The causes of *Pseudomonas* diversity. *Microbiology* **146**, 2345–2350.

Spiro, S. (2007). Regulators of bacterial responses to nitric oxide. *FEMS Microbiol Rev* **31**, 193–211.

Srour, N., Chaparro, C., Vandemheen, K., Singer, L. G., Keshavjee, S. & Aaron, S. D. (2014). Effect of infection with transmissible strains of *Pseudomonas aeruginosa* on lung transplantation outcomes in patients with cystic fibrosis. *J Heart Lung Transplant Off Publ Int Soc Heart Transplant*.

Stamatakis, A. (2006). RAxML-VI-HPC: maximum likelihood-based phylogenetic analyses with thousands of taxa and mixed models. *Bioinforma Oxf Engl* **22**, 2688–2690.

Stanier, R. Y., Palleroni, N. J. & Doudoroff, M. (1966). The aerobic pseudomonads a taxonomic study. *J Gen Microbiol* **43**, 159–271.

Stelitano, V., Giardina, G., Paiardini, A., Castiglione, N., Cutruzzolà, F. & Rinaldo, S. (2013). C-di-GMP hydrolysis by *Pseudomonas aeruginosa* HD-GYP phosphodiesterases: analysis of the reaction mechanism and novel roles for pGpG. *PLoS ONE* **8**, e74920.

Stevanin, T. M., Ioannidis, N., Mills, C. E., Kim, S. O., Hughes, M. N. & Poole, R. K. (2000). Flavohemoglobin *Hmp* affords inducible protection for *Escherichia coli* respiration, catalyzed by cytochromes *bo'* or *bd*, from nitric oxide. *J Biol Chem* **275**, 35868–35875.

Stevanin, T. M., Moir, J. W. & Read, R. C. (2005). Nitric oxide detoxification systems enhance survival of *Neisseria meningitidis* in human macrophages and in nasopharyngeal mucosa. *Infect Immun* **73**, 3322–3329.

Stöhr, C., Strube, F., Marx, G., Ullrich, W. R. & Rockel, P. (2001). A plasma membrane-bound enzyme of tobacco roots catalyses the formation of nitric oxide from nitrite. *Planta* **212**, 835–841.

Stover, C. K., Pham, X. Q., Erwin, A. L., Mizoguchi, S. D., Warrener, P., Hickey, M. J., Brinkman, F. S., Hufnagle, W. O., Kowalik, D. J. & other authors. **(2000).** Complete genome sequence of *Pseudomonas aeruginosa* PAO1, an opportunistic pathogen. *Nature* **406**, 959–964.

Strehmel, J., Neidig, A., Nusser, M., Geffers, R., Brenner-Weiss, G. & Overhage, J. (2014). The sensor kinase PA4398 modulates swarming motility and biofilm formation in *Pseudomonas aeruginosa* PA14. *Appl Environ Microbiol*.

Strube, K., de Vries, S., & Cramm, R. (2007). Formation of a dinitrosyl iron complex by NorA, a nitric oxide-binding di-iron protein from *Ralstonia eutropha* H16. *J Biol Chem* **282**, 20292–20300.

Sudhamsu, J. & Crane, B. R. (2009). Bacterial nitric oxide synthases: what are they good for? *Trends Microbiol* **17**, 212–218.

Su, S., Panmanee, W., Wilson, J. J., Mahtani, H. K., Li, Q., VanderWielen, B. D., Makris, T. M., Rogers, M., McDaniel, C. & other authors. **(2014).** Catalase (KatA) plays a role in protection against anaerobic nitric oxide in *Pseudomonas aeruginosa*. *PLoS ONE* **9**, e91813.

Svartengren, M., Strand, V., Bylin, G., Järup, L. & Pershagen, G. (2000). Short-term exposure to air pollution in a road tunnel enhances the asthmatic response to allergen. *Eur Respir J* **15**, 716–724.

Taber, H. W., Mueller, J. P., Miller, P. F. & Arrow, A. S. (1987). Bacterial uptake of aminoglycoside antibiotics. *Microbiol Rev* **51**, 439–457.

Takaya, N., Catalan-Sakairi, M. A. B., Sakaguchi, Y., Kato, I., Zhou, Z. & Shoun, H. (2003). Aerobic denitrifying bacteria that produce low levels of nitrous oxide. *Appl Environ Microbiol* **69**, 3152–3157.

Talavera, G. & Castresana, J. (2007). Improvement of phylogenies after removing divergent and ambiguously aligned blocks from protein sequence alignments. *Syst Biol* **56**, 564–577.

Tamir, S., Burney, S. & Tannenbaum, S. R. (1996). DNA damage by nitric oxide. *Chem Res Toxicol* **9**, 821–827.

Tao, Y., Xie, Z., Chen, W., Glazebrook, J., Chang, H.-S., Han, B., Zhu, T., Zou, G. & Katagiri, F. (2003). Quantitative nature of *Arabidopsis* responses during compatible and incompatible interactions with the bacterial pathogen *Pseudomonas syringae*. *Plant Cell* **15**, 317–330.

Thomas, D. D., Ridnour, L. A., Isenberg, J. S., Flores-Santana, W., Switzer, C. H., Donzellie, S., Hussain, P., Vecoli, C., Paolocci, N. & other authors. **(2008).** The chemical biology of nitric oxide. Implications in cellular signaling. *Free Radic Biol Med* **45**, 18–31.

Tocchetti, C. G., Stanley, B. A., Murray, C. I., Sivakumaran, V., Donzelli, S., Mancardi, D., Pagliaro, P., Gao, W. D., van Eyk, J. & other authors. **(2011).** Playing with cardiac 'redox switches': the 'HNO way' to modulate cardiac function. *Antioxid Redox Signal* **14**, 1687–1698.

Trunk, K., Benkert, B., Quäck, N., Münch, R., Scheer, M., Garbe, J., Jänsch, L., Trost, M., Wehland, J. & other authors. **(2010).** Anaerobic adaptation in *Pseudomonas aeruginosa*: definition of the Anr and Dnr regulons. *Environ Microbiol* **12**, 1719–1733.

Tsay, Y.-F., Chiu, C.-C., Tsai, C.-B., Ho, C.-H. & Hsu, P.-K. (2007). Nitrate transporters and peptide transporters. *FEBS Lett* **581**, 2290–2300.

UNECE. **(2015).** Protocol concerning the Control of Emissions of Nitrogen Oxides. *U N Econ Comm Eur UNECE*.

Uratani, Y. & Aiyama, A. (1986). Effect of phospholipid composition on activity of sodium-dependent leucine transport system in Pseudomonas aeruginosa. *J Biol Chem* **261**, 5450–5454.

Uwate, M., Ichise, Y., Shirai, A., Omasa, T., Nakae, T. & Maseda, H. (2013). Two routes of MexS-MexT-mediated regulation of MexEF-OprN and MexAB-OprM efflux pump expression in *Pseudomonas aeruginosa*. *Microbiol Immunol* **57**, 263–272.

Valko, M., Leibfritz, D., Moncol, J., Cronin, M. T. D., Mazur, M. & Telser, J. (2007). Free radicals and antioxidants in normal physiological functions and human disease. *Int J Biochem Cell Biol* **39**, 44–84.

Vallet-Gely, I., Sharp, J. S. & Dove, S. L. (2007). Local and global regulators linking anaerobiosis to *cupA* fimbrial gene expression in *Pseudomonas aeruginosa*. *J Bacteriol* **189**, 8667–8676.

Vanounou, S., Pines, D., Pines, E., Parola, A. H. & Fishov, I. (2002). Coexistence of domains with distinct order and polarity in fluid bacterial membranes. *Photochem Photobiol* **76**, 1–11.

van der Veen, S. & Tang, C. M. (2015). The BER necessities: the repair of DNA damage in human-adapted bacterial pathogens. *Nat Rev Microbiol* **13**, 83–94.

Vincent, J.-L., Sakr, Y., Sprung, C. L., Ranieri, V. M., Reinhart, K., Gerlach, H., Moreno, R., Carlet, J., Le Gall, J.-R. & other authors. **(2006).** Sepsis in European intensive care units: results of the SOAP study. *Crit Care Med* **34**, 344–353.

van Vliet, P., Knape, M., de Hartog, J., Janssen, N., Harssema, H. & Brunekreef, B. (1997). Motor vehicle exhaust and chronic respiratory symptoms in

children living near freeways. *Environ Res* **74**, 122–132.

Vollmer, W., Blanot, D. & de Pedro, M. A. (2008). Peptidoglycan structure and architecture. *FEMS Microbiol Rev* **32**, 149–167.

Vos, P. D. & Ley, J. D. (1983). Intra- and intergeneric similarities of *Pseudomonas* and *Xanthomonas* ribosomal ribonucleic acid cistrons. *Int J Syst Bacteriol* **33**, 487–509.

Vos, P. D., Goor, M., Gillis, M. & Ley, J. D. (1985). Ribosomal ribonucleic acid cistron similarities of phytopathogenic *Pseudomonas* species. *Int J Syst Bacteriol* **35**, 169–184.

Vos, P. D., Landschoot, A. V., Segers, P., Tytgat, R., Gillis, M., Bauwens, M., Rossau, R., Goor, M., Pot, B. & other authors. **(1989).** Genotypic relationships and taxonomic localization of unclassified *Pseudomonas* and *Pseudomonas*-like strains by deoxyribonucleic acid: ribosomal ribonucleic acid hybridizations. *Int J Syst Bacteriol* **39**, 35–49.

Vromman, F. & Subtil, A. (2014). Exploitation of host lipids by bacteria. *Curr Opin Microbiol*, Host–microbe interactions: bacteria **17**, 38–45.

Wahl, A., My, L., Dumoulin, R., Sturgis, J. N. & Bouveret, E. (2011). Antagonistic regulation of *dgkA* and *plsB* genes of phospholipid synthesis by multiple stress responses in *Escherichia coli*. *Mol Microbiol* **80**, 1260–1275.

Walsh, U. F., Morrissey, J. P. & O'Gara, F. (2001). *Pseudomonas* for biocontrol of phytopathogens: from functional genomics to commercial exploitation. *Curr Opin Biotechnol* **12**, 289–295.

Wang, Y.-Y., Hsu, P.-K. & Tsay, Y.-F. (2012). Uptake, allocation and signaling of nitrate. *Trends Plant Sci* **17**, 458–467.

Watmough, N. J., Butland, G., Cheesman, M. R., Moir, J. W. B., Richardson, D. J. & Spiro, S. (1999). Nitric oxide in bacteria: synthesis and consumption. *Biochim Biophys Acta BBA - Bioenerg* **1411**, 456–474.

Wei, Q. & Ma, L. Z. (2013). Biofilm matrix and its regulation in *Pseudomonas aeruginosa*. *Int J Mol Sci* **14**, 20983–21005.

Weller, D. M., Landa, B. B., Mavrodi, O. V., Schroeder, K. L., De La Fuente, L., Blouin Bankhead, S., Allende Molar, R., Bonsall, R. F., Mavrodi, D. V. & Thomashow, L. S. (2007). Role of 2,4-diacetylphloroglucinol-producing fluorescent *Pseudomonas* spp. in the defense of plant roots. *Plant Biol Stuttg Ger* **9**, 4–20.

Wenk, M. R. (2006). Lipidomics of host–pathogen interactions. *FEBS Lett*, Lipidome and Disease **580**, 5541–5551.

Whitesides, G. M. (2003). The 'right' size in nanobiotechnology. *Nat Biotechnol* **21**, 1161–1165.

White-Ziegler, C. A., Um, S., Pérez, N. M., Berns, A. L., Malhowski, A. J. & Young, S. (2008). Low temperature (23 degrees C) increases expression of biofilm-, cold-shock- and RpoS-dependent genes in *Escherichia coli* K-12. *Microbiol Read Engl* **154**, 148–166.

Willumeit, R., Kumpugdee, M., Funari, S. S., Lohner, K., Navas, B. P., Brandenburg, K., Linser, S. & Andrä, J. (2005). Structural rearrangement of model membranes by the peptide antibiotic NK-2. *Biochim Biophys Acta BBA - Biomembr* **1669**, 125–134.

Wink, D. A. & Mitchell, J. B. (1998). Chemical biology of nitric oxide: Insights into regulatory, cytotoxic, and cytoprotective mechanisms of nitric oxide. *Free Radic Biol Med* **25**, 434–456.

Womack, A. M., Bohannan, B. J. M. & Green, J. L. (2010). Biodiversity and biogeography of the atmosphere. *Philos Trans R Soc Lond B Biol Sci* **365**, 3645–3653.

van Wonderen, J. H., Knight, C., Oganesyan, V. S., George, S. J., Zumft, W. G. & Cheesman, M. R. (2007). Activation of the cytochrome *cd1* nitrite reductase from *Paracoccus pantotrophus*. Reaction of oxidized enzyme with substrate drives a ligand switch at heme *c*. *J Biol Chem* **282**, 28207–28215.

Woodmansee, A. N. & Imlay, J. A. (2003). A mechanism by which nitric oxide accelerates the rate of oxidative DNA damage in *Escherichia coli*. *Mol Microbiol* **49**, 11–22.

Wu, G., Wainwright, L. M. & Poole, R. K. (2003). Microbial globins. *Adv Microb Physiol* **47**, 255–310.

Yang, W., Rogers, P. A. & Ding, H. (2002). Repair of nitric oxide-modified ferredoxin [2Fe-2S] cluster by cysteine desulfurase (IscS). *J Biol Chem* **277**, 12868–12873.

Yoon, S. S., Hennigan, R. F., Hilliard, G. M., Ochsner, U. A., Parvatiyar, K., Kamani, M. C., Allen, H. L., DeKievit, T. R., Gardner, P. R. & other authors. **(2002).** *Pseudomonas aeruginosa* anaerobic respiration in biofilms: relationships to cystic fibrosis pathogenesis. *Dev Cell* **3**, 593–603.

Zajicek, R. S., Allen, J. W. A., Cartron, M. L., Richardson, D. J. & Ferguson, S. J. (2004). *Paracoccus pantotrophus* NapC can reductively activate cytochrome *cd1* nitrite reductase. *FEBS Lett* **565**, 48–52.

Zhang, Y.-M. & Rock, C. O. (2008). Membrane lipid homeostasis in bacteria. *Nat Rev Microbiol* **6**, 222–233.

Zheng, H., Wisedchaisri, G. & Gonen, T. (2013). Crystal structure of a nitrate/nitrite exchanger. *Nature* **497**, 647–651.

Zottini, M., Formentin, E., Scattolin, M., Carimi, F., Schiavo, F. L. & Terzi, M. (2002). Nitric oxide affects plant mitochondrial functionality in vivo. *FEBS Lett* **515**, 75–78.

Zumft, W. G. (2005). Nitric oxide reductases of prokaryotes with emphasis on the respiratory, heme–copper oxidase type. *J Inorg Biochem*, Heme-diatomic interactions, Part 1 **99**, 194–215.

Zumft, W. G. & Kroneck, P. M. H. (2007). Respiratory transformation of nitrous oxide (N_2O) to dinitrogen by Bacteria and Archaea. *Adv Microb Physiol* **52**, 107–227.

Zumft, W. G. (1997). Cell biology and molecular basis of denitrification. *Microbiol Mol Biol Rev* **61**, 533–616.

***Review of the Gothenburg Protocol. Report of the Task Force on Integrated Assessment Modelling and the Centre for Integrated Assessment Modelling*. (2007).** ask Force on Integrated Assessment Modelling (TFIAM) and the Centre for Integrated Assessment (CIAM).

WHO | Ambient (outdoor) air quality and health. (2015). *WHO*.

Reduction of pollutant emissions from light vehicles. (2015, July 23). *Access Eur Union Law*.

VIII. Annexes

Supplementary data

Chapter 4 Study of lipidome of airborne *P. fluorescens*

A new study of the bacterial lipidome: HPTLC-MALDI-TOF imaging enlightening the presence of phosphatidylcholine in airborne *Pseudomonas fluorescens* MFAF76a

Table S1. Fatty acid composition of airborne *P. fluorescens* MAFA76a

Peak identity	Fatty acids, %
C14:0	1.0±0.1
C16:0	37.7±4.4
C16:1*trans*	10.7±3.8
C16:1*cis*	31.5±2.1
C17cyclo	1.2±0.3
C18:0	2.4±0.3
C18:1*trans*	1.9±1.7
C18:1*cis*	13.1±2.2
C19cyclo	0.5±0.1

The analyses were performed for three independent bacterial lipid extracts. Analysis of fatty acids in hexane was performed using a quadruple GC System (HP5890, Hewlett &Packard, Palo Alto, USA). The fatty acids were identified by GC and co-injection of authentic reference compounds obtained from Supelco (Bellefonte, USA). The peak areas of the fatty acids were used to determine their relative amounts.

Chapter 5 Effect of stress factors on membrane of *P. fluorescens*

1. Effect of air pollution on membrane of airborne bacteria: NO2 modifies both *Pseudomonas fluorescens* glycerophospholipids and membrane electron-accepting character

Table S1. Effect of increasing temperature and nitrogen dioxide on fatty acid composition of airborne *P. fluorescens* MFAF76a

Experimental conditions		Area, %[a]						
		16:0	16:1 *trans*	16:1 *cis*	17cyclo	18:0	18:1 *trans*	18:1 *cis*
28°C	EGP[b]	37.7±2.19	10.7±1.91	31.5±1.03	1.2±0.16	2.4±0.17	1.9±0.85	13.1±1.08
	SGP[c]	41.1±5.18	6.2±1.94	20.2±6.88	10.1±4.52	2.1±0.22	0.4±0.14	15.8±3.02
37°C	EGP	41.8±0.67	4.7±2.24	35.1±2.17	0.3±0.15	3.4±0.52	0.2±0.09	13.1±1.24
	SGP	49.5±3.42	2.0±0.86	16.2±7.27	9.0±5.04	3.2±0.30	0.1±0.01	12.6±0.69
NO_2 level,	0	35.95±0.28	3.74±0.80	33.55±0.80	5.33±0.17	3.97±0.24	1.27±0.86	16.19±0.35
	0.1	35.85±0.02	5.47±0.10	32.83±0.29	4.29±0.24	3.29±1.05	2.34±0.65	15.93±0.01
	5	35.36±0.14	11.86±2.06	29.89±2.16	2.55±0.13	1.62±0.06	1.73±0.57	17.00±0.85
	45	35.99±0.13	4.27±0.19	35.62±0.40	3.31±0.18	3.77±0.22	1.23±0.11	15.81±0.15

[a] The fatty acids were identified and quantified by the GC in at least three replicates. The peak areas of fatty acids were used to determine their relative amounts. The results are presented as the percentage of average value relative to the sum ± SEM. [b]**EGP**: exponential growth phase; [c]**SGP**: stationary growth phase.

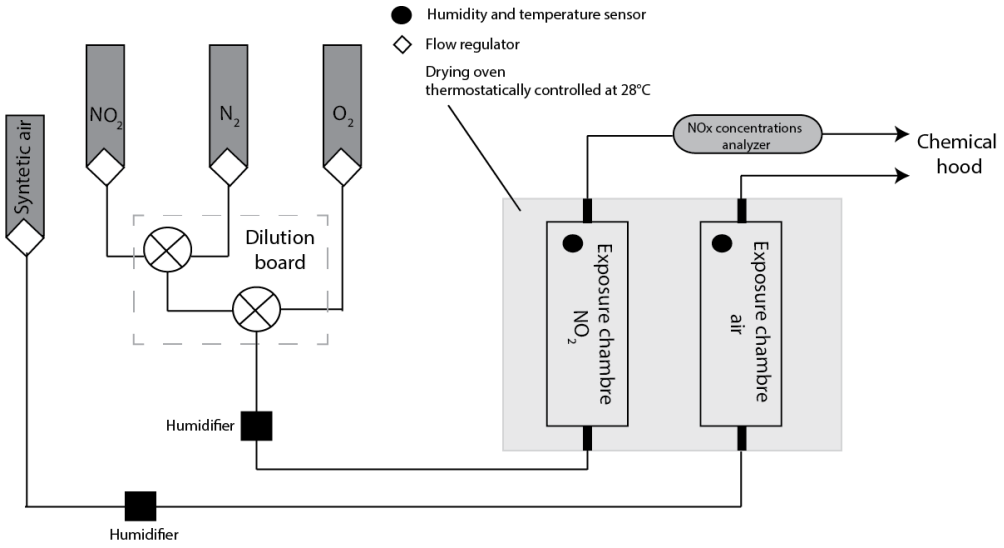

Figure S1. Schematic representation of NO_2 gas delivery system
Bacterial NO_2 exposure was done in gas phase for 2 h, according (Ghaffari *et al.*, 2005). Two exposure chambers (one for the NO_2 exposure, the second one for the control simple - exposure to the synthetic air) were used. The gases NO_2, N_2 and O_2 were mixed together to obtain pre-calculated concentration of NO_2 and maintain the O_2/N_2 ratio at 2/8, (v/v). All experimental parameters (NO_2 concentration, temperature, relative humidity) were controlled.

References

[1] Ghaffari A, Neil DH, Ardakani A, Road J, Ghahary A, Miller CC. A direct nitric oxide gas delivery system for bacterial and mammalian cell cultures. Nitric Oxide 2005;12:129-40. doi:10.1016/j.niox.2005.01.006

2. Effect of temperature and NO_2 on membrane glycerophospholipids of clinical *Pseudomonas fluorescens* strain MFN1032

Table S1. Effect of increasing temperature and nitrogen dioxide on fatty acid composition of clinical *P. fluorescens* MFN1032

Experimental conditions[a]		Area, %[b]						
		16:0	16:1 *trans*	16:1 *cis*	17cyclo	18:0	18:1 *trans*	18:1 *cis*
28°C	EGP	36.±1.0	10.0±0.6	27.3±1.3	0.7±0.1	6.4±2.0	1.2±0.3	15.1±1.3
	SGP	38.4±0.7	6.1±1.8	22.3±0.9	6.3±0.1	7.8±1.0	0.8±0.1	15.6±0.8
37°C	EGP	44.2±1.5	0.7±0.2	28.2±3.4	3.6±0.2	6.6±1.4	0.2±0.1	13.1±0.6
	SGP	42.4±1.6	0.7±0.2	17.5±2.1	10.0±0.2	8.1±0.8	0.3±0.2	15.0±1.1
NO_2 level. ppm	0	35.6±0.1	4.7±0.4	31.9±0.4	5.1±0.17	3.4±0.2	0.7±0.2	18.6±0.1
	0.1	36.5±0.7	5.5±0.2	30.0±0.4	6.4±0.4	3.8±0.1	0.4±0.03	17.5±0.3
	5	34.3±0.2	1.4±0.05	35.9±0.2	4.2±0.1	2.0±0.1	0.1±0.003	22.1±0.1
	45	35.7±0.3	3.1±0.1	32.7±0.2	5.6±0.2	3.8±0.1	0.9±0.1	18.2±0.1

[a]The fatty acids were identified and quantified by GC in at least three replicates. The peak areas of the fatty acids were used to determine their relative amounts[b]. The results are presented as the percentage of average value relative to the sum ± SEM.

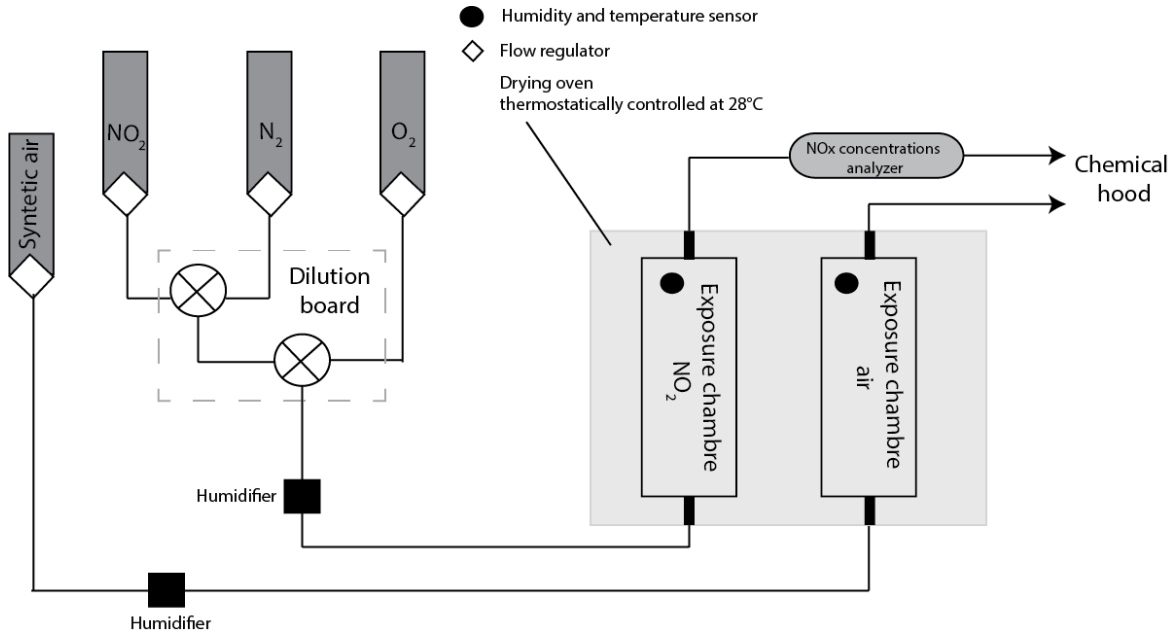

Figure S1. Schematic representation of NO_2 gas delivery system

Bacterial NO_2 exposure was done in gas phase for 2 h, according (Ghaffari *et al.*, 2005). Two exposure chambers (one for the NO_2 exposure, the second one for the control simple - exposure to the synthetic air) were used. The gases NO_2. N_2 and O_2 were mixed together to obtain pre-calculated concentration of NO_2 and maintain the O_2/N_2 ratio at 2/8. (v/v). All experimental parameters (NO_2 concentration, temperature, relative humidity) were controlled.

References

[1] Ghaffari A, Neil DH, Ardakani A, Road J, Ghahary A, Miller CC. A direct nitric oxide gas delivery system for bacterial and mammalian cell cultures. Nitric Oxide 2005;12:129-40. doi:10.1016/j.niox.2005.01.006

Chapter 6 *Pseudomonas fluorescens* response to NO_2 toxicity

P. fluorescens airborne strain MFAF76a and clinical strain MFN1032 response to NO_2 stress

Table S1. Genes identified with the Blast 2.2.30+ software

	Gene name	GenBank accession number		Protein name	Protein description	References	
		MFAF76a	MFN1032			Strain	Bibliographies
NO_2 detoxificatio	*hmp*	KR818822	KR818823	flavohemoglobin	nitric oxide dioxygenase	*E. coli* *P. aeruginosa*	Arai et al., 2005; Poole et al., 1996; Gardner et al., 1998
	Pfl76a_nirB *Pfl1032_nirB*	KT186428	KT070320	putative nitrite reductase large subunit NirB	assimilatory nitrite reductase	*P. aeruginosa*	Romeo et al., 2012
Biofilm and motility	*bdlA*	KT186436		putative protein BdlA	biofilm dispersion protein BdlA	*P. aeruginosa*	Petrova and Sauer, 2012b
	dipA		KT186437	putative phosphodiesterase DipA	protein, possessing EAL domain and involved in biofilm dispersion	*P. aeruginosa*	Roy et al., 2012
	mucR		KT186445	putative phosphodiesterase MucR	protein possessing both GGDEF and EAL domains and involved in NO-mediated biofilm dispersion	*P. aeruginosa*	Li et al., 2013
	ndbA	KT186444		putative phosphodiesterase NdbA	protein possessing both GGDEF and EAL domains and involved in NO-mediated biofilm dispersion	*P. aeruginosa*	Li et al., 2013
Antibiotic resistance	*mexE*	KT070324	KT070323	putative membrane fusion protein MexE	RND family efflux transporter	*P. aeruginosa*	Maseda et al., 2000; Fetar et al., 2011; Poole K., 2005b
	mexF	KT070321	KT070322	putative cation efflux protein MexF	multidrug efflux transporter		
	oprN	KT070325	KT186432	putative multidrug efflux RND transporter, outer membrane factor lipoprotein OprN	outer membrane component of multidrug efflux system		
	mexX	KT070313	KT186462	putative MexX	MexX family efflux pump subunit	*P. aeruginosa*	Poole, 2005a; Morita et al., 2014; Sobel et al., 2003
	mexY	KT070314	KT070315	putative MexY	multidrug efflux protein		

Supplementary Table S2. Primer sequences of the indicated genes used for quantitative RT-PCR assay.

Gene	Forward primer (5'-3')	Reverse primer (5'-3')
***Pseudomonas fluorescens* MFAF76a**		
hmp	AAACCGCGATCTATGACCAG	GCTTCATGCCGATGTACTGA
Pfl76a_nirB	AATTGAAAGTCACCGGCATC	GAATCTGCCGGAAATACCAA
bdlA	ACATTCTTACCGCCAACCAG	ACTGTCCGTGGAAGAACTCG
ndbA	AGATGAAAGAGCCGATCGAA	TGAAGAAGTGCAGACCGTTG
mexE	ACTCAAACATTTGCGCTTCC	AATTCGTCCCACTCGTTGAC
mexF	GAGTGGACCGACCTGACCTA	GCAAGTCCCACCAGTACGAT
oprN	ACCTCAACAACCAGCAGGAG	AGGTCGACGGTCAGTTTGTC
mexX	CGCAGCGAGTTTCCCAAT	TGGATGGTTGCCTGCTCAA
mexY	GGCTGGGTCGGCTATGC	TCAGCAGGACCACGTAGATCAT
***Pseudomonas fluorescens* MFN1032**		
hmp	GATAAACCGCTGGTGCTGAT	ATCCTCGGCGTAGCAGTAGA
Pfl1032_nirB	CGCCCTATGTGCTGGTGTT	ATCTGCCGGGCCATCTC
dipA	ACGAAGACATCACCCAGACC	TTGATGCGCTTGAAGTTGTC
mucR	CCTTGTCGTGATTTCCCTGT	GCCAACATCCCGATAAAGTG
mexE	CCGACAAGGTTTACGCCTAC	GTGTATTCGCCCTTGCTGTT
mexF	CTGACCCTGACCATCACCTT	ATTGAGGATCGCGTAGTTGG
oprN	GTTGCTGGCATTGGAAGAGT	GTCGAGCAACACCAGGAAGT
mexX	CCGTTGCCGGGTAAATTG	GAACTCGCTGCGCAGGAT
mexY	CAGTGGTTTTGAGTTCCGTTTG	GCAGCGTCCAGCAATTCAGT

Scientific contributions

1. Publications

Airborne fluorescent pseudomonads: What potential for virulence?

Cécile Duclairoir Poc, Julien Verdon, Anne Groboillot, Magalie Barreau, Hervé Toucourou, Lily Mijouin, Camille Leclerc, Olivier Maillot, **Tatiana Kondakova**, Cristian Hulen, Jean-Paul Morin, Marc GJ Feuilloley, Annabelle Merieau, Nicole Orange

International Journal of Current Microbiology and Applied Sciences 3 (2014) 708-722

Int.J.Curr.Microbiol.App.Sci (2014) 3(8) 708-722

International Journal of Current Microbiology and Applied Sciences
ISSN: 2319-7706 **Volume 3 Number 8 (2014) pp. 708-722**
http://www.ijcmas.com

Original Research Article

Airborne fluorescent pseudomonads : What potential for virulence?

Cecile Duclairoir Poc[1*], Julien Verdon[1,2], Anne Groboillot[1], Magalie Barreau[1], Hervé Toucourou[1], Lily Mijouin[1], Camille Leclerc[1], Olivier Maillot[1], Tatiana Kondakova[1], Christian Hulen[1], Jean-Paul Morin[3], Marc GJ Feuilloley[1], Annabelle Merieau[1] and Nicole Orange[1]

[1]Normandie University, France; University of Rouen, LMSM, EA 4312, 55, rue St Germain, F-27000 Evreux, France
[2]University of Poitiers, F-86034 Poitiers Cedex, France ; Lebi, UMR CNRS 7267, MDE, F-86022 Poitiers Cedex, France
[3]Normandie University, France ; University of Rouen, ABTE-ToxEMAC, EA 4651, F- 76183 Rouen Cedex, France
**Corresponding author*

Keywords

Fluorescent pseudomonads; *Pseudomonas fluorescens*; *Pseudomonas putida*; air; airborne; bio-contamination, virulence; exoproducts

A B S T R A C T

The presence of human pathogens in the environment is a key concern, therefore the air needs to be evaluated as a potential source of bio-contamination. This study dealt with the characterization of fluorescent pseudomonads strains isolated from air in order to evaluate their factors of virulence. 19 strains were identified by API® strips, by MALDI-Biotyper and by 16S rDNA gene sequencing. Their growth at 30°C and 37°C, biosurfactant and biofilm production, motility and production of exoproducts were tested. A *Pseudomonas fluorescens* clinical strain was used as reference. By comparison with the virulence factors of this climical strain, most of these strains isolated from air did not produced highly virulent factors. However a bacterial couple : *P. fluorescens* MFAF76a and *P. putida* MFAF88, was selected thanks to their observed characteristics linked to virulence quite similar with traits of the clinical reference. The cytotoxicity of their culture supernatant was investigated toward human epithelial pulmonary cells. Results revealed that these airborne fluorescent *Pseudomonas* strains secreted exoproducts, such as enzymes, surfactants and siderophores, highly virulent against the studied pneumocytes.

Introduction

For environmental policies, air quality is generally related to the presence of chemicals and particulate matter and its pollution is correlated with uncontroversial health impact. According to a survey in European intensive care units, 68% of sepsis are lung infections and *Pseudomonadaceae* are the second most common organisms (14%), but the only ones that induce rising mortality rates (Vincent et al., 2006).

Gram-negative *Pseudomonadaceae* bacteria

present a great adaptive ability related to their large genome (Stover et al., 2000). *P. aeruginosa* is well known as prevalent pathogen in acute and chronic infections (Clifton & Peckham, 2010; Fernstrom & Goldblatt, 2013), although other fluorescent *Pseudomonas* species are ubiquitous. In fact, *Pseudomonas* are widespread Gram-negative bacteria present in various ecological niches: soil, water (Rajmohan et al., 2002), care units (Vincent et al., 2006), humans (Chapalain et al., 2008; Donnarumma et al., 2010) and air (AFSSET, 2010; Morin et al., 2013).

Moreover, some strains, isolated from a clinical environment, are able to grow at or above 37°C (Chapalain et al., 2008). *P. fluorescens* MFN1032, a clinical strain, was recently isolated from a patient with a lung infection (Chapalain et al., 2008) and induces cytotoxic responses (Rossignol et al., 2008; Madi et al., 2010; Sperandio et al., 2010; Sperandio et al., 2012). The pathogenicity of *Pseudomonas* bacteria is correlated with their enzymatic secretion (Gessner & Mortensen, 1990 ; Rossignol et al., 2008 ; Strateva & Mitov, 2011).

The purpose here was, after identification, to assess the potential for virulence of 19 airborne fluorescent pseudomonads strains, selected from Gram-negative oxidase-negative strictly aerobic rods collected during a previous study (AFSSET, 2010; Duclairoir Poc et al., 2011a ; Morin et al., 2013). For each of them, physiological characterization and determination of virulence factors were confronted. Two airborne bacteria appeared to have great similarities with the clinical standard, *P. fluorescens* MFN1032.

To compare the cytotoxicity of their secreted factors, A-549 human pulmonary type II-like epithelial cell line was implemented in order to assess their potential virulence toward human by airways. Those cells play a critical role in coordinating both innate defence and inflammatory responses (Hawdon et al., 2010) and make it suitable to study virulence in conditions fairly close to *in vivo*.

Materials and Methods

19 airborne fluorescent *Pseudomonas* strains

In a previous study (AFSSET, 2010; Morin et al., 2013), more than 3000 bacteria were collected in air samples between June 2008 and September 2009 in 3 areas : in peri-suburban Evreux (Normandy, France), in the suburbs of Rouen (Normandy, France) and in dust clouds generated during crop ship loading in Rouen harbor installations (Normandy, France). About 3000 bacterial isolates were stored and then frozen at -80°C. Morphological characters, Gram staining and biochemical tests used to separate this bacterial population into 8 groups, which included a Gram-negative oxidase-positive strictly aerobic rods group containing *Pseudomonas* spp.

This group appeared among the most predominantly collected groups of airborne Gram-negative bacteria on harbor installations. Proportionally to their relative sample representation, 19 fluorescent *Pseudomonas* strains were randomly selected.

Clinical standard strain, MFN1032

P. fluorescens MFN1032 is a clinical strain isolated after a lung infection, related to biovar I of *P. fluorescens* species (Chapalain et al., 2008).

Int.J.Curr.Microbiol.App.Sci (2014) 3(8) 708-722

Identification of the 19 airborne strains API® identification

The 19 representative strains were submitted to metabolic characterization using API® 20NE strips. API® kits were operated according to the manufacturer's instructions (BioMérieux, France).

Mass spectrometric MALDI-Biotyper bacterial identification

These isolates were submitted to bacterial identification by MALDI mass spectrometry (MS) based on the total proteome screening analyzed using an algorithmic method to identify bacterium. The bacterial proteomes were obtained using an Autoflex III Matrix-Assisted Laser Desorption/Ionization-Time-Of-Flight mass spectrometer (MALDI-TOF) (Bruker, Germany) coupled to the MALDI-Biotyper 3.0 algorithmic system for microbial identification (Hillion et al., 2013). Before MS analysis, the bacterial material was spotted onto a MALDI target plate and overlaid by matrix ($10 g.L^{-1}$ α-cyano-4-hydroxycinnamic acid in 50% acetonitrile, 2.5% trifluoroacetic acid provided by Sigma-Aldrich, France).

The software generated scores evaluating the probability of correct identification of the microorganism. The species identification is considered acceptable for score values over 2.0 and, between 1.7 and 2.0, the genus identification is assumed confident. (Hillion et al., 2013)

16S rDNA gene sequencing and identification

The same isolates were identified by 16S ribosomal DNA gene sequencing. For amplification of the complete 16S RNA gene, universal primers UNI_OL (AGAGTGTA GCGGTGAAATGCG) and UNI_OR (ACGGGCGGTGTGTACAA) were used as already described (Duclairoir Poc et al., 2011a). The nucleotide sequences were registred on GenBank, NCBI (http://www.ncbi.nlm.nih.gov/genbank/submit/) and were compiled in Table 1.

Partial 16S rRNA gene sequences were aligned with reference sequences using BLAST data bank (http://blast.ncbi.nlm.nih.gov/Blast.cgi?PROGRAM=blastn&PAGE_TYPE=BlastSearch&LINK_LOC=blasthome).

The minimum similarity among all members of the *Pseudomonas* genus is assumed at 77% (Balet et al., 2010). Over 95% of similarity, the species is considered surely identified.

Physiological characterization of airborne bacteria: Growth conditions

The bacteria were cultured in Luria Bertani medium (LB) (AES Chemunex, France) under shaking (180 rpm) at 30°C, close to optimum growth temperatures of *Pseudomonas fluorescens* species, i.e. 28°C (Merieau et al., 1993), and at 37°C, i.e. human body temperature. The bacterial density was determined by measuring optical density (OD) at 580 nm (Helios ε, Thermo Spectronic,USA) during at least 120h. Thanks to these growth kinetiks curves, the maximum growth rate, μ_{max}, was calculated for each strain.

Determination of virulence factors of airborne bacteria

Bacterial enzymatic characterization

Several methods were used to screen enzymatic activities. Each test was done at 30°C and 37°C.

Int.J.Curr.Microbiol.App.Sci (2014) 3(8) 708-722

Proteolytic activity was determined on Trypticase soy agar (TSA) (AES Chemunex, France) with skimmed milk 20%. Esterase was detected by growth on TSA (AES Chemunex, France) containing Tween 80 1% colored with Phenol red (1%).

Lecithinase and lipoproteolytic activities were analyzed by growth on TSA (AES Chemunex, France) with egg yolk 50% (VWR, Germany). Bacteria hydrolyse lecithin contrasting medium next to the inoculated streak. On the contrary a lighter colored zone shows lipoproteolytic activity.
In the secreted hemolysis test, bacterial strains were streaked onto a 2% sheep red blood cell plates, whose were visually inspected the zones of clearing around the colonies. The pyoverdine production was observed by growth on King B Agar plates (AES Chemunex, France). After 48h incubation, the plates were observed with Ultra-Violet light at 365nm (VL-6LM, Vilber Lourmat, France), as the produced pyoverdine induces fluorescence.

Biosurfactant production

Surface tension measurement of a rinsing solution of bacteria cultured on solid agar medium is a direct method for determining global biosurfactant production, in ideal conditions for biosurfactant production and was done as previously described (Duclairoir Poc et al., 2011b).

Bacterial motility

Motility characters were observed through the evaluation of swim, swarm, twitch deplacements after 40h at 30°C and 37°C. These motilities were obtained thanks to specific agar concentrations: 0.3% for the swim deplacement, 0.5% for the swarm and 1% for the twitch. Initially, the plates were inoculated with overnight culture in LB at 30°C and 37°C (Rossignol et al., 2008).

Adhesion assays on abiotic surface

The bacterial adhesion was evaluated in triplicate in polystyrene microtitration plate at 30°C and 37°C incubated in LB during 24h and 48h. The adherent bacterial population was estimated by direct measurement (quantification) of absorbance at 595 nm after 0.1% crystal violet coloration and after cell lysis by sodium dodecylsulfate 1% (Duclairoir Poc et al., 2011b).

Evaluation of supernatant virulence using the A549 pneumocyte model

The cytotoxicity of *P. fluorescens* MFN1032, MFAF76a and MFAF88 culture supernatants, in LB at 30°C and 37°C, was evaluated toward A-549 human pulmonary type II-like epithelial cell line as described elsewhere (Pimenta et al., 2006).

The percentage (%) of total lysis was calculated as follows:
$\%LDH = 100 \times (OD_{sample} - OD_{0\%}) / (OD_{100\%} - OD_{0\%})$

A percentage as lower than 20% could be assumed linked to an avirulent strain. Four other classes were defined : 20-40%: weak virulence, 40-60%: virulence, 60-80%: highly virulent and greater than 80%: extremely virulent.

Results and Discussion

Identification of airborne fluorescent pseudomonads : preponderance of

***Pseudomonas fluorescens* cluster**

The *Pseudomonas* genus is splitted into three well-supported clusters in the 16S rRNA phylogeny named aeruginosa, putida and fluorescens r-clusters (Bodilis et al., 2012). Different approaches : API/ MALDI

–Biotyper/ 16S rRNA gene sequencing, were done to identify the 19 airborne selected strains. According to the classification stated by Bodilis (Bodilis et al., 2012), a putative identification was proposed for each strain based on the more reliable identification by 16S rRNA sequencing (homology>95%) and /or by MALDI-Biotyper (score>2). The three strains : MFAE20, MFAB75 and MFAK14, were stated as *Pseudomonas* spp., their genus was surely identified, but their species could not confidently assumed. The majority of the 19 airborne strains are identified as *Pseudomonas fluorescens*.

The preponderance of *Pseudomonas fluorescens* species among the airborne Gram-negative bacteria was no surprise, due to their ubiquitous character created by their large genome (Stover et al., 2000). Morever *P. fluorescens* is observed as the most common *Pseudomonas* species (at least 42%) in outdoor air, as already reported by Nevalainen (Nevalainen et al., 1990).

Although the pathogenicity of *P. aeruginosa* is largely described and cause several human diseases, specially in lung infections (Clifton & Peckham, 2010), the literature on other fluorescent *Pseudomonas* is poorly documented in airways transmitting route, even if such bacteria are able to induce pulmonary pathologies such as *P. fluorescens* strains (Chapalain et al., 2008).

This study aimed to contribute on a better knowledge of the impact of fluorescent pseudomonads on the safety of the air, that we breathe. To evaluate the potential of virulence on this panel of 19 airborne strains, two contamination situations were explored. Firstly, conventional airway infections at 37°C, corresponded to an internal infection such as pulmonary, and, at 30°C, temperature of an external infection such as burned dermal injuries (Church et al., 2006) or as contamination of medical devices (Gershman et al., 2008).

Physiology of the 19 airborne bacteria : overall able to growth at 37°C

The growth rate for each of 19 airborne *Pseudomonas* strains, compiled in Table 1, was evaluated in LB medium at 30 and 37°C. Most of them were able to grow at 37°C, except MFAH4a and MFAD21c. Twelve other strains had an higher grow rate at 30°C, similar to the optimal growth temperature for *P. fluorescens* species, 28°C (Merieau et al., 1993). The first 5 strains, namely, MFAF76a, MFAF49a, MFAF88, MFAO2 and MFAF80b, presented an equivalent or increasing growth rate between 30 and 37°C. In addition to survival, they were able to multiply at human physiological temperature, which could facilitate the infectious processes.

Characterization of bacterial extracellular virulence factors : all the airborne strains produce several factors of virulence

MFN1032 was introduced in the panel to have a standard of virulence with a clinical origin that assures its pathogenic potential (Chapalain et al., 2008, Rossignol et al., 2008; Rossignol et al., 2009; Madi et al., 2010; Sperandio et al., 2010; Sperandio et al., 2012) and then makes a possible comparison of studied airborne *Pseudomonas* spp.

The 19 airborne *Pseudomonas* strains showed different patterns of secretion, as tabulated in Table 2. All strains synthesized lipoproteolytic enzymes and, except for MFAE48, induced clearing zones on sheep red blood cell plates revealing secreted hemolysis *a minima* incomplete for at least

one growth temperature. According to conventional microbiological nomenclature, the secreted hemolysis could be categorized as complete (β), incomplete (α) or no hemolysis (Luo et al., 2001). In any case, hemolytic phenomenon could result from synergy between activity of several hydrolysases, such as proteases, lecithinases, lipoproteases, and biosurfactants (Rossignol et al., 2008; Zhang et al., 2009). The hemolysis was complete for MFAF49a, MFAF80b and MFAD21c at 30°C and for MFAO2, MFAO39, MFAB75 and MFAH4a at 37°C.

Some virulence factors could be, on the one hand, strain-dependant: no protease and no lecithinase for MFAF49a, MFAF80b and for several strains less adapted at 37°C, no esterase for MFAF88 and MFAO39, no pyoverdine production for MFAF80b, MFAE88, MFAE20 and MFAH106a. On the another hand, some virulent exoproducts were strain- and temperature-dependant in the case of MFAF88 and the most of the strains were more adapted at 30°C than at 37°C.

Surprisingly, both strains, MFAH4a and MFAD21c, were not able to grow at 37°C in broth, but presented virulence factors at 37°C. To stimulate enzymatic secretion, bacterial growth was done on agar medium, promoting sessile lifestyle (i.e. in a surface adherent community). Such conditions seemed to facilitate the growth of MFAH4a and MFAD21c, contrary to more planktonic and less protective cell growth in broth. An other common character for this couple was their secretion of biosurfactant, as for MFN1032, MFAF88, MFAO2, MFAA66a, and MFAK14. This surfactive production was established through a surface tension lowered above 45mN/m (Carillo et al., 1996). Biosurfactants favor bacterial displacement, but may be affecting adhesion, even colonisation of the host (37°C) or of a medical device or even burn injuries (30°C) (Van Hamme et al., 2006).

To conclude, only MFAF76a, MFAO2 and MFAO40 exhibit activity for all the tested enzymes like the clinical strain *P. fluorescens* MFN1032, but, among them, only MFAO2 produces biosurfactant as MFN1032.

Bacterial motility : some strains swim, all swarm and none twitch

Infection deals in part with bacterial motility to allow their colonisation in the host.

The 3 motile types : twitch, swim and swarm, were tested at 30 and 37°C.

No twitching, but swarming motility was noted for any strain at either temperature, as shown in Table 3. The swarming motility is a collective microbial motility resulting from, at least, one functional flagella, often completed by biosurfactant production (Kearns, 2010).

Although all strains were able to swim at 30°C, only 6 of them maintained the swimming mode at 37°C. This displacement allows bacteria to individually move towards the host with the help of functional flagella.

The flagella dependant motilities, i.e. swim and swarm, are involved in the development of biofilms (O'Toole & Kolter, 1998). For instance, functional flagella are needed for swarming mobility, which is related to the surface movement in the case of bacterial groups. This mobility is favored by biosurfactive production or by lipopolysaccharides, outer membrane components, for some Gram-negative bacteria (Kearns, 2010).

Bacterial adhesion on abiotic surface: different behaviours

As noted in Table 3, thicker biofilms were observed at 30°C than at 37°C. For MFAF76a, MFAF88, MFAE48 and MFAE8b, their biofilm were observed at 24h and 48h at either temperature. When the biofilm evolved between 24h and 48h, most of the time it increased, the mature structure was not yet reached, the biofilm seemed still under edification. However, for both temperatures, MFN1032 had a lowest ability to form biofilm at 48h than at 24h, this phenomenon was already reported about *P. fluorescens* biosurfactant production (Duclairoir Poc et al., 2011b). This biofilm reduction was noted at 30°C for MFAF88, MFAF80b and MFAO29 and at 37°C for MFAH4a.

Concerning contamination, the bacterial presence on biofilm is stabilized in the host or on a surface, and even protects from hostile microenvironment behind its shelf-shielding extracellular polymeric substances. Nevertheless, a biofilm could reduce over the time and persists slimmer; the lacking cells could be assumed in dispersing and colonising elsewhere in host (McDougald et al., 2012).

Selection of two airborne strains: *P.fluorescens* MFAF76A and *P. putida* MFAF88

In *P. aeruginosa* infections, tissue damage is due to the production of several extracellular and cell-associated virulence factors (Strateva & Mitov, 2011), similar exoproducts are produced by all *Pseudomonas* species and also known as factors of virulence.

Through the obtained results, two airborne strains, MFA76a and MFAF88, are of particular interest: they are able to grow at 37°C and possibly better than at 30°C. They swim and swarm, thanks to their flagella and completed for MFAF88 by its biosurfactant production, as shown in Table 2. They present some virulent factors and form biofilm at either temperature. *P. fluorescens* MFA76a is very close to MFN1032 except for biosurfactant production and *P. putida* MFAF88 had an enzymatic pattern very different from MFN1032, but produced biosurfactant, as MFN1032.

Virulence of culture supernatant of MFN1032, MFAF76a, MFAF88 toward A-549 pneumocytes : strain-dependant virulence

Exoproducts such as lipases and proteases produced by *P. fluorescens* are known for their virulence (Rossignol et al., 2008; Zhang et al., 2009). Thus testing the growth supernatant could have a promising outcome. The need of an adequate cytotoxic model was crucial at this point and had to be ideally close to *in vivo* contamination by airway or pulmonary infection mode. The evaluation of virulence toward pneumocytes, such as cellular line A549 was assayed. The cytotoxic mechanism involved only the action of exoproducts, such as enzymes, siderophores or biosurfactants. All the supernatants, resulting from bacterial growth at 30°C and 37°C, induced lysis of the pulmonary cells by contact for 12h. Supernatant of MFAF88 induced a strong virulent response, in similar range (around 80%) at 30°C and 37°C. Furthermore, surpernatants of MFN1032 and MFAF76a had significantly changed their virulence towards epithelial cells for both growth temperatures. MFN1032 was extremely virulent at 30°C and MFAF76a at 37°C and their virulence was less severe, i.e. only highly virulent, at 37°C for MFN1032, and at 30°C for MFAF76a, respectively.

Int.J.Curr.Microbiol.App.Sci (2014) 3(8) 708-722

Table.1 Characterization of the 19 airborne fluorescent *Pseudomonas* spp. strains

Strain	Sampling localisation & season	API® 20NE identification	MALDI Biotyper: total proteomic comparison (score)	Identity percentage of 16S ribosomial RNA sequence <GenBank accession numbers>	Putative identification	μ_{max} at 30°C (h^{-1})	μ_{max} at 37°C (h^{-1})
MFAF76a	Rouen Harbor, Summer	*P. fluorescens* (excellent)	*P. koreensis* (2.122)	*P. koreensis* strain AGB-1 (96%) <KJ470785>	fluorescens r-cluster	1	1.08
MFAF49a	Rouen Harbor, Summer	*P. fluorescens* (excellent)	*P. abietaniphila* (2.094)	*P. lundensis* (85%) <KJ470784>	fluorescens r-cluster	0.79	1.05
MFAF88	Rouen Harbor, Summer	*Bulkholderia pseudomallei* (very good)	*Pseudomonas* spp. (1.982)	*P. putida* strain CG29 (99%) <KJ470787>	putida r-cluster	0.47	1.01
MFAO2	Rouen Harbor,Winter	*P. fluorescens* (excellent)	*P. koreensis* (2.001)	*Pseudomonas* sp. strain E1 (86%) <KJ470791>	fluorescens r-cluster	0.93	0.88
MFAF80b	Rouen Harbor, Summer	*P. fluorescens* (excellent)	*P. abietaniphila* (2.152)	*P. abietaniphila* strain HMGU118 (99%) <KJ470786>	fluorescens r-cluster	0.71	0.77
MFAE88	Rouen Harbor, Summer	*P. oryzihabitans* (very good)	*Pseudomonas* spp. (1.866)	*P. rhizosphaerae* strain BKB1(95%) <KJ470782>	fluorescens r-cluster	0.83	0.38
MFAO39	Rouen Harbor,Winter	*P. fluorescens* (excellent)	*Pseudomonas* spp. (1.962)	*P. putida* strain bD1 (100%) <KJ470793>	putida r-cluster	0.84	0.35
MFAA66a	Surburban Rouen, Summer	*P. oryzihabitans* (good)	*P. congelans* (2.164)	*P. syringae pv. Syringae* strain XJLX-2-2 (99%) <KJ470777>	fluorescens r-cluster	0.68	0.32
MFAO40	Rouen Harbor,Winter	*P. fluorescens* (excellent)	*P. koreensis* (2.149)	*P. fluorescens* strain TCA33 (99%) <KJ470794>	fluorescens r-cluster	0.85	0.3
MFAE20	Rouen Harbor, Summer	*P. oryzihabitans* (very good)	*Pseudomonas* spp. (1.917)	*P. graminis strain 8B2* (84%) <KJ470780>	*Pseudomonas* spp.	0.64	0.26
MFAE48	Rouen Harbor, Summer	*P. oryzihabitans* (very good)	*P. graminis* (2.403)	*P. graminis* strain R5SpM3P2C1 (99%) <KJ470781>	fluorescens r-cluster	0.59	0.22
MFAB75	Surburban Rouen, Summer	*P. oryzihabitans* (very good)	*Pseudomonas spp.* (1.728)	*P. plecoglossicida* strain ETLB-3 (78%) <KJ470778>	*Pseudomonas* spp.	0.8	0.22

Int.J.Curr.Microbiol.App.Sci (2014) 3(8) 708-722

MFAE8b	Rouen Harbor, Summer	*P. fluorescens* (excellent)	*Pseudomonas* spp. (1.856)	*P. rhizosphaerae* strain - Y12 (79%) <KJ470783>	fluorescens r-cluster	0.82	0.21
MFAO48	Rouen Harbor,Winter	*P. oryzihabitans* (very good)	*P. savastanoi* (2.098)	*P. syringae* CC1557 (99%) <KJ470795>	fluorescens r-cluster	0.6	0.19
MFAK14	Surburban Rouen, Winter	*P. fluorescens* (good)	*Pseudomonas spp.*(1.923)	*P. putida strain SCR2* (78%) <KJ470790>	*Pseudomonas* spp.	0.62	0.17
MFAO29	Rouen Harbor,Winter	*P. fluorescens* (good)	*P. chlororaphis* (2.006)	*P. thivervalensis* strain BD2-26 (99%) <KJ470792>	fluorescens r-cluster	0.6	0.15
MFAH106a	Rouen Harbor, Summer	*P. oryzihabitans* (excellent)	*Pseudomonas* spp. (1.821)	*P. rhizosphaerae* strain R2-255 (99%) <KJ470788>	fluorescens r-cluster	0.64	0.14
MFAH4a	Rouen Harbor, Summer	*P. fluorescens* (excellent)	*P. poae* (2.255)	*P. fluorescens strain RK2* (83%) <KJ470789>	fluorescens r-cluster	0.79	No growth
MFAD21c	Residential Evreux, Summer	*P. fluorescens* (very good)	*P. poae* (2.147)	*P. fluorescens strain RK2* (86%) <KJ470779>	fluorescens r-cluster	0.78	No growth

Score >1.700 : probable genus
Score >2.000 : probable species, secure genus

Air sample localisation and season; bacterial identification by API®20NE strips, by MALDI-Biotyper and by16S rDNA gene sequencing after matching with NCBI data bank (http://blast.ncbi.nlm.nih.gov/Blast.cgi?PROGRAM=blastn&PAGE_TYPE=BlastSearch&LINK_LOC=blasthome); and maximum specific growth rate (μ_{max}) at 30 and 37°C in LB medium, 180rpm, classified by decreasing μ_{max} at 37°C.

Int.J.Curr.Microbiol.App.Sci (2014) 3(8) 708-722

Table.2 Extracellular virulence factors, at 30°C and 37°C, and biosurfactant production for MFN1032 (clinical strain) and for each airborne strain

The observed characters were proteolytic, esterase lecithinase, lipoproteinase and hemolytic activities, after 5 days, or pyoverdine production, after 2 days. The biosurfactant production was observed on Davis Minimum medium after 5 days. Experiments done in three independant assays.

Activity	Proteolytic		Esterase		Lecithinase		Lipoproteolytic		Secreted hemolytic		Pyoverdin production		Biosurfactant
Incubation temperature (°C)	30	37	30	37	30	37	30	37	30	37	30	37	production
MFN1032	++	++	++	++	++	++	+	+	α	α	++	++	+
MFAF76a	++	++	++	++	++	++	++	++	α	α	++	++	-
MFAF49a	-	-	++	++	-	-	++	+	β	α	++	++	-
MFAF88	-	+	-	-	-	++	+	++	α	α	++	+	+
MFAO2	++	++	++	++	++	++	++	+	α	β	++	++	+
MFAF80b	-	-	++	++	-	-	++	++	β	α	-	-	-
MFAE88	-	-	-	++	-	-	++	++	α	-	-	-	-
MFAO39	-	+	-	-	++	-	+	++	β	β	++	-	-
MFAA66a	+	+	+	-	-	-	+	++	β	α	++	++	+
MFAO40	++	++	++	++	++	++	++	++	α	α	++	++	-
MFAE20	++	-	++	++	-	-	++	++	α	α	-	-	-
MFAB75	-	-	+	-	-	-	+	++	β	β	++	++	-
MFAE48	-	V	++	V	-	V	++	V	-	-	-	+	-
MFAE8b	-	-	++	++	-	-	++	+	α	α	++	-	-
MFAO48	-	-	++	++	-	V	++	V	-	α	++	-	-
MFAK14	-	+	++	-	-	-	+	++	α	α	+	-	+
MFAO29	+	V	++	V	-	V	++	V	β	α	++	-	-
MFAH106a	++	++	++	++	-	+	++	++	-	α	-	-	-
MFAH4a	++	++	++	++	-	-	+	+	β	β	++	++	+
MFAD21c	++	++	++	++	-	-	++	++	β	α	++	++	+

++: important activity
+: light activity
V: weak and variable
-: no activity

α: partial hemolysis
β: complete hemolysis

Int.J.Curr.Microbiol.App.Sci (2014) 3(8) 708-722

Table.3 Motility and biofilm ability, at 30°C and 37°C, for MFN1032 (clinical strain) and for each airborne strain. The observed motility characters were swim, swarm, twitch, after 40h. The biofilm formation was observed after 24h and 48h

Activity	Swim		Swarm		Twitch		Biofilm formation after 24h		Biofilm formation after 48h	
Incubation temperature (°C)	30	37	30	37	30	37	30	37	30	37
MFN1032	++	++	+	+	-	-	++	+	+	-
MFAF76a	++	++	+	+	-	-	++	+	++	+
MFAF49a	+	-	+	+	-	-	-	-	+	+
MFAF88	++	++	+	+	-	-	++	+	+	+
MFAO2	++	+	+	+	-	-	+	-	+	-
MFAF80b	+	-	+	+	-	-	++	-	+	-
MFAE88	+	-	+	+	-	-	+	-	+	-
MFAO39	+	-	+	+	-	-	++	-	++	-
MFAA66a	+	-	+	+	-	-	-	-	-	-
MFAO40	+	-	+	+	-	-	++	-	++	-
MFAE20	+	-	+	+	-	-	+	-	+	+
MFAB75	+	-	+	+	-	-	-	-	+	-
MFAE48	+	-	+	+	-	-	+	+	+	+
MFAE8b	++	+	+	+	-	-	++	+	++	+
MFAO48	+	-	+	+	-	-	-	-	-	-
MFAK14	+	+	+	+	-	-	-	-	-	-
MFAO29	+	-	+	+	-	-	+	-	-	-
MFAH106a	+	-	+	+	-	-	+	-	+	-
MFAH4a	V	-	+	+	-	-	-	+	+	-
MFAD21c	V	-	+	+	-	-	-	-	-	-

++: deplacement upper than 30mm
+: deplacement upper than 10mm
=: deplacement lower than 10mm
V: weak and variable

++: OD595 higher than 0.200
+: OD595 higher than 0.050
-: OD595 lower than 0.050

Int.J.Curr.Microbiol.App.Sci (2014) 3(8) 708-722

Figure.1 Virulence towards A549 pneumocytes exposed to culture supernatants obtained at 30°C and 37°C

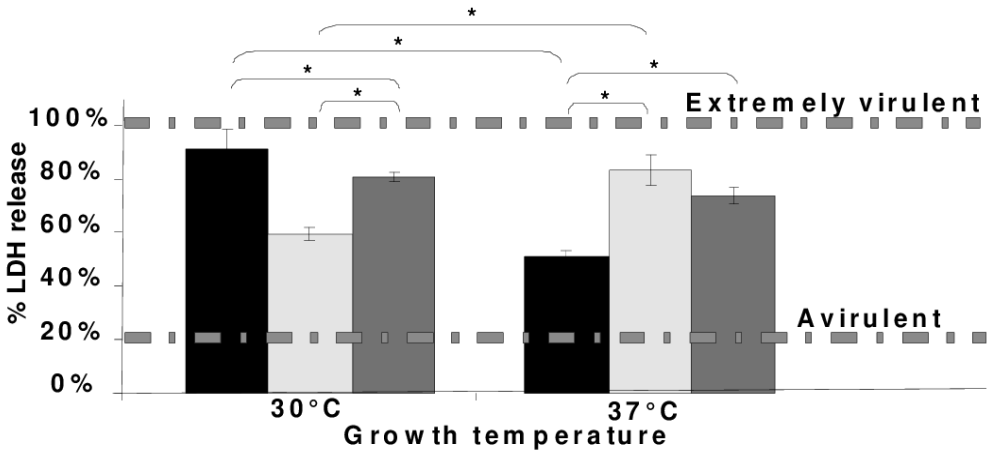

The virulent pattern is strain- and temperature-dependant. In fact, *P. putida* MFAF88 shows a constant virulence, its secretion varies nevertheless with temperature. Virulence could then be attributed to the common production at 30 and 37°C, i.e. lipoproteases, siderophores, and may be completed by biosurfactants, even if their quantities could be secreted quite variably at the two temperatures.

This variability in intensity of secretion could also explain the decrease in virulence for MFN1032. As shown in Table 2, all the enzymes and pyoverdine were expressed at 30°C as well as at 37°C, but no evidence was given about quantity. Rossignol and cowokers rightly note, at 37°C, a weaker production of phospholipase C, than at 28°C (Rossignol et al., 2008). This enzyme is known as a major factor of virulence.

Like MFN1032, the same families of exoproducts are secreted by *P. fluorescens* MFAF76a at both temperatures. However a slightly significative increase in virulence is noted at 37°C and again might be due in the exoproducts secretion modulation in concentration or in nature.

In any case, airborne *P. fluorescens* MFAF76a and *P. putida* MFAF88 may induce by their secretion, especially at 37°C, cytotoxic responses from A549 airway epithelial cells. Thus the biohazard, that they create as biocontamination, must be identified and not ignored. Moreover the virulence of these airborne strains and of the clinical standard, *P. fluorescens* MFN1032 operates on different ways from each other. To better understand these virulent mechanisms, an exoproteomic study would create insight.

Acknowledgements

This study was supported by grants from Grand Evreux Agglomération, AFSSET, and FEDER "*Pseudomonas* Virulence". We wish to thank Christine Farmer for linguistic insight for this manuscript.

References

Agence française de Sécurité Sanitaire de l'environnement et du travail (became ANSES-Agence nationale de sécurité sanitaire de l'alimentation, de

l'environnement et du travail), 2010. Project PUC2MP : Particules Urbaines et Céréalières, Microorganismes Mycotoxines et Pesticides (AFSSET-07-CRD-30) Supervisor Jean-Paul Morin, Partners: Normandie Univ, France ; Univ Rouen, INSERM U644, LMSM, CERTAM, Air Normand.

Bodilis, J., Nsigue-Meilo, S., Besaury, L., Quillet, L. 2012. Variable Copy Number, Intra-Genomic Heterogeneities and Lateral Transfers of the 16S rRNA Gene in *Pseudomonas*. PLoS ONE. 7(4): e35647.

Carrillo, P.G., Mardaraz, C., Pitta-Alvarez, S.I., Giulietti, A.M. 1996. Isolation and selection of biosurfactant-producing bacteria. Journal of Microbiology and Biotechnology. 12: 82-84.

Chapalain, A., Rossignol, G., Lesouhaitier, O., Merieau, A., Gruffaz, C., Guerillon, J., Meyer, J.M., Orange, N., Feuilloley, M.G. 2008. Comparative study of 7 fluorescent pseudomonad clinical isolates. Canadian Journal of Microbiology 54(1): 19-27.

Church, D., Elsayed, S., Reid, O., Winston, B., Lindsay, R. 2006. Burn wound infections. Clin Microbiology Reviews 19(2): 403-434.

Clifton, I.J., Peckham, D.G. 2010. Defining routes of airborne transmission of *Pseudomonas aeruginosa* in people with cystic fibrosis. Expert Review of Respiratory Medicine. 4(4): 519-529.

Donnarumma, G., Buommino, E., Fusco, A., Paoletti, I., Auricchio, L., Tufano, M.A. 2010. Effect of temperature on the shift of *Pseudomonas fluorescens* from an environmental microorganism to a potential human pathogen. International Journal of Immunopathology and Pharmacology. 23(1): 227-234.

Duclairoir Poc, C., Groboillot, A., Lesouhaitier, O., Morin, J.P., Orange, N., Feuilloley, M.J.G. 2011a. *Caenorhabditis elegans:* a model to monitor bacterial air quality. BMC Research Notes 4: 503.

Duclairoir Poc, C., Ngoya, S., Groboillot, A., Bodilis, J., Taupin, L., Merieau, A., Feuilloley, M.G., Orange, N. 2011b. Study of the influence of growth temperature on cyclolipopeptides production in environmental strains of *Pseudomonas fluorescens*. Journal of Bacteriology and Parasitology S1:002. Available http://dx.doi.org/10.4172/2155-9597.S1-002. Accessed 23 July 2014.

Fernstrom, A., Goldblatt, M. 2013. Aerobiology and Its Role in the Transmission of Infectious Diseases. Journal of Pathogens, Article ID 493960, Available : http://dx.doi.org/10.1155/2013/493960 . Accessed 23 July 2014.

Gershman, M.D., Kennedy, D.J., Noble-Wang, J., Kim, C., Gullion, J., Kacica, M., Jensen, B., Pascoe, N., Saiman, L., McHale, J., Wilkins, M., Schoonmaker-Bopp, D., Clayton, J., Arduino, M., Srinivasan, A., *Pseudomonas fluorescens* Investigation Team. 2008. Multistate outbreak of *Pseudomonas fluorescens* bloodstream infection after exposure to contaminated heparinized saline flush prepared by a compounding pharmacy. Clinical Infectious Diseases. 47(11):1372-9.

Gessner, A.R; and Mortensen, J.E. 1990 Pathogenic factors of *Pseudomonas cepacia* isolates from patients with cystic fibrosis. Journal of Medical Microbiology. 33 : 115-120.

Hahn, H.P. 1997. The type-4 pilus is the major virulence-associated adhesin of *Pseudomonas aeruginosa*--a review.

Gene 192(1): 99-108.

Hawdon, N.A., Aval, P.S., Barnes, R.J., Gravelle, S.K., Rosengren, J., Khan, S., Ciofu, O., Johansen, H.K., Høiby, N., Ulanova, M. 2010. Cellular responses of A549 alveolar epithelial cells to serially collected *Pseudomonas aeruginosa* from cystic fibrosis patients at different stages of pulmonary infection. FEMS Immunology & Medical Microbiology. 59(2): 207-220.

Hillion, M., Mijouin, L., Jaouen, T., Barreau, M., Meunier, P., Lefeuvre, L., Lati, E., Chevalier, S., Feuilloley, M.G.J. 2013. Comparative study of normal and sensitive skin aerobic bacterial populations. MicrobiologyOpen 2(6):953-961.

Kearns, D.B. 2010. A field guide to bacterial swarming motility. Nature Reviews Microbiology. 8(9): 634-644.

Luo, G., Samaranayake, L.P., Yau, J.Y. 2001. *Candida* species exhibit differential in vitro hemolytic activities. Journal of Clinical Microbiology. 39(8):2971-4.

Madi, A., Lakhdari, O., Blottière, H.M., Guyard-Nicodème, M., Le Roux, K., Groboillot, A., Svinareff, P., Doré, J., Orange, N., Feuilloley, M.G., Connil, N. 2010. The clinical *Pseudomonas fluorescens* MFN1032 strain exerts a cytotoxic effect on epithelial intestinal cells and induces Interleukin-8 via the AP-1 signaling pathway. BMC Microbiology. 10(10): 215.

McDougald, D., Rice, S.A., Barraud, N., Steinberg, P.D., Kjelleberg, S. 2011. Should we stay or should we go: mechanisms and ecological consequences for biofilm dispersal. Nature Reviews Microbiology. 10(1): 39-50.

Merieau, A., Gügi, B., Guespin-Michel, J.F., Orange, N. 1993. Temperature regulation of lipase B. secretion by *Pseudomonas fluorescens* strain MF0. Applied Microbiology and Biotechnology. 39: 104-109.

Morin, J.-P., Preterre, D., Gouriou, F., Delmas, V., François, A., Orange, N., Grosboillot, A., Duclairoir-Poc, C., Moretti, M., Maillot, O., Lesouhaitier, O. 2013. Particules urbaines et céréalières, micro-organismes, mycotoxines et pesticides. Pollution atmosphérique. 217, Available: http://lodel.irevues.inist.fr/pollution-atmospherique/index.php?id=759.

Mulet, M., Lalucat, J., García-Valdés, E. 2010. DNA sequence-based analysis of the Pseudomonas species. Environmental Microbiology. 12(6): 1513–1530.

Nevalainen, A., Savolainen, R., Heinonen-Tanski, H.1990. Indoor and outdoor occurrence of Pseudomonas bacteria. Proc. of the 5th International Conference on Indoor Air Quality and Climate, Toronto, Canada 29.07.-03.08.1990

O'Toole, G.A., Kolter, R. 1998. Flagellar and twitching motility are necessary for *Pseudomonas aeruginosa* biofilm development. Molecular Microbiology. 30: 295-304.

Pimenta, A.L., Di Martino, P., Blight, M.A. 2006. Positive correlation between *in vivo* and *in vitro* assays for the evaluation of *Pseudomonas* virulence. Research in Microbiology. 157(9): 885-890.

Prüss-Ustün, A., Vickers, C., Haefliger, P., Bertollini, R. 2011. Knowns and unknowns on burden of disease due to chemicals: a systematic review. Environmental Health-Glob 10:9. Available: http://www.ehjournal.net/content/10/1/9. Accessed 23 July 2014..

Rajmohan, S., Dodd, C.E., Waites, W.M.

2002. Enzymes from isolates of *Pseudomonas fluorescens* involved in food spoilage. Journal of Applied Microbiology. 93(2): 205-213.

Rossignol, G., Merieau, A., Guerillon, J., Veron, W., Lesouhaitier, O., Feuilloley, M.G., Orange, N. 2008. Involvement of a phospholipase C in the hemolytic activity of a clinical strain of *Pseudomonas fluorescens*. BMC Microbiology 30(8): 189.

Rossignol, G., Sperandio, D., Guerillon, J., Duclairoir Poc, C., Soum-Soutera, E., Orange, N., Feuilloley, M.G., Merieau, A. 2009. Phenotypic variation in the *Pseudomonas fluorescens* clinical strain MFN1032. Research in Microbiology. 160(5): 337-344.

Semmler, A.B.T., Whitchurch, C.B., Mattick, J.S. 1999. A re-examination of twitching motility in *Pseudomonas aeruginosa*. Microbiology+. 145: 2863-2873.

Sperandio, D., Rossignol, G., Guerillon, J., Connil, N., Orange, N., Feuilloley, M.G., Merieau, A. 2010. Cell-associated hemolysis activity in the clinical strain of *Pseudomonas fluorescens* MFN1032. BMC Microbiology. 24(10): 124.

Sperandio, D., Decoin, V., Latour, X., Mijouin, L., Hillion, M., Feuilloley, M.G., Orange, N., Merieau, A. 2012. Virulence of the *Pseudomonas fluorescens* clinical strain MFN1032 against Dictyostelium discoideum and macrophages in relation with type III secretion system. BMC Microbiology. 12: 223.

Stover, C.K., Pham, X.Q., Erwin, A.L., Mizoguchi, S.D., Warrener, P., Hickey, M.J., Brinkman, F.S., Hufnagle, W.O., Kowalik, D.J., Lagrou, M., Garber, R.L., Goltry, L., Tolentino, E., Westbrock-Wadman, S., Yuan, Y., Brody, L.L., Coulter, S.N., Folger, K.R., Kas, A., Larbig, K., Lim, R., Smith, K., Spencer, D., Wong, G.K., Wu, Z., Paulsen, I.T., Reizer, J., Saier, M.H., Hancock, R.E., Lory, S., Olson, M.V. 2000. Complete genome sequence of *Pseudomonas aeruginosa* PAO1, an opportunistic pathogen. Nature. 406(6799): 959-964.

Strateva, T. and Mitov, I. 2011. Contribution of an arsenal of virulence factors to pathogenesis of *Pseudomonas aeruginosa* infections. Annals of Microbiology. 61(4): 717-732.

Van Hamme, J.D., Singh, A., Ward, O.P. 2006. Physiological aspects. Part 1 in a series of papers devoted to surfactants in microbiology and biotechnology. Biotechnology Advances. 24(6): 604-620.

Vincent, J.L., Sakr, Y., Sprung, C.L., Ranieri, V.M., Reinhart, K., Gerlach, H., Moreno, R., Carlet, J., Le Gall, J.R., Payen, D. 2006. Sepsis in European intensive care units: results of the SOAP study. Critical Care Medicine. 34(2): 344-353.

Zhang, W.W., Hu, Y.H., Wang, H.L., Sun, L. 2009. Identification and characterization of a virulence-associated protease from a pathogenic *Pseudomonas fluorescens* strain. Veterinary Microbiology. 139(1-2): 183-188.

2. Oral communications

1. Kondakova T., Merlet-Machour N., Preterre D., Dionnet F., Feuilloley M., Orange N., Duclairoir Poc C. "**A new study of the bacterial lipidome: HPTLC-MALDI TOF Imaging**" - Seminar at Réseau Sécurité Sanitaire GRR Chimie, Biologie, Santé, Rouen (France). November 28, 2013.

2. Kondakova T., Merlet-Machour N., Preterre D., Dionnet F., Orange N., Duclairoir Poc C. "**Study of the virulence of airborne *Pseudomonas* with a new lipidomics tool**" – Day of Air Quality, Villeneuve d'Ascq (France). February 10-11, 2014.

3. Kondakova T., Merlet-Machour N., Preterre D., Dionnet F., Orange N., Duclairoir Poc C. "**Study of the airborne *Pseudomonas* lipidome with HPTLC-MALDI TOF Imaging tools**" – 17th Seminar of PhD School EdNBISE: Le Havre (France). Avril 10, 2014.

4. Kondakova T., Merlet-Machour N., Bodilis J., Dionnet F., Feuilloley M., Orange N, Heipieper H.J., Duclairoir Poc C. "**Bacterial phospholipid adaptation to human temperature"** – Euro Fed Lipid Congress, Florence (Italy). September 27-30, 2015.

3. Posters

1. Kondakova T., Merlet-Machour N., Preterre D., Dionnet F., Orange N., Duclairoir Poc C. "**Lipidome of airborne *Pseudomonas* sp. by HPTLC-MALDI TOF MSI: remarkable presence of eukaryotic lipid – phosphatidylcholine**" – 3rd scientific day of IRIB (Institute for Research and Innovation in Biomedicine), Manoir Henri IV de Caugé (France), June 20, 2014.

2. Kondakova T., Merlet-Machour N., Bodilis J., Dionnet F., Feuilloley M., Orange N., Heipieper H.J., Duclairoir Poc C. "**Effect of temperature on *Pseudomonas* phospholipid composition**" – 18th Seminar of PhD School EdNBISE, Rouen (France), April 26-27, 2014.

3. Kondakova T., Dionnet F., Feuilloley M., Orange N., Heipieper H.J., Duclairoir Poc C. "**The nitrogen dioxide modifies *Pseudomonas fluorescens* biofilm? Identification of the bacterial response to air pollutant**" - 6th Congress of European Microbiologists, Maastricht (Netherlands), June 7-11, 2015.

4. Kondakova T., Merlet-Machour N., Bodilis J., Dionnet F., Feuilloley M., Orange N, Heipieper H.J., Duclairoir Poc C. "***Pseudomonas fluorescens* lipidome screening: effect of temperature and growth phase on *Pseudomonas* phospholipids"** – 6th Congress of European Microbiologists, Maastricht (Netherlands), June 7-11, 2015.

Lipidome of airborne Pseudomonas *sp. by HPTLC-MALDI-TOF MSI : remarkable presence of eucaryotic lipid - phosphatidylcholine*

T. KONDAKOVA[1,3], N. MERLET-MACHOUR[2], D. PRETERRE[3], F. DIONNET[3], N. ORANGE[1] , C. DUCLAIROIR POC[1]

[1] Normandie University of Rouen, Laboratory of Microbiology Signals and Microenvironment, Research Team 4312, 55 rue St. Germain F 27000 Evreux

[2] Team Modified to Surface and Interface Analysis (SIMA), UMR 6014 COBRA, Research Institute of Fine Organic Chemistry of Rouen, 55 rue St. Germain F 27000 Evreux

[3] Aerothermic and Internal Combustion Engine Technological Research Center (CERTAM), 1 rue Joseph Fourier, F 76800 - Saint Etienne du Rouvray

Introduction

Over the past years, in addition to terms such as "proteomics", "genomics", and "metabolomics", "lipidomics" was introduced and confirmed also the widespread interest in the development of methods for analyzing bacterial lipid profiles. Lipids are major compounds of bacterial cell that exhibit a variety of biological functions (metabolism, membrane integrity, nutrient transport …)

This study investigates lipids of airborne bacterium *Pseudomonas* sp. MFAF76a with a modern and easy analytical method coupling of HPTLC and MALDI TOF MS.

Developed methodology: HPTLC-MALDI-TOF MSI

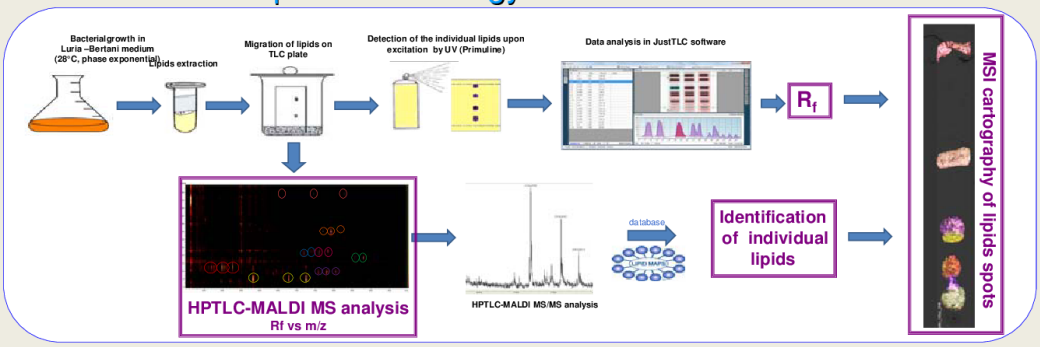

Lipidome of airborne *Pseudomonas* sp. MFAF76a using HPTLC-MALDI-TOF MSI

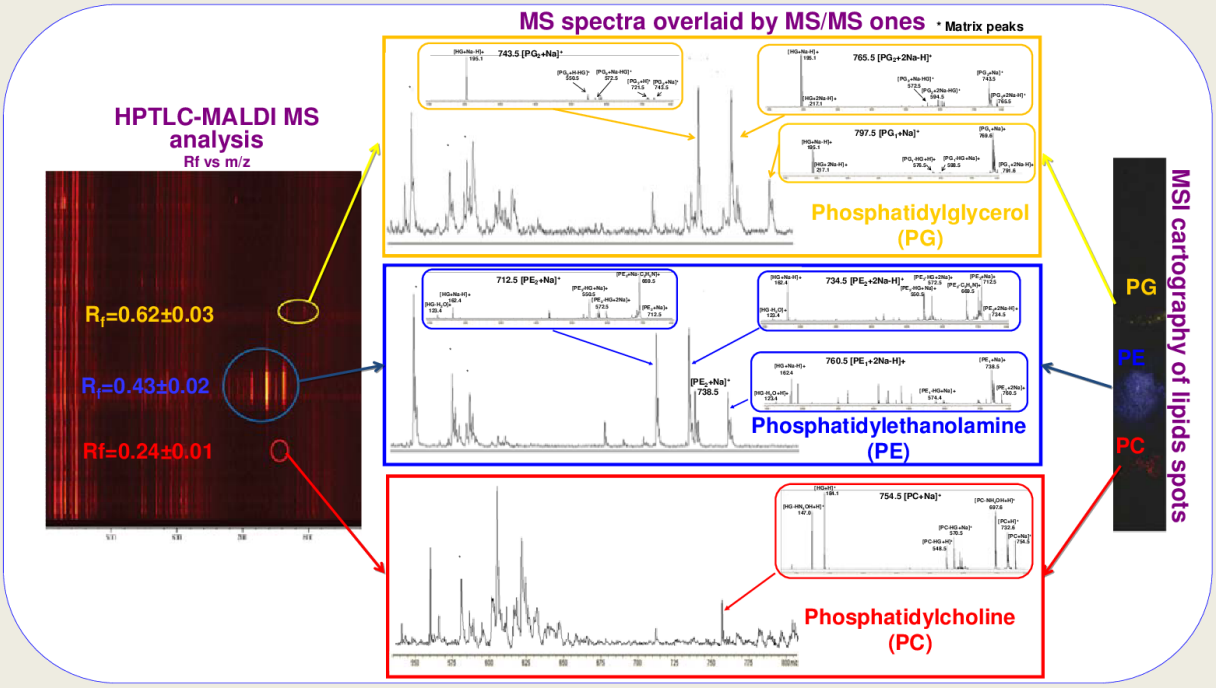

This study of bacterial lipidome using HPTLC MALDI TOF MSI method shows the screening of bacterial lipids in a very short time and with a modest cost.

Thanks to this method, various species of phosphatidylethanolamine and phosphatidylglycerol are identified in the lipidome of the airborne *Pseudomonas* sp. MFAF76a.

Moreover, unusual presence of phosphatidylcholine, as major eukaryotic lipid, speculates its important role during pathogen/symbiont – host interaction.

Effect of temperature on *Pseudomonas* phospholipid composition

T. Kondakova[1,3], N. Merlet-Machour[2], J. Bodilis[1], F. Dionnet[3], M. Feuilloley[1], N. Orange[1], H.J. Heipieper[4], C. Duclairoir Poc[1]

[1] Laboratory of Microbiology Signals and Microenvironment EA 4312, Normandie Univ., Univ. Rouen, IRIB, 27000 Evreux, France
[2] Team Modified to Surface and Interface Analysis (SIMA), UMR 6014 COBRA, Normandy Univ., Univ. Rouen, 55 rue St Germain, 27000 Evreux, France,
[3] Aerothermic and Internal Combustion Engine Technological Research Centre (CERTAM), 1 rue Joseph Fourier, 76800 Saint Etienne du Rouvray, France,
[4] Department of Environmental Biotechnology, UFZ Helmholtz Centre for Environmental Research, Permoserstr. 15, 04318 Leipzig, Germany.

Introduction

Pseudomonas are present in all natural environments, and able to quickly adapt to environmental modifications. Physiologically, this adaptation depends essentially to the structure and organization of their envelope. The membrane functions are traditionally attributed to proteins that are immersed in the lipid bilayer, but lipids are not only a matrix to accommodate proteins, but play a major role in bacterial functioning. *P. fluorescens* is a psychrophilic bacterium commonly found in soil and water. Some of *P. fluorescens* members are able to growth at the human temperature, as members of the skin microbiota or as opportunistic pathogens.

The aim of this work is:

1. Characterization of the phospholipid composition of *P. fluorescens* using an adapted HPTLC-MALDI-TOF MS Imaging tool,
2. Establish if the response to human temperature involves changes in *P. fluorescens* phospholipids,
3. Study of lipidomes of two *P. fluorescens* strains from different ecological niches: one clinical MFN1032 and one airborne MFAF76a.

1. Adaptation of *P. fluorescens* to human temperature by membrane phospholipid modifications

Temperature and phospholipid composition

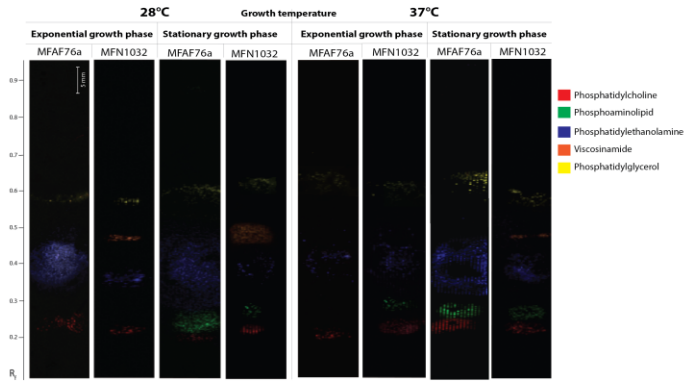

1. At 37°C the both strains product more zwitteronic phospholipids, like phosphatidylethanolamine and phosphatidylcholine.
2. The phosphatidylethanolamine is the major structural component of *P. fluorescens* membrane. Its quantity determines the membrane charge.
3. The phosphatidylcholine is the major eukaryotic phospholipid. This phospholipid may be involved in *P. fluorescens* - host interactions.

Temperature and degree of fatty acids' saturation

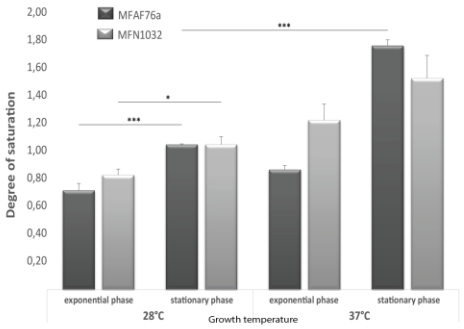

1. The temperature augmentation increases membrane fluidity.
2. To adapt to human temperature *P. fluorescens* products more phospholipids with unsaturated alkyl chains, increasing the degree of phospholipid saturation.
3. The synthesis of unsaturated phospholipids allows *P. fluorescens* to control the membrane fluidity.

2. New phospholipid class identification

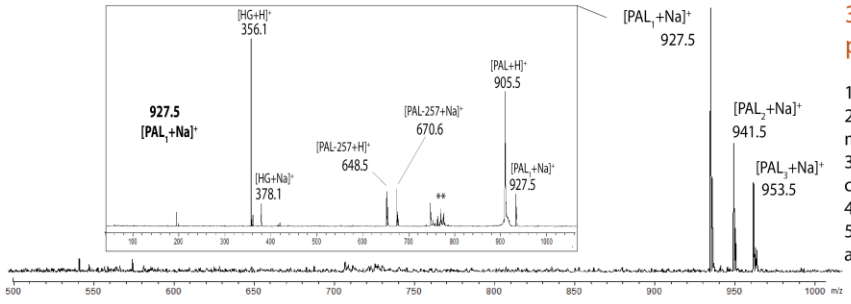

3 molecules of phosphoaminolipid (PAL):

1. Retention factor 0.26
2. Three MS peaks with Na^+ adducts: m/z 927.5; m/z 941.5; m/z 953.5.
3. Mechanism of PSD fragmentation characteristic for phospholipid
4. Two alkyl chains 16:/18:0
5. Head group (HG) peaks at m/z 195.5 and m/z 356.1

Conclusions

1. *P. fluorescens* is able to adapt to human temperature using two lipidic pathways:
1) the increase of degree of fatty acid unsaturation controls the membrane fluidity,
2) the increase of the synthesis of zwitteronic phospholipids results in the membrane charge changes.
2. The phosphatidylcholine overproduction may facilitate *P. fluorescens* - host interactions.
3. The new lipid class PAL is identified. The role of this phospholipid in *P. fluorescens* temperature adaptation is unknown.

Open questions

1. The phosphatidylcholine role in *Pseudomonas* adaptation to human temperature
2. The PAL complete identification
3. The role of PAL in *P. fluorescens* functionning and temperature adaptation

Supported by

The nitrogen dioxide modifies *Pseudomonas fluorescens* biofilm formation? Identification of the bacterial response to air pollutant

T. Kondakova[1,3], T. Kentache[2], A. Garreau[1], M. Barraud[1], A. Groboillot[1], J. Hardouin[2], F. Dionnet[3], M. Feuilloley[1], N. Orange[1], H.J. Heipieper[4], C. Duclairoir Poc[1]

[1] Laboratory of Microbiology Signals and Microenvironment EA 4312, Normandie Univ., Univ. Rouen, IRIB, 27000 Evreux, France
[2] 2 CNRS UMR 6270, Laboratory Polymères, Biopolymères, Surfaces, University of Rouen, 76820 Mont-Saint-Aignan, France,
[3] Aerothermic and Internal Combustion Engine Technological Research Centre (CERTAM), 1 rue Joseph Fourier, 76800 Saint Etienne du Rouvray, France,
[4] Department of Environmental Biotechnology, UFZ Helmholtz Centre for Environmental Research, Permoserstr. 15, 04318 Leipzig, Germany.

Introduction

Air pollution is a major environmental worldwide concern. Motor traffic is a major source of air pollutants such as nitrogen dioxide (NO_2) and particle aerosol. *Pseudomonas fluorescens* are found in all natural environments, and able to quickly adapt to environmental modifications. However, the influence of air pollutants on bacteria stills poorly studied. Our researches have focused on the impact of traffic-related air pollution on *P. fluorescens*. Thus, two *P. fluorescens* strains were studied: airborne strain MFAF76a and clinical strain MFN1032. In this project, the mechanism of *P. fluorescens* response to NO_2 in different concentrations was evaluated. Three NO_2 concentrations were studied: 100 ppb as environmental NO_2 rate; 5 ppm as regylatory limit; and 45 ppm as high NO_2 concentration.

1. Does NO_2 can freely penetrate into bacterial cells?

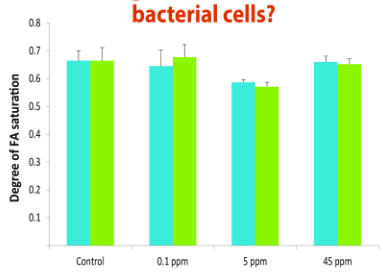

2. Does NO_2 modify *P. fluorescens* gene expression?

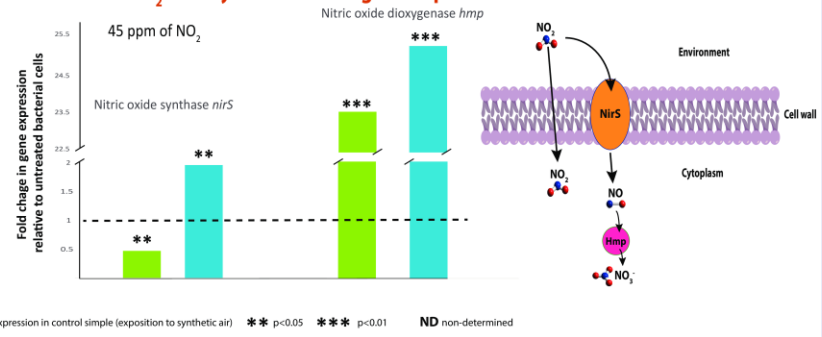

3. Does NO_2 modify *P. fluorescens* biofilm ?

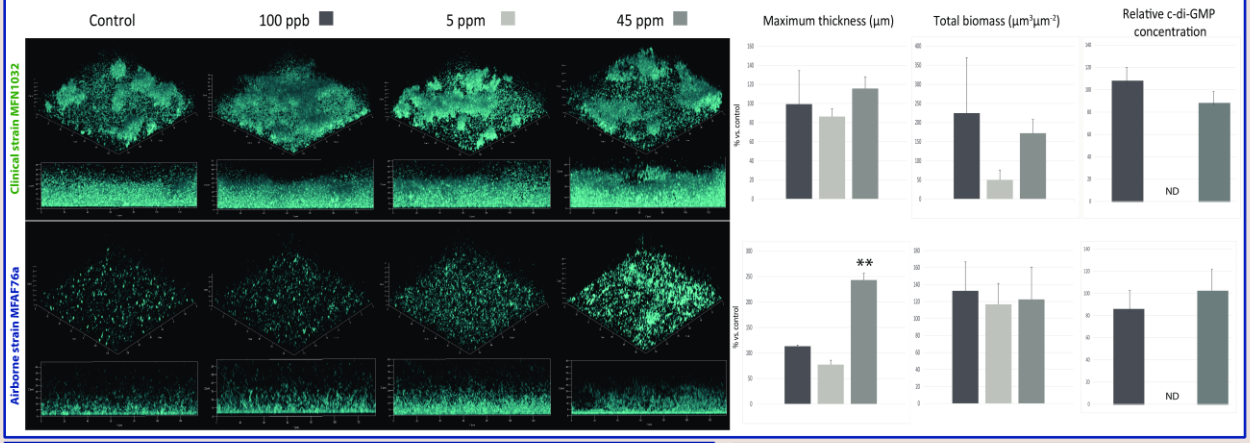

4. How *P. fluorescens* eliminates NO_2 stress ?

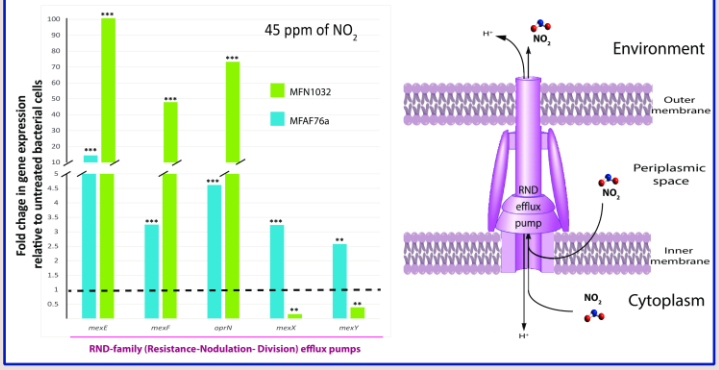

Conclusions

1. ***P. fluorescens*** **is able to adapt to NO_2 stress. Even the highest studied NO_2 concentration allows bacterial growth.**
2. **NO_2 molecules can freely penetrate *P. fluorescens* cell wall.**
3. ***P. fluorescens*** **transform the NO_2 to nitrate (NO_3^-) thanks to nitric oxide synthase (NirS) and nitric oxide dioxygenase (Hmp) enzymes. Thus, *P. fluorescens* prevent NO_2 toxicity (otherwise known as "nitrosative stress").**
4. **NO_2 in three tested concentrations does not modify *P. fluorescens* biofilm biomass, but causes the increasing in biofilm thickness. The thickness increasing was observed only for 45 ppm of NO_2 for airborne strain MFAF76a, and may result from the overproduction of NirS enzyme.**
5. **To eliminate unmodified NO_2, *P. fluorescens* cells use the RND efflux pumps, like MexE/F or MexX/Y.**

Open questions

1. **NO is known to disperse *P. aeruginosa* biofilm. Does its analog, NO_2 modify the expression of genes coding to biofilm dispersion?**
2. **Efflux pumps are involved in bacterial antibiotic resistance. Does NO_2 stress allow increasing in *P. fluorescens* antibiotic resistance?**

Pseudomonas fluorescens lipidome screening: effect of temperature and growth phase on *Pseudomonas* phospholipids

T. Kondakova[1,3], N. Merlet-Machour[2], J. Bodilis[1], F. Dionnet[3], M. Feuilloley[1], N. Orange[1], H.J. Heipieper[4], C. Duclairoir Poc[1]
[1] Laboratory of Microbiology Signals and Microenvironment EA 4312, Normandie Univ., Univ. Rouen, IRIB, 27000 Evreux, France
[2] UMR 6014 COBRA, Normandy Univ., Univ. Rouen, 55 rue St Germain, 27000 Evreux, France,
[3] Aerothermic and Internal Combustion Engine Technological Research Centre (CERTAM), 1 rue Joseph Fourier, 76800 Saint Etienne du Rouvray, France,
[4] Department of Environmental Biotechnology, UFZ Helmholtz Centre for Environmental Research, Permoserstr. 15, 04318 Leipzig, Germany.

Introduction

Pseudomonas fluorescens are found in all natural environments, and able to quickly adapt to environmental modifications. Physiologically, these adaptations depend essentially on the structure and organization of their envelope. Its protective functions are traditionally attributed to proteins that are immersed in the lipid membrane, but lipids also play a major role in bacterial functioning. *P. fluorescens* is a psychrophilic bacterium commonly found in soil and water. Some of *P. fluorescens* members are able to grow at the human temperature (37°C), as opportunistic pathogens.

The aims of this work are:

1. Characterization of the glycerophospholipid (GP) membrane composition of *P. fluorescens* using an adapted HPTLC-MALDI-TOF MS Imaging tool,
2. Establishing of membrane lipids response of *P. fluorescens* to human temperature,
3. Study of lipidomes of two *P. fluorescens* strains from different ecological niches: one clinical MFN1032 and one airborne MFAF76a.

1. Adaptation of *P. fluorescens* to human temperature by membrane glycerophospholipid modifications

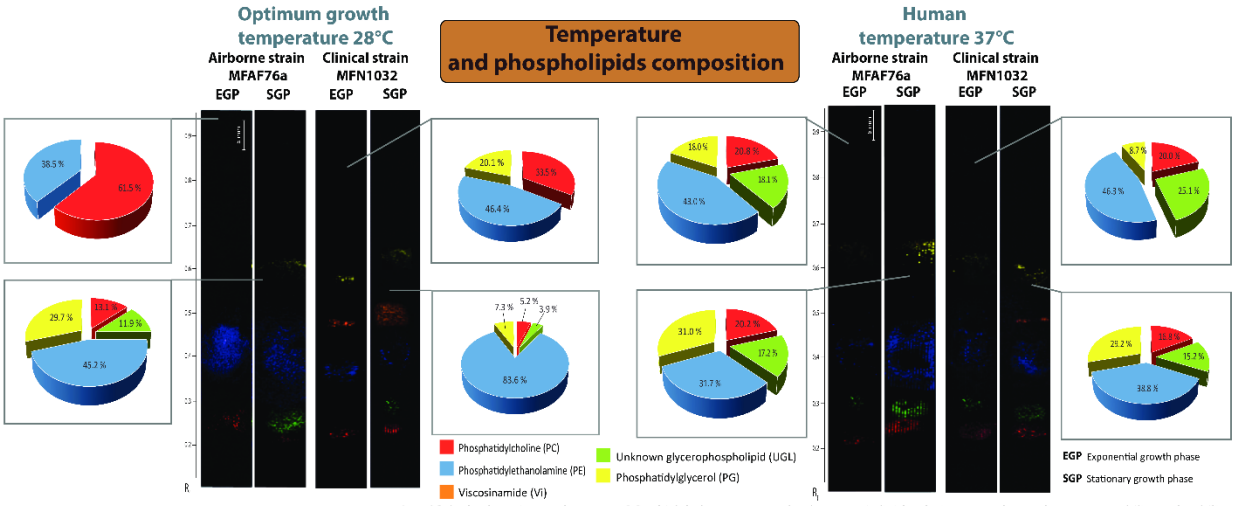

1. At 37°C the both strains product more PG, which helps to counter the decreases in lipid ordering, controls membrane permeability and stability
2. The PC is the major eukaryotic phospholipid. This GP is found in all experimental conditions, indicating its structural membrane role. The quantity of this GP does not related with temperature effect, but with growth phase. PC is much more produced in exponential growth phase. Thus, thanks to its chemical composition, PC production regulates the membrane fluidity.

Temperature and degree of fatty acids saturation

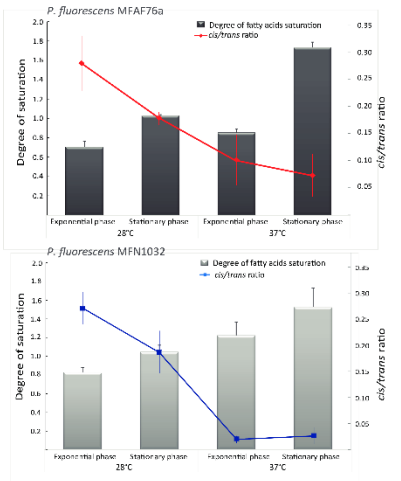

1. The temperature augmentation increases membrane fluidity.
2. To adapt to human temperature *P. fluorescens* products more GPs with unsaturated alkyl chains, increasing the degree of GPs saturation.
3. The synthesis of unsaturated GPs allows *P. fluorescens* to control the membrane fluidity.

2. New phospholipid class identification

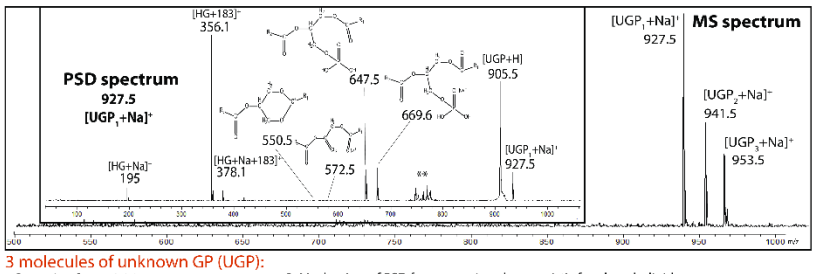

3 molecules of unknown GP (UGP):

1. Retention factor 0.26.
2. Three MS peaks with Na^+ adducts: m/z 927.5; m/z 941.5; m/z 953.5.
3. Mechanism of PSD fragmentation characteristic for phospholipid.
4. Two alkyl chains 16:/18:0.
5. Head group (HG) peaks at m/z 195.5 and m/z 356.1.

Conclusions

1. ***P. fluorescens* is able to adapt to human temperature using two lipidic pathways:**
   1) **increase of degree of fatty acid saturation controls the membrane fluidity,**
   2) **increase of PG synthesis controls lipid ordering, membrane stability and permeability.**
2. **PC production is independent on temperature, but growth phase. The PC overproduction in exponential growth phase can increase *P. fluorescens* membrane fluidity.**
3. **The new GP class is identified. The role of this GP in *P. fluorescens* membrane is unknown.**

Open questions

2. **UGP complete identification**
3. **Role of UGP in *P. fluorescens* functionning and temperature adaptation**

Normandie Université

THESE

Pseudomonas adaptation to stress factors: role of membrane lipids and *Pseudomonas fluorescens* response to NO_2

The high distribution of *Pseudomonas fluorescens* group is linked to its ability to adapt to stress factors. This work goaled the response of an airborne *P. fluorescens* MFAF76a, and its clinical standard *P. fluorescens* MFN1032 to environmental changes in order to refine the specific adaptation of airborne bacteria. First the HPTLC-MALDI TOF MSI tool defined glycerophospholipid (GP) composition of both strains. In stationary growth phase, an unknown GP, in short UGP, was found and seemed to be involved in temperature adaptation for the clinical strain. After exposure to 0.1, 5 and 45 ppm concentrations, the bacterial response to NO_2 was defined through motility, biofilm formation, antibiotic resistance and expression of several chosen target genes. While no change in parameters was seen in bacteria exposed to 0.1 and 5 ppm of NO_2, several alterations were occurred with a bacterial exposure to 45 ppm. NO_2 seemed to bias the UGP production, reduced *P. fluorescens* swim and decreased swarm only for MFN1032 strain. Biofilm formed by NO_2-treated MFAF76a showed increased maximum thickness, with no change in c-di-GMP intracellular level. Expression of the *hmp*-homologue gene involved in NO detoxification was upregulated in response to NO_2, suggesting a possible common pathway between NO and NO_2 detoxification. Finally, NO_2 was found to increase bacterial resistance to ciprofloxacin and chloramphenicol. Thus the resistance nodulation cell division (RND) MexEF-OprN efflux pump encoding genes were highly upregulated in both strains. Together these findings implement the first model of bacterial response to NO_2 toxicity and the role(s) of GP in bacterial adaptation to environmental changes.

Keywords: *Pseudomonas fluorescens*, adaptation, glycerophospholipid, fatty acids, pollution, nitrogen oxides

Adaptation de *Pseudomonas* aux facteurs de stress : rôle des lipides membranaires et réponse de *Pseudomonas fluorescens* au NO_2

La large distribution des *Pseudomonas fluorescens* est liée à leur grande adaptabilité aux facteurs de stress tels que les variations environnementales. Ce travail avait pour objet la réponse spécifique au milieu aéroporté de *P. fluorescens*, comme l'aéroportée MFAF76a et la clinique MFN1032, comme standard. La technique récente HPTLC-MALDI-TOF MSI a permis de caractériser les divers glycérophospholipides (GP) des deux souches. En phase stationnaire de croissance, un GP inconnu (UGP - unknown GP) a été isolé et semble intervenir dans l'adaptation à la température de la souche clinique MFN1032. Quant au stress NO_2 gaz, les deux souches ont été exposées aux concentrations: 0.1, 5 et 45 ppm. Leurs phénotypes ont été confrontés à l'expression de quelques gènes ciblés. Pour les valeurs standard 0,5 and 5 ppm en NO_2, aucun paramètre n'est modifié. Par contre, une réponse bactérienne est constatée suite à l'exposition à 45 ppm de NO_2. Cette exposition semble impacter la production d'UGP. De plus *hmp* et *mexEF-oprN*, codant respectivement pour la flavohémoglobine et pour la pompe à efflux RND, se trouvent surexprimés, corroborant l'évolution de la résistance bactérienne aux antibiotiques. Contrairement au NO, aucune altération de la biomasse de biofilm n'est observée pour le NO_2, qui favorise, cependant, l'augmentation de son épaisseur chez MFAF76a, mais aussi l'inhibition du swarming et la diminution du swimming, avec un taux de c-di-GMP stable. Ce faisceau de résultats offre, pour la première fois, la réponse bactérienne et le rôle des GP lors de stress comme NO_2 ou à la température, autre modification environnementale.

Mots clefs: *Pseudomonas fluorescens*, adaptation, glycérophospholipide, acides gras, pollution, oxydes d'azote, détoxification